MINISTRY OF EDUCATION AND SCIENCE OF UKRAINE

NATIONAL TECHNICAL UNIVERSITY OF UKRAINE
"IGOR SIKORSKY KYIV POLYTECHNIC INSTITUTE"

Y. Poplavko, S. Voronov, Y. Yakymenko

SELECTED PROBLEMS OF MATERIALS SCIENCE

Recommended by the Academic Council of the National Technical University of Ukraine "Igor Sikorsky KPI" as a textbook for bachelors / masters / doctors of philosophy in the educational program "Applied Physics" specialty 105 "Applied Physics and Nanomaterials"

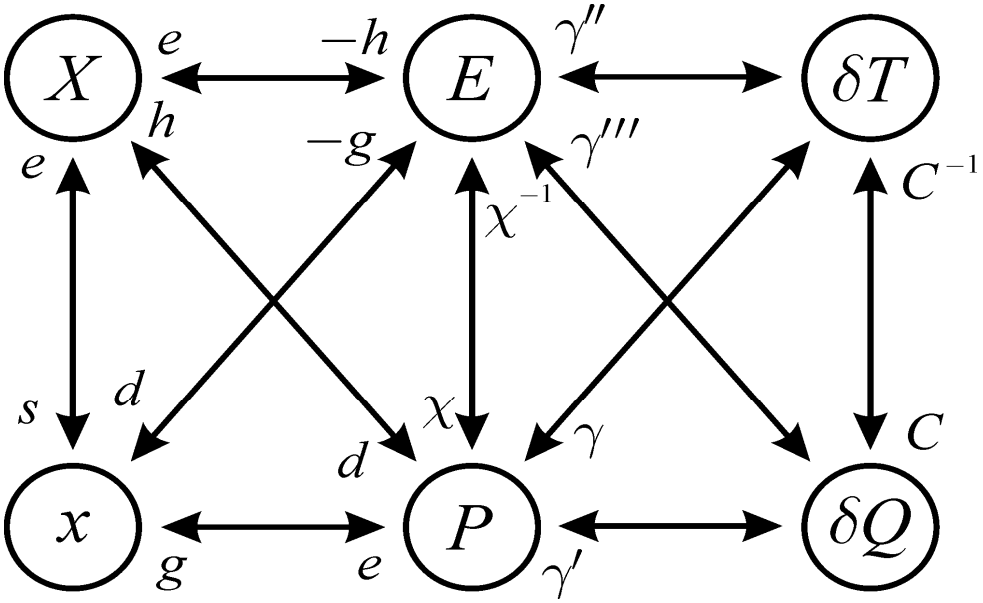

Kyiv
Igor Sikorsky KPI
2021

Reviewer: *O. Stronsky*, Dr. Phys.-Math. Sciences, Professor,
Institute of Semiconductor Physics V.Y. Lashkareva
National Academy of Sciences of Ukraine;

V. Kotovsky, Dr. Technical Sciences, Professor,
Head of the Department of
General Physics and Solid State Physics
"Igor Sikorsky Kyiv Polytechnic Institute"

General editor *N. Gordiyko*, Phd in Technical Sciences,
Associate Professor,
Department of Applied Physics
"Igor Sikorsky Kyiv Polytechnic Institute"

The stamp was provided by the Methodical Council. Igor Sikorsky KPI
(protocol № 8 from 24.06.2021)
at the request of the Academic Council of the Institute of Physics and Technology
(protocol № 12 of 14.06.2021)

Educational edition

Y. Poplavko, Dr. Tech. Sciences, Prof.,
S. Voronov, Dr. Tech. Sciences, Prof.,
Y. Yakymenko, Dr. Tech. Sciences, Prof., Academician of the National Academy of Sciences of Ukraine

SELECTED PROBLEMS OF MATERIALS SCIENCE

Selected problems of materials science [Text]: textbook. way. for students. specialty 105 "Applied Physics and Nanomaterials" / Y. Poplavko, S.Voronov, Y. Yakymenko; "Igor Sikorsky KPI". – K.: "Igor Sikorsky KPI", 2021. – 390 p.

Abstract. The textbook discusses the physical foundations and practical application of functional dielectrics and simiconductors. Theories, experimental data and also specifications of basic materials, necessary for practical application, are considered. The results of modern research in the field of microelectronics and nanophysics are taken into account, with a special attention paid to the influence of the internal structure on the physical properties of materials and prospects for their use. The textbook is based on the authors' many years of experience in teaching physical materials science, intended for the students of higher educational institutions with specializations in the fields of "Applied Physics" and "Microelectronics". The book can also be used by the graduate students, engineers and researchers specializing in materials science.

CONTENT

PREFACE

The relevance of the publication of this tutorial is due to the fact that *Materials sciences* are very important for specialists in the applied physics. It is also supported by the fact that at present not only the educational but also the monographic literature cannot keep pace with rapid development of materials science, in other words, of applied solid-state physics. In this context, the applied physics and, especially, microelectronics with nanoelectronics are particularly fast-growing areas, so it is clear that they are not mentioned in well known books on material science and solid-state physics issued 20–40years ago. This concerns many areas of physics and technology—from the materials elaboration to the devices realization.

The features of the presentation of the *Material Science* in this book are significantly simplified mathematical interpretation of theories, with an emphasis on the basic concepts of physical phenomena in the electronic and other materials, and their simple explanation. Most of the chapters are devoted to the advanced scientific and technological issues; in addition, some new theoretical facts related to the properties of materials are presented, which are important for their use in modern technical devices. This approach of the presentation is due to modern tendency towards the interpenetration and synthesis of various fields, at first glance, belonging to the different fields of science.

This training course might be a key reference in the application of physics for advanced fundamental understanding of the physical mechanisms in micro- and nanomaterials and their electronic applications. It examines the modern methods of studying these materials properties that are needed by researchers and engineers working in the field of electronics. The *purpose* of the book is to form students' abilities for practical use of modern models and research tools in solving scientific and technical problems; learn to independently develop models of the latest electronic processes, as well as technological processes of electronics. Main *objectives* of the tutorial, according to the requirements of the curriculum, students after mastering the discipline must demonstrate the following learning outcomes: knowledge of the physical foundations of processes in micro- and nanostructures, as well as tools and methods for calculating the characteristics of correspondent devices.

Key features: (1) Provides students with a scientifically based understanding of the micro- and nanomaterials and their practical applications. (2) Takes a simplified mathematical approach to theories, essential to understanding of micro- and nanomaterials, and summarizes at the end of each chapters. (3) Interweaves modern experiments and theories in topics such as micro- and nanomaterials.

INTRODUCTION

The present time of universal communication obliges us to teach students special subjects in English. The need to use English in modern technical education of students is very relevant. In the course of modern interactive learning, students should be prepared for both individual work and work with a teacher and in a team; they must also be active in perception, communication and sociality. It goes without saying that such interactive learning should be provided with high-quality didactic material in modern scientific and technical English. To this end, the authors of this book have revised their textbooks previously published in Ukrainian into a textbook in English, intended for masters and doctoral students. The presented textbook belongs to the field of materials science physics, and is focused mainly in the direction of electronic engineering.

The complex and important issue of higher education pedagogy is the optimization of the process of future specialists training, the development of professional qualifications, the creation of a new system of vocational guidance, and the training of competent specialists. For the training of such personnel it is necessary to activate the process of education, to develop new forms and methods of teaching. When activation of educational process is understood the construction of such training, which involves the organization of the educational process on a scientific basis, the creation of conditions for creative thinking, research work of students, that generates interest in their future specialty, etc.

Use of information technologies in preparing competent specialists is one of the main requirements set for educational institutions in the context of development of the information society. Improvement of the educational process is associated with the informatization of education and the effective implementation of special methods and techniques in the educational process. An important element in formation of student’s higher competence is information technology tools. Under information technology refers to modern equipment and systems that allow you to manage information processes. Authors consider the effective use of various teaching methods, including interactive methods: readiness for cognitive actions from position of independence; willingness to solve problems; willingness to effectively use information and communication technologies at the user level; readiness for interpersonal oral and written relations (as in Ukrainian so in English). Interactive methods are based on the relationship between the student and the student, as well as methods that create conditions for joint activities. In other words, the word "interactive" means joint activities, the establishment of cooperation

procedure. And "interactive learning" means learning based on joint communication, learning through dialogue, "teacher-student", "student-student", "self-learner" relations in the following formats: conversation, dialogue, discussion, joint actions. Thus, interactive teaching methods built on interpersonal relationships satisfy the paradigm of modern education aimed at "personal development". At the same time, interactive methods not only form the activity of perception and personal significance in learning, but also develop them. Through the interactive methods, students master new knowledge, qualifications, skills and abilities: development of critical thinking, reflexive abilities; analysis and evaluation of their ideas and actions; independent understanding, comprehensive analysis and the ability to select information; independent formation of new knowledge; participation in discussions, defending their opinions; decision making and solving complex issues. In the process of interactive learning, the student learns to formulate his opinion, correctly convey his thoughts, substantiate his opinion, lead a discussion, listen to others, respect and reckon with other opinions and points of view.

Modern education of students in the Technical university puts forward the requirement to teach not only the characteristics of the profession but also the ability to work with scientific and technical literature, which is presented now mainly in English. Our practice shows that only a part of students are able to use technical English at their end in technical university study.

The contents of this book takes into account a rapid progress in the field of material sciences to reflect latest achievements. Below is a list of the modern advances in electronic materials science, presented in this book, that have not previously been described in the educational literature.

Chapter 1. Thermodynamics of dielectrics is dedicated to materials thermal properties, which are conditioned by the interaction energy of molecules, atoms and electrons. In addition to a general description of thermodynamics applied to the electrical properties of materials, the original research results are presented.

Adiabatic and isotermal permittivity. Research and application of materials is generally held under the adiabatic conditions, when during the change of applied voltage a thermal equilibrium between dielectric and surrounding environment can not be installed in time, so any alteration of entropy is absent: $\delta S = 0$. Therefore, from experiments, the *adiabatic permittivity* ε^S is generally determined. In such dielectrics, which polarization depends on temperature (paraelectrics, ferroelectrics, pyroelectrics, and others), an another – isothermal – process of polarization might be important, when $\delta T = 0$ and permittivity is *isothermal*: ε^T. Analytical determination of relationship between ε^T and ε^S may be important both to explain

the frequency dependence of permittivity in range of subsonic frequencies, and for theoretical calculations. Isothermal dielectric permittivity is always greater than adiabatic one: $\varepsilon^T > \varepsilon^S$. In most cases this difference is small and can be neglected. However, in the pyroelectrics, and, especially, in the vicinity of ferroelectric phase transition, the difference between ε^T and ε^S can reach 10–50%, so it should be taken into account.

Temperature coefficient of permittivity ($TC\varepsilon$) is very important for practical application, and it is very important that thermodynamics gives a convincing prediction on this quession, linking the sign of $TC\varepsilon$ to the mechanisms of polarization. If the dielectric permittivity increases during dielectric heating, i.e., when $TC\varepsilon > 0$, then the change in entropy $S - S_0(T)$ during polarization must be positive. Thus, not discussing the details of processes which occur in a dielectric, only from general thermodynamic considerations, it can be concluded that in the dielectric with $TC\varepsilon > 0$, when it is placed in the electrical field, such physical processes occur, which *reduce* the degree of molecular or atomic structure ordering. Conversely, if in the dielectric possessing $TC\varepsilon < 0$, i.e., when its permittivity decreases with heating, the change in entropy is negative. This means that basic mechanisms, which determine electrical polarization, the external electrical field application results in the *increase* in the ordering of molecules (ions, atoms) in a dielectric.

Explanation of second order phase transition. Degrees of a freedom while atomic particles movement in solids can be divided into two groups. If the interaction energy of particles U_{int} is small in comparison with thermal motion energy k_BT, namely $U_{int} << k_BT$, then the appropriate degrees of freedom behave as the *collection* of quasi-particles, i.e., as "almost ideal gas" of phonons; this refers to ordinary non-polar dielectrics. In the opposite case, when, conversely, $U_{int} >> k_BT$, then appropriate degrees of freedom are usually quite ordered, but their movement, too, can be described by the introduction of phonons. These substances include majority of functional polar-sensitive dielectrics (piezoelectrics and pyroelectrics), so the application of phonons concept to them in most cases can be considered justified. Much more complicated cases arise if interaction energy $U_{int} \sim k_BT$. In this case, the theoretical description of solids becomes complicated, especially at phenomenon of phase transition, when the non-polar phase is turning into the polar phase. At that, polar-sensitive crystal behaves by such a way, when any conventional concept, based on phonons, can not adequately describe experimental situation. Particles interaction has special character: the probability of collective movements is bigger then the probability of individual movements. Abnormal increased role of collective

movements is confirmed by experiments in the vicinity off phase transition: at temperature $T = T_C$ crystal shows the maximum of specific heat, the minimums of thermal expansion and thermal diffusion coefficients.

Specific heat of polar crystals contains an additional contribution due to the disordering-disordering processes of their polar-sensitive bonds. It is discovered and explained that in the polar crystals specific heat exceeds this parameter as compared with the non-polar crystals: this is clearly expressed in the vicinity of phase transitions, where the maximum of specific heat capacity can be several times higher than its average value. It might be supposed that an additional contribution to the specific heat in the ordering phase is due to the configurational entropy. Statistical possibility of several states realizing increases the total entropy of a system: such *configuration entropy* is related to the position of constituent particles rather than to their velocity or momentum. It is physically related to number of ways of arranging all particles of a system while maintaining some overall set of specified system properties, such as energy. Change in the configuration entropy corresponds to the same change in macroscopic entropy.

Slowed thermal diffusion. At normal temperatures, the heat transfer in crystals is curried out mainly by the shortwave acoustic phonons, ("heat phonons"), which wavelength is commensurable with crystal lattice parameter, and propagation velocity is much less as compared with the long-length “sound phonons”. To describe the mechanisms of heat transfer, two important parameters, reflecting the peculiarities of material internal structure, are used: thermal *conductivity* (η) and thermal *diffusivity* (ξ). The first parameter has the meaning mainly for the technical properties of materials (for example, to predict their overheating), while the second parameter is the best for the interpretation of heat transfer mechanisms. In the *polar crystals*, both these parameters are noticeably less than in the common dielectrics, and thermal diffusion looks like strongly slowed down. The point is that polar crystals are the piezoelectrics, in which an association of acoustic phonons with optical phonons is clearly expressed. Indeed, in the phonons spectrum of polar crystals, when acoustic phonons branch approaches to the boundary of Brillouin zone, it bends down due to acoustic-optical interaction, so the group velocity of heat phonons greatly reduced. That is why, the polar crystal which are well-transparent for the long-waves sound phonons, for the short-waves heat phonons looks like a turbid medium. At that, some of optical phonons have large spatial dispersion so that they can make a significant positive contribution to the heat transfer. But in the most cases, their spatial dispersion is small, so the optical phonons give only an additional

contribution only to the phonons scattering, which substantially decreases as the thermal conductivity so the thermal diffusivity.

In the *ferroelectrics*, the heat phonons are scattered by the dynamically ordering polar clusters; therefore, when study heat transfer, it is possible to trace as the polar bonds self-ordering so their forced ordering (by applied electrical field), obtaining amazing results in the vicinity of phase transitions. The strongest scattering of a diffuse-type occurs, when phonons wavelength becomes comparable with the size of fluctuating polar clusters: the smaller wavelength the stronger wave scattering in the polar structure. In the ferroelectrics, the $\xi(T)$ dependence shows a sharp minimum in the Curie point, indicating a large decrease of heat phonons wavelength in the vicinity of phase transition due to the deposit of optical phonons into process of phonons scattering. In contrast, the *antiferroelectric* shows an acute maximum of $\xi(T)$ in the Curie point due to optical phonons actively mix with the acoustic phonons thereby participating in the heat transfer. The point is that in the antipolar crystal a special arrangement of polar-sensitive bonds can lead not only to the increase crystal density but also facilitates the participation of optical phonons in phenomenon of heat transfer. This effect becomes especially noticeable in antiferroelectric phase transition, when multiplication of crystal lattice parameter happens. In them, the spatial dispersion of optical phonons is particularly large near the boundary of Brillouin zone due to critical decrease of their frequency; so optical phonons actively mix with acoustic ones, participating in the heat transfer.

Thus, the mechanism of thermal conductivity in the polar crystals is predominantly phononic, since the electrical conductivity in these materials is very small. The interaction of the acoustic and optical phonons in the polar crystals manifests itself in two ways: (1) it gives an additional deposit into the phonons scattering, observed as a deep minimum of diffusivity; (2) it makes the contribution to heat transfer with an acute maximum of diffusivity seen in the antiferroelectric phase transition.

Negative thermal expansion. Thermal expansion coefficient α, reflecting peculiarities of crystal inter-atomic bonds, in most crystals *increases* with temperature rise. That is why, the *negative value* of $\alpha(T)$, seen in as a rule in the polar crystals in certain temperature interval, appears to be an unusual phenomenon. In such crystals, the negative coefficient of thermal expansion testifies to the dynamic self-ordering of the polar bonds in crystals, and is seen not only in the piezoelectrics, but also in the semiconductors (like Si) that might be due to the ordering of the virtual hexagonal polar phase. Note that features of inter-atomic interactions, which are of special importance for the polar crystals, are better

revealed under the scalar (homogeneous) influences on crystal, such as the uniform change of temperature δT. The point is that the vector or tensor (non-scalar) actions are added to the symmetry of a response (Curie principle).

The increase in the crystal volume with temperature rise (usual for most of solids), in the polar crystals at low temperatures slows down, since the increase in the intensity of thermal motion stimulates the self-ordering of polar bonds, increasing the rigidity of their structure and even leading to a small compression. But next, with significant increase in temperature, the more intense thermal movement violates this ordering, and, therefore, the volume of crystal continues to increase again, as in the ordinary crystals. In this case, the coefficient of thermal expansion α_V in the polar crystals at low temperatures changes its sign twice, forming a region of negative α_V. Its extended minimum means that initially (when a noticeable thermal motion appears) the polar bonds gradually acquire their partial ordering: in this case, the stronger the interatomic bonds, the lower thermal expansion coefficient, up to its negative value. The point is that polar structures in crystals arise due to the structural compensation of the electronegativity of different neighboring atoms. A negative value of $\alpha_V(T)$ corresponds to such particular case, when the entropy grows with pressure increasing, which is the characteristic of configurational entropy: the region of negative expansion coefficient corresponds to the processes of self-ordering of polar bonds. Since the minimum $\alpha_V(T)$ of polar crystals is explained by the ordering of polar bonds, this concept can be extending to some semiconductors. In them, it can be assumed that some polar tendencies, fluctuating in the structures, become consolidated at low temperatures.

In connection with the discussion of dynamic ordering in the polar crystals, the conditional division of the entropy into the "vibrational entropy" and the "configurational entropy" becomes relevant. The vibrational entropy can be thought of as the *number of microstates*, through which the thermal energy is distributed between particles. The higher the temperature, the greater the vibrational entropy, but with the increasing of pressure it becomes smaller since the binding energy of particles increases. Consequently, with pressure increases, the vibrational entropy *decreases*. The configurational entropy is that part of the entropy of a system, which is due to the different *positions* of some parts of a system, which are applicable to all possible configurations in a system. This entropy characterizes the number of ways, in which *related groups* of atoms can be distributed in a space. With the increasing of pressure, the possibility of partial ordering of dynamic orientation of nanoscale groups becomes limited, so the mutual chaos increases. Thus, a distinctive

feature of the configurational entropy is its *growing* with pressure increase. Negative thermal expansion correlates to the configurational entropy.

Strain engineering technology for polar films is based not only on the mismatch of thermal expansion, but to a greater degree on the difference in permanent lattices of film and substrate. According to principle of La Chatelier, if during formation of polar phase one of crystal size increases, then the forced change in this size of crystal should lead to the change in crystal polar state. In the *biaxially stressed films*, such materials are obtained that in the bulk state are not ferroelectrics at any temperature. The biaxial deformations of films make it possible to increase the Curie point by hundreds of degrees with a simultaneous increase in the polarization directed perpendicular to film thickness. Deformations, reaching value of several percents, have a great influence on the properties of polar-sensitive thin films so it becomes possible to obtain films with such properties that are not found in the natural materials. Thus, the difference in thermal expansion as well as the mismatch between lattice parameter of film and substrate can be used in modern technologies of microelectronics.

Chapter 2. Interdependence of electrical conductance and polarization is devoted to the problem of a complex description of the electrical response of the material under study to an electric field applied to it. In the alternating electrical field, the electrically induced displace and move of charged particles lead to both an active and a reactive electrical current that is characterized usually by the *complex* permittivity, but also can be described by the *complex* conductivity. Between these complex parameters an unambiguous relationship can be established: both of these methods of a describing of electrical reaction of substance to applied electrical field, in principle, are equivalent.

Electrical polarization is the charge separation while electrical conductivity is the charge transfer. At an alternating voltage, the connection between conductivity and polarization is obvious, since both of these phenomena are due to limited (polarization) and almost-free (conductivity) movement of electrical charges in a matter, and in both cases the inertial phenomena affect these movements. To be described in the *sinusoidal* electrical field both the dielectric displacement and the conduction can be represented by the complex parameters and Maxwell-Lorentz equations shows that the ohmic current density and the time derivative of electrical displacement are the *additive quantities*. That is why, the current density and bias current might be represented as the equivalent functions, if the complex values will be used to describe them. Material's properties are usually characterized by the complex permittivity $\varepsilon^*(\omega)$, but can also be described by the complex conductivity

$\sigma^*(\omega)$. When these functions are represented by their real and imaginary parts, the complex conductivity is connected to the complex permittivity. However, mostly to describe materials parameters frequency dependence the complex *permittivity* is used.

Thermally activated motion of charged particles, whose localization is determined by a set of potential minima and barriers, in the external electrical field give rise to both conduction and polarization. Polarization process predominates at lower frequencies, but when frequency grows the permittivity decreases that is accompanied by the correspondent increase of conductivity; it looks like as if polarization is turned into conductivity. Frequency dependence of effective conductivity can be useful evidence of physical nature of the polarization mechanisms. Inertia of charge transfer mechanisms can be clearly detected by dielectric spectroscopy methods, including the movement of electrons in metals. When charge carries show their inertia, the conductivity decreases; in metals conductivity decreases in the ultraviolet wavelength range so even the electronic polarizability of deep ionic shells in ionic lattice of metal becomes noticeable. In the doped semiconductors, the presence of free charge carriers decreases the refractive index: this negative contribution of plasma to the permittivity is seen at optical frequencies. In dielectrics, due to a low concentration and small mobility of charge carriers, the plasma oscillations are practically imperceptible.

Chapter 3. Dynamics of electrical polarization describes the main physical property of dielectrics. For the application of dielectric materials in high-frequency electronics and information technology, the dynamic properties of polarization are most important, which can be described by both phenomenological and models representations.

Relaxor model is discussed as a physical concept which it that coordinated response-polarization function of a system of dipoles, when their forced ordering by electrical field action is opposed by the chaotic disordering thermal motion. Justification of a relaxor model of dielectric spectra is given on the base of Debye formula of permittivity dispersion in the polar dielectrics. According to relaxor model, the electrical polarization of polar complexes is late as the frequency of electrical field grows; as a result, permittivity decreases while dielectric loss factor shows a maximum. In other words, at rather high frequencies the equilibrium distribution of the relaxing electrons, ions and dipoles has not enough time to be established. This effect is peculiar for the relaxation spectra, whose main characteristic is their diffusivity in rather broad frequency range.

Oscillator model, describing the resonant dispersion of permittivity, is another key model in dielectric spectroscopy. This is physical model characterizing a

dynamic reaction of the system of elastically coupled electrical charges to the externally applied electrical field, whose action is opposed by the internal elastic force tending to return quasi-elastic system into the non-polarized state. Permittivity dispersion and corresponding losses, conditioned by quasi-elastic polarization, usually are observed at much higher frequencies then the relaxation processes; nevertheless in some dielectrics these losses become significant at microwaves, being important for some electronic components. At that, the presence of a minimum in the permittivity frequency dependence is principal sign of resonance dispersion that distinguishes it from relaxation dispersion.

Dielectric spectra described by both relaxor model and oscillator model are very useful as a method, known in the electrical engineering as the Nyquist charts. When the polarization response is normalized to the value of the dielectric contribution, in the case of the relaxation dispersion the imaginary and the real part of permittivity on a complex plane are the Cole-Cole semi-circle. The resonant dispersion on the complex plane demonstrates more complex figure with a characteristic loop in the range of negative permittivity.

Ferroelectrics new description makes it possible to refuse the concept of "spontaneous polarization", i.e., to the imagine that in polar crystal the "permanent polarization" *exists*. It looks more reasonable the assumption that electrical polarization *appears* as a response to external (not even electrical). This is due to a peculiar distribution of polar-sensitive internal bonds having distinction in ions affinity for electrons, i.e., electronegativity. In the ferroelectrics of *order-disorder type* large microwave absorbance is seen as in the ferroelectric phase, so in the paraelectric phase. Ferroelectrics of *displace type,* above their phase transition, practically have no dielectric dispersion (i.e., in their paraelectric phase); correspondingly, their losses above Curie point are small that might have application in the microwave tuneable devices. Below Curie point microwave absorbance of ferroelectrics is increased owing to domain walls relaxation (although dielectric losses in the single domain crystals of displace type ferroelectrics remain small).

Chapter 4. Dielectric properties models explaining is given with considering of valence of elements constituting the crystal (taking into account the magnitude of their electronegativity) and by the quantum states of the electronic shells of atoms. In according to electronic theory of a *valence*, the inter-atomic bonds are due to the redistribution of electronic density in the outer orbitals, usually resulting in a stable electronic configuration of noble gas (octet) due to formation of ions (or shared electronic pairs between atoms).

Any dielectric is able to polarization in the external *electrical* field, but only some of dielectrics – polar types – can be polarized in *non-electrical* manner. Unique properties of polar crystals (pyroelectrics, piezoelectrics, etc.) can be described by a peculiar polar-sensitive internal structure, capable to generate electrical response onto non-electrical homogeneous (scalar) actions. Electrical polarization means that electrical charges separation occurs (which however remain non free). Electrons, ions and dipoles can acquire induced electrical moment (i.e., polarized state) through various mechanisms: (1) elastic reversible displacement of bound electric charges, (2) displacement of weakly bound charges with participation of their thermal motion, and (3) macroscopic displacement of free charges that later localize on defect places in dielectric. It should be noted that in the polar dielectrics all this processes can occur *without* external electrical field application but under the action of varying temperature, pressure, mechanical stress, exposition by sufficiently high energy irradiation, etc.

Polar dielectrics-pyroelectrics have an ability to make the electrical moment $P_i = \gamma_i \cdot \delta T$ induced in them by the change of temperature δT; this property is described by the first rank material tensor: *pyroelectric coefficient* γ_i, i.e., electrical susceptibility to the change of temperature. Pyroelectrics also have an ability to create in them induced electrical moment $P_i = \zeta_i \cdot p$ due to the change of hydrostatic pressure p, described by first rank material tensor: piezoelectric pressure coefficient ζ_i, i.e., they have sensitivity to the change in pressure. Polar *dielectrics-piezoelectrics* show the ability to create in them electrical moment induced by the mechanical stress: $P_i = d_{ikl} \cdot X_{kl}$. This property is described by third rank material tensor: the *piezoelectric module* d_{ikl} (it can also be called as the susceptibility to mechanical stress). In fact, any experimental investigations of pyroelectric or piezoelectric effects do not allow determine directly the value of their "spontaneous polarization", but experiments characterize only the magnitude of *dynamic response* of peculiar polar-sensitive internal crystalline structure.

Spontaneous polarization presence in the pyroelectrics is questionable, since always existing free electric charges make it impossible availability of any equilibrium and unchanging polarized state. That is why, to explain the pyroelectricity and piezoelectricity in polar crystals, it is assumed that they contain the hybridized ionic-covalent polar-sensitive bonds that do not create any internal field, but are capable of electrical response generation to uniform non-electrical effect (heat, pressure, etc.). This response is described by the generalized electrical moment, which varies critically with temperature change. Ferroelectrics in electrical

field reorient polar-sensitive couplings with the nonlinear response, which gives different meaning of their spontaneous polarization.

Polar crystals are characterized by a finely balanced structure of interatomic bonds, which is highly sensitive to the external influences. The mixed ionic-covalent polar-sensitive bonds make it possible for polar crystals to generate electrical response onto non-electrical influences (thermal, mechanical, optical, chemical, etc.). This response on scalar impact can be described by the generalized electrical moment, critically changing with temperature: $M_{ijk}(T) \sim (\theta - T)^n$ (at temperature θ response disappears). In the case of three-dimensional arrangement of polar bonds, the critical parameter is $n = 2$; for their two-dimensional expansion $n = 1$, and in the one-dimensional case (ferroelectrics), $n = 0.5$ (this is critical Landau index). Thus, distinction between pyroelectrics and piezoelectrics is not fundamental, and it consists in different spatial distribution of polar bonds. In the ferroelectrics, polar-sensitive bonds are capable of changing their orientation with a nonlinear response to electrical field (hysteresis). At the same time, to explain the unique properties of polar crystals, it is not necessary to use the hypothesis of spontaneous polarization, which would be forcedly accompanied by the internal field that is difficult to explain in the equilibrium state. The reason for the existence of polar bonds (as well as the formation of crystals with non-centrosymmetric structure) is structural compensation for difference in electronegativity of neighboring atoms.

Linear electromechanical effect (which is a peculiar property of polar crystals) can be interpreted as the *linearized electrostriction*. The point is that electrical field changes original *symmetry* of a crystal due to its electrical polarization. In this way, under fixed external voltage, the structure of a crystal turns into the *artificially created polar* structure (it becomes electrically-induced non-centrosymmetric structure). In dielectrics which have large permittivity, electrically induced piezoelectric effect can become "gigantic", and this feature is really used now in electronics. Similarly, in the presence of electrical bias field in *any* crystal the *pyroelectric* effect also can be induced, that finds application in modern thermal sensors. In compliance with such electrically induced piezoelectric and pyroelectric effects, one can suppose that *usual* piezoelectric effect also can be explained as the “linearized electrostriction”. This assumption might be advanced according to the conception that fundamental reason of crystal intrinsic polar-sensitivity is the asymmetry in the electronic density distribution along the polar bonds between ions, which have different electronegativity (this mechanism replaces externally applied field).

Mixed covalent-ionic bonds, which in polar crystals is main property, guarantee piezoelectric and pyroelectric properties without external electrical field application to a crystal. In this way, instead of external electrical field, which need to be applied to ionic or covalent crystals in order to force them to have polarized state (although non-equilibrium), in the case of mixed covalent-ionic crystals their polar-sensitive state *remains stable* without any external field, being ensured by the fundamental property of ions – their *electronegativity*. Polar-sensitive bonds usually arise in such crystals, which have small coordination number (CN) which shows the number of nearest neighbors to given atom. Thus, to polar dielectrics and semiconductors an "open" structures correspond: they provide sufficient space for electronic orbits interaction. If in usual densely-packed crystalline structures this number is large (CN = 12 for metals and CN = 8–6 for ordinary dielectrics), then, for example, the coordination number in piezoelectric sphalerite structure and in pyroelectric wurtzite structure CN = 4.

Chapter 5. Polar crystals peculiarities are seen in various experimental evidences of polar-sensitivity existence in the crystals: the similar structures of piezoelectrics and pyroelectrics; the chemical features of polar crystals confirming proximity of their properties; the increase in volume while polar-sensitive bonds self-ordering; the piezoelectric and electrocaloric contributions to the permittivity of polar crystals; the high-frequency dielectric absorption; the dependence of polar crystal elastic properties on various electrical boundary conditions, etc. Features of the charge transfer in polar-sensitive crystals are explained: physical nature of giant change of conductivity in the critistors, posistors and varistors, as well as in the others field-controllable switching elements, the particularly those which exhibit the colossal magnetoresistance; the nature of high sensibility of nanostructured sensors based on zinc oxide are discussed.

Polar-sensitivity in crystals manifests itself in the *structural affinity* of piezoelectrics and pyroelectrics with an example of zinc sulfide uniting in polymorphic structure the regions with sphalerite and wurtzite symmetry; as well as in the *chemical features* of polar crystals demonstrating different chemical sensitivity on the surfaces of opposite polarity. Moreover, polar-sensitive bonds ordering leads to the *increased volume* at the transition into polar phase; such crystals are characterized by the electromechanic and electrocaloric *contributions* into the *permittivity* as well as big high-frequency dielectric *absorption*.

Charge transfer in some polar-sensitive crystals may depend on the symmetry of the polar phase: the large *decrease* of resistance in the *critistors* of vanadium dioxide type occurs from its triclinic (piezoelectric) symmetry; while large *increase*

of resistance in the *posistors* is due to doped barium titanate transition from the polar tetragonal (pyroelectric) structure into the non-polar cubic phase. Zinc oxide being best material for *varistors* (with giant change in resistance) has polar wurtzite (pyroelectric) structure with possible transformation into another but also polar sphalerite (piezoelectric) state. Others field-controllable switching elements, which exhibit the colossal magnetoresistance as well as high sensibility of nanostructured sensors based on the zinc oxide also belong to the polar-sensitive crystals.

Electrical control by piezoelectric effect is very interesting for practical application in electronics: this opens possibility to implement tunable piezoelectric resonators and filters as well as various SAW devices. *Mechanically induced* pyroelectricity (and the volumetric piezoelectric effect) is possible to obtain in any polar-neutral piezoelectric (which is not pyroelectric). For this, an original method of partial limitation of thermal (or elastic) deformations is applied, due to which one of the *polar-neutral* axes is transformed into the *polar axis*. Obtaining the artificial pyroelectric effect (or the volumetric piezoelectric effect) is achieved in a composite system "non-deformable substrate – oriented plate of polar-neutral crystal". These studies can be realized in two- and three-dimensional structural arrangements of polar-sensitive bonds; as a result, the artificial pyroelectric effect is calculated for all 10 classes of polar-neutral piezoelectric crystals.

Special boundary conditions can be created for piezoelectric crystal to obtain the “pyroelectric effect” in 10 polar-neutral classes of crystals. Therefore, in any polar crystals, the changes in the polar-sensitivity under thermal (δT) or pressure (δT) variation provide the pyroelectric effect ($P_i = \gamma_i \delta T$) or the volumetric piezoelectric effect ($P_i = \zeta_i \delta p$). At that, the pyroelectric coefficient γ_i as well as the volumetric piezoelectric coefficient ξ_i are the *material vectors*, which inherent to the polar crystals only. That is why, the polar-sensitive crystal can transform the scalar influences (δT or δp) into the vector type of responses, which are electrical voltage or electrical current. Temperature dependence of polar-sensitivity in the piezoelectric can be used in microelectronics for thermal sensors. By similar way, polar-sensitivity dependence on pressure can by applied in the mechanical sensors. Significant polar sensitivity in crystals of $A^{III}B^{V}$ group can be observed along any of [111] directions, whereas in the standard-used direction of [100] type does not respond to mechanical vibrations and temperature changes.

Chapter 6. Piezoelectrics: physics and applications. Mechanical property (elasticity) and electrical property (polarization) of piezoelectric crystals are interrelated, and, therefore, they can be *considered together*. This relationship is characterized by electromechanical coupling coefficient K_{EM} – one of most

important parameters of piezoelectric materials and devices. In case of direct piezoelectric effect, the applied to piezoelectric mechanical energy is spent not only on elastic deformation, but also creates electrical polarization, which causes electrical energy accumulation. Conversely, supplied to piezoelectric electrical energy (in case of converse piezoelectric effect) is spent not only for its polarization, but also to its elastic deformation and elastic energy accumulation. The square of electromechanical coupling factor K_{EM}^2 shows what part of energy, attached to piezoelectric, is converted into the energy of other kind in a static mode. However, this parameter is not a performance factor: firstly, because the losses of electrical or mechanical power are not considered, and, secondly, actual conversion efficiency of piezoelectric depends not only the K_{EM}, but largely is on the shape, orientation and other peculiarities of piezoelectric element.

Polar crystals and textures are distinguished by the fact that their electrical, elastic and thermal characteristics are interdependent. Moreover, during the study (or the use of devices) of only electrical effect (for example, polarization) reveals that corresponding electrical parameters depend on the mechanical and thermal boundary conditions: for example, permittivity of mechanically free crystal (ε^X) differs from permittivity of clamped piezoelectric crystal ε^x (which can not be deformed), and always $\varepsilon^X > \varepsilon^x$. By the same way, elastic stiffness of piezoelectric (or its elastic compliance) depends on its electrical state (short-circuited or open-circuited) and therefore $c^E \neq c^D$; in some cases they differ several times.

Thermodynamic theory (phenomenological) allows, without specifying the molecular mechanisms, obtain all basic equations, describing direct and converse piezoelectric effect at the macroscopic level. These equations are used in engineering calculations, and parameters of these equations can be the basis for comparing the properties of different piezoelectric materials. For application in electronics and instrumentation, many piezoelectrics of different structures have been developed: crystals, ceramics, polymer materials, films, composites. One of most important piezoelectric crystals is quartz, which combines large mechanical *Q*-factor ($Q_m \sim 10^7$) with high thermal stability of resonant frequency in the operating temperature intervals. In electronics, piezoelectric crystals niobium tantalite, lithium tantalite and langasite, whose unique characteristics provide wide implementation of acousto-electronic devices, are widely employed.

The chapter deals with properties of piezoelectric ceramics, polymer piezoelectric films, electrostriction materials and others. A description of the features is given for piezoelectric sensors, devises using converse piezoelectric effect, piezoelectric actuators, piezoelectric motors, piezoelectric transformers of voltage and current.

Chapter 7. Pyroelectrics: physics and applications. Transformative function of polar crystals is due to their peculiar physical structure and chemical composition. Several mechanisms of thermoelectric transformation in the polar dielectrics are discussed: the pyroelectric effect and converse to it electrocaloric effect are reviewed in the aspects of their use in electronic devices at various *boundary conditions* (adiabatic and isothermal development, mechanically free or clamped crystals study, short-circuited or open-circuited circumstances). The nature of thermoelectric coupling in polar-sensitive crystals as wellas its influence on the dielectric permittivity and thermal properties crystals are also described by various models and by thermodynamic calculations. The principles of operation of main types of pyroelectric sensors are considered: the motion detector sensors, infrared thermometers for high precision pyrometery; pyroelectric vidicons in both vacuum and microelectronic design, etc. Physical mechanisms and applications of *electrically induced* pyroelectric and electrocaloric effects at various conditions are also depicted. The possibilities of electrocaloric effect using are discussed in connection of its possible application in miniature solid-state refrigeration systems.

Pyroelectricity is the property of a polar crystal to *produce electrical energy* when it is subjected to the *change* of thermal energy. It is possible also to define *pyroelectric* effect as the ability of crystals to generate electricity, when they are *dynamically* heated or cooled; at that, pyroelectric becomes polarized positively or negatively in proportional to the *change* of its temperature. Pyroelectricity looks like *thermoelectric* power conversion; at that, this effect is a linear one, so, according to Curie principle, a reversed effect must exist, namely, the *electrocaloric* effect, which the *electrothermal* energy conversion characterises. Physical mechanism of pyroelectric effect is as follows: under constant external conditions (temperature, pressure, etc.), the structure of polar crystal corresponds to its energy minimum. At the same time, the polar-sensitive interatomic bonds, striving for their mutual ordering, are in the *subtle equilibrium* with the thermal chaotic motion of atoms in crystal lattice. When this equilibrium changes, caused for example by the change in temperature (i.e., change in thermal energy), the polar crystal immediately reacts by the appearance of electrical polarization — bound charges appearance on the crystal surface.

Electrocaloric effect is characterized by next physical mechanism: electrical field applied from the outside to a polar crystal violates its equilibrium state, which was previousy established thermodynamically under certain conditions at given temperature and pressure, which corresponds to the energy minimum. Applied field changes mutual ordering of polar-sensitive interatomic bonds, existing in the equilibrium structure. If applied electrical field is directed accordingly to the internal

orientation of polar bonds, then it increases total energy of a crystal and it heats up. If this field is directed oppositely, then crystal energy decreases, which is expressed in its cooling. Electrocaloric effect has a certain prospects for use in the miniature solid-state refrigeration systems. Using electrically induced phase transition from ferroelectric into anti-ferroelectric phase, a cooling up to 4 °C can be obtained in the single transition period.

Thermoelectrical coupling in polar-sensitive crystals can be described by various models: the *primary* pyroelectric effect and the pyroelectric *secondary* effect; moreover, the electrically and mechanically induced *artificial* pyroelectric effects are possible. Hidden (or latent) intrinsic polarity in pyroelectric is only their *ability* to provide electrical (vector) response to any non-electrical (scalar) *dynamic* influence (such as uniform change of temperature). *Primary* pyroelectric effect reflects the strength of bonding energy of polar bonds and their resilience to the chaotic thermal motion: these bonds react to external action by such a change, which is accompanied by the electrical response, i.e., by the induced polarization. *Secodary* pyroelectric effect is the piezoelectrically transformed thermal deformation.

Electrically induced artificial pyroelectric effect is possible in all solid dielectrics, but it has practical meaning only in the dielectrics with very high permittivity (10^3–10^5). Electrical field keeps induced polar state of dielectric in the opposition to the thermal motion in crystal; any violation of this equilibrium with temperature change leads to the electrical response: i.e., artificial pyroelectricity. *Thermomechanically induced* pyroelectric effect manifests itself in any piezoelectric material and arises along the *polar-neutral* axes (in pyroelectrics – along the special polar axis, being in this case the secondary pyroelectric effect). Partial limitation of thermal deformation turns the polar-neutral axis into the polar one. This effect can be of practical importance in wide-band semiconductors-piezoelectrics of $A^{III}B^{V}$ type, allowing in the monolithic (one-crystal) devices combining pyroelectric element with amplifier.

Infrared sensors use very small changes in temperature which can produce perceptible pyroelectric potential: are designed from such pyroelectric materials, when heat of a human or animal from several feet away is enough to generate voltage. Among wide variety of thermal sensors, using pyroelectric effect, *motion detector* sensors can be identified as well as *infrared thermometers* for high precision pyrometery, *pyroelectric vidicons* in both vacuum and microelectronic design, etc.

CHAPTER 1. THERMODYNAMICS OF DIELECTRICS

Content

Many phenomena and effects could be attributed to the *thermal properties* of electronic materials conditioned by the thermal motion which determines important features in the electrical, magnetic, and other properties. Start with the fact that already the synthesis of crystals, arising their microsized and nanosized structures, next their alloying, annealing and quenching, as well as many other technological operations occur under the special thermal conditions. Thermal energy determines many properties of crystals; for example, generation and recombination of charge carriers as well as their equilibrium concentration setting in the *semiconductors* are due to thermal motion in lattice. In the different phase transitions, the dielectric-to-metal transformations, various transitions in the ferromagnetic and ferroelectric states, as well as such noticeable phenomena as pyroelectricity, electrocaloric effect, magnetic cooling, thermostriction and others directly relate to the thermal properties.

Thermodynamic approach to description of *dielectric properties* is important, particularly, for understanding of temperature, frequency and field dependences of dielectric permittivity, as well as for ferroelectric phase transitions analyzing, for energetic theories of piezoelectric and pyroelectric converters, as well as for the explanation of such phenomena as heat capacitance, thermal expansion and thermal diffusivity and conductivity in the polar dielectrics.

The *specific heat* in the polar crystals contains an additional contribution due to the disordering-disordering processes of their polar-sensitive bonds. Statistical possibility of several states realizing increases the total entropy of a system: such *configuration entropy* is a part of total entropy of a system that is related to the *position* of constituent particles rather than to their velocity or momentum. It is physically related to the number of ways of arranging all the particles of a system while maintaining some overall set of specified system properties, such as energy. The change in configurational entropy corresponds to same change in macroscopic entropy.

Thermal *expansion coefficient*, reflecting the peculiarities of crystal interatomic bonds, in most of crystals increases with temperature rise. The negative value of this coefficient, seen in the polar crystals in a certain temperature interval, correlates to the configurational entropy, which in opposed to vibrational entropy increases as pressure grows. Negative coefficient of thermal expansion testifies to dynamic self-ordering of polar bonds in crystals, and is seen not only in the piezoelectrics, but also in the semiconductors (like Si) that might be due to ordering of the virtual hexagonal polar phase.

Thermal diffusivity coefficient is measured directly using a spread of plane temperature waves excited by Peltier element. By this way, both self-ordering of polar bonds and their forced ordering in the bias electrical field are studied. The interaction of acoustic and optical phonons in the polar crystals manifests itself in two ways: (1) it gives an additional deposit into phonons scattering, observed as a deep minimum of diffusivity; (2) it makes contribution to heat transfer with an acute maximum of diffusivity seen in the antiferroelectrics, in which soft phonon mode vanishes in the middle of Brillouin zone and phase transition occurs with multiplication of lattice unite cell, so the optical phonons actively mix with the acoustic ones, participating in the heat transfer.

1.1 Thermodynamic functions

A description of thermodynamic state in any system or material (particularly, in dielectrics) is dependent on the purpose of theory application, i.e., what kind of physical properties of a substance needs to be predicted or explained. In the case of dielectric, the thermodynamics allows to describe processes of dielectrics polarization and many other properties and features in terms of energy: the dielectric is regarded as the thermodynamic system, which equilibrium state can be changed as by electrical field application so due to many other factors.

At that,

· Thermodynamic *state* is determined by the combination of thermodynamic parameters and it is characterized by the internal energy of a system.

· Thermodynamic *parameters* are the temperature (T), pressure (p), volume (V) and others;

· Thermodynamic *process* is the change in the state of a system; depending on the conditions (the constancy of certain parameters), this process can be isothermal $T = const$, adiabatic $\delta Q = const$, isobaric $p = const,$ and isochoric $p = const$;

· *Absolute temperature T* measured in {K] (Kelvin degree) characterizes the state of a body at the thermodynamic equilibrium (this temperature is proportional to average kinetic energy of particles);

· *Heat Q* measured in [J] (joule) is the energy absorbed by a system when its temperature increases when system does not perform work (heat represents energy of thermal motion of particles forming a body);

· *Specific heat C* measured in [J/deg] or in [cal/(deg□mol)], is the absorbed (or released) heat when temperature changes: it is the ratio of heat (given to a body from outside) to corresponding increase in temperature.

· *Internal energy* (*U*) is that part of the total energy of a thermodynamic system, which does not depend on the choice of the frame of reference, but can change within the framework of the problem under consideration. *Potential energy* is a part of the energy of system or body that depends on the positions of particles in body in force fields. In solids, the sources of potential energy are Coulomb forces that cause the attraction of opposite sign charges and the repulsion of same sign charges. *Kinetic energy* (or energy of particles motion in solids) is due to the fact that atoms and ions continuously oscillate due thermal excitation. Internal energy is a collection of those variable components of the total energy of system that should be taken into account in a particular situation. Therefore, the internal energy is an additive quantity, that is, the internal energy of system is equal to the sum of internal energies of its subsystems, i.e., internal energy of system includes the energy of various types of motion and interaction of particles included in the system: the energy of translational, rotational and vibrational movements of atoms and molecules, the energy of intra- and intermolecular interactions, the energy of the electronic shells of atoms, etc. When temperature rises, the internal energy increases, and when temperature decreases, it decreases, but the constancy of the temperature of a system does not mean the invariability of its internal energy, for example, the temperature of the system is unchanged during phase transitions, but the energy changes.

· *Enthalpy* (*H*) is the isobaric-isentropic potential, the thermal Gibbs function, which determines the heat content of system by doing constant pressure and corresponds to the amount of energy that is available for conversion into heat at a certain temperature and pressure. Enthalpy is the extensive quantity, i.e., for a composite system, it is equal to the sum of the enthalpies of system's independent parts; in this case, like the internal energy, the enthalpy is determined up to arbitrary constant term. Being general energetic function, the enthalpy is such property of thermodynamic system that is defined as the sum of system's internal energy and the

product of pressure p on volume V. As temperature increases from T_1 to T_2, the enthalpy increases: $H_2 = H_1 + \int_{T_1}^{T_2} C_P \partial T$, where H_1 is the enthalpy at initial temperature T_1, and H_2 is the enthalpy at final temperature T_2 and C_p is the specific heat under constant pressure p.

The enthalpy can be defined in two ways. The first method is based on the *internal energy* U and the *work* pV performed by a system relatively to the environment:

$$H = U + pV,$$

where P is the *pressure* and V is the *volume* of a material. The second method of enthalpy definition is based on the Helmholtz free energy F

$$H = F + pV + TS,$$

where $F = U - TS,$ or on the Gibbs free energy G: $H = G + TS,$ where $G = F + pV$ (or $G = H - TS$) while TS represents the energy conditioned by internal disordering in a matter, i.e., the energy assessment of a chaos.

It is appropriate here to clarify some of introduced concepts:

· The *Helmholtz free energy* ($F = U - TS$) is the isothermal-isochoric thermodynamic potential that measures useful work obtainable from thermodynamic system at constant temperature (isothermal processes) and constant volume (isochoric processes). Note that at constant temperature and in equilibrium state system Helmholtz free energy is minimized.

· The *Gibbs free energy* ($G = F + pV$) is isobaric-isothermal thermodynamic potential is a quantity whose change in the course of transformations is equal to the internal energy change of a system. The Gibbs energy shows what part of the total internal energy of a system can be used for the transformations (or obtained as a result of them) and makes it possible to establish the fundamental possibility of thermodynamic process under specified conditions. Mathematically, this is a thermodynamic potential of the following form:

$$G = H - TS = U + pV - TS.$$

The spontaneous course of this isobaric-isothermal process is determined by two factors: the enthalpy, associated with its decrease in system, and due to increase in its entropy (system disordering). It is the difference of these thermodynamic factors that is a function of the state of the system, called the isobaric-isothermal potential or Gibbs free energy. In solids, when thermodynamic processes studying, the more expedient is to take into account not a pressure, but the *volume* of a system, so the preference is given to the Gibbs free energy, $G = F + PV$. Its minimum

corresponds to the equilibrium state of a system, changing at *constant temperature* and *constant volume*.

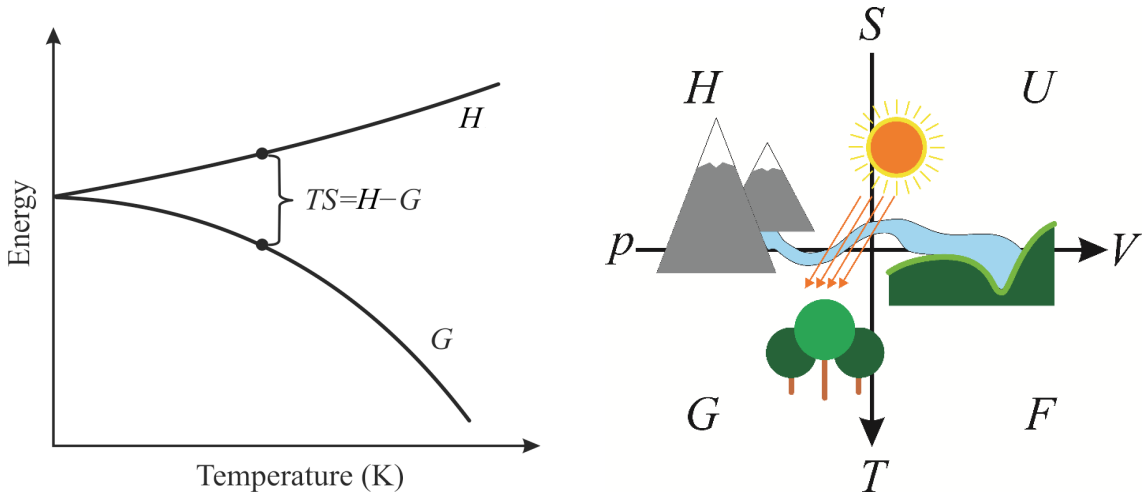

(A) (B)

Fig. 1.1. Thermodynamic potentials: A – temperature dependence of enthalpy and Gibbs energy *G;* B – diagram connected different thermodynamic functions (following Max Born)

As seen in Fig.1. 1, the enthalpy in all cases increases with temperature, but the value of entropy (*TS*) *increases faster*. Consequently, the Gibbs free energy *decreases* with temperature rise. Since it is the *free energy* that used in subsequent discussions below, it should be noted that at zero absolute temperature Gibbs free energy equals enthalpy: $G = H$. At the same time, the free energy decreases with temperature increase, but the rate of free energy decrease is associated with the entropy, Fig. 1.1.

The e*ntropy* (*S*) is the meaningful property of thermodynamic system denoting the measure of irreversible energy dissipation using to describe the *equilibrium* (reversible) processes. Besides, in the nonequilibrium (irreversible) processes, the entropy serves as a measure of the proximity of the state of a system to equilibrium: the greater the entropy, the closer the system is to the equilibrium; it is obvious that in the state of thermodynamic equilibrium, the entropy of the system has maximum. The physical meaning of entropy is the logarithm of the number of available microstates of the system; entropy dimension in SI units is [kg□m^2□s^{-2}□K^{-1}] or the "joules per kelvin", [J□K^{-1}]. Entropy is defined as function of the state of a system; the difference of entropy in two equilibrium states 1 and 2 equals to the reduced amount of heat $\delta Q/T$, which system needs to give in order to be transfered from state 1 to state 2 along any but quasi-static path: $\Delta S = S_2 - S_1 = \int \delta Q/T$. Since the entropy is determined as to arbitrary constant, then in initial state it is possible to set $S_1 = 0$, then $\Delta S = \int \delta Q/T$. This integral is taken for the

arbitrary quasi-static process. The *differential function* of the entropy has a form d$S = \delta Q/T$. Also, since the entropy is always *positive* and increases with temperature rise, the slope of free energy plot on temperature continuously increases as seen in Fig. 1.1A, where no phase transformations are implied in a given substance. However, when in the studied material the *different phases* are possible, the value of free energy shoes anomalies which gives important information about correspondent phase transformation, at that, the lower is the free energy the more resistant is the phase.

[***Useful note.*** Figure 1B shows a helpful mnemonic Max Born diagram, which might be used for better imagination of the entire picture of thermodynamic potentials. It is written in such way: the vertical $S \rightarrow T$ means "Sun shines onto Trees), the horizontal $p \rightarrow V$ can be identified with "water flows from peak to Valley). Next, following clock-arrow, put *U,* and then in the alphabet order *F, G, H*. If it's needed to find the *full differential* of any thermodynamic potential, it's going to be consist of two sums of multiplication of neighbor's variables differentials multiplied on another two variables, which stand at *another side* of appropriate arrow. The pointed by the arrows variables (*T* and *V*, when one looks for their neighbor potentials, such as *U, F* and *G*), it should be written minus "–" before it. For example: $dF = -S dT - p dV$, $dG = V dp - S dT$, $dH = V dp + T dS$ and $dU = T dS - p dV$. And if one wants to find differense between *F* and *G* (for instance), subtract d*G* from d*F*: $dF - dG = -S dT - p dV - V dp + S dT = -d(pV)$, and next integrate: $F = G - pV$. Or for difference between *F* and *U*: $dF - dU = -S dT - p dV - T dS + p dV = -d(TS)$, and after integration get: $U = F + TS$].

1.2 Dielectric permittivity temperature dependence

Electrical polarization of dielectrics is characterized by the relative dielectric permittivity, which is dimensionless parameter corresponding to ratio of the electrical induction *D* to the electrical field strength *E*: $\varepsilon = D/\varepsilon_0 E$. Dielectric permittivity characterizes also the density of electrical energy in the polarized dielectric; depending on the mechanisms of polarization, permittivity varies in different ways on temperature and also on intensity and frequency of changing electrical field acting on dielectric. Further it will be shown that without going into the details of physical mechanisms of polarization, only from the *general* thermodynamic provisions, it is possible to make the important predictions and conclusions as to these mechanisms peculiarities.

Next the only most general energy relations that characterize the phenomenon of polarization in dielectric will be considered. To describe the state of polarized dielectric, the correspondent thermodynamic *functions* might be selected: free energy F, internal energy U and entropy S. At that, the thermodynamic *parameters* (independent variables) should be temperature T and electrical field E that allows the best possible way to describe permittivity temperature variation $\varepsilon(T)$. With this choice of parameters, it is supposed that the *volume* of a dielectric maintains constant; therefore, this approach does not include as thermal expansion so electrostriction of a dielectric, supposing that these effects are too small (however, if need, these restrictions also might be considered when using the energy relations obtained below).

The ***first law*** of thermodynamics (the law of energy conservation) for dielectric polarization process is:

$$\mathrm{d}U = \mathrm{d}Q + E\mathrm{d}D \tag{1.1}$$

where $\mathrm{d}U$ is the change in internal energy per unit volume of dielectric and $\mathrm{d}Q$ is the change of a heat. Equation (1.1) means that the increase in energy $\mathrm{d}U$ during thermodynamic process, at which an electrical field E or temperature T are changing (or both changing simultaneously), the equals to heat $\mathrm{d}Q$ obtained by dielectric, and work $E\mathrm{d}D$, which is performed by the electrical field during polarization process in a dielectric. The free energy which characterizes the maximal work which system can run at constant temperature is: $F = U - TS$.

In compliance with the ***second*** *law* of thermodynamics, the alteration of entropy equals: $\mathrm{d}S = \mathrm{d}Q/T$, where $\mathrm{d}S$ can be expressed in terms of parameters E and T. However, instead of E, the E^2 should be selected as the independent variable, because the energy is a quadratic function of the field strength:

$$\mathrm{d}S = \frac{\partial S}{\partial T}\mathrm{d}T + \frac{\partial S}{\partial\left(E^2\right)}\mathrm{d}\left(E^2\right).$$

It is important to note that entropy of reversible thermodynamic processes is the total differential. This means that for reversible process the value of integral from dS does not depend on the path of integration, but it is determined only by the limits of integration, i.e., by the initial and final state of a system in the thermodynamic process. So to get the differential equations for internal energy, it needs to use this property:

$$\mathrm{d}S = M\left(T, E^2\right)\mathrm{d}\left(E^2\right) + N\left(T, E^2\right)\mathrm{d}T;$$

$$\frac{\partial N}{\partial\left(E^2\right)} = \frac{\partial M}{\partial T}.$$

The following are the main defining cases.

1. The case ∑= Const needs to be considered in order to obtain the baseline data for subsequent consideration of dielectric permittivity changing with the temperature and the electrical field.

In view of D = ∑0∑E, the change of electrical induction, taking into account the energy conservation law (1.1), is:

$$\mathrm{d}D = \varepsilon_0\varepsilon\mathrm{d}E + \varepsilon_0 E\mathrm{d}\varepsilon = \varepsilon_0\varepsilon\mathrm{d}E.$$

Turning to the variable E2 and using the relationship $\mathrm{d}\left(E^2\right) = 2E\mathrm{d}E$, it is possible to obtain:

$$\mathrm{d}D = -\frac{\varepsilon_0\varepsilon}{2E}\mathrm{d}\left(E^2\right).$$

Dy substituting this expression into the above equations, and with regard to dependence of internal energy on selected variables *T* and E^2, it is possible to get:

$$\mathrm{d}U = \mathrm{d}Q + \frac{1}{2}\varepsilon_0\varepsilon\mathrm{d}\left(E^2\right) = \frac{\partial U}{\partial E^2}d\left(E^2\right) + \frac{\partial U}{\partial T}dT.$$

From right side of this equation, the *dQ* can be determined, and next find *dS*:

$$\mathrm{d}S = \frac{\mathrm{d}Q}{T} = \frac{1}{T}\left(\frac{\partial U}{\partial\left(E^2\right)} - \frac{1}{2}\varepsilon_0\varepsilon\right)\mathrm{d}\left(E^2\right) + \frac{1}{T}\frac{\partial U}{\partial T}dT.$$

According to the property of total differential

$$\frac{1}{T}\frac{\partial^2 U}{\partial\left(E^2\right)\partial T} - \frac{1}{T^2}\left(\frac{\partial U}{\partial\left(E^2\right)} - \frac{1}{2}\varepsilon_0\varepsilon\right) = \frac{1}{T}\frac{\partial^2 U}{\partial T\,\partial\left(E^2\right)},$$

Now the next differential equation for internal energy can be obtained:

$$\frac{\partial U}{\partial\left(E^2\right)} = \frac{1}{2}\varepsilon_0\varepsilon.$$

After integration, it is possible to get an important formula, which expresses the change in the internal energy during polarization in the case of constant permittivity:

$$U = U_0(T) + \frac{1}{2}\varepsilon_0 \varepsilon E^2 \quad . \tag{1.2}$$

From these expressions it follows: $\partial S / \partial(E^2) = 0$. Therefore:

$$\begin{aligned} S &= S_0(T); \\ F &= F_0(T) + \frac{1}{2}\varepsilon_0 \varepsilon E^2 . \end{aligned} \tag{1.3}$$

So, while the polarization occurs in the dielectric which has $\varepsilon = Const$ the entropy is not changing, while the change in the *internal energy U* equals to the change in *free energy F.*

2. *The case* $\varepsilon = \varepsilon(T)$ *regardless of polarization mechanisms* is the next important point actual for many dielectrics used in electronics, because in most of them their permittivity varies with temperature. It is all the more important that the developers of dielectrics for their use in electronics usually strive to eliminate the temperature dependence of permittivity by investigating different mechanisms of polarization.

In a given case the change of electrical induction is

$$\mathrm{d}D = \varepsilon_0 \varepsilon \mathrm{d}E + \varepsilon_0 E \frac{\partial \varepsilon}{\partial T} dT = \frac{\varepsilon_0 \varepsilon}{2E} \mathrm{d}(E^2) + \varepsilon_0 E \frac{\partial \varepsilon}{\partial T} dT \quad .$$

Consequently, the change of internal energy equals to:

$$\mathrm{d}U = \mathrm{d}Q + \frac{1}{2}\varepsilon_0 \varepsilon \mathrm{d}(E^2) + \varepsilon_0 E^2 \frac{\partial \varepsilon}{\partial T} \mathrm{d}T = \frac{\partial U}{\partial T} \mathrm{d}T + \frac{\partial U}{\partial (E^2)} \mathrm{d}(E^2) \quad .$$

Defining dQ, it needs to get

$$\mathrm{d}S = \frac{\mathrm{d}Q}{T} = \frac{1}{T}\left(\frac{\partial U}{\partial (E^2)} - \frac{1}{2}\varepsilon_0 \varepsilon \right) \mathrm{d}(E^2) + \frac{1}{T}\left(\frac{\partial U}{\partial T} - \varepsilon_0 E^2 \frac{\partial \varepsilon}{\partial T} \right) \mathrm{d}T \quad .$$

To obtain the differential equation for energy change, the property of total differential dS is used. After transformations:

$$\frac{\partial U}{\partial (E^2)} = \frac{1}{2}\varepsilon_0 \varepsilon + \frac{1}{2}\varepsilon_0 T \frac{\partial \varepsilon}{\partial T} \quad .$$

The integration of this differential equation needs to use nest expression for internal energy:

$$U = U_0(T) + \frac{1}{2}\varepsilon_0 \left(\varepsilon + T \frac{\partial \varepsilon}{\partial T} \right) E^2 \quad .$$

After integration it can be obtained:

$$\frac{\partial S}{\partial\left(E^2\right)}=\frac{\varepsilon_0}{2T}\left(T\frac{\partial\varepsilon}{\partial T}\right);$$

$$S=S_0\left(T\right)+\frac{1}{2}\varepsilon_0\frac{\partial\varepsilon}{\partial T}E^2.$$

Therefore, the free energy is

$$F=F_0\left(T\right)+\frac{1}{2}\varepsilon_0\varepsilon E^2 \qquad (1.4)$$

These relations for U, S and F are significantly different from the expressions characterizing dielectrics with constant permittivity. In particular, from comparison of these expressions, it is seen that well-known formula $\frac{1}{2}\varepsilon_0\varepsilon E^2$ for the energy of polarization characterizes the only free energy F change of dielectric in the electrical field but not the change in its internal energy U.

Turning to the new thermodynamic parameters T and S (instead of T and E), it is possible to derive formula that links εT and εS:

$$\frac{\varepsilon^T-\varepsilon^S}{\left(\varepsilon^T-1\right)\left(\varepsilon^S-1\right)}=\frac{\varepsilon_0 T}{C_P}\left(\frac{\partial E}{\partial T}\right)_P^2, \qquad (1.5),$$

where C is the specific heat while the index P means that heat capacity (as well as derivative дE/дT) is determined at the condition, when the polarization is constant. As follows from the equation (1.5), the isothermal permittivity is always bigger than the adiabatic permittivity: εT > εS.

Obtained energy relations can be used to analyze many properties of dielectrics which are associated with the process of polarization. In particular, it is possible to determine whether the way of thermodynamic process of polarized state establishing has any influence on the magnitude of permittivity.

If the process of polarization is considered as the isothermal (dT = 0), the internal energy of polarization equals $\frac{1}{2}\varepsilon_0\varepsilon E^2$, so its temperature dependence can be not taken into account during the determination of polarization energy. In practice, however, isothermal process is difficult to implement, since it is possible only at a very slow change of the electrical field and in the case of very good heat-conducting contact of test dielectric and environment (that is the "thermostat"). Measuring studied sample should be provided only in the subsonic frequency range

and only for rather thin films deposited on the massive metallic substrate. In other cases, it is impossible for usual bulk sample to meet the basic requirement of isothermal process when the establishment of thermal equilibrium between sample and thermostat needs in all stages of experiment (such studies are difficult to achieve in practice). However, as will be noted earlier, in the case of nanoscale samples, the isothermal process takes place under the normal conditions.

Usually most research of dielectrics are carried out under the adiabatic conditions ($dS = 0$) when at time of voltage change any thermal equilibrium between the dielectric and environment has no time to install. Already at 50 Hz electrical field changes 100 times per second; in addition, dielectrics have low thermal conductivity that makes difficult to heat exchange with the environment. Thus, in the most cases, real energy of dielectric polarization is described by the relation (1.4). From resulting expressions for *U, F* and *S*, it follows that the change in *free energy* during polarization does not depend on the changes $\varepsilon(T)$, and always equals $\frac{1}{2}\varepsilon_0\varepsilon E^2$. However, the temperature dependence of permittivity significantly impact on the change in *entropy*. If the permittivity increases during the heating of a dielectric, that is, when the temperature coefficient of permittivity is positive ($TC\varepsilon > 0$), the change in entropy $S - S_0(T)$ during polarization must be *positive*. Thus, not discussing details of physical processes that occur in the dielectric, only from general thermodynamic considerations, it can be concluded that:

If the dielectric, characterizing by $TC\varepsilon > 0$ *(that means permittivity increase with temperature rise), is placed in the electrical field, the change in the entropy is positive, so such physical processes occur, which reduce the degree of ordering in the molecular or atomic structure in the dielectric.*

Conversely, if in the dielectric $TC\varepsilon < 0$*, that is, if its permittivity decreases with heating, the change in the entropy is negative: it means that basic mechanisms, which determine polarization in case of external electrical field application, results in the increase of ordering of molecules (ions, atoms) of a dielectric.*

These important conclusions are applicable to the ferroelectrics and paraelectrics, but the most convincing are their application to the relaxation polarization.

3. ***The case ε = ε(T) applied to thermally activated polarization****,* takes into account the feature that *thermal motion* of the particles in a dielectric may greatly affect on the polarization process (if dipoles, ions or electrons are weakly bound in dielectric structure). Remaining localized in the nano-size regions, these particles under the influence of thermal motion can make thermally activated jumps, moving

within atomic-dimension distances. Relaxation time of thermally activated polarization is strongly dependent on temperature, that is why dielectric contribution and losses generated by thermally activated polarizations essentially changes with temperature and frequency: at higher temperatures and frequencies, the permittivity decreases with temperature so $TC\varepsilon < 0$, while at lower temperatures and frequencies the permittivity increases with temperature so $TC\varepsilon > 0$. Let's start with the first case when Curie's law is satisfied (by analogy with paramagnetics),

$$\varepsilon = \varepsilon_1 + \frac{K}{T} \qquad (1.6)$$

where T is the absolute temperature, K is the Curie constant, and ε_1 characterizes the fast processes of polarization which only a little depends on temperature (this dependence is neglected). Calculated from formula (1.4), the internal energy is:

$$U = U_0(T) + \frac{1}{2}\varepsilon_0\varepsilon_1 E^2 .$$

Therefore, it turns out that the contribution into *internal energy* is possible only from the temperature-independent part of polarization. On the contrary, the change in the entropy is due to the contribution from those polarization which varies with temperature: $S = S_0(T) - \frac{1}{2}\varepsilon_0 \frac{K}{T^2} E^2$.

Since entropy is a measure of disorder of the molecules, and suggesting that the specific mechanism of thermal polarization is the orientation of dipoles in the electrical field, obtained expressions can be interpreted as follows: in the absence of electrical field the dipoles are oriented randomly, while the electrical field influence results in *partial ordering* of dipoles orientation, and the greater the field strength, the more dipoles are oriented.

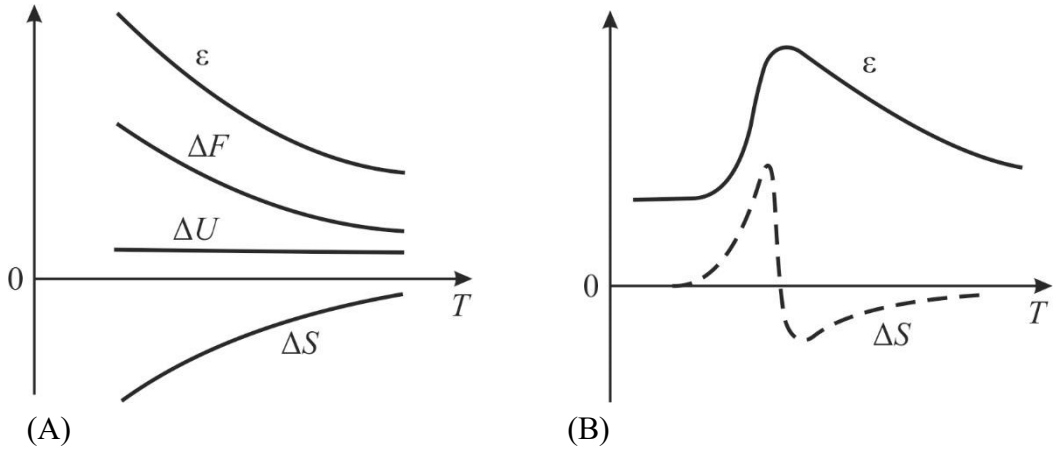

Fig. 1.2. Temperature dependence of permittivity and main thermodynamic functions for dielectrics with thermal polarization prevailing: A – within the limits of Curie law; B – in the wide temperature range

Temperature dependence of permittivity and main thermodynamic functions of ΔS, ΔU and ΔF for dielectric with thermally activated polarization are shown in Fig. 1.2A. Free energy changes with temperature, because it contains not only the temperature-independent contribution from internal energy, but the contribution from the entropy that is dependent on temperature and electrical field:

$$F = F_0(T) + \frac{1}{2}\varepsilon_0\left(\varepsilon_1 + \frac{K}{T}\right)E^2 . \qquad (1.7)$$

From thermodynamic analysis of this example it follows that the expression (1.7), which characterizes the temperature dependence of permittivity, in principle can not be true at very low temperatures. This would be in contradiction to the ***third law*** of thermodynamics, which states that the entropy of any system in the absolute zero is the universal constant that can be set equal to zero. From formula (1.7) it follows that the entropy in electrical field might increase at low temperatures.

Therefore, at very low temperatures the Curie formula (1.6) can not hold true.

Indeed, in the description of thermal polarization, the expression (1.6) is a special case of more general relationship

$$\varepsilon = \varepsilon_1 + \frac{K}{T\left[1 + B\exp\left(\frac{b}{T}\right)\right]}, \qquad (1.8)$$

from which it implies that in broad temperature range thermally activated polarization is characterized by the *asymmetric maximum* of permittivity (Fig.1. 2B). It is easy to show that the change in entropy in this case is different in different parts of shown temperature dependence of permittivity.

In those temperature range, where the permittivity increases with temperature, the electrical polarization leads to entropy increase.

4. *The case $\varepsilon = \varepsilon(E,T)$ describes the non-linearity* of thermally activated polarization, i.e., takes into account not only dynamic properties of thermally activated polarization, but also the *nonlinear responses* of this polarization seen in strong electrical field.

The dielectric nonlinearity may be of interest for some applications in electronics, e.g. the nonlinearity of paraelectrics at ultrahigh frequencies. But as an illustrative example, it is possible to analyze dielectric non-linearity at different temperature for the thermally-activated polarization.

From elementary models of this polarization (for example, the thermal-electronic or thermal-ionic polarization, occurring in solid dielectrics having high concentration of crystal defects), the dependence of the permittivity at the same time

on temperature and electrical field, in a simple approximation can be represented as follows:

$$\varepsilon(T,E) \approx \varepsilon_1 + \frac{K\left(1-\frac{a}{3}E^2\right)}{T\left[1+B\exp\left(\frac{b}{T}\right)\right]\left(1-aE^2\right)},$$

where ε_1 characterizes the fast (deformation types) polarization, which is lightly affected by T and E, and coefficient B depends on the parameters of molecular models of polarization.

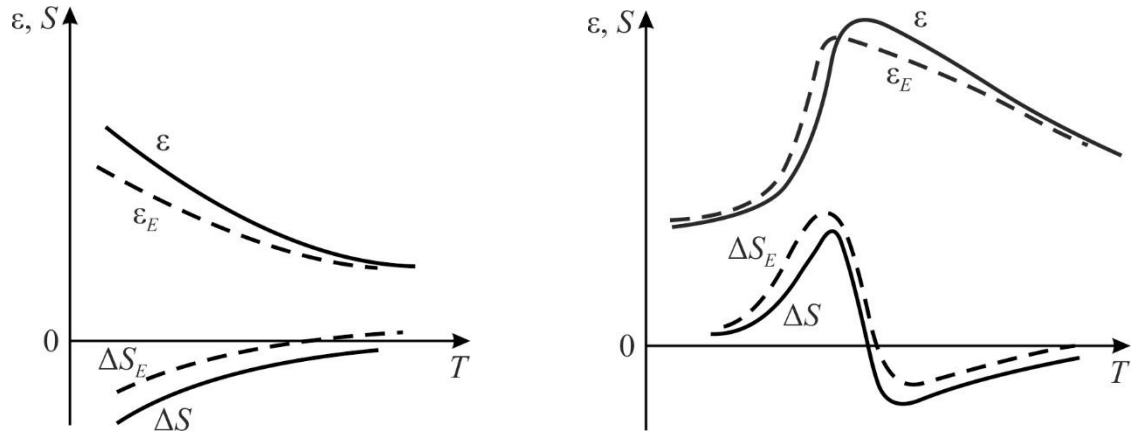

(A) (B)

Fig. 1.3. Temperature dependence of permittivity and entropy for dielectrics with thermally activated polarization in strong electrical field: A – within the limits of Curie law; B – in the broad temperature range; ε_E and ΔS_E are determined in the strong electrical field

A joint temperature and field dependence of permittivity and entropy is shown in Fig.1. 3. In this case, $\varepsilon(E)$ dependence influences on the thermodynamic functions as follows: *in the strong electrical field*, *the internal and free energy reduces while the entropy increases*.

Specific issues related to the thermodynamic description of thermodynamics application to the *ferroelectrics*, *piezoelectrics* and *pyroelectrics* will be discussed further.

1.3 Specific heat and configurational entropy

A solid is characterized by the strength, hardness and rigidity that seemingly exclude the possibility of any internal movement. However, in solids there are many different types of microscopic motions and displacements. Firstly, there is a movement of *structural defects*: the displacement of interstitial atoms, dislocations

and vacancies). In the vicinities of defects the energy of crystal is increased, so defects can move (very slowly) in order to find energetically more favourable configuration. Secondly, a *diffusion* is another type of atoms or ions motion in solids.

This mechanism is a result of thermal fluctuations: the kinetic energy of some particles due to fluctuations can get so big that particle can overcome potential barrier that separates one particle from another however, in most cases the probability of such processes at normal temperature is small.

Thirdly, the *electrons* can move in solids, and just their movement determines many electrical and magnetic properties of a matter. It is obvious that in the case of ionic conductivity *cations* and *anions* show the directional move in a crystal.

However, in the listed cases, microscopic movements in solids are not limited. Despite the fact that a solid the aggregate of regularly spaced and strongly interacting with each other particles, they particles are subjected to the microscopic oscillations and other excitations, which extend through crystal in a form of *weakly interacting waves*.

To explain main characteristics of solids, in this case the ***heat capacity***, it is considered that solids contain some "hidden" states – *quasiparticles*, which are the collective movement of many closely located atoms (such as local vibrations in crystal lattice).

Although in each excitation many atoms are involved, this movement, nevertheless, has the atomic scale. For such quasiparticles, which number in any state is unlimited, the Bose-Einstein distribution is valid, and these particles are the *bosons*.

If quasiparticles are a subject of Pauli principle, to them the Fermi-Dirac distribution is applicable, and these particles are *fermions*. The main contribution to the heat capacity of crystals is made by the bosons (only at very low and at very high temperatures, the contribution of fermions to the heat capacity can turn out to be significant).

Quantum mechanics describes microscopic objects only mathematically, and, certainly, any classic model of quasiparticle is not adequate.

However, it is possible to keep an idea of quasiparticles as some mobile "clusters" in crystal which might be described by the overall picture of waves that looks like "wave-clots" or “wave-packets”, Fig. 1.4. With some caution, one can assume that this is how the phonons that determine the heat capacity of the crystal look like.

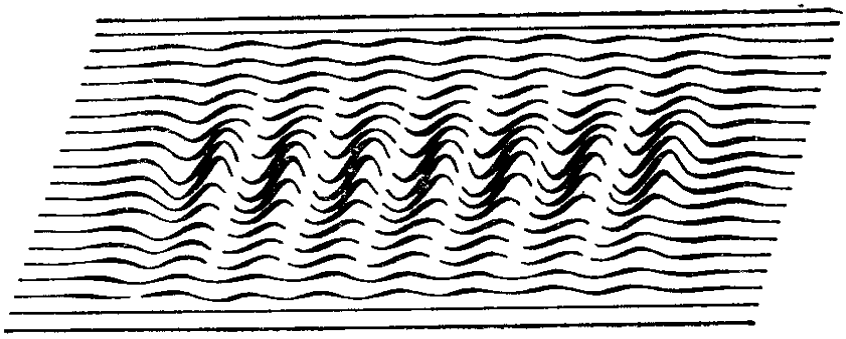

Fig. 1.4. Wave packet in two-dimensional presentation

1. ***Basic definitions.*** It is worth recalling that the specific value of heat capacity of a body is the physical quantity defined as a ratio of the amount of heat dQ obtained by a body to the its temperature increase by dT: C = dQ/dT, so the commonly used unit of specific heat in SI is [J/K]. However, the studied substance can be measured in the kilograms, cubic meters or moles. Correspondingly, the *mass* specific heat C_m is the amount of heat given to the unit mass of a material to increase it temperature by one Kelvin, so and specific heat is measured in [J□kg^{-1}□K^{-1}]. Respectively, the *volumetric* specific heat C_v is the amount of heat necessary to bring it to the unit volume of material, and it is measured in [J□m^{-3}□K^{-1}]. By the same way, the *molar* specific heat C_μ is measured in [J/(mol□K)], and, at last, in the *Gauss system,* the specific heat is determined in [cal/(g-mol□K)].

The heat capacity might be dependent on:

- various *mechanical* boundary conditions, which lead to difference between the C^X peculiar for the free crystal (stress X = 0), and C^x for the clamped crystal (strain x = 0);

- various *electrical* boundary condition when C^E is defined for the short circuited crystal (E = 0) while C^D is measured in the close circuited crystal (D = 0);

- different *thermodynamic processes,* at which the C^T corresponds to the isothermal process (T = *Const*), the C^S is defined during the adiabatic process (S = *Const*), the C_V is defined while isochoric process (with constant volume of a system, V = *Const*) and the C_p in peculiar for the isobaric process, at which the pressure remains unchanged (p = *Const*).

Historically, several theories of the lattice specific heat were developed. The first was the law of specific heat *constancy* (Dulong-Petit's law) that corresponds to the *classic* ideas, but with some accuracy is valid at *room temperature and higher*. The second was the Einstein's quantum theory of heat capacity, and it was first successful attempt to use quantum mechanics to describe specific heat in solids at *low-temperatures*. The third was the Debye's quantum theory of heat capacity based

on the model of the *constrained* atomic vibrations, and showed better correspondence to low temperature experimental data than the Einstein's theory. The fourths was the Born's theory of lattice dynamics that represents the most advanced method to describe crystal lattice dynamics, including theory of heat capacity.

· *The classic law of specific heat constancy* states that the *molar* heat capacity of different solids is the same (at room temperature and increased temperature) and equals $C_{solid} = 3R$, where R is the universal gas constant. Very important is that molar heat capacity in solids at ambient temperature more is twice as high in comparison with heat capacity of ideal gas: $C_{gaz} = 3/2$ R, Fig. 1.5. It should be remind that one mole of *any substance* contains the same number of atoms determined by the Avogadro number: $N_A = 6.02 \cdot 10^{23}$ mol^{-1}.

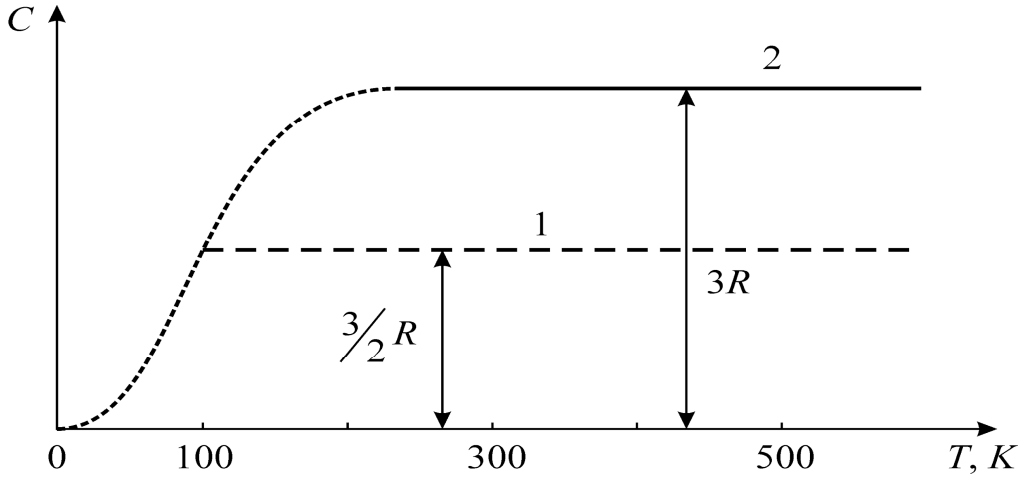

Fig. 1.5. Dependence of molar heat capacity of temperature: *1* – ideal gas; *2* – solid body

According to classic statistics, each degree of freedom of a gas particle makes same contribution to the molar heat capacity. This rule is the *law of equipartition*. Any particle of monatomic gas has only three degrees of freedom; according to this the molar heat capacity of a gas should be equal to 3/2 R, that is, about 13.5 J/(kmol·K); in Gauss units this is 3 cal/(mol·K) that is in good agreement with experiments. The reason is that the free atoms of gas have exclusively the *kinetic energy*; each gas atom has three degrees of freedom and the contribution to energy of each degree is $(k_BT)/2$ that is just $(3/2)k_BT$ in total. Since one mole contains of N_A atoms, the molar specific heat of a gas equals 3/2 R, Fig. 1.5. Often used in the solid state theories *Boltzmann constant* $k_B = R/N_A$ defines the relationship between temperature and energy: $k_B = 1.4 \cdot 10^{-23}$ J/K = $8.6 \cdot 10^{-5}$ eV/K).

[***Note.*** The universal gas constant $R = 8.314$ J·mol^{-1}K^{-1} equals to the expansion of one mole of ideal gas in the isobaric process with the increase in temperature by 1 K. It enters into equation of the state of ideal gas: $pV = RT$, and equals the difference between molar specific heat of ideal gas at constant pressure

and constant volume: $R = C_p - C_V$. The Avogadro number $N_A = 6{,}022 \cdot 10^{23}$ mol^{-1} is the physical quantity numerically equal to the number of specified structural units (atoms, molecules, ions) in 1 mole of substance].

The atom, being *constrained* in the crystal lattice, during its vibration possesses not only the *kinetic* but also the *potential* energy, which equals to kinetic energy on average; that is, each atom in a lattice has the twice as much energy in comparison with same atom in a gas: $3k_BT$. Exactly because of this fact the law of specific heat *constancy* follows. The Dulong-Petit's law, in a dynamic formulation of a problem, is derived by the assuming that crystal lattice consists of atoms, and each atom is the *harmonic oscillator in the three dimensions* (due to 3D lattice structure), whereby the fluctuations in the three orthogonal directions are independent. This means that each atom can be associated with a superposition of three oscillators with energy E that satisfies to following formula: $E = k_BT$. This formula follows from the theorem of *energy equipartitioning* among the degrees of freedom. Each oscillator has one degree of freedom, and, therefore, its average kinetic energy equals to $k_B/2$ per temperature unit. Since the oscillations are *harmonic,* the average potential energy equals to the average kinetic energy, so the total energy, respectively, equals to their sum. The number of oscillators in one mole of substance is $3N_A$, and their total energy per one Kelvin equals to the specific heat of a solid; just from this reasoning the law of constant specific heat follows directly. Thus, the classic (and the simplest) idea as to the thermal motion in the crystal lattice can be reduced to the model of *independent* oscillators.

Note that law of the molar specific heat constancy in crystals does not depend on the type of atoms (or ions) of a solid body and does not depend on temperature; it should be noted, that even this relatively simple model of equal and independent oscillators is capable to explain this feature. However, the low temperature investigations of specific heat demonstrates a *fast decline* of $C_{solid}(T)$ characteristic, shown in Fig.1.5 by dotted line. Moreover, while approaching to absolute zero, the specific heat vanishes: $C_{solid} \rightarrow 0$. All this testifies a shortcomings of the simple model of *classic* oscillator. The temperature dependence of the specific heat in solids at low temperatures is explained in the *quantum models* of Einstein and Debye.

Einstein's quantum theory of specific heat. Main assumption of this theory is that atom-oscillator in crystal lattice is the *quantum object*, not the classic one. However, as in the previous model, these oscillator again is considered as *independent*. The quantum oscillator with frequency v can absorb (or emit) energy only by portions – by the quanta: $h\nu = \hbar\omega$. This is shown schematically in Fig.1. 6 (see left chart). In the case of relatively high temperature (T_3), when thermal motion

is rather intense, the average thermal energy of oscillator (k_BT_3) is much greater than quantum of oscillator energy ($k_BT_3 >> \hbar\omega$), so the fact, that oscillator is the *quantum* oscillator, is not significant, and, therefore, the classic Dulong-Petit's law is satisfactory.

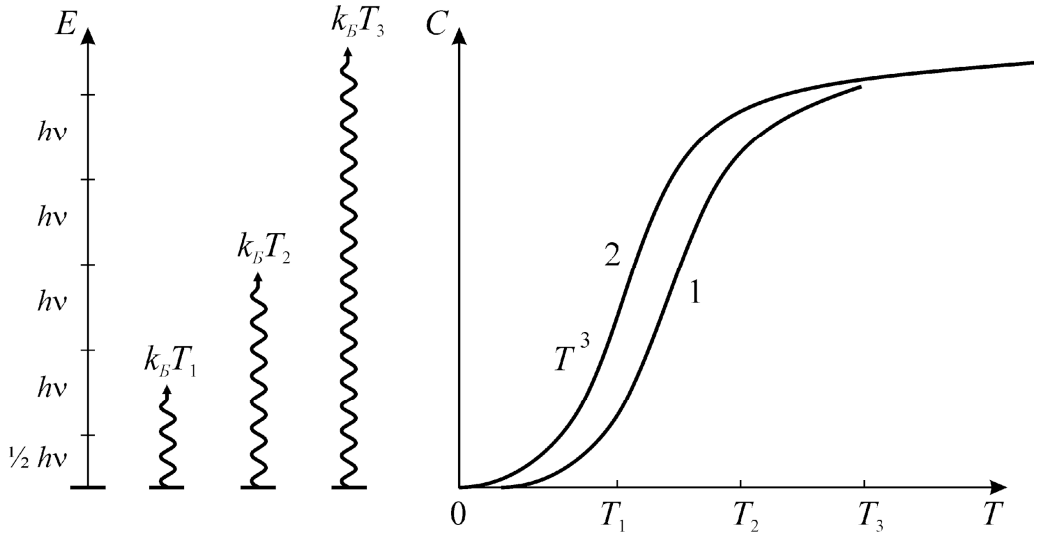

Fig. 1.6. Specific heat quantum model for independent oscillators (curve 1) and more correcr model of coupled oscillators (curve 2)

In case of low temperature, the average energy of thermal motion becomes approximately same as energy of quantum oscillator: $k_BT_1 \sim \hbar\omega$. Of course, energy distribution between lattice vibrations is chaotic, but when crystal is getting cooled, the number of quantum oscillators (which do not accept and do not radiate energy) increases, so the specific heat should be reduced with temperature decrease. This result was obtained by Einstein. His theory is based on the assumption that atoms in the crystal lattice behave as harmonic oscillators which do not interact with each other. The number of oscillators in one mole of substance is equal $3N_A$ and their energy is quantized. According to the model, proposed by Einstein, close to absolute zero of temperature the specific heat tends to zero, but at high temperatures the law of Dulong-Petit's holds true. The temperature dependence of $C_{lattice}$ in the Einstein's model is described by the *exponential* law (Fig. 1.6. curve 1). However, subsequent experiments have shown that in fact this dependence is described by a *cubic parabola*: $C \sim T^3$. As it turns out, it is necessary to consider the *interaction* between adjacent atoms; such calculations is made by Debye.

Debye's model of specific heat takes into account the contribution to heat capacity from the lattice of *interacting* atoms. This model correctly predicts the low-temperature specific heat proportionality to T^3, and considers that atoms-oscillators in crystal lattice are *elastically connected* to each other, so their vibrations are

interdependent. To explain the influence of atoms interaction on the frequencies of their oscillations, two models are shown in Fig. 1.7*a*: free and bound pendulum. In the case of *free* pendulum the eigenfrequency of oscillations ω is dependent only on the length of pendulum – this model corresponds to the case of independent oscillators discussed before. The constrained pendulums, Fig. 1.7*a*, can serve as a model to explain simplest two-atom bonding. In the case of two resiliently connected pendulums, the oscillation process becomes more complicated, as each pendulum has same eigenfrequency ω but there is also the additional *combinational* frequency Ω. If there would be three pendulums, then such a system would have three characteristic frequencies. Obviously, for n pendulums (that mimics crystal lattice of n atoms) number of characteristic vibration frequencies will be $n + 1$.

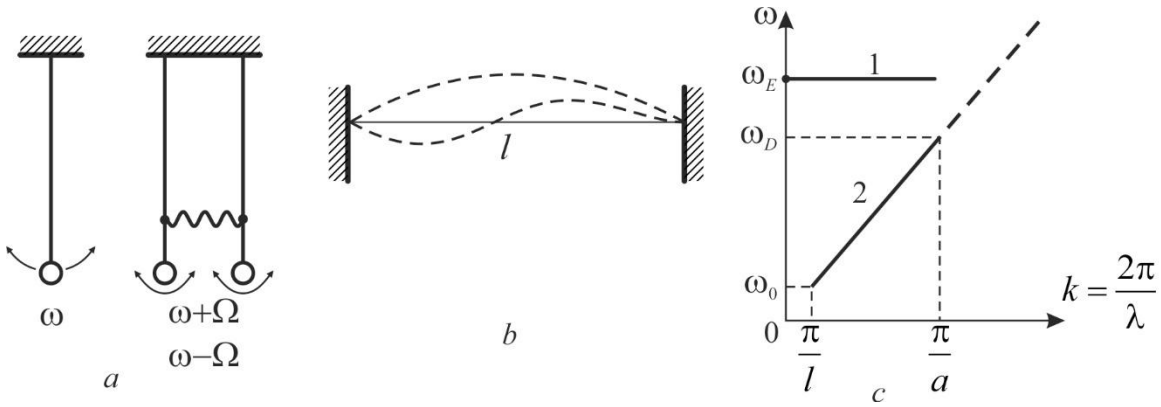

Fig. 1.7. Explanations related Debye model: *a* – single and two connected pendulums, *b* – string oscillations (primary tone and first overtone), *c* – $\omega(k)$ dependence of oscillator frequency of string on its length (dotted line); 1 – Einstein's mode ω_E of free oscillators; 2 – Debye mode of bounded oscillators with maximal frequency ω_D

To illustrate the Debye's model, it is possible to consider oscillations of a *string* with the length l and attached on the ends, Fig. 1.7*b*. The main tone has frequency ω_0 that corresponds to wavelength $\lambda = 2l$ of the elastic string. The overtones are $2\omega_0$, $3\omega_0$, … and so on, and they are located on same line $\omega(k)$ with wavelengths l, $2/3l$, …, and so on. The dependence of oscillation frequency ω on the reverse wavelength (wave vector) $k = 2\pi/\lambda$ is shown in Fig. 1.7*c*. In the Debye's model, the movement of the *centre of masses* of inter-connected lattice with N elements is considered. It is assumed that this complex movement (lattice vibrations) is equivalent to the $3N$ harmonic oscillators. Coordinates of these oscillators are the *normal coordinates*, and their fluctuations are termed the *normal modes*.

The internal energy and the specific heat of a solid consists of additive contributions of energies from individual normal vibrations. To derive the formula that describes specific heat dependence on temperature, it is necessary to know

frequency spectrum of normal vibrations. This spectrum can be calculated theoretically, whereby in the case of simplest lattice this solution contains three *acoustic modes*, with $\omega(k)$ dependence corresponding to three possible independent orientations of wave polarization vector (two transverse modes and one longitudinal mode). The relationship $\omega(k)$ is the *dispersion law*. In case of Einstein's model, frequency ω_E does not depend on the wave vector k – see line 1 in Fig. 1.7*c*. On the contrary, according to Debye's model, these relationship exists, and it is characterized by the *sloping line* 3. In this model the dependence $\omega(k)$ is *linear* (in same way as for a string), however, there is one important *restriction*: this line ends at the abscissa value π/a. This means the limiting of the wave length: $\lambda = 2a$, because there is no physical carrier for shorter wavelengths.

At low-temperatures the energy of crystal increases with temperature due to two factors: firstly, due to the *increase in average energy* k_BT of normal vibrations (that is proportional to T) and, secondly, due to the *increase excited oscillations number* proportionally to T^3. Therefore, the total energy of a crystal increases with temperature proportionally to fourth power of temperature: $E_{lattice} \sim T^4$. Accordingly, the specific heat of a lattice (which is determined as derivative; $C \sim dE_{lattice}/dT$) is proportional to temperature in a cubic power: $C \sim T^3$, that is in good agreement with experiments. At high temperatures, all normal lattice vibrations are already excited, and, therefore, further temperature increase does not a result of phonons number increase. Consequently, at relatively high temperatures, the growth of solids energy can only take place due to the increase in the degree of excitation of normal vibrations that causes the increase of their average energy proportionally to temperature (k_BT); so energy increase in solid must be proportional to temperature: $E_{lattice} \sim T$, while specific heat of lattice ($C \sim dE_{lattice}/dT$) should not depend on temperature: $C = const$.

Thus, above Debye temperature θ_D the specific heat tends to a constant value "$3R$" accordingly to the Dulong-Petit's law. Below θ_D the quantum nature of lattice vibrations becomes decisive, that is why, Debye temperature approximately indicates such temperature limit, below which the quantum effects become *non-negligible*. On the basis of other fundamental constants (Planck's constant h and Boltzmann's constant k_B), the Debye temperature can be expressed in terms of Debye frequency: $\omega_D = 2\pi\nu_D$. Indeed, by the analogy with equation $k_BT = h\nu$, it is possible to define similar equation $k_B\theta_D = h\nu_D$, so $\theta_D = (h/k_B)\nu_D$.

In different crystals, the value of Debye frequency is located in the range of $\nu_D = 10^{13}$–10^{14} Hz. These frequencies of lattice elastic vibrations correspond to the far infrared range of the electromagnetic spectrum. It is assumed that at Debye

temperature almost all oscillatory modes (types of oscillations) in a crystal are excited. During further increase of temperature new oscillatory modes do not appear any longer, but, instead, the existing modes increase their amplitude, that is, the average energy with increasing temperature rises linearly. In various crystals the value of Debye temperature are diverse, but typically $\theta_D \sim 200$ –400 K. For most of important in electronics crystals these temperatures are: in silicon $\theta_D = 650$ K, in germanium $\theta_D = 380$ K, in quartz $\theta_D = 250$ K. In the alkali halide crystals θ_D varies from $\theta_D = 730$ K in the LiF till $\theta_D = 100$ K in the RbJ; the highest Debye temperature $\theta_D = 1860$ K is seen in the diamond. At that, Debye temperature characterizes not only the specific heat, but also some other thermal properties of a solid (such as thermal conductivity, thermal expansion, melting points, etc.).

· *Born's dynamic theory* gives a chance to calculate the specific heat and many other parameters of solids even more accurately than Debye's theory, using peculiarities of the atomic structure of crystals. The solid body is treated as a lattice composed of elastically interconnected point masses. Not only the forces closest to a given atom are taken into account, but also the forces, acting between atoms located at larger distances. Even in the case of simplest model (one-dimensional model, i.e., the series of elastically joint atoms), it may be shown that Debye's result of the *linear* dependence $\omega(k)$ should be corrected: in the Born's dynamic theory the *dispersion* of elastic waves is predicted (that comes in very good agreement with experiments). However, in the case of low temperatures, the only *lowest-energy phonons* can be excited, so the Born's $\omega(k)$ dispersion is negligible. Therefore, the low temperature dependence of lattice specific heat in the Born's theory is also cubic: $C \sim T^3$.

In the considered *harmonic approximation*, the thermal expansion of a solid is absent, epy adiabatic and isothermal elastic constants are equal to each other and do not depend on epy pressure and temperature, elastic waves propagating in the lattice do not interact. In real conditions, all this is not fulfilled because in the harmonic approximation the nonlinearity of atomic vibrations is not taken into account. Taking into account the anharmonicity, it is also possible to explain the cases temperature anomalies in the specific heat capacity.

2. *Deviations from law of specific heat constancy* look very unusual above the Debye temperature, since the specific heat is a very *conservative parameter* determined by the fundamental physical laws. In most crystals, at normal temperatures and higher (when $T > \theta_D$) all possible lattice vibrations are already excited; therefore, the energy of a crystal increases with temperature rise as the *average energy* k_BT of normal vibrations; therefore, the specific heat of a crystal

would not be dependent on temperature: $C \approx Const$ (but in fact, specific heat *slightly rises* with temperature increase due to *anharmonicity* of lattice vibrations). Therefore, any significant change or leap in the temperature dependence of specific heat is associated with the *restructuring* of the crystal lattice.

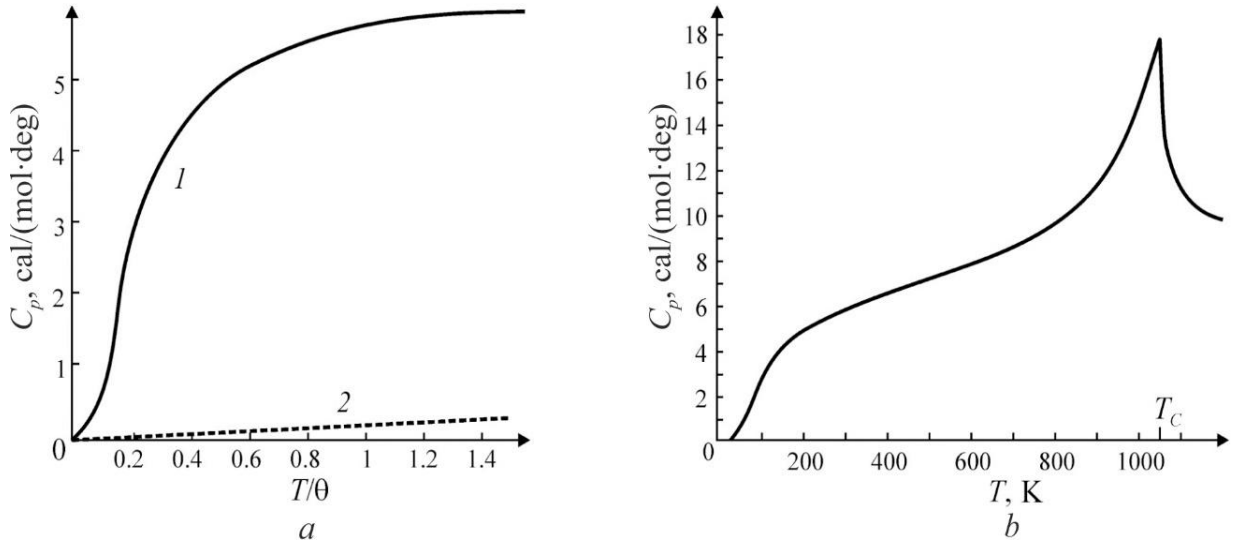

Fig. 1.8. Temperature dependence of heat capacity for the lattice (*1*) and the electronic (*2*) contributions in metal: A – nonmagnetic metal; B – ferromagnetic metal (iron)

Almost the only exception are the magnetics, where in the partially ordered ferromagnetic phase the *magnons* contribution to the heat capacity is significant (but it disappears above Curie point), Fig. 1.8B. Specific heat behaviour of ferromagnetic shows a pronounced deviation of usual $C(T)$ dependence which is quite different from a smooth curve with saturation at high temperatures, observed in the non-magnetic metals. It means that inherent to ferromagnetic *destruction* of spin ordering adds some energy throughout temperature range. Therefore, heat capacity of ferromagnetic, as shown in Fig. 1.8B, is significantly increased in comparison with usual metals. Especially noticeable effect of the increased heat capacity is seen in the vicinity of ferromagnetic phase transition followed by fast decrease of specific heat with temperature.

If one heats a ferromagnetic above the Debye temperature, its specific heat looks much bigger than in non-ferromagnetic crystal. The point is that the contribution to the specific heat in the magnetic materials is due not only to phonons, but also to magnons, at that summary specific heat substantially surpasses this parameter seen in the conventional metals. The increased heat capacity is especially noticeable at temperatures below Curie point, because in this region spontaneous magnetization decreases, so a peak-type anomaly of the specific heat near the critical point is caused by elementary magnetic moments disordering that is seen in rather narrow temperature interval below Curie temperature.

In the ordering polar crystals, their specific heat similar to ferromagnetic but in much narrow temperature interval also *exceeds* the "normal specific heat" as compared with the non-polar crystals. This is most clearly expressed near the ferroelectric phase transitions, where the maximum of the specific heat can be more than two times higher than its average value. A convincing example of internal polarity disordering influence on thermo-physical properties is their change at phase transition from *non-polar* (high-temperature centrosymmetric) phase into the *polar* (low-temperature ferroelectric) phase in the TGS crystal (triglycinesulphate, $(NH_2CH_2COOH)_3 \cdot H_2SO_4$), Fig. 1.9.

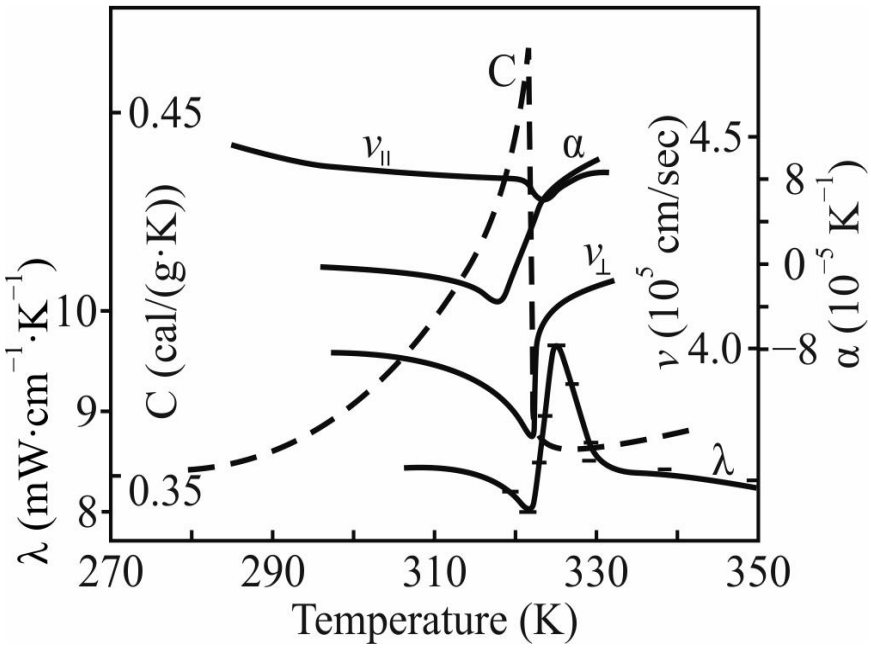

Fig. 1.9. Temperature dependence of main TGS parameters: specific heat C, ultrasound speeds v_1 in [010] direction and v_3 along [001] direction, linear expansion coefficient α_1 along [010] direction and thermal conductivity λ_1 along [010] direction

The point is that in the polar crystals their specific heat contains an additional contribution due to processes of polar bonds ordering-disordering. Implementation of statistical possibility of several states increases the total entropy of a system: this is the *configurational entropy* which is a part of total entropy of a system relating to the *positions* of constituent particles rather than to their velocity or momentum. It is explained by the number of ways of all the particles mutual arranging in a system while maintaining some overall set of specified system properties, such as energy. The change in the configurational entropy corresponds to same change in the macroscopic entropy.

In connection with given in Fig. 1.9 example note the following. In the vicinity of phase transitions, the substance, firstly, shows the anomalies in its main physical

properties; secondly, allows a considerable control of physical parameters by not very strong external influences that is widely used in the electrically controlled devices; third, the substance is very sensitive to the changes in temperature, pressure, humidity, etc., that is used in various sensory devices.

To understand physical causes of polar crystals peculiarities, it is necessary to compare the basic energy characteristics of solids with special properties arising due to phase transition into the phase having internal polarity. In this regard, recall that one of important crystal physical quantity is *Debye energy* $\hbar\omega_D$.

It becomes equal to *thermal energy* k_BT at a certain temperature called *Debye temperature* and denoted by θ_D; therefore $\hbar\omega_D = k_B\theta_D$ and $\theta_D = \hbar\omega_D/k_B$. Thus, the very important characteristics - Debye frequency $\omega_D = 2\pi\nu_D$ and Debye temperature - are connected with each other by two fundamental constants: Planck constant $\hbar$ and Boltzmann constant k_B.

The degrees of freedom at atomic particles movement in solids can be divided into two groups. In some degrees of a freedom, the interaction energy of particles U_{int} is small in comparison with thermal motion energy k_BT. At that, when $U_{int} << k_BT$, the appropriate degrees of a freedom behave as the *collection* of particles, i.e., as the "almost ideal gas" of phonons; at that, applicability to use the model of *quasi-particles* is earnestly justified. In given discussion, this refers to the ordinary non-polar dielectrics.

In the opposite case, when conversely $U_{int} >> k_BT$, the appropriate degrees of freedom are usually quite ordered, so their movement, too, can be described by the introduction of the quasi-particles, in a given case by the phonons. These substances include the majority of functional polar dielectrics (piezoelectrics and pyroelectrics), so the concept of phonons application to them, in most cases, can be considered justified.

However, in a given discussion, the much more complicated situation arises: when the interaction energy is close to the averaged energy: $U_{int} \sim k_BT$. In this case, any theoretical description of solids becomes very complicated, especially at the phenomenon of *phase transition*.

In the vicinity of *second-order phase transition* the crystal behaves by such a way when any, based on the quasi-particles, conventional concept can not adequately describe the experimental situation. Normally, the interaction of *closest neighbouring* particles in a crystal is considered as dominating, while the interaction of *distant particles* might be neglected. However, near the phase transition, in contrast, the interaction of neighbouring particles *compensates one another*, and on this background the interaction of those particles, which are located at some distance

from one another, appears *dominant*. This interaction has a very special character: the probability of *collective movements* is bigger then the probability of *individual movements*. It is possible that such a situation contributes to the aggregation of groups of atoms into clusters, which presupposes the creation of the basis for configurational entropy.

Abnormally increased role of the collective movements is confirmed by experiment, Fig.1. 10: at temperature $T = T_C$ crystal shows the maximum of specific heat, also the dielectric permittivity in the ferroelectric tends to infinity, as well as the maximum of permeability in the ferromagnetic (in superconductors their conductivity actually becomes infinite), and so on.

The crystals possessing polar bonds, in the certain conditions, behave in complex way: the lifetime of some phonons is commensurate with the inverse frequency of oscillation; that is, the oscillators, which characterize these phonons, turn out to be over-damped.

At the first glance, an amazing situation arises when the crystal of excellent quality, being ideally transparent in the optical wavelength range and having small attenuation of transmitting long acoustic (ultrasonic) waves, for the short (heat) waves turns out to be an almost opaque (turbid) environment, in which phonons of a certain frequency getting stuck like feet in a swamp.

Another striking feature of the polar crystals is their *compression* when being heated (in contrast to usual crystals extension) that is observed in the low-temperature interval. To explain the physical nature of such negative thermal expansion of polar crystals, a comparison will be carried out of two different scalar influences on polar crystals: the homogeneous change of temperature and the homogeneous (hydrostatic) change of pressure.

These actions are uniting by the fact that, being scalar, both these influences lead to a *natural* (not distorted by the symmetry of external action) change in the crystal size, which reflecting exactly the peculiarities of crystal internal bonds. Later in Section 1.4 it will be shown that the main thermal effects in crystals are interdependent, and expedient to begin consideration with the specific heat.

As opportune example of specific heat increasing in the polar-sensitive crystals, the ferroelectrics can be chosen, in which one can compare the heat capacity of *polar* and *nonpolar* phase (above phase-transition temperature). As an example, the TGS crystal is elected again, which is non-polar above its Curie point, its heat capacity and internal electrical moment ΔM is shown in Fig. 1.10.

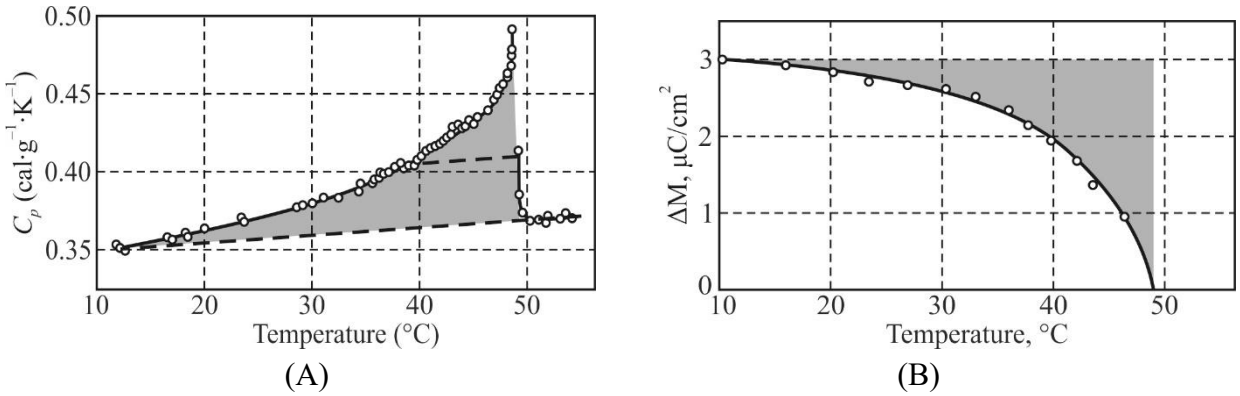

Fig. 1.10. Temperature dependence of heat capacity (A) and averaged electrical moment of polarization fluctuations (B) in TGS = $(NH_2CH_2COOH)_3 \cdot H_2SO_4$

The fact is that the *gradual increase* and the *maximum* in $C(T)$ dependence is necessarily manifested in the ferroelectric crystals when their phase transition temperature T_C is approached, Fig. 1.10A. Fundamental part of the heat capacity, which is practically temperature-independent, is shown by the bottom dotted line. Above the upper dotted line, the λ-type maximum of $C(T)$ is seen, which in this case reaches 50% of the fundamental specific heat (in some ferroelectrics it might be much times greater). This maximum is due to the nature of ferroelectric phase transition and corresponds to the latent heat releasing at phase transition.

However, discussed here $C(T)$ anomaly looks like a rather big region of the excess heat capacity. Below the Curie point, with decreasing temperature, the internal (spontaneous) polarization changes very gradually as seen in Fig. 1.10B. At that, the complete ordering could occur only at an unattainable absolute temperature $T = 0$ K; the unordered part is shown by the shaded area which quite corresponds to those temperature interval where specific heat is increased. It might be supposed that the contribution to the heat capacity in the gradually ordering phase is due to the configurational entropy. It is pertinent to note that such deviation from the linearity of $C(T)$ dependence above Debye temperature occurs very rarely in solids. As noted, the analogous case of specific heat capacity increase is seen it the ferromagnetic, in which an additional contribution to the $C(T)$ is due to the *collective excitation*, associated with the electronic spins structure in the partially ordered magnetic lattice, i.e., magnons.

Shown in Fig. 1.10A specific heat increase, peculiar to the ordering polar crystals, requires an explanation. Need to mark that a significant *smoothing* of temperature maxima elastic stiffness s_{11} and s_{33} in TGS is seen under the influence of a strong CD electric field. Besides, the experiment in ultrasound absorption in TGS crystal near its phase transition shows the decrease of sound absorption in the

polar phase and its increase in the non-polar phase while DC electrical field application.

All this indicates that the gradual increase in $C(T)$ and its temperature peak shown in Fig. 1.10A is due to the reorganization in the arrangement of polar-sensitive bonds, and can be explained by thermal fluctuations of disordered (nonpolar) phase in the depths of ordered polar phase. Probably, these fluctuations are concentrated in the domain walls, which dynamically can expand and contract. It is possible to offer another explanation to the fact that below phase transition the ordering of polarity in ferroelectrics occurs gradually. Statistical possibility of several states realizing increases the total entropy of a system: such *configurational entropy* is a part of total entropy of a system that is related to the position of the constituent particles rather than to their velocity or momentum. It is physically related to the number of ways of arranging all the particles of a system while maintaining some overall set of specified system properties, such as energy. Change in the configuration entropy corresponds to the same change in macroscopic entropy.

From point of view of macroscopic theory, due to existing electrical, thermal and mechanical properties *interconnection* in the polar crystals, the dependence of their thermal properties on mechanical and electrical boundary conditions of a crystal is not surprising: heat capacity of mechanically clamped crystal C^x differs from heat capacity of free crystal C^X, just as the heat capacity of short-circuited crystal C^E is not equal to the heat capacity of electrically free (opened circuit) crystal C^D. At that, the temperature anomaly of TGS heat capacity, shown in Fig.1. 10A, corresponds to the property of electrically and mechanically free crystal.

Further it will be shown that specific features of polar crystals have noticeable effect on the heat exchange processes. However, the most impressive difference between polar and non-polar crystals is their negative thermal deformation at low temperatures interval, when thermal motion in crystals weakens that allows observe the details of structural peculiarities.

1.4 Thermal expansion and entropy

From the point of view of thermodynamics, the dynamic changing in the own structural ordering, taking place in the polar dielectrics and magnetics, need more detailed consideration of the *entropy conception*, namely, not only use traditional account of "kinetic" part of entropy, associated with the individual particles dynamics, but also the *configuration* entropy, since the directional inter-atomic polar bonds, during their ordering-disordering process, spontaneously form a lot of

various nanoscale configurations. A statistical possibility of several states realizing increases the entropy of a system: such a *configurational entropy* is the part of total entropy of system, and it relates to the *position* of groups of particles rather than to their velocity or momentum. This contribution to the entropy is due to a number of ways of mutual arrangement of particles contained in the system while maintaining some overall set of specified system properties, such as kinetic energy. The change in configuration entropy corresponds to same change in the general entropy.

A number of physical phenomena, observed in the polar dielectrics, directly indicate a large role of the configuration part of entropy: the *negative* coefficient of thermal expansion, the *maximum* of heat capacity at phase transition from disordered phase to ordered phase, the *increase* of polar phase volume when it arises from the non-polar phase (and the *decrease* of anti-polar phase volume), the drastic changes of phonons *scattering* during the heat transfer, etc.

1. *Coefficient of thermal expansion* (denoted α and measured in the $[\text{deg}^{-1}] = [\text{K}^{-1}]$ represents the alteration of relative dimensions of a solid body when its temperature changes by 1 K. The thermal deformation of crystal is a characteristic feature of the *internal connections* of atoms, ions or molecules; thermal deformation depends also on the energy value of these bonds. At that, coefficient α reflects the features of interatomic bonds in a crystal; particularly, in the polar dielectrics, this is a peculiar polar-sensitive structure arisen due to structural compensation of atoms electronegativity. It is pertinent to recall that relative deformation of a solid is the dimensionless parameter described by the second-rank tensor x_{ij}. This deformation can occur not only under the influence of the *mechanical stress* X_{kl} (also second rank tensor), but under various other external influences as well: the electrical action described by *polar vector* E_k, the magnetic influence described by *axial vector* H_k, as well as by the *scalars* (homogeneous) influences such as the uniform change of temperature δT or hydrostatic change of pressure δp. In all listed cases, the character and the symmetry of parameters which link the various actions (X_{kl}, E_k, H_k,δT,δp) and the linear response – strain x_{ij} – induced by these actions are very different:

$$x_{ij} = s_{ijkl}X_{kl}, \quad x_{ij} = d_{ijk}E_k, \quad x_{ij} = \varsigma_{ijk}H_k, \quad \boldsymbol{x_{ij} = \alpha_{ij}\delta T}, \quad x_{ij} = \xi_{ij}\delta p,$$

where s_{ijkl} is the elastic compliance (fours rank tensor), d_{ijk} is the piezoelectric module (third rank tensor), ς_{ijk} is the piezomagnetic module (third rank tensor) and α_{ij} is the coefficient of *thermal expansion* (second rank tensor), exactly the parameter discussing in this Section.

It is noteworthy that first three of above parameters characterize those properties of a crystal which can be obtained by the external action of *fields* possessing vector symmetry, so the symmetry of a response (in this case, the strain

x_{ij}) is *composed* of symmetry of actions and symmetry of crystal. Therefore, in case of multifaceted study of crystal properties, the tensors s_{ijkl}, d_{ijk}, ς_{ijk} can only *indirectly* characterize the nature of internal bonds of atoms (ions) in a crystal. At the same time, the *scalar* action on a crystal (which has symmetry of a *sphere*) gives such parameter (α_{ij}), which reflects the *intrinsic properties* of interatomic bonds *directly seen* in the response.

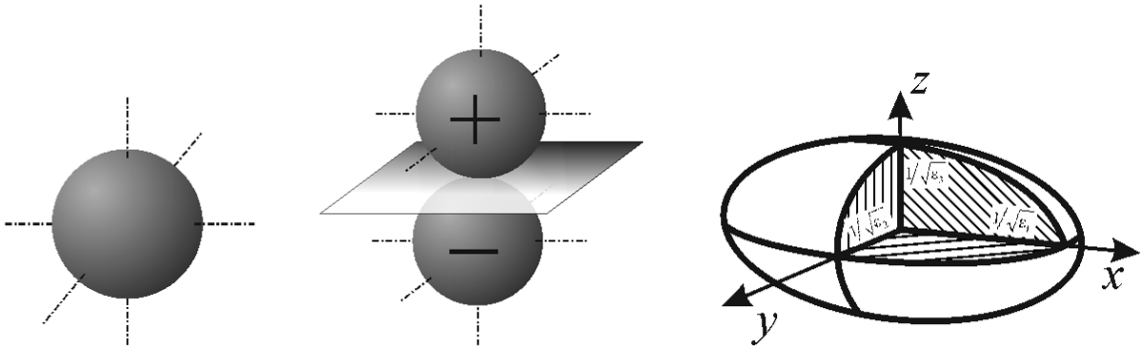

(A) (B) (C)

Fig. 1.11. Images of material tensors of various ranks: A – zero rank tensor (*scalar*, such as density, temperature, specific heat, etc.); B – first rank material tensor (*vector,* such as pyroelectric coefficient or volumetric piezoelectric modulus); C – second rank material tensor (electrical permittivity, electrical conductivity, magnetic permeability, etc.)

The second-rank material tensor seen in Fig. 1.11C most often describes the vector response to the vector action ($D_i \sim \varepsilon_{ik}E_k$, $j_i = \sigma_{ik}E_k$, etc.), so it is characterized by the second-order surface (ellipsoid), while its components form the symmetric matrix (3×3 = 9 components). But in the case of thermal expansion, the action is the scalar quantity (δT) while the response x_{ij} is the second rank tensor (deformation), which, depending on symmetry of crystal, leads to a great variety in the combination of different components for tensor α_{ij}. At that, the *anisotropy* of thermal expansion characterizes the anisotropic properties of atomic bonds in a crystal. It can be argued that it is the internal polarity, which is one of reasons for both the anisotropy of thermal expansion and negative deformation when crystal temperature increases in certain range.

$$\begin{pmatrix} \alpha_{11} & 0 & 0 \\ 0 & \alpha_{11} & 0 \\ 0 & 0 & \alpha_{11} \end{pmatrix} \quad \begin{pmatrix} \alpha_{11} & 0 & 0 \\ 0 & \alpha_{11} & 0 \\ 0 & 0 & \alpha_{33} \end{pmatrix} \quad \begin{pmatrix} \alpha_{11} & 0 & 0 \\ 0 & \alpha_{22} & 0 \\ 0 & 0 & \alpha_{33} \end{pmatrix} \quad \begin{pmatrix} \alpha_{11} & \alpha_{12} & 0 \\ \alpha_{12} & \alpha_{22} & 0 \\ 0 & 0 & \alpha_{33} \end{pmatrix} \quad \begin{pmatrix} \alpha_{11} & \alpha_{12} & \alpha_{13} \\ \alpha_{12} & \alpha_{22} & \alpha_{33} \\ \alpha_{13} & \alpha_{23} & \alpha_{33} \end{pmatrix}$$

(A) (B) (C) (D) (E)

Fig. 1.12. Matrices of thermal expansion coefficient in crystals of various classes of symmetry: A – cubic; B – hexagonal; C – rhombic; D – monoclinic; E – triclinic

This anisotropy is clearly seen from α_i matrix representation in Fig. 1.12, where various matrices for crystals of different symmetry are presented. In the most common *ionic* and *covalent* crystals, the coefficient of thermal expansion is *isotropic* and can be represented by the scalar value $\alpha_{ij} = \alpha$; at that, components located in main diagonal of matrix α_{ij} are same, Fig. 1.12A. The ball made of such crystal, being exposed by uniform heating or cooling, will change its radius but will not change its shape. It would be seem that in the hexagonal crystals (Fig.1. 12B) this ball will turn into the ellipsoid of rotation, and in the case of rhombic or monoclinic crystals initial ball will be transformed into a three-axis ellipsoid.

In the lower symmetry crystals, their diagonal components α_{11}, α_{22} and α_{33} can have not only different values, but also *different signs*. Therefore, instead of second rank surface (the ellipsoid seen in Fig. 1.11C), the indicatrix of thermal expansion coefficient is symmetrical but *very complex surfaces,* Fig. 1.13.

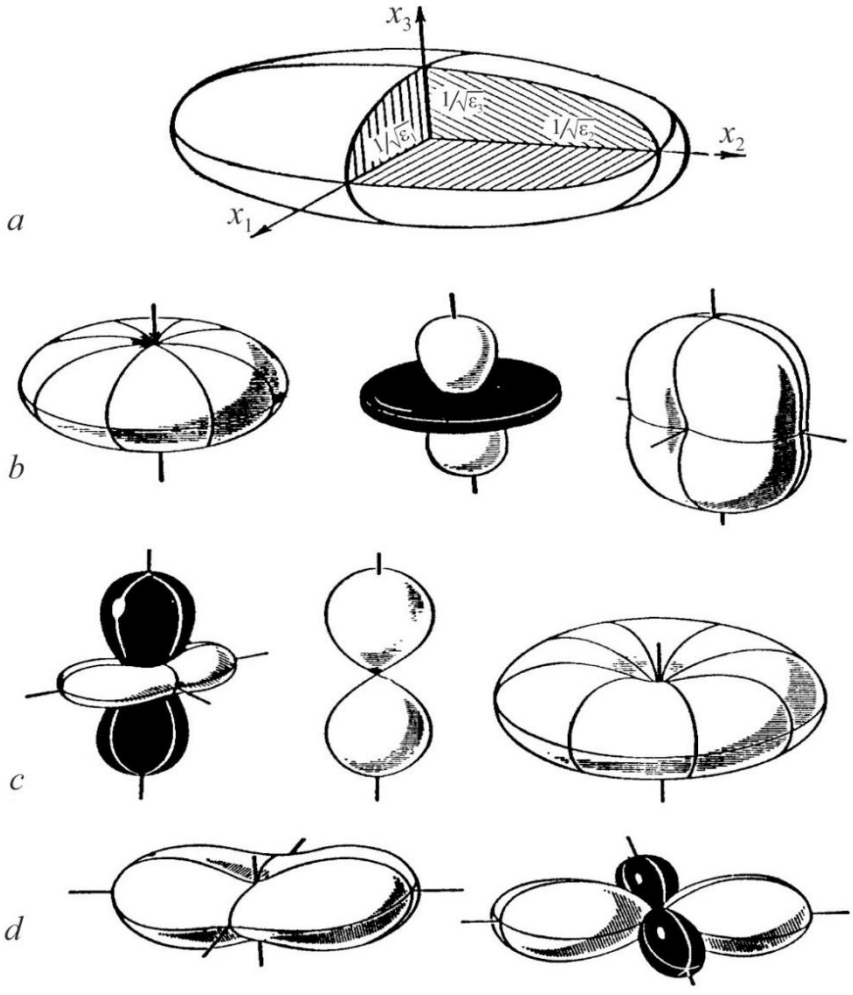

Fig. 1.13. Characteristic surfaces that exhibit anisotropy of physical quantities described by second-rank material tensor; *a* – ellipsoid of permittivity of biaxial crystal symmetry; *b, c, d* – figures describing thermal expansion coefficient in crystals of different symmetry, black shows negative value of α (according to A.V. Shubnikov)

In a general case, with possibly different signs of components of thermal expansion tensor, the characteristic surfaces in Cartesian coordinates are not ellipsoids, and, generally, they are not even a surface of second order. Nevertheless, the knowledge of characteristic surfaces is important for anisotropic crystals applications. For example, in the calcite crystals, the expansion coefficient in the direction of principal axis of a crystal is positive, but in the directions perpendicular thereto it is negative. This means that in some oblique directions, the expansion coefficient *should be zero,* and, hence, in a certain direction the radius vectors of indicatory surface should be zero (this case is impossible for ellipsoid).

A. Shubnikov considered *all possible forms* of indicatory surfaces of thermal expansion coefficients in the crystals in the condition when linear expansion coefficients α_1, α_2 and α_3 differ both in magnitude and in sign, Fig. 1.13. Positive values of α are shown on these figures by t *white surfaces* while negative values of α are shown by *black surfaces*. As it was noted above, in the crystals of cubic symmetry, all three major expansion coefficients are equal, and all three of them are usually positive. Corresponding surface in this case is obviously the sphere with positive radius: this is "white-colored sphere", but this simplest case is not shown in Fig. 1.13. In case, when $\alpha_3 \neq \alpha_1 = \alpha_2$ and $\alpha_3 > 0$, the surface describing expansion coefficients is similar to oval; it can be either flattened (at $\alpha_3 < \alpha_1$, Fig. 1.13*b* or elongated along axis *3*. These surfaces describe simple cases of thermal expansion of optically *uniaxial crystals* that are often found in practice. In the calcite crystal, for example, the component α_3 has positive sign, while components $\alpha_1 = \alpha_2$ have negative signs. The surface that corresponds to case is also shown in Fig. 1. 13*b*. It is composed of two egg-shaped positive (white) surface and torus-like negative (black) surface. The most complex forms of the indicatrix of thermal expansion can be observed in the triclinic crystals, in which matrix α_{ij} can not be reduced to a diagonal form. Characteristic surfaces of thermal expansion tensor shown in Fig.1.13 exhaust all possible combinations of main components of α_{ij} tensor.

Thus, the anisotropy of thermal expansion reflects the complex distribution of the hybridized ionic-covalent interatomic bonds in the polar crystal, while the simple ionic and covalent bonds in crystal are usually characterized by the isotropic (scalar) thermal expansion coefficient. It can be seen from the data presented that the nature of thermal expansion is quite complex, but it is this that reveals the nature of intter-atomic bonds.

2. *Physical nature of thermal expansion.* The change in volume (or in the linear dimensions) of a crystal with temperature alteration is a result of the

asymmetry in the interaction law of the neighboring particles. This asymmetry can be easily traced in the main types of inter-tone connections, Fig. 1.14.

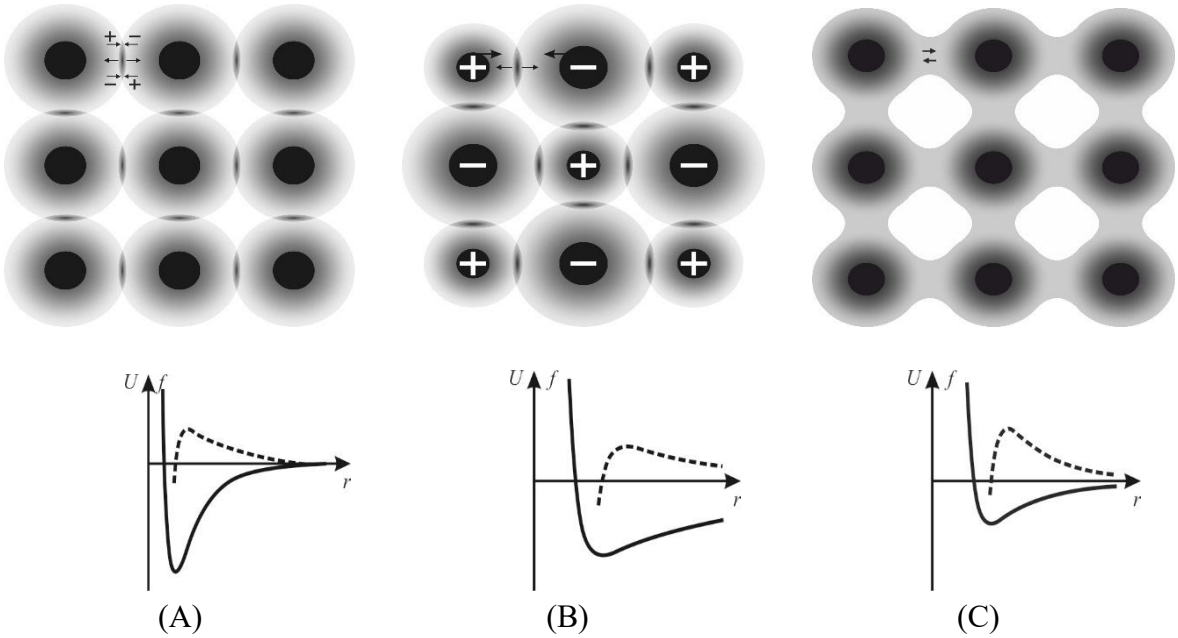

Fig. 1.14. Two-dimensional image of electrical charge distribution: A – molecular crystal, in which the quadrupole electronic fluctuation (+ − … − +) causes the attraction of atoms while partial overlapping of the electronic shells leads to repulsion (←…→) compensating this attraction;
B – ionic crystal where ions attraction is compensated by partial overlapping of electronic shells;
C – covalent crystal (in graphs, solid curves show the interaction energy while dotted curves show the inter-atomic force)

Quantitatively the degree of volume (V) change is characterized by the *volumetric coefficient* of thermal expansion (α_V). According to conventional definition, this coefficient is a relative change of volume when body is heating/cooling by one degree of temperature at constant pressure p, and it can be written as: $\alpha_V = (1/V)\cdot(\partial V/\partial T)_p$. As noted, the thermal expansion of polar crystals might be anisotropic and can be even negative. The last means that when temperature increases the crystal widens (or compresses) differently in various crystallographic directions. Therefore, besides the volumetric expansion coefficient, the *linear* thermal expansion coefficient α_l is widely used: $\alpha_l = (1/l)\cdot(\partial l/\partial T)_p$, where l is the linear dimension of tested sample. Coefficient of thermal expansion can be presented as a matrix (Fig. 1.12), at that, the sum of three diagonal matrix elements approximately equals to the volumetric expansion coefficient: $\alpha_V \approx \alpha_1 + \alpha_2 + \alpha_3$.

Occasionally observed negative value of α corresponds to a such particular case, when the entropy of crystal *increases* with the rise of a pressure that can occur

only in the case of configurational entropy: the temperature interval of negative thermal expansion corresponds to the processes of *own structural ordering* in crystal structure (at that, it should be noted that $\alpha(T)$ negative minimum, typical for polar crystals, can be seen in the semiconductors as well). With regard to practical applications, it should be noted that the difference in thermal expansion coefficients can create the mismatch between lattice parameters of deposited film and its substrate that is used in modern technologies of microelectronics.

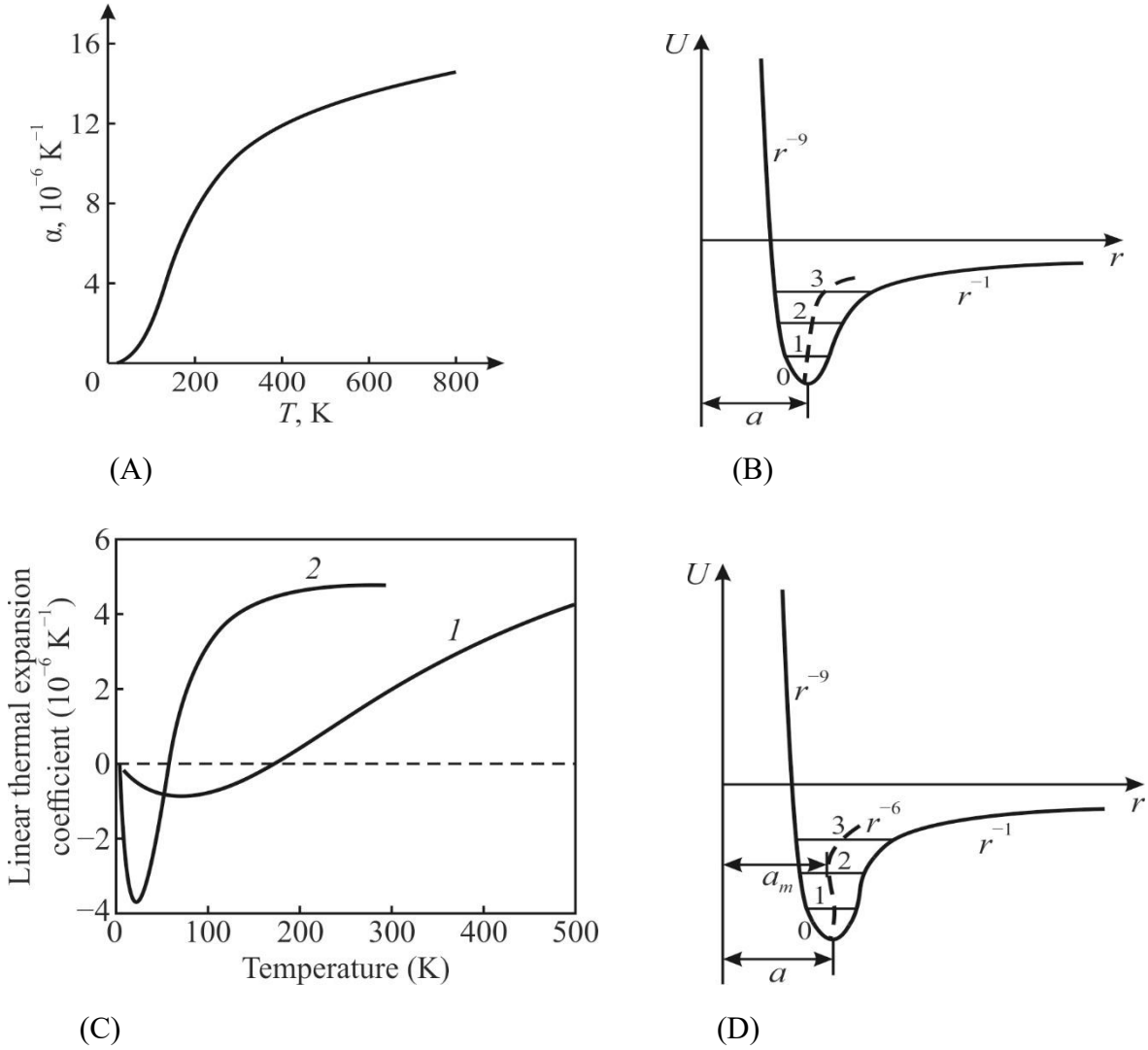

Fig. 1.15. Thermal expansion in different crystals: A – typical temperature dependence of expansion coefficient with example MgO; B – typical thermal expansion approximate explanation: increase in amplitude of ions oscillations as temperature rise shown by horizontals 0-1-2-3 leads to the gradual increase of lattice constant *a* shown by dotted line (in fact, roughly shown situation develops only in the narrow interval of interatomic distance *r,* very deep near the bottom of energy minimum); C – thermal expansion in the polar crystals with examples ZnO (*1*) and HgTe (*2*); D –symbolic explanation of negative thermal expansion; in fact, shown situation develops deeply, near the very bottom of energy minimum

The typical for vast majority of solids example of $\alpha(T)$ dependence is shown in Fig. 1.15A: coefficient α *increases* with temperature rise according to cubic law $\alpha \sim T^3$, like specific heat C changes with temperature. An explanation is that the change in the volume or in the shape of a solid body with temperature alteration is due to the *different nature* of the forces acting between atoms. Here it is pertinent to note the *striking difference* in the temperature dependence of thermal expansion coefficient of most crystals (with ordinary entropy), Fig. 1.15A, and the crystals with a self-ordering structure, Fig. 1.15C, characterized by *configurational* entropy and negative $\alpha(T)$ dependence in a certain temperature interval.

The energy of atoms interaction, Fig. 1.14 and Fig. 1.15B, consists of attraction (negative) and repulsion (positive) components. When the distance between interacting particles changes, these components vary in different ways. The repulsive force operates at a *very short distance,* because their potential energy decreases very fast with distance r between particles as r^{-8}–r^{-12} (the nature of these force is that electronic shells of neighboring atoms or ions can only a little penetrate each other). Conversely, the attraction forces operate at a rather *long distance*, as their energy changes with interatomic distance approximately like r^{-1}–r^{-6} depending on the nature of attraction (i.e., on the type of atomic bonds: ionic, covalent or molecular of mixed).

The total energy versus distance dependence $U(r)$ always is characterized by the *asymmetric* minimum, Fig. 1.14 and Fig. 1.15B. At lowest temperature, the bottom of potential well can be approximated by symmetric parabola, so that, when temperature changes near the absolute zero, no noticeable alteration in crystal size occurs: $r = a$. This explains why the coefficient of thermal expansion for *quite different solids* tends to zero in the region of absolute zero, Fig. 1.15A. However, as the amplitude of thermal oscillations increases, the middle distance between atoms (shown by dotted line) increases: exactly this is the evident cause of thermal expansion. Different energy levels are depicted in Fig. 1.15B by the horizontal lines 1-2-3: as far as thermal oscillations amplitude increases starting from zero; at that, the displacement of oscillating atoms to the left becomes less than their displacement to the right. As a result, the time-average equilibrium position of atom $(a+x)$ shown by dotted line in Fig.1.15B shifts to the right, and this effect becomes the stronger the higher is the energy of atom oscillation. In this argument, a special moment is the concept of time-average displacement of vibrating atoms $\langle x \rangle$, which actually determines the temperature dependence of the expansion coefficient. According to given description, the physical meaning of thermal expansion coefficient) can be described as *a reciprocal value of the slope of a curve, which expresses the*

dependence of bonding energy on the interatomic distance (a + x) at the point corresponding to time-average position of atom: dU(a + x)/d(a + x) ~ 1/α.

[***Note.*** *This* ***formal feature*** can be justified microscopically. In case of small enough oscillations of atoms around its equilibrium position, the potential energy $U(x)$ can be expanded in the Taylor series in terms of atom displacement x with the respect to atom equilibrium position. To describe the specific heat, it was enough to take into account only first term of this expansion $U = ½cx^2$, i.e., to consider atoms oscillations as a harmonic. However, when analyze the thermal expansion, the *anharmonicity* of the atoms vibrations should be taken into account, at least by one subsequent term of Taylor series: $U = ½cx^2 – (1/3)bx^3$, where coefficient c charaterizes elastic bonding, while the coefficient b is referred to as coefficient of *anharmonicity*. Accordingly, the force that acts between oscillating atom and fixed atom is given by: $f = – dU/dx = – cx + bx^3$. In this equation, a non-linear term "+ bx^2" is added to the linear term "– *cx"*. The new term takes into account the asymmetry as to interaction forces, acting between atoms, and it is the *anharmonicity coefficient b*. Role of anharmonicity becomes more significant the greater is the displacement x. With this term, a time-dependent displacement of the oscillating atom is no longer sinusoidal (i.e., not harmonic); that is why, this approximation is called as anharmonic. This simple model can explain the thermal expansion of solids. The average potential energy of thermal fluctuations ($½ cx^2$) at a given temperature equals $½ k_BT$, where k_B is the Boltzmann constant. One can show that the average shift of atom in this model is $x_{aver} = (b/c^2)□k_BT$. Thus, in the considered diatomic model, the thermal expansion coefficient α is defined as the ratio of average shift x_{aver} to the equilibrium distance r_0: $\alpha = k_Bb/r_0c^{1.}$ It follows that in the absence of anharmonicity (when $b = 0$) the thermal expansion coefficient $\alpha = 0$. The asymmetry of the resultant interatomic interaction force in crystal lattice is considered further as main cause of the phonons *interaction* in a lattice].

Below Debye temperature, the intensity of thermal oscillations increases nonlinearly, and, in accordance with the theory discussed here, parameter $\alpha(T)$ should be proportional to the specific heat $C(T) \sim T^3$ (above Debye temperature $\alpha(T)$ dependence, like the specific heat dependence, reaches a plateau, Fig. 1.15A). The cubic increase of the thermal expansion coefficient is performed for most crystals of chemical elements and for most simple chemical compositions, for example, for halide salts and most oxides. Moreover, the *increase* of thermal expansion coefficient with temperature rise corresponds to the Grüneisen law, which establishes the similarity in the temperature dependence of specific heat C_V and thermal expansion coefficient α of solid dielectrics: $\alpha = \gamma□C_V/3K$. Here K is the

modulus of bulk elasticity[*)] (i.e., all-round compression modulus) and γ is the Grüneisen constant[**)] which enters in the *state of equation* for solids, being a measure of anharmonicity of interatomic forces acting in a crystal. However, the application of the Grüneisen relation in the case of negative expansion seems unconvincing, since it assumes a negative value of the parameter γ. It is possible that this ratio does not take into account the possibility of the presence of sonfiguration entropy, giving preference only to kinetic phenomena.

[***Note.*** The ***compressibility*** K is an important parameter of solids; for example, it allows make a estimation as to inter-atomic (intra-molecular) distances. The greatest compressibility is observed in the crystals with long and weak bonding. The compressibility characterizes the dependence of relative change ΔV of crystal volume under hydrostatic pressure p: $\Delta V = - Kp$. Scalar parameter K is formed as the invariant of elastic compliance tensor: $K = s_{11} + s_{22} + s_{33} + 2(s_{12} + s_{13} + s_{31})$. In the cubic crystals and in other isotropic solids, the compressibility equals: $K = 3(s_{11} + 2s_{12})$. It should be noted that the compressibility is strongly dependent on the atomic bonds energy.

The dimensionless ***Grüneisen parameter*** γ describes the effect of dependence of crystal volume on vibrational properties of crystal lattice, as a consequence, the effect of temperature change on the volume or dynamics of crystal lattice. The same temperature dependence of the specific heat C_V and the coefficient of thermal expansion α of solid dielectrics is established. At normal and elevated temperatures, the Gruneisen constant is close to unity, but it is pertinent to note that some experimental data indicate the deviations from Grüneisen law: at low temperatures $\gamma(T)$ decreases somewhat more rapidly than predicts cubic law, while at high temperatures, instead of remaining constant value, $\gamma(T)$ slowly grows].

The correlation of *temperature expansion coefficient a* with crystal's *compressibility K,* showing crystal deformation under the *uniform* (hydrostatic) compression is very important. The relationship $\alpha \Leftrightarrow K$ is due to the fact that both the thermal action and the homogeneous compression are the *scalar actions* on a crystal, and, therefore, corresponding reaction of crystal (its deformation which is the second rank tensor) in both cases relates to the crystal *elastic properties* and reflects the peculiarities of the internal atomic bonds. Therefore, it is not surprising that during further discussion about the nature of the *negative* coefficient of thermal expansion this property will be compared with the modulus of crystal *bulk elasticity*, which characterizes the response of a crystal to hydrostatic compression.

A convincing example of strong influence on the polar dielectric (barium titanate, $BaTiO_3$) two different but *scalar impacts*: the uniform change of

temperature and the uniform hydrostatic (all-round) compression is shown in Fig. 1.15 (permittivity measurements were carried out in weak electrical field which practically does not affect the phase transition). At normal pressure and temperature less than 400 K (as well as at normal temperature and pressure less than 1.5 GPa), a predominantly *ordered* phase occurs in $BaTiO_3$ (in this phase, the dynamically flickering nano-islands with a disordered structure remain, while the atomic bonding in crystal tends to full ordering when approaching unattainable absolute zero).

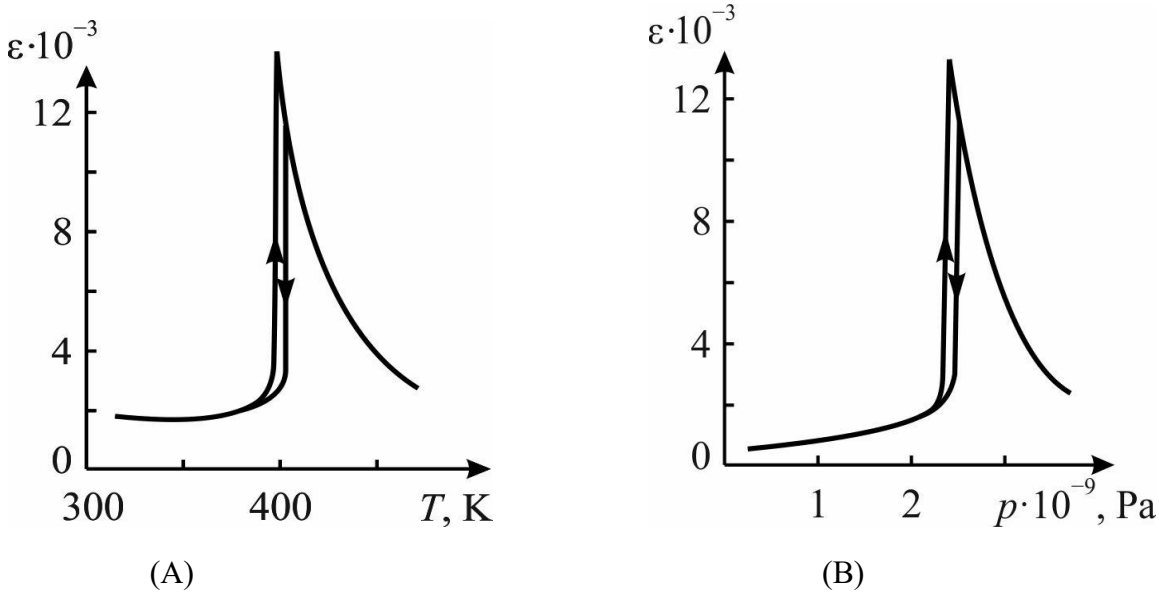

Fig. 1.16. Barium titanate dielectric permittivity dependence on *temperature* (A) at constant atmosphere pressure, and on *hydrostatic pressure* (B) at constant temperature near 300 K/

With the increase in temperature (or pressure), the degree of ordering in the polar phase decreases, and at critical temperature (or critical pressure) the middle ordering disappears, nevertheless, the shimmering of nanosized dynamically ordered islands remain. It is important to note that in the almost-ordered phase, with increasing pressure the entropy *increases*, while in the disordered phase, the entropy *decreases* with pressure (by the way, this corresponds to the very general conclusions made in Section 1.2 in connection with Fig. 1.2). An increase in the entropy with increasing pressure in the polar phase also corresponds to thermal expansion coefficient decrease, which goes over to its sharply negative value in the vicinity of the phase transition.

The point is that the *homogeneous* scalar actions (temperature or pressure), possessing the *highest type of symmetry* (spherical), makes it possible experimentally identify namely the *intrinsic symmetry* of the atomic bonds of a crystal. At that, the others methods of research tend to *violate* the intrinsic symmetry of any object under study. For instance, in case of *vector* type action on a crystal

(such as temperature *gradient*, electrical or other *field*), as well as in case when external influence corresponds to the second rank tensor (for instance, the *directional* mechanical stress), the symmetry of such actions *mixes* with internal symmetry of a crystal, so the response (received information) gives a distorted view as to *own* internal properties of a crystal.

In the overwhelming majority of cases, the crystal *expands* when being heated. This means that the coefficient of thermal expansion is *positive* ($\alpha > 0$), and this is *thermodynamically connected* with that circumstance, when under the *increase* of homogeneous pressure the entropy *S decreases*. On the contrary, in the *polar* crystals, at relatively low temperatures the exactly *negative* value ($\alpha < 0$) is observed that thermodynamically corresponds to a such peculiar case, when the entropy *S increases* with pressure rising (it will be shown that it is possible only for the *configurational* entropy). Therefore, by thermal expansion investigating, one can draw a certain conclusion about the nature of atomic interactions in studied crystal. It will be further shown that temperature region of negative $\alpha(T)$ corresponds to thermally activated processes of structural ordering of polar bonds that arises as a result of structural compensation of atoms electronegativity.

3. *Negative thermal deformation.* As already mentioned (and this is the main subject of this discussion), in the polar crystals in a certain temperature range the parameter $\alpha(T)$ takes negative value; at that, as seen in Fig. 1.15C, the dependency graph $\alpha(T)$ twice passes through a zero before it shows usual for most crystals growing by the law $\alpha \sim T^3$. Typical for the polar crystals $\alpha(T)$ dependence is shown in Fig. 1.15C by the examples of hexagonal crystal ZnO having polar wurtzite structure of 6*m* symmetry and cubic crystal HgTe, which has the polar sphalerite structure of 43*m* symmetry. It should be noted that at very low temperatures their thermal expansion coefficient again becomes positive, so it approaches to zero from its *positive* side (although this is invisible in the rough scale of Fig. 1.15C but can be seen in the insert of Fig. 1.16B for Ge crystal). In this case, the negative contribution to $\alpha(T)$ disappears, because the quantum oscillations break any ordering of the polar sensitive bonds in the crystal lattice (like in the virtual ferroelectrics $KTaO_3$ and $SrTiO_3$).

Formal explanation of negative thermal expansion coefficient (which at lower temperatures is typical for any polar crystal) is given in Fig. 1.15D (note that roughly shown situation develops only in a narrow interval of interatomic distance *r,* located very deep near the bottom of energy minimum). A special characteristic of ions attraction in the polar crystals occurs due to the hybridization of ionic and covalent bonds, which becomes so complicated that leads to the *specific profile* of

attraction energy in its dependence in the vicinity of the inter-atomic distance $r = a \pm x$. The anharmonic vibrations in the hybridized covalent-ionic bonds become dependent in complex way on vibrational energy; as a result, average in time mutual displacement of ions changes its sign: first it decreases ($r = a - x$) reaching a minimum, and then it increases ($r = a + x$). All this occurs below Debye temperature when lattice vibrations obey quantum laws. As a result, when temperature increases, the volume of crystal, after initial small growth, next decreases (levels 0-1-2 in Fig.1. 1D) so the lattice parameter reaches the value a_m. Only then one can see increase $\alpha \sim T^3$ (on levels 2-3 and higher) that is usual for temperature expansion coefficient of any solid. The points of dotted curve in Fig. 1.15D, when $r = a_m$, corresponds to the minimum in the $\alpha(T)$ dependence seen in Fig. 1.15C.

Table 1.1 gives some experimental data as to temperature minimum of thermal expansion coefficient in the polar substances. In most cases, α_{min} is about 20% of its value in the saturation region of $\alpha(T)$ characteristic. The effect of negative expansion is very strongly pronounced in mercury telluride crystal due to its special structure, which determines a very low sound velocity. For comparison, in Table 1 the low-temperature properties of the ice are given, although the arrangement of polar bonds in H_2O crystal is substantially different.

Table 1.1

Minimal value of thermal expansion coefficient (α_{min}), its value (α_{300}) at temperature near 300 K, and temperature $T_{\alpha\, min}$ at which α_{min} is observed in different polar crystals

Material	$\alpha_{min} \cdot 10^{-6}$, K^{-1}	$T_{\alpha\, min}$, K	$\alpha_{300} \cdot 10^{-6}$, K^{-1}
HgTe	– 8	25	8
InSb	– 1.4	27	1
ZnO	– 1.2	75	5
InAs	– 0.9	35	–
InP	– 0.5	45	8
H_2O	– 8	40	–
Fused quartz	– 9	40	6

It is interesting to note that the fused quartz also belongs to the substances with negative values of α at low temperatures. In this material, the pronounced anisotropic polar properties of *crystalline* quartz are averaged; as a result $\alpha_{min} = -9 \cdot 10^{-6}$ K^{-1} at temperature about 40 K that is 1.5 times higher than $\alpha_{300} = +6 \cdot 10^{-6}$ K^{-1}. After, at higher temperatures, fused quartz thermal expansion *changes* its sign to the positive near 190 K. It should be noted that a small minimum at 550–600 K is

also seen on $\alpha(T)$ characteristic in the region of α–β quartz transition. It can be concluded that negative value of α is a general property of substances with *small coordination number* (with the open structure), which are characterized by tetrahedral arrangement of atoms: in them, the ordering of polar-sensitive bonds becomes easier. In contrast, in structures with a tight packing, thermal expansion coefficient is always positive[).

[***Note.*** It is impossible to ignore the fact that the transition to one peculiar ordered structure may not lead to a minimum but to the *maximum* intemperature depemdence of thermal expansion coefficient $\alpha(T)$: this is observed in the antiferroelectrics. The point is that antiferroelectric type ordering is specific - it does not lead to a "softening" of the structure that promotes dynamic self-ordering-disordering in the expanded lattice, but, on the contrary, suppresses these processes in a "toughened", compressed lattice. Important fact is also that antiferroelectric phase transition occurs with *multiplication* of crystal lattice parameter in the ordered phase that is accompanied by the *increase* of crystal density at that $\alpha(T)$ *maximum* is seen (but not $\alpha(T)$ minimum usual for ferroelectric phase transitions].

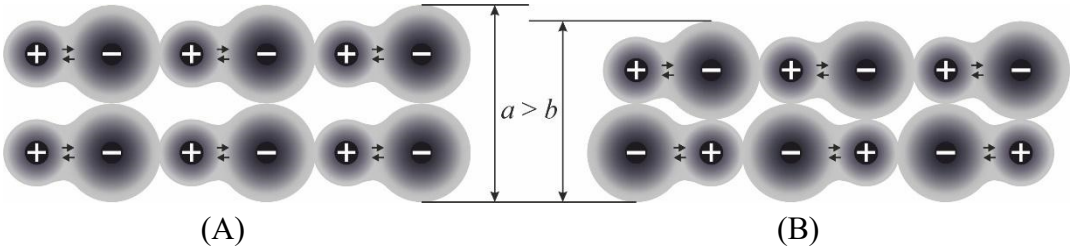

Fig. 1.17. Comparison of polar ordering (A) lattice with antipolar ordering (B): it is seen that $a > b$

Simplest model of this feature is given in Fig. 1.17, where differently located polar-sensitive bonds give an opportunity to explain how the size of crystal lattice might be changed under different phase transitions. In the case of ferroelectric (polar) ordering, the crystal lattice occupies a larger volume than in the case of anti-ferroelectric ordering. In this regard, it is necessary to take into account that the concept of configurational entropy should include not just a "static" concept of the existence of various locations of the groups of atoms, but precisely of their *dynamically changing* configurations.

4. *Thermodynamic explanation* of negative thermal expansion in a certain temperature range is based on the Gibbs function concept using the *isobaric-isothermal* thermodynamic potential: a quantity which changing in the course of a thermodynamic process is equal to the change in the internal energy of a system.

Gibbs energy shows how much of total internal energy of system can be used for transformations or obtained as a result of them under specified conditions, and allows establish fundamental possibility of occurrence of changes in specified conditions. Mathematically, this is potential of form: $G = U + pV - TS$, where U is the internal energy, p is the pressure, V is volume, T is the absolute temperature, and S is the entropy. Minimum of Gibbs potential corresponds to the stable equilibrium of thermodynamic system with fixed temperature, pressure and number of particles. For further calculations, to describe system with constant number of particles, it is important to express the *differential* of Gibbs energy:

$$\mathrm{d}G = -S\mathrm{d}T + V\mathrm{d}p \qquad (1.9)$$

Volumetric thermal expansion coefficient is defined as the *relative* change in volume with temperature at constant pressure: $\alpha = (\partial V/\partial T)_p/V$. At that, the change in the volume can be expressed through the Gibbs potential as well as the pressure (1.9) at constant temperature: $V = (\partial G/\partial p)_T$, and obtain following expression:

$$\alpha = \frac{1}{V}\left(\frac{\partial\left(\partial G \big/ \partial p\right)_T}{\partial T}\right) = \frac{1}{V}\left(\frac{\partial^2 G}{\partial T\,\partial p}\right).$$

By the replacing variables in this expression, it is possible to get final result linking the nature of thermal expansion with entropy and pressure

$$\alpha = \frac{1}{V}\left(\frac{\partial\left(\partial G \big/ \partial T\right)}{\partial p}\right) = \frac{-1}{V}\left(\frac{\partial S}{\partial p}\right)_T. \qquad (1.10)$$

In almost all solids, as temperature rises, the *increase* in their volume occurs, and parameter $\alpha > 0$ because the repulsive forces of atoms in the crystal lattice act at short-range distance while attraction forces act at long-range distance. Expression (1.10) means that the entropy is less the greater is pressure, and this correlation corresponds to the *normally observed* temperature expansion in solids.

On the contrary, in the dynamically ordering systems, for example, in the polar crystals, a certain temperature interval exists, in which the coefficient $\alpha < 0$; that means the *rise of entropy with the increasing pressure*. Such unusual phenomenon, which is the characteristic of, particularly, polar crystals, requires deeper understanding of entropy. Of all properties of thermodynamic system, the entropy S looks like difficult to explain property: the point is that temperature T, pressure p and volume V is easy to measure, while the entropy can not be measured directly. As is known, the entropy characterizes the inaccessibility of part of thermal energy of a system for conversion into work, in other words, it is a measure of

thermal energy of system per unit temperature, which is not available for performing useful work. Often, entropy is interpreted as a degree of disorder or randomness in system, namely, entropy is due to number of microscopic configurations, which are consistent with the macroscopic quantities (*p, V, T*) characterizing system.

As noted, entropy is a function of state, because it does not depend on how the transition from one state of system to another state is accomplished, but it is determined only by initial and final states of a system. At that, the entropy establishes a connection between macro- and micro- states. It is believed that particular arrangement of particles, which characterized by average quantities, is the *macrostate*, while the individual arrangement, defining properties of all particles for a given macrostate, is the *microstate*. Entropy is related to number of ways, in which the microstate can rearrange itself without affecting the macrostate. At that, for microstates, for example, for the system of *N* particles, it is possible to specify coordinates and velocities of the particles. It's obvious that macroscopic state of system can be described using several macroscopic parameters, for example, *p, T, V*.

Therefore, peculiarity of entropy is that it is the only function, which shows the *direction* of thermodynamic processes. During ideal *reversible* process the entropy does not change, while the *irreversible* process always increases total entropy. In connection with the study of dynamically ordering polar crystals, the *conditional* separation of entropy into "vibrational" and “configurational” becomes important.

The *vibrational entropy* can be thought of as the number of microstates through which the thermal energy can be shared between particles. The higher the temperature, the greater the vibrational entropy, but with increasing pressure it becomes smaller, since the binding energy of the particles increases. Therefore, with increasing pressure, the vibrational entropy decreases.

The *configurational entropy* is those part of system entropy, which is due to the *various positions* of some parts of a system, and this rule is applicable to all possible configurations of a system. This entropy characterizes the number of ways in which the groups of atoms can be distributed in the space. With increasing pressure, the possibilities of partial ordering of the *dynamic nanoscale clusters* collapses, and the mutual chaos increases. That is why, a distinctive feature of the *configurational entropy is its growth with increasing pressure*.

With regard to dynamically ordering in polar crystals, then when discussing the relationship of entropy and pressure, the Le Chatelier’s principle can be applied: the ordering of polar bonds leads to the decrease in entropy and increase in volume;

therefore, the increase in pressure (which decreases volume) should lead to the disordering of the polar bonds and, accordingly, to entropy increase. Thus, the negative coefficient of thermal expansion proves the importance of configurational entropy accounting, when polar crystals properties description. In turn, the negative expansion indicates the presence of self-ordering-disordering processes in the polar crystals.

5. ***Polar structures with negative thermal expansion*** are no special exception. Since here the properties of polar crystals are discussed, a convincing example, which shows the direct relationship of negative expansion coefficient with the structural ordering, may be given. This is a well-studied barium titanate crystal, passing while cooling from its non-polar to the polar phase at temperature ~ 400 K. During the phase transition from disordered paraelectric phase into ordered polar phase, the volume of $BaTiO_3$ crystal *increases* while the configurational entropy *decreases* due to the *suppression* of polar fluctuations (which is peculiar to higher temperature disordered paraelectric phase). As seen in Fig.1. 17A, in the $\alpha(T)$ dependence a deep minimum is observed, i.e., the negative thermal expansion is characteristic of certain temperature range, where an intense process of ordering of polar bonds occurs, and this is known property of ferroelectrics.

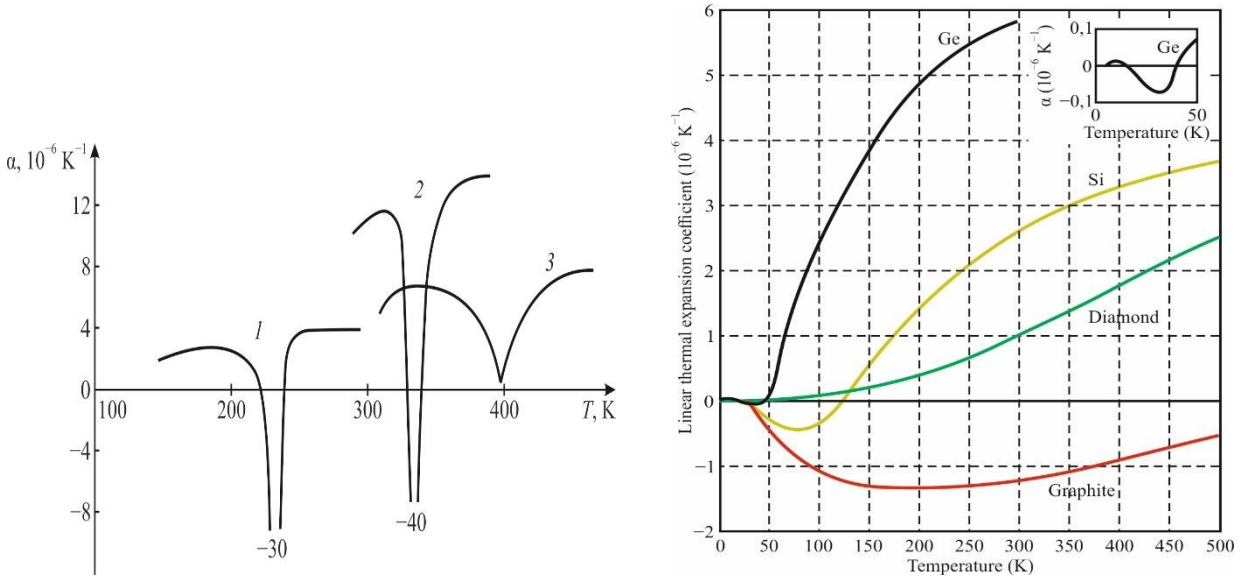

(A) (B)

Fig. 1.18. Thermal expansion coefficient temperature dependence: A – in ferroelectrics KDP (*1*), TGS (*2*) and $BaTiO_3$ (*3*); B – in semiconductors Ge, Si, C-diamond and C-graphite

If one touch on the specific microscopic mechanisms of ordering in certain ferroelectrics, then it was established that in $BaTiO_3$ the fluctuations of the internal polarity exists along four symmetry axes of third order ([111]-type) i.e., in $BaTiO_3$ structure, dynamically appears and disappears (flashes) most stable lowest

temperature rhombohedral phase. In the polar phases of barium titanate, as the temperature rises, the rhombohedral, orthorhombic, and tetragonal phases dominate sequentially, but the rhombic fluctuations remain as flickering impurity in all phases, including the non-polar high-temperature cubic phase. The hydrostatic pressure applied to $BaTiO_3$ below its Curie point (i.e., in its polar phases) returns this crystal to its paraelectric (non-polar) phase, Fig. 1.16, in which, however, the fluctuations of [111]-type *persist*, and, naturally, configurational entropy becomes larger.

Other well known example of the configurational entropy connection with pressure is the phase transition in H_2O at 273 K: freezing of water leads to the ice, which has increased volume, but externally applied pressure returns ice into the disordered structure of a water with more pronounced configurational entropy due to polar phase fluctuations.

Thus, when discussing negative thermal deformation in the polar crystals, one should pay attention to the fact that $\alpha(T)$ takes negative value in the vicinity of ferroelectric phase transitions, since the volume of low-temperature predominantly *ordered* phase becomes greater than the volume of same crystal but in its *disordered* phase (however, in case of antiferroelectric phase transition, the volume of antipolar phase, on the contrary, decreases; correspondingly, at phase transition $\alpha(T)$ shows maximum). From the point of crystal lattice dynamics, negative value of $\alpha(T)$ corresponds to such features in polar crystal phonon spectrum, which leads to the negative value of Grüneisen constant. Since this effect is observed at low temperatures, such singularities are due to the *acoustic* vibrational modes; in polar crystals the branch of transverse acoustic oscillations bends downward when its approaching boundary of Brillouin zone. Therefore, this branch can be represented as two parts: Debye-type mode in the beginning of spectrum and Einstein-type mode at its end, exactly last part of *TA* branch near boundary of Brillouin zone corresponds to a negative $\alpha(T)$.

In connection with negative $\alpha(T)$ that is seen at low temperatures in the polar crystals, it is important to keep in mind other cases of negative thermal expansion coefficient observations. In dielectrics and semiconductors such cases are known among the crystals that have the *layered* and *chain* structures. Typical examples of such crystals are the rhombohedral tellurium and selenium, which, among other things, refers to the piezoelectrics of the polar-neutral class 32 (same as quartz). In Te crystal *transversal* thermal expansion coefficient is positive: $\alpha_1 = \alpha_2 = +27 \cdot 10^{-6}$ K^{-1}, while *along* the chains this coefficient is *negative*: $\alpha_3 = -1.6 \cdot 10^{-6}$ K^{-1}. In the Te and Se crystals the helical chains Te–Te (or Se–Se) are elongated in parallel to the axis *3*. Pronounced anisotropy and negative value of α_3 are due to the fact that

inter-atomic bonds along the chains are much stronger than the interaction between chains. Therefore, with heating, the crystal contracts in the direction *3* but it expands in perpendicular *1* and *2* directions.

The example of *layered crystal* is the *hexagonal graphite*, in which in the direction perpendicular to the plane of layers (where inter-atomic bonds are weak), a rather big and *positive* thermal displacement of atoms are observed, so in this direction graphite expands with heating: $\alpha_3 = +30 \cdot 10^{-6}$ K^{-1}. However, *along the layers of graphite* (where atomic bonds are very strong) at lower temperatures, the *negative* thermal expansion coefficient is seen: $\alpha_1 = \alpha_2 = -5 \cdot 10^{-6}$ K^{-1}, i.e., in this plane, while heating, the graphite becomes more compressed. The point is that in the graphite layers, the covalent bonds are so strong that at low temperatures the thermal vibrations can be excited mostly *perpendicularly* to the rigid layers (along *3* axis). In this case, a lateral compression appears, characterized by the negative $\alpha_1 = \alpha_2$ along the layers. At low temperatures (up to about 300 K), in graphite layers the transverse acoustic vibrations dominate, being polarized perpendicularly to the layers of carbon: this corresponds to negative expansion. Only at a temperature of 650 K the parameters $\alpha_1(T) = \alpha_2(T)$ acquire their positive value – when the *intensity* of thermal movement becomes significant. Note that *large negative* coefficient of thermal expansion is observed also in the graphene and nanotubes.

Thus, through temperature dependence of thermal expansion, the features of crystal inter-atomic bonds are manifested. In the layered crystals, the positive thermal displacements of atoms is seen perpendicularly to the planes of layers, while in the chain crystals they are pronounced perpendicularly to the axis of chains. In both cases, in the directions of the *strong bonds*, the coefficient of thermal expansion is negative. The conclusion is obvious:
the stronger inter-atomic bonds, the less thermal expansion coefficient, down to its negative value.

By comparing these data with temperature properties of polar crystals, there is a reason to believe that when temperature decreases below a certain limit, the intensity of thermal oscillations becomes so weak that a self-ordering of polar bonds starts that gradually leads to their strengthening. Caused by this ordering with temperature decrease, the widening of crystal lattice results in the negative sign of thermal expansion coefficient. The foregoing makes it possible to affirm that negative value of thermal expansion coefficient at low temperatures in the polar crystals is due to the increase in *partial ordering* of polar-sensitive bonds.

Above considerations provide a basis for explanation of negative expansion coefficient in the polar crystals at low temperatures: it is the polar bonds self-

ordering which intensifies when the thermal oscillations in a crystal become weakened. In this connection, it is necessary to compare the uniform *temperature* scalar action (which leads to the crystal widening or compression), and the uniform scalar action of a pressure (*hydrostatic* action). By different ways, both effects give rise to same result: the change of crystal volume. As is known from thermodynamics, the thermal expansion coefficient is related to entropy S changing with pressure: $\alpha_V = -(\mathrm{d}S/\mathrm{d}P)_T/V$. In this way, the *negative* value of $\alpha(T)$ corresponds to such an unusual case, when the entropy *increases* with increasing pressure. (Usual is phenomenon when entropy *decreases* with pressure rise, correspondingly to a common case of *positive* thermal expansion coefficient).

Thus possible explanation of negative thermal expansion coefficient is reduced to finding out a reason why entropy can increase with uniform pressure rise. The fact is that entropy depends not only on dynamic characteristics of particles (their velocity or momentum), but also depends on particles *equiprobable locations*: exactly this determines the *configurational entropy*, i.e., the number of ways of particles arranging, maintaining specific system properties. With increasing pressure *only configurational entropy increases*.

Therefore, comparison of two different scalar influences on thermal and elastic properties of polar crystals shows a compelling correlation: negative thermal expansion is observed, if increase of homogeneous pressure *increases* configurational entropy (that, in turn, is due to the presence of metastable microscopic states) [7]. It can be argued that they are precisely those states that correspond to the ambiguity in the *orientations* of internal polarity. Indeed, polar bonds ordering leads to increase of crystal volume and to decrease of configurational entropy. The fact is that hydrostatic compression suppresses the ordering processes and thereby increases entropy.

6. ***Negative thermal expansion in semiconductors.*** As can be seen from Table 1, many polar crystals are semiconductors. In fact, the compounds of $A^{III}B^{V}$ group have polar sphalerite structure and they belong to the piezoelectrics, while semiconductors of $A^{II}B^{VI}$ group are the pyroelectrics. It is pertinent to note that exactly polar semiconductors are the *direct band* semiconductors, while monoatomic semiconductors of diamond symmetry are the *nondirect band* semiconductors. By the way, it should be noted that at low temperatures (where *negative* $\alpha(T)$ is seen) the concentration of free charge carriers in semiconductors is very low and charge carries can not screen possible polar fluctuations in a structure. Therefore, the cause of the negative thermal expansion observed at low temperatures

has to be sought not in electrical conductivity but in the phenomenon of electrical polarization.

In connection with foregoing, the low-temperature minimum in coefficient of thermal expansion is not surprising. With temperature decrease, the thermal chaotic motion freezes, and existing polar bonds becomes ordered (configurational entropy decreases), so the crystal occupies bigger volume, demonstrating negative $\alpha(T)$. However, with further cooling to a very low temperature, the inescapable quantum oscillations in the crystal lattice prevent further ordering of fluctuating polarity, so with the approach to zero of Kelvin the crystal again compresses a little (by similar way exactly the quantum oscillations impede the transition to ferroelectric phase in the *virtual ferroelectrics* $KTaO_3$ and $SrTiO_3$).

If in *polar* $A^{III}B^{V}$ and $A^{II}B^{VI}$ semiconductors, which have non-centrosymmetric structure, the minimum of $\alpha(T)$ can be considered as explained before, then for *atomic* semiconductors of diamond type this minimum needs special explanation. As seen from Fig.1. 17B, in germanium, a small minimum of $\alpha(T)$ is observed at temperature round 35 K (~ 0.1 θ_D) while in silicon a much deeper minimum $\alpha(T)$ is seen at temperature near 60 K (~ 0.1 θ_D). At the first glance, it is difficult to suspect any natural polarity in atomic semiconductors consisting of only one chemical element and, naturally, possessing only by covalent bonds. Nevertheless, mentioned above single element crystals of tellurium and selenium have even a pronounced piezoelectric effect and belong to the hexagonal symmetry class 32 (like quartz). Probably, the reason for this internal polarity lies in the significant complications of covalent bonds distribution in their structure.

As was shown theoretically, the negative coefficient of thermal expansion is due to the change in *configurational entropy.* Obviously, that it is necessary to indicate, which kind of the ordering process is possible in the crystals of diamond type. Here is assumed that the reason of negative $\alpha(T)$ in germanium and silicon is the fluctuations in the partial ordering of *hexagonal* polar phase, when the double bonds becom mixed with single covalent bonds. This assumption is based on the fact of *hexagonal diamond* existence: initially it was discovered in the meteorites but later is synthesized in the laboratory as well. Having appeared in peculiar technologic conditions, the hexagonal phase can remain stable only in the super hard and super stable diamond ($\theta_D \sim 1900$ K and $T_{metling} \sim 4000$ K) being observed throughout temperature range due to a very small concentration of charge carriers, which cannot screen the possible polar interactions. However, in the silicon ($\theta_D \sim 600$ K and $T_{metling} \sim 1700$ K) and in the germanium ($\theta_D \sim 360$ K and $T_{metling} \sim$ 1200 K) the hexagonal phase apparently can exists only in a form of the polar

fluctuations in the [111]-type of directions; at that, any polar interactions are screened by the charge carriers. It is pertinent to note that the direction of natural growth of these crystals from their melt is the polar [111]-direction; moreover, these crystals can float in their own melt (like the ice floats in water) that indicates the *decrease* of material density during crystallization. The same property is possessed, for example, gallium arsenide, which is a polar crystal of sphalerite symmetry.

The hexagonal structural feature that accidentally arising in the diamond and, probably, weakly fluctuating in silicon and germanium, is fully implemented in the graphite and graphene, which cellular plane is characterized by the *negative* $\alpha_1 = \alpha_2$ with explicit minimum at temperature 180 K (~ 0.1 θ_D, Fig. 1.17B). As mentioned earlier, crosswise to the layers of graphite is characterized by a positive $\alpha_3(T)$. In the Fig. 1.17B there is not by chance the curve *4* is shown, demonstrating thermal expansion $\alpha(T)$ in the plane of graphite, in which at a temperature of about 200 K the minimum are seen: $\alpha_{1min} = \alpha_{2min} = -1.5\times10^{-6}$ K^{-1}. The structural basis in the graphite planes is carbon hexagons, in which three single covalent bonds alternate with three double bonds. It should be noted that more strong C=C double bond is much shorter than single C–C bond, and it can be assumed that arising with increasing temperature from absolute zero thermal motion stimulates the formation and hardening of double covalent bonds. In favor of this assumption, it needs to note that temperature minimum of the thermal expansion in the *graphene* is even deeper than in graohite: $\alpha_{min} = -5.5\times10^{-6}$ K^{-1} at 300 K, and in carbon *nanotubes* at temperature 240 K it reaches $\alpha_{min} = -9.5\times10^{-6}$ K^{-1}. One could assume that, in general, in crystals with negative thermal expansion at low temperatures, a strong (resulting in compression) covalent bond formation occurs.

Study of the features of thermal expansion in various crystals has not only scientific but technical interest also. In vast majority of cases, as the temperature rises the solid expands. Therefore, the exceptional case of negative expansion coefficient has a particular interest. Physical nature of negative thermal expansion in polar crystals corresponds to a special case when the entropy increases with increasing pressure that is possible only in case of configurational entropy. In turn, the presence of this entropy testifies to the processes of structural ordering-disordering in the crystal. Discussed model, based on the asymmetry in the electronic density distribution along atomic bonds, is free from assumption of any internal electrical field existence in crystals. Although polar-sensitive bonding is not a result of internal field in crystal, it can provide an electrical response onto the non-electrical external action that is impossible in the centrosymmetric crystals. It is assumed that physical basis of natural polarity is a distinction in the electronegativity

of ions forming a crystal. Since the temperature minimum of thermal expansion coefficient in the polar crystals is explained by the polar bonds ordering at low temperatures, a proposed concept can be extended to the non-polar semiconductors. In them, too, it can be supposed that fluctuating in structure polar tendencies become consolidated at low temperatures.

Thus, in the polar crystals at low temperatures the coefficient of thermal expansion α changes its sign twice, forming a region of α negative values. The nature of the negative thermal expansion is explained by partial ordering of the polar-sensitive bonds at low temperatures, leading to their long-range interaction and, a result, to flattening of the transverse acoustic mode of lattice vibrations near the boundary of Brillouin zone. The above-described features of thermal expansion in both conventional and polar crystals can be used in development of new technologies for microelectronic materials.

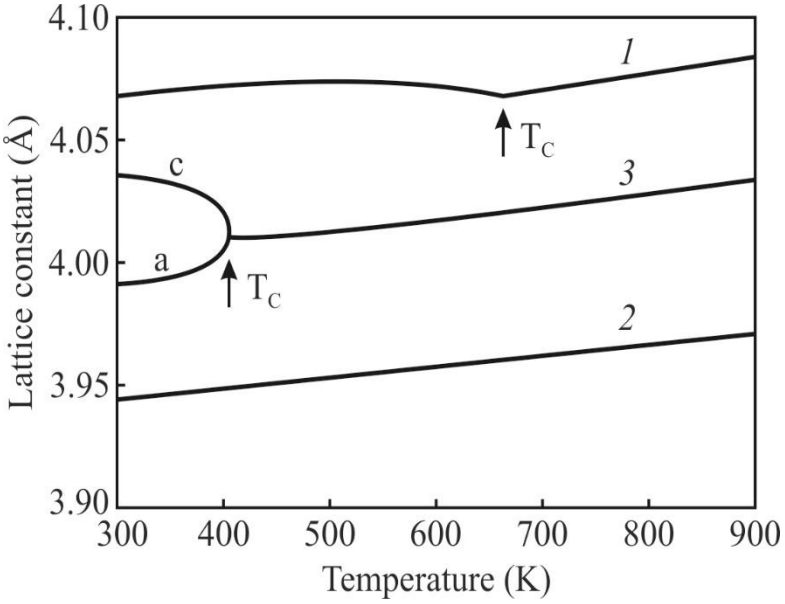

Fig. 1.19. Lattice parameters temperature dependence in strained $BaTiO_3$ film out-of-plane (*1*) and in-plane (*2*) in comparison with single crystal $BaTiO_3$ (*3*)

7. ***Lattice strain engineering using polar-sensitive films*** is based not only on the mismatch in thermal expansion, but to a greater degree in the difference of permanent lattices of the film and substrate. As known, the occurrence of internal polarity in a crystal is accompanied by the anisotropic change in its size: the elongation along the axis of polarization and the compression in the perpendicular direction (at that, the volume of ferroelectrics increases but in the anti-ferroelectrics it decreases). According to principle of La Chatelier, if during polar phase formation one of crystal size increases, so forced the change in this size of crystal should lead

to the change in its polar state. For example, in the ferroelectric their phase transition temperature should change.

In the functional dielectrics, possessing polar-sensitive properties, the coupling between the polarization and mechanical strain is strongly manifested. The external mechanical action not only leads to a piezoelectric effect, but can also changes the temperature of ferroelectric phase transition T_C. For example, hydrostatic pressure can lower the phase transition point by tens of degrees and greatly change the dielectric properties of a bulk ferroelectric, Fig. 1.15. It is important to note that much greater possibilities of the mechanical control by the polar crystal parameters appear in the *epitaxial thin films,* which allow *large* biaxial (plane) deformations without film destruction. The highly perfect ferroelectric thin films, which are synthesized on the suitable substrates, demonstrate that the *strained* ferroelectric thin films can exhibit the properties which are greatly superior the possibilities of their bulk.

This phenomenon may be demonstrated by the example of most well studied ferroelectric – barium titanate, Fig. 1.19. The *epitaxial* films of $BaTiO_3$ were deposited at high temperature on the isomorphic substrate $GdScO_3$, which have same perovskite structure but quite different lattice parameter. The mismatch in the lattice parameters leads to a *forced biaxial compression* of a film that leads to the increase of its deformation perpendicularly to its plane that contributes to more stable polarized state of $BaTiO_3$ that persists at much higher temperatures. The biaxial strain can be defined as $x_s = (a_{\|} - a_0)/a_0$, where a_0 is the lattice parameter of ferroelectric material in its cubic state under the stress-free conditions (free-standing) and $a_{\|} = a_{subs}$ is in-plane lattice parameter of the biaxially strained ferroelectric film.

The limit of strain can be given by Griffith criteria for crack formation: $x_s = (1 - v)\square(2\xi/(\pi\square E\square t)$, where v is the Poission's ratio, ξ is the surface energy, E is the Young's modulus, and t is film thickness (biaxial strain x_s arises from lattice mismatch with underlying substrate for fully coherent epitaxial growth). With this limit, it is quite possible to largely control the properties of polar-sensitive materials. In addition to above example with Curie point temperature shift in barium titanate, another impressive example is the conversion of virtual ferroelectric film of strontium titanate into the *ferroelectric* film, with sufficiently high Curie temperature (increased from 35 to 300 K). Thus, in the biaxial stressed films, such materials can be obtained that in the bulk state are not ferroelectrics at any temperature. Biaxial deformations of films make it possible to increase the Curie point by hundreds of degrees with a simultaneous increase in the polarization in

direction perpendicular to film thickness. Such films have great advantages for use in microwave technology.

In the strain engineering, it is necessary to use only high quality films, obtained, as a rule, by the molecular-beam epitaxy: the growth of such film on substrate means the arrangement of film atoms similarly to the arrangement of substrate atoms. This technology makes it possible to convert the virtual ferroelectric into the ferroelectric, potential ferromagnetic into the ferromagnetic, and even to obtain ferroelectric and ferromagnetic properties together in one film.

Summing up, it should be noted that biaxial deformations, created for control of polar-sensitive film properties, can be obtained by the essential mismatch of lattice parameters between film and substrate, and the different in the thermal expansion coefficient. (It should be recalled that bulk crystals usually break down long before the deformation of percentage levels is reached.). The deformations reaching a value of several percent have a great influence on the properties of polar-sensitive thin films and superlattices. Coherent epitaxial films have the advantage that they have very few dislocations. In addition, thr epitaxial films allow create the superlattices: both from layers of different polar-sensitive dielectrics and alternating layers of polar dielectrics and ferromagnetics, thus obtaining films with properties that are not found in natural materials.

1.5 Thermal conductivity and thermal diffusivity

A thermal conductivity characterizes the ability of material to conduct heat in the course of chaotic thermal movement material's particles (electrons, ions, molecules). In a steady state, the directed heat flux q_i is proportional to the temperature gradient: $q_i = -\lambda_{ij}\nabla T_j$, where the second rank tensor λ_{ij} is the thermal conduction coefficient, (this tensorial description only becomes necessary in the anisotropic materials while for isotropic media the scalar equation can be used: $q = -\lambda \square \text{grad}\, T$). This relation is known as Fourier's heat conductivity law, where q_i is the heat flux vector, which magnitude is the amount of energy that passes in unit time through the unit area, oriented perpendicularly to the direction of heat transfer. Like dielectric permittivity ε_{ij} or conductivity σ_{ij}, the tensor λ_{ij} can be described by a second-order surface, which usually has a form of ellipsoid.

Various solids can have quite different thermal conductivity that can vary in thousands of times. In *metals* the thermal energy can be transferred predominantly by the electrons while in dielectrics and semiconductors by phonons. At that, in metals their electronic thermal conductivity is big: λ = 400–200 W/(m·K) at 300 K.

In the *semiconductors*, the heat transfer is carried out basically by the phonons being greatly dependent on temperature, at 300 K usually λ = 150–50 W/(m·K). In the *non-polar covalent dielectrics,* the thermal conductivity also has phonon nature with λ = 80–30 W/(m·K); newly developed aluminium nitride AlN shows λ = 180 W/(m·K) while the diamond at 300 K shows λ > 1000 W/(m·K). Most of mentioned materials have increased Debye temperature and, correspondingly, high velocity of sound waves.

At that, relatively big thermal conductivity in the *covalent* crystals is due to the fact that in them the heat carriers (short-wave acoustic phonons located near the boundary of Brillouin zone) practically not interact with the optical phonons. In majority of *ionic* dielectrics, the phonon type of thermal conductivity at normal temperature not only significantly lesser than in metals, but much smaller than in covalent crystals: λ = 15–10 W/(m·K). It can be assumed that the ionic bonding in these crystals contributes to the *deceleration* of thermal phonons through the mechanism of their interaction with optical phonons. Such interaction even more enhanced in the polar-sensitive (non-centrosymmetric) crystals, in which the intra-atomic bonding has the *mixed* ionic-covalent character, so the thermal conductivity in these crystals at 300 K usually is less than λ = 10 W/(m·K).

Heat transfer is described phenomenologically in the non-equilibrium thermodynamics, while in the microscopic theory heat transfer in the dielectrics is determined mainly by the phonons mutual scattering. At normal temperatures, the heat transfer is carried out by the *shortwave phonons,* which wavelength is commensurable with the parameter of crystal lattice. Therefore, the polar-sensitive bonds, which characterize many features of noncentrosymmetric crystals, should clearly manifest themselves in the heat transfer.

Indeed, the difference in thermal conductivity λ of polar and nonpolar crystals clearly follows from its comparison with the coefficient of thermal expansion. Figure 1.20A demonstrates the dependence of λ on α^2 (causal relationship of these parameters will be explained below).

When further discussions of heat transfer mechanisms, two parameters are used: the *thermal conductivity* (λ) and the *thermal diffusivity* (ξ). The first of these parameters is important mostly for assessing the *technical properties* of electronics material, for example, to predict possible overheating of this or that structure, while the second parameter is better to use in the *interpretation* of experimental data. In the polar crystals, both these parameters are noticeably less than that of common crystalline dielectrics and semiconductors.

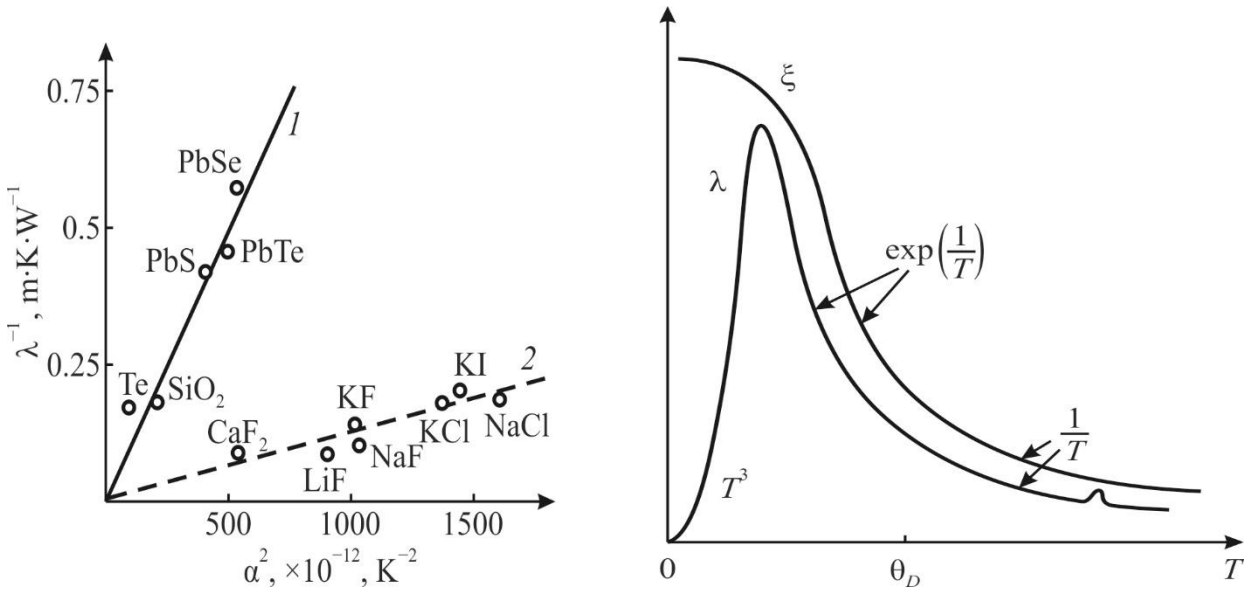

Fig. 1.20. Main features of heat transfer in crystals: A – comparison of thermal resistance in the polar (curve *1*) and in the nonpolar (curve *2*) crystals at normal temperature; B – comparison of temperature dependence of thermal diffusivity ξ and thermal conductivity λ

For research methods of λ and ξ investigation compare, the following should be noted.

1. ***Thermal conductivity coefficient*** λ, defined in SI units by watts per metre-kelvin [W·m^{-1}·K^{-1}], as shown by kinetic theory, depends on crystal specific heat *C,* phonons average free path <*l*> (i.e., distance between one phonon collision with another phonon) and average velocity υ of phonons: $\lambda = (1/3)\square\upsilon\square l = (1/3)C\square\upsilon^2\square\tau$, where τ is the free path time which is time between collisions. It can be shown that the time of average free path is determined by the *square* of anharmonicity coefficient. Therefore, thermal conductivity is related to thermal expansion coefficient, which also is determined by the coefficient of anharmonicity, but in its *first degree*. Measurements really show that the *inverse* thermal conductivity is proportional to the *square* of thermal expansion coefficient: $1/\lambda \sim \alpha^{1\cdot}$ Experimental data obtained from comparison of different dielectrics and semiconductors (polar and nonpolar) shows that such a relationship really exists, Fig. 1.20A. On the line *2,* which has smaller slope, the crystals with increased thermal conductivity are grouped: they have predominantly covalent or ionic bonding. The upper curve *1* possessing larger slope characterizes the crystals with reduced thermal conductivity: they are the polar crystals, in which the *mixed* ionic-covalent bonds predominate. The ratio $1/\lambda \sim \alpha^2$ is determined by the peculiarities of interatomic bonds. In this case, it can be considered that crystals with larger expansion coefficient have smaller thermal conductivity.

It is important to note that temperature dependence of thermal conductivity follows rather complicated law, Fig. 19B, since it is determined by a *product* of specific heat C by phonons average free path $\langle l \rangle$. As a result, at very low temperatures, the thermal conductivity *tends to zero* and with temperature increase $\lambda(T)$ fast increases, following Debye specific heat law: $C \sim T^3$. At that, the $\lambda(T)$ dependence reaches a maximum at temperature $T \sim 0.1\theta_D$, and only then decreases in connection with the temperature dependence of average free path of thermal phonons. It should be noted also that when studying the anomalies of thermal conductivity (common in the polar crystals, especially near phases transition), true form of the anomalies $\lambda(T)$ can be somewhat distorted by the unavoidable *temperature gradient* while measurements. In this respect, temperature dependence of another parameter – *thermal diffusivity* $\xi(T)$ can be studied with greater accuracy.

2. *Thermal diffusivity coefficient* ξ is measured in SI units by [m^2/s] and defined as the thermal conductivity divided by material's density ρ and specific heat at constant pressure: $\xi = \lambda/(C_p \cdot \rho)$. It characterizes the *rate of the heat transfer* of a material from its hot side to the cold side. In a sense, the thermal diffusivity is a measure of the *thermal inertia*; so in the substance with high thermal diffusivity the heat moves more rapid through it. At that, the thermal diffusivity is determined mainly by the average free path $\langle l \rangle$ of thermal phonons propagating in crystal ($\xi \sim \langle l \rangle$). At very low temperatures the density of phonons is so small that they do not interact, and their free path is large being dependent mostly on the macroscopic-size defects including crystal boundaries. At that, the parameter ξ remains nearly constant, keeping its greatest value, Fig. 1.20B. However, ξ decreases hundreds of times as temperature increases: the point is that the intensity of phonons interaction becomes larger as it is determined by the anharmonicity of lattice vibrations, which is measured by the Grüneisen parameter γ.

Thus, average free path of phonons is $\langle l \rangle \sim a/(\alpha \cdot \gamma \cdot T)$, where a is the lattice constant and α is the thermal expansion coefficient. As temperature increases, thermal diffusivity falls very fast: $\xi(T) \sim \langle l \rangle \sim \exp(T^{-1})$, since the average free path of phonons becomes limited by the intra-phonon umklapp processes (U-processes), which occur with the loss of quasi-momentum. Next, with subsequent increase of temperature (when $T > \theta_D$), just in the temperature interval that will be discussed below, the lowering in the $\xi(T)$ dependence follows the Aiken law: $\xi(T) \sim T^{-1}$.

To identify the physical mechanisms of heat transfer, an analysis of *thermal diffusivity* temperature dependence seems much simpler than the analysis of thermal conductivity. For example, in the non-polar silicon crystal and in the polar quartz, the speed of sound (determined by the long-wave phonons spread) is approximately

the same: ~ 5000 m/s. on the contrary, the speed of short-wave thermal phonons differs greatly, however: at temperature of 300 K in silicon $\xi = 88$ mm^2/s while in quartz only $\xi = 1.4$ mm^2/s.

Therefore the coefficient of thermal diffusion is a more strong criterion for phonons kinetics then the thermal conductivity: thermal diffusion characterizes not a total heat flux but exactly the kinetics of energy carriers.

The upper limit of the thermal diffusion is determined by so-called folding umklapp processes (*U*-processes), while the lower boundary corresponds to the amorphous solids, where the energy transfer occurs only between the *nearest* neighboring cells. It should be noted that such limits is difficult to indicate for the thermal conductivity coefficient, since there are no restrictions as to density of energy states.

3. *Thermal transfer features in polar crystals*. In the dielectrics and semiconductors, the main contribution into thermal conductivity is given by the acoustic phonons, which group velocity slows down, when acoustic branch of spectrum approaches to the boundary of Brillouin zone. However, main feature of polar crystals (as all of them are piezoelectrics!) is that the *acoustic phonons are associated with the optical phonons*. If the optical phonons have large spatial dispersion, they can make a significant *positive* contribution to the heat transfer. But in most cases spatial dispersion is small, so the optical phonons give an additional contribution only in the phonons scattering, which substantially *decreases* thermal conductivity. Exactly this decrease due to the inhibitory interference of optical phonons explains the difference in thermal conductivity of polar and nonpolar crystals, shown in Fig. 1.20A.

As already indicated, the thermal energy in dielectrics is transferred by the *short-length* lattice waves ("heat waves"), which propagation velocity in a crystal is significantly lesser as compared with the long-length “sound waves”. That is why the crystals which are well-transparent for long elastic waves (sound waves), in case of short length waves looks like a turbid medium, because short lattice waves are characterized by the strong scattering of a diffuse-type, when their wavelength is comparable with the value of intra-atomic distances. The smaller wavelength the stronger wave scattering by the nano-inhomogeneous structure; therefore, in the polar-sensitive crystals the main interaction of phonons is determined by the polar-sensitive bonds.

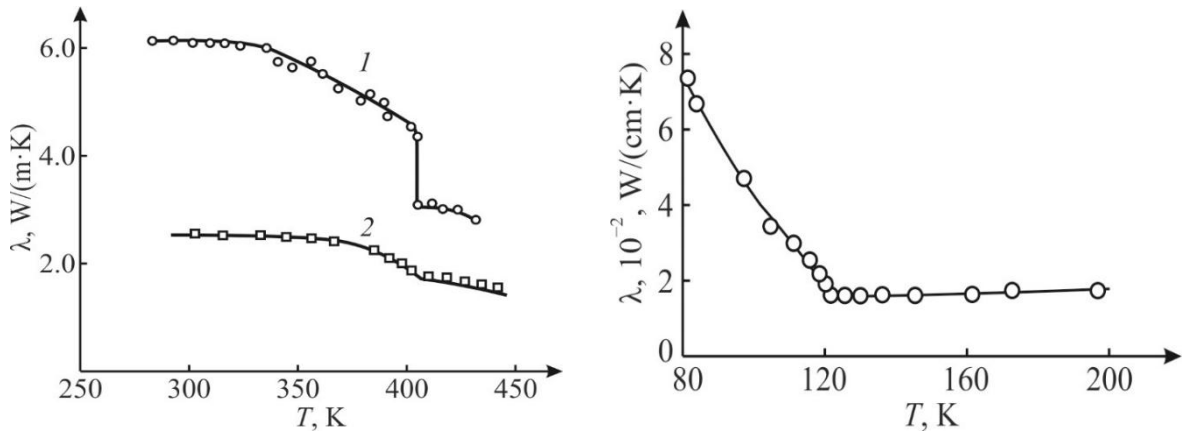

Fig. 1.21. Thermal conductivity of ferroelectrics near their transition from higher temperature disordered phase into lower temperature ordered phase: A – barium titanate crystal (*1*) and ceramics (*2*); B – potassium dihydrogen phosphate (KH_2PO_4 = KDP) crystal

The fact that the value of thermal conductivity is dependent on the degree of ordering of polar-sensitive bonds is clearly seen with the example of ferroelectrics, Fig. 1.21. In the polycrystalline barium titanate, its thermal conductivity in 1.5 times less than in single crystal, both above and below Curie point (400 K), because ceramics have macroscopically disordered structure. However, as in $BaTiO_3$ crystal so in its ceramics, in the *ordered* ferroelectric phase the thermal conductivity almost doubles in comparison with the nano-scopic disordered paraelectric phase. At that, the jump of thermal conductivity at a phase transition (especially noticeable in the crystal) indicates a first-order phase transition. It is also interesting to note that in the KH_2PO_4 (KDP) crystal below its Curie point (T_C = 122 K) the thermal conductivity increases linearly with cooling, reflecting gradual process of structural ordering in the ferroelectric phase in accordance with the second order phase transition. However, thermal conductivity of KDP also slightly increases when crystal is heated above Curie point. In all likelihood, the fluctuations of intrinsic polarity are the main scattering factor for phonons which carry heat.

Significantly decreased thermal conductivity in the polar crystals is due to the peculiarities of phonon dissipation process: i.e., by the perceptible binding of acoustical and optical phonons. This special feature of crystals, which possess the polar-sensitive bonds, correlates with their phonon spectrum near the *boundary* of Brillouin zone, where transverse acoustic mode has anomaly, as example, shown in Fig. 1.22 for GaAs (similar bending in the v_{TA} mode is seen in quartz). This is the evidence of such interaction between nearest atoms that can be described by the *mixing* of acoustic and optical phonons.

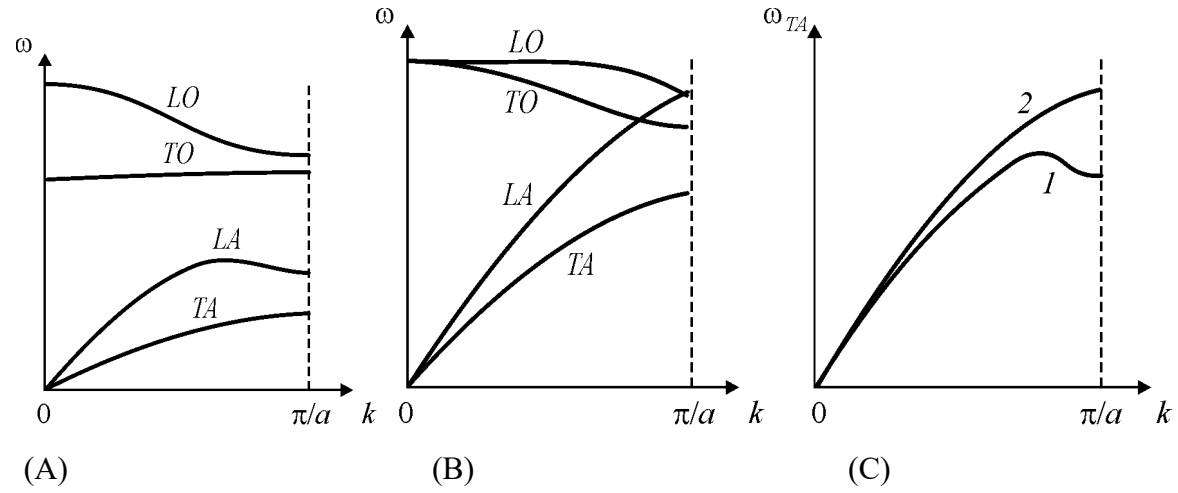

Fig. 1.22. Phonons spectrum for: A – ionic crystal NaI; B – covalent crystal diamond; C – TA (transverse acoustic mode) in polar GaAs crystal (*1*) and in non-polar NaCl crystal (*2*)

4. ***Thermal conductivity in the vicinity of phase transition*** demonstrates peculiarities that are seen when the non-polar (centrosymmetric phase) is turning into the polar ferroelectric phase. These crystals include the triglycinesulphate (TGS) and its isomorphs, which thermal conductivity is shown in Fig. 1.23 together with the reciprocal dielectric permittivity which tends to zero in the phase transition.

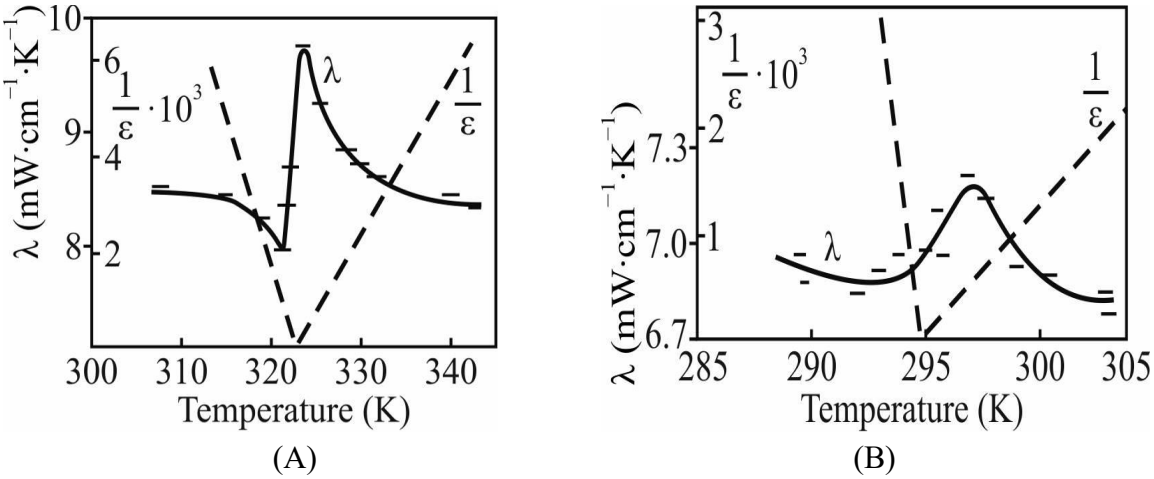

Fig. 1.23. Thermal conductivity (λ) temperature dependence and inverse value of permittivity ($1/\varepsilon$) along the [010] direction for single crystals TGS (A) and TGSel (B); small dashed lines show the inevitable temperature gradient while measurements

As could be foreseen, in the vicinity of phase transition, the anharmonicity of intra-atomic interactions clearly manifests itself, so the anomalies in phonons kinetics are expected. The density of elementary excitations increases, so the specific heat (one of components of thermal conductivity) increases as well. At that, the maximum of specific heat corresponds to the maximum of energy fluctuations; therefore, the relaxation time changes critically. The density of excitations and the

growth of anharmonicity lead to a decrease in the *diffusion length* of energy carriers and to the decrease in the intensity of heat transfer.

To explain such anomaly of thermal conductivity, refer again to Fig. 1.23, where the value of thermal conductivity in the [010] direction in the TGS crystals is compared with others physical parameters which determine the phonon thermal conductivity, namely, with the temperature dependence of specific heat C, with the speed of acoustic waves propagation in longitudinal v_{lon} and transverse v_{tr} orientation, and with the thermal expansion coefficient α along [010]. As can be seen, the Aiken's law $\lambda(T) \sim T^{-1}$ for thermal conductivity of TGS in the studied temperatures region is not satisfied that is due to a small average free path of phonons, scattering centers for which are commensurable with the order of lattice constant. Therefore, temperature-variation of thermal conductivity should follow the change in heat capacity. But in this case the minimum of thermal conductivity would not be observed, since the main investment in $\lambda(T)$ is made by specific heat change, as can be seen from Fig. 1.23.

It is possible that the phonon scattering in the vicinity of phase transition is due not only to anharmonicity of lattice vibrations, but also to other additional phonon-scattering mechanisms, for example, the scattering on structural heterogeneities. It is possible to came to conclusion that the minimum of thermal conductivity in phase transition region is due to mechanism of phonon scattering considering *interaction* of acoustic and optical phonons. It is also possible that below T_C in temperature interval of 40–50 °C there is a noticeable additional scattering of phonons on domain walls. In the TGS-family crystals the anomalies of thermal conductivity in vicinity of phase transition are also observed in the (100) and (001) directions. The absolute values of thermal conductivity of TGS, TGFB and TGSel, as expected, are of same order of magnitude. Anisotropy of the thermal conductivity is observed in all crystals: largest value of $\lambda(T)$ is seen in the [100] direction while the smaller are in (010) and (001) directions. The anisotropy of thermal conductivity in the TGS is consistent with the anisotropy in the velocity of ultrasound propagation.

5. *Thermal diffusivity in polar crystals*. As already mentioned above, during study of thermal conductivity, the anomalies in polar crystals display simultaneously two important factors. First is the temperature anomaly of *specific heat* $C(T)$ at phase transition (this is manifestation of *latent heat* of transition). Second is the change in the *average free path* of phonons $\langle l \rangle \sim \xi(T)$ due to polar-sensitive bonds ordering. As a result, it turns out that heat transfer is determined by the product: $\lambda(T) = \xi(T) \times C(T)$. To avoid the influence of heat capacity on the heat transfer analysis and

to separate out the processes of phonons scattering, another method of thermal diffusion $\xi(T)$ measure is developed, which indicates just the average free path of phonons without taking into account heat capacity $C(T)$.

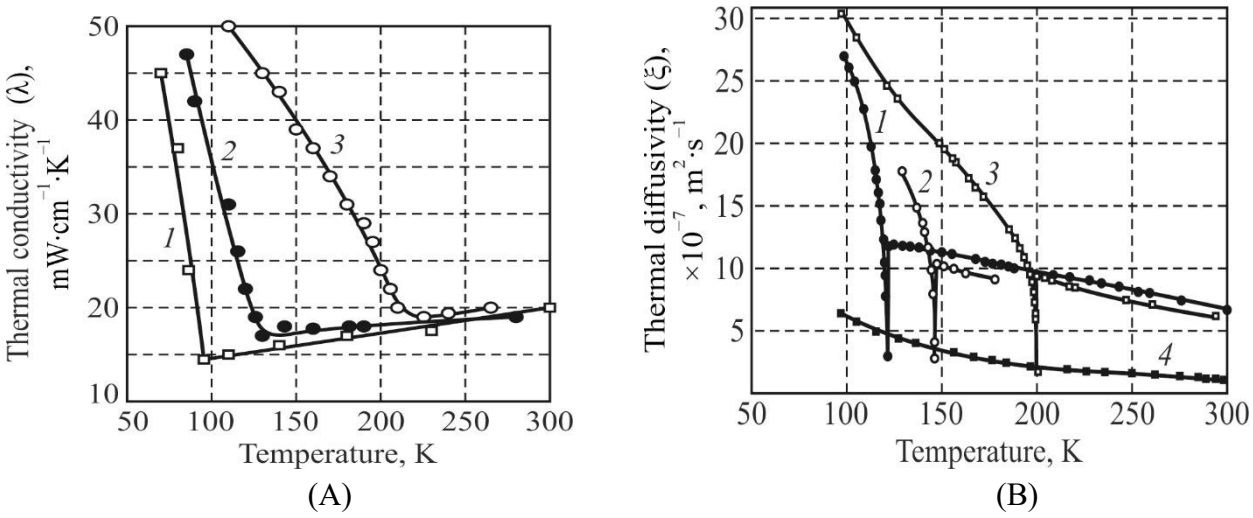

Fig. 1.24. Thermal conductivity (A) and thermal diffusivity (B) in ferroelectrics: phosphates *1* – KH_2PO_4, *2* – KH_2AsO_4, *3* – KD_2PO_4 and Rochelle Salt *4* – $\underline{KNa}C_4H_4O_6 \cdot 4H_2O$

The temperature dependence of thermal conductivity is compared to the thermal diffusivity in the crystals of KDP group, Fig. 1.24. These dependences are significantly different. In the $\lambda(T)$ dependence at phase transition point, the only a bend is seen followed by the essential $\lambda(T)$ increase at low temperature due to strengthening in ordering of polar bonds. However, in all studied crystals of phosphates in the vicinity of phase transition the thermal diffusivity $\xi(T)$ curves show the sharp minima that indicates a fast shortening in average *wavelength* of heat phonons. Such large difference between the $\lambda(T)$ and $\xi(T)$ dependences is due to the fact that in $\lambda(T)$ characteristic the decrease in phonons wavelength is compensated by the large maximum of the specific heat.

Ferroelectric phosphates, which investigations are shown in Fig. 1.24, are the piezoelectric (polar) crystals in *all temperature range*; however above the Curie point they belong to the *polar-neutral* symmetry class 42*m* (piezoelectrics) while below Curie point they belong to the *polar* pyroelectric class *mm*1. Thermal diffusion coefficient of in phosphates at temperature close to 300 K equals approximately $\xi \approx 7 \cdot 10^{-7}$ m^2s^{-1} that considerably exceeds the value $\xi \approx 2 \times 10^{-7} m^2 s^{-1}$ seen in the Rochelle salt crystals. The appearance of new collective excitations in the vicinity of phase transition leads to the fact that kinetics of acoustic phonons changes: an additional scattering leading to heat flux suppression is observed but

under the condition of increased specific heat. Exactly this factor is manifesting in the form of heat transfer poorly expressed minimum.

However, the sharp anomalies in the $\xi(T)$ dependence are observed only in the phosphates, in which the diffusion coefficient passes through a deep minimum (30–50% of ξ value), and its temperature interval is narrow (20–30 K). This minimum in the diffusion is due to the increase in crystal's anharmonicity, which leads to enlargement of inter-phonon interactions, as well as to the increase of ultrasound attenuation and the increase in dielectric losses. Increase in the relaxation time of thermal phonons also affects the anomaly of thermal diffusion.

As above so below the Curie point, the acoustic vibration modes (phonons) in the polar crystals are mixed with the optical phonons; therefore, the optical phonons also participate in a heat transfer. In the polar crystals, the process of heat transfer is significantly influenced by the optical phonons, since they are associated with the acoustic phonons. A prerequisite for the participation of optical phonons in the phenomenon of heat transfer is the spatial dispersion of optical modes. The interaction of acoustic phonons with the soft transverse optical mode (peculiar to ferroelectrics) leads to a significant decrease in the average free path of phonons. It is obvious that at the point of phase transition the average free path of heat phonons is reduced to the possible minimal level. In different crystals and at various temperatures (and even in case of KDP deuterization – DKDP) this level remains almost same, Fig. 1.24B. It was also established that in a wide temperature range same very low level of thermal diffusion is seen in the Rochelle salt crystal, so it is not surprising that sharp dips in the $\xi(T)$ curve at Curie points are not seen in this crystal.

On the basis of established lowest limit of the wavelength of thermal phonons (which, apparently, reaches the value of unit cell parameter of a crystal), one can come to conclusion that in the disordered phase (above the phase transition temperature) this wavelength still remains an order of magnitude larger and then continues to drop with temperature – as it is usual for all crystals. Below the phase transition temperature, the role of structural ordering of polar crystals becomes very noticeable (apart from Rochelle salt, in which a particularly complex structure makes it almost heat-impermeable (resembling glass). As temperature lowers starting from Curie point, the essential increase of thermal phonons wavelengths is observed, which indicates a substantial ordering in the polar-sensitive bonds. Since in this temperature range there are no noticeable anomalies in the specific heat, so the same dependence is reproduced in the temperature dependence of thermal conductivity.

6. *Electrical field influence on thermal transfer*. The ability to control the heat flow by the electrical field has not only a scientific, but also technical interest. Therefore, in seen in Fig. 1.25 first experiments, this question was studied on the example of a polycrystalline ferroelectrics with a diffuse phase transition, in which dielectric permittivity can be changed approximately 10 times by the electrically displacement field in a considerable temperature range. The measurements were carried out in the vicinity of phase transition.

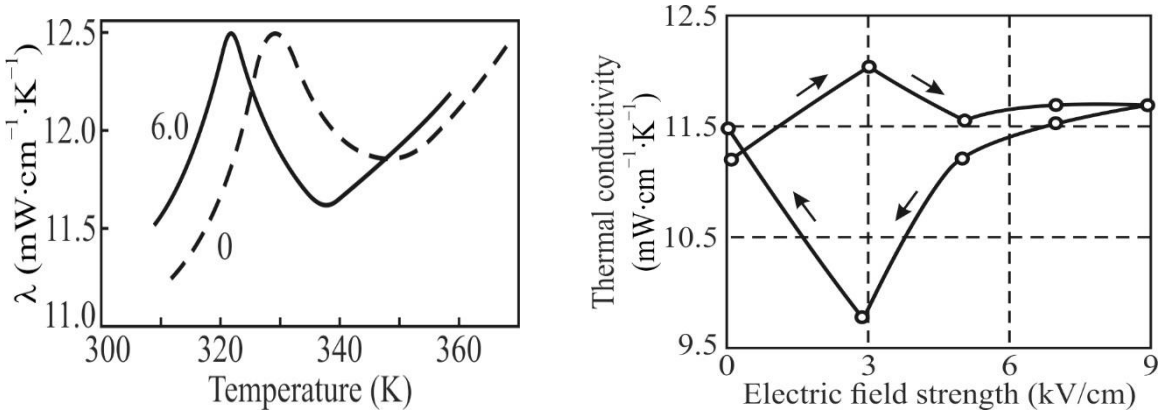

Fig. 1.25. Influence of bias electrical field on thermal conductivity coefficient (λ) of nonlinear ferroelectric near phase transition: A – λ temperature dependence at E = 0 (1) and E = 6 kV/cm (2): B – λ dependence on electrical field at 48 °C

The results of study of polycrystalline ferroelectric Ba(Ti,Zr,Sn)O_3 are shown in Fig. 1.24. When constant electrical field is applied, the maximum of thermal conductivity in the region of phase transition remains, but it shifts by 5–8 °C towards lower temperatures. This corresponds to the increase in thermal conductivity in the ferroelectric phase near phase transition. The phenomenon of thermal conductivity hysteresis with the change in magnitude and sign of electrical field strength is also observed, Fig. 1.24B and indicates that phonons scattering is to some extent due to the domain structure of ferroelectric. However, for technical applications, the effect of thermal conductivity control seems to be too small.

To clarify the mechanism of field effect on the thermal conductivity, the single crystals were studied. Very convenient object for more detailed studies of thermal diffusion is the TGS crystal, which is ferroelectric with hydrogen bonds that occupies middle position in terms of thermal diffusion coefficient: it has no large anomalies near its phase transition at Curie temperature T_C = 49°C ≈ 323 K. The peculiarities in the $\xi(T)$ variations at the phase transition from nonpolar (high-temperature) phase to the polar (low-temperature) phase are shown in Fig. 1.26. It is found that the electrical bias field significantly changes the anomalies of thermal

conductivity and thermal diffusion at the phase transition (electrical field is applied along the polar axis of a crystal, where it shows greatest impact on the degree of polar bonds ordering).

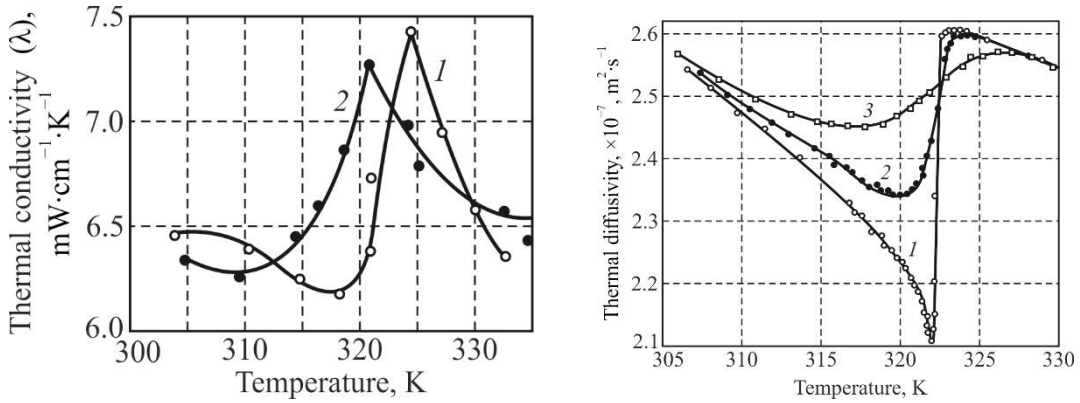

Fig. 1.26. Thermal conductivity (A) and thermal diffusivity (B) of TGS crystal near phase transition
under bias electrical field influence; A: curve *1*– $E = 0$; curve *2* – $E = 6$ kV/cm;
B: *1*– curve *1*– $E = 0$. curve *2* – $E =$ 3.4 kV/cm, curve *3* – $E = 10$ kV/cm

The free path of phonons in the TGS, calculated from the thermal conductivity ($\lambda \approx 2\times10^{-3}$ cal□cm^{-1}□s^{-1}□deg^{-1}), the specific heat capacity ($C_V \approx 0.6$ cal□deg^{-1}□cm^{-3}) and the speed of ultrasound propagation ($v \approx 4\times10^{3}$ cm□s^{-1}), has the value of 3×10^{-8} cm, i.e. it is of lattice constant order. When the electrical field is applied, the condition of phonon scattering changes, for example, by scattering on the domain walls, which in the ferroelectrics in have the length on the order of lattice constant. As noted, the thermal conductivity depends not only on the conditions of phonon scattering, but also on specific heat and elastic properties of a crystal. As indicated above in connection with Fig. 1.9, the specific heat of TGS crystal increases as Curie point approaches, and its sharp maximum is observed exactly at transition point. Under the influence of electrical field, the "smearing" in $C_V(T)$ dependence appears and a decrease in specific heat maximum is seen, but its temperature is not shift. The displacement of thermal conductivity maximum in the ferroelectrics, in particular, in TGS single crystals, is probably due to a change in not only conditions of phonon scattering, but also by changing in the elastic properties of a crystal under the influence of electrical field in the region of Curie point.

In the temperature dependences of thermal *conductivity* and thermal *diffusion* a big difference is obvious. The influence of the applied electrical field on the thermal conductivity can be explained by the shift in the frequency of optical phonons branch. In the absence of bias field, a small minimum accompanied by the maximum of $\lambda(T)$ is observed, which in the electrical field becomes blurred and

shifted to low temperatures (it should be noted also that magnitude of these anomalies also depends on unavoidable temperature gradient, at which measurements should be provided). However, any interpretation for alteration in the $\lambda(T)$ dependence is complicated also by the fact that the thermal conductivity is affected not only by average free path of thermal phonons, but also by the change in specific heat.

As a rule, the group velocity of optical phonons is small and their contribution to the heat transfer is small also, so thermal excitation of the optical phonons leads only to an *additional scattering* of thermal phonons on them.

However, one must also take into account the fact that the *spatial dispersion* of the optical phonons leads to the appearance for them the group velocity near the *boundary* of Brillouin zone.

Note that when approaching to the boundary of Brillouin zone, the group velocity of acoustic phonons decreases substantially for such a "heat" phonons, and exactly this region of spectrum defines the heat transfer. In the polar crystals, the acoustic and optical phonons are connected, so that the optical phonons can participate in the *heat transfer*: this is confirmed by the electrical field influence as on thermal conductivity so on thermal diffusion.

The double mechanism of optical phonons participation (scattering and participation) in the process of heat transfer can compensate each other in the case of thermal *conductivity*, but not in the process of thermal *diffusion*.

It can be seen that thermal diffusion coefficient increases substantially in the ordered phase, indicating the decrease of polar-sensitive bonds disordering which hinders the diffusion of a heat: in the electrical bias field the wavelength of thermal phonons increases. In a certain sense, it is possible to control the heat flux by means of electrical field, although for practical significance of this effect is too small: it occurs in a narrow temperature range and allows heat flux controlling in the range of only 20%.

It is noteworthy that above the Curie temperature (in the disordered phase) the influence of electrical field shows the opposite effect: the thermal diffusion coefficient somewhat decreases. Apparently this is due to the blurring of phase transition and its displacement in the electrical field to higher temperatures.

7. *Thermal diffusion in antiferroelectrics.* The most impressive feature of thermal diffusion is seen in the relatives to polar crystals: in the antiferroelectrics, Fig. 1.26. Instead of deep minimum in $\xi(T)$ dependence the sharp *maximum* is observed at Curie point, for example, in ammonium dihydrophosphate (ADP). At the first glance, this behavior of $\xi(T)$ may seem quite unusual. However, the matter

is that to the heat transfer in the antiferroelectrics the *optical phonons* is substantially added, especially in the vicinity of phase transition.

In this crystal, the frequency of optical vibration mode of a lattice near the boundary of Brillouin zone *decreases critically* to the frequency of the acoustic modes, leading to their mixing.

This occurs precisely with the short-wave (thermal) phonons, which ensure heat transfer. As a result, the coefficient of thermal diffusion increases critically precisely in the Curie point, as seen in Fig. 1.27, curve *1*.

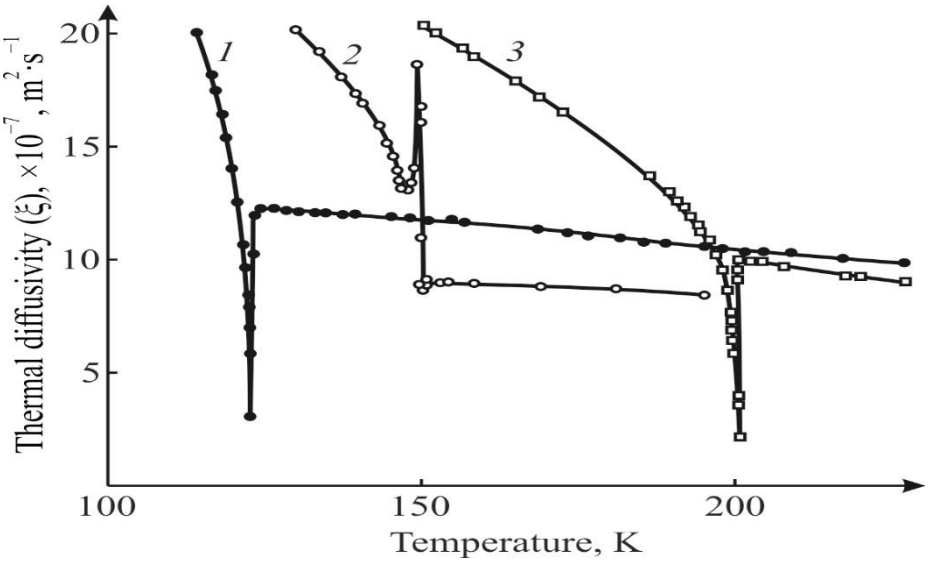

Fig. 1.27. Thermal diffusion comparison in ferroelectrics KDP (*1*) and DKDP (*3*) in comparison with antiferroelectric ADP (*2*)

In contrast, in the *ferroelectric* crystals of KDP and DKDP the effect of $\xi(T)$ increase does not exist, because in them the optical lattice mode decreases critically *near the center* of Brillouin zone, i.e. in the region of long-wavelength phonons. This decrease strongly affects the speed of sound, i.e., long-wavelength phonons as well as leads to the large permittivity in Curie point: at frequency of 10 GHz in the ferroelectric KDP $\varepsilon_{max} \approx 1000$ while in the antiferroelectric ADP at 10 GHz $\varepsilon_{max} \approx 90$.

Inasmuch as in the ferroelectrics (like KDP) near the center of Brillouin zone only the *long-wave* optical phonons show anomalies decrease in frequency, so this critical phenomenon have only little effect on the heat transfer realized by the short-wave "thermal" phonons; that is why the *scattering* effect of thermal phonons dominates.

It is seen especially in vicinity of phase transition when the *structural rearrangemen*t of crystal occurs: the wavelength of thermal phonons becomes minimal, leading to a deep minimum of $\xi(T)$ seen in Fig. 1.27, curves *1* and *3*.

Because of additional influence of optical phonons, the temperature dependence of thermal conductivity can not uniquely reflect the change in optical phonons kinetics. Such a parameter is the thermal diffusion coefficient, which mainly reflects the dependence of the phonon mean free path on temperature.

Thus, the mechanism of thermal conductivity in polar-sensitive crystals is predominantly phonons scattering; since the electrical conductivity of these materials is very small it can be assumed that there are no other heat transfer mechanisms (electronic, excitonic or photonic).

Consequently, discussed peculiarities of thermal conductivity can only be due to the change in the phonon scattering conditions. The influence of the polar-sensitive (mixed ionic-covalent) bonds greatly affects the phenomenon of heat transfer in crystals: their thermal conductivity is noticeably lower than that in simple covalent or ionic crystals.

Studies of the anomalies of *thermal diffusion* in the vicinity of ferroelectric phase transitions, where their disordered non-polar structure changes to ordered polar structure, make it possible to clarify some features in the behavior of polar-sensitive bonds.

1.6 Summary and self-test questions

1. *Thermal properties* of a material are due to interaction energy of molecules, atoms and electrons. Thermodynamic function called the *enthalpy* (heat content) characterizes the energy state of system or material; enthalpy increases with temperature rise. The *entropy* is the measure of internal disordering (chaotic) in a system. The Helmholtz's *free energy* has its minimum in the equilibrium state of system, in which any changes occur at constant volume and temperature.

2. Research and application of dielectrics is generally held under the *adiabatic* conditions, when during the change of applied voltage a thermal equilibrium between dielectric and surrounding environment can not be installed in time, so any alteration of entropy is absent: $\delta S = 0$. Therefore, from experiments, the *adiabatic permittivity* ε^S is generally determined. In such dielectrics, which polarization depends on temperature (paraelectrics, ferroelectrics, pyroelectrics, and others), another – isothermal – process of polarization might be important, when $\delta T = 0$ and permittivity is isothermal: ε^T. Analytical determination of relationship between ε^T and ε^S may be important both to explain the frequency dependence of permittivity in range of subsonic frequencies, and for theoretical calculations. Isothermal dielectric permittivity is always greater than adiabatic one: $\varepsilon^T > \varepsilon^S$. In most cases this

difference is small and can be neglected. However, in the pyroelectrics, and, especially, in the vicinity of ferroelectric phase transition, the difference between ε^T and ε^S can reach 10–50%, so it should be taken into account.

3. If the dielectric permittivity increases during dielectric heating, i.e., when the temperature coefficient of permittivity is positive ($TC\varepsilon > 0$), then the change in entropy $S - S_0(T)$ during polarization must be positive. Thus, not discussing the details of processes which occur in a dielectric, only from general thermodynamic considerations, it can be concluded that in the dielectric with $TC\varepsilon > 0$, when it is placed in the electrical field, such physical processes occur, which *reduce* the degree of molecular or atomic structure ordering. Conversely, if in the dielectric possessing $TC\varepsilon < 0$, i.e., when its permittivity decreases with heating, the change in entropy is negative. This means that basic mechanisms, which determine electrical polarization, the external electrical field application results in the *increase* in the ordering of molecules (ions, atoms) in a dielectric.

4. Basic energy characteristics of solids are the *Debye energy* $\hbar\omega_D$ and the *thermal energy* k_BT. Debye temperature $\theta_D = \hbar\omega_D/k_B$ and Debye frequency $\omega_D = 2\pi\nu_D$ are connected with each other by two fundamental constants: Planck constant $\hbar$ and Boltzmann constant k_B.

5. Degrees of a freedom while atomic particles movement in solids can be divided into two groups. If interaction energy of particles U_{int} is small in comparison with thermal motion energy k_BT, namely $U_{int} << k_BT$, then the appropriate degrees of freedom behave as the *collection* of quasi-particles, i.e., as "almost ideal gas" of phonons; this refers to ordinary non-polar dielectrics.

6. In the opposite case, when, conversely $U_{int} >> k_BT$, then appropriate degrees of freedom are usually quite ordered, but their movement, too, can be described by the introduction of phonons. These substances include majority of functional polar-sensitive dielectrics (piezoelectrics and pyroelectrics), so the application of phonons concept to them in most cases can be considered justified.

7. Much more complicated cases arise if interaction energy $U_{int} \sim k_BT$. In this case theoretical description of solids becomes complicated, especially at phenomenon of phase transition, when the non-polar phase is turning into the polar phase. At that, polar-sensitive crystal behaves by such a way, when any conventional concept, based on phonons, can not adequately describe experimental situation. Particles interaction has special character: the probability of collective movements is bigger then the probability of individual movements. Abnormal increased role of collective movements is confirmed by experiments in the vicinity off phase

transition: at temperature $T = T_C$ crystal shows maximum of the specific heat, the minimums of thermal expansion ant thermal diffusion coefficients, and so on.

8**.** Peculiar properties of the polar crystals are manifested in their specific heat, thermal expansion and thermal conductivity. Crystals possessing polar-sensitive bonds in certain conditions behave in a complex way: for some phonons, for example, the thermal ones, their lifetime is commensurate with the inverse frequency of oscillation; that is, characterized them oscillators turn out to be overdamped. That is why, the crystal of excellent optical quality, which are good optically transparent and have small attenuation for *long* acoustic (ultrasonic) waves transmission, in case of the *short* (heat) waves transmission turns out to be almost opaque environment, in which the phonons of certain frequency get stuck.

9. The *specific heat* in the polar crystals contains an additional contribution due to the disordering-disordering processes of their polar-sensitive bonds. Statistical possibility of several states realizing increases the total entropy of a system: such *configuration entropy* is a part of total entropy of a system that is related to the *position* of constituent particles rather than to their velocity or momentum. It is physically related to the number of ways of arranging all the particles of a system while maintaining some overall set of specified system properties, such as energy. The change in configurational entropy corresponds to same change in macroscopic entropy.

10. In the polar crystals, their specific heat somewhat exceeds this parameter as compared with the non-polar crystals: this is clearly expressed in the vicinity of phase transitions, where the maximum of specific heat capacity can be several times higher than its average value. It might be supposed that an additional contribution to the specific heat in the gradually ordering phase is due to the configurational entropy.

11. The statistical possibility of several states realizing increases the total entropy of a system: such *configuration entropy* is related to the position of constituent particles rather than to their velocity or momentum. It is physically related to number of ways of arranging all particles of a system while maintaining some overall set of specified system properties, such as energy. Change in the configuration entropy corresponds to the same change in macroscopic entropy.

12. The thermal expansion reflects the features of inter-atomic bonds in crystals. Without matching between the thermal expansions coefficients, technologically obtained microelectronics structures would be mechanically stressed that affects their properties and even might lead to the local destruction. However, there are some important cases, when exactly the difference in thermal expansion is used for managing of combined structures properties.

13. In the polar dielectrics, their peculiar polar-sensitive structures arisen due to structural compensation of atoms electronegativity. Negative value of $\alpha(T)$ corresponds to such particular case, when the entropy of crystal *increases* with the rise of pressure that is possible only in the case of configurational entropy: the negative expansion region in the $\alpha(T)$ dependence corresponds to the processes of polar bonds self-ordering.

14. Low-temperature minimum of thermal expansion coefficient can be explained: when temperature decreases, the thermal chaotic motion freezes, and existing in crystal polar-sensitive bonds become partially ordered (configurational entropy decreases). As a result, crystal occupies bigger volume, demonstrating negative $\alpha(T)$. With further cooling to a very low temperature, the quantum oscillations in the crystal lattice prevent the further ordering of fluctuating polarity, so with the approach to zero crystal again compresses a little before $\alpha(T) \rightarrow 0$ at $T \rightarrow 0$.

15. Low temperature negative thermal expansion in semiconductors of $A^{III}B^{V}$ and $A^{II}B^{VI}$ types is not surprising as they belong to the polar groups of crystals. However, in the *atomic* semiconductors of a diamond type, the $\alpha(T)$ minimum needs explanation. It might be assumed that the reason of negative $\alpha(T)$ in germanium and silicon is the fluctuations of partial ordering of the *virtual* hexagonal polar phase (this assumption is based on the fact of hexagonal diamond existence).

16. The s*train engineering* technology for polar-sensitive films is based not only on the mismatch of thermal expansion, but to a greater degree on the difference in permanent lattices of film and substrate. According to principle of La Chatelier, if during formation of polar phase one of crystal size increases, then the forced change in this size of crystal should lead to the change in crystal polar state.

17. In the *biaxial stressed films*, such materials are obtained that in the bulk state are not ferroelectrics at any temperature. The biaxial deformations of films make it possible to increase the Curie point by hundreds of degrees with a simultaneous increase in the polarization directed perpendicular to film thickness. Deformations, reaching value of several percents, have a great influence on the properties of polar-sensitive thin films so it becomes possible to obtain films with such properties that are not found in the natural materials. Thus, the difference in thermal expansion as well as the mismatch between lattice parameter of film and substrate can be used in modern technologies of microelectronics.

18. *The heat transfer* in the polar crystals is provided mostly by the short lattice waves having low velocity, so the polar crystals look like turbid medium. Short lattice waves demonstrate strong diffuse-type scattering by nano-size

inhomogeneous of structure, in which phonons interaction is determined mostly by the polar-sensitive bonds, because the wavelength of heat phonons is commensurable with the parameter of crystal lattice.

19. *The thermal conductivity* depends on the crystal specific heat *C,* on the free path between phonon collisions $<l>$, and on the average velocity υ of phonons: $\lambda = (1/3)\cdot\upsilon\cdot l$. In the usual temperature interval, the dependence of $\lambda\,(T)$ goes down following Aiken law: $\lambda\,(T) \sim T^{-1}$. the thermal conductivity corresponds to the thermal expansion coefficient: $1/\lambda \sim \alpha^2$ that determined by the peculiarities of inter-atomic bonds. Therefore, crystals with larger thermal expansion coefficient have smaller thermal conductivity.

20. The thermal conductivity in the polar crystals, in comparison with usual crystals, is significantly decreased that is conditioned by the peculiarities of phonon dissipation process: i.e., by the perceptible binding of acoustical and optical phonons. This special feature of crystals having polar-sensitive bonds correlates with their phonon spectrum near the boundary of Brillouin zone, where the transverse acoustic mode noticeably reduced. This is the evidence of such interaction between nearest atoms that can be described by the mixing of acoustic and optical phonons.

21. The *thermal diffusivity* coefficient ξ is the thermal conductivity divided by the crystal density ρ and by its specific heat C at a constant pressure: $\xi = \lambda/(C_p\cdot\rho)$. It measures the rate of heat transfer of a material from the hot side to the cold side. In a sense, the thermal diffusivity is the measure of the *thermal inertia*; in the substance possessing higher thermal diffusivity, the heat moves more rapidly through it. At that, the thermal diffusivity is determined mainly by the mean free path $<l>$ of thermal phonons propagating in crystal ($\xi \sim <l>$). At normal and increased temperatures (when $T > \theta_D$) with the increase of temperature the $\xi(T)$ dependence slows down following Aiken law: $\xi(T) \sim T^{-1}$. In all studied ferroelectrics the sharp minimum are observed on $\xi(T)$ curves, which indicate fast shortening of average wavelength of phonons in the vicinity of phase transition.

22. In contrast to the ferroelectrics, where the thermal diffusivity shows a sharp and deep maximum at the Curie point, in the antiferroelectrics it demonstrates a sharp maximum, because due to the peculiarities of the antiferroelectric phase transition in the kinetics of phonons, the optical phonons are actively involved.

23. Electrical field influence on the thermal transfer has not only scientific, but also technical interest. When the constant electric field is applied to ferroelectric, the maximum of its thermal conductivity in the region of phase transition remains, but it shifts towards the lower temperatures. This corresponds to the increase in thermal conductivity in the ferroelectric phase near phase transition. The

phenomenon of thermal conductivity hysteresis with electrical field changing is also observed, that indicates that the scattering of phonons is to a some extent due to the domain structure of ferroelectric. However, for technical applications, effect of thermal conductivity control seems to be too small.

24. Thus, polar-sensitive (mixed ionic-covalent) bonds strongly affect the processes of heat transfer in polar crystals: their thermal conductivity is much less than that in the pure-ionic or pure-covalent crystals. The anomalies of thermal diffusion in the vicinity of ferroelectric and antiferroelectric phase transitions are described by the change of ordered polar structure to disordered non-polar structure. In the ordered phase the thermal diffusion coefficient increases; this indicates that disordering of polar-sensitive bonds hinders the diffusion of heat.

Chapter 1. Self-assessment questions

1. How experimentally compare adiabatic and isotermal permittivity?
2. How is the temperature dependence of permittivity related to the change in entropy during electrical polarization?
3. Why is it difficult to use quasiparticle model to explain the second-order phase transitions?
4. What is the physical meaning of configuration entropy and when should it be used?
5. What is the physical meaning of electronegativity and when should it be used?
6. How to explain the difference in thermal diffusivity anomalies at the Curie points of ferroelectrics and antiferroelectrics?

CHAPTER 2. INTERDEPENDENCE OF ELECTRICAL CONDUCTANCE AND POLARIZATION

Content

In any substance, the applied electrical field affects existing in it charged particles, which might be as bound so relatively free. Their reaction (electrical polarization or electrical conductivity) on the *permanent* (constant) field is possible to consider separately and characterize by the conductivity and dielectric constant. However, in the *alternating* electrical field, the electrically induced displace and free move of charged particles lead to both reactive and active a electrical current, that is characterized usually by the *complex permittivity*, but also can be described by the *complex conductivity*. At that, between these two complex parameters the unambiguous relationship can be established. Both of these methods of electrical reaction of a substance onto the applied electrical field describing are equivalent, but more common parameter is the complex permittivity, although sometimes the complex conductivity can be more informative.

2.1 Complex permittivity and conductivity

1. ***Different responses of a substance*** onto the applied electrical field are listed symbolically in Fig. 1A. Several reversible and irreversible physical phenomena are seen – not only of *electrical* nature but also the *mechanical* and *thermal* responses. Among them are not only electrical responses – electrical induction $D(E)$ and current $j(E)$, but also the mechanical effects: electrostriction $x(E^2)$ and piezoelectric effect $x(E)$ as well as some thermal effects: Joule heat from dielectric losses $\delta Q(E^2)$ and the heat or cold from the electrocaloric effect $\delta Q(E)$.

However, only the *electrical responses* are discussed below.

The *electrical polarization*, among many others phenomena, can be noted as the first. In dielectrics, the electrical *displacement D* (otherwise known as electrical *induction* (measured in [D] = C/m^2) appears, which in dielectric is greater than in

vacuum owing to the electrical *polarization P*. Indeed, if there is no dielectric between the metallic electrodes of a capacitor (the case of a vacuum), the value of the electrical induction equals $D = \varepsilon_0 E$, where $\varepsilon_0 = 8.854 \cdot 10^{-12}$ F/m is the electrical constant ([F] = *C/V* is the farad, unit of electrical capacitance *C* measure). Parameter ε_0 in SI agrees the units of *D* and *E*, characterizing the *absolute permittivity* of vacuum.

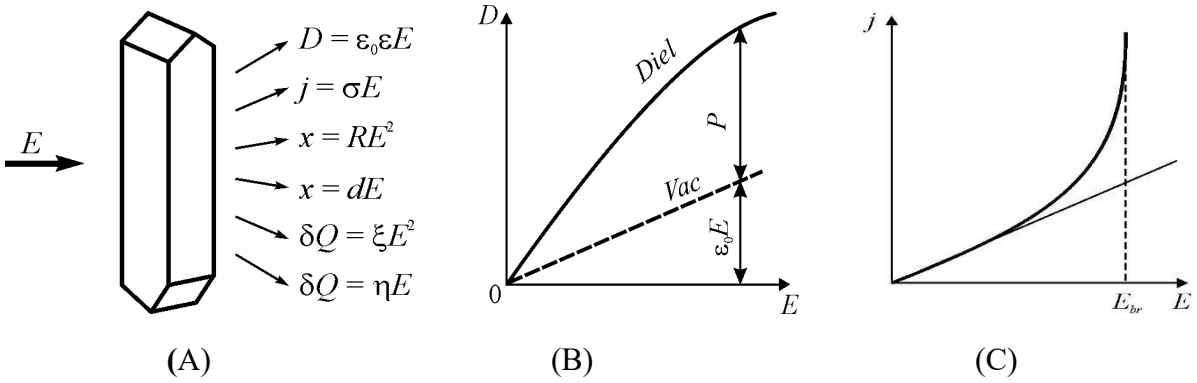

Fig. 2.1. Classification of polar crystal responses on electrical field influence: A – classification of electrical (*D, j*), mechanical (strain *x*) and thermal (δQ heat) effects (ε is permittivity, σ is conductivity, *R* is electrostriction coefficient, *d* is piezoelectric module, ξ is generalized loss factor,
η is electrocaloric coefficient; B – electrical induction dependence on electrical field in dielectric compared with vacuum; C – electrical current density *j* dependence on electrical field *E*

When dielectric is placed between the electrodes of a capacitor, then, under the action of electrical field, the bounded positive and negative charges of atoms, ions and molecules of a material becomes slightly shifted relatively to each other, creating the overall electrical moment. The *specific electrical moment* (i.e., the moment per unit of volume) is the polarizability tradionally called as the *polarization P.* The stronger electrical field the larger is the value of *P*, Fig. 2.1B. The *electrical displacement D* (otherwise called induction) is the sum, determined as $D = \varepsilon_0 E + P$.

The ability of dielectric to polarization in the electrical field is characterized by the *relative permittivity* ε (commonly referred to as dielectric constant), which shows how much more the electrical induction in a dielectric is greater than in the vacuum: $D = \varepsilon_0 \varepsilon E$. It should be noted, however, that in the strong electrical field a deviation from this linear dependence of $D(E)$ can be observed, shown in Fig. 1B. This dielectric *nonlinearity* usually is bigger in the dielectrics possessing higher permittivity, which in this case depends on the magnitude of electrical field: $\varepsilon = \varepsilon(E)$. As a matter of fact, the temperature usually affects the polarization process that results in the temperature dependence of permittivity: $\varepsilon = \varepsilon(T)$. Furthermore, when

dielectric is studied at the AC voltage, the permittivity can vary with frequency, so $\varepsilon = \varepsilon(\omega)$. Thus, very important for dielectrics parameter can be a function of several external influences: $\varepsilon = \varepsilon(\omega, E, T)$.

The *conduction,* Fig. 1C, is the second important phenomenon, which arises in a material under the action of electrical field. If this field is not very big, then the current density, according to Ohm's law, is proportional to voltage: $j = \sigma E$, where σ is the *specific conductivity* (otherwise called simply as conductivity). However, in the strong electrical fields, the Ohm's law in dielectrics and semiconductors is violated, resulting in the *nonlinear* conductivity, so that $\sigma = \sigma(E)$, Fig. 1C. The increase in conductivity in strong electrical field plays a decisive role in material *electrical durability* (a steady state with small and time-independent conductivity). In strong electrical field conductivity increases with voltage growing, and becomes so big that the phenomenon of *electrical breakdown* occurs. Just before breakdown, the electrical current increases sharply due to the ionization effect, when electrons moving in the electrical field interact with molecules, ions or atoms, adding them a sufficient energy to generate new electrons.

Electrical conductivity depends also on temperature, since thermal motion of atoms and molecules leads to the activation of new free charge carriers, so that $\sigma = \sigma(T)$. In most dielectrics and semiconductors, the frequency dependence of conductivity is also observed: $\sigma = \sigma(\omega)$. This dependence can be absent only in those cases, when the electrical current is carried by the untied electrons – particles with a very high mobility. However, electronic conductivity in dielectrics, predominantly, has the hopping (polaron) character, when charge carriers have large effective mass and, hence, a low mobility. In the case of ionic conduction, as well as in the case of charge transfer by the micro-particles (molions), charge carriers have rather big inertia; consequently, the frequency dependence of electrical conductivity becomes evident. Thus, the bulk specific conductivity of dielectrics and semiconductors, same as their permittivity, is dependent not only on temperature but also on the electrical field intensity and frequency: $\sigma = \sigma(\omega, E, T)$.

Below only the *frequency dependence* of permittivity and conductivity is considered, since they turn out to be mutually dependent

2. *Complex permittivity and conductivity* are introduced for the convenience of their interdependence describing, since only at a constant voltage these parameters can be considered as independent. Polarization is the charge separation, and electrical conductivity is the charge transfer. At an alternating voltage, the connection between conductivity and polarization is obvious, since both of these phenomena are due to the limited (polarization) and the almost-free (conductivity)

movement of the electrical charges in a matter, and in both cases the inertial phenomena affect these movements. In connection with detailed analysis, one should refer to the fundamental definitions.

In the physics and materials sciences, a conception of *dielectric permittivity* ε (dielectric constant) appears in three fundamental laws: (1) filled by dielectric electrical capacitor, in comparison with vacuum capacitor, increases its capacitance in ε times (established by Faraday); (2) mechanical strength of electrical charges interaction reduces in ε times (Coulomb's law); (3) electromagnetic waves velocity in the dielectric decreases in $\sqrt{\varepsilon}$ times, as follows from Maxwell-Lorentz equations. It is clear that all three cases regard to same physical parameter, and each of above said laws can be derived one from the other.

It is also appropriate to recall that the value of relative dielectric permittivity (ε), as well as the relative magnetic permeability (μ) and the electrical conductivity (σ) in a classic understanding of these *electrodynamics parameters* of a substance follows from the homogenization of Maxwell equations derived by Lorentz more than 100 years ago. To obtain these three parameters of a medium, the averaging-out was performed, using two microscopic quantities: "the physically infinitesimal time interval" and "the physically infinitesimal volume". At that, the smallest time interval is considered as $\tau \leq 10^{-14}$ s while the physically small volume of a substance is estimated of about a dozen of inter-atomic distances.

Grounded by this way, the classic concept of permittivity needs to be detailed and might be perceived differently, because of appearance of a huge variety of modern experimental data, obtained by quite different methods in the various crystals, ceramics, polymers, composites and nano-materials. In assessing this diversity, it must be guided by the fundamental relationships.

The interaction of electrical and magnetic fields E and H in a matter has been described by the Lorentz-Maxwell's equations:

$$\text{rot } E = -\partial B/\partial t, \qquad \text{rot } H = j + \partial D/\partial t,$$
$$\text{div } D = \rho, \qquad \text{div } B = 0, \qquad (2.1)$$

where B is the magnetic induction), j is the current density, D is the dielectric displacement, and ρ is the density of electrical charges).

[***Note.*** The relationship between magnetic field H and magnetic induction B is defined as $B = \mu_0 \mu^* H$, where μ_0 is the magnetic permeability of vacuum, while $\mu^* = \mu' - i\mu''$ is the complex magnetic permeability denote the real and the loss part (taking into account not only magnetization, but also any energy loss in alternating field). However, in the case under consideration, i.e., for the diamagnetics and weak

paramagnetics, it can be set $\mu^* = \mu' = 1$ and $\mu'' = 0$; therefore, any magnetic processes are no longer taken into account in future considerations].

Next only the *electrical polarization* and the *electrical conductivity* will be considered. Both of these processes occur due to electrical field effect on the charged particles movement in a substance, so in the AC polarization and conduction are usually *interdependent* (they can be separated only in DC electrical field). To be described in the *sinusoidal* electrical field $E(\omega) = E_0\exp(i\omega t)$, both the dielectric displacement and the conduction should be represented by the <u>*complex parameters*</u>. In the Maxwell-Lorentz equations (1), the second one (rot $H = j + \partial D/\partial t$) shows that the current density j and the time derivative of electrical displacement $\partial D/\partial t$ are the *additive quantities*. That is why, the current density $j = \sigma^* E$ and $\partial D/\partial t = i\omega\varepsilon_0\varepsilon^* E$ would be represented as the *equivalent functions*, if the complex values will be used to describe them. When these functions are described by the real and imaginary parts, the complex conductivity σ^* is connected to the complex permittivity ε^*:

$$\sigma^*(\omega) = \sigma'(\omega) + i\sigma''(\omega) = i\omega\varepsilon_0\varepsilon^*(\omega),$$
$$\varepsilon^*(\omega) = \varepsilon'(\omega) - i\varepsilon''(\omega), \qquad (2.2)$$

where ε_0 is the dielectric permittivity of vacuum. Hence, in the sinusoidal electrical field, the complex conductivity σ^* and the complex dielectric function ε^* are interconnected. It follows that the real and imaginary part of dielectric permittivity can be expressed through the components of complex conductivity:

$$\varepsilon'(\omega) = \sigma''(\omega)/(\varepsilon_0\omega);$$
$$\varepsilon''(\omega) = \sigma'(\omega)/(\varepsilon_0\omega). \qquad (2.3)$$

Similarly, the real and imaginary part of complex conductivity can be expressed through the components of complex permittivity:

$$\sigma'(\omega) = \varepsilon_0\omega\varepsilon''(\omega);$$
$$\sigma''(\omega) = \varepsilon_0\omega\varepsilon'(\omega). \qquad (2.4)$$

Thus, *in principle*, any of aforementioned complex parameters can describe <u>*completely*</u> the frequency dependence of electrical response of a substance to the alternating voltage. Nevertheless, exactly the frequency dependence of *permittivity* is traditionally used in most researches. However, it should be noted that in some cases, when obtained experimentally data processing, the more informative parameter is turned out the frequency dependence of *conductivity;* for example, to determine accurately the natural frequency of a damped oscillator: it corresponds exactly to the $\sigma'(\omega)$ maximum.

In conclusion of above discussion, it should be noted that formally established connections between $\sigma^*(\omega)$ and $\varepsilon^*(\omega)$ is expedient to be explained by the

microscopic mechanisms of substance responses, both from the side of polarization processes, which means the *separation* of bound electrical charges, so from the side of electrical conduction, which means the *transfer* of the non-bound charge.

3. *Electrical polarization mechanisms* explain an occurrence of *electrical moment* arising in a dielectric when electrical field E is applied to it: $P = \varepsilon_0 \chi E$, where ε_0 is the electrical constant and χ is the susceptibility of a dielectric. Electrical polarization means the *separation* of bound electrical charges: for example, on the opposite surfaces of plane-parallel dielectric sample the electrical charges of different signs appear; at that, these charges are not free but closely bound in a dielectric. As noted before, polarization is bound with electrical displacement: $D = \varepsilon_0 \varepsilon E = \varepsilon_0 E + P$, which includes the induction of vacuum $\varepsilon_0 E$, and the actual polarization of dielectric is $P = \varepsilon_0 \chi E$. At that, the dielectric permittivity $\varepsilon = 1 + \chi$ takes into account both processes.

At the moment of electrical voltage switching on, through a dielectric (included in the electrical circuit) a *reactive current* of electrical charges displacement flows; next it terminates, if the voltage remains unchanged and conductivity is insignificant. The voltage switching off also is accompanied by a jump of the electrical current of *depolarization,* which has an opposite sign as to charging current; in this way, the electrical polarization reacts *only to the change* of electrical voltage.

The lower the inertia of polarization processes, the lower dielectric losses and the wider range of operating frequencies, that is very important for dielectrics used in high-speed electronic equipment. When electrical field is applied to a dielectric, the associated charges of structural units displace relative to each other, leading to the electrical polarization. This mechanism looks like electrical field induces in the dielectric a set of elementary electrical moments $p = qx$, where q is the charge of bound units and x is their mutual displacement. The electrical moment, induced by the external field, has contributions from the *electrons* (moving from their equilibrium positions in atoms) and from the *ions* (deviating from their equilibrium state in crystal lattice). The *dipoles* (polar molecules), which change the orientation of their moments in the electrical field, and the *macro-dipoles*, which are the electrically charged radicals or complexes in the heterogeneous structures, also lead to the induced polarization.

At that, the electrons, ions and dipoles (including macro-dipoles) can acquire the induced electrical moment (i.e., polarized state) by the various mechanisms: (1) the *elastic* reversible displacement of tightly connected electrical charges, (2) the displacement of *weakly bound* charges during their participation in the chaotic

thermal motion, and (3) the *macroscopic* displacement of semi-free charges that later localize on the defects in a dielectric. Due to the large difference in the *characteristic times*, at which these mechanisms take place, it is possible to distinguish their contributions to the permittivity and to the delay frequencies of different polarization mechanisms.

Note that only the first of above-mentioned mechanisms is considered to be such ones that determine those properties of dielectrics, which are necessary for their functioning in high speed electronic devices. In this case, particles should be tightly connected in a structure, so the external electrical field or any other impact cause only a *very small* deviations (as compared with atomic dimensions) from the non-polarized equilibrium state. However, since in this process of the polarization *all particles* of a dielectric are involved, even these small displacements of charges result in a significant integral effect. That is why, the only mechanisms of *quasi-elastic polarization* can give need permittivity with a minimal dielectric losses necessary for the most modern applications of dielectrics. On the contrary, significantly slower mechanisms of the *thermal* (relaxation) polarization and the *migration* (space-charged) polarization can manifest themselves in a very broad frequency band – from infra-low frequencies to radio frequency range. At that, although these mechanisms increase permittivity, they show its decrease with frequency growing and give significant dielectric losses in both sound and radio frequency ranges.

4. *Electrical conductivity* appear, when the electrical field E is applied to a substance which have N *free* charge carriers per volume possessing by the charge q. Current density j, i.e., the electrical charge flowing per unit time through a unit area (oriented perpendicular to field direction) equals to $j = Nq\upsilon$, where υ is the speed of the *orderly* movement of charge carriers due to the action of electrical field. This *drift speed* is much less than the velocity of chaotic motion of charge carriers in a material being proportional to the electrical field strength: $\upsilon = uE$, where u is the *mobility* of charge carriers. According to Ohm's law, current density is proportional to the electrical field: $j = \sigma E$, where $\sigma = Nqu$ (measured in [S/m]) is the specific electrical conductivity. This quantitative characteristic of charge transport in matter determines the current density in a fixed electrical field.

Electrical field acts on the charge carrier by the force qE, therefore, carrier's movement increases its kinetic energy. However, the path and the time of charge carriers free movement in a material are limited by the "collisions" of carriers with atoms (molecules or ions); that is, by the interaction of charge carriers with the particles of a matter. In the crystalline dielectrics these collisions are described as

interaction with the phonons (lattice vibrations) or with the charged impurities, as well as with other electrically active structural defects. As a consequence, an accelerated motion of charge carrier is interrupted, and the energy acquired by it in the electrical field is dissipated. The average time of electrons free acceleration before the collision is the *relaxation time* (τ), becouse during this time the charge carrier returns to its state of thermodynamic equilibrium with a matter.

Due to the variety types of charged particles possible existing in a material, the quite different mechanisms of their generation (excitation) and the different mechanisms of charges move, the transfer of charged particles might be rather complicated physical phenomenon. In fact, among the *charge carriers,* the electrons, polarons, ions and molions (charged complexes of molecules) are distinguished. Their *generation* process might be thermal, optical, radiation or initiated by the electrical field, as well as the *recombination* process of charge carriers can be also realized through many different mechanisms. The peculiarities of charge carrier *movement* in the electrical field can also be different: drift, diffusion and hopping.

It is appropriate to note here that two important properties of dielectrics – the polarization and the conduction – are *largely interdependent*.

Firstly, the electrons or holes, appearing in a dielectric as a result of various activation processes, usually become less mobile, because their own electrical field *polarizes* the surrounding nano-size areas in a dielectric, so they are forced to move together with these polarized regions (creating polarons). Consequently, even such a small amount of free electrons, which appear in dielectric due to thermal activation of impurities, may not cause any appreciable charge transfer just because the *local polarization* clouds around the charge carriers arises, which reduce their mobility in the electrical field.

Secondly, low concentration of the charge carriers and their low mobility, in its turn, are responsible for a *long time existence of electrostatic field* in the dielectrics. In conductors this field is screened by the free charge carriers (in metals, for example, screening radius is approximately equals to inter-atomic distance). Thus, the electrical polarization contributes to the emergence and existence in the dielectrics a *relatively stable state with low electronic conduction*. However, this stability may be broken in dielectric by its heating or by the high intensity irradiation, particularly, by the coherent optical (laser) irradiation. At that, charge carriers are generated in a very high concentration, shielding electrical field, so the dielectric can be converted into a conductive medium. Stability of the non-conducting state of dielectrics may be compromised also by the strong electrical field, which accelerates freed electrons (or holes) up to the energy, at which they can no longer be "captured"

by the polarization of nano-size surroundings. These *fast electrons* cause the percussive ionization in a dielectric, resulting in the number of free electrons growing that ultimately gives rise to electrical breakdown, and insulator changes into a conductor.

2.2 Frequency dispersion of conductivity and permittivity

Changes in the electrical response parameters with increasing frequency is an inevitable process due to the inertia of particles, involved in the electrical charge transfer. In accordance with physical nature of charge carries and depending on properties of a material, the conductivity can both increase or decrease during frequency growth. The increase of $\sigma(\omega)$ is usually caused due to *delay of polarization mechanism*. This effect is conditioned by the close connection between processes of polarization and conduction, which, in principle, can be completely separated only at the direct voltage.

Two typical cases of interdependent changing with frequency of permittivity and effective conductivity in dielectrics are shown in Fig. 2.2 (it is assumed that conductivity at direct voltage is so small that it can be neglected).

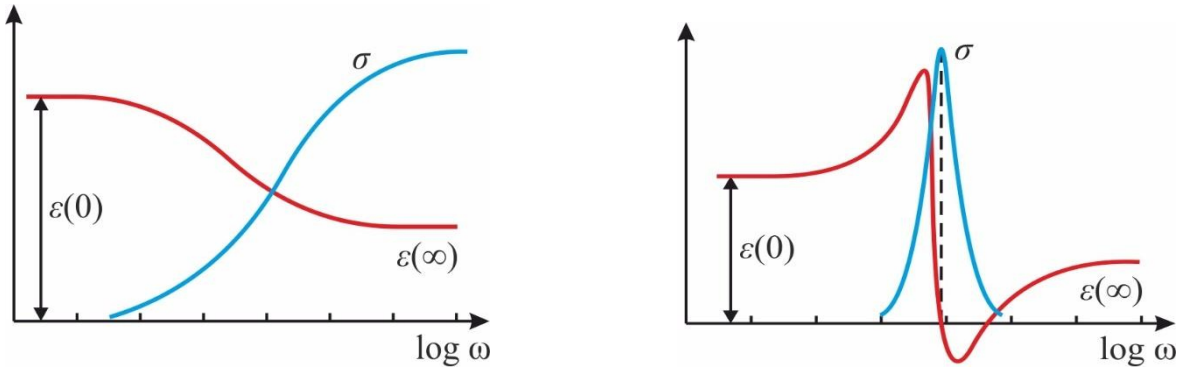

Fig. 2.2. Comparison of frequency dependence of permittivity and effective conductivity for two main models describing dielectric permittivity dispersion: A – relaxation, B – resonance

1. ***The relaxation dispersion*** of permittivity, Fig. 2.2A, consists in the $\varepsilon'(\omega)$ gradual decrease from its initial value of $\varepsilon(0)$ to the end value of $\varepsilon(\infty)$, when the relaxing polarization mechanism, giving the contribution $\Delta\varepsilon = \varepsilon(0) - \varepsilon(\infty)$, is completely delayed. At that, a gradual increase in the effective conductivity from almost zero to the constant value of $\sigma'_{ef} = \varepsilon_0\Delta\varepsilon/\tau$ is seen (τ is the relaxation time). This dependence of conductivity in the dielectrics and in wide-gap semiconductors usually are observed in a *broad* frequency range (10^{-4}–10^{8} Hz), being typical for quite different structures and various chemical compositions. Such a common

property of $\sigma(\omega)$ dependence is described by power law: $\sigma \sim \omega^n$, where $0.7 < n < 1$, established by A. Ionscher. This law is peculiar to low frequency polarization mechanisms, at which charged particles *move in a local area* in the dielectrics or semiconductor under the influence of *alternating* electrical field.

The fact is that some ions and polarons (i.e., electrons or holes bound in ionic lattice) while their "hopping" movement between the states of self-trapping (as well as dipoles in process of their rotational vibrations between several equilibrium positions separated by potential barriers) simulate the *increase* of effective conductivity when frequency grows. In the same way, other charged particles and complexes at their moving in the limited space under the influence of electrical field also bring to the frequency dependence of conductivity, described by formula $\sigma \sim \omega^n$. This means that directed by the electrical field thermally activated motion of partially bound charged particles (whose localization are determined by a set of potential barriers) gives rise to *both the polarization and the conduction.*.

At that, polarization predominates at comparatively low frequencies, since the entirely free movement of charged particles in almost constant electrical field is *limited* by the existing potential barriers (arising from structural defects and interfaces), which prevent the free carry of electrical charges from one electrode to another. Most of ions in a crystal (their concentration is $n \sim 10^{22}$ cm^{-3}) are located at their lattice sites; this position is rather stable and can not be disturbed by applied to crystal electrical field which causes only a slight shift of ionic sub-lattices (that constitutes the quasi-elastic polarization). However, any crystal, almost inevitably, contains a certain concentration ($n_0 << n$) of impurities or structural defects, so charged particles are loosely bound in crystal lattice. They can be located in the interstices (Frenkel defects) or represent the charged vacancies (Schottky defects). Just these weakly constrained ions cause the electrical conductivity, Fig. 2.3.

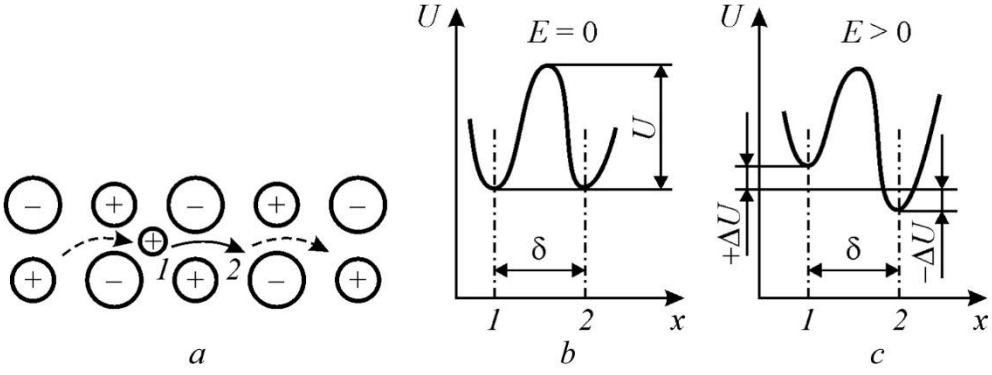

Fig. 2.3. Ionic conduction: *a* – small cation jumps over interstices, *b* – potential barrier in absence of electrical field; *c* – change in potential barrier in electrical field

Stimulating by thermal movement, the ionic conductivity is similar to the ionic polarization (which is thermally induced polarization). In fact, both

mechanisms (such as the ionic thermal polarization so the ionic electro-conductivity) are due to the *ions diffusion, supported by the electrical field*. The polarization prevails, if the potential barrier is big, but if the potential barrier is small the conductivity prevails. It should be noted that in real crystals structures, due to many reasons, there is a broad distribution of the heights of potential barriers, and it makes no sense to separate these processes.

In the case of a higher barriers (with predominance of polarization), with frequency grows at first one and then others kinds of charged particles do not have enough time (during a quarter of applied voltage period) to reach places of their next localization, and, therefore, they continuously follow *in phase* with the changing electrical field, already contribute to the conductivity. For this reason, the contribution of their motion tothe polarization is ceased, resulting in the dispersion (reduction) of the permittivity: $\varepsilon'(\omega)$ decreases with $\varepsilon''(\omega)$ increase, inasmuch as conductivity increases: $\sigma'(\omega) = \varepsilon_0\omega\varepsilon''(\omega)$. It looks as if the *polarization turned into conductivity*. Very flat increase of conductivity $\sigma'(\omega)$ in very broad frequency range, Fig. 2A, can be explained by the essential difference in the heights of potential barriers and sizeable distinction in the length of free paths of charged particles.

2. ***The resonant dispersion*** of permittivity, Fig. 2B, is characterized by the fact that at first the derivative $d\varepsilon'/d\omega$ is positive and next (at the resonance point) it changes sign to the negative value, but after the anti-resonance the derivative $d\varepsilon'/d\omega$ again becomes positive. Therefore, the permittivity passes through the maximum and minimum. In the region of resonance dispersion of permittivity, the effective conductivity is characterized by a sharp maximum $\sigma'_{max} = \varepsilon_0\Delta\varepsilon\omega_0/\Gamma$, locating *exactly at the resonance frequency* ω_0 of the oscillator describing this dispersion, Γ is the relative damping factor and $\Delta\varepsilon = \varepsilon(0) - \varepsilon(\infty)$ is the dielectric contribution of resonant polarization mechanism.

When resonant dispersion occurs, in its initial stage, the dielectric losses and effective conductivity increase due to a weakening of elastic bonds between ions of a lattice when resonance approaches. As a result, at same value of electrical field, the mutual shift of ions increases critically, and permittivity has a maximum. In the resonance frequency, the elastic bonds between ions no longer have enough time to manifest itself in a rapidly changing alternating electric field, so that the system of cations and anions looks like the “electrolyte” (so a maximum of conductivity is seen). Then, the phase of mutual displacement of ions changes in such a way that in the external alternating field the anti-resonance occurs, at which the dielectric contribution of oscillator becomes negative while the effective conductivity decreases. With the further increase in frequency the ionic lattice no longer manages

to respond to the rapid change of electrical field, but still the *electronic* quasi-elastic polarization of ionic cores establishes and provides a certain value of $\varepsilon(\infty)$.

Summing up, it should be noted that in case of gradual increase in frequency (that means the more rapid changing of electrical field) the *inertia* of charge carriers begins to affect, so their usual mode of movement at sufficiently high frequencies becomes impossible. At that, the large *charged complexes* have not enough time to move in phase with the applied electrical field already at subsonic frequencies (that is why the electrophoresis is used mainly at the direct voltage). The *ionic-type* conduction in dielectrics is late regarding the change in electrical field at radio frequencies, so that already at microwaves this conduction practically has no effect. The less inertia mechanism is the *electronic* conduction, but in the dielectrics this mechanism, for the most part, has the polaron character, so it is late at much lower frequencies than in the semiconductors.

Charge transfer mechanism in the weakly ordered systems (doped wide-gap semiconductors and dielectrics, as well as the polymeric materials) gradually changes with increasing frequency from the infra-low frequency range via the sound-frequency range (10^{-5}–10^{3} Hz) up to the radio frequency range (up to 10^{8} Hz). In this case, the mean free path of charge carriers movement in the electrical field varies from the *macroscopic* value (charge carries move from electrode to electrode) to the *microscopic* value (charge carries move between inter-atomic distances). When studying two complex parameters $\varepsilon^*(\omega,T)$ and $\sigma^*(\omega,T)$ in a broad range of frequencies and temperatures, we have:

$$\varepsilon^*(\omega,T) = \varepsilon'(\omega,T) - i\varepsilon''(\omega,T),$$
$$\sigma^*(\omega,T) = \sigma'(\omega,T) + i\sigma''(\omega,T),$$

The obtained dependences allow analyze the main mechanisms of charge transfer accompanied by the dielectric relaxation.

At that, in the solids with weakly ordered structure, the charge transfer occurs mostly due to the *hopping conduction*, which includes several mechanisms (the variable free pass when charge carrier hopping, the phonons assistance during hopping, etc.). It is important to note that charges motion in the disordered systems is obviously accompanied by the *electrical polarization* of a relaxation type that is clearly recorded in the dielectric spectra. One of the highly possible mechanisms is as follows: the ion or polaron, being weakly bound in a lattice and surrounded by the *screening cloud* of opposite sign charges, moves in a lattice by the jumps. At that, any jump of this polaron to a new position leads to the charge transfer only in those case, when it is followed by screening cloud of polarization, otherwise surrounding environment of such charge carrier counteracts directed jumps (in fact,

same jumps semi-free ion makes). The mobility of these partially bound charge carriers is hundreds of times less than the mobility of free charge carrier, i.e., their relaxation time τ is large in comparison with free charge carriers. Hopping conductivity is small until frequency of applied electrical field is lower than relaxation time ($\omega < 1/\tau$).

Although the conductivity of weakly ordered systems at low frequencies is small, a perceptible *electrical polarization* is created by them due to the displacement of semi-connected charges relatively its screening environment. So that the polarons or weakly bound ions contribute to the relaxation polarization, which manifests itself at low frequencies, but when frequency grows this polarization decreases, being accompanied by the increase in conductivity, Fig. 2A. The fact is that for the time, at which polaron under the influence of higher-frequency field manages to shift from its equilibrium position (or weakly bound ion displaces in a lattice), the *electrical field changes its sign*, so that all these charge carriers now are moving practically *in phase* with the applied alternating electrical field that in essence is the electrical conduction.

When discussing various aspects of conductivity, it should be noted that the *electronic conduction* can not be discovered in dielectrics in the infrared and optical frequencies: it is negligibly small as compared to bias (reactive) current conditioned by the polarization. However, the dispersion of electronic conductivity is clearly manifested in the metals. The normal (described by electronic band theory) electronic conduction in metals does not lead to any frequency dependence of conductivity over entire frequency range (up to terahertz) that is used in electronics. Nevertheless, when the frequency of electromagnetic field extremely increases, eventually the movement of electrons also *manifests their inertia*, but the dispersion of conductivity in metals has another character as compared to the dielectrics and semiconductors.

2.3 Conductivity and permittivity at plasma resonance in conductors

The resonant changes in the electrical response at optical frequencies can be seen in the metals, in other conductors (graphite, nanotubes, graphene, etc.) and in the semiconductors. In the above discussed cases, the $\sigma(\omega)$ *increase* (possible, of course, up to certain limit) was discussed due to the time-delay of the electrical polarization; however, next conductivity *decreases* with frequency rise. In what follows, the various mechanisms of $\sigma(\omega)$ decrease will be discussed, which become

apparent, as a rule, in the highest frequency region. In a rapidly changing electrical field, the *inertia* of charge carriers begins to affect, that is why, their movement at sufficiently frequency electrical field becomes no longer possible[).

[***Note.*** For comparison, it should be noted that the very slow *molions* do not have time to move in the electrical field already at sound-range frequencies, while the much faster ionic conductivity in solid and liquid dielectrics can hardly be detected already at microwave range. Since both the activation and motion of molions, ions and polarons in the dielectrics are caused by the chaotic thermal motion of these charge carriers (which in this case must overcome local potential barriers with relaxation time τ), then, with the increase in electrical field frequency ω, the situation inevitably changes when $\omega > 1/\tau$, and aforementioned charge carriers simply do not have time to move, so the conductivity decreases with increasing frequency, rarely remaining at frequency of 10^9 Hz].

Quite different situation arises with the highly mobile electrons in metals and semiconductors. Exposure to them by a high-frequency electrical field leads to the *plasma resonance,* and to dispersion of electronic gas conductivity (in dielectrics, electronic conduction has a polaronic nature and "lags" at lower frequency). The least inertia of "free" electrons is a characteristic of metals and other conductors (graphite, graphene, etc.), which widely used in electronics as inter-connectors and components of absorbing microwave composites. In the semiconductors, the *more less dense* electronic plasma leads to the resonance phenomena and dispersion at the *optical* frequencies.

It is important to note that the inertia of electrons can be detected by the dielectric spectroscopy methods. When the charge carries show their inertia, the *decrease* of conductivity is seen; at that, in usual metals their conductivity decreases in the *ultraviolet* wavelength range (above 10^{16} Hz), so the *electronic polarizability of the deep ionic shells* in the ionic lattice of metal becomes noticeable. Nevertheless, in the *weakly conducting* metals and, especially, in the finely *dispersed* metals (usually used in the absorbing composites), the inertia of electronic conductivity may appear already in the range of millimeter waves and even at microwaves.

The following is a simplified model, which describes the conductivity by using a conception of the *electronic plasma in solids*. The plasma is a system of positive and negative charge carriers; at that, the plasma can be *charged* (like electronic plasma in the metals) or *neutral* (like the electron-hole plasma in the semiconductors). The density of the charge carriers in charged plasma can reach 10^{22} cm^{-3}, while in the case of neutral plasma charge carries density might be 10^{15}–10^{18} cm^{-3}. The plasma can be considered as a subsystem, which can interact with crystal

lattice that facilitates its properties study. Characteristic property of plasma is the presence of the *collective excitations* – plasma oscillations.

The model of Langmuir oscillations in the electronic plasma of metals supposes that the *returning force* arises, when the group of electrons possessing charge *e,* mass *m,* and density *N* shifts from their equilibrium position on a some distance relatively to positively charged "non-moving" ionic lattice (in particular, this displacement can be induced by the external electrical field). The returning force, acting on the displaced group of electrons, causes the oscillations of electrons around their equilibrium position with a plasma frequency $\omega_{pl} = (Ne^2/m\varepsilon_0)^{1/2}$.

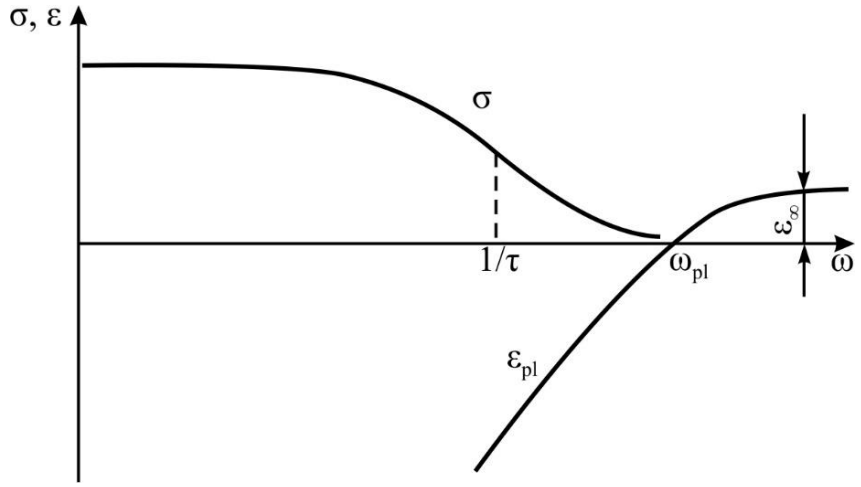

Fig. 2.4. Conductivity σ and effective permittivity ε_{pl} frequency dependence in metals in the vicinity of plasma resonance

Experiment indicates that electronic gas in metals demonstrates its inertia at frequencies of 10^{16}–10^{17} Hz: at higher frequencies electrons have no time to follow electromagnetic field changing. That is why, *above* the plasma frequency it is possible to determine in metal the *dielectric permittivity* ε_{uv} arising due to the elastic displacement of the non-collectivized electrons (bound electronic shells inside ionic cores).

Thus, the conductivity $\sigma(\omega)$ of metals (and other high-conductive materials used in electronics as the inter-connectors, in waveguides, antennas and as components of absorbing microwave composites) has almost *constant value* $\sigma(0)$, which defines the *ohmic losses* of conductor in the broad frequency range including the terahertz range. With a further increase in frequency, a smooth *decrease* of conductivity up to zero is observed (in metals it is seen in the ultraviolet part of a spectrum), accompanied by the increase of permittivity, which from their negative value becomes positive.

The high-frequency properties of metals can be found using simple Drude-Langmuir model for free charge carriers absorption in metals, from which for *complex permittivity* follows:

$$\varepsilon^*(\omega) = -(Ne^2/m\varepsilon_0)/(\omega^2 - i\omega\gamma) = -\omega_{pl}^2/(\omega^2 - i\omega\gamma) \qquad (2.5)$$

where N is the concentration of charge carries, e is their charge, m is the effective mass, $\gamma = 1/\tau$ is the damping factor of plasma oscillation, τ is the scattering (life) time of charge carries, ω_{pl} is plasma resonant frequency, and ω is angular frequency.

Accordingly, from the above model, the *complex conductivity* can be determined: $\sigma^*(\omega) = i\omega\varepsilon_0\varepsilon^*(\omega)$, or otherwise

$$\sigma^*(\omega) = \frac{\sigma(0)}{1 + i\omega\tau}, \text{ where } \sigma(0) = \frac{Ne^2\tau}{m} = \varepsilon_0\omega_{pl}^2\tau \qquad (2.6)$$

The lower frequency conductivity $\sigma(0)$ remains frequency independent in the case when $\omega << 1/\tau$, i.e., practically in the entire frequency range used in electronics. At that, the conductivity makes contributions both to the real and the imaginary parts of permittivity:

$$\varepsilon'_{pl}(\omega) = \varepsilon_{uv} - (\omega_{pl}\tau)^2,$$

$$\varepsilon''_{pl}(\omega) = \omega_{pl}^2\tau/\omega, \qquad (2.7)$$

where ε_{uv} is the contribution to permittivity given by the polarization of deep electronic shells of ions making up metal crystal lattice (ε_{uv} is detectable only in the ultraviolet frequencies). Thus, in the metals and other conductors, the plasma contribution to the permittivity is *negative,* while the plasma contribution to losses, of course, is positive but at low frequencies (far from resonance) it is very small.

Graphs of the $\sigma(\omega)$ and $\varepsilon(\omega)$ changing are shown in Fig. 2.4: frequency behavior of *conductivity* resembles the *relaxation* dispersion of permittivity: at the frequency $\omega = 1/\tau$ conductivity decreases by a half while near the frequency of plasma resonance conductivity vanishes. However, the frequency dependence of plasma contribution to *permittivity* resembles the *resonance* dispersion, but only *above* the natural frequency of correspondent oscillator. The fact is that in electrically conductive media below the frequency of plasma resonance the charge carriers *shield electrical field*, so the phase of their displacement in the applied alternating field corresponds to *negative* contribution into permittivity, which is the greater the higher concentration of charge carriers and lower frequency.

In the frequency of plasma resonance ($\omega = \omega_{pl}$), the permittivity of metal equals zero: $\varepsilon'(\omega) = 0$ due to the *compensation* of negative dielectric contribution from free charge carriers by the positive contribution to permittivity from the polarization of ionic cores: $\varepsilon_{cor} = \varepsilon(\infty)$. When frequency increases above ω_{pl}, the

permittivity ε_{cor} gradually gets its full value; next, with a subsequent increase in the frequency and its approach to the *X*-ray values, *any* polarization mechanism has no time for establishing, so $\varepsilon'(\omega) \to 1$.

It is worth noting that plasma oscillations of electrons can be *quantized,* so the model of quasi-particle can be introduced: the *plasmon*, which is the elementary excitation of plasma oscillations. The formula for the plasma resonance frequency $\omega_{pl} = (Ne^2/m\varepsilon_0)^{1/2}$ shows that it is proportional to the square root of charge carriers concentration. In the highly conductive metals ($N \sim 10^{22}$ cm^{-3}), this frequency is located in the ultraviolet part of a spectrum, but for the weakly conducting metals the frequency ω_{pl} is lower. In the semiconductors, which have charge carrier concentration of 10^{15}–10^{17} cm^{-3}, the plasma resonance frequency is seen in the visible optical range. At that, the *effective mass* of charge carriers has an essential influence on the resonance frequency, so that in the semiconductors, possessing small effective mass of electrons, the frequency of plasma resonance is increased.

Since at the frequency of plasma resonance, dielectric permittivity $\varepsilon(\omega)$ vanishes, the reflection of the electromagnetic waves from crystal, when $\varepsilon(\omega) = 1$, is absent; in practice, this means that a quasi-particle – plasmon – leads to a minimum of reflection coefficient of semiconductors in the optical range. That is why, the frequency ω_{pl} can be determined from a minimum of optical reflection, characterizing by the ratio of charge carriers *concentration* to their *effective mass*.

Besides, in the *heavily doped* semiconductors, the presence of free charge carriers *decreases* their optical refractive index. Such a negative contribution of electronic plasma to the permittivity at optical frequencies is especially significant in those semiconductors, in which the effective mass of electrons is small (usually these are the semiconductors of $A^{III}B^{V}$ type). Effect of plasma onto the refractive index decrease is used in the integrated optics to obtain the planar optical light guides. All these features are manifested in the semiconductors but in the dielectrics, due to a low concentration and very small mobility of charge carriers, the plasma oscillations are practically irrelevant.

2.4 Permittivity and conductivity interconnection at dielectric polarisation

As already noted, in the electrical field applied to dielectric, both free and bound electrical charges move. If electrical field is alternating, and especially in the case high-frequency variation external field, the motion of charged particles, which can be as bound in the structure so relatively free, makes the contributions to both

active and reactive electrical currents, that is, it affects both the dielectric permittivity and conductivity.

1. ***Dielectric losses conditioned by DC conductivity*** can be described by next simple mechanism. While directed movement of charges carriers (i.e., their drift or diffusion in the external field), the carriers at their free path get energy from electrical field. Acquired energy is spent in the "collisions", that are, actually, the interactions of charges carriers with the atoms, ions or molecules, which are in a state of thermal motion.

Giving back acquired energy during these collisions, charge carriers increase the intensity of chaotic motion of particles of matter; therefore, the temperature of dielectric increases. For this reason, the electrical conductivity σ increases the dielectric loss factor ε'', loss tangent $\tan\delta$ and loss specific power p (energy dissipation per unit volume). Corresponding formulas are:

$$\varepsilon'(\omega) = \varepsilon(0) = \varepsilon(\infty); \qquad \varepsilon''(\omega) = \sigma/(\varepsilon_0\omega);$$

$$\tan\delta(\omega) = \sigma/(\varepsilon_0\varepsilon\omega); \qquad p(\omega) = E^2\varepsilon_0\varepsilon\omega\tan\delta = \sigma E^2.$$

It follows that conductivity determines the loss factor ε'' and the loss tangent $\tan\delta$ mainly at *lower frequencies*: both of these parameters decrease with frequency as $1/\omega$.

However, the loss specific power $p \sim \sigma$ in this case does not depend on frequency, because it is a product of the frequency independent conductivity and squared electrical field ($p = \sigma E^2$). Thus, the reducing of ε'' and $\tan\delta$ with increasing frequency no means the reduction of loss specific power p with increasing frequency, as this parameter does not depend on frequency.

Frequency characteristics of considered parameters are shown in Fig. 2.5A. In the case when no absorption mechanisms exists other than the electrical conductivity, the permittivity is determined only by the fast polarization processes: $\varepsilon(\omega) = \varepsilon(\infty)$, being independent on frequency. Temperature dependences of losses parameters in the case, when the predominant mechanism of losses is the electrical conductivity, are shown in Fig. 2.5B. All of them, except $\varepsilon(\omega) = \varepsilon(\infty)$, show the exponential increase with temperature, since just by this law the conductivity varies with temperature. It is seen also that the electrical conductivity contributes significantly to the $\tan\delta$ and ε'' at *higher temperatures* and at *lower frequencies*.

At very low temperatures and at very high frequencies the contribution of conductivity to the dielectric losses usually is so small that it can be neglected.

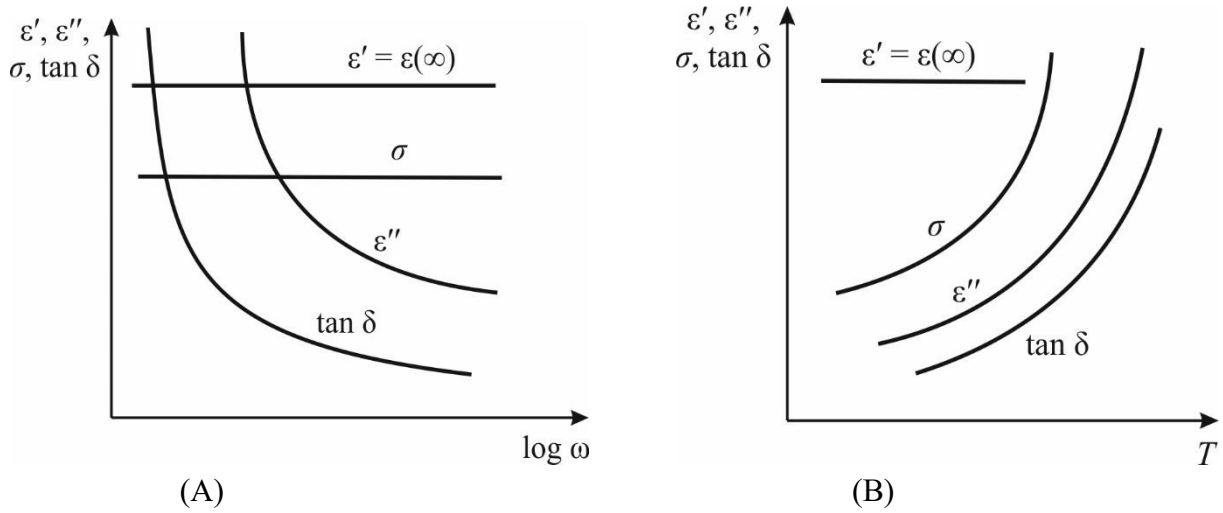

Fig. 2.5. Frequency (A) and temperature (B) dependence of dielectric basic parameters (losses due conductivity dominate in ε'' and tanδ

In the present-day electronics, the dielectrics and semiconductors are widely used in the microwave technique. Usually their permittivity ($\varepsilon = \varepsilon'$) is independent on frequency. For the losses of semiconductors the conductivity dominates; at that, their high frequency conductivity due to high mobility of electrons is independent on frequency including terahertz range. The loss coefficient $\varepsilon'' = \sigma/(\varepsilon 0\omega)$ and the $\tan\delta = \sigma/(\varepsilon 0\varepsilon'\omega)$ decrease with frequency, Fig. 2.5A, because the active component of current ja is frequency independent, while the reactive component jr linearly increases with frequency while tanδ = ja/jr. If in specified frequency range given dielectric has no relaxation or resonant ε-dispersions, the parameter $\varepsilon'(\omega)$ remains constant, while the loss factor $\varepsilon''(\omega)$ depends on the conductivity σ and decreases with increasing frequency:

$$\varepsilon^*(\omega) = \varepsilon' - i\frac{\sigma}{\omega\varepsilon_0},$$

This equation is not a dispersion one, inasmuch as describes only the $\varepsilon''(\omega)$ dependence that is *not concerned* with ε' = const. Therefore, in the case when σ is independent on frequency, the conductivity *does not contribute to the real part of permittivity*.

2. ***Effective conductivity conditioned by thermally activated polarization.*** In this model, it is assumed that the DC electrical conductivity is absent, but at the alternating voltage the active current in a dielectric appears due to the polarization lagging in time. Relaxation polarization is caused by a local electro-diffusion process, at which weakly bounded charges are accumulated in localized states (or dipoles are directionally oriented). Being supported by thermal movement, this type of polarization is settled rather slowly. Relaxation time of this polarization varies

with temperature but lies in the limits of 10^{-3}–10^{-9} s. Thus, distinguishing frequency of molecular relaxation processes in such dielectrics may be located just in a such frequency range, where dielectrics are used in electrical engineering and electronics (50 Hz–100 GHz).

Dielectric relaxation at thermal and migration polarization is described by the Debye equations

$$\varepsilon^*(\omega) = \varepsilon' - i\varepsilon'' = \varepsilon(\infty) + \frac{\varepsilon(0) - \varepsilon(\infty)}{1 + i\omega\tau}$$

where $\varepsilon(0)$ is the permittivity before dielectric dispersion (at $\omega \to 0$) while $\varepsilon(\infty)$ is the permittivity after this dispersion (at $\omega \to \infty$) while τ is the relaxation time. After dividing on real and imaginary parts, Debye equation looks like:

$$\varepsilon'(\omega) = \varepsilon(\infty) + \frac{\varepsilon(0) - \varepsilon(\infty)}{1 + \omega^2\tau^2}, \quad \varepsilon''(\omega) = \frac{\left[\varepsilon(0) - \varepsilon(\infty)\right]\omega\tau}{1 + \omega^2\tau^2} = \sigma ef(\omega)/(\varepsilon 0\omega),$$

where $\sigma ef(\omega)$ simulates electrical conductivity of a dielectric, i.e., characterizes the active component of electrical current arising due to polarization time-lag (in the accepted notation $\sigma ef(\omega) = \sigma'(\omega)$, Fig. 2.6B.

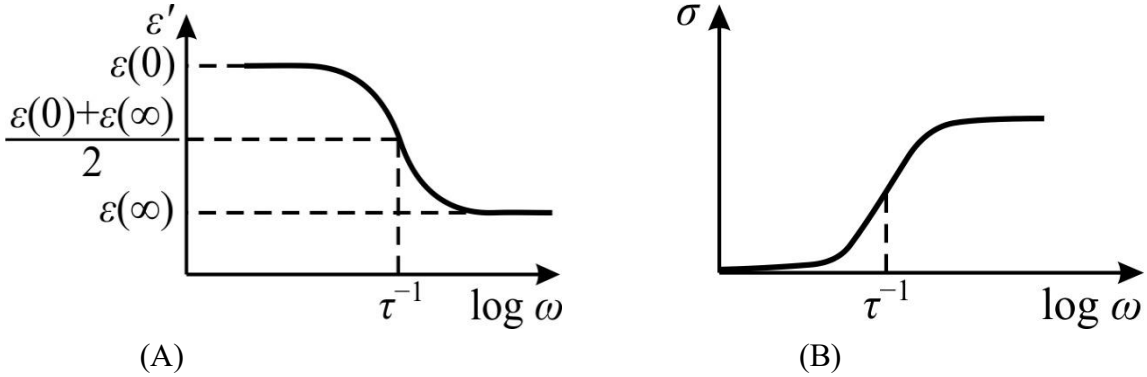

(A) (B)

Fig. 2.6. Permittivity (A) and effective conductivity (B) at relaxation polarization dispersion

From Fig. 6 it follows that at low frequencies (when relaxation polarization is totally settled in time and $\varepsilon'(\omega) \approx \varepsilon(0)$), the effective conductivity $\sigma'(\omega)$ vanishes; next it increases with frequency growing and when $\omega = 1/\tau$ (in centre of dispersion) $\sigma' = \varepsilon_0\Delta\varepsilon/2\tau$ where $\Delta\varepsilon = \varepsilon(0) - \varepsilon(\infty)$. At higher frequencies, when $\varepsilon'(\omega) \approx \varepsilon(\infty)$, the effective conductivity reaches its saturation: $\sigma' = \varepsilon_0\Delta\varepsilon/\tau$, and next becomes independent on frequency (of course, within certain limits).

3. ***Effective conductivity conditioned*** by resonant polarization. As in previous model, it is further assumed that DC electrical conductivity is absent but at the alternating voltage an active current (and hence the effective conductivity) arises in

the vicinity of polarization resonance. Resonant dispersion at oscillator frequency ⎤0 = ⎤TO can be described by the Lorentz expression:

$$\varepsilon^* = \varepsilon' - i\varepsilon'' = \varepsilon(\infty) + \frac{\varepsilon(0) - \varepsilon(\infty)}{1 - \left(\frac{\omega}{\omega_{TO}}\right)^2 + i\Gamma\frac{\omega}{\omega_{TO}}}$$

where ω_{TO} is the transverse optical frequency, Γ is the relative attenuation and the difference $\varepsilon(0) - \varepsilon(\infty) = \Delta\varepsilon$ characterizes the dielectric contribution of resonant polarization mechanism. Turning to the analysis of frequency dependence of $\varepsilon'(\omega)$ and $\sigma'(\omega) = \omega\varepsilon_0\varepsilon''(\omega)$, it is necessary to separate in the above equation real and imaginary parts of complex permittivity:

$$\varepsilon'(\omega) = \varepsilon(\infty) + \frac{\left[\varepsilon(0) - \varepsilon(\infty)\right]\left(1 - \frac{\omega^2}{\omega_{TO}^2}\right)}{\left(1 - \frac{\omega^2}{\omega_{TO}^2}\right)^2 + \Gamma^2\frac{\omega^2}{\omega_{TO}^2}}; \quad \varepsilon''(\omega) = \frac{\left[\varepsilon(0) - \varepsilon(\infty)\right]\Gamma\frac{\omega}{\omega_{TO}}}{\left(1 - \frac{\omega^2}{\omega_{TO}^2}\right)^2 + \Gamma^2\frac{\omega^2}{\omega_{TO}^2}};$$

from which it follows that effective conductivity is

$$\sigma(\omega) = \frac{\left[\varepsilon(0) - \varepsilon(\infty)\right]\omega_0\varepsilon_0}{\Gamma}\frac{\Gamma^2\left(\frac{\omega}{\omega_0}\right)^2}{\left[1 - \left(\frac{\omega}{\omega_0}\right)^2\right]^2 + \Gamma^2\left(\frac{\omega}{\omega_0}\right)^2}$$

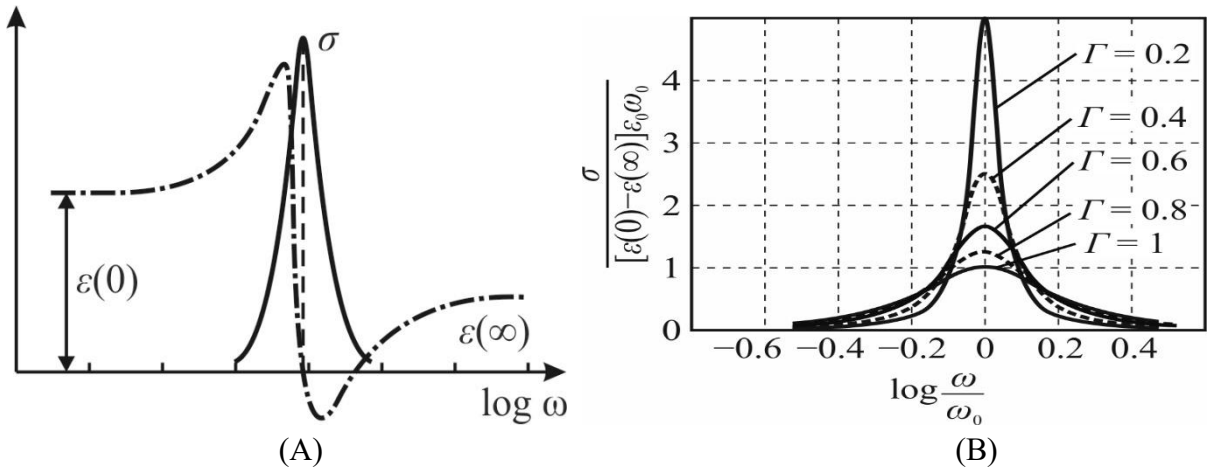

Fig. 2.7. Permittivity (ε) and effective conductivity (σ) frequency dependence for resonance mechanism of polarization (A) and conductivity maximum dependence on damping coefficient (B)

Analysis shows that the maximum of effective conductivity for any amount of attenuation is located exactly at the resonant frequency of the oscillator, Fig. 2.7A. The frequency dependence of oscillator effective conductivity normalized to the dielectric contribution in case of different values of relative attenuation is shown in Fig. 2.7B.

2.5 Summary and self-test questions

1. In the alternating electrical field, the electrically induced displace and move of charged particles lead to both an active and a reactive electrical current, that is characterized usually by the *complex* permittivity, but also can be described by the *complex* conductivity; between these complex parameters an unambiguous relationship can be established. Both of these methods of a describing of electrical reaction of substance to applied electrical field are equivalent.

2. Electrical field E applied to a substance induces in it several reversible and irreversible physical phenomena: not only of electrical nature but also the mechanical and thermal responses. Among the *electrical* responses, one is the reversible: the electrical induction $D(E)$ describing by the dielectric permittivity $\varepsilon = D/(\varepsilon_0 E)$ while another is the irreversible response - the electrical current $j(E)$ described by the conductivity $\sigma = j/E$.

3. Electrical polarization is the charge separation while electrical conductivity is the charge transfer. At an alternating voltage, the connection between conductivity and polarization is obvious, since both of these phenomena are due to limited (polarization) and almost-free (conductivity) movement of electrical charges in a matter, and in both cases the inertial phenomena affect these movements.

4. To be described in the *sinusoidal* electrical field $E(\omega) = E_0 \cdot \exp(i\omega t)$, both the dielectric displacement and the conduction can be represented by the *complex parameters.* One of Maxwell-Lorentz equations: rot $H = j + \partial D/\partial t$) shows that current density j and time derivative of electrical displacement $\partial D/\partial t$ are the *additive quantities*. That is why, the current density $j = \sigma^* E$ and $\partial D/\partial t = i\omega\varepsilon_0\varepsilon^* E$ would be represented as the *equivalent functions*, if the complex values will be used to describe them.

5. Material's properties are usually characterized by the *complex permittivity* $\varepsilon^*(\omega)$, but can also be described by the *complex conductivity* $\sigma^*(\omega)$. When these functions are represented by their real and imaginary parts, the complex conductivity is connected to the complex permittivity:

$$\sigma^*(\omega) = \sigma'(\omega) + i\sigma''(\omega) = i\omega\varepsilon_0\varepsilon^*(\omega), \quad \sigma'(\omega) = \varepsilon_0\omega\varepsilon''(\omega); \quad \sigma''(\omega) = \varepsilon_0\omega\varepsilon'(\omega).$$

$$\varepsilon^*(\omega) = \varepsilon'(\omega) - i\varepsilon''(\omega), \quad \varepsilon'(\omega) = \sigma''(\omega)/(\varepsilon_0\omega), \quad \varepsilon''(\omega) = \sigma'(\omega)/(\varepsilon_0\omega).$$

Mostly, to describe materials parameters frequency dependence the complex *permittivity* is used.

6. Thermally activated motion of charged particles, whose localization is determined by a set of potential minima and barriers, in the external electrical field

give rise to *both conduction and polarization*. Polarization process predominates at lower frequencies, but when frequency grows the permittivity decreases that is accompanied by the correspondent increase of conductivity; it looks as if polarization turned into conductivity.

7. Frequency dependence of effective conductivity $\sigma'_{ef}(\omega)$ can be useful evidence of physical nature of the polarization mechanisms. In the case of relaxation polarization, in the region of dispersion $\sigma'_{ef}(\omega)$ gradually increases to a certain limiting constant value: $\sigma'_{ef} = \varepsilon_0 \Delta\varepsilon / \tau$. In the case of resonant polarization $\sigma'_{ef}.(\omega)$ also increases, but it quickly reaches a maximum $\sigma'_{max} = \varepsilon_0 \Delta\varepsilon\omega_0 / \Gamma$ at the resonance frequency ω_0, and then decreases with frequency grows.

8. Inertia of charge transfer mechanisms can be clearly detected by dielectric spectroscopy methods, including movement of *electrons in metals*. When charge carries show their inertia, the conductivity decreases; in metals conductivity decreases in the ultraviolet wavelength range so even the electronic polarizability of deep ionic shells in ionic lattice of metal becomes noticeable. In the doped semiconductors, the presence of free charge carriers decreases the refractive index: this negative contribution of plasma to the permittivity is seen at optical frequencies. In dielectrics, due to a low concentration and small mobility of charge carriers, the plasma oscillations are practically imperceptible.

Chapter 2. Self-test questions

1. Why is there a reciprocal relationship between complex permittivity and complex conductivity?
2. Under what conditions can the dielectric constant and the conductance be completely separated?
3. Under what conditions can the dielectric constant of different metals be compared?
4. Which of the field-induced displacements of charged dielectric particles are related to polarization and which to conductivity?
5. In what sense can the dielectric permittivity of a metal be interpreted as "negative"?

CHAPTER 3. DYNAMICS OF ELECTRICAL POLARIZATION

Contents

The main physical property of dielectrics is their *electrical polarization*. For the application of dielectric materials in high-frequency electronics and information technology, the dynamic properties of polarization are most important, which can be described both phenomenological and through the models representations. Dynamic polarization models are applicable to the rather complex objects - ferroelectrics.

Ferroelectric materials are widely used in electronics in hundreds of different devices. The requirements for the properties of these materials can be very diverse, and therefore, when developing their composition and technology, it is necessary to use various physical research methods, including dielectric spectroscopy. To evaluate the obtained spectra, it is necessary to know the fundamentals of physical mechanisms that determine certain parameters of the materials under study. A brief description of these mechanisms, based on the classical and modern concepts as to the nature of polarization, precedes the description of selected dielectric spectra.

The necessary information and examples of dynamic properties of basic ferroelectrics with an *order-disorder* phase transition are given. Rather complete consideration is devoted to the dynamic properties of polarization and the main parameters of the *paraelectrics*. A brief description of the physical properties of ferroelectrics with a phase transition of the *displacive* type is given, with the illustrations of how these properties are reflected in the dynamic properties that is necessary to predict application of electronic materials based on these ferroelectrics.

Dielectric properties and mechanisms of polarization of *antiferroelectrics* can also be of interest not only for the physics of condensed matter, but also for their use as the components of piezoelectric and thermoelectric materials. The *relaxor ferroelectrics*, in which the record dielectric, electromechanical and electro-optical

parameters have been achieved, are of greatest scientific and technical significance and, at the same time, the greatest difficulty for research.

3.1 Polarization based on relaxor model

Since not empirical but the model approach is discussed later for the description dielectric permittivity and loss factor frequency and temperature dependence, it is reasonably to start this discussion with the essence of the elementary model of dielectric relaxation.

1. ***Frequency dependence of main relaxor parameters.*** The "*relaxor"* is idealized physical model, which describes an electrical response, characterizing a *gradual* establishment of equilibrium in the system of dipoles perturbed by the electrical field in a condition of thermal chaotic motion. Main parameters of relaxor are the contribution to dielectric permittivity $\Delta\varepsilon$ (*dielectric strength*) and the characteristic time τ (*relaxation time*) of a response to disturbance (or relaxation frequency $\Omega = 1/\tau$). To describe frequently observed in experiments broadband frequency dispersion of dielectric permittivity $\varepsilon(\omega)$, the parameter of the relaxation time *distribution* ς can be added to listed parameters.

The dependence of relaxor parameters ($\Delta\varepsilon.$, τ and ς) on the intensity of thermal motion in a system of dipoles (or polar complexes) means their strong dependence on the temperature. Indeed, the overcoming potential barriers during reorientation of dipoles, or jumps of weakly bound electrons and ions is energetically provided by the fluctuations of thermal motion, while the electrical field only creates the directionality of these transitions. At the sufficiently low temperatures any thermal motion almost ceases, so that relaxation time increases extremely, usually going beyond experimental possibilities of its definition. On the other hand, at the sufficiently high temperatures, very intense thermal motion converts the relaxation polarization into the ionic or electronic conductivity, since local potential barriers already cannot keep free movement of charged particles. Therefore, the temperature interval of 100–600 K can be considered as a limit for relaxor model application to describe dielectrics polarization. Another important consequence of chaotic nature of the relaxation polarization is extended frequency range of its manifestation.

When relaxor model justifying, it is supposed that in the dielectric a system of *non-interacting* dipoles exists, characterizing by dipole moment and subjected to the chaotic thermal motion, causing these dipoles *dynamic reorientation*. If the constant electrical field $E = E_0$ acts on such dielectric, then it forces the orientation of definite part of dipoles, creating the induced electrical polarization $P = P_0$, Fig.

3.1A, where exact moment of electrical field switching on is not considered. In the applied electrical field E_0 a lot of dipoles in a dielectric are continuously orienting and disorienting, however, in average, the polarized state with the value P_0 remains thermodynamically stable.

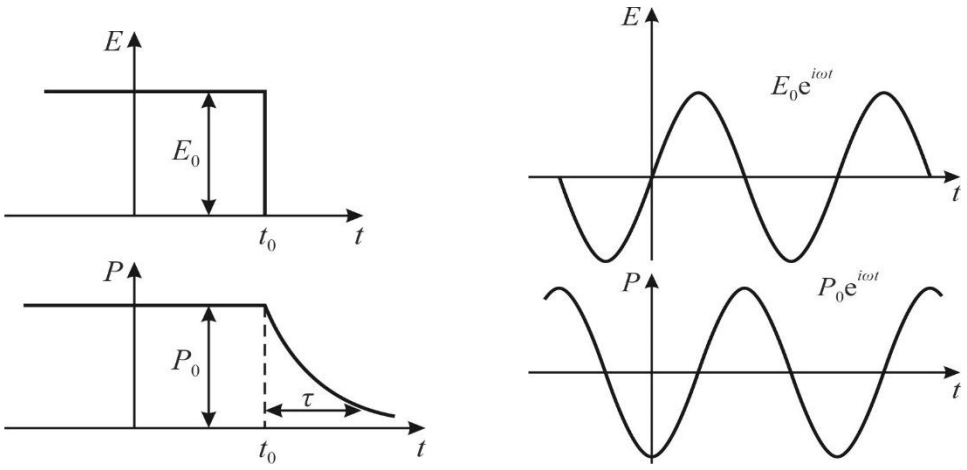

Fig. 3.1. Time-dependence of relaxor polarization *P* under the influence of constant (A*a*) and alternating (B) electrical field *E*

Suppose that at the moment $t = t_0$ the electrical field is turned off; as a result, the chaotic thermal motion leads to a gradual *depolarization* of dielectric. At that, a new equilibrium state (not disturbed by electrical field) will be already non-polarized. The principle of thermodynamics states that the *rate of recovery* of the equilibrium state is proportional to the magnitude of a deviation from this state, i.e., $dP/dt = -kP$. The dimension of proportionality coefficient k is the inverse value to time so it can be denoted as $k = \tau^{-1}$. Therefore, differential equation, describing the gradual decrease of polarization when it approaches to the equilibrium state, is $dP/dt = -(1/\tau)P$. The solution of this equation results in description of the time-dependent *gradual decay* of polarization:

$$\frac{dP}{dt} = -\frac{1}{\tau}P; \qquad \frac{dP}{P} = -\frac{dt}{\tau}; \qquad P(t) = P_0 e^{-\frac{t}{\tau}}$$

Frequency dependent dielectric permittivity can be found, if the *alternating* electrical field $E(\omega)$ acts on the model under consideration (system of non-interacting dipoles), taking into account the definition of permittivity as the proportionality coefficient between the electrical displacement (induction) D and electrical field E:

$$D = \varepsilon_0 \varepsilon E = \varepsilon_0 E + P; \quad \varepsilon = 1 + P/\varepsilon_0 E. \qquad (3.1)$$

where ε_0 is the *electrical constant* used in SI system. Thus, to determine permittivity, it is necessary to find the ratio $P/\varepsilon_0 E$. For this purpose, as shown in Fig. 3.1B, the

sinusoidal (harmonic) dependence of electrical field of frequency ω should be used: $E(\omega) = E_0\exp(i\omega t)$, which in the *linea*r case (correspondent to weak electrical field) leads to similar dependence of induced polarization $P(\omega) = P_0\exp(i\omega t)$.

To find the frequency dependence of permittivity, it is necessary to solve first-order inhomogeneous differential equation:

$$\frac{dP}{dt} + \frac{1}{\tau}P = gE_0e^{i\omega t}$$

where coefficient g is the *reactive conductivity*, which, as seen from the dimension of dP/dt, is the *density of current* while E is the electrical field (Ohm's law). When solving this equation, the transient processes are not considered, so by substituting $P(\omega) = P_0\exp(i\omega t)$ it is possible to get

$$\varepsilon(\omega) = 1 + \frac{P}{\varepsilon_0 E} = 1 + \frac{g\tau\ /\ \varepsilon_0}{1 + i\omega t}$$

Relative permittivity of vacuum is $\varepsilon = 1$, but it should be replaced by the contribution to the permittivity of fast polarization $\varepsilon(\infty)$, because the relaxor is located in dielectric medium, which is characterized, except slow dipole polarization, by others high frequency polarization processes. The numerator $g\tau/\varepsilon_0$ in the above formula is the dielectric contribution of relaxor: $\Delta\varepsilon = \varepsilon(0) - \varepsilon(\infty)$, while $g = n_0\alpha_T$ is determined by dipoles concentration n_0 while their temperature-dependent polarizability is α_T. The *dipole* relaxation polarization equals $\alpha_{dT} = \mu_0^2/3k_BT$, for the *electronic* relaxation polarization it is $\alpha_{eT} = e^2\delta^2/12k_BT$ while for the *ionic* relaxation polarization polarizabily equals $\alpha_{iT} = q^2\delta^2/12k_BT$ (i.e., the polarizability in all listed cases *decreases with temperature*: $\alpha_T \sim T^{-1}$). This feature should be taken into account when studying dielectric properties in the temperature range.

The obtained result corresponds to the *Debye formula*, which describes the frequency dependence of *complex permittivity* consisting of real $\varepsilon'(\omega)$ and imaginary $\varepsilon''(\omega)$ parts:

$$\varepsilon^*(\omega) = \varepsilon(\infty) + \frac{\varepsilon(0) - \varepsilon(\infty)}{1 + i\omega\tau} \qquad (3.2)$$

From expression (3.2) the main formulas describing frequency dependence of tangent of dielectric loss angle (tanδ) and the specific power of losses p follow:

$$\varepsilon'(\omega) = \varepsilon(\infty) + \frac{\varepsilon(0) - \varepsilon(\infty)}{1 + \omega^2\tau^2}; \qquad \varepsilon''(\omega) = \frac{\left[\varepsilon(0) - \varepsilon(\infty)\right]\omega\tau}{1 + \omega^2\tau^2}.$$

$$\tan\delta = \frac{\left[\varepsilon(0)-\varepsilon(\infty)\right]\omega\tau}{\varepsilon(0)+\varepsilon(\infty)\omega^2\tau^2}; \qquad p(\omega) = \varepsilon_0\varepsilon''\omega E^2.$$

These expressions can be used for ε', ε''', tanδ and p frequency dependences investigation. When describing the $\varepsilon'(\omega)$ dependence, one can see that at low frequency $\varepsilon'(\omega) \to \varepsilon(0)$, while at higher frequency $\varepsilon'(\omega) \to \varepsilon(\infty)$. At the frequency $\omega = 1/\tau$ the dielectric contribution of relaxor $\varepsilon_{rel} = \varepsilon(0) - \varepsilon(\infty)$ is halved, Fig. 3.2A. From $\varepsilon'''(\omega)$ dependence it follows that $\varepsilon''' \to 0$ both at very low frequencies (when $\omega \to 0$) and at very high frequencies (when $\omega \to \infty$), Fig. 2C. By examining the derivatives $d\varepsilon'''/d\omega$ and $d^2\varepsilon'''/d\omega^2$, it is easy to show that $\varepsilon'''(\omega)$ has the *maximum* at frequency $\omega = 1/\tau$, i.e., exactly at the frequency, when dielectric contribution of relaxor ε_{rel} reduced by half with frequency rise, Fig. 2C.

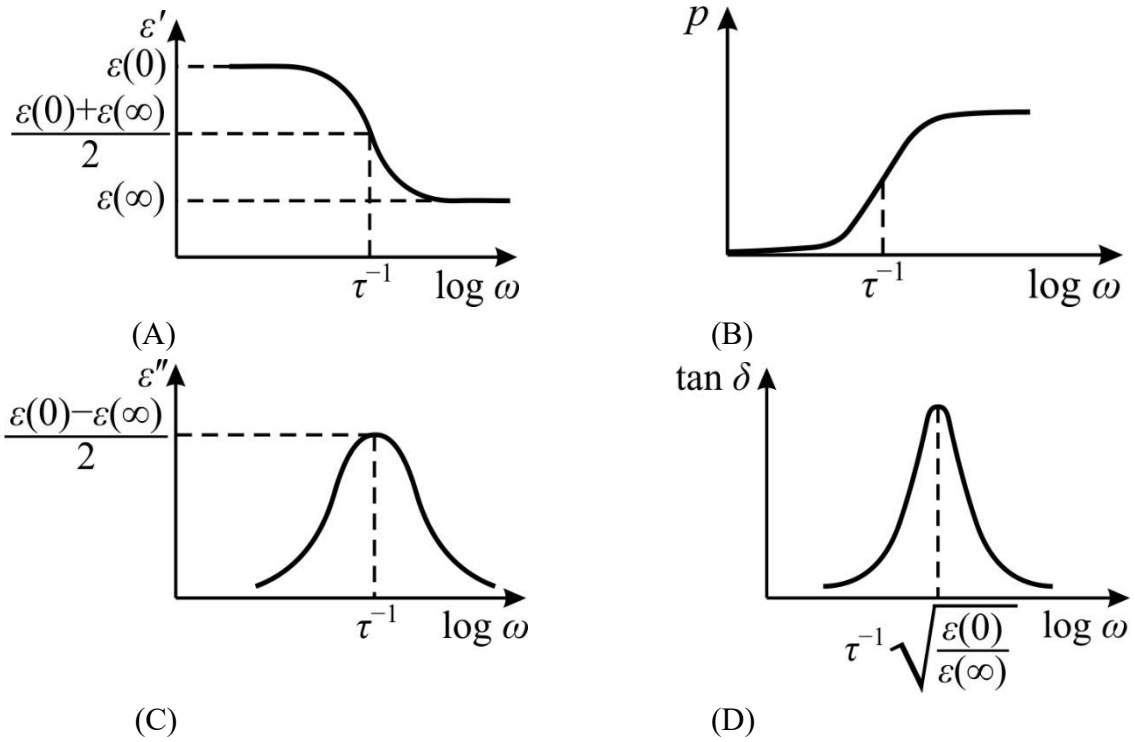

Fig. 3.2. Relaxation polarization in dielectric spectra: A – permittivity; B – absorbed energy power; C – loss coefficient; D – loss tangent delta. (The change of permittivity with frequency increase can be presented most expediently by the Bode plots, when the abscissa is the frequency in logarithmic scale; in this presentation many physical processes might be reflected, but in case of dielectric spectroscopy this is a permittivity conditioned by different polarization mechanisms)

The frequency dependence of loss tangent angle tanδ is also characterized by the *maximum* in the region of permittivity relaxation dispersion. Exploring above expression on extremes, it is possible to get

$$\tan\delta_{\max} = \frac{\varepsilon(0) - \varepsilon(\infty)}{2\sqrt{\varepsilon(0)\cdot\varepsilon(\infty)}}, \qquad \omega_{\tan\delta\max} = \frac{1}{\tau}\sqrt{\frac{\varepsilon(0)}{\varepsilon(\infty)}}$$

Thus, the maximum of tanδ(ω) is observed at a frequency somewhat larger than the $\varepsilon''(\omega)$ maximum. It is interesting to note that the maximum of loss tangent angle depends only on the $\varepsilon(0)$ and $\varepsilon(\infty)$ values.

The *average power* of electrical losses also can be found from above expressions

$$p = \frac{g\omega^2\tau^2}{1+\omega^2\tau^2}E^2 = \varepsilon_0\varepsilon''\omega E^2 . \qquad (3.3)$$

where g is the reactive conductivity. From this formula it follows that at low frequencies (when relaxation polarization completely establishes in time) the specific power of relaxation losses practically do not manifest itself. At that, in the centre of permittivity dispersion, when $\omega\tau = 1$, the specific power of losses reaches the value $p = \frac{1}{2}gE^2$. Very remarkable is the fact that at higher frequencies (when $\omega\tau >> 1$), the specific power of losses reaches its saturation value $p = gE^2$ and then does *not depend on frequency*. Thus, although the relaxation polarization at higher frequencies is late and has no influence on the value of permittivity, the specific power of relaxation processes at high frequencies remain maximal, Fig. 3.2B.

The fact is that at rather high frequencies the equilibrium distribution of relaxing electrons or ions has no time for establishing. Therefore, their movement in the electrical field through the potential barriers affects the losses in same way as the ordinary (DC) electrical conductivity. Same happens with the dipoles relaxation polarization: if frequency is so high that polar molecule does not have enough time to reorient, then the bonding of opposite charges of dipole is late to manifest. As a result, the effect of dipole polarization on the losses becomes the same as the effect of two opposite-charged ions involved in the electrical conductivity. This circumstance is clearly seen experimentally when permittivity frequency dependence is studied.

2. *Temperature dependence of main relaxor's parameters* describing thermally activated polarization in dielectrics is discussing. For this purpose, it is necessary to find out the temperature dependence of the coefficients included in the Debye equation (1). For this it needs to introduce base notations, which simplify this consideration: coefficients *A, B* and *K,* which do not depend on temperature:

$$\tau = \frac{1}{2\nu}\exp\left(\frac{U}{kT}\right) = A\exp\frac{B}{T} \qquad g\tau = \frac{n_0 q^2\delta^2}{12kT} = \frac{K}{T}.$$

By writing temperature dependences of ε' and ε'' with new coefficients, obtain

$$\varepsilon' = \varepsilon(\infty) + \frac{K}{T\left(1 + \omega^2 A^2 \exp\frac{2B}{T}\right)}; \qquad \varepsilon'' = \frac{\omega K A \exp\frac{B}{T}}{T\left(1 + \omega^2 A^2 \exp\frac{2B}{T}\right)}$$

Initially, such a case is considered, which corresponds to the relatively *higher temperatures* or/and *lower frequencies*, i.e., when $\omega\tau < 1$ so thermally activated polarization has enough time for its establishing. Then term "$\omega\tau$" in denominators of above expressions can be neglected in comparison with "1":

$$\varepsilon' \approx \varepsilon(\infty) + \frac{K}{T}; \qquad \varepsilon'' \approx \frac{A_1}{T}\exp\left(\frac{B}{T}\right).$$

As seen from first expression, the temperature change of permittivity occurs according to so-called *Curie law*: $\varepsilon'(T) = \varepsilon(\infty) + K/T$, where dielectric contribution from fast mechanism of polarizations $\varepsilon(\infty)$ is assumed to be weakly dependent on temperature, Fig. 3.3A. Curie law is explained by the fact that the increase in the intensity of thermal oscillations of atoms, ions or molecules of a matter hinders to the ordering of relaxing particles in electrical field, thereby reduces their contribution to permittivity.

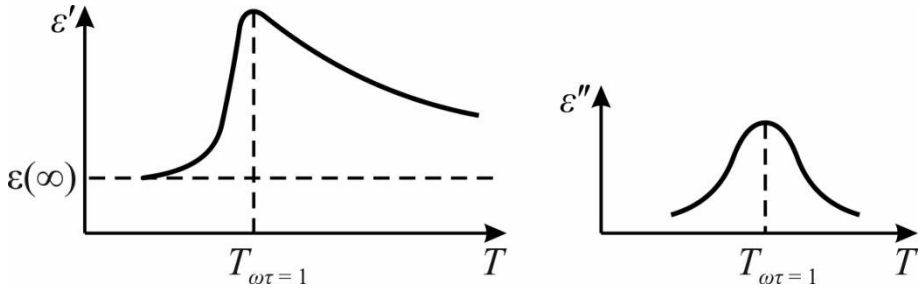

(A) (B)

Fig. 3.3. Temperature dependence of base parameters of dielectric possessing relaxation polarization

At that, as follows from the expression for loss factor $\varepsilon''(T)$, the contribution of relaxation polarization to the dielectric loss factor also decreases with temperature rise, and faster than for $\varepsilon'(T)$. The fact is that as temperature grows both the relaxation time of thermal polarization and the number of particles actually participating in the relaxation process decrease. Let us discuss the opposite case: when $\omega\tau > 1$.

This case is characterized by the fact that the process of thermal polarization doed not have enough time to be developed over the quarter-period of electrical field

changing. The delay of polarization is observed at relatively higher frequencies or/and at relatively lower temperatures, when the relaxation time is long enough. In this case one needs to *neglect the unit* as compared to value of $\omega^2\tau^2$ in the denominator of the above expressions.

In addition, linear temperature dependence of discussed parameters can be ignored as compared with much sharper exponential one. As a result, when temperature grows, the increase is observed both in $\varepsilon'(T)$ and $\varepsilon''(T)$ in such temperature range, where thermal polarization due to the decrease in relaxation time ceases to lag at given frequency ω, i.e., when $1/\tau \rightarrow \omega$, Fig. 3.3.

By performing complete analysis of above formulas, it can be shown that the temperature changing of complex permittivity, conditioned by thermal polarization, is characterized by non-symmetric maximum in $\varepsilon'(T)$ curve and almost symmetrical maximum in $\varepsilon''(T)$ dependence; at that, both maximums are seen exactly at $\omega\tau = 1$.

Consequently, the location of relaxation maxima in the dependences $\varepsilon'(T)$ and $\varepsilon''(T)$ is determined by the value of frequency at which the measurements are made. Since the relaxation time decreases with temperature grows, both *maximums* $\varepsilon'(T)$ and $\varepsilon''(T)$ *shift toward more high temperature* when frequency increases.

The specific power of dielectric losses also has temperature maximum, which is dependent on frequency. Frequency and temperature dependences of permittivity and losses are mutually connected with each other: the family of temperature characteristics of various parameters in the case of relaxation polarization is shown in Fig. 3.4.

When experimental studies of many dielectrics, the dependence of $\tan\delta(T)$ can be affected by conductivity. The effect of conductivity is especially noticeable at low frequencies and at high temperatures.

In Fig. 3.4 both frequency and temperature dependences of ε and $\tan\delta$ are given for the dielectrics, in which not only a thermal polarization but also the electrical conductivity is noticeably manifested.

Experimental study of $\varepsilon'(T)$ and $\tan\delta(T)$ dependences, conducted at several fixed frequencies in the region of relaxation, as well as the study of frequency characteristics $\varepsilon'(\omega)$ and $\tan\delta(\omega)$ at different temperatures can serve as a basis for determining the *height* of potential barrier U overcame by the electrons, ions or dipoles in the process of their thermal (relaxation) polarization establishing.

In principle, for such calculation, any pair of curves shown in Fig. 3.4 can be used.

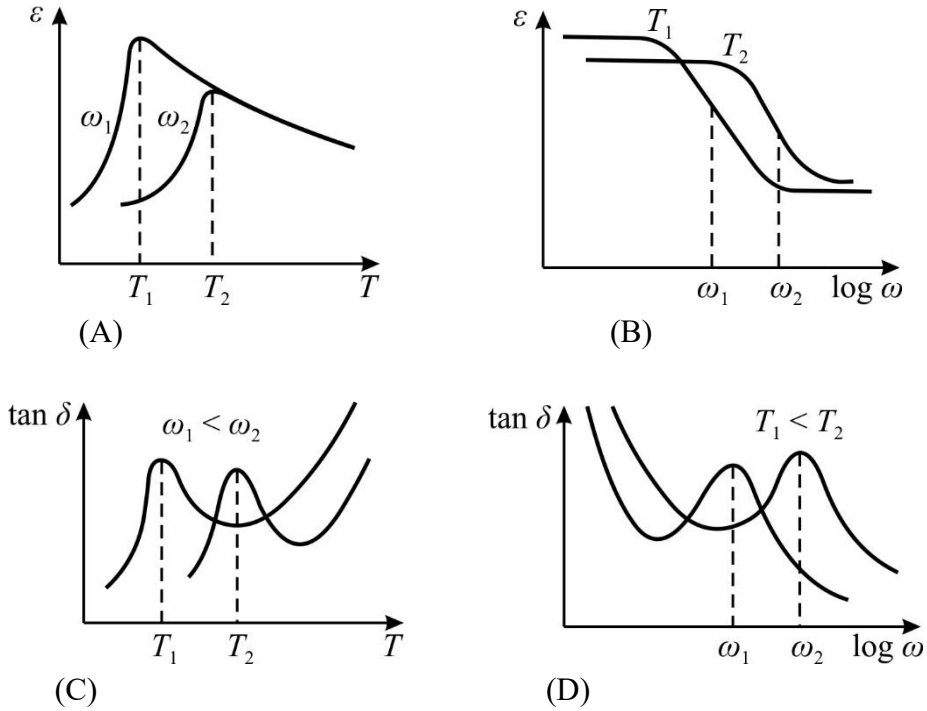

Fig. 3.4. Thermally activated polarization and conductivity manifestation in frequency-temperature dielectric spectra

It should be noted that dielectric permittivity dispersion studies and interpretation of correspondent parameters in broad frequency range take more laborious as compared to $\varepsilon'(T)$ and $\tan\delta(T)$ investigations in wide temperature interval, because to get frequency dependencies a set of experimental setups and different sized samples are required. Moreover, the characteristics $\varepsilon'(\omega)$ and $\tan\delta(\omega)$, as a rule, are not used when finding the value of U, since anomalies in temperature-frequency dependency of permittivity usually are small because its frequency dependency is flattened. That is why, for investigation of dielectrics characterized by thermal polarization combined with electrical conductivity, methodologically, exactly the temperature dependences of $\tan\delta(T)$ at several (at least two) frequencies are the most convenient for potential barrier definition.

Thus, experimental dependences of $\tan\delta(T)$ at different frequencies can serve as the base data for the height of potential barrier determining. For its calculation, it is sufficient to obtain experimentally two temperatures T_1 and T_2, which correspond to two values of frequency ω_1 and ω_2 when the peaks of losses are observed:

$$\frac{\exp\left(\frac{U}{kT_1}\right)}{\exp\left(\frac{U}{kT_2}\right)} = \frac{\omega_2}{\omega_1}$$

, from this it follows: $$U = \frac{kT_1T_2}{T_2 - T_1}\ln\frac{\omega_2}{\omega_1}. \qquad (3.4)$$

Stated above simple theory of the relaxation polarization is confirmed by many experiments conducted with different dielectrics.

3. Representation of Debye dispersion formula on complex plane leads to the significant simplification of permittivity dispersion analysis based on the equation:

$\varepsilon^*(\omega) = \varepsilon'(\omega) - \varepsilon''(\omega) = \varepsilon(\infty) + [\varepsilon(0) - \varepsilon(\infty)]/(1 + i\omega\tau)$.

After dividing on the real and imaginary parts it looks:

$$\varepsilon'(\omega) = \varepsilon(\infty) + \frac{\varepsilon(0) - \varepsilon(\infty)}{1 + \omega^2\tau^2}; \qquad \varepsilon''(\omega) = \frac{\left[\varepsilon(0) - \varepsilon(\infty)\right]\omega\tau}{1 + \omega^2\tau^2};$$

To simplify these formulas, introduce the "normalized" designation:

$$\xi^* = \xi' - i\xi'' = \frac{\varepsilon^* - \varepsilon(\infty)}{\varepsilon(0) - \varepsilon(\infty)}.$$

After that Debye dispersion formula looks like:

$(\xi^*)^{-1} = 1 + i\omega\tau$.

Then by entering notation $\omega\tau = z$ and dividing real and imaginary parts of ξ^*, obtain:

$$(\xi^*)^{-1} = 1 + iz; \qquad (\xi')^{-1} = 1 + z2; \qquad (\xi'')^{-1} = (1 + z2)/z. \qquad (3.5)$$

For the further analysis, it is convenient to introduce the concept of dispersion frequency $\Omega = 1/\tau$, which corresponds to the frequency of absorption maximum. From expressions (5) it is possible to find the frequency of $\xi''(z)$ maximum by usual analysis, using expressions: $d\xi''/dz = 0$ and $d2\xi''/dz2 < 0$.

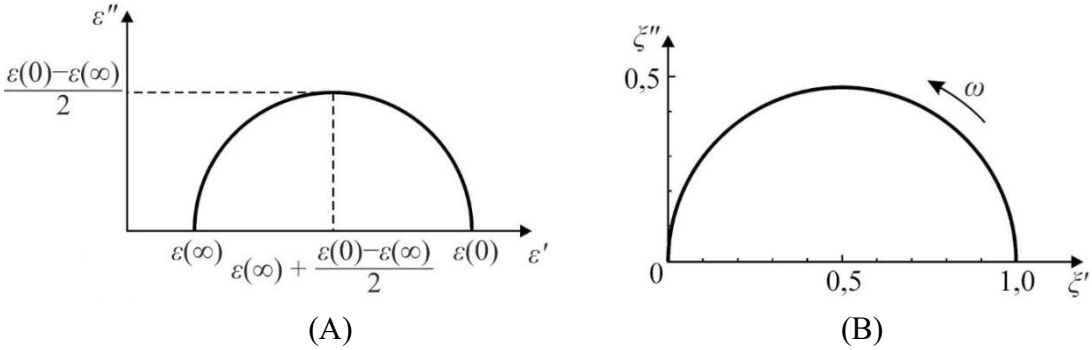

(A) (B)

Fig. 3.5. Coal-Cole plots: A – Debye equation in usual coordinates; B – Debye equation in normalized coordinates

The maximum of "normalized" absorption is $\xi''max = 0.5$ and is seen at normalized frequency $z = 1$. The width of Debye spectrum is characterized by parameter $\Delta\omega/\Omega$, where $\Delta\omega = \omega2 - \omega1$; the frequencies $\omega2$ and $\omega1$ are determined

at both sides of ξ″max = 0,5. From equation z/(1 + z2) = 0,25 find $z_{1,2} = 2 \pm \sqrt{3}$; hence spectrum width of Debye equation equals to $\frac{\Delta\omega}{\Omega} = 2\sqrt{3} = 3.5$ .It is important to note that Debye formula, describing the relaxation spectrum of permittivity dispersion, has an interesting feature: in the rectangular coordinates iξ″□ξ′ it is the circle equation:

$$\left(\xi' - 0.5\right)^2 + \left(\xi''\right)^2 = \left(0.5\right)^2 \tag{3.6}$$

This circumstance was first noted in works of K. Cole and R. Cole [4]. Their diagrams are shown in Fig. 3.5 as for usual coordinates ε' and ε", so for normalized dielectric contribution in coordinates ξ′ and ξ″. When frequency dispersion of ε*(ω) is well described by the Debye equation, then the experimental data really "lie" on a semicircle. If experimental studies can not be conducted in all necessary frequency range, then the Cole-Cole diagram allows make corresponding approximations of spectrum to the semicircle. Such a method is very useful and it is widely used in the description of the relaxation dielectric spectra.

3.2 Polarization based on oscillator model

The oscillator model is often used at dielectric properties description when electronic materials are studied or applied. Compared to the relatively “slow” processes of the relaxation polarization, the establishing of quasi-elastic polarization occurs almost instantly. That is why, in the equations describing thermal relaxation polarization the dielectric contribution of these fast processes to the value of permittivity is taken into account as the $\varepsilon(\infty)$, and it was assumed that in a very broad frequency range this value remains constant, while dielectric losses are attributed only to slow polarization processes and to electrical conductivity.

Indeed, the dielectric losses conditioned by the *quasi-elastic polarization* are observed at much higher frequencies; nevertheless, in some dielectrics already at microwaves the losses from the *soft modes* of ionic polarization become significant. In case of ionic lattice polarization, this loss factor gradually increases with frequency grows but fully manifests itself only in the far infrared frequency range (and in the ultraviolet range for the electronic polarization).

In case of the quasi-elastic polarization, at which electrical field acts on ions (bound in crystal lattice) or electrons (bound in atom), they only *slightly displace* while a returning force arises, which is proportional to ions or electrons elastic shifting from their equilibrium positions. Obviously, discussed in the previous

section *exponential law* of polarization establishing, which is valid for the relaxation processes, is not applicable here, but it should be expected the appearance of *oscillations* of all particles forcibly deviating by the applied field from their equilibrium position. Undoubtedly, to describe the dynamic properties of quasi-elastic polarization, it is expected to use the model of *harmonic oscillator,* taking into account dielectric losses by the introduction of damping factor. The elastic polarization is distinguished by the linear dependence of *restoring force* on displacement x induced by external field: $f = -cx$. At that, the polarizability α_{elas} can be calculated for any model of elastic polarization as $\alpha_{elas} = q^2/c$, where the elastic force cx resists to the displacement x of the charge q.

1. ***Frequency dependence of main oscillator parameters.*** Suppose that in the unit volume of dielectric n elastically bound charged particles are displacing that define the induced polarization $P = nqx,$ where q is the charge shifting on distance x. Each of particles is characterized by the mass $m,$ by the coefficient elasticity c and by the damping factor λ' of oscillation. If the constant electrical field $E = E_0$ acts on such dielectric, then it forces the charged particles to be displaced, i.e., the constant shifting x_0 for each charges is induced, resulting in the polarization $P_0 = nqx_0$ (at that, the initial time of electrical field switching on is not considered).

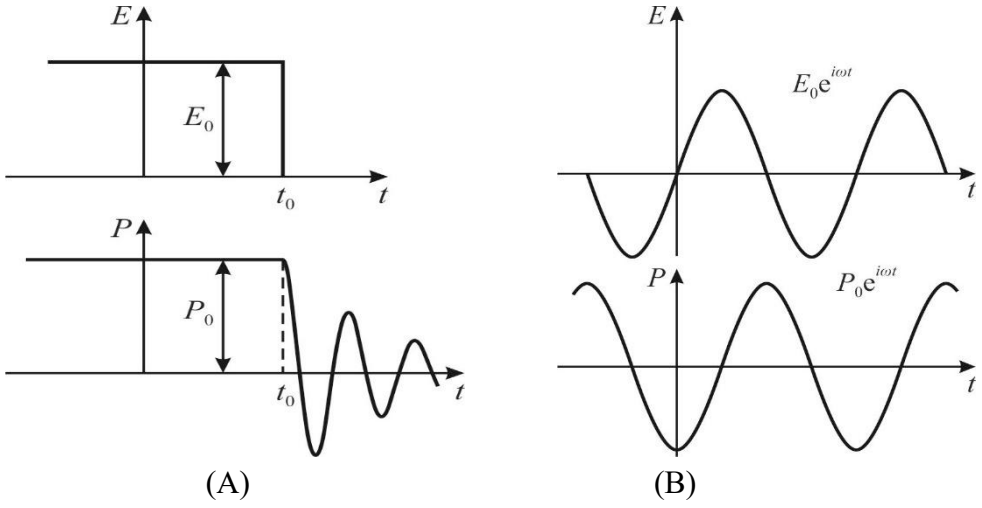

Fig. 3.6. Time-dependent polarization $P(t)$ of oscillators system under the influence of constant (A) and alternating (B) electrical field $E(t)$

Suppose also that in some moment $t = t_0$ long time applied electrical field E_0 is turned off, Fig. 6A, so elastic forces seeks to return the non-polarized (equilibrium) state of dielectric. This process occurs with the damped oscillations, and can be described by differential equation

$$m(\mathrm{d}^2x/\mathrm{d}t^2) + \lambda'\mathrm{d}x/\mathrm{d}t) + cx = 0,$$

in which $m(d^2x/dt^2)$ is the inertia force, $\lambda'(dx/dt)$ is the friction force, and cx is the elastic returning force. Dividing all members of this equality by m and taking into account the fact that $c/m = \omega_0^2$ is the oscillation frequency (if neglect friction), from above equation it is possible to get second order differential equation:

$$d^2x/dt^2 + \lambda(dx/dt) + \omega_0^2 x = 0, \quad (3.7)$$

where the damping coefficient is $\lambda = \lambda'/m$. Taking into account that $P = nqx$, the received equation of particles oscillations can be rewritten for the *polarization*:

$$d^2P/dt^2 + \lambda(dP/dt) + \omega_0^2 P = 0, \quad (3.8)$$

characterizing the damped oscillations of the polarization around fast established non-polarized state with $P = 0$, as shown in Fig. 3.6A.

The last equation characterizes the oscillator which describes the resonant type dielectric dispersion. It is a physical model characterizing dynamic reaction of a system of elastically coupled electrical charges to the externally applied electrical field, which is opposed by the internal elastic force tending to return the system into the non-polarized state. The *dielectric dispersion oscillator* is characterized by the resonant frequency ω_0, wave vector $k = 2\pi/\lambda$ and relative damping factor Γ. To describe the broadband resonant dielectric spectra that are often observed in experiments, the parameter of oscillator *frequency distribution* can be added to above listed dielectric dispersion oscillator parameters.

In this model, the scattering of energy during oscillations is taken into account by the introducing a certain coefficient λ' at the derivative dx/dt, i.e., representing a kind of "friction" (such force, as known, is proportional to the velocity of movement: dx/dt). The microscopic mechanisms that lead to this “friction” can be varied and complex. For example, in case of ionic quasi-elastic polarization in crystals, losses are characterized by the energy exchange between the optical and acoustic modes of oscillations in crystal lattice (optical and acoustic phonons). With this exchange, electrical energy dissipates turning into a heat. The point is that electrical field acts on the neighboring positive and negative ions in the opposite directions and thus initiates their optical (polarization) oscillations.

The energy dissipation of these oscillations is stimulated by various mechanisms.

First of all, any crystal has some structural defects which are any deviations of crystal structure from the ideal: any type of dislocations, grain boundaries, ionic vacancies and other low-mobility (“static”) structure deformations. Defects lead to the so-called *two-phonon interaction,* when optical phonons are scattering on the static fields of deformations. However, this is not the only mechanism of losses. Even if one assumes crystal structure being ideal, losses are also possible due to the

manifestation of oscillations *anharmonicity*. Depending on specific structure of a crystal the *three-phonon* or *four-phonon* interactions may prevail. Three-phonon interaction occurs, when the oscillations are described by cubic equation. In this case, two phonons — one of two different optical oscillation modes — generate phonon in the third mode. At that, transverse low-frequency wave interacts with two high-frequency waves belonging to same polarization branch. The four-phonon process is in many respects similar to three-phonon process. These and similar processes in oscillator model are taken into account by the introducing damping factor: λ' or $\lambda = \lambda'/m$.

The *frequency dependence of permittivity* in the oscillatory model of electrical polarization can be found on the base of equation (7), if one add the alternating electrical force $qE_0e^{i\omega t}$ acting on the oscillator:

$$m(d^2x/dt^2) + \lambda' dx/dt) + cx = qE_0e^{i\omega t}.$$

If not consider the transient processes and considering only the *stationary regime* of forced oscillations, the solution of this equation is:

$$x(\omega) = [qE_0e^{i\omega t})]/[\omega_0^2 - \omega^2 + i\lambda\omega].$$

The displacement x of charged particles in the electrical field ultimately determines polarization of dielectric, if n particles in unit volume are shifted in same way: $P = nqx$. Therefore, above equation can be rewritten for polarization:

$$P(\omega) = P_0\, e^{i\omega t} = \frac{\frac{nq^2}{m} E_0\, e^{i\omega t}}{\omega_0^2 - \omega^2 + i\lambda\omega}.$$

This formula shows that in the alternating electrical field $E_0e^{i\omega t}$ the polarization varies with same frequency as electrical field, but the polarization turns out to be the *complex parameter* having another phase in comparison with exciting electrical field. At last, at higher frequencies, the elastic polarization does not have time to be established, which leads to permittivity dispersion, while the presence of "friction coefficient" λ results in dielectric losses.

The frequency dependent dielectric permittivity can be found from a definition of permittivity as the proportionality coefficient between electrical displacement and electrical field: $D = \varepsilon_0\varepsilon E = \varepsilon_0 E + P$, from which $\varepsilon = 1 + P/\varepsilon_0 E$. Thus, to determine the permittivity, it is necessary to find the ratio $P/\varepsilon_0 E$, i.e., to get from above formula the complex parameter $\varepsilon^*(\omega) = 1 + nq^2/[\varepsilon_0 m(\omega_0^2 - \omega^2 + i\lambda\omega]$. To simplify this equation, the ideas of the "*dielectric strength"* of oscillator $\varepsilon_q = nq^2/\varepsilon_0 m$ and the *relative attenuation* $\Gamma = \lambda/\omega_0$ should be used. Suppose also that some different processes of elastic polarization occur in a dielectric, due, for example, to

the rapid displacement of valence electrons and other higher modes of ionic oscillations, etc. It is assumed that frequencies of corresponding oscillators are substantially different and oscillators are *independent*. Therefore, the process of elastic polarization should be described by the *various oscillators*, the number of which is equal to k, with a result that formula of dielectric permittivity dispersion will take following form:

$$\varepsilon^* - 1 = \sum_k \frac{\varepsilon_{qk}}{1 - \left(\frac{\omega}{\omega_{0k}}\right)^2 + i\Gamma_k \frac{\omega}{\omega_{0k}}}$$

To describe the permittivity dispersion in the simplest (cubic) ionic crystal by above formula, it needs to highlight the contribution of electronic polarization $\varepsilon_{el} = \varepsilon_{opt} = \varepsilon(\infty)$ from above sum. Then, for ionic polarization of crystal lattice the frequency dependence of permittivity can be described by following expression

$$\varepsilon^* = \varepsilon' - i\varepsilon'' = \varepsilon(\infty) + \frac{\varepsilon(0) - \varepsilon(\infty)}{1 - \left(\frac{\omega}{\omega_{TO}}\right)^2 + i\Gamma \frac{\omega}{\omega_{TO}}} \tag{3.9}$$

where ω_{TO} is the transverse optical frequency, Γ is the relative attenuation and the difference $\Delta\varepsilon = \varepsilon(0) - \varepsilon(\infty)$ characterizes the dielectric contribution of ionic polarization mechanism. This equation, which is usually called Drude–Lorentz equation, describes the resonance spectrum of permittivity dispersion. Turning to the analysis of frequency dependence of ε' and ε'', it is necessary in the above equation to separate the real and imaginary parts of complex permittivity:

$$\varepsilon'(\omega) = \varepsilon(\infty) + \frac{\left[\varepsilon(0) - \varepsilon(\infty)\right]\left(1 - \frac{\omega^2}{\omega_{TO}^2}\right)}{\left(1 - \frac{\omega^2}{\omega_{TO}^2}\right)^2 + \Gamma^2 \frac{\omega^2}{\omega_{TO}^2}}; \quad \varepsilon''(\omega) = \frac{\left[\varepsilon(0) - \varepsilon(\infty)\right]\Gamma \frac{\omega}{\omega_{TO}}}{\left(1 - \frac{\omega^2}{\omega_{TO}^2}\right)^2 + \Gamma^2 \frac{\omega^2}{\omega_{TO}^2}};$$

To simplify analysis of obtained relations, it needs first assume that damping is small ($\Gamma << 1$), then

$$\varepsilon'(\omega) \approx \varepsilon(\infty) + \frac{\left[\varepsilon(0) - \varepsilon(\infty)\right]\omega_{TO}}{\omega_{TO}^2 - \omega^2}; \quad \varepsilon''(\omega) \approx \frac{\left[\varepsilon(0) - \varepsilon(\infty)\right]\omega\Gamma\omega_{TO}^3}{\left(\omega_{TO}^2 - \omega^2\right)^2};$$

$$\tan(\delta) = \Gamma \frac{\omega}{\omega_{TO}} \frac{\varepsilon(0) - \varepsilon(\infty)}{\varepsilon(0)}. \tag{3.10}$$

It can be seen from formulas obtained that the value of permittivity $\varepsilon'(\omega)$ can be both positive and negative, while the loss coefficient is positive at any frequency: $\varepsilon''(\omega) > 0$. Indeed, the losses, characterizing heat release in dielectric due to the dissipation of electrical energy, always must have *positive value* according to the second law of thermodynamics.

The above relations show that in the frequency range $\omega < \omega_{TO}$ both $\varepsilon'(\omega)$ and $\varepsilon''(\omega)$ *increase* with frequency grows and in the vicinity of $\omega \sim \omega_{TO}$ both reach maximums. With further growing in frequency, the $\varepsilon'(\omega)$ and $\varepsilon''(\omega)$ dependences become different. The value of $\varepsilon'(\omega)$, after reaching its maximum value at frequency ω_1, decreases sharply, and at frequency ω_2 reaches minimum value, Fig. 7A and B. Then, as can be seen from above formulas, in the frequency range $\omega > \omega_{TO}$ the magnitude of $\varepsilon'(\omega)$ gradually increases with frequency and, when $\omega \to \infty$, the permittivity $\varepsilon'(\omega) \to \varepsilon(\infty)$. The positions of $\varepsilon'(\omega)$ and $\varepsilon''(\omega)$ maximum and minimum can be obtained through the studies on extremes: $\omega_{2,1} = \omega_{TO}(1 \pm \Gamma)^{1/2}$. In a particular case of small attenuation, i.e., at $\Gamma < 1$, the frequencies $\omega_{2,1} \approx \omega_{TO}(1 \pm \Gamma/2)$. Maximum and minimum values of permittivity at frequencies ω_1 and ω_2 respectively equal

$$\varepsilon_{\max} = \varepsilon(\infty) + \frac{\varepsilon(0) - \varepsilon(\infty)}{(2-\Gamma)\Gamma};\ \varepsilon_{\min} = \frac{\varepsilon(0) - \varepsilon(\infty)}{(2-\Gamma)\Gamma}$$

Describing the features of $\varepsilon'(\omega)$ dependence, it should be noted that when frequency of alternating electrical field equals to own oscillator frequency, i.e., in case of $\omega = \omega_{TO}$, the contribution to dielectric permittivity, as can be seen from above formula, becomes zero; in Fig. 3.7A this frequency is indicated as ω_3.

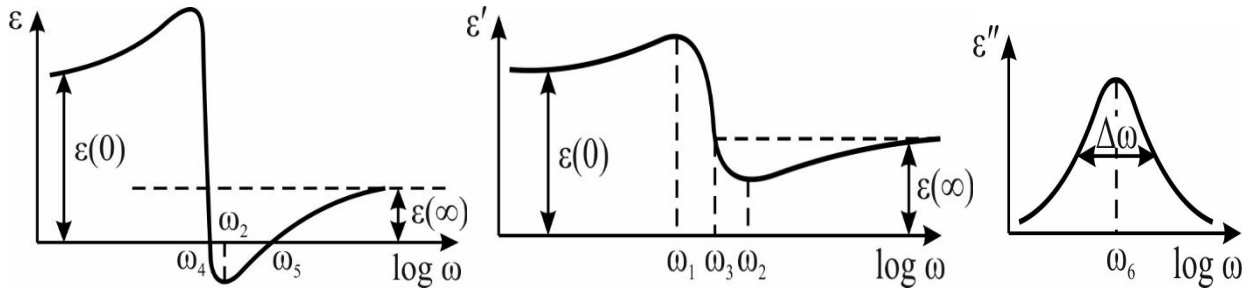

(A) (B) (C)

Fig. 3.7. Oscillator damping influence on permittivity dispersion: A – small damping; B – big damping; C – losses maximum

In this figures, two variants of permittivity frequency dependence are shown. It may be that in a certain frequency range $\omega_4 < \omega < \omega_5$ permittivity becomes negative; this case is favored by big dielectric contribution of oscillator and small

damping of oscillations. Characteristic points ω_4 and ω_5, at which the curve $\varepsilon'(\omega)$ intersects abscissa axis, can be determined from above equations:

$$\omega_4 \approx \omega_{TO}(1 + \Gamma^2/2)^{1/2}, \quad \omega_4 \approx \omega_{TO}[\varepsilon(0)/\varepsilon(\infty) - \Gamma^2/2]^{1/2}.$$

These cases are relevant in the study of dielectric spectra, when the attenuation can already be estimated by the form of frequency dependence of permittivity.

Now turn to the frequency dependence of loss coefficient $\varepsilon''(\omega)$. As shown in Fig. 3.7C, in this case the maximum is observed at frequency ω_6 in the vicinity of resonance dispersion of permittivity. When attenuation is small, this frequency can be easily obtained from above approximate formula, moreover, when analyzing any dispersion spectrum, the important characteristic is the *width of spectral line*, which directly characterizes the damping of oscillations. This parameter equals to the difference in frequency $\Delta\omega$ on the level $\varepsilon''_{max}/2$. In the case of small attenuation the maximal losses equals $\varepsilon''_{max} \approx [\varepsilon(0) - \varepsilon(\infty)]/\Gamma$; besides that the width of resonant spectrum is determined by relative attenuation: $\Delta\omega/\omega \approx \Gamma$. In the experimental study of dielectric spectra, as a rule, the frequency dependence of *loss coefficient* is determined. The frequency, at which losses maximum is observed and the width of $\varepsilon''(\omega)$ curve ($\Delta\omega$) make it possible to determine such important parameters of oscillator model as ω_{TO} and Γ. But all above calculated ratios are correct only in condition of $\Gamma < 1$.

The analyses of *exact formula* for $\varepsilon''(\omega)$ dependence show that, in reality, the frequency of loss factor maximum is lower than the oscillator own frequency ω_{TO} and in the case of large attenuation this difference can be significant:

$$\omega_6 \approx \omega_{TO}(1 - \Gamma^2/6) \text{ and } \varepsilon''_{\max} \approx \frac{\varepsilon(0) - \varepsilon(\infty)}{\Gamma\left(1 - \Gamma^2/6\right)}.$$

But these relations are also approximate and case of oscillator possessing very high damping can lead to the error in ω_{TO} determination. Therefore, in case of large attenuation of oscillations others experimentally determine parameters should be used to analyze the resonant dispersion spectra.

It should be noted that the value of *tangent* of dielectric loss angle is easily determined from relation: $\tan\delta = \varepsilon''(\omega)/\varepsilon'(\omega)$. However, parameter $\tan\delta$ cannot serve a convenient characteristic when *resonance* dispersion analyzing: the point is that this parameter can change its sign (together with permittivity); at that, at the points of $\varepsilon'(\omega)$ zeros, the $\tan\delta$ becomes infinite. Moreover, even in case of small dielectric contribution of equivalent oscillator, the maximum of $\tan\delta$ significantly shifts towards the higher frequencies in comparison with ω_{TO}. Therefore, to interpret resonance spectra, it is not advisable to use the concept of dielectric loss tangent.

Nevertheless, it is important to note that above formulas make it possible to use tanδ to *estimate* the contribution of far infrared permittivity dispersion to microwave losses. Assuming that $\omega << \omega_{TO}$, for this contribution the following expression can be obtained:

$$\tan\delta \approx \Gamma \frac{\omega}{\omega_{TO}} \frac{\varepsilon(0)-\varepsilon(\infty)}{\varepsilon(0)} \qquad (3.11)$$

In the case of large attenuation, when processing experimental data related to the resonance dispersion of permittivity, it is convenient to determine the frequency of equivalent oscillator by the maximum of "*effective conductivity*" using the connection $\sigma(\omega)$ and loss factor, established as $\sigma(\omega) = \varepsilon_0\omega\varepsilon''(\omega)$. Substituting loss factor $\varepsilon''(\omega)$ into this expression and investigating the resulting expression to extreme, it can be shown that in case of resonant dispersion the frequency of "effective conductivity" maximum $\sigma_{max}(\omega)$ at *any value of damping* corresponds to the frequency of equivalent oscillator ω_{TO} describing this dispersion.

Note that at relaxation dispersion of permittivity study, much attention is paid to changing of these spectrum with temperature. In the case of resonance dispersion, the simple models of elastic polarization (electronic and ionic) used here to describe resonance spectrum do not provide grounds for conducting any detailed analysis of resonant frequency and losses temperature dependence. Nevertheless, it is obvious that dielectric losses due to the elastic polarization depend on temperature. In the ionic crystals, for example, such dependence is caused by the scattering of optical phonons on the structural defects or on other phonons. However, significant dependence of resonant polarization on temperature is observed only in the paraelectrics and ferroelectrics that will be described in detail later.

2. Representation of Lorentz dispersiom formula on complex plane ***is convenient to describe dielectric spectra. To this end, the Lorentz oscillator formula should be modified by the introducing of "normalized" designations:***

$$\varepsilon^*(\omega) = \varepsilon' - i\varepsilon'' = \varepsilon(\infty) + \frac{\varepsilon(0)-\varepsilon(\infty)}{1-(\omega/\omega_0)^2 + i\Gamma(\omega/\omega_0)}, \quad \longrightarrow \quad \xi^* = \xi' - i\xi'' = \frac{\varepsilon^* - \varepsilon(\infty)}{\varepsilon(0)-\varepsilon(\infty)}.$$

After new notation introducing for frequency: x = ⁄0, the normalized equations for real and imaginary part of permittivity are:

$$\xi'(x) = \frac{1-x^2}{\left(1-x^2\right)^2 + \Gamma^2 x^2}; \quad \xi''(x) = \frac{x\Gamma}{\left(1-x^2\right)^2 + \Gamma^2 x^2}. \qquad (3.12)$$

The minimum and maximum $\xi'_{1,2}(x) = [\Gamma(2 \pm \Gamma)^{-1}$ are observed at normalized frequencies $x_{1,2}^2 = 1 \pm \Gamma$. In the case of a large attenuation ($\Gamma > 1$), the maximum $\xi'(x)$ will be absent, but the minimum $\xi'(x)$, which *distinguishes resonance spectrum* with a large attenuation from relaxation spectrum, does not disappear at any value of attenuation Γ. The $\xi''(x)$ maximum is seen at normalized frequency x_3:

$$x_3^2 = \frac{1}{6}\left\{2 - \Gamma^2 + \left[\left(\Gamma^2 - 2\right)2 + 12\right]\right\},$$

so that only for $\Gamma < 1$ it can be assumed that x_3 determines the frequency of dispersion oscillator.

The location of ξ' and ξ'' on the complex plane taking into account various relative attenuations Γ is shown in Fig. 3.8. The form of these curves differs significantly from the arcs of Cole-Cole circles, Fig. 3.8A, because in the case of resonant spectrum for any Γ the region of negative permittivity ($\xi'(\omega) < 0$) is observed. As attenuation increases, as $\xi'(\omega)$ so $\xi''(\omega)$ maximums become blurred, while the latter are noticeably *shifted* to lower frequencies. Indeed, when some dielectrics studies there are cases of a large relative attenuation. The critical value of attenuation is $\Gamma = 2$, Fig. 3.8; this means that only at $\Gamma < 2$ the quasi-elastic system, being exited by the external force from its equilibrium position and left unaffected, will carry out oscillations with its own frequency ω_0. At $\Gamma > 2$ the oscillator is called "over-damped", because the equilibrium state of a system in this case rehabilitates itself aperiodically.

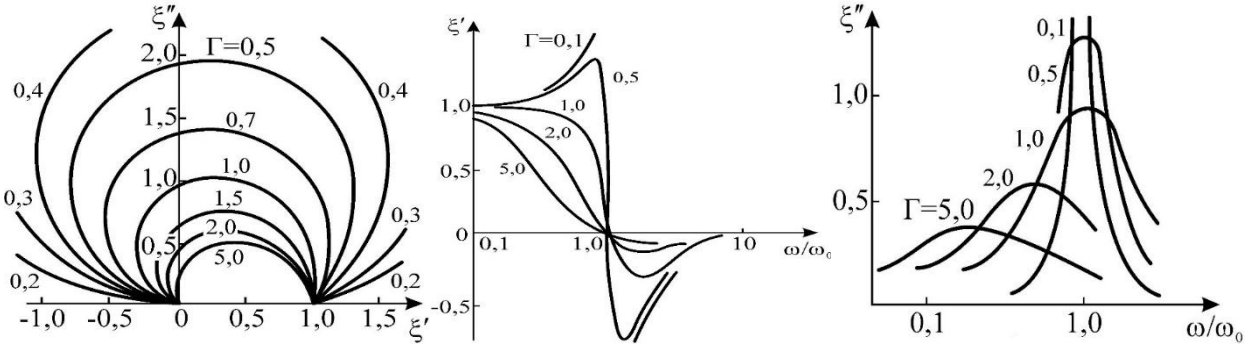

(A) (B) (C)

Fig. 3.8. Diagram $\xi''(\xi')$ at different values of attenuation of oscillator Γ (A), and frequency dependence of ξ' (B) and ξ'' (C)

Different relative attenuation significantly affects the character of dispersion spectrum. The maximum in a curve $\xi'(\omega)$, observed at the beginning of frequency dispersion at $\omega_1 = \omega_0\sqrt{1-\Gamma}$ and with increasing attenuation moves towards lower frequencies becomes smoothed out and disappears at $\Gamma = 1$. The minimum with increasing Γ moves towards higher frequencies and decreases; however, this minimum in the frequency dependence of permittivity is retained even in case of

large attenuation. The frequency of this minimum is $\omega_2 = \omega_0\sqrt{1+\Gamma}$, while its disappearance is possible only under condition of $\Gamma \to \infty$.

Thus, the presence of a minimum in the ε′(ω) frequency dependence is a principal sign of resonance dispersion that distinguishes it from the model of relaxation dispersion.

Important task for dielectric permittivity dispersion study and for mathematical processing of correspondent experimental data is to determine the basic parameters of the dispersion equation (10), that is, the values $\varepsilon'(0)$, $\varepsilon'(\infty)$, ω_0 and Γ. The first two parameters are easy determined from $\varepsilon'(\omega)$ dependence at such frequencies, when dielectric losses (absorption) are small, so the error of permittivity determination is little. However, there may be some difficulties in case of parameters ω_0 and Γ determining from experimental data.

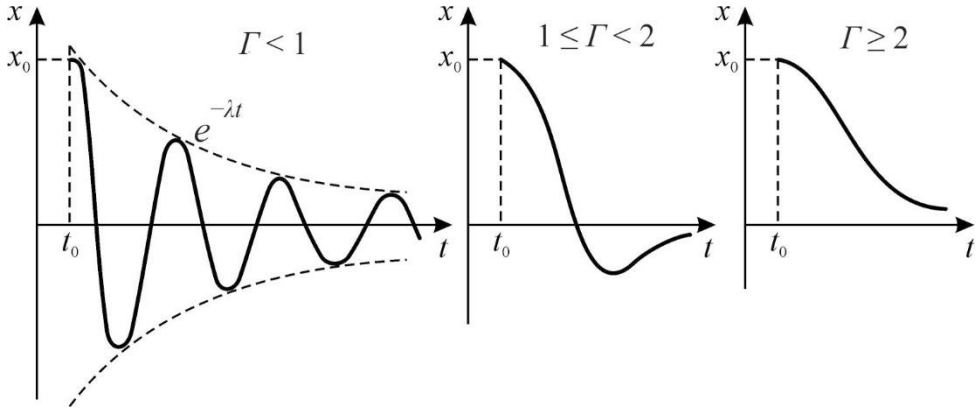

Fig. 3.9. Influence of relative attenuation Γ on oscillatory process

In Fig. 3.9, the time variation of the amplitude of the damped oscillator perturbed by the electric field with a different parameter Γ. is explained. When the field is turned off, in the case Γ < 1 the oscillations are still observed, at 1 δ Γ < 2 some trace of a resonance is still preserved (the amplitude becomes negative), but at $\Gamma \geq 2$ only the aperiodic process is visible.

In problems related to dielectric spectroscopy, it can be important to establish which polarization mechanism — relaxation or resonance — must describe the permittivity dispersion in the object under study. In case of small attenuation, parameters ω_0 and Γ can be found quite accurately using formulas given above. However in the case of *highly damped* oscillator, to express these parameters one needs to use following:

• *Resonance frequency* ω_0 of dispersion oscillator can be found from the dependence $\varepsilon'(\omega)$, if use the fact that in the dispersion region $\varepsilon'(\omega) = \varepsilon(\infty)$. If this

method of frequency determining looks difficult (for example, in case of complex multi-oscillators spectrum), then ω_0 can be found from the frequency of conductivity ($\sigma = \varepsilon_0 \varepsilon'' \omega$) maximum, which at any damping value is located exactly at ω_0.

• *Relative attenuation* Γ can be determined from $\varepsilon'(\omega)$ dependence at permittivity minimum ($\omega_{\varepsilon' min}$), because $\Gamma = (\omega_{\varepsilon' min}/\omega_0) - 1$. If this method is uncomfortable for some reasons (it leads to errors for "over-damped" oscillator), then the value of Γ can be found using position of absorbance maximum: $\omega_{\varepsilon'' max}/\omega_0$ (at that ω_0 corresponds to the $\sigma(\omega)$ maximum).

Discussing the ways how to obtain information about fundamental properties of dielectrics from permittivity dispersion spectra, it is worth noting a comparative complexity of data processing with resonance spectra. At that, the *relaxation dispersion* of permittivity is usually observed at not very high frequencies, so for their research, as a rule, it is quite sufficient to provide dielectric measurements at frequencies up to 10^{10} Hz. Lucky is that in this frequency range the values of $\varepsilon'(\omega)$ and $\varepsilon''(\omega)$ are determined *directly from measurements* without complex processing (for example, no using Kramers-Kronig method, commonly used when dielectrics study in far infrared range). However, the *resonance dispersion* of permittivity is usually observed in the far infrared wavelength range or sometimes even in millimeter range, when it is necessary to perform some rather complicated preliminary calculations before obtaining dependence $\varepsilon^*(\omega)$. In this case, a particular complexity is observed with such dielectrics, whose dispersion spectra can be represented by the model of oscillators with high attenuation.

In this regard, it is necessary to note several *simple experimental features* that characterize the dispersion spectra with large attenuation of equivalent oscillator:

• High attenuation affects the curve $\varepsilon'(\omega)$ by the fact that at $\Gamma > 1$ there is no longer any maximum in the initial dispersion region, Fig. 3.8B.

• Similar condition can be obtained also in the case, when a certain parameter associated with the modulus $|\varepsilon^*|$ when microwave measurement methods are applied. In this case, it can be shown that maximum in the $|\varepsilon^*|(\omega)$ dependence in the initial region of dispersion is absent for $\Gamma \geq \{2\varepsilon_0[\varepsilon(0) - \varepsilon(\infty)]\}^{-1/2}$, i.e., with greater value of relative attenuation as it was in case of dependence $\varepsilon'(\omega)$. If assume that $\varepsilon(0) >> \varepsilon(\infty)$, which is a characteristic of some polar dielectrics and ferroelectrics, given condition is simplified: $\Gamma \geq \sqrt{2}$.

• In the far infrared reflection spectra, as well as when use in study quasi-optic methods in the sub-millimeter wavelength range, the increase of $\varepsilon'(\omega)$ and $\varepsilon''(\omega)$ in the initial region of resonant dispersion must lead to corresponding increase in

reflectance coefficient $R(\omega)$, i.e., with the increase of frequency the reflection of electromagnetic waves from dielectric grows. Approximately (in case of small attenuation) this relation is expressed by formula: $R = \dfrac{\left(\sqrt{\varepsilon}-1\right)^2}{\left(\sqrt{\varepsilon}+1\right)^2}$, from which it is evident that when $\omega \to \omega_0$ in the initial region of permittivity dispersion $R(\omega)$ increases. Really, the higher attenuation the weaker manifestation of resonant properties is seen in $R(\omega)$ dependence. However, for some value of attenuation the growth of $R(\omega)$ in initial region of permittivity dispersion will be absent. In case of $\varepsilon(0) >> \varepsilon(\infty)$ this criterion is reduced to simple inequality $\Gamma \geq 2$, which coincides with definition of "over-damped" oscillator.

Thus, from some direct experiments by observing the very form of spectra $\varepsilon'(\omega)$, $|\varepsilon^*|(\omega)$ or $R(\omega)$ it is possible to judge which model is suitable for experimental data interpretation. In case of oscillator model application for permittivity dispersion one can even previously estimate the amount of attenuation of dispersion oscillator.

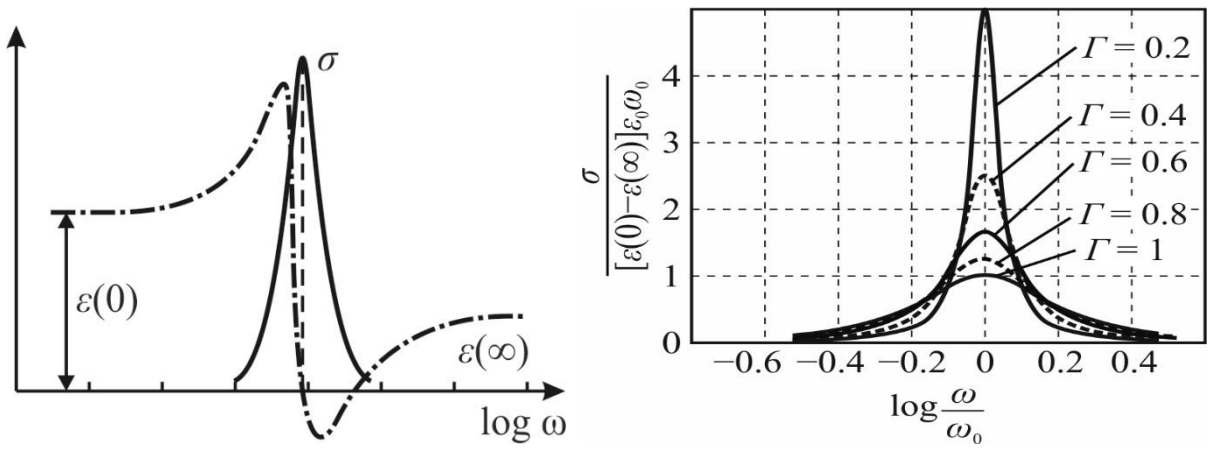

(A) (B)

Fig. 3.10. Permittivity (ε) and effective conductivity (σ) frequency dependence for resonance mechanism of polarization (A) and conductivity maximum dependence on damping coefficient (B)

In conclusion, it should be noted that the attenuation of oscillator can be determined by the value of effective conductivity:

$$\sigma(\omega) = \frac{\left[\varepsilon(0)-\varepsilon(\infty)\right]\omega_0\varepsilon_0}{\Gamma} \frac{\Gamma^2\left(\dfrac{\omega}{\omega_0}\right)^2}{\left[1-\left(\dfrac{\omega}{\omega_0}\right)^2\right]^2 + \Gamma^2\left(\dfrac{\omega}{\omega_0}\right)^2}$$

The dependence of the oscillator effective conductivity normalized to the dielectric contribution for different values of the relative attenuation is shown in Fig. 3.10.

Due to the fact that $\varepsilon^*(\omega)$ dependence in case of large attenuation of the oscillator becomes close to the relaxation type of dielectric spectrum, one should consider whether a single microscopic approach to permittivity dispersion can be found, which includes both resonance and relaxation.

Turning to the analogy of well-developed problem of resonance absorption in gases, it should be noted three main mechanisms of spectral line expansion in gases, i.e., three mechanisms of attenuation: radiation ($\Gamma \sim \lambda^{-1}$), Doppler's effect ($\Gamma \sim T^{1/2}$), collision of particles ($\Gamma \sim \lambda_0 T^{1/2}$).

In a given case of relatively long waves λ, high temperature T and condensed matter (solid dielectric), the most important of these mechanisms is the *collision of particles*. For example, A. Hippel considered the case of transition of resonant spectrum to the relaxation by increasing gas pressure – when frequency of collisions exceeds the rotational speed of a rotator (dumbbell molecule).

The density of solid dielectric corresponds to density of strongly compressed gas, and high frequency of collisions prevents the formation of discrete quantum states. As a result, the uncertainty in the presence of energy state becomes equal to $\Delta E = h\nu$, i.e., this uncertainty has the order of magnitude of energy of quantum.

The resonant state in this case disappears, and the spectral line expands into a continuous spectrum, that is, the oscillator becomes "over-damped".

The theories combining the models of oscillator and relaxor were developed in works of L. van Fleck and H. Frohlich.

In essence, the rotator model was developed in the state of continuous collisions, i.e., a rotator located in the "viscous environment" was studied. It was shown that Debye dispersion formula is imperfect in the region of higher frequencies (above dispersion frequency).

The correction to Debye formula sometimes is referred to the "inertial correction" that leads essentially to dispersion equation of the "over-damped" oscillator.

The above comparison of the oscillator and relaxor models might be important for choosing a more adequate model when analyzing the spectra of permittivity dispersion.

3.3 Ferroelectrics conception

Ferroelectricity is one of the most important and very complex areas of condensed matter physics. Dielectric spectroscopy of ferroelectrics is used not only as an instrument of scientific research but also in the development of diversified components with the necessary parameters.

The traditional theory suggests that ferroelectrics are a subclass of *pyroelectrics,* which can be defined as the crystals of 10 polar classes of symmetry possessing spontaneous polarization P_S. In the "hard" pyroelectrics, this polarization changes with temperature (which is used in electronics) and the polar structure is retained until crystal melts. However, in the ferroelectrics their polarized state is not stable enough: it disappears at the Curie temperature T_C and can be changed also by many external influences: electrical field, pressure, etc. In particular, thr electrical field switches the direction of polarization to opposite, demonstrating hysteresis loop, Fig. 3.11A.

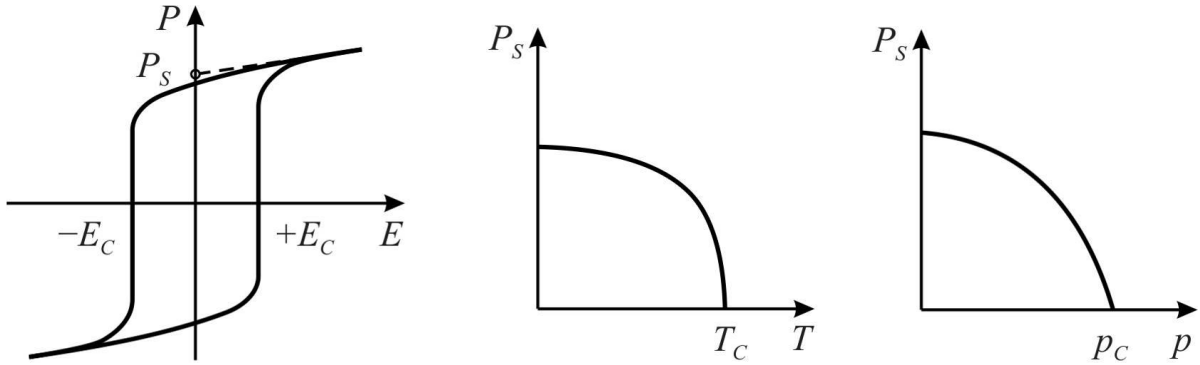

Fig. 3.11. Ferroelectric spontaneous polarization dependence: A – on electrical field; B – on temperature; C – on pressure

In connection with various possibilities for dielectric spectra interpretation in the ferroelectrics, it is appropriate to mention also other views about physical nature of ferroelectrics. In particular, when explaining various properties of polar crystals, one can do without the concept of "spontaneous polarization" (i.e., without imaging that in the polar crystal "own polarization" *exists*). Alternative reasonable assumption might be that the electrical polarization *appears* as a response to external action (not even electrical). Microscopically, this property is due to a peculiar distribution of polar-sensitive interatomic bonds in polar crystals whose ions have different affinity for electrons, i.e., different electronegativity.

To discuss the latter approach, following should be noted. In fact, any experimental investigations of pyroelectric or piezoelectric effects do not allow determine directly the value of their “own polarization”, because any experiment

characterizes only the magnitude of *dynamic response* of a peculiar polar-sensitive internal crystalline structure. To explain such manifestations of crystals properties, it needs to take into account the special structure of atomic external structure: total number of electrons in atom, degree of screening of electrons from action of nucleus, etc. The electronegativity is a property of atom to attract electrons; it depends on the atomic number (number of protons in nucleus), on the degree of internal electrons screening, as well as on the structure features of the external electron orbitals. The *excess* electronegativity means that given atom stronger attracts electrons while *insufficient* electronegativity means less affinity atom for electrons.

Non-centrosymmetric structures are formed owing to the compensation of atomic electronegativity by the polar-sensitive bonding emerging in the process of polar crystal formation (while it is growing from the liquid or steam state of a material). At that, dependently on the chemical composition of a crystal, the variety of combinations may occur between the ions of crystals possessing by two- or three-dimensional polar-active constructions (which, when external actions exerts on them, can produce the electrical responses, describable by the tensors of different ranks). Polar structures of crystals are the demonstration of *mixed ionic-covalent bonds* between their ions.

These bonds are strongly directional and, therefore, such structures lead to the different manifestations of the asymmetry and complexity of polar crystal structures. When electrical field is affected on the "persistantly arranged" polar structure, its electrical polarization usually looks like a linear effect (as in the ordinary dielectrics). However, the exception are the ferroelectrics, in which the *switching* of their “gently arranged" polarization is seen: their low-stable enantiomorphic structure can change its polar-sensitive direction. Outwardly this event manifests itself as dielectric *hysteresis loop*, Fig. 3.11A, which allows measure the ability of polar-sensitive structure to react on the external actions and indirectly can characterize its features. An increase in the intensity of thermal motion in the crystal lattice leads to the destruction of polar-sensitive bonds strength in ferroelectrics, Fig. 3.11B, while in the pyroelectrics they remain until the crystal melts. An increase in pressure also leads to the destruction of these bonds, Fig. 3.11C since ferroelectricity is accompanied by the increase in crystal volume. The increased sensitivity to pressure should be taken into account when examining the dielectric spectra of ferroelectric samples, so that they do not appear when measured under conditions of exposure to mechanical stresses.

1. *Multidomain structure*. When analyzing dielectric spectra, one should take into account that important feature of ferroelectrics (suggesting them as the electrical

analogue of ferromagnetics) is their spontaneous division into a plurality of domains. Within each domain the spontaneous polarization P_S same direction, but in neighboring domains it has different orientation. The subdivision of ferroelectric structure into great number of domains is energetically advantageous, since the single-domain crystal would create in the environment external electrical field (as in the case of electrets). Obviously, energy of this field decreases with diminution of size of domains.

Externally applied electrical field causes, at first, the junction of randomly oriented ferroelectric domains into one domain; next its polarization reaches saturation. As it can be seen in Fig. 3.11A, after external field switching off polarization tends to maintain its constant direction. If the polarity of externally applied field would be changed, the polarization, without changing its absolute value, will change its direction abruptly. For such "forced" change in the direction of P_S, i.e., for ferroelectric polarization reversal, it is necessary to apply electrical field of certain value, which is the *coercive field* E_C. Sometimes the value of this field reaches very large values, and then ferroelectric cannot be re-polarized and behaves like the pyroelectric.

However, during a heating of such "hard" ferroelectric, as it approaches to Curie point T_C, the coercive field E_C mush reduces, and, therefore, close to Curie point it becomes possible to observe the hysteresis. In the ferroelectric, both coercive field E_C and polarization P_S becomes zero at $T = T_C$. The pyroelectric, however, has no Curie point, and until electrical breakdown its internal polarisation does not change direction – such crystal rather can be destroyed than change the direction of polarization. It is therefore believed that theavailability of dielectric hysteresis is *necessary and sufficient property* of ferroelectric state. If temperature exceeds the critical value T_C then as the hysteresis loop so the ferroelectric state disappears. In same way on ferroelectric polarization affects the increase of hydrostatic pressure, Fig. 3.11C. In contrast, linear pyroelectric does not change its polarized state under pressure up to being destroyed. Summarizing, it might be concluded that *ferroelectric is the nonlinear pyroelectric*.

Ferroelectrics properties are considerably dependent on the domain structure**.** The origin of multidomain structure in ferroelectric crystal below phase transition is energetically favourable. Single-domain crystal shown in Fig. 3.12A, in principal, would create electrical field in the surrounding space (like electrets), to which an energy W_1 will be spent. As can be seen from Fig. 6.2B, the energy of external field in two-domain crystal would be smaller than in single-domain crystal. Thus, in case of many-domain structure total energy of crystal must be reduced. However, this

reduction in energy is limited by the growth of energy W_2 expended on domain walls formation, which separate the regions with different directions of P_S, Fig. 3.12C. The average size of domains (at which the sum $W_1 + W_2$ is minimal) depends on temperature, structural defects and electrical conductance of dielectric, as well as on environment properties. Multidomain structure in ferroelectrics is relatively stable; at that, the equilibrium state of ferroelectric domains usually corresponds to domain size from a few hundredths of millimetre to several millimetres.

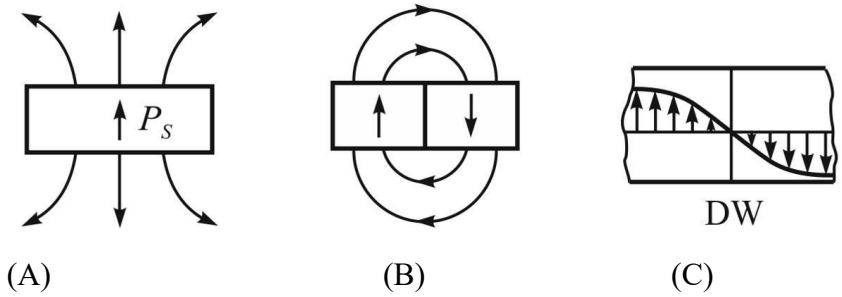

Fig. 3.12. Domain structure of ferroelectrics: A – single-domain crystal creates depolarizing electrical field in surrounding area; B – in two-domain crystal depolarizing field is reduced; C – domain wall (DW) in vicinity of which P_S gradually changes its direction to opposite

The possibility of spontaneous splitting into the domains is caused by the changeableness of "soft" ferroelectric state in comparison with "hard" pyroelectric state. In this regard, sometimes ferroelectric is defined as *pyroelectric which divides into domains.*

2. *Two types of phase transitions.* In the vicinity of phase transitions, the substance, firstly, allows considerable control of its parameters by the not very strong fields that is used in electrically and magnetically controlled devices; secondly, the substance is very sensitive to changes in temperature, pressure, humidity, etc. that is used in various sensory devices. Due to enormous anomaly of dielectric properties observed at phase transitions, dielectric spectroscopy requires special measurement methods and software for obtaining information about physical properties of the object under study (critical frequency and attenuation, critical relaxation time, etc.).

It seems appropriate to discuss how fundamental theory of phase transitions can provide for physical interpretation of experimentally observed dielectric spectra.

According to the *condensed state physics*, the nature of phase transitions can be like that. The degrees of freedom of atomic particles in solids can be divided into two groups. For some degrees of freedom the interaction energy of particles U_{int} is smaller in comparison with thermal motion energy k_BT. In this case, i.e, at $U_{int} << k_BT$ the appropriate degrees of freedom behave as the collection of particles, i.e., as

the "almost ideal gas", and the applicability to use the model of *quasi-particles* is justified. Conversely, when $U_{int} >> k_BT$, then appropriate degrees of freedom are ordered, but their movement, too, can be described by the introduction of quasi-particles. In other words. both of these cases correspond to the ordinary state of crystals and it is possible to describe, for instance, the phenomena of electric charge transfer (electronic or impurity ionic), as well as the phenomena of electrical polarization, by involving the dynamics of the crystal lattice (phonons).

However, if the energy of particles interaction approaches to changing with temperature thermal motion energy ($U_{int} \sim k_BT$), the theoretical description of dynamic phenomena in a solid becomes complicated: exactly this case usually corresponds to the *phase transitions*.

As known, in almost all substances at a definite temperature the significant change in physical properties occur and as a rule it is not a gradual but *abrupt*: this spasmodic change of properties is a phase transition. The “liquid ⇔ steam” (vaporization) phase transition is a typical example while another example is the "liquid ⇔ crystal" transition (crystallization). Both transitions refer to the *first order* (PT-I), in which the phases before and after transition point *differ significantly* from each other. At that, one phase replaces another phase just because it is more favourable energetically. To make this change happen, the essential energy barrier, separating these phases, should be overpass so the *stepped changing* of entropy should take place with a heat release (or absorption). Moreover, in the neighbourhood of first order phase transition the overcooling (or the overheating) is theoretically expected and seen experimentally. Methods of dielectric spectroscopy in such studies are not appropriate to use.

However, for solid state physics, more ordinary are the phase transitions within same physical state, which takes place as in the crystals so in the liquid crystals. Of particular interest are the phase transitions, at which a *new property* appears in crystal, for example, polar phase with the ability to electrical controlling (hysteresis loop) in case of transition from paraelectric phase to ferroelectric phase. This type of transitions is related to PT-II model: at Curie temperature ($T = T_C$) one phase ceases to exist, but it is replaced by another phase. In the point of transition both phases can not be clearly distinguished, but when system moves away from this point, the difference between properties of phases gradually increases. Second-order transitions are gradual and smooth; they do not show any temperature hysteresis and not accompanied by the discontinuous jump in the energy or in the volume of a crystal. Nevertheless, as a result of this transition, the new physical property appears: crystal becomes ferroelectric, ferromagnetic, ferroelastic, superconductive, etc.

When a ferroelectric phase transition is studied by the dielectric spectroscopy, the sample is exposed to the external electrical field and the “uncertainty” of phases at Curie point of ferroelectrics is expressed as a huge maximum of permittivity (as well as in the point of ferromagnetic phase transition the maximum permeability is huge).

When microscopic characteristics of any phase transition are discussed, a *regulating* (*ordering*) *parameter* η should be considered. In crystals, it is the measure of structural deviation from the state of highest symmetry. Depending on what kind of microscopic interactions gives rise to the PT and what changes of structure take place, the ordering parameter η acquires different physical meaning. For example, in ferroelectrics ordering parameter may correspond to the degree of electrical dipoles regularity, in ferromagnetics parameter η describes the ordering in system of magnetic moments (spins), etc. Ordering parameter may have also broader content; for example, in case of PT with the aggregate conversion this parameter characterizes the degree of regularity in a mutual arrangement of atoms or molecules [3].

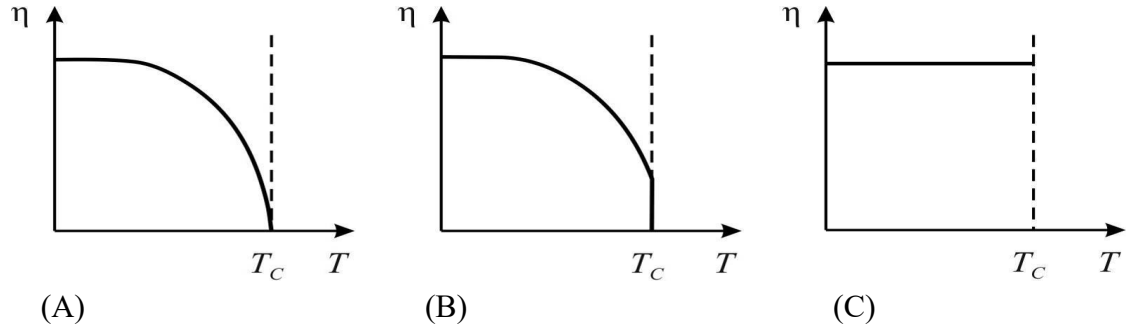

Fig. 3.13. Temperature dependence of ordering parameter for PT-II (A); PT-I close to PT-II (B) and for PT-I (C)

Ordering parameter η may vary differently with temperature changing, as it is illustrated in Fig. 3.13. The characteristic feature of PT-II is the *continuous* change of this parameter with temperature in the ordered phase Fig.3.13A. On the contrary, idealized case of PT-I corresponds to the case when ordering parameter changes by *jump*, Fig. 3.13C. But it should be noted that in many experimental situations the $\eta(T)$ dependence very often changes by one of "*intermediate*" ways, shown in Fig. 3.13B. In this case, the phase transition is the *transition of first order, close to transition of second order*. Here the ordering parameter η first changes with temperature increase gradually, but than abruptly falls down to the disordered phase.

Phase transition of second order can be accompanied by the multiplication of the size of crystal unit cell. Then the volume of unit cell of low-symmetry phase (more ordered) increases in 2, 4, 8 times, as well as the translational symmetry of unit cell also changes. Based on microscopic changes in a structure, the phase transitions are divided into *order-disorder type* and *displacive type:* theoretical

justifications for this division will be given below. Nevertheless, it should be noted here that a clear border between the displacesive and order-disorder types of PT can not be determined. In terms of crystal symmetry, there are no differences between them: when analizing structure, always an average position of atoms is taken in consideration.

So it is no matter how this averaging is performed: by the discrete way or by the continuous way. As to some other properties, especially, the dynamics of PT in case of displacive type of transition and in order-disorder type of transition vary considerably. When using dielectric spectroscopy, the most impressive results can be obtained for ferroelectrics.

3. *Simplest model of ferroelectrics.* The main cause of the appearance of ferroelectric state in a crystal can be explained on the base of *mixed* ionic-covalent bonds. They lead to *anharmonicity* of ions vibrations in a lattice and provide substantial non-linearity in the law of reciprocal displacement of neighboring ions in crystal lattice. The energy, describing vibrations in linear chain of ions, can be expanded in series by the dynamic displacement x:

$$U(x) = \tfrac{1}{2}\, cx^2 + \tfrac{1}{4}\, bx^4 + \ldots \qquad (3.13)$$

where x is the ion deviation from its equilibrium state. When considering electrical polarization of the ordinary ("linear") dielectric, the sufficient approximation is to take into account only the first term of this expansion: $U(x) = \tfrac{1}{2}\, cx^2$, where c is the coefficient of elasticity.

Here to determine the role of anharmonicity it is enough to account only next (anharmonic) term $\tfrac{1}{4}bx^4$ with coefficient of anharmonicity $b > 0$, which must be *positive* to guarantee lattice stability in case of large fluctuations. As to the coefficient of elasticity, it might be as positive ($c > 0$) so negative ($c < 0$).

The equation (3.13) corresponds to the fact that ferroelectric is found *above* the Curie point (T_C), i.e., in its non-polar (paraelectric) phase, which has centrosymmetric structure. Below T_C this model crystal passes into non-centrosymmetric (ferroelectric) phase, for which the energy of ion spontaneous displacement $-F\,x$ should be added to the series (3.13):

$$U(x) = \tfrac{1}{2}\, cx^2 + \tfrac{1}{4}\, bx^4 - Fx, \qquad (3.14)$$

where F is driving electrical field. Figure 6.4 shows the functions $U(x)$ for both cases: $c > 0$ and $c < 0$. To a complex parabola ($\tfrac{1}{2}\, cx^2 + \tfrac{1}{4}\, bx^4$) driving field energy is added in the form of an inclined straight line. It is seen that below Curie point the spontaneous deformation x_S arises at which total energy $U(x)$ shows a minimum.

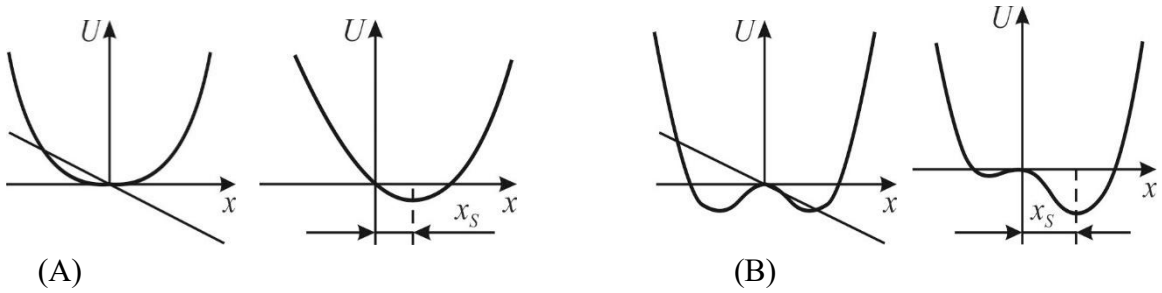

(A) (B)

Fig. 3.14. Energy dependence on "ferroelectric-active" ion deviation from equilibrium state in lattice with different elasticity coefficient: A – $c > 0$; B – $c < 0$

Since the polarized state at $x = x_S$ now is the equilibrium state, a total force acting on system of charges in this state equals zero: $\partial U(x)/\partial x = 0$ that means $cx + bxc^3 - F = 0$. Electrical field F (called the coercive field) is associated with spontaneous polarization: $F_C = \beta P_S$, where β is the Lorentz factor. In case of one-dimensional model of ferroelectric, represented by a simple linear chain of ions, polarization equals $P_S = nqx_S$, where n is ions concentration and q is ions charge. By substituting this data to equation (3.14) the cubic equation can be obtained

$$cx_S + bx_S^3 - nq^2\beta x_S = 0, \qquad (3.15)$$

where term cx_S describes the "elasticity" while member bx_S^3 characterizes "anharmonicity". This equation has three roots:

$$x_1 = 0; \quad x_{2,3} = \pm\,[(nq^2\beta - c)/b\,]^{1/2} \qquad (3.16)$$

As far as the only *spontaneously polarized phase* (with spontaneous deformation $x_S \neq 0$) is taken into consideration, first solution $x_1 = 0$ in (3.16) is a side root and will not be implemented here.

The analysis of other two obtained solutions provides an opportunity to make following conclusions. Firstly, the signs «±» means two equivalent possible directions of the spontaneous polarization, which corresponds to two equal in magnitude but opposite in direction ions displacements: $\pm x_S$: the areas of opposite direction of polarization are called domains. Secondly, in the crystals possessing small anharmonicity (when $b \approx 0$), spontaneous displacement of ions is impossible. Therefore, the anharmonicity of ionic displacements is one of *defining properties* of ferroelectricity existence in crystals. Third, the equation (6.4) has real roots $x_{2,3}$ only at the conditions when $nq^2\beta > c$ (because $b > 0$). By multiplying left and right side of this inequality on deformation x, obtain its physical meaning:

$$nq^2\beta x > cx. \qquad (3.17)$$

Right-hand side of this inequality corresponds to *elastic force,* which counteracts ferroelectric spontaneous displacement x_S: the overlap of electronic shells of neighboring ions seeks to *return* the non-polar state. The left side of the

inequality (3.17) has also the dimension of a force, and it is the *leading interaction* (i.e., leads to ferroelectricity). Thus, the ferroelectricity occurs in such crystals, in which the *leading interaction exceeds returning interaction*. The further analysis of inequality (6.5) shows that to the ferroelectric state in crystals contribute the *high density* of crystal (represented by parameter n), the *big charge* q of shifting ions and the increased *Lorentz factor* β.

Obtained with the above simple reasoning qualitative results are consistent generally with the actual situation. Indeed, among large number of well-studied alkali halide crystals (such as NaCl) no one ferroelectric exist: ions in these crystals are *single charged* (Na^{+1} and Cl^{-1}), while the Lorentz factor is small: $\beta = 1/3\varepsilon_0$ (ε_0 is the permittivity of free space). At the same time, in the *oxygen-octahedral* ferroelectrics with a general formula ABO_3, the "ferro-active" ion has the valence of +4 or +5 while in the inequality (6.5) charge enters as q^2: i.e., in 16−25 times over than in alkali halides. The Lorentz factor in the ABO_3 perovskites is also in five times higher than in the simple cubic ionic crystals. Therefore, for the fulfilment of the inequality (6.5) the ABO_3 type ferroelectrics have all reasons.

Returning to above description of phase transitions in the condensed matter physics, note that near the point of *second-order phase transition* the crystal behaves by such a way when a conventional concept based on quasi-particles can not adequately describe the experimental situation. Normally, the closest neighbouring particles in a crystal are considered as the *strongly interacting* particles, while the interaction of distant particles might be neglected. In this case, the harmonic approximation turns out to be rather good, so that in model described above in Fig. 3.4 and in formula (3.13) it is possible to put $b \approx 0$ and naturally in this case $c > 0$.

However, near the phase transition, in contrast, the interaction of neighbouring particles *compensates one another*, and, on this background, the interaction of those particles which are *at a distance* from one another appears dominant. This interaction has a special character: the probability of *collective movements* is bigger then the probability of *individual movements*. In the described above model it means that the elasticity coefficient is so small that both cases $c > 0$ and $c < 0$ are possible, so the anharmonicity comes to the fore: system stability is provided by $b > 0$. Unusually increased role of collective movements is confirmed by experiments: at the Curie temperature crystal shows maximum of specific heat, the permittivity in ferroelectrics tends to infinity as well as the permeability in ferromagnetic, and so on.

Shown in Fig. 3.44 two possible cases of anharmonicity quite meet the requirements of inequality (6.5) which also find confirmations in properties of

different ferroelectrics (number of which at present far exceeds hundred). In a theoretical approach is common to describe phase transitions to ferroelectric state using two models: the *displacement* of crystal sublattices that in a simplest case corresponds $c > 0$, and the *order-disorder* phase transition, which in some sense is close to case with $c < 0$. The difference in the physical nature of these two models of phase transition is large enough to consider corresponding dielectric spectra in the different cases.

3.4 Order-disorder ferroelectrics

It was in such ferroelectrics about a hundred years ago that the phenomenon of *dielectric hysteresis* (similar to magnetic hysteresis) was first discovered, which led to the name of this entire class of materials. Previously piezoelectric and pyroelectric effects were widely used in them, but even now the nonlinear optical, electrooptical, and piezooptical properties of these crystals are of interest in electronics. To diagnose physical phenomena in the ordered ferroelectrics and to determine their parameters over a wide frequency range, the dielectric spectroscopy is used. For example, when studying the frequency spectra in the temperature range, a low-temperature transition was first detected in the Rochelle salt, as well as the high-temperature transitions in the crystals of potassium dihydrogen phosphate (KDP) type.

In many cases dielectric spectra of ferroelectric crystals can be very complex, especially for order-disorder polar crystals. Depending on the orientation of studied crystal the dispersion of permittivity is observed at sound frequencies, at radio frequency range, at microwaves and up to the infrared region. The reason for such complexity is contributions to permittivity from various polarization mechanisms, as well as large dielectric anisotropy: main components of permittivity tensor ε_1, ε_2 and ε_3 can differ hundreds of times. High frequency properties of ferroelectrics, which show the phase transition of order-disorder type (most of them have the hydrogen bonds), are quite different from displacive ferroelectrics properties. Although in both cases above the phase transitions the Curie-Weiss law holds: $\varepsilon(T) \approx C/(T-\theta)$, parameter C in the ordering ferroelectrics by two orders of magnitude *lesser* than in the displacement ferroelectric. Moreover, the phase transition temperature T_C in the ordering ferroelectrics is very close to the Curie-Weiss temperature θ.

Experimental characteristics of key representatives of the order-disorder type ferroelectrics, taken from author measurements, are listed in Table 3.1.

Table 3.1

Ferroelectric crystals of order-disorder type and their properties according to microwave research

Ferroelectric	P_S, ⌈Q⊕sm□2	T_C, K	⟨, K	$C \cdot 10^{-4}$, K	W_g, eV	$A/2$□, GHz·K□1/2
Roshelle Salt	0,25	297	291	0,17	–	–
(two transitions)	–	255	257	0,14	–	–
Deuterated Roshelle Salt	–	308	300	–	–	–
(two transitions)	0,35	251	253	–	–	–
TGS	2,8	322,7	322	0,28	–	8,1
DTGS	3,2	327,5	327	0,27	–	10
KDP	4,7	123	118	0,28	–	180
DKDP	4,8	216	208	0,31	–	37
Chalcogenides:						
SbSI	50	295	285	23	1,9	–
SbSBr	10	95	82	12	2,2	–
PbTe	–	–	–	14	0,2	–

1. ***Thermodynamic theory*** predicts that in the ordering type ferroelectrics an availability is required of such active structural elements (polar radicals or groups of ions), which possess different equilibrium positions, whose changes can be described by dipole moments orientation. At higher temperature (in the paraelectric phase), the energy of thermal motion in a crystal exceeds the energy of dipole-dipole interactions and, therefore, the orientation of dipoles is chaotic and does not lead to any total polarization ($P_S = 0$). However, with decreasing temperature, in the vicinity of phase transition, interactions energy of dipoles begin to exceed thermal disordering, and the self-ordering of polar elements prevails, so spontaneous polarization appears ($P_S > 0$).

Curie-Weiss law, characterizing the temperature change of permittivity, clearly seen in the dielectric spectra, can be obtained in the Landau theory [1], in which the thermodynamic potential is written in a form: $\Phi(T,P) = \Phi_0(T) + \frac{1}{2}\alpha P^2 + \frac{1}{4}\beta P^4 + ...$, where α and β are the coefficients in series of thermodynamic potential.

Considering that electrical field can be defined as derivative $\partial\Phi/\partial P$, above expression can be rewritten as $E = \alpha P + \beta P^3$.

So the inverse susceptibility is $\chi^{-1} = \frac{\partial E}{\partial P} = \frac{\partial^2 \Phi}{\partial P^2} = \alpha + 3\beta P^2$ that defines permittivity $\varepsilon \approx \chi$, since $\varepsilon = 1 + \chi$ and in ferroelectrics $\varepsilon >> 1$.

In the ***non-polar phase*** *(paraelectric)*, where first term in Landau polynomial is negative ($\alpha > 0$ when $T > T_C$), main conditions of phase sustainability are: $\frac{\partial \Phi}{\partial P} = 0$, $\frac{\partial^2 \Phi}{\partial P^2} > 0$. First of these expressions can be reduced to the cubic equation $\alpha P + \beta P^3 = 0$ which has only one valid root: $P_1 = 0$, because high-temperature phase is disordered (other roots $P_{2,3} = \pm\sqrt{-\alpha/\beta}$ are imaginary since for PT-II parameter $\beta > 0$ and above T_C also $\alpha > 0$). Permittivity temperature dependence in the paraelectric phase, Fig. 3.15E, is described by the Curie-Weiss law: $\frac{1}{\varepsilon} = \alpha_0 (T - \theta)$, $\varepsilon = \frac{C}{(T - \theta)}$.

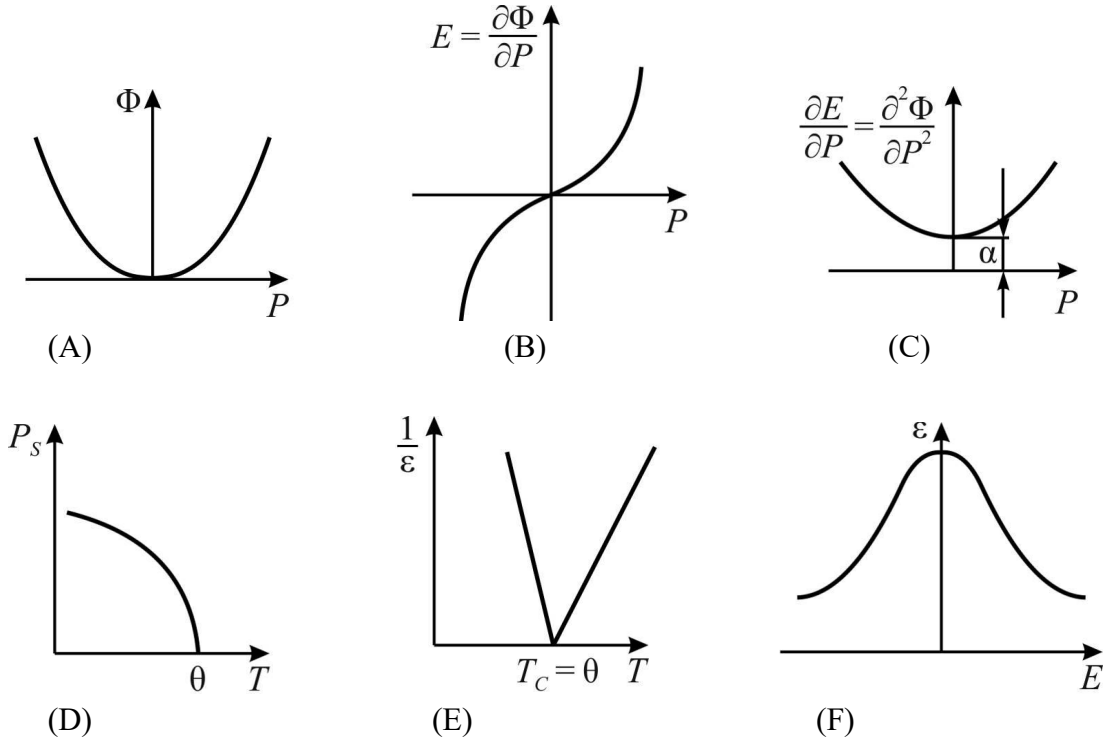

Fig. 3.15. Order-disorder phase transition description: thermodynamic potential (A) and its derivatives (B,C) dependence on ordering parameter P above T_C; temperature dependence of polarization (D) and inverse permittivity (E); dielectric nonlinearity in non-polar phase (F)

In *nonlinear dielectric spectroscopy* is important that in the non-polar phase permittivity depends not only on temperature but also on *electrical field strength*. Thermodynamics predicts significant *dielectric nonlinearity*, Fig. 3.15F at that $P(E)$

dependence is characterized by the saturation area. Therefore, the permittivity in the paraelectrics *decreases* in strong electrical field, because $\varepsilon \sim \partial P/\partial E$. General formula, that takes into account both ε-non-linearity and ε-temperature dependence is

$$\varepsilon\left(T, E\right) = \frac{C}{\left(T - \theta\right)}\left[1 + 3\beta\,\varepsilon_0^3 E^2 \frac{C^3}{\left(T - \theta\right)^3}\right]^{-\frac{1}{3}}.$$

It is seen that nonlinearity in the non-polar phase the higher the closer temperature to phase transition point.

In the ***polar phase,*** below Curie point the spontaneous polarization appears, so all roots of cubic equations $\partial\Phi/\partial P = \alpha P + \beta P^3 = 0$ are valid. However, since $\alpha < 0$ the root $P_1 = 0$ now corresponds to the $\Phi(P)$ *maximum*, Fig. 3.16. At that, by definition, polar phase is stable if value $\Phi(P)$ is minimal, i.e., at $P_{2,3} = \pm\sqrt{-\alpha/\beta}$. By substituting $\alpha = \alpha_0(T - \theta)$ in this expression, it is possible to find temperature dependence of spontaneous polarization: $P_c^2 = \frac{\alpha_0\left(\theta - T\right)}{\beta}$ shown in Fig. 6.5D. Temperature dependence of permittivity is $\frac{1}{\varepsilon} = 2\frac{\left(\theta - T\right)}{C}$; $\varepsilon = \frac{C}{2\left(\theta - T\right)}$. Thus, thermodynamic theory predicts that below Curie point, at the same distance from T_C, the value of permittivity is *twice smaller* than in paraelectric phase at $T > T_C$, Fig. 3.15E.

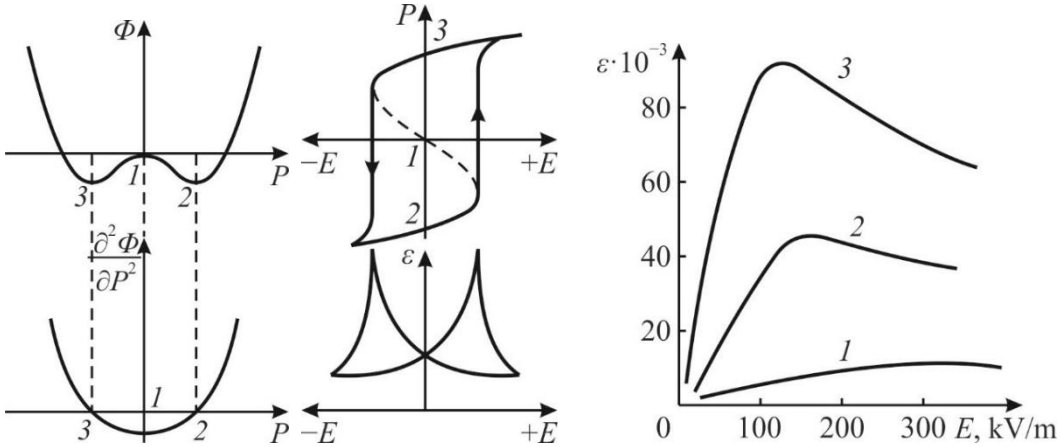

(A) (B) (C)

Fig. 3.16. Non-linearity in polar phase: A – thermodynamic potential and its derivatives, points *1, 2* and *3* indicate roots of equation; B – polarization and dynamic permittivity field dependence; C – effective permittivity field dependence: *1* – $BaTiO_3$, *2* – $Ba(Ti,Zr)O_3$, *3* –$Ba(Ti,Sn)O_3$

Now the nonlinear properties of ferroelectrics in the polar phase will be discussed. Describing the polar phase PT-II ferroelectric thermodynamic potential and its derivatives are shown in Fig. 3.17A. The $\Phi(P)$ dependence denotes the extreme points at which this function and its second derivates intersects the axis P. Correspondent dependence $P(E)$, Fig. 3.17B, is characterized by the *unstable* region shown by the dashed line where permittivity $\varepsilon \sim dP/dE$ would be negative. To restore the stability, the *dielectric hysteresis* occurs, corresponding to it *differential* permittivity $\varepsilon(E)$ passes through two maximums when polarization switches its direction at the coercive field. The *effective* permittivity measured at alternating voltage, averaged over the period of electrical voltage changing is given, as example, for various ferroelectrics in Fig. 3.17C.

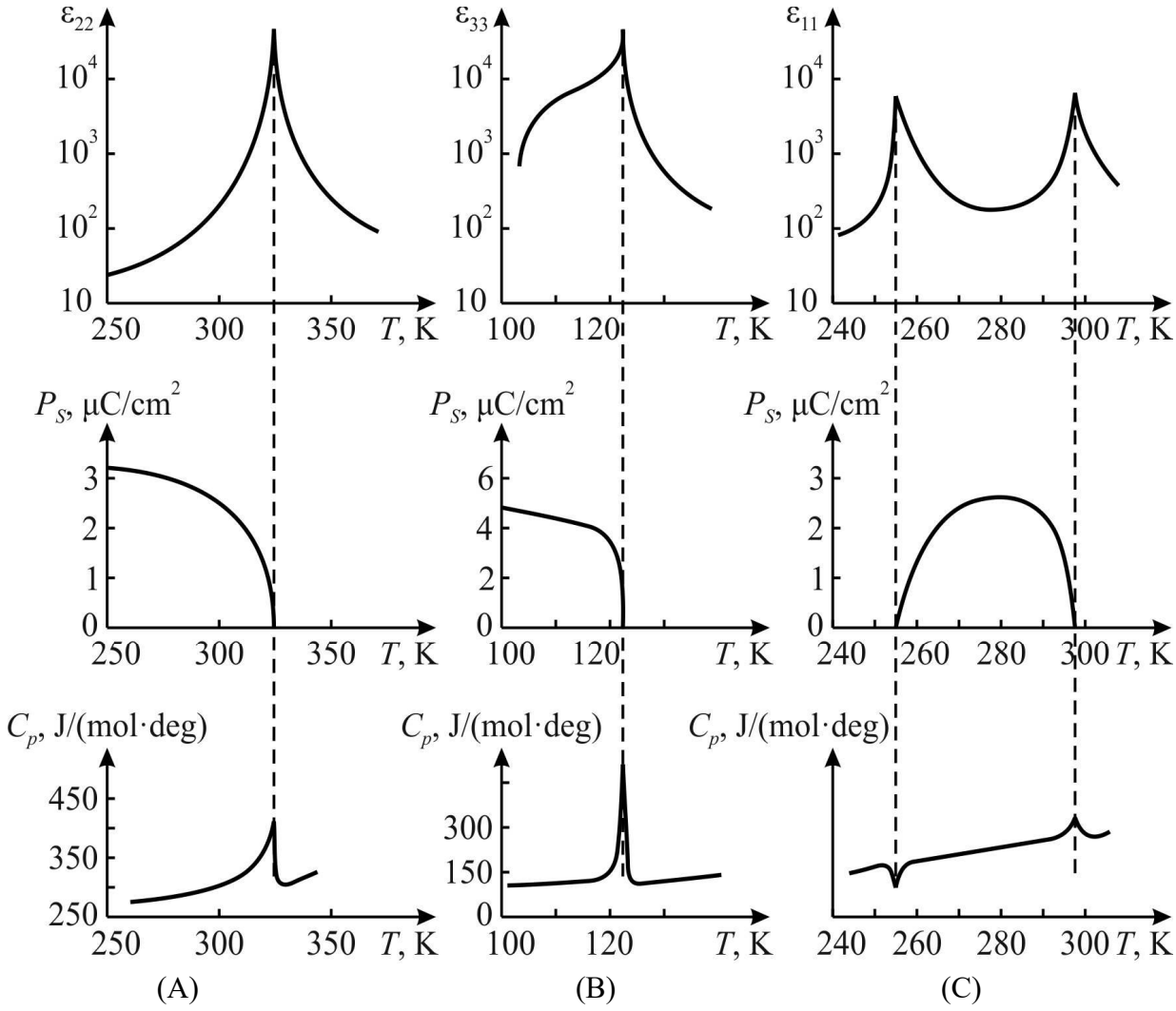

Fig. 3.17. Temperature dependence of relative dielectric constant ε, spontaneous polarization P_S and specific heat C_p for ferroelectric which are close to model of order-disorder phase transition:

A – TGS = triglycinesulphate (NH_2CH_2□$(COOH)_3H_2SO_4$); B – KDP = potassium dihydrogen phosphate (KH_2PO_4); C – Rochelle salt (RS) $KNaC_4H_4O_6$□$4H_2O$

All predictions of theory is well confirmed by the experiments. Temperature dependence of permittivity, spontaneous polarization and specific heat of major representatives of order-disorder type ferroelectrics shown in Fig. 3.17 corresponds to the thermodynamic theory of phase transitions of second order. The change in the permittivity with temperature in ferroelectrics is so great that a logarithmic scale should be applied.

Dynamic properties of all these crystals differ from same properties of ferroelectrics possessing displacement-type phase transition. Among other features, special and interesting property of crystals with order-disorder transition is the *isotopic effect* – the displacement of Curie point in case when hydrogen replacing by deuterium (Table 3.1). This peculiarity demonstrates the importance of hydrogen bonds for majority of these types of ferroelectrics. The study of dielectric spectra is one of important methods for obtaining information on the polarization mechanisms of such dielectrics. Studying the dispersion of permittivity allows evaluate the conclusions of various theories and hypotheses about the nature of ferroelectricity, as well as to obtain information about the characteristic frequencies and dielectric contributions of various polarization mechanisms.

3.5 Dynamics of dipole-ordering ferroelectrics

In the previous sections, the application of dielectric spectroscopy to the study of the *frequency* characteristics of materials is mainly considered. But there are some cases of significant (even critical) changes in the dielectric properties with *temperature* that also substantially affects the frequency characteristics.

The frequency characteristics of *ferroelectrics* are very diverse, nevertheless, since many components of electronics use ferroelectric materials, their properties on radio frequencies and microwaves are of particular interest. Most ferroelectrics are characterized by high absorption coefficient at microwaves, especially near ferroelectric phase transitions. At that, in the order-disorder type ferroelectrics, the fundamental mechanism of polarization is seen exactly on microwaves due to *critical slowing down* of relaxation time (that in the end results in the phase transition of order-disorder type).

In the process of dielectric spectra investigation, it is important to keep in mind that many of ferroelectric crystals have a pronounced *anisotropy* of their dielectric properties; at that, exactly *ferroelectric* properties are maximally manifested only in a single (polar) direction, whereas in other directions these crystals behave like ordinary ionic or molecular crystals. The difference in the

absorption in the range of millimeter waves may reach thousand times, so these crystals are natural polarizers.

Almost all polarization mechanisms, which characterize ferroelectrics, are strongly dependent on temperature, including the change of their permittivity and characteristic frequency of relaxation. Therefore, permittivity dispersion in the ferroelectrics must be investigated in connection with the temperature dependence of their parameters. In this section, only those mechanisms that lead to permittivity dispersion of *relaxation type* are considered. In the *polar* phase of ferroelectric (below Curie point) dispersion of permittivity is observed due to the irreversible (in strong electrical fields) and reversible (in weak fields) motion of domain walls. In the *non-polar* phase of ferroelectric (above Curie point), the relaxation spectra describe the main contribution to permittivity conditioned by self-ordering of polar clusters, which dielectric response varying accordingly to Curie-Weiss law: $\varepsilon(T) = C/(T - \theta)$.

In the *ordinary* polar dielectrics, when temperature decreases, the relaxation time of polarization mechanism grows up exponentially: $\tau \sim \exp(U/k_B T)$ and tends to the infinity at zero temperature, Fig. 3.17A, *curve 1*. At that, correspondent activation energy U can be found from the loss factor $\varepsilon''(T)$ maximum *shifting to lower frequencies* as temperature decreases (more precisely, from linear dependence of $\ln(\omega_{\varepsilon''max}/\omega_0)$ on $1/T$). However, in the order-disorder type *ferroelectrics*, their relaxation type dispersion of permittivity does not obey this temperature dependence, especially in the vicinity of phase transitions, Fig. 3,18A, *curve 2*. In experiments, this corresponds to a sharp $\varepsilon''(T)$ maximum at the temperature of ferroelectric phase transition, which, when frequency changes, *does not shift* on a temperature scale but remains at the phase transition point.

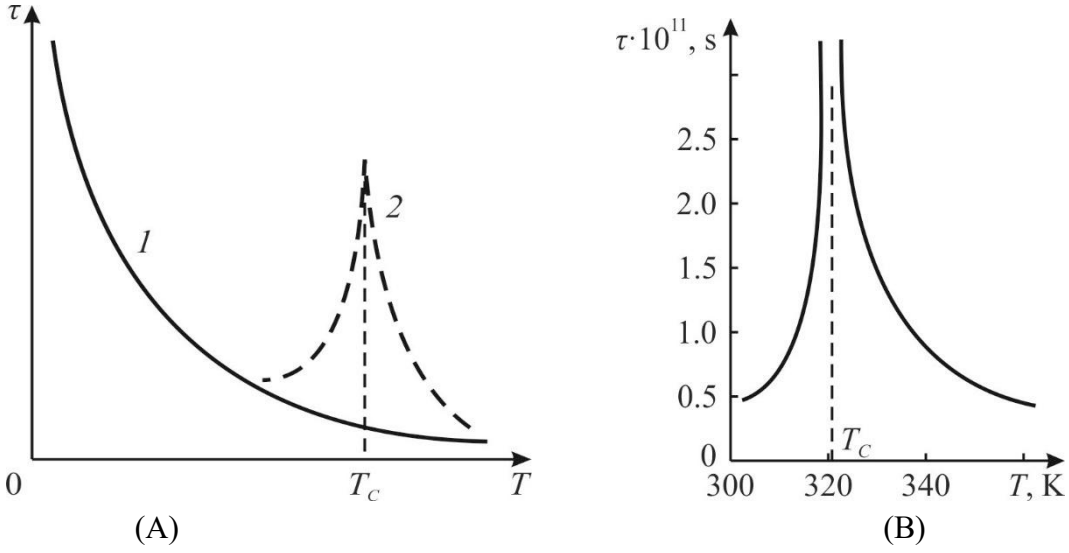

Fig. 3.18. Temperature dependence of relaxation time in polar dielectrics: A – comparison of ordinary dielectric (*1*) with ferroelectric (*2*), B –$\tau(T)$ maximum for triglycine sulfate near Curie point

This indicates quite different dynamics of relaxation processes due to *critical change* of relaxation time with temperature (in ordinary polar dielectrics relaxation time changes gradually as shown by *curve 1* in Fig. 3.18A). The dynamics of polarization in order-disorder (dipole) type ferroelectrics supposes that the temperature dependence of the *inverse* relaxation time is close to law: $\tau^{-1} = (T - \theta)/\tau_0$.. Here θ describes the Curie–Weiss law for permittivity (note that θ might be a little different from phase transition temperature T_C). As for the base parameter τ_0, it is determined as $\tau_0 = (2\nu_D)^{-1}\exp(U/k_BT)$, i.e., by usual exponential dependence, where U is the potential barrier overcoming by dipoles when orientation, ν_D is the Debye frequency of atomic oscillations in crystal lattice and k_B is the Boltzmann constant. However, within the limits of *critical change* of $\tau(T)$, as can be seen from Fig. 3.18A, the value of τ_0 can be considered approximately as a constant (in the vicinity of phase transition).

When properties of order-disorder type ferroelectrics describing, it is supposed that they have some groups of atoms (clusters) containing equally directed dipoles. In the paraelectric phase (above Curie point) these clusters are small and disordered, i.e., they have equally probable orientations of dipole moments for a lot of polar groups, which are randomly distributed along these directions under the influence of thermal vibrations of crystal lattice. As temperature decreases, the interaction of these polar groups leads to their grows and partial ordering, until finally the mess gives way to ordering and phase transition to the ferroelectric (polarized) state occurs. In this case, however, even inside polar phase not all polar groups are completely ordered, especially near the phase transition. Therefore, the clusters of disordered phase exist even below the phase transition point, which leads only to a gradual decrease in permittivity with decreasing temperature.

To analyze these processes by applying dielectric spectroscopy methods, it is necessary to study exactly the *frequency-temperature* dependence of permittivity and loss factor, since these experiment can determine relaxation time of the process leading to the spontaneous ordering of polar groups. It is notable that *in the vicinity of dispersion* the temperature dependence of permittivity is characterized by a sharp *minimum* $\varepsilon'(T)$ in the Curie point, instead of usual sharp maximum of permittivity (which is seen in all ferroelectrics but at much lower frequencies). This phenomenon was first discovered in microwave studies of Rochelle Salt, but later similar minima were found at ultrahigh frequencies in other ferroelectrics.

In the microwave range, starting with a frequency of about 10^8 Hz, a *sharp minimum* of permittivity appears in the place of permittivity maximum seen at lower frequencies. As frequency increases, this minimum expands and deepens. When

dispersion of permittivity ends, temperature anomaly of $\varepsilon(T) = C/(T - \theta)$ gradually disappears. The relaxation time in the phase transition region has a maximum, Fig. 3.18B. On the side of *paraelectric* (non-polar) phase, when temperature decreases, a *critical increase* in the relaxation time is seen due to the size of polar micro-regions (clusters) growing. At phase transition point (when $T = T_C$), the number of equally oriented clusters dominates and they confluent together. Nevertheless, below the phase transition an inevitable thermal fluctuations continue destroy partially the ordering, although the fraction of disordered regions little by little decreases during cooling. Correspondingly, the value of $\varepsilon'(T)$ in the *ferroelectric* phase below the phase transition also decreases: $\varepsilon(T) = C/2(T_C - T)$, see the left dashed curve in Fig. 3.18A below temperature T_C.

The dispersion equation for critically dependent on temperature permittivity can be obtained from theDebye formula, assuming in it $\varepsilon(0) - \varepsilon(\infty) = C/(T - \theta)$, where $\varepsilon(\infty)$ is the contribution of fast mechanisms of polarization, which is only slightly dependent on temperature:

$$\varepsilon^*(\omega, T) = \varepsilon(\infty) + \frac{C}{(T - \theta) + i\omega\tau_0} \qquad (3.18)$$

The appearance of minimum in permittivity dependence at phase transition at a certain frequency means the presence of a *singular point* on the curve $\varepsilon'(T)$ in the paraelectric phase just at given frequency. This frequency can be found from the derivative $d\varepsilon'(\omega, T)/dT = 0$ under the conditions $\omega \geq \omega_C$ and $T \geq T_C$, where ω_C is the frequency when permittivity temperature minimum occurs. Extracting the real part from expression (3.18) and producing this differentiation, the following formula for such frequency can be obtained: $\omega_C = (T_C - \theta)/\tau_0$, above which the *minimum* $\varepsilon'(T)$ should appear instead of usual for ferroelectrics maximum (T_C and θ are two parameters of crystal that are independent from temperature).

Permittivity minimum at the Curie point T_C, in fact, means the *splitting* of seen at lower frequencies maximum of permittivity as well as the occurrence of *two* $\varepsilon'(T)$ maximums, shifting to the right and to the left from Curie point, i.e., both in the paraelectric and ferroelectric phases. Above the Curie point, in the paraelectric phase, when $T_p > T_C$, the temperature of shifted $\varepsilon'(T)$ maximum is determined by formula: $T_p = \theta + \omega_p\tau_0$, where ω_p is the frequency at which $\varepsilon'(T)$ maximum in a paraelectric phase observed.

Therefore, from the description of permittivity dispersion by the Debye equation in the vicinity of order-disorder ferroelectric phase transition, it follows that a *minimum* in the temperature dependence of permittivity should appear, starting

from frequency equal $1/\tau$, i.e., in the center of Debye dispersion region. To analyze obtained experimental data, it is important to note that the equation describing $\varepsilon^*(\omega,T)$ variance allows determine the relaxation time τ_0. In fact, the temperature maximum of permittivity in the vicinity of permittivity dispersion is associated with the order-disorder type mechanism, and it can be described as

$$\varepsilon'_{\max} = \varepsilon(\infty) + \frac{C}{2\omega\tau_0}; \qquad \tau_0 = \frac{T-\theta}{\omega_C}; \qquad \tau_0 = \frac{C}{2\omega\left[\varepsilon'_{\max} - \varepsilon(\infty)\right]}.$$

In the cases, where in the experiment it is possible to observe confidently only a *beginning* of permittivity dispersion in the vicinity of phase transition (providing measurements near the "center" of dispersion are difficult due to large attenuation), there is an opportunity to find the relaxation time, using experimentally observed $\varepsilon'(\omega)$ decrease at different temperatures:

$$\tau_0 \approx \frac{T-\theta}{\omega_1}\sqrt{\frac{\varepsilon(0)-\varepsilon'(\omega_1)}{\varepsilon(0)-\varepsilon(\infty)}},$$

where ω_1 is a measurement frequency in the initial region of permittivity dispersion, when permittivity decreases by 5–30% from its initial value. To determine τ_0, it is possible to use also the data on magnitude of dielectric losses, increasing in the initial dispersion region at frequency ω_1:

$$\tau_0 \approx \frac{\varepsilon''(\omega_1)}{\varepsilon'(\omega_1)-\varepsilon(\infty)}\frac{T-\theta}{\omega_1}.$$

Usually, all three listed above ways of relaxation time definition lead to same result (within the limits of experimental error). The dielectric *loss factor* $\varepsilon''(\omega,T)$ also can be found from above expressions.

It is appropriate to recall that in the case of *classic* relaxation mechanism the temperature maximum of loss factor *shifts* towards the higher temperatures with increasing frequency. On the contrary, in the ferroelectrics, described by the model of order-disorder type phase transition, *no temperature shift* of loss maximum with the change in frequency is seen. When frequency grows, these maximums first increases (reaching a certain limit value) and then decreases with frequency, remaining located in phase transition point. This fact is opposed, firstly, to the usual dipole-type dielectrics and, secondly, opposed to the considering further displacement type ferroelectrics possessing resonant polarization. In other words, in the entire frequency range, where the relaxation type permittivity dispersion is observed, the maximums of $\varepsilon''(T)$ are always located at the temperature of phase transition, i.e., at $T = T_C$. Moreover, unlike the loss factor maximums observed in

usual dipole dielectrics, the maximums of $\varepsilon''(T)$ in the ferroelectrics usually are higher and sharper. Due to mechanical stresses, structural defects or impurities, the dispersion spectrum $\varepsilon^*(\omega,T)$ in the ferroelectrics becomes broadened, so sometimes the $\varepsilon'(T)$ maximum is not so sharp. Moreover, in the ferroelectric crystals with imperfect structure this maximum looks as a little diffuse and even *no minimum* in temperature dependence of permittivity is seen.

3.6 Displacive ferroelectrics

The most studied of ferroelectrics, which corresponds to a displacive phase transition model, is barium titanate, $BaTiO_3$. This is one of many ferroelectrics with perovskite structure, which can be characterized by the first order phase transition. Unlike uniaxial ferroelectrics, barium titanate just like most related ferroelectrics and antiferroelectrics is the triaxial crystal so in the paraelectric (cubic) phase in all crystalline directions it is characterized by same permittivity.

1. ***Main experimental characteristics*** of displacive ferroelectrics is advisable to cite as an example of barium titanate shown in Fig. 3.19.

Depending on temperature or hydrostatic pressure, the permittivity of $BaTiO_3$ passes through acute maximum $\varepsilon_{max}(T)$ which in normal pressure is seen at Curie temperature T_C = 400 K. Note that at normal temperature same $\varepsilon_{max}(p)$ is observed under pressure of p = 2.5 GPa. The temperature hysteresis in the dependence $\varepsilon(T)$ as well as hysteresis in the dependence $\varepsilon(p)$ in the vicinity of phase transition indicates that phase transition in $BaTiO_3$ is close by its nature to the *first-order* transition.

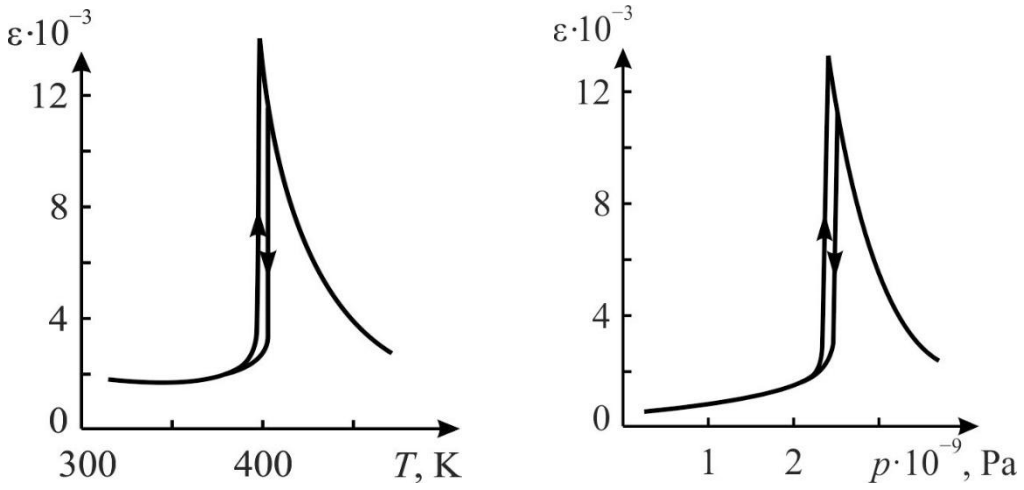

(A) (B)

Fig. 3.19. Barium titanate permittivity dependence on temperature (A) and pressure (B)

From shown in Fig. 3.19 characteristics, the following important conclusions can be made as to the study of polar materials by dielectric spectroscopy: first, when measuring temperature dependences, the direction of temperature change is important: is it cooling or heating; secondly, the mechanical conditions (fixing) of the test sample are important, since the mechanical stress (for example, due to a difference in the coefficients of thermal expansion of holder and sample) can significantly affect the results.

The parameters of several other relative to $BaTiO_3$ materials, obtained experimentally at microwave measurements. are given in Table 3.2. However, the calcium titanate (perovskite, $CaTiO_3$) shown in this table is only a *paraelectric*, and therefore it has no parameters P_S and T_C. The strontium titanate ($SrTiO_3$) can become the ferroelectric, but only in externally applied electrical field: it is the *virtual ferroelectric*. Other crystals in Table 3.2 are the ferroelectrics; in addition to phase transition temperature, parameters C and θ from the Curie-Weiss law: $\varepsilon \approx C/(T-\theta)$, are shown, which describes the temperature dependence of permittivity above phase transition.

Table 3.2

The main parameters of complex oxides - ferroelectric crystals of the barium titanate type obtained accordingly to the author's microwave research

Crystal	P_S, ⌈Q/sm^2	T_C, K	(, K	$C\oplus10^{\square4}$, K	W_g, eV	$A/2\square$, GHz⊕ K$^{\square1/2}$
$CaTiO_3$	–	–	– 90	4,5	3,2	170
$SrTiO_3$	–	–	35	8,4	3,2	180
$BaTiO_3$	30	400	388	12	3,3	75
$PbTiO_3$	80	780	730	15	3,1	90
$KNbO_3$	30	685	625	18	3,4	95
$LiNbO_3$	70	1500	–	–	3,6	–

The electronic band gap energy W_g is also given in Table 3.2 to characterize electronic conductivity of given crystals. The coefficient A describes temperature dependence of ferroelectric "soft mode" frequency ω_{TO},which determines permittivity dispersion in paraelectric phase: $\omega_{TO} = A\sqrt{(T-\theta)}$. It is seen that frequency of transverse optical phonon ω_{TO} would be zero, when crystal at its cooling from paraelectric state reaches temperature θ. However, in the experiment this is not observed due to phase transition occurs *before*: at temperature $T_C > \theta$.

However, it should be noted that the difference $T_C - \theta$ usually is little so the frequency ω_{TO} turns out to be very small in comparison with other frequencies of crystal lattice.

2. *Thermodynamic theory* based on the Landau's theory supposes that thermodynamic potential of ferroelectric $\Phi(T,P)$ can be represented as a series in powers of ordering parameter P (polarization):

$$\Phi(P) = \Phi_0(T) + \frac{\alpha}{2}P^2 + \frac{\beta}{4}P^4 + \frac{\gamma}{6}P^6, \qquad (3.19)$$

where α, β, and γ are coefficients of series. Analyzing this expansion, it is possible to make a conclusion as to *critical dependence* of parameter α on temperature: $\alpha(T) = \alpha_0(T - \theta)$, where α_0 is independent of temperature coefficient.

Due to polynomial form of free energy presentation, Landau's theory allows not only quantitatively describe changes of crystal properties near phase transitions, but also predict many physical characteristics.

At that, according to Landau's theory, the type of phase transition (PT-I or PT-II) is determined by the *sign* of coefficient β at the fourth degree of ordering parameter. In previous Section 6.2 where the phase transition PT-II was considered, ssecon Landau parameter β is positive so in this case the parameter γ in polynomial (6.6) becomes unnecessary and one can put $\gamma = 0$ as well as $\beta = const > 0$.

The ***first-order*** phase transition (PT-I) is characterized by polynomial (3.19) with parameters $\beta < 0$, $\alpha = \alpha_0(T - \theta)$ and $\gamma > 0$. In this case, the sustainability of a studied system is provided by next term $\frac{1}{6}\gamma P^6 > 0$ in the expansion, because just this ensures stability of all phases.

When these relationships detailed study, some special points for $\Phi(P)$ function and for its derivatives can be found. If instead of the image of the function $E(P)$ the more convenient coordinates $P(E)$ would be used, polar phase existence will be explained by the region of instability, that corresponds to dielectric hysteresis loop like in Fig. 3.13A and Fig. 3.16. Accordingly, the permittivity depends on the field strength. Thus, main characteristics of ferroelectrics in their *polar phase* (hysteresis loop and $\varepsilon(E)$ dependence) do not depend on what type of phase transition undergoes in the Curie point.

To study the polynomial (3.19) describing PT-I, it is necessary to find singular points for both the function $\Phi(P)$ and its derivatives:

$$\partial\Phi/\partial P = E = \alpha P + \beta P^3 + \gamma P^5; \qquad (3.20)$$

$$\partial^2\Phi/\partial P^2 = \partial E/\partial P = 1/\chi \approx \varepsilon = \alpha + 3\beta P^2 + 5\gamma P^4; \qquad (3.21)$$

$$\partial^3\Phi/\partial P^3 = \partial^2 E/\partial P^2 = 6\beta P + 20\gamma P^3; \qquad (3.22)$$

$$\partial^4\Phi/\partial P^4 = \partial^3 E/\partial P^3 = 6\beta + 60\gamma P^2 \qquad (3.23)$$

The first condition for the phase stability $\partial\Phi/\partial P = 0$ leads to equation of fifth degree (3.20); its roots are equal to:

$$P_1 = 0; P_{2,3,4,5} = \pm\sqrt{\frac{-\beta \pm \sqrt{\beta^2 - 4\alpha\gamma}}{2\gamma}} \qquad (3.24)$$

To analyze the second stability condition $\partial^2\Phi/\partial P^2 = 0$ it is necessary to study the conditions for the extrema of equation $E(P) = 0$ which can be found from (6.8):

$$P_{6,7,8,9} = \pm\sqrt{\frac{-3\beta \pm \sqrt{9\beta^2 - 20\alpha\gamma}}{10\gamma}} . \qquad (3.25)$$

In turn, extrema of dependence $\partial E/\partial P$ are special points of expression (6.9):

$$P_{10} = 0; P_{11,12} = \pm\sqrt{\frac{-3\beta}{10\gamma}} . \qquad (3.26)$$

And finally, from expression (3.23) it is possible to obtain

$$P_{13,14} = \pm\sqrt{\frac{-\beta}{10\gamma}} . \qquad (3.27)$$

Fourteen special points (extremes, kinks, intersections with axes) characterize many different variants of $\Phi(P)$ dependence, which arise in the vicinity of PT-I when the ratio between coefficients α, β and γ changes.

Before further analysis, it is advisable to introduce the generalized parameter $\varsigma = \alpha\gamma/\beta^2$, which makes it possible to trace how the thermodynamic potential and its derivatives change (depending on the combination of Landau parameters). It should be noted that this investigation might have grate interest for the *nonlinear dielectric spectroscopy*, when exactly the dependence of dynamic permittivity on electrical field is important.

As seen in Fig. 3.20, just at phase transition point, i.e., at $T = T_C$, the parameter $\varsigma = 0.2$, while at Curie-Weiss temperature $T = \theta$ this parameter is zero ($\varsigma = 0$). In the Fig. 3.20 it is shown how, starting from high-temperature nonpolar (paraelectric) phase (when $\varsigma = 0.4$) when the crystal gradually is cooling to the ferroelectric phase ($\varsigma = 0.2$) the change in $\Phi(P)$ and its derivatives occur, when generalized parameter passes through the values $\varsigma = 0.4, 0.3, 0.2, 0$.

Continuing above analysis, note that all the roots of equations (6.9) and (6.10) are valid are determined by formulas (6.13) and (6.14) since $\beta < 0$ and $\gamma > 0$. Therefore, equations roots P_{13} and P_{14} determine respectively the minimum and maximum of the function $\partial^2\Phi/\partial P^2$, while the roots of P_{10}, P_{11} and P_{13} determine the maximum and two minimums of $\partial E/\partial P$ function as shown in Fig. 3.21.

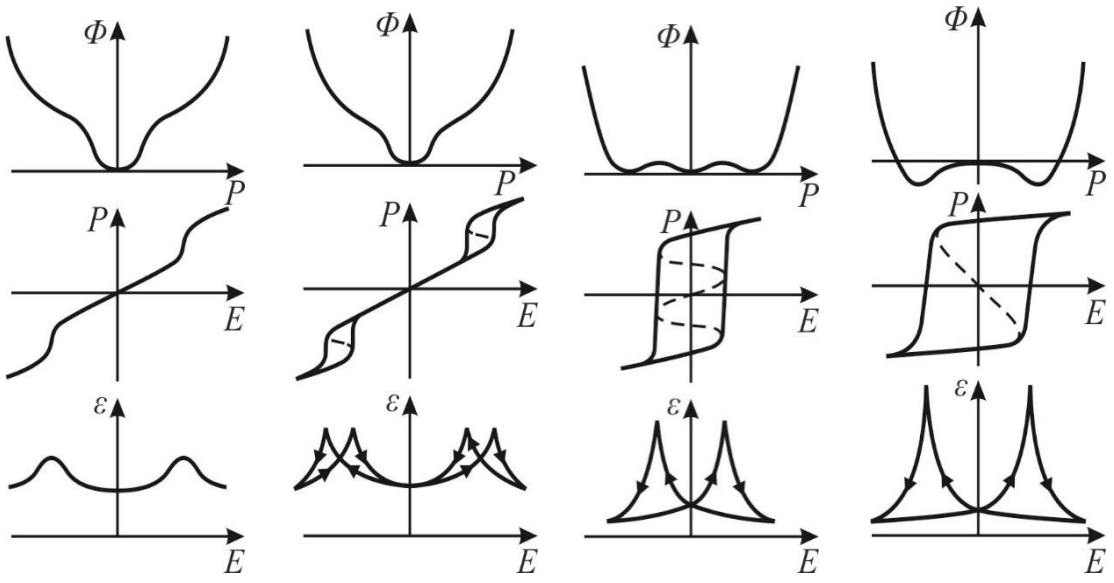

Fig. 3.20. Dependence of Φ(*P*) characteristic on generalized parameter $\varsigma = \alpha\gamma/\beta^2$

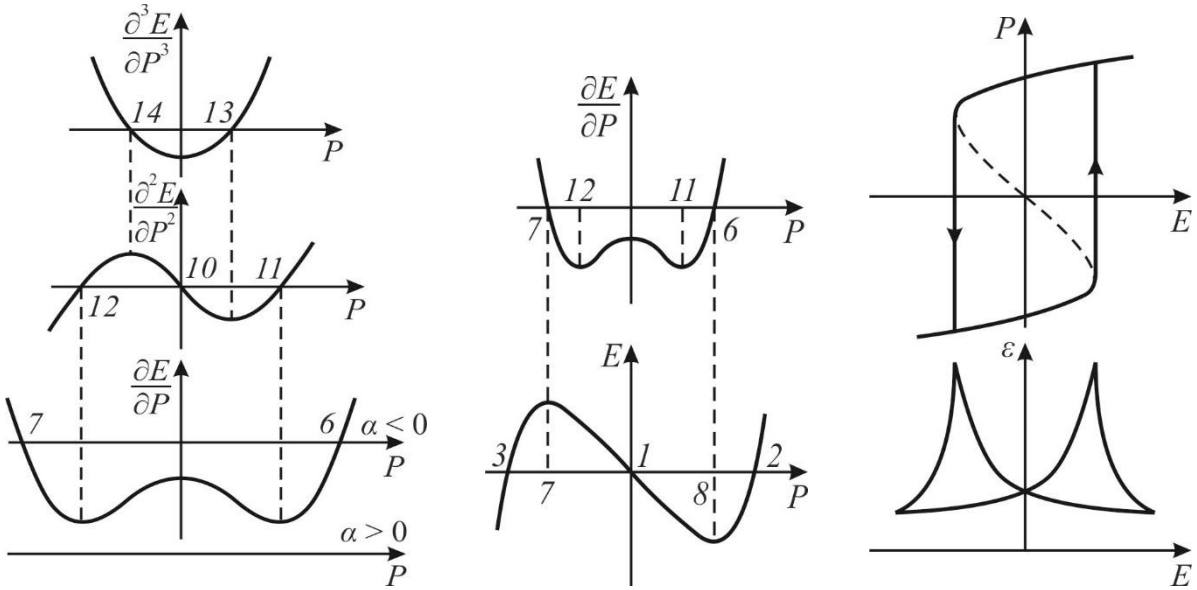

Fig. 3.21. Thermodynamic analysis of ferroelectric phase transition of first kind: A, B − derivatives describing phase transition parameters, numbers at intersections correspond to roots of equations (3.21−2.23); C − explanation of dielectric hysteresis and dynamic dielectric permittivity ε(*E*)

Further analysis depends on Landau parameter α temperature changing.

In the ***polar phase*** of the PT-I ferroelectric, at a *sufficient distance* from the critical point T_C (when $T < \theta$ and $\alpha < 0$), as follows from formula (3.25), the equation (3.21) has only two real roots (P_6 and P_7) of the four. In this case, the dependence $E(P)$ is characterized by a minimum at P_6 and a maximum at P_7 and also intersects

the P axis at three points: $P_1 = 0$; $P_{2,3,4,5} = \pm [-\beta \pm (\beta^2 - 4\alpha\gamma)^{1/2}/2\gamma]^{1/2}$ (the other roots P_4 and P_5 in the expression (3.24) are imaginary since $\alpha < 0$.

Characteristics $\partial E/\partial P$ and are given in Fig. 3.21B. Further, presenting the functional dependence $E(P)$ as $P(E)$, obtain a situation that is similar to PT-II and shown in Fig. 3.16B. with the instability region and hysteresis loop. Accordingly, the dynamic permittivity also changes, but in the *vicinity* of PT-I variations of polarization $P(E)$ and permittivity $\varepsilon(E)$ are much more complicated than in the case of PT-II. But far from the phase transition, both the hysteresis loop and the dynamic permittivity nonlinearity in the PT-I and PT-II ferroelectrics are qualitatively similar.

Now discuss spontaneous polarization and permittivity temperature dependence, Fig. 3.22. At the phase transition point, the potentials of the polar and nonpolar phases should be the same, i.e. $\Phi(P) = \Phi_0$ at $P = 0$. Therefore, from equation (3.19) it follows $\alpha + 1/2\beta + 1/3\gamma = 0$. Substituting into this expression the value for P_S obtained from formula (6.11) while note that the roots $P_{2\text{-}5}$ and the root P_1 are side solutions, we can obtain an equation relating all three parameters $\alpha_C = \frac{3\beta^2}{16\gamma}$, where α_C is first parameter Landau at $T = T_C$. When dielectric spectroscopy application to PT-I ferroelectrics study, it should be noted that first order phase transition occurs not at the temperature $T = \theta$ (when parameter $\alpha(T) = 0$) but at the value α_C That is why, in case of PT-I the transition temperature T_C is *higher* than Curie-Weiss temperature θ. At that, the spontaneous polarization arises at $T = T_C$ by a *jump* (unlike the PT-II), and the size of this jump equals $\Delta P_S = \frac{3\beta}{4\gamma}$, Fig. 3.22A.

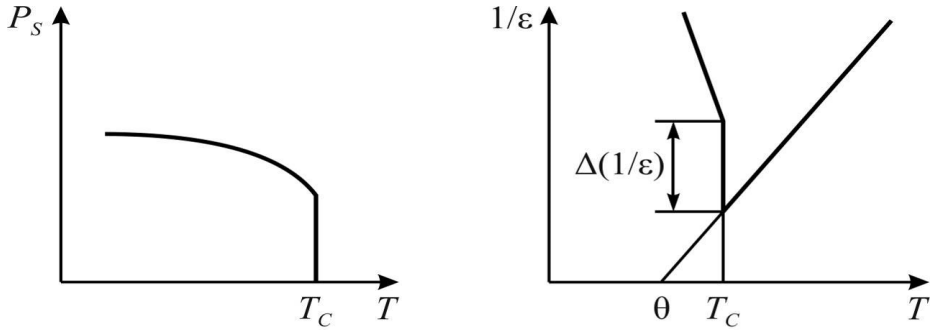

(A) (B)

Fig. 3.22. Temperature dependence of spontaneous polarization (A) and inverse permittivity (B) in ferroelectrics possessing PT-I

Permittivity also shows a jump at temperature T_C, and its graded change is $\Delta\varepsilon = \frac{4\gamma}{3\beta^2}$; correspondingly, at PT-I is not expected that permittivity becomes

infinite (as predicted in case of PT-II) but has a maximum seen at T_C which equals $\frac{16\gamma}{3\beta^2}$. Most studied ferroelectric which has phase transition nature close to PT-I is barium titanate. The temperature maximum of permittivity in pure $BaTiO_3$ occurs at T_C = 400 K, while Curie-Weiss temperature (θ = 388 K) is below on 12 K. Curie-Weiss constant in barium titanate equals $C = 1.2 \cdot 10^5$ K and temperature maximum of permittivity is $\varepsilon_{max} = 10^5$.

3.7 Dynamics of displacive ferroelectrics

The frequency of fundamental dielectric dispersion in these ferroelectrics is two orders of magnitude higher than in the order-disorder type ferroelectrics. Therefore, if they would be considered as potential components to be used in the microwave electronic devices (or absorbing composites), it should be taken into account that the maximal absorption of electromagnetic waves in the displacement type ferroelectrics is located in the region of the millimeters and sub-millimeters waves.

From a large number of experimental dependences of $\varepsilon^*(\omega,T)$, obtained by the dielectric measurements using millimeter, sub-millimeter and far infrared waves, it is possible to get reliable information about natural frequency $\omega_0(T)$ and damping factor $\gamma_0(T)$ of "soft" vibration modes of ferroelectric lattice. Permittivity dispersion is due to the quasi-elastic displacement of ions that usually is observed in the crystals at frequencies 10^{13}–10^{14} Hz, but in some ferroelectrics near their phase transition the frequency of their "soft mode" of lattice vibrations can decrease down to 10^{11}–10^{12} Hz. The change of permittivity in this frequency range can be described by the model of damped oscillator. At that, a general tendency is noticeable: the higher permittivity the lower dispersion frequency and greater attenuation of the oscillator, which describes corresponding mode of oscillation in a crystal lattice.

In the *paraelectric phase* of displacement type ferroelectrics, i.e., above the ferroelectric phase transition, the temperature dependence of frequency of oscillator describing "soft mode" is determined by a *critical dependence*, i.e., by Cochran ratio $\omega_0(T) = A(T - \theta)^{1/2}$, while the characteristic *attenuation frequency* rather weakly depends on temperature: $\gamma(T) = \gamma_0 + aT + bT^2 + cT^3$. Here the first term is caused by two-phonon scattering on static fields of lattice defects, while the second and next terms correspond respectively to three- and four-phonons processes in the

anharmonic crystal. Near the phase transition weak temperature dependence of $\gamma(T)$ can be neglected, however, the *relative attenuation* $\Gamma(T) = \gamma/\omega_0(T)$ depends on temperature critically: $\Gamma(T) = B(T - \theta)^{-1/2}$ that is due to critical dependence of oscillator frequency.

The *permittivity* temperature-frequency dependence of ferroelectrics, possessing phase transition of displacement type, can be describe by the Drude–Lorentz equation and the Cochran ration, taking into account also Curie–Weiss law:

$$\varepsilon^*(\omega,T) = \varepsilon(\infty) + \frac{C}{T-\theta}\frac{\omega_0^2}{\omega_0^2 - \omega^2 + i\gamma\omega} \qquad (3.28)$$

where $\varepsilon(\infty)$ characterizes the optical and other higher-frequency contributions to permittivity, C and θ are Curie–Weiss constants; the temperature dependence of damping factor γ is weak and can be neglected.

Dividing the real and imaginary parts in equation (14), it can be obtained:

$$\varepsilon'(\omega,T) - \varepsilon(\infty) = CA^2\frac{A^2(T-\theta) - \omega^2}{\left[A^2(T-\theta) - \omega^2\right]^2 + \gamma^2\omega^2}; \qquad (3.29)$$

$$\varepsilon''(\omega,T) = CA^2\frac{\gamma\omega}{\left[A^2(T-\theta) - \omega^2\right]^2 + \gamma^2\omega^2}; \quad \tan\delta \approx \frac{\gamma\omega}{A^2(T-\theta)}. \qquad (3.30)$$

It follows from these equation that in the region of dielectric dispersion the temperature dependence of permittivity in the paraelectric phase can be described by equation $\varepsilon'_{max} = \varepsilon(\infty) + CA^2/(2\omega\gamma)$. The temperature at which the anomaly of of permittivity is seen corresponds to $T = \theta + [\omega(\gamma + \omega)]A^2$. This means that at sufficiently high frequency at the point of phase transition the *minimum* of permittivity should be observed at temperature $T \approx T_C$, as well as in the ferroelectrics of order-to-disorder phase transition type.

Thus, ε'(T) minimum in the dispersion region is seen in all ferroelectrics (with the exception of improper ferroelectrics).

Figure 3.23A shows the temperature dependence of permittivity in the barium titanate, calculated above Curie point, i.e, in the paraelectric phase. It is seen that, starting from a certain frequency, the $\varepsilon''(T)$ maximum *shifts* with the increase of frequency to higher temperatures, forming the minimum of permittivity in the Curie point. As it follows both from calculations and experimental data, in the region of dielectric dispersion the *temperature maximum* of loss factor: $\varepsilon''_{max,T} = CA^2/(\gamma\omega)$ should also be observed at frequency $\omega_1 = A\,(T_1 - \theta)^{1/2}$.

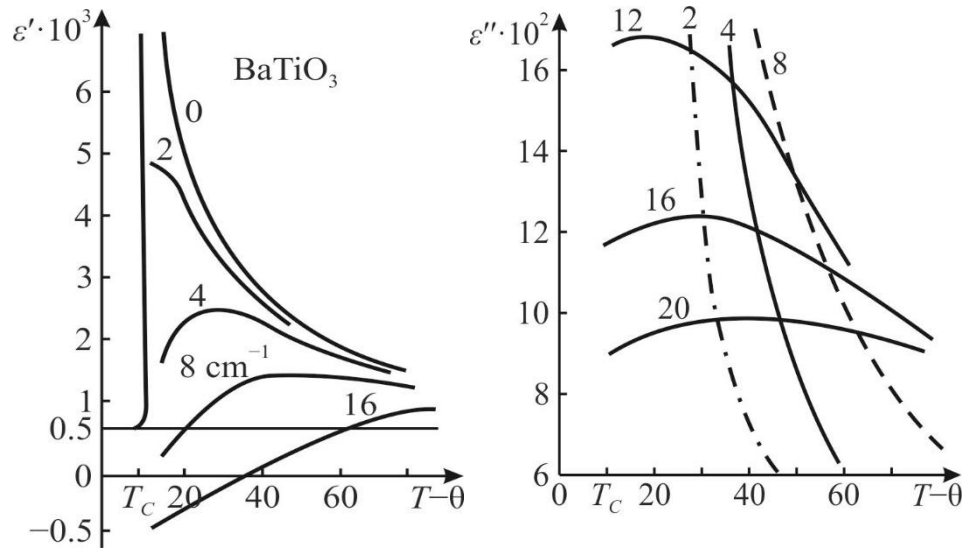

(A) (B)

Fig. 3.23. Temperature dependence of real (A) and imaginary (B) parts of permittivity in barium titanate paraelectric phase described by: $C = 2.1 \cdot 10^5$ K, $A = 3$ cm^{-1}K$^{-1/2}$ and $\gamma = 50$ cm^{-1} (near curves the frequency is shown in cm^{-1}), vertical line at Curie point characterizes ε' jump, minimum of $\varepsilon'(T)$ is formed above 2 cm^{-1}; maximum $\varepsilon'(T)$ shifts in range of 4–16 cm^{-1} while maximum of $\varepsilon''(T)$ is clearly expressed at frequencies of 12–20 cm cm^{-1} (1 cm^{-1} = 30 GHz)

Therefore, the *loss factor* $\varepsilon''(T)$ in the paraelectric phase of displacement type ferroelectrics in the vicinity of permittivity dispersion demonstrates the *maximum,* which at sufficiently high frequency *shifts to higher temperatures* when frequency growing. Note that this is qualitatively distinguished from the family of curves $\varepsilon''(T)$ describing permittivity dispersion in relaxation model. This circumstance can be used in the dielectric spectroscopy to select one or another model when describing polarization in ferroelectrics.

The equations (3.29) and (3.30) make it possible to find main parameters of dispersion oscillator from the experimental data; namely the frequency $\omega_0(T)$ and the damping factor $\gamma_0(T)$ of the "soft" vibration mode. In the case when only a beginning of permittivity dispersion can be investigated, i.e., the significant increase of tanδ is found followed by frequency change of $\varepsilon'(T)$, next simple formulas for attenuation value calculating can be obtained from above expressions:

$$\gamma \approx \frac{A^2(T-\theta)}{\omega}\tan\delta \approx \frac{A^2(T-\theta)}{\omega}\sqrt{\frac{\varepsilon(0)-\varepsilon'_{hf}}{\varepsilon(0)-\varepsilon(\infty)}}$$

where ω is the measurement frequency; $\varepsilon(0)$ is the permittivity before dispersion; ε'_{hf} is the high-frequency decrease of permittivity in the initial region of dispersion.

In the polycrystalline ferroelectrics, as well as in the crystals possessing by high concentration of structural defects, when studying the temperature-frequency dependence of permittivity describing in the framework of oscillator model, the *distribution* of frequency of oscillators can also be taken into account (as in the case of relaxor).

Thus, when experimental study of high-permittivity materials by dielectric permittivity frequency dispersion method, it is possible to make reliable selection between relaxor and oscillator models.

3.8 Polarization dynamics in paraelectrics

Paraelectrics are of interest for the use in the electronic components as materials combining high permittivity and low dielectric loss with dielectric non-linearity found in the microwave range. The disadvantage of paraelectrics is their temperature instability, as a result of which the compromise solutions have to be applied at technical devices elaboration with use of paraelectric components.

In solid state physics, the term "paraelectric" appeared as an analogue to the "paramagnetic", although this analogy is very arbitrary.

The fact is that magnetic permeability μ of most paramagnetics is very small ($\mu = 1 + æ \approx 1$), and only the temperature dependence of their *susceptibility* $æ$ obeys the Curie law $æ = K/T$. However, the permeability is great in the *paramagnetic phase* of ferromagnetics and antiferromagnetics, where it is described by the Curie-Weiss law $\mu \approx æ = C/(T - \theta)$. On the contrary, in the *paraelectrics* their permittivity is always high and in all cases can be described by the Curie-Weiss law $\varepsilon \approx C/(T - \theta)$.

Note that in most paraelectrics Curie-Weiss temperature is positive ($\theta > 0$ K), and these materials tend to go into the polar on antipolar phase when temperature decreases (however, the electrically ordered phase in them can also appear under the influence of external electrical field or inhomogeneous mechanical stresses.

If the paraelectrics are determined as the crystals with high permittivity obeyed Curie Weiss law, then it should be noted that there exist paraelectrics, in which this critical temperature looks negative ($\theta < 0$ K) and they could be called as "stiff" paraelectrics, because they have never been transformed into polar phase (incidentally, interesting case when $\theta < 0$ K is also known in magnetism when describing paramagnetic phase of antiferromagnetics).

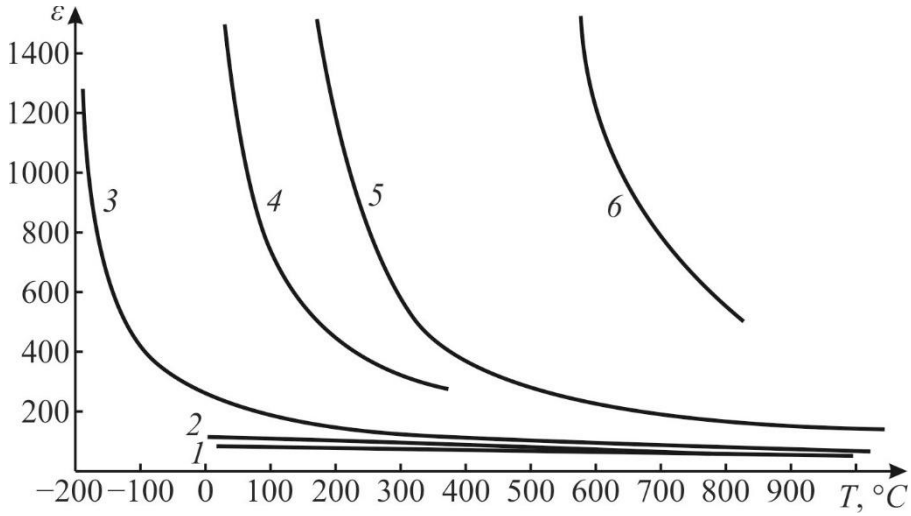

Fig. 3.24. Temperature dependence of permittivity in various paraelectrics at frequencies of 37 GHz and 77 GHz: *1* – TiO_2 polycrystal, 2 – $CaTiO_3$ polycrystal, 3 – $SrTiO_3$ single crystal, 4 – $Ba(Ti_{0.6}Sn_{0.4})0_3$ polycrystal, $Ba(Ti_{0.9}Sn_{0.1})0_3$ polycrystal, 6 – $PbTiO_3$ single crystal [15]

1. Theoretical notes. In most of paraelectrics, at temperature T = Tc ≈ θ (critical temperature) the phase transition occurs to ferroelectric (or antiferroelectric) phase. That is why the paraelectricity usually is associated with the ferroelectricity; for this reason, just as the ferroelectrics, the paraelectrics can be divided into two basic classes.

The paraelectrics of *order-disorder type* (reviewed in previous Section 3.4) are crystals containing dipoles. As temperature decreases, the dipole-dipole interaction gives rise to a gradual ordering of dipole orientations, until, finally, when temperature becomes $T_c \approx \theta$ the ferroelectric phase arises, at which most of dipoles are *steadily* oriented. Such paraelectrics near their second-order phase transition are characterized by an acute $\varepsilon(T)$ maximum and rather fast decrease of permittivity with temperature rise that signifies the *small* Curie-Weiss constant ($C \approx 10^3$ K). At that, at high frequencies, especially in the microwave range, the order-disorder type paraelectrics have *huge losses* and therefore very limited prospects for application.

The paraelectrics of the *displacment type* are the ionic (not dipole) crystals, in which, however, the ionic-covalent bonding between atoms is very significant. Most of these paraelectrics demonstrate the *first-order* phase transition to the ferroelectric phase with a relatively *flatter* $\varepsilon(T)$ dependence that is characterized by *big* Curie-Weiss constant: $C \approx 10^5$ K. In electronic materials, contemporary technology of *polycrystalline solid solutions* enables to obtain quite different ε and $TC\varepsilon$. This is especially important at high frequencies (microwave ε_{mic}). While technical dielectrics designing, it is considered that the change in the magnitude and sign of $TC\varepsilon$ depends on what type of polarization dominates – electronic or ionic. It is

important to note that the ionic (lattice) polarization depends also on the atomic electronic shells displacement, but the frequency characteristic of this mechanism of polarization is given by the inter-atomic elastic forces and the masses of ions. Therefore, this frequency is much less than the optical frequency but remains quite enough for microwave electronics applications.

The role of electronic shells displacements is especially important for *high permittivity* dielectrics. Note that because of electronic (optical) polarization affects ionic (infrared) polarization, instead of simple expression for polarization: $P = N\alpha F$ (where α is polarizability, N is concentration of polarizable particles, and F is acting Lorentz force) one has to write:

$$P = \left[a + \frac{nq^2}{m} \frac{1}{\left(\omega_0^2 - \omega^2\right)} \right] \left(E + \frac{1}{3\varepsilon_0} P \right),$$

where $1/(3\varepsilon_0)$ is the Lorentz factor and a takes into account *optical polarization*. After some transformations, for frequencies of transverse and longitudinal optical phonons as well as for dielectric contribution from infrared polarization following expressions it can be obtained:

$$\omega_{TO}^2 = \frac{c}{m} - \frac{nq^2}{3\varepsilon_0 m} \frac{\varepsilon(\infty) + 2}{3};$$

$$\omega_{LO}^2 = \frac{c}{m} + \frac{2nq^2}{3\varepsilon_0 m} \frac{\varepsilon(\infty) + 2}{3};$$

$$\varepsilon(0) - \varepsilon(\infty) = \frac{nq^2}{\varepsilon_0 m \omega_{TO}^2} \frac{\left(\varepsilon(\infty) + 2\right)^2}{9}.$$

Expression for frequency ω_{LO} is the sum, therefore, the influence of electronic polarization almost does not change the frequency ω_{LO} (as opposed to value of ω_{TO}). From above equations it is seen that the lower frequency ω_{TO} the greater the value of $\varepsilon_{mic} = \varepsilon(0) - \varepsilon(\infty)$ and measured at microwave frequencies. Formula for frequency ω_{TO} shows that with temperature increase, due to thermal expansion, on one hand, the term c/m reduces, but, on other hand, the subtrahend decreases being dependent on $\varepsilon(\infty)$. In the expression for ω_{TO}, the temperature variation of the difference can be various depending on what effect predominates, and it defines value $\varepsilon_{mic}(T)$.

To describe the paraelectricity, one needs to express the Curie-Weiss constant through the parameters of above discussed model. The approximate form of Curie-Weiss law $\varepsilon(T) \approx C/(T - \theta)$ can be obtained, if the following formula is substituted:

$$\frac{m\omega_{TO}^2}{c} = 1 - \frac{nq^2\left(\varepsilon(\infty) + 2\right)^2}{9c\varepsilon_0} = \gamma\left(T - \theta\right).$$

By substituting of this value into the expression for permittivity, obtain

$$\varepsilon(0)-\varepsilon(\infty)=\frac{nq^2\left(\varepsilon(\infty)+2\right)^2}{9c\gamma\varepsilon_0}\frac{1}{T-\theta};\qquad A=\sqrt{\frac{c\gamma}{m}};\qquad C=\frac{nq^2\left(\varepsilon(\infty)+2\right)^2}{9c\gamma\varepsilon_0}.$$

The main contribution to ε_{mic} is given by the far infrared (lattice) polarization. Formally it is mentioned as the "ionic" polarization, but in fact it is associated with the susceptibility of ions electronic orbitals. It is found that most part of ε_{mic}, for example, in the "stiff" paralectrics (such as rutile and perovskite) is caused by the highly polarizable oxygen octahedrons TiO_6 connected by their vertices. In this case, the electronic clouds, which link ions in the system of octahedrons, provide enough freedom for easy polarization that leads to $\varepsilon_{mic} > 100$.

2. *"Stiff" paraelectrics* are attractive to technology due to not only in them, but also in their solid solutions the microwave dielectric losses are small. These *non-polar* ionic crystals with $\varepsilon \sim 100$ (and some above) occupy special place among dielectrics with high permittivity. Typical representatives of such dielectrics are the rutile (TiO_2) and perovskite ($CaTiO_3$). It should be noted that these crystals are characterized by the increased electronic (optical) polarization: $\varepsilon_{opt} > 5$. Moreover, the microwave permittivity of rutile and perovskite is strongly temperature dependent with the *negative TC*ε. The dependence $\varepsilon(T)$ in $CaTiO_3$ (perovskite) can be described in the broad temperature range, if in formula $\varepsilon(T) = \varepsilon_1 + C/(T - \theta)$ one put $\varepsilon_1 = 60$, $C = 4 \cdot 10^4$ K and $\theta = -90$ K.

The explanation of frequency ω_{TO} reducing when temperature decreases and the high polarization in crystals of *perovskite* structure may be as follows. Each ion is in the equilibrium position under the action of long-range electrical forces of attraction and short-range forces of repulsion. High polarization means that application of even a weak electrical field leads to the unusually large displacements of ions from their equilibrium position (or, according to model of "soft" ions, to the large deformation of the electronic shell of ions). This also means that the elastic force of repulsion of ions is small (i.e., it corresponds to lower oscillation frequency). It is logical to assume that in the perovskite-type structures the such conditions are created for some ions, when the compensation of short-range repulsion forces and long-range attraction forces occurs. Thus, the effects, caused by the interaction of electronic shells of ions, lead to a large value of permittivity with the anomalous temperature dependence as well.

Figure 3.24 shows the fulfillment of Curie-Weiss law in the paraelectrics at millimeter waves (when the influence of conductivity and low-frequency relaxation processes is excluded). At that, the strontium titanate refers to the *virtual*

ferroelectrics (which can be easily turned to the ferroelectric phase under the influence of electrical field or non-uniform mechanical stress) while both solid solutions Ba(Ti,Sn)0_3 and $PbTiO_3$ refers to the *ferroelectrics* with various Curie point. At the scale selected in Figure 3.24 it is difficult to judge the properties of lower permittivity "stiff" these paraelectrics, so their characteristics at millimeter waves are given more detail in Fig. 3.25A,B. As it follows from crystal lattice dynamics, the microwave permittivity is proportional to the square of frequency of transverse optical vibration mode determined from infrared spectra. The experiment clearly indicates that the Curie-Weiss law with a negative value of the temperature parameter θ in the "stiff" paraelectrics is good satisfied.

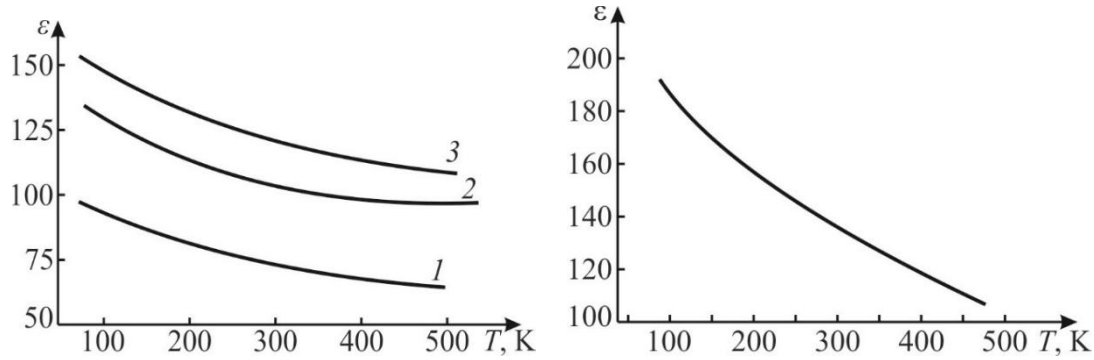

(A) (B)

Fig. 3.25. Permittivity and "soft" lattice mode temperature dependence of "stiff" paraelectrics: A – rutile, TiO_2, at 37 GHz, *1* – ε_1 for crystal, *3* – ε_3 for crystal, *2* – ε for ceramics; B – perovskite, $CaTiO_3$, ceramics at 77 GHz

The correlation of the “soft” mode frequencies and their dielectric contribution, which varies according to the Curie-Weiss law, can be seen in Fig. 3.26.

3. *"Soft" paraelectrics* of displacive type may be represented by strontium titanate, $SrTiO_3$. In the frequency dependence of reflection coefficient, all three vibration modes are clearly expressed both for $SrTiO_3$ single crystal and for the polycrystal. Complex permittivity of $SrTiO_3$ temperature and frequency dependence can be described by the equations

$$\varepsilon'(\omega,T)-\varepsilon_\infty = CA^2\frac{A^2(T-\theta)-\omega^2}{\left[A^2(T-\theta)-\omega^2\right]^2+\gamma^2\omega^2}, \quad \varepsilon''(\omega,T)-\varepsilon_\infty = CA^2\frac{\gamma\omega}{\left[A^2(T-\theta)-\omega^2\right]^2+\gamma^2\omega^2},$$

where $C = 8.4\cdot10^4$ K, (= 35 K, $A/2$□ = 180 GHz·K□$^{1/2}$, ∑(□) = 40 and © = 0.6. The temperature dependence of $SrTiO_3$ “soft” mode frequency $\omega_{TO} = A\sqrt{T-\theta}$ is shown in Fig. 6.21B.

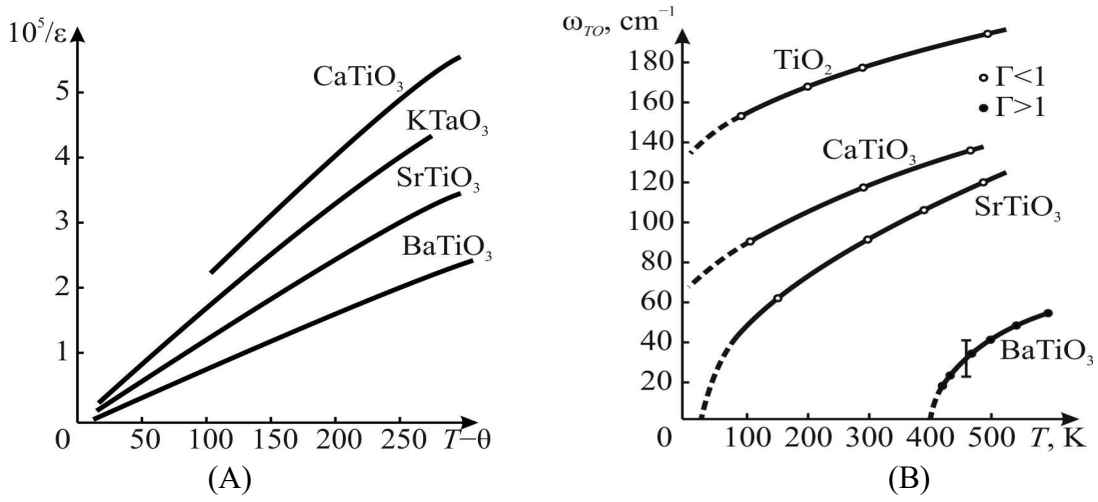

Fig. 3.26. Temperature dependence of inverse permittivity (A) and frequency ω_{TO} (B) for paraelectrics TiO_2, $CaTiO_3$, $SrTiO_3$ and ferroelectric $BaTiO_3$ (in its paraelectric phase); Γ is correspondent oscillator damping factor, 1 cm^{-1} = 30 GHz [14]

Thus, from experimental dependences $\varepsilon^*(\omega,T)$ obtained by dielectric measurements on millimeter, sub-millimeter and infrared waves, it is possible to obtain important data on the frequency of "soft" mode ($\nu = \omega/2\pi$) of crystal lattice vibrations and its damping. Permittivity dispersion caused by the elastic displacement of ions in the ordinary crystals occurs at frequencies of about 10^{13} Hz, but in the “soft” paraelectrics, when approaching the phase transition, the frequency of “soft mode” of these oscillations can decrease to 10^{11} Hz. A noticeable general trend: the higher dielectric permittivity, the lower frequency and the greater attenuation of the oscillator, which describes the vibration mode of crystal lattice corresponding to main dispersion of permittivity.

While study "soft" paraelectrics by the dielectric spectroscopy method, it is important to keep in mind their increased sensitivity not only to the impurities, structural defects and electrical field strength, but also to the *mechanical conditions* in which the sample under study is located. It is known, for example, that a planar mechanical deformation of a film sample, caused, for example, by the difference in the coefficients of thermal expansion of studied paraelectric film and its substrate, can cause the *phase transition* of soft paraelectric into the ferroelectric phase.

3.9 Dynamics of antiferroelectrics, ferr*i*electrics, etc

In electronics, the antiferroelectrics are used, firstly, as important components of piezoelectric ceramic materials, secondly, for components of high-permittivity low-loss microwave devices, and, thirdly, they are promising materials for

electrocaloric coolers. In the dynamics of dielectrics, the antiferroelectrics are noteworthy because despite their high permittivity most of them do not experience any microwave dispersion in both the paraelectric and antipolar phases.

1. *Physical basis.* The antiferroelectrics are close to the ferroelectrics by their physical nature, structure and chemical composition. As in the ferroelectric, in the antiferroelectric paraelectric phase, the Curie-Weiss law is fulfilled that leads to the maximum of permittivity in the Curie point, where the first-order phase transition occurs, usually with a temperature hysteresis, Fig. 3.27A,B,D.

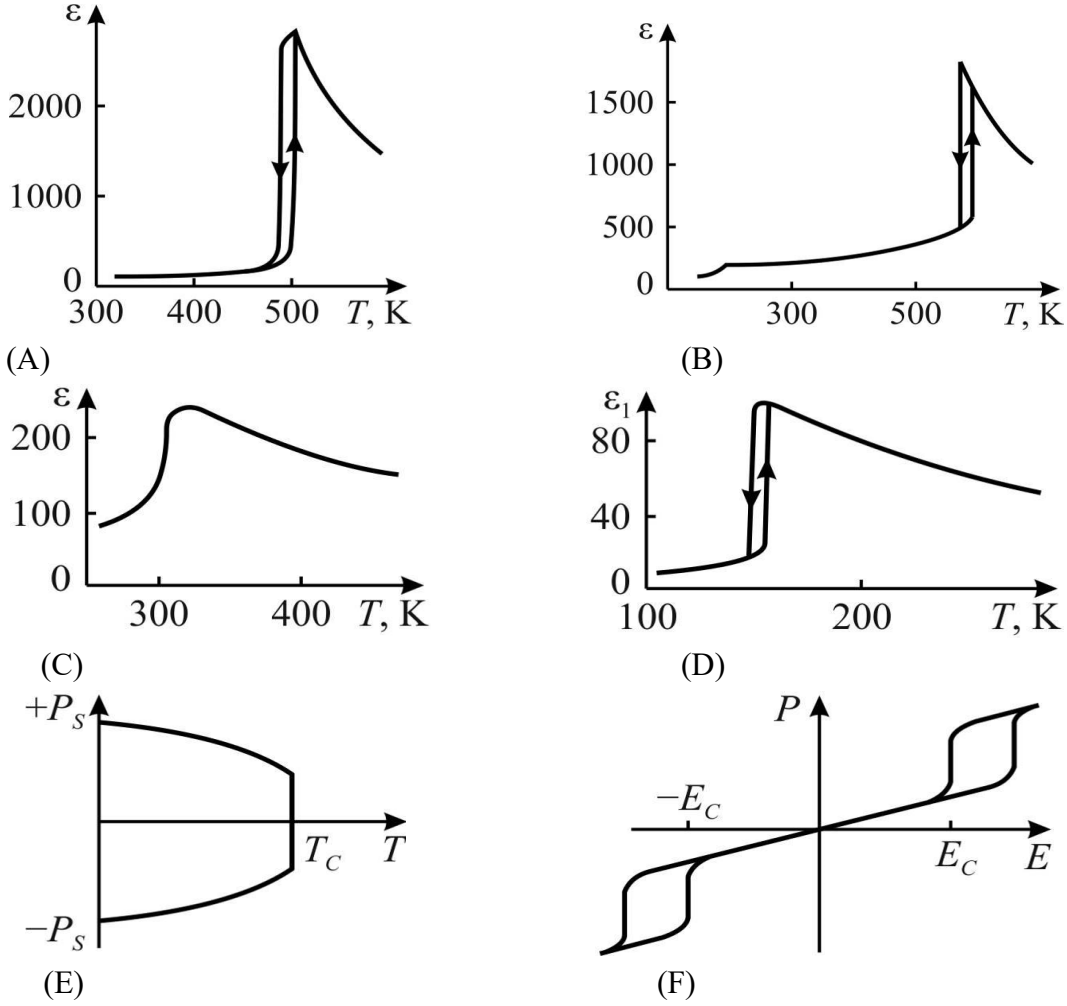

Fig. 3.27. Temperature dependence of permittivity in antiferroelectrics $PbZrO_3$ (A), in $NaNbO_3$ (B), $PbMgWO_6$ (C) and NH_4PO_4 (D), as well as model of spontaneous polarization compensation in unit cell of antiferroelectric (E) and double hysteresis loop (F)

However, any spontaneous polarization in the antiferroelectric is absent since below their phase transition from the paraelectric state crystal polarization is totally compensated *within a single unit cell*. The fact is that in the antiferroelectric not a parallel (like ferroelectric) but the antiparallel displacement of same sort ions occurs. In this case, the multiple increase in the size of crystal unit cell is observed. Inasmuch as the energy of the *centrosymmetric* antipolar state is not very different from the

energy of the non-centrosymmetric polar state, so external influences usually can turn antiferroelectric into the ferroelectric. For example, the phase transition from the antipolar to the polar state can be induced by the strong electrical field ($E > E_{cr}$); in this case the *double hysteresis loop* is observed, Fig. 3.27F.

The phase transition between the antiferroelectric and ferroelectric phases can occur not only under the influence of electrical field, but also by the introducing impurities, by the formation of solid solutions with ferroelectric, and, sometimes, even as a result of temperature change. Last situation is observed, for example, in sodium niobate ($NaNbO_3$, Fig. 3.27B), in which the antiferroelectric phase exists in a limited temperature interval from 630 K to 80 K: below temperature of 80 K crystal $NaNbO_3$ turns into ferr*i*electric phase, in which the ferroelectric and antiferroelectric states coexist.

It is noteworthy that while phase transition from their paraelectric phase, the antiferroelectric phase arises with the "*multiplication"* of crystal unit cell. As a result, below Curie point the size of unit cell of the antipolar phase becomes in 2, 4 or 8 times bigger than the unit cell of paraelectric phase. Simplifying situation, it is possible to assume that so called "spontaneous polarization" in the antiferroelectric is compensated by the opposite charges displacement within new enlarged unit cell. In this connection, it is necessary to note that in at the phase transition from the paraelectric into the *ferroelectric state,* the multiplication of the elementary unit cell usually is not observed: each unit cell below Curie point becomes polarized in a same way, and this effect is summarized in crystal, forming $P_S > 0$.

Thus, in the antiferroelectric, owing to unit cell multiplication in comparison with original (non-polar) phase, "polar" shifts of ions during phase transition are compensated at the *elementary level*, so total spontaneous polarization in a crystal is absent. Important fact is that the antiferroelectric type phase transition occurs with the *increase* in crystal density, so that in the vicinity of antiferroelectric phase transition the *maximum* of thermal expansion coefficient $\alpha(T)$ is observed (but not a minimum $\alpha(T)$ usual for ferroelectric phase transitions).

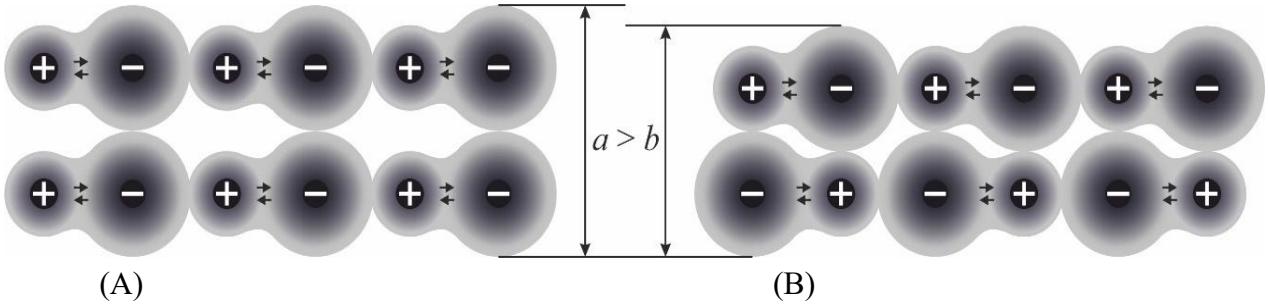

Fig. 3.28. Comparison of polar ordering lattice (A) and antipolar ordering lattice (B): it is seen that lattice parameters $a > b$

Simplest explanation of this feature is given in Fig. 3.28, where differently located polar-sensitive bonds give an opportunity to explain how the size of crystal lattice might be changed under different phase transitions. In the antipolar crystals, a special arrangement of polar-sensitive bonds can lead not only to increase of crystal density, but also facilitates optical phonons participation in the electrical properties of crystal. This becomes especially noticeable near the antiferroelectric phase transition, in which a *spatial dispersion* of optical phonons is large exactly at the boundary of Brillouin zone, since a *critical decrease* in their frequency occurs. Moreover, in the antiferroelectric a critical reduction in the frequency of vibrational "soft" mode occurs not in the center of Brillouin zone (as in displacive ferroelectric) but on the *boundary* of Brillouin zone, and, therefore, the Brillouin zone shrinks that is followed by change of crystal symmetry below the phase transition.

Dielectric spectroscopy has shown that it is possible (but very conditional) to divide the antiferroelectrics into two groups. In the first of them ("soft"), the dielectric permittivity at the Curie point reaches several *thousands,* and they, like similar oxygen-octahedral ferroelectrics, experience the *dispersion* of permittivity in their paraelectric phase at millimeter waves. In the second group ("stiff" antiferroelectrics) the permittivity at Curie point has the order of two to three *hundreds*, and no dielectric dispersion is observed in them even at sub-millimeter waves. In the both groups of antiferreelectrics, in their *antipolar phase,* there is no dielectric dispersion up to far infrared range; therefore, not only at radio frequencies but also at microwaves the dielectric losses in the antiferroelectrics are small (in contrast to ferroelectrics).

2. *"Soft" antiferroelectrics* can easily form solid solutions with ferroelectrics; moreover, a *morphotropic boundary* is created, in which the piezoelectric properties are strongly pronounced (this circumstance is widely used in electronic materials technology). Besides, at a not very large distance from Curie point, the strong external electrical field can transform "soft" antiferroelectric into the ferroelectric phase, showing the double-hysteresis loop, Fig. 3.27F (at that, the heat is absorbed, which can be used for the electrocaloric cooling).

If the reversibility of spontaneous polarization would be considered as a necessary property of ferroelectric, then it will be logical to think the possibility of a forced transition to the ferroelectric state as the necessary condition for the antiferroelectric state existence (due to the proximity of these states energy). Since the antiferroelectric phase transition occurs with a multiplication of crystal unit cell, from the point of view of lattice dynamic theory, such a transition should result in the condensation of the lattice “soft mode” not in the center of Brillouin zone (as in

the displacive ferroelectric), but at the *nonzero* wave vector. Moreover, the proximity of energies of polar and antipolar phases means that at least two lattice critical oscillations are necessary for the antiferroelectric phase transition, as well as the proximity of temperature at which these modes condense. At that, one of these lattice vibration modes is characterized by a wave vector close to zero that leads to the anomaly of permittivity and to Curie-Weiss law in the paraelectric phase.

The most studied representative of antiferroelectrics is the lead zirconate ($PbZrO_3$, T_C = 230 ºC, θ = 190ºC, $C = 1.7\times10^5$), the basic dielectric characteristics of which are given in Fig. 3.24; similar properties shows lead hafnat, $PbHfO_3$ in the vicinity of its phase transition at temperature T_C = 160ºC.

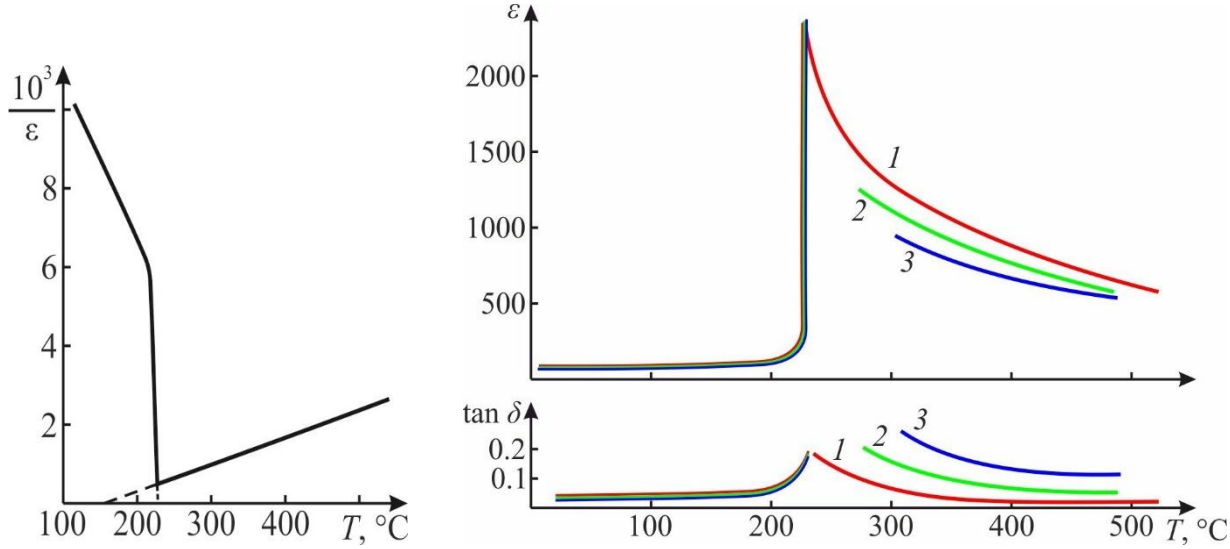

Fig. 3.29. Temperature dependence of permittivity and losses of lead zirconate at millimeter wave frequencies: A — Curie-Weiss law at 36 GHz; B — permittivity dispersion in paraelectric phase at frequencies: *1* — (36–46) GHz, *2* — 66 GHz, *3* — 78 GHz

In these antiferroelectrics, the same dispersion of permittivity in the paraelectric phase is found as in the $BaTiO_3$. As can be seen from Fig. 3.29B, up to the frequency of about 50 GHz the $\varepsilon(T)$ curve at microwaves practically does not differ from the measured at frequency 1 MHz. However, at the millimeter waves, above T_C a noticeable decrease in permittivity is observed, which manifests itself all the more, the closer is phase transition; accordingly, the losses increase. Like in barium titanate, this indicates a very low frequency "soft" mode of lattice vibrations: $\nu = A(T - \theta)^{1/2}$ in the $PbZrO_3$, where A = 140 GHz×K$^{-1/2}$. This vibration mode is overdamped with the attenuation coefficient $\Gamma > 2$, because in the beginning of $\varepsilon(\nu)$ the dielectric permittivity decreases.

It is important to note that below the phase transition, in contrast to the multidomain *ferroelectrics* (like barium titanate), the *antiferroelectrics* (lead

zirconate and all others) shows no traces of any microwave dispersion of the permittivity, and their dielectric losses at microwaves are small.

3. *"Stiff" antiferroelectrics* represent a large group of substances of oxygen-octahedral structure with increased permittivity, which demonstrates a maximum at the Curie point, Fig. 3.30. The dielectric permittivity of "stiff" antiferroelectrics surpasses the permittivity of ordinary dielectric oxides by more than an order of magnitude, but it rarely exceeds the $\varepsilon_{max}(T) \approx 200$ in its temperature peak that is about a dozen times less than such peak value of "soft" antiferroelectrics.

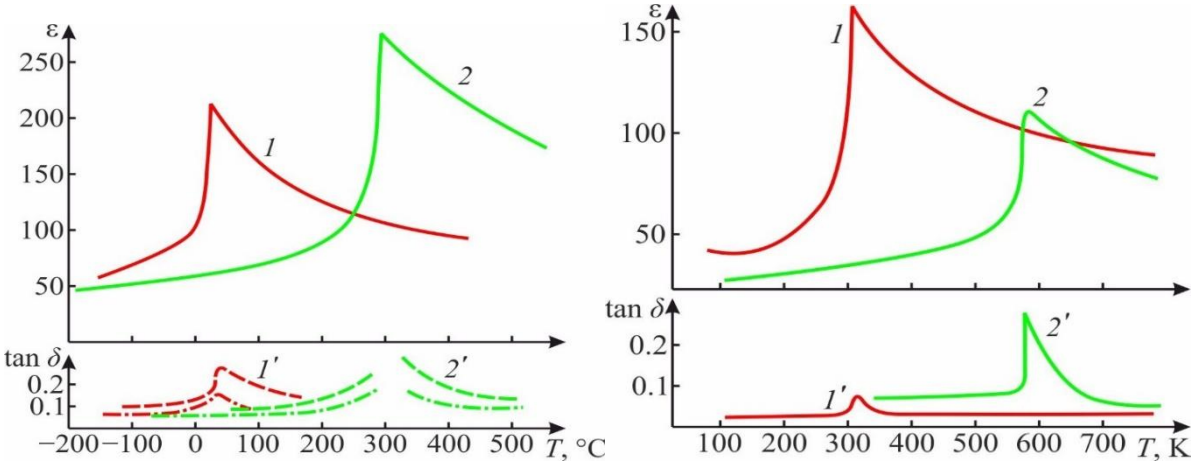

Fig. 3.30. Temperature dependence of permittivity (*1, 2*) and loss tangent (*1′, 2′*)of four antiferroelectrics at frequencies 37–78 GHz: A – Pb_2MgWO_6 (*1, 1′*); Pb_2YbNbO_6 (*2, 2′*); B – Pb_2YbTaO_6 (*1, 1′*); Pb_2YbNbO_6 (*2, 2′*)

The nature of the increased dielectric permittivity in the antiferroelectrics can be revealed by the dielectric spectroscopy. It's obvious that the vibrational modes of crystal lattice of the antiferroelectrics, possessing by the wave vector other than zero ($q \neq 0$), can be detected only by the neutron spectroscopy. However, the accompanying them "soft" vibrations with $q \approx 0$ can be detected in the far infrared region, since these modes cause large contribution to thr permittivity and therefore in the magnitude of far infrared reflection coefficient.

4. *Ferrielectrics* are the crystals, in which their internal polarization is compensated only partially – by the analogy with ferr*i*magnetics, which are characterized by partial compensation of their spontaneous magnetization. Therefore, the ferr*i*electric is *not entirely compensated antiferroelectric.* To the ferr*i*electrics the sodium niobate ($NaNbO_3$ below 80 K), tungsten oxide WO_3, Pb_2CdWO_6 and some other isostructural compounds are related.

In the *sodium niobate*, as in most antiferroelectrics, any dispersion of permittivity is not observed even at millimeter waves. It is noteworthy also that at the Curie point of $NaNbO_3$ dielectric permittivity is of the same order of magnitude

as in the "soft" antiferroelectrics with Curie-Weiss parameters C = 2.8×J0^5 and θ = 415 K, Fig. 3.31A. Unlike $PbZrO_3$, the dispersion of permittivity at millimeter waves in the paraelectric phase of $NaNbO_3$ is absent – as in the "stiff" antiferroelectrics. However, the strong electrical field applied to the antiferroelectric phase of sodium niobate induces in it the ferroelectric phase (however, it also appears even without bias field application when this crystal is cooled below 80 K).

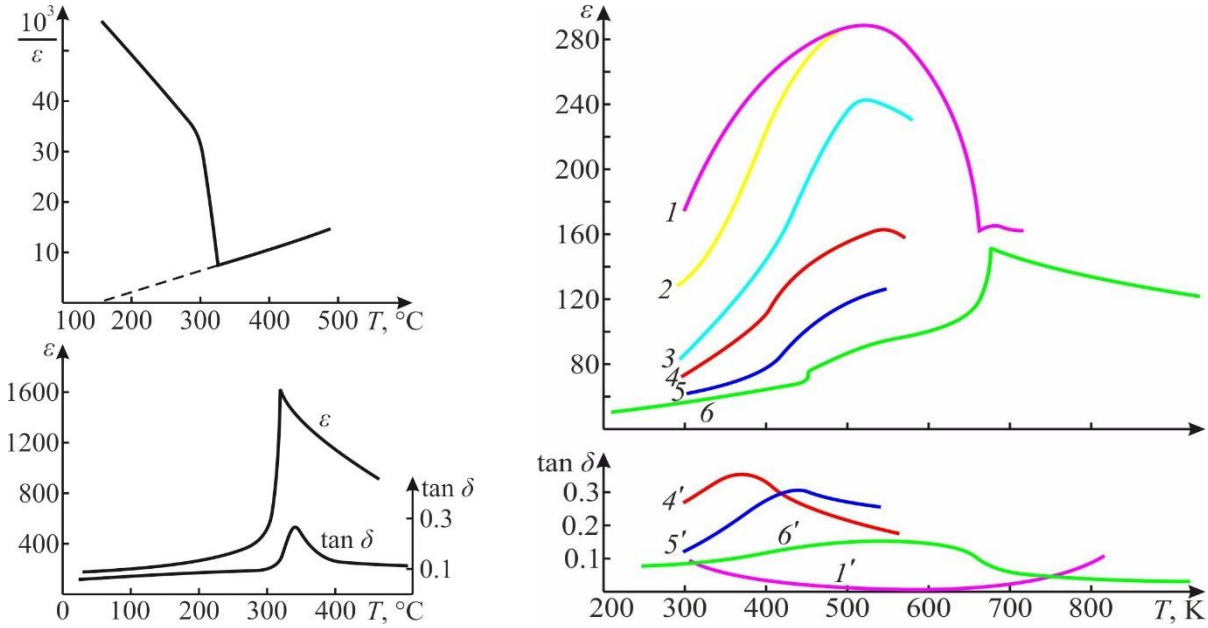

Fig. 3.31. Dielectric dispersion in ferr*i*electrics: A – determination of Curie-Weiss law parameters for $NaNbO_3$ at frequency of 37 GHz; B – temperature-frequency dependence of permittivity and loss tangent for Pb_2CdWO_6 at frequencies: *1* – 10^5 MHz, *2* – 3.7 MHz, *3* – 135 MHz,
4 and *4′* – 300 MHz; *5* and *5′* –1.5 GHz; *6* and *6′* – 37 GHz [34]

In the ferr*i*electric *lead cadmium-tungstate*, Pb_2CdWO_6, dielectric spectroscopy made it possible to detect some phenomenal properties shown in Fig. 3.31B. In this unusual for the accepted models of ferroelectricity material, temperature dependence of permittivity at radio frequencies differs significantly from $\varepsilon(T)$ of other compounds of this type shown before in Fig. 3.30 antiferroelectrics Pb_2MgWO_6 Pb_2YbNbO_6, Pb_2YbTaO_6 and Pb_2YbNbO_6, in which there is an acute maxima ε_{max} = 100–250 at Curie point are seen at frequencies of 10^5–10^{11} Hz while no permittivity dispersion is observed. The peculiarity of Pb_2CdWO_6 lies in the fact that at frequencies of 0.1–70 MHz the maximum $\varepsilon(T)$ is blurred and gradually decreases with increasing frequency. The situation becomes clearer when measurements are provided in millimeter waves: permittivity temperature dependence indicates clear antiferroelectric phase transition at

temperature 700 K. At that, however, another step-like ε-anomaly at millimeter waves is seen at temperature of about 450 K, Fig. 3.31B, which correlates with lower frequency $\varepsilon(T)$ blurred maximum.

Additional studies have shown that in the region of $\varepsilon(T)$ the blurred maximum when strong electrical field application only leads to the increase in dielectric losses, but hardly affects the permittivity that is not typical for ferroelectrics. The frequency-temperature characteristics, observed in lead cadmium-tungstate, partially resemble relaxor ferroelectrics properties, although do not fully meet their definition. Thus, the nature of ferroelectricity is very diverse, and sometimes it is far from always observable properties can be squeezed into predetermined models.

3.10 Summary and self-test questions

1. The change of both permittivity and conductivity with frequency increase can be presented most expediently by the Bode plots, when the abscissa is the frequency in logarithmic scale; in this presentation many physical processes might be reflected, but in case of dielectric spectroscopy this is a permittivity conditioned by different polarization mechanisms.

2. The *relaxor model* is discussed as physical concept which it that coordinated response-polarization function of a system of dipoles, when their forced ordering by electrical field action is opposed by the chaotic disordering thermal motion. Justification of a relaxor model of dielectric spectra is given on the base of Debye formula of permittivity dispersion in the polar dielectrics.

3. According to relaxor model, the electrical polarization of polar complexes is late as the frequency of electrical field grows; as a result, permittivity decreases while dielectric loss factor shows a maximum. In other words, at rather high frequencies the equilibrium distribution of the relaxing electrons, ions and dipoles has not enough time to be established. This effect is peculiar for the relaxation spectra, whose main characteristic is fuzziness in rather broad frequency range.

4. The Lorentz oscillator, describing the resonant dispersion of permittivity, is another key model in dielectric spectroscopy. This is physical model characterizing a dynamic reaction of the system of elastically coupled electrical charges to the externally applied electrical field, whose action is opposed by the internal elastic force tending to return quasi-elastic system into the non-polarized state.

5. Permittivity dispersion and corresponding losses, conditioned by quasi-elastic polarization, usually are observed at much higher frequencies then the

relaxation processes; nevertheless in some dielectrics these losses become significant at microwaves, being important for some electronic components. At that, the presence of a minimum in the permittivity frequency dependence is principal sign of resonance dispersion that distinguishes it from relaxation dispersion.

6. When analyzing fragments of the dielectric spectra described by both the relaxor model and the oscillator model, it turns out to be a very useful the method, known in the electrical engineering as the Nyquist charts. When the polarization response is normalized to the value of the dielectric contribution, in the case of the relaxation dispersion the imaginary and the real part of permittivity on a complex plane are the Cole-Cole semi-circle. The resonant dispersion on the complex plane demonstrates more complex figure with a characteristic loop in the range of negative permittivity.

7. Ferroelectrics are characterized by spontaneous polarization, which direction can be changed by externally applied electrical field. The steady polarization is inherent to the pyroelectric crystal; however, ferroelectric differs from pyroelectric by its ability to re-polarization, i.e., spontaneous polarization switching in applied electrical field (dielectric hysteresis). Also the definition of ferroelectrics may be such: ferroelectric is pyroelectric that divides on domains.

8. By analogy with magnetism (where ferromagnetics, antiferromagnetics and ferr*i*magnetics can exist), not only the ferroelectrics but *antiferroelectrics* and *ferrielectrics* are known. Spontaneous polarization of antiferroelectric is compensated already in the crystal unit cell, while in the ferr*i*electrics their antipolarization is not totally compensated.

9. When explaining various properties of polar crystals, it is possible to refuse the concept of "spontaneous polarization", i.e., to imagine that in polar crystal the "permanent polarization" *exists*. It looks also reasonable the assumption that electrical polarization *appears* as a response to external (not even electrical). This is due to a peculiar distribution of polar-sensitive internal bonds having distinction in ions affinity for electrons, i.e., electronegativity.

10. In the ferroelectrics of *order-disorder type* large microwave absorbance as in the ferroelectric so in the paraelectric phase is seen. Dielectric spectra make it possible to study in all details the critical dynamics of second-order phase transitions/ Many examples demonstrate the wide capabilities of microwave spectroscopy for the detection and study of subtle physical phenomena in crystals.

11. In the ferroelectrics characterized by the order-disorder type at phase transition point, a sharp minimum of $\varepsilon'(T)$ appears instead of usual maximum of permittivity. Former maximum splits into two maximums, and the characteristic

temperature of each of them shifts with increasing frequency in different directions. On the other hand, the temperature of loss maximum ε″(T) remains at the point of phase transition: firstly the loss factor increases with frequency growing but then it decreases staying at same temperature (these dependencies are fundamentally different from conventional relaxor). All these data are preferably taken into account when studying ferroelectrics by dielectric spectroscopy.

12. Ferroelectrics of *displace type* above their phase transition practically have no dielectric dispersion (in paraelectric phase); correspondingly, their losses above Curie point are small that might have application in the microwave tuneable devices. Below Curie point microwave absorbance of ferroelectrics is increased owing to domain walls relaxation (losses in single domain crystals in displace type ferroelectrics remain small).

13. In the ferroelectrics with the phase transition of *displacement type*, at sufficiently high frequency in the point of phase transition the *minimum of permittivity* can be observed at Curie point (like in ferroelectrics of order-disorder type phase transition). Thus, the $\varepsilon'(T)$ minimum in the dispersion region is seen in *all ferroelectrics* (with the exception of improper ferroelectrics). However, the maximum of loss factor $\varepsilon''(T)$, observed in paraelectric phase when frequency grows, shifts in the direction of higher temperatures. This is qualitatively distinguished from the family of curves $\varepsilon''(T)$ described by the relaxation model of dispersion and can be used to select one or another model when describing polarization in various ferroelectrics using dielectric spectroscopy.

Chapter 3. Self-test questions

1. What is the fundamental difference between the relaxor and oscillator models?
2. What is the reason for the blurring of the relaxation spectrum of permittivity dispersion?
3. How to distinguish the spectrum of an over-retarded oscillator from a relaxor?
4. What parameters of ferroelectric currents can be obtained from their dispersion spectrum?
5. What is the difference between the dielectric spectra of displacement ferroelectrics from order-disorder ferroelectrics?

CHAPTER 4. MODELS EXPLAINING DIELECTRIC PROPERTIES

Content

Formation of the crystals, amorphous and other substances from the individual atoms is accompanied by the *energy decrease* in resulting system as compared to the unconnected atoms. Energy minimization is accompanied by a regular arrangement of atoms what is achieved by a peculiar distribution of electronic density between particles. This distribution is influenced by the valence of elements constituting the crystal (taking into account the magnitude of their electronegativity) and by the quantum states of the electronic shells of atoms. In according to electronic theory of a *valence*, the inter-atomic bonds are due to the redistribution of electronic dencity in the outer orbitals, usually resulting in a stable electronic configuration of noble gas (octet) due to formation of ions (or shared electronic pairs between atoms).

4.1 Inter-atomic bonds classification

The connections of atoms, molecules or ions are conditioned by their electrical and magnetic interaction. At the increased inter-atomic distance, the forces of *attraction* dominate while at the short distance the *repulsion* of particles sharply increases. Exactly the balance between long-range attraction and short-range repulsion is a cause of this or that structure as well as base properties of substances. Therefore, the inter-atomic connection creates the *chemical bonds,* which are due to atoms interaction by means of the overlap of their electronic clouds.

1. *Chemical bonding* is characterized by the *energy* and by the *length.* A measure of bonds strength is the energy expended in the case of bond destruction, or the energy gained during compounds formation from individual atoms. Consequently, the energy of chemical bonds equals to the work that must be expended to separate particles that are constrained, or alienate them from each other on the infinite distance. While chemical bonds formation, exactly those electrons which belong to the *valence* shells take a major part, since their contribution to solid

body formation is much greater than the contribution of inner electrons of atoms. However, the division into ionic residues and valence electrons is a matter of convention. For example, in the metals, it is sufficient to consider that valence electrons are transformed into the *conduction* electrons while all other electrons belong to the ionic residues.

The fact is that in the *atoms* of metal the outer electronic orbits are filled with a relatively small number of electrons which have *low ionization energy*. When these atoms come together (that is, when the crystal is formed from individual atoms), the orbits of the valence electrons strongly overlap. As a result, the valence electrons in metals become uniformly distributed in a space inside cationic lattice, and these electrons have the *common wave function*. Therefore, valence electrons in most of metals are fully collectivized, and, therefore, such crystals constitute a lattice of positively charged ions crowded by the “electronic gas”. Unlike, for example, the covalent bonds, the complete delocalization of electrons is a distinctive feature of metallic bonds.

In this way, at the heart of solids classification (dielectrics, semiconductors and metals) the spatial distribution of valence electrons lies. Division of crystals into the classes suggests that solids consist of:

· *ionic residues*, i.e., nuclei themselves and those electrons that are so strongly associated with their nuclei that formed the residues which cannot significantly change their configuration;

· *valence electrons*, i.e., electrons, which distribution in solids may differ significantly from their configuration existing in isolated atoms.

Shown in Fig. 4.1 spatial distribution of electronic density in the *s-, p-* and *d*-orbitals of a certain atom has a strong influence on the strength and direction od inter-atomic bonding. At that, only the *s*-orbital is characterized by a spherical symmetry. In contrast, already the *p*-orbital has a very specific form, and this is especially true for the *d*-orbitals: their forms are considered as one of causes of *transition metals* specific properties. In the *rare earth metals*, the *f*-electrons are present, and they may play a double part: as the residues electrons of "atomic core" and as the "free" electrons (note that *f*-orbitals are too complicated, and they are not shown in Fig. 4.1).

Thus, when chemical bonds formation, the valence electrons play a main part, because at crystal growth their contribution is much greater than the contribution of electrons which form atomic internal orbitals in the residues. Complex configurations in the distribution of the electron density, which is especially characteristic of the *d-* and *f*-states of the outer electron shells, have a noticeable

effect on the future crystal structure. This effect is especially pronounced in the nanoscale structures, when part of the bonds of atomic shells are located on the surface of nanopartles and turns out to be, as it were, "free".

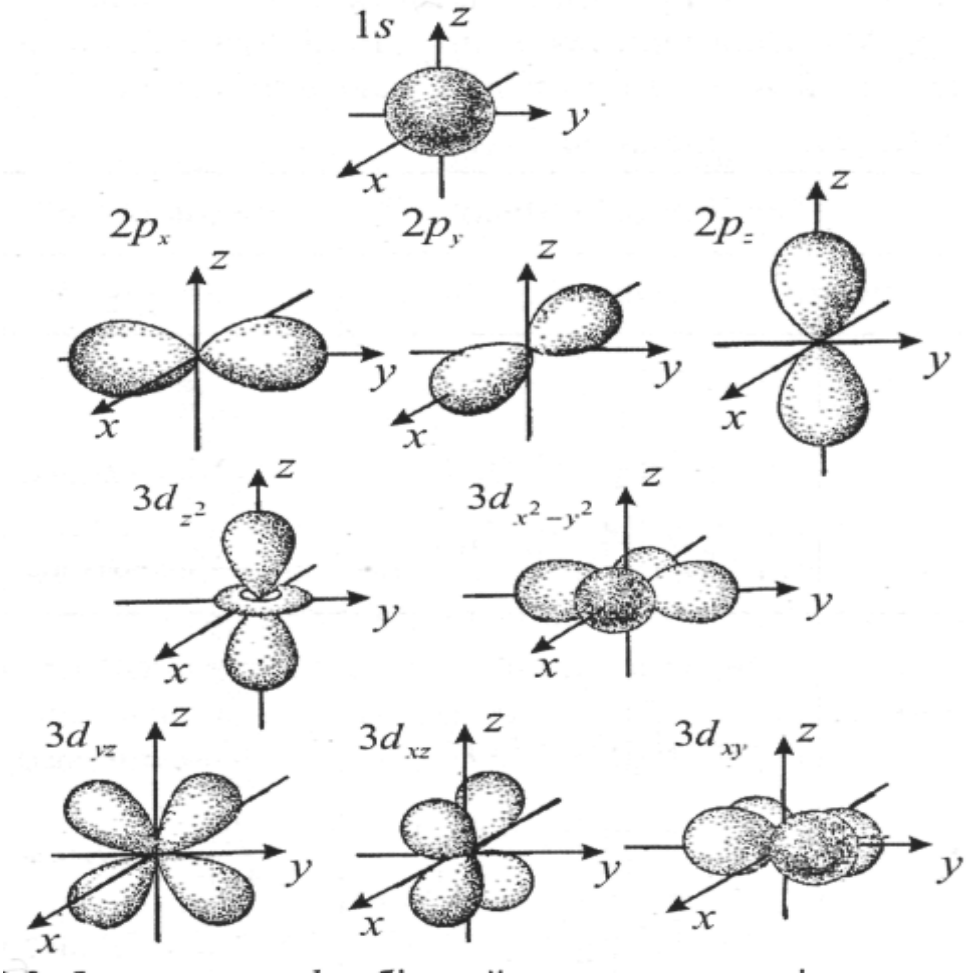

Fig. 4.1. Calculated forms of *s-*, *p-*, and *d-* orbitals: angular dependence of square wave functions

2. *Electronegativity* is another important factor when formation of complex atomic bonds. It's obvious that primary cause of some crystals peculiarities is the *asymmetry of electronic density distribution* along atomic bonds. Being fundamental chemical property, the electronegativity characterizes the tendency of atom to attract the *shared pair of electrons* (or electronic density). This property manifests itself in the chemical bonds as a displacement of bonding electrons towards more electronegative atom. The highest degree of electronegativity is in the halogens and strong oxidants (F, O, N, Cl), and the lowest is in active metals (s-elements of group I). An atom's electronegativity is affected by both its atomic number and the distance at which its valence electrons reside from the charged nucleus. The higher the associated electronegativity, the more an atom or a substituent group attracts electrons. The electronegativity is determined by factors like the nuclear charge (the

more protons atom has, the more "pull" it will have on electrons) and the number and location of other electrons in the atomic shells (the more electrons an atom has, the farther from the nucleus the valence electrons will be, and as a result, the less positive charge they will experience (both because of their increased distance from nucleus and because other electrons in lower energy core will act to shield the valence electrons from the positively charged nucleus).

Electronegativity depends on atomic number, as well as on size and structure of outward (valence) electronic orbitals. The higher is atomic electronegativity, the stronger atoms attract electrons towards themselves. The difference of atoms by electronegativity might be very substantial. At that, atom with higher electronegativity strongly attracts conjunctive electrons, so his true charge becomes more negative. Conversely, the atom with lower electronegativity acquires increased positive charge. Together these atoms create polar connection and, correspondingly, the *non-centrosymmetric structure*. At the same time, such connections do not lead to the appearance of any internal fields, but it can provide peculiar response to external impact that is quite different in various non-centrosymmetric crystals. For example, in case of *directional* mechanical influence onto polar crystal the *electrical* response arises (direct piezoelectric effect). The point is that elastic displacement of atoms compresses (or stretches) their asymmetric connections, and by this way induces the electrical charges on the crystal surface (piezoelectric polarization). On the contrary, if the atomic connections in crystal are the centrosymmetrical, no electrical response is possible to any *uniform* mechanical impact (however, the *inhomogeneous* thermal or mechanical impact artificially makes the atomic bonds asymmetrical that results in the electrical response appearance in any crystal).

3. *Differentiation* of possible bonds between particles in crystals is shown in Fig. 4.2A. In fact, this division of real inter-atomic connections into elementary models is not strict. Moreover, the very nature of bonds in certain chemical compounds can change depending on external conditions. It is noteworthy that in the conditions of *very high pressure* any material with ionic or covalent bonding would acquire a property of *metal bond,* so any material will be turning into a "metal".

The point is that the very high pressure leads to the forced convergence of atoms with a great overlap of their outer electronic shells and all valence electrons are collectivized into an electronic gas. (It should be noted that in some but rear cases even at normal pressure the phase transition of "dielectric-metal" is possible; this transition might be stimulated by the change in temperature or by the external electrical or magnetic field).

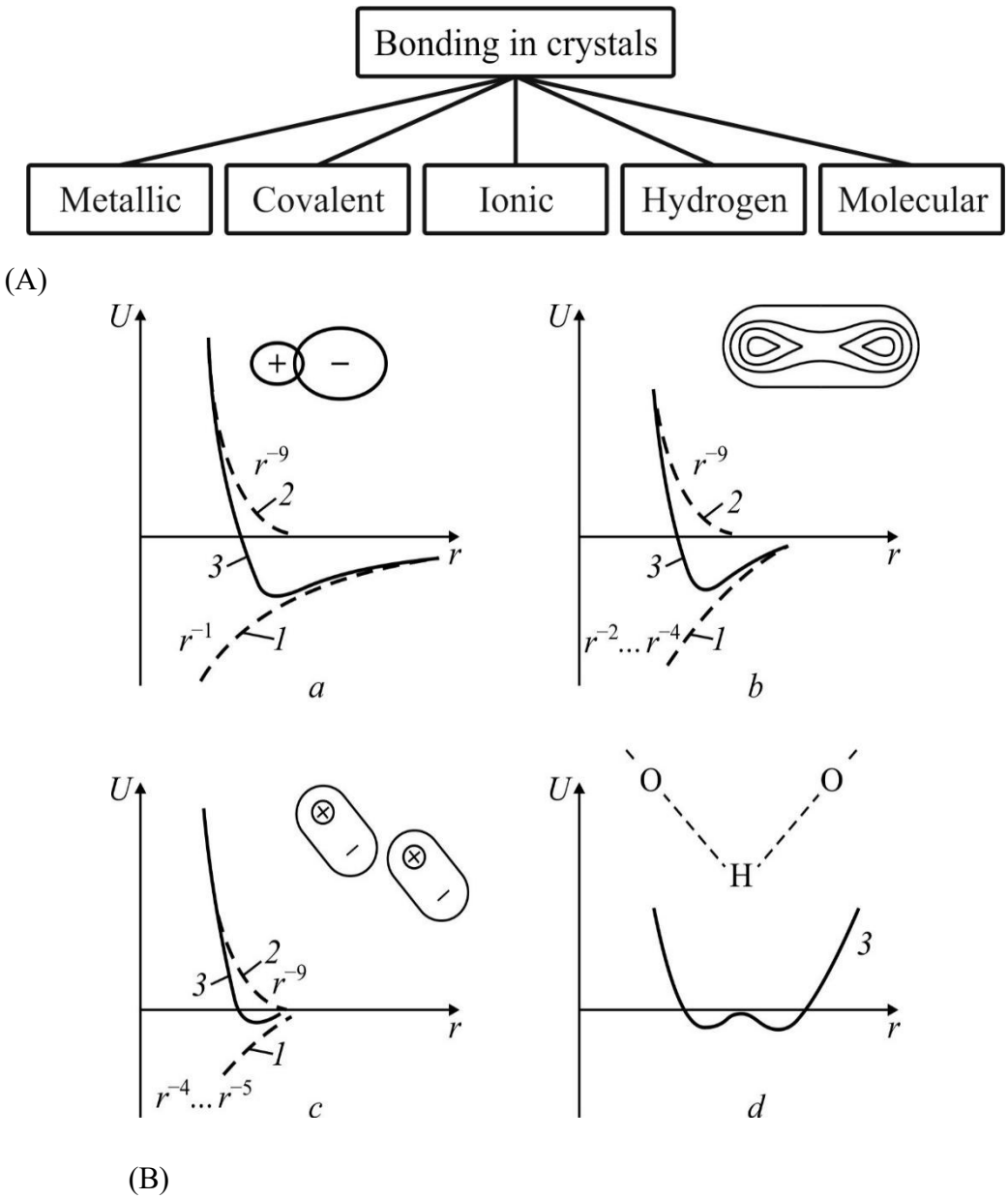

Fig. 4.2. Various models for atomic bonds in crystals: A – classification; B – dependence of attraction energy (*1*), repulsion energy (*2*) and total energy (*3*) on inter-atomic distance *r*: *a* – ionic bond, *b* – covalent bond; *c* – molecular (quadrupole) bond; *d* – hydrogen bond

Such a division is rather conditional, since it corresponds to simplified models: it should be noted that in many cases actual bonding might be more complicated, and the intermediate cases between simple model representations often take place. Figure 4.2B schematically shows the dependence of *energy* on inter-atomic distance for bonds in base types of dielectrics and semiconductors (metal bonds are not shown). Between particles (atoms, molecules or ions), creating crystal, at relatively big distances the forces of attraction dominate: corresponding energy is *negative* and characterized by curves *1*. At short distances the force of repulsion becomes much more powerful; its energy is *positive* and characterized *curves 2*. The

total potential energy of inter-atomic interaction is shown by *curves 3* which minimum corresponds to the stable distance between the interacting particles (this is the *parameter of lattice*).

Strong repulsion between the approaching atoms or ions can be modeled by the drastic energy dependence: $U_{rep} \sim r^{-8}$–r^{-12}; this dependence characterizes the mutual *impenetrability* of electronic orbitals: electronic shells of the neighbor atoms or ions can penetrate each other only a very slightly. This is a reason while the atoms, ions or molecules can be presented by the "hard spheres" of certain radiuses, the size of which remains practically unchanged. The attraction forces that tie together atoms, ions and molecules in solids have electrical nature. It should be noted that crystals are classified just by the *nature of attraction forces*. As it can be seen from Fig. 4.2, main types of chemical bonds in dielectrics and semiconductors are: *covalent, ionic, molecular,* and *hydrogen* bonds. *Metallic* bonding (not shown in Fig. 2B) can be considered as limiting case of covalent bond.

The molecular and the metallic bonds are shown in the opposite sides of a scheme in Fig. 2A, because they are absolutely contrary. The *molecular bonding* is a main type of inter-atomic connection in the molecular crystals, in which all electrons are *completely locked* in their molecules (or atoms), Fig. 4.3A.

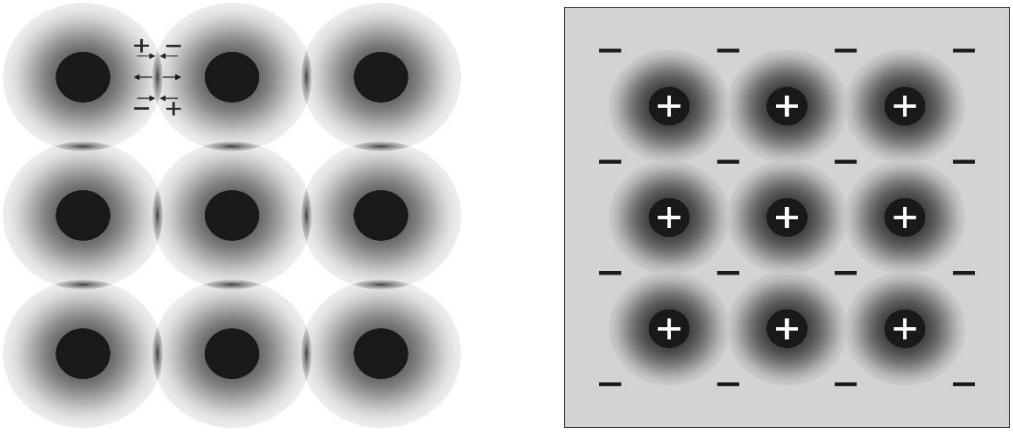

(A) (B)

Fig. 4.3. Two-dimensional image of electrical charge distribution: A – molecular crystal, in which quadrupole electronic fluctuation (+ – … – +) causes the attraction of atoms while partial overlapping of electronic shells leads to repulsion (←…→) balancing this attraction; B – metal crystal, black circles represent positively charged atomic residues, immersed in electronic gas

The nucleus are surrounded by the spaces (shown as black balls), where the density of electronic cloud reaches significant values. The spindle-shaped shaded areas between the atoms symbolically represent dynamically self-induced dipole or quadrupole inter-atomic (or intermolecular) *attractive* forces, which provide molecular crystals a certain (generally low) strength. It is pertinent to note that this

type of bonding is present in all compounds, but since it is weak in comparison with other types of bonds, it is usually neglected. Only in the absence of other types of bonds the molecular bonding becomes decisive.

Simplest examples of pure molecular bonding are the atomic crystals of *solid inert gases*: neon, argon, krypton and xenon. They have completely filled electronic shells, which stable electronic configuration undergoes only a minor change while solids formation. Therefore, the crystal of inert gas is the example of rigid body, in which strong electronic bonding exists exclusively *inside* atoms (or molecules), while the electronic density between atoms is rather small, because all electrons are well-localized near their own nucleuses. On going to the nanosize, this "conservative" type of bonding changes very little, because the electron shells for any particle size remain tightly bound in their atoms.

4. ***Metallic bonding,*** as already noted, are formed by the outer electronic orbitals are incomplete, containing rather small amount of electrons which have low energy of ionization. When such atoms approach closer together (that is, when metal crystal is formed), the orbitals of valence electrons largely overlap each other. As a result, these electrons become distributed nearly uniformly in the space between ions, Fig. 4.3B. Indeed, the *X*-ray studies of metals indicate practically *uniform* electronic density in their lattice. Usually the valence electrons in metals are the joint collective in the crystal as a whole, and metal represents the lattice of positively charged ions, in which the “electronic gas” exists. This is a reason of the *delocalization* of metal bonds; moreover, metallic bonds are *unsaturated* and *non-directional*. For the same reasons, the vetals are characterized by highest among crystals *coordination number* of ions (usually in metals this number is 12, it is the quantity of nearest neighbors to given particle). For comparison, it should be noted that in the ionic crystals this number is often 6 or 8 while coordination number in the covalent crystals even smaller – it is only 4 in the semiconductors of diamond structure.

It is noteworthy that already in the *micro-sized* metallic particles an increasing role plays the *peculiar* electronic states of atoms located on the surface of metal particles that noticeably affects the properties of such material. With a further decrease in the size of metallic particles and the transition to *nanoparticles*, the formation of common electronic gas throughout nanoparticle becomes problematic, and the metallic bonding degenerates.

5. ***Ionic bonding*** is peculiar mostly for ionic crystals (such as sodium chloride (Na^+Cl^-), which are the chemical compounds formed from the metal and non-metal elements. The energy of different ions attraction varies with distance rather slowly,

so the ionic bonds are the most *long-ranging* in comparisons with others. Like atomic or molecular crystals (shown before in Fig. 4.3A), the ionic crystals can be characterized by such a distribution of electronic charge, which is almost completely *localized near the ions*. In the simplest model of ionic crystal shown in Fig. 3.4A the ions look like the “nearly impenetrable charged balls". This approximation is rather good for those ions which possess the *completely filled* electronic shells.

Typically, the cations and anions acquire the electronic configuration of *inert gases,* and, therefore, the distribution of electronic charge in them has almost *spherical symmetry.* Ions with the opposite charges attract each other due to the long-range Coulomb forces, so the energy of their attraction varies with distance very slowly: $U_{att} \sim r^{-1}$, Fig. 4.2B. At the same time, the *short-ranging* repulsive energy of ions is inversely proportional to inter-atomic distance: $U_{rep} \sim r^{-8}$–r^{-12} (exponent depends on properties of given crystal). It might seem that ionic crystal can be considered as molecular crystal which lattice is built not from the atoms but from ions (as, for example, ions Na^+ and Cl^- in the rock salt). The point is that charge distribution between the ions, located in a solid body, is only a slightly different as if it were for isolated ions. However, the particles which form ionic crystal are not the neutral atoms: between ions the *large attraction forces* exist, which play major role and determine main properties of the ionic crystals (which differ significantly from properties of molecular crystals).

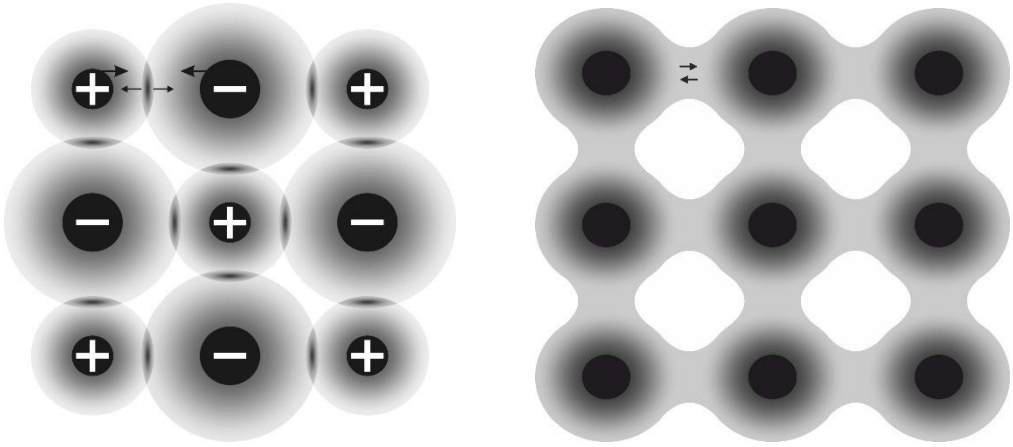

(A) (B)

Fig. 4.4.Two-dimensional image of electronic charge distribution in: A – ionic crystal, where ions attraction is balanced by partial overlapping of electronic shells; B – covalent crystal, black diffused circles represent atomic residues surrounded by the regions, where electronic density reaches significant values

In Fig. 4.4A demonstrating simplest model of ionic crystal, all ions are presented as "interacting nearly impenetrable charged spheres", and this

approximation is quite sufficient for ions possessing entirely filled electronic shells. While in the molecular crystals all electrons remain *locked* in their native atoms, in the ionic crystals the valence electrons, during crystal formation, passed to the neighboring atoms, forming the cations and anions with a strong electrostatic interaction. The ionic bonding occurs between the particles of two types, one of which easily loses electrons, forming positively charged ions (cations) and other atoms that are readily get electrons, forming, respectively, negatively charged ions (anions). Most of electropositive cations belong to groups I and II of the Periodic System, while most of anions belong to the groups VI and VII. As a rule, the ions in crystals are packed tightly, as each of them is surrounded by the *largest number* of oppositely charged ions. Stabilization of ionic solids structure takes place at *coordination number* 6, 8 and, occasionally, even 12. It should be noted that ionic radiuses varies noticeably with value of coordination number. Ionic bonds, unlike metallic bonds, are *saturated*, but like in metals they are *not directed*.

Like other types of bonds, ionic bonding is very sensitive to the size of particles, since the role of surface states in the microparticles and especially in the nanoparticles sharply increases. A decrease in size leads to a change in the symmetry of micro-crystals in comparison with bulk crystals of the same chemical composition; the properties of films of ionic compounds also change significantly.

6. *Covalent bonding* in crystals is typical for *semiconductors*. Dependence of binding energy on the inter-atomic distance is shown in Fig. 4.2B; the attractive forces in case of covalent bonds are *not so long-ranging* as in case of ionic bonding: their energy changes with distance as r^{-2}–r^{-4}. In principle, the nature of covalent bond is close to the metallic bond, but in the covalent crystals the valence electrons are shared only between the *nearest neighboring atoms* while in metals their valence electrons are shared within crystal lattice. Usually covalent bond (which is also called the *homeopolar* bond) is formed with a pair of valence electrons which have opposite directions of spins (one such pair is shown by 2 arrows in the upper part of Fig. 4.4B, in fact, each atom is surrounded by four such pairs). While covalent chemical bond formation, the reduction of total energy is achieved by a quantum effect of *exchange interaction*: simplest example of covalent bond is hydrogen molecule H_2, in which two electrons belong simultaneously to both atoms).

Classic example of covalent crystal is the *diamond,* Fig. 4B*,* where carbon atoms are located rather roomy: their coordination number is only 4. The inter-atomic space in such a crystal seems to be very free (it is enough to compare it with the metal in Fig. 4.3B, where the coordination number is 12). It is possible that this is the reason for the high mobility of electron freed from covalent bond (the effective

mass of such electron in some semiconductors turns out to be three orders of magnitude less than in metals and vacuum). At that, the diamond (as semiconductors of similar structure – germanium and silicon) is characterized by a comparatively *high density* of electronic cloud in the atomic interstitials: electrons are concentrated mainly near the lines connecting each *atom* with its four nearest neighbors. Although the diamond is a dielectric, the high charge density in the areas between atoms is the characteristic feature of semiconductors.

Covalent bonds, unlike metallic bonds, are *strongly directed*, moreover, they are *saturated*. Saturation of the covalent bond is the ability of atoms to form only *limited number* of covalent bonds. The number of bonds formed by each atom is determined by its outer electronic orbital. Directivity of the covalent bond is caused by their peculiar electronic structure and geometrical shape of electronic orbitals (angles between two bonds are the *valence angles*). Sometimes, covalent bonding might have a pronounced *polarity* and increased *polarizability,* which determines many chemical and physical properties of correspondent compounds. The polarity of covalent bond formed by different atoms is due to uneven distribution of electronic density due to difference in *electronegativity* of generating atoms (just on this basis the covalent bonds are divided into the non-polar and polar). The polarizability of bonds can be expressed by non-symmetrical self-displacement of binding electrons.

The following types covalent connections are distinguished:

· The *non-polar* (simple) covalent bond arising from the fact that each of atoms provides one of its unpaired electrons, but formal charge of atoms remains unchanged, since the atoms which forming a bond equally have socialized electronic pair (it is this type of connection that is shown in Fig. 4.4B).

· The *polar* covalent bond, in which generating atoms are different and the degree of covering of socialized pair of electrons is determined by difference in electronegativity both atoms. Atom with a greater electronegativity stronger attracts electrons, so its real charge becomes more negative. Less electronegative atom acquires, respectively, the positive charge of same magnitude.

· The *donor-acceptor* bond arises, when *both* connecting electrons are provided by one of atoms (called the *donor*) while the second atom, involved in the formation of a bond, is the *acceptor*. When creating this pare, the formal charge of donor is increased by one while the formal charge of acceptor is reduced by one. The electronic pair of one atom (donor) goes into a common use, while another atom (acceptor) provides its free orbital. As donor atoms, usually serve the atoms, which have more than 4 valence electrons.

· The *σ-bond* and *π-bond* are the approximate description of some types of covalent bonds in some compounds. At that, the *σ*-bond is characterized by a maximum of electronic cloud density along the axis joining the nuclei of atoms. Formation of the *π*-bond is characterized by the lateral overlap of electronic clouds "above" and "below" plane of *σ*-bond.

Unlike metallic coupling, the emergence of covalent bond is accompanied by such a redistribution of electronic density, when its maximum localizes *between* the interacting atoms. As in metals, in the case of covalent bond, a *collectivization* of outer valence electrons is seen, but the nature of electronic allocation is another than in metals. In the ground state of covalent crystals, i.e., at temperature $T = 0$ K, there are no partially filled electronic energy bands and the conductivity tends to zero (on the contrary, in the metals at $T \to 0$ conductivity tends to infinity). In other words, the covalent crystal can not be described by the uniform distribution of electronic density between atoms, as it is typical for simple metals. Conversely, in the covalent crystals, their electronic density is increased along the "best destinations" leading to the *chemical bonds*. Covalent bond is the stronger the greater is the overlap of electronic clouds of interacting atoms. If this bond is formed between similar atoms, the covalent connection is called the *homeopolar,* and when generating atoms are different – the *heteropolar*.

In the case when two interacting atoms shares one electronic pair, the connection is *single*, when there are two electronic pairs, this is the *double* bond, and when there are three electronic pairs the bond is *triple*. The distance between bound nuclei is the *length* of covalent bond; at that, bond length decreases, when the order of bond increases. For example, the length of "carbon-to-carbon" bond depends on the multiplicity: for C–C bond its length is $1.54 \cdot 10^{-1}$ nm, in case of C=C bond the length is $1.34 \cdot 10^{-1}$ nm while for C≡C it is only $1.20 \cdot 10^{-1}$ nm. With the increase of bond order its energy increases.

The *directivity* of covalent bond characterizes the features of electronic density distribution in atoms. For instance, in the germanium and silicon crystals (which have diamond structure) each atom is located in the centre of tetrahedron, formed by four atoms – closest neighbors. In this case, the tetrahedral bonds are formed so that each atom has only four nearest neighboring atoms. Most of covalent bonds are created by *two* valence electrons (hybridized) – one from each of interacting atom. In case of such connection, these electrons are localized in the space between two atoms; at that, the spins of these electrons are anti-parallel. In Fig. 4.5C, where the main types of inter-atomic bonds of dielectrics and

semiconductors are compared, different directions of electronic spins are conventionally shown by opposite arrows.

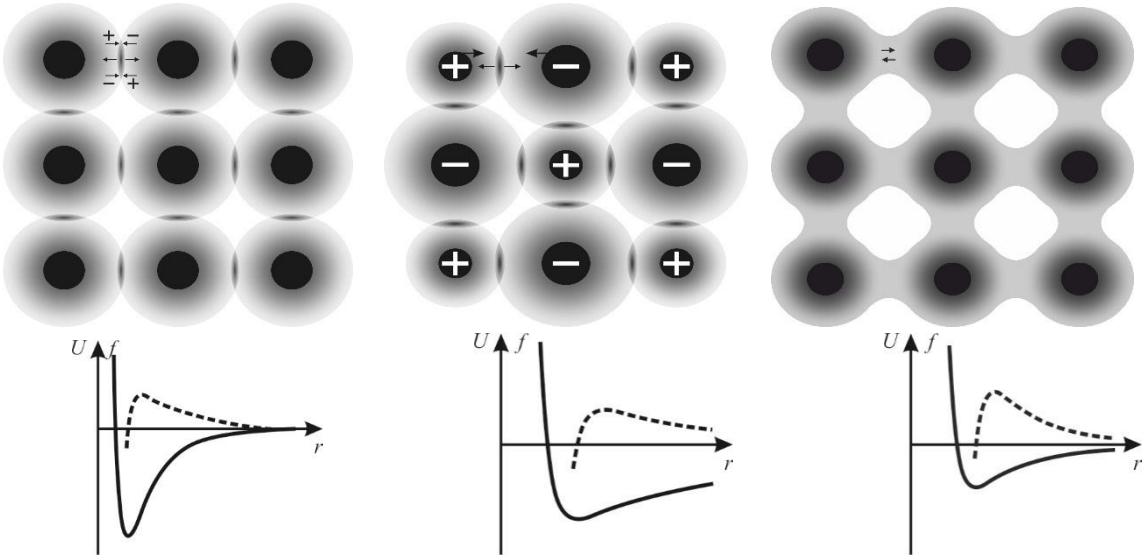

(A) (B) (C)

Fig. 4.5. Two-dimensional image of electrical charge distribution: A – molecular crystal, in which the quadrupole electronic fluctuation (+ – … – +) causes attraction of atoms, while partial overlapping of electronic shells leads to their repulsion (←…→) compensating this attraction; B – ionic crystal where the attraction of ions is compensated by partial overlapping of electronic shells; C – covalent crystal; in graphs, solid curve shows interaction energy while dotted curve shows inter-atomic force

Shown in Fig. 4.5 plane scheme can give only approximate representation of actual location of atoms. In fact, these atoms relative position in real crystals can be quite complex.

7. ***Hybrid ionic-covalent bond*** is schematically shown in Fig. 4.5C. As the model of "purely covalent" so the model of "purely ionic" crystal are too idealized. In the real crystals (let us say, in some $A^{III}B^{V}$ and $A^{II}B^{IV}$ types of semiconductors and in polar dielectrics) an *intermediate* case between the ionic and covalent bonds exists. In the covalent silicon crystal, see Fig. 4.6A, the electrons, on average, are equally distributed around atoms; at that, electronic density *between* atoms is rather big (the small coordination number 4 leaves enough room for a noticeable concentration of electronic density in the interatomic space). In the ionic crystal, see Fig. 6B, the attraction of cathion and anion is compensated by the repulsion force creating due to the partial overlapping of electronic shells.

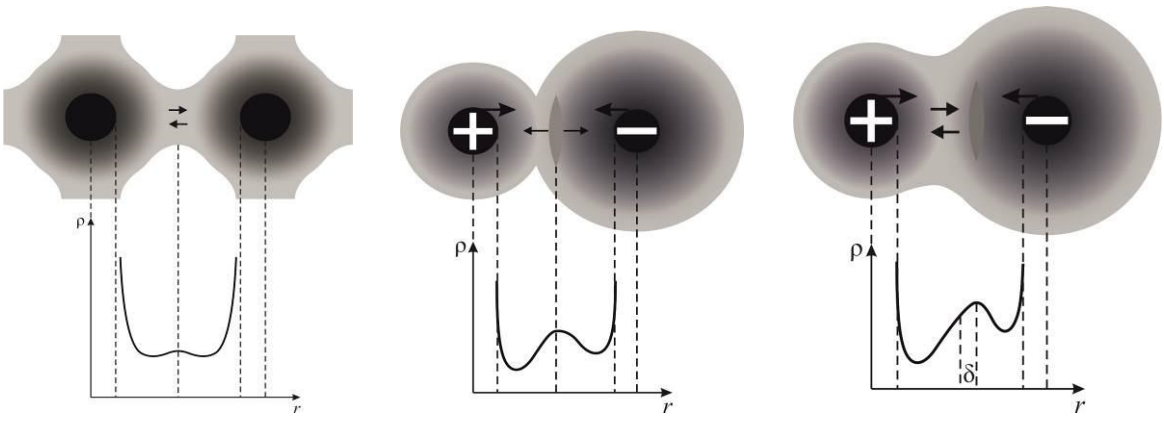

(A) (B) (C)

Fig. 4.6. Simplified scheme of the transition from covalent and ionic bonds to the mixed polar bond: A – in covalent bond the electronic density (ρ) distribution is quite symmetrical (arrows symbolize opposite orientation of spins in connecting electrons pair); B – in ionic bond the cation and anion attract (big arrows) and small overlap of electronic shells ensures the repulsion (small arrows) while electronic density distribution is almost symmetrical, C – asymmetric mixed bond leading to polar properties of crystals, both attraction and repulsion are seen: covalent bond is formed by electronic pair with opposite spins; electronic density distribution is asymmetric that can be characterized by displacement δ

The conception of intermediate type bonds agrees with the imagination of ions deformation due to their polarization. This may occur, for example, by the distortion of anion's electronic orbital mainly by a different *electronegativity* of adjacent ions. At that, the electronic density between the ionic residues increases, i.e., the mixed covalent-ionic bond by peculiar charge separation becomes the *polar bond*. It is pertinent to note that exactly the presence of such bonds determines the non-centrosymmetric structure of some crystals; i.e., hybrid ionic-covalent bonding is a main cause of the pyroelectric, ferroelectric and piezoelectric properties. Most of such *active dielectrics* belong to such crystals or to other ordered polar systems (liquid crystals, electrets, polar polymers, etc.). That is why, a physical hypothesis, relevant to the nature of the *internal polarity* (that is not caused by external electrical field) deserves particular attention. This *hidden* (or latent) polarity manifests itself in the polar crystals as the ability to provide electrical (vector) response to any non-electrical scalar, vector or more complicated tensor impacts.

The tendency of *polar crystals* to electrical response onto non-electrical impact leads to the fact that they can generate electrical potential due to the uniform heating or cooling of crystal (pyroelectricity) or under uniform deformation (piezoelectricity). They are mostly the crystals with a *hybrid ionic-covalent bonding*. Just this peculiarity causes the reduction in crystal symmetry, so polar crystals always belong to the non-centrosymmetric classes. On the contrary, crystals with the

exclusively ionic bonds, as well as the crystals with the exclusively covalent bonds are non-polar ones. Usually they belong to the centrosymmetric classes of crystals: in typically ionic crystals the *central symmetry* exists, i.e., no special orientations in the atomic connections exists. In the same way, the *simple* covalent crystals also belong to the centrosymmetric structures: each atom provides for bonding one unpaired electron, at that, four socialized electronic pairs are located symmetrically.

The fact that in many crystals (for example, in some semiconductors) the type of bonding has an intermediate character between covalent and ionic bonds. At that, the energy of ionic, covalent and metallic chemical bonding is characterized by similar order of magnitude; in this respect they are much inferior to molecular bonds.

8. ***Molecular (Van der Waals) bonds*** exist always, but only when much stronger valence bonds are absent the molecular bonds become main type of chemical connecting, firstly, in the molecular crystals. The forces of attraction in this case are relatively small being very *short-ranging*: energy of intermolecular attraction varies with distance as $U_{att} \sim r^{-4} - r^{-6}$, Fig. 4.2B*c*. It is evident that this kind of attraction is weak in comparison with ionic and covalent forces; at that, the Van der Waals bonds are *additive* and *non-saturated*.

In case of non-polar molecules, the attractive forces are due to the *accidental deformations* of electronic shells. Quantum fluctuations of electronic density in the molecules exists always; thereby, spontaneously arising (virtual) electrical dipoles or quadrupoles lead to the attraction of molecules (in Fig. 4.B,*c* the Van der Waals bonding is shown schematically and only as dipole-to-dipole interaction). Electronic polarizability of orbitals determines the optical dispersion in the materials; that is why, the forces of attraction of this type sometimes are called as *dispersion* forces.

In the case of *polar* molecules, the *orientation interaction* also contributes to the usual molecular interaction. The influence of intrinsic (permanent) dipole onto induced polarity of another molecule is the *inductive interaction*. In general, in case of Van der Waals bonding, main contribution is given by the dispersion forces, but when molecules have large dipole moments a contribution of orientation effect might be significant. As a rule, inductive interaction is negligible.

9. ***Hydrogen bond*** appears between the hydrogen atoms and electronegative atoms P, O, N, Cl, S belonging to other molecule. The nature of this bond lies in the redistribution of electronic density between atoms, conditioned by the hydrogen ion H^+ (proton), Fig. 4.2B,*d*. The crystals possessing hydrogen bonds (dielectrics and semiconductors) show the properties similar to the molecular crystals, but there is a reason to allocate them in special class. The point is that hydrogen is unique in following respects:

· the residue of hydrogen ion is "bare" proton, which size is of about 10^{-13} cm (i.e., in 10^5 times smaller than any other ion);
· the hydrogen needs only one electron to constitutethe stable helium-type electronic shell (that is a unique case among other stable configurations having only two electrons in outer shell);
· the ionization potential (energy required to remove electron from atom) in the hydrogen is vey big: 13.6 eV (in alkali-halide metals it is ~ 4 eV).

Because of these properties, during formation of correspondent crystalline structure, the effect of hydrogen may differ significantly from the influence of other elements. Due to the large ionization potential of hydrogen atom it is difficult to remove completely its alone electron. Therefore, the formation of ionic crystals with hydrogen occurs differently than, for example, in the case of alkali-halide crystals. Hydrogen atom may not behave in a crystal as typical covalent atoms: when H atom loses its electron, it can create only a *single* covalent bond, shared with another atom.

Because the size of proton is about 10^{-13} cm, it is localized on the surface of large negative ions; thereby such a structure arises that can not be formed with any other positive ions. The energy of hydrogen bond is less by order of magnitude than covalent bond energy, but it is greater than the energy of Van der Waals interactions in the order of magnitude. Although hydrogen bonds are not very strong, they plays important role in the properties of correspondent crystals. Hydrogen bonds are *directional*; molecules that form hydrogen bonding tend to have *dipole moment* that indicates polar nature of this bonding. In some crystals, exactly hydrogen bond leads to the piezoelectric, pyroelectric and ferroelectric properties; it should be noted also that the molecular and hydrogen bonds are very important in the various structures of *liquid crystals*.

10. ***Effect of structural defects*** that violate strict periodicity of crystal lattice can lead not only to the *local polar properties* of ionic and covalent crystals, but in some rare cases even lead to formation of *polar-sensitive crystal lattice*.

First, the appearance of a *local polarity* in crystals containing *semi-free* (localized) electrons (or electronic holes) will be discussed. They are concentrated in the vicinity of structural defects of a dielectric, allowing the localization of electrons (holes) in *two or more equivalent positions*, which are separated by low potential barriers. Thus, structural defects centers are the places of irregularity in the distribution of electric charge in the crystal lattice.

This type of local electron polarization is characteristic of many technically important dielectrics, such as rutile (TiO_2), perovskite ($CaTiO_3$), and similar complex oxides of titanium, zirconium, niobium, tantalum, lead, cerium, and

bismuth. A high concentration of structural defects such as an *anion vacancy* is the structure peculiarity of these substances, especially in their polycrystalline state.

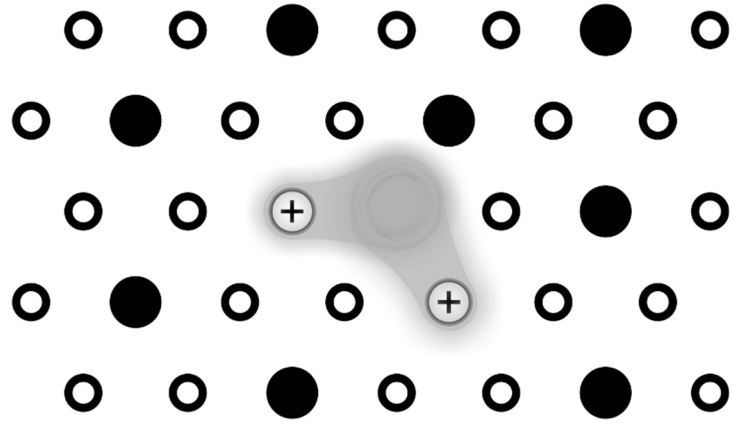

Fig. 4.7. Local polar centres in rutile: planar lattice model of titanium dioxide with oxygen anion vacancy located at the intersection of electron clouds; **O** – oxygen, O^{-2}; • – Ti^{+4}; □ – Ti^{+3}

During high-temperature synthesis of ceramics from mixture of oxides (or while crystal growth) appearance of anionic vacancies is very likely. Electrical compensation of these defects occurs by the lowering of valence of cations located near anion vacancy. Figure 4.7 shows one of possible case of partially-bound electrons location near ionic vacancy in rutile. In selected part of TiO_2 crystal there are three titanium ions as the nearest neighbours to anion vacancy (in 3D crystal the number such neighbours are five). Charge compensation of oxygen vacancy carried out by the fact that two of five adjacent to the anion vacancy titanium ions become trivalent: each of them contains in its outer shell one weakly bound electron; at that probability density of these electrons wave function is increased in the place of missing oxygen. Under the influence of chaotic thermal lattice vibrations these polar centres are oriented randomly that do not lead to regularly oriented polarization in crystal: concentration of anion vacancies in crystal can not be very large; so these pseudo-dipoles can not become self-organized into the polar lattice.

Second example that might have of particular interest is that local polarity can be artificially created by *irregular disposition of ions* in crystal. In simple case, this can be obtained in the solid solutions of crystals that have *different sizes of ions:* in them, smaller ion occupies not its geometrically-central position, but shifts to one of nearest ions of opposite polarity. At that, polar moment is formed, which can change its direction in a lattice, when small ion jumps closer to another neighboring ion. Figure 1.7 symbolically shows, for example, potassium chloride crystal that forms solid solution with lithium chloride $(K_{1-x}Li_x)Cl$, where index x is Li^{+1} volumetric concentration.

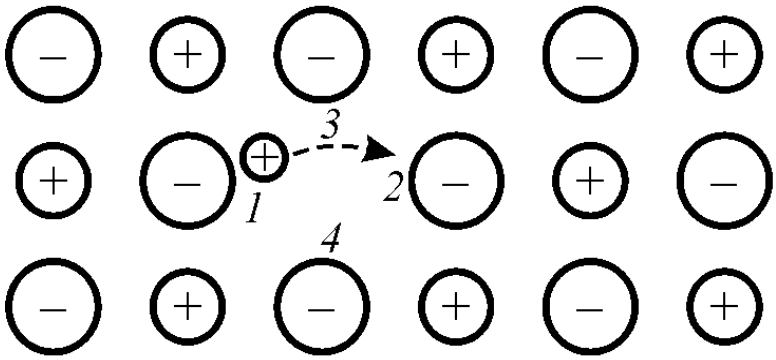

Fig. 4.8. The ability to create polar cluster in simple cubic ionic crystal: small positive ion localizes nearby one (*1*) of possible negative ions, having the ability to jump in other position (*2*)

In cubic lattice of KCl crystal, small cation Li^{+1} jump closer to one of six neighboring ions Cl^{-1}, thereby forming local dipole moment embedded in lattice. In Fig. 4.8 such equiprobable positions are four, but there are six of them in the volume of a crystal. The solubility of LiCl in the KCl is limited, so that the distance between these dipoles is not enough to create by their interaction polar lattice able to overcome energy of thermal vibrations (especially since permittivity in alkali halide crystals is rather small; $\varepsilon < 10$). That is why in others similar crystals it is also not possible to obtain by this way any polar lattice.

However, some experiments with the *non-central cations*, imbedding into crystal matrix with *higher permittivity*, namely, in non polar (paraelectric) crystal $KNbO_3$ in which $\varepsilon \sim 200$ turned out to be more successful: crystal $(K_{1-x}Li_x)Nb_3$ looks like *artificial ferroelectric* with Curie point round 300 K. The interaction of embedded dipoles, formed by the non-central location of Li^{+1} ions partially replacing K^{+1} ions, in the *highly polarized lattice* opened up a possibility for formation of *self-ordered polarization*.

4.2 Electrical properties explanations by inter-atomic bonds

The electrical properties of a material include the electrical conductivity, electrical polarization, electrostriction, piezoelectric, pyroelectric and electrothermal effects. Different responses of crystal onto the applied electrical field are listed symbolically in Fig. 1A. Several reversible and irreversible physical phenomena are seen – not only of *electrical* nature but also the *mechanical* and the *thermal* responses.

Among responses there are the electrical displacement (induction) $D(E)$ and the electrical current $j(E)$, among mechanical effects the electrostriction $x(E^2)$ and

the piezoelectric effect $x(E)$, among thermal effects the Joule heat from dielectric losses $\delta Q(E^2)$ so the heating or cooling due to the electrocaloric effect $\delta Q(E)$.

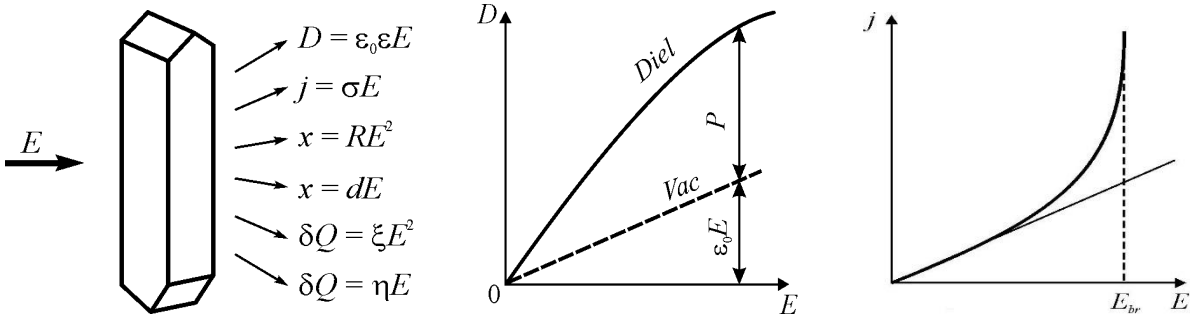

(A) (B) (C)

Fig. 4.9. Classification of polar crystal responses on electrical field influence:
A – classification of electrical (D, j), mechanical (strain x) and thermal (δQ heat) effects (ε is permittivity, σ is conductivity, R is electrostriction coefficient, d is piezoelectric module, ξ is generalized loss factor, η is electrocaloric coefficient;
B – electrical induction dependence on electrical field in dielectric compared with vacuum; C – electrical current density j dependence on electrical field E

1. ***Electrical polarization and electrostriction*** will be discussed as priority. The *electronic quasi-elastic* (optical) polarization is considered using Fig. 4.9. In the non-polarized state ($E = 0$) the electronic shells of atoms are located symmetrically with respect to their nuclei, Fig. 4.9A, so that the *effective centre* of negative charge (q^-) creating by the electronic shells coincides with positively charged (q^+) nucleus. Accordingly, when electrical field is absent, the elemental dipole moment is zero ($p = 0$), since it is determined by the product $qx = p$, but any relative displacement of charges q^+ и q^- is absent: $x = 0$.

2. ***Electronic shells polarization*** (otherwise known as "optical" polarization) is simplified shown in Fig. 4.10. The system of positive charges (nuclei) and negative charges (electronic shells) is balanced, and in the one-dimensional chain of atoms with length l there is no polarization, Fig. 4.10A.

If the electrical field acts on this model, the electrical force influences on each atom, molecule or ion, and their electronic shells displace with respect to the correspondent nucleus, Fig. 4.10B,C whereby the centre of negative charge shifts relatively to the positively charged nucleus, so that in each atom *elementary polar moment* appears: $p = qx > 0$.

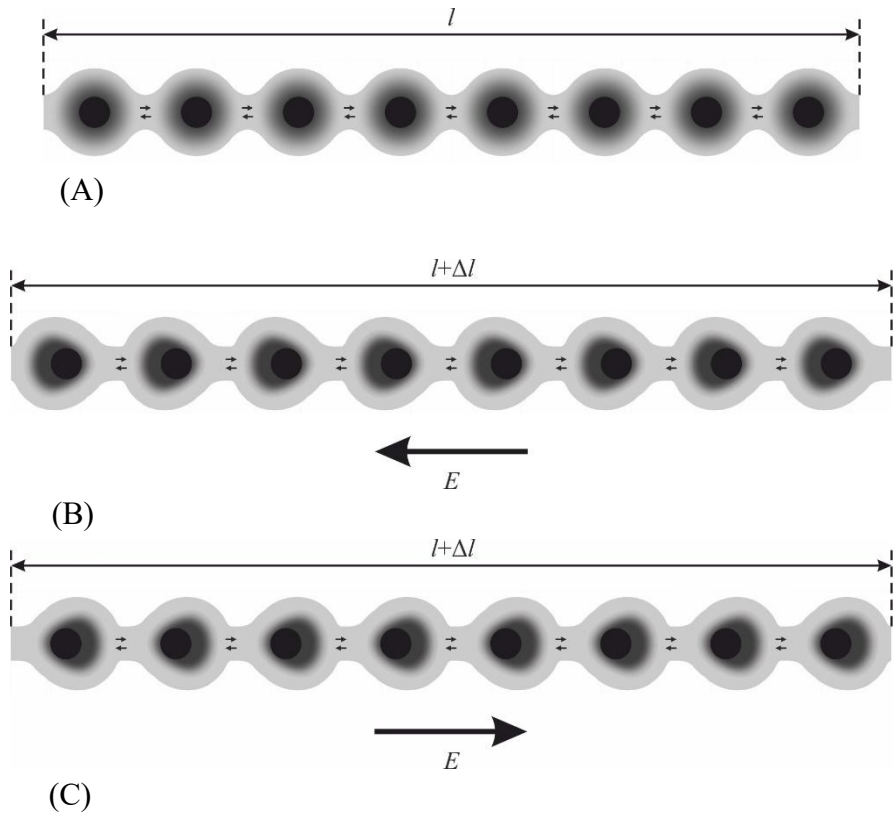

Fig. 4.10. Electronic (optical) polarization: A – 1D covalent crystal simplified model as a chain consisting of alternate covalently linked atoms; B, C – electrical field influence

The elementary electric moment depends on the electric field: $p(E)$ and *changes its sign* when the electrical field changes its sign. This means that the dependence $p(E)$ is an odd function, which, when expanded in a series at the condition of the smallness of electrical field, allows restrict to the first term of this series $p(E) = \alpha E$ where α is polarizability – the microscopic parameter. When macroscopic description, if electrical field E is applied to a dielectric, than an electrical polarization arises: $P = \varepsilon_0 \chi E$, where P is the ***polarization*** (macroscopic electrical movent), ε_0 is electrical constant and χ is dielectric susceptibility. Electrical polarization means that the *separation of electrical charges* occurs: for example, on the opposite surfaces of plane-parallel dielectric sample the electrical charges of different signs appear; at that, these charges are not free but closely bound to dielectric. Traditionally polarization process is described by the electrical induction

$$D = \varepsilon_0 \varepsilon E = \varepsilon_0 E + P,$$

which includes the induction of vacuum $\varepsilon_0 E$ and the polarization of dielectric $P = \varepsilon_0 \chi E$; at that, dielectric permittivity $\varepsilon = 1 + \chi$ takes into account both processes.

Electrical polarization is accompanied by the deformation: $x = \Delta l/l$; it is noteworthy that the magnitude and the sign of relative deformation (strain) does not depend on the sign of applied electric field (that is seen from Fig. 4.10B,C); that is,

the dependence of deformation on the field $x(E)$ is described by an even function. When expanding this function in a series, the smallness of the value of deformation allows restrict to the first term of this series: $x(E) = RE^2$ where R is the coefficient of ***electrostriction***.

3. ***Ionic lattice*** polarization (otherwise known as "far-infrared" polarization) is modelled by simplified model of 1D ionic crystal chain with length l shown in Fig. 4.11A.

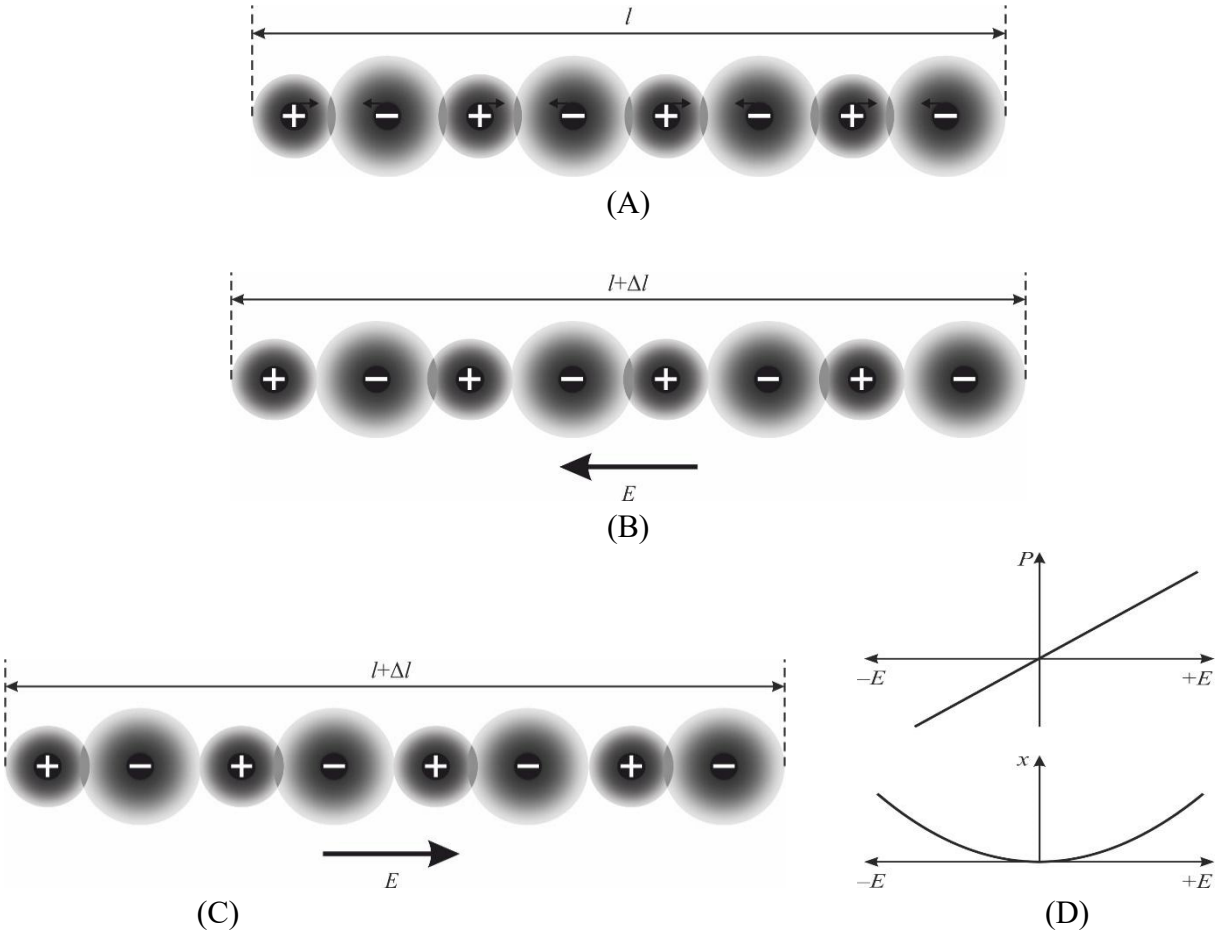

Fig. 4.11. Ionic polarization: A – 1D ionic crystal as chain consisting of alternate one positive and one negative ion; B, C – electrical field influence, D – polarization and strain field dependence

When electrical field is absent, the lattice is balanced by the cations and anions interaction and is not electrically polarized: the system of different signs charges is electrically neutral, and it does not show any own electrical moment (polarization) in the absence of external influences. But under applied external electric field, Fig. 4.11B,C the cations and anions mutually displace forming polarized lattice of $q^+ \downarrow q^-$, in which induced elementary electrical moment is $p = qx > 0$. By this way, the ionic polarization arises, and it determines many electrical properties of ionic crystals.

Exactly, as in the case of electronic polarization, the ionic polarization is accompanied by electrostriction $x(E) = RE^2$. In an ionic crystal, both electronic polarization and electrostriction (caused by electronic shells) are inappropriately present. However, in the ionic crystals, the electrostriction is much higher than the electronic electrostriction and sometimes (in crystals with high permeability) is an important electromechanical effect for practical application. In Fig. 4.11D the odd effect (linear) of polarization and the even effect (quadratic) of electrostriction effect are compared.

However, the electromechanical effect, as seen in Fig. 4.9, can be not only a quadratic ($x = RE^2$), but also the linear, i.e. *converse piezoelectric effect:* $x = dE^2$. Simple systems of covalent (electronic) and ionic bonds shown in Figs. 4.10 and 4.11 cannot explain the linear piezoelectric effect, so it is necessary to consider more complex types of inter-atomic bonds.

4.3 Polar-sensitive atomic bonds

For further consideration of internal polarity nature, turn to possibility of creating polar properties in dielectric *artificially* in uniform impurity-less non-polar crystal. In fact, in ordinary ionic or covalent crystals *polar* properties can be obtained by applying to them electrical field E. At that, resulting induced polarization $P = \varepsilon_0(\varepsilon - 1)E$ is accompanied by electrostriction, which is the quadratic effect when relative deformation x of crystal increases in the applied field by *parabolic* law: $x = R \square E^2$ (in contrast to polar crystals, in which field-induced deformation depends on applied field *linearly*, showing piezoelectric effect: $x = d \square E$). It is seen that strain x in the case of electrostriction does not change its sign with change electrical field sign – unlike piezoelectric effect.

1. ***Linearized electrostriction***. It is quite remarkable that the *linear* electromechanical effect (which is a peculiar property of *polar* crystals) can be interpreted as the linearized electrostriction, Fig. 4.12. Suppose that external direct electrical field (bias field E_b) is applied to the usual centrosymmetric crystal which is non-piezoelectric at $E_b = 0$. Applied electrical field changes the original symmetry of a crystal due to its electrical polarization: as seen from Fig. 4.12, the strain x_b increases quadratically in dependence on the bias field E_b. In this way, under the *fixed* external direct voltage, the structure of a crystal turns into *artificially created* polar structure (it is turning into the "*electrically induced* non-centrosymmetric" structure).

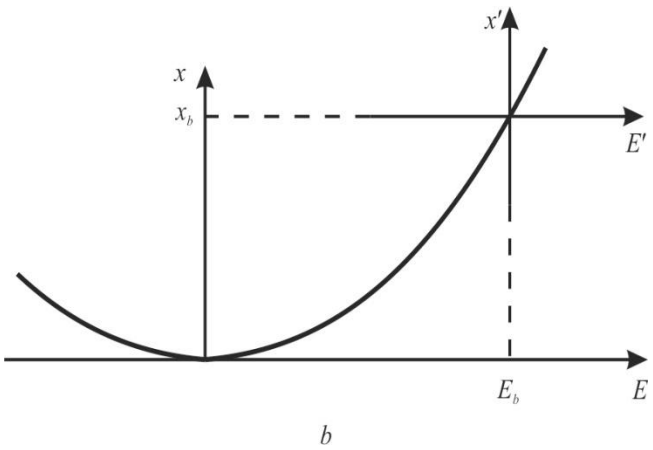

Fig. 4.12. Representation of piezoelectric effect as the linearized electrostriction; in bias field E_b quasi-linear dependence $x'(E')$ imitates the piezoelectric effect [4]

If that's the case, than the *imitation* of linear electromechanical response (piezoelectricity) can be observed on a wing of the electrostriction parabola: at the presence of bias field, the alternating electrical filed E' generates practically linear mechanical response: $x' \approx d' \square E'$, where d' is *electrically induced* piezoelectric module. Calculations shows that $d' \approx 2Q'\varepsilon_0^2\varepsilon^2 E_b$, where ε is the permittivity and Q' is the electrostriction parameter. It should be noted that in those dielectrics which have very large permittivity ($\varepsilon = 10^4$–10^5) this effect can be "gigantic", Fig. 4.13B, that is really used now in electronics.

Similarly, in the presence of electrical bias field, the *pyroelectric effect* can be also induced in *any* crystal, that also finds some application in modern thermal sensors. In the dielectrics possessing large permittivity, the electrically induced pyroelectric effect can be so great that it exceeds in the sensitivity the natural pyroelectricity in polar crystals. In compliance with such electrically induced piezoelectric and pyroelectric effects (that are possible in any solid dielectric but applicable in the dielectrics possessing large permittivity), one can suppose that the *usual* piezoelectric effect also can be explained as the "*linearized electrostriction*", Fig. 4.13. This assumption might be advanced according to conception that fundamental reason of crystal intrinsic polar-sensitivity is the asymmetry in electronic density distribution along polar bonds between such ions possessing different electronegativity which *replaces the externally applied field*. In extremely simplified form, two linear models of electronic density distribution (covalent, ionic and mixed bonding) are shown in Figs. 4.10 and 4.11: both given in the normal state and under electrical field influence.

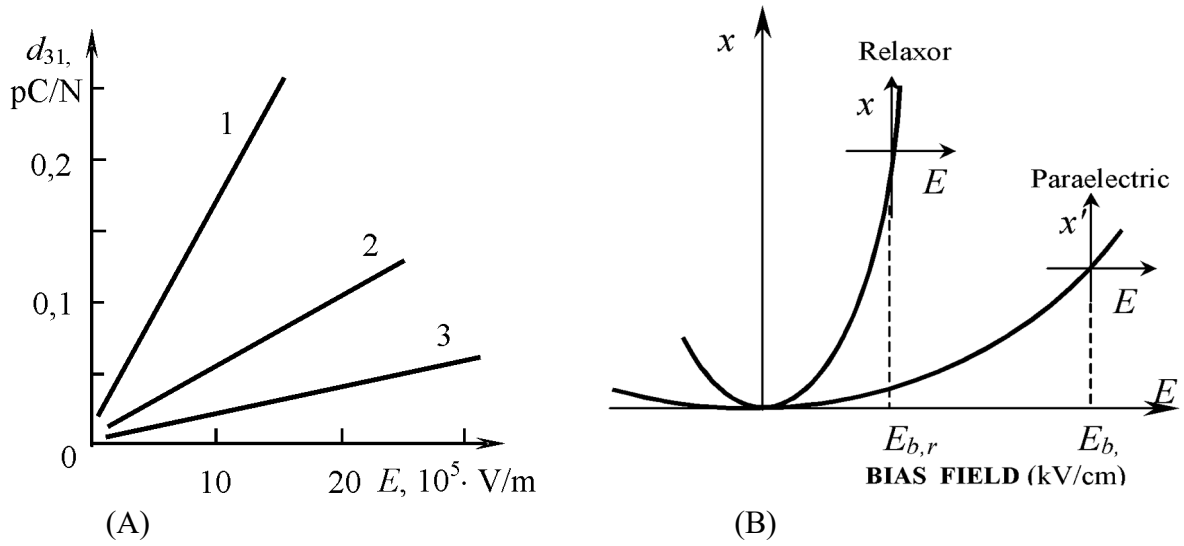

Fig. 4.13. Electrically induced piezoelectric effect in high-∑ dielectrics: A – line *1* is $SrTiO_3$ with
$\sum$= 300; line *2* – $CaTiO_3$ with $\sum$= 150; line *3* – TiO_2 with $\sum$= 100); B – comparison of relaxor-ferroelectric and paraelectric

It is pertinent to recall that in the *covalent* crystal the electrons are equally distributed around their atoms; at that, the electronic density between atoms is rather big. The most important property of covalent structure is the *openness* of their structure, due to a small number of neighboring atoms (four in total) and mutual coupling of electronic pairs having opposite spin. From this it follows, by the way, the increased electronic polarizability of covalent crystals (ε_{opt} = 7–15) and highest possible mobility of free electrons in them. It is important here that the externally applied field *deforms* the electronic shells of atoms by the stretching them that leads both to electrostriction $x = \Delta l/l \sim E^2$ and to the increased polarization due to the relatively free displacement of the electronic density clots, Fig. 4.6A.

In the *ionic crystals,* the mutual attraction of cations and anions is compensated by the repulsion of partially overlapping of electronic shells as well as by the essential deformation of the electronic shells of ions. In contrast to covalent (atomic) crystals, in which magnetic attraction of spins dominates in the outer shells, in the ionic crystals the outer electronic shells are under the action of electrical field of dissimilar ions, Fig. 4.6B. In the external electrical field, the cations and anions are forced to be displaced that gives such a *deformation* of electronic shells of ions, at which virtual formations of *electronic pairs* become possible. That is why, the application of external field is accompanied by the electrostriction, the value of which is proportional not only to E^2 but also to ε^2. If in the covalent dielectrics and semiconductors, as a rule, $\varepsilon \sim 10$, then in some highly polarizable non-polar ionic

crystals (paraelectrics) ε reaches 10^2–10^4 that leads to very large and even gigantic electrostriction.

Therefore, being in the *non-equilibrium* polarized state, under the influence of externally applied field, both covalent and especially ionic crystals *acquire the properties of polar crystals*, namely, the ability to show piezoelectric, pyroelectric, linear electrooptical and others special effects.

2. ***Mixed covalent-ionic bonding,*** shown in Fig. 4.6C, is the *distinctive feature* of models under discussion, as well as main property of polar crystals guarantee the piezoelectric and pyroelectric effects *without* external electrical field application. In this way, instead of external electrical field, which need to be connected to ionic or covalent crystals and forcing them to be in the polarized but nonequilibrium state, in the case of mixed covalent-ionic crystals their polar-sensitive state is a stable property without any external field, being ensured by one of fundamental properties of ions – their electronegativity. Exactly the distinction in the *affinity to electrons* in various ions leads to formation of hybridized polar-sensitive bonds, which determine crystal's own polarity, replacing in this way external electrical field, which can polarize any crystal. In polar crystal its state: "able to polarization by non-electrical way" is entirely equilibrium state at certain temperature (T_1) and pressure (p_1), and it is stored in absence of external influences as much as one wants. If any external acting on polar crystal occurs (changing in temperature, mechanical stress, etc.), then a new stable state arises, already at T_2 and p_2. At that, change in state ($T_1 \rightarrow T_2$ or $p_1 \rightarrow p_1$) is accompanied by surface electrical charges dynamic appearance (in other words, thermally or mechanically induced polarization arises), i.e., pyroelectric or piezoelectric effect becomes apparent.

3. ***Longitudinal piezoelectric effect*** (as well as the secondary pyroelectric effect) can be explained by a simple one-dimensional model which is the chain of ions with a hybrid (mixed) bonding, Fig. 4.14. In this simplified model internal polar-sensitive bonds are "persistant", but they can be deformed as by mechanical stress (producing piezoelectric effect) so by the thermal expansion due to temperature change (generating secondary pyroelectric effect). Such intrinsic polar-sensitivity in the linear pyroelectric usually is conserved up to crystal melting. Under the action of external *electrical* field, in such a model only *linear* polarization (as in any dielectric) arises with a value of permittivity typical for ordinary ionic crystals ($\varepsilon \sim 5$–10).

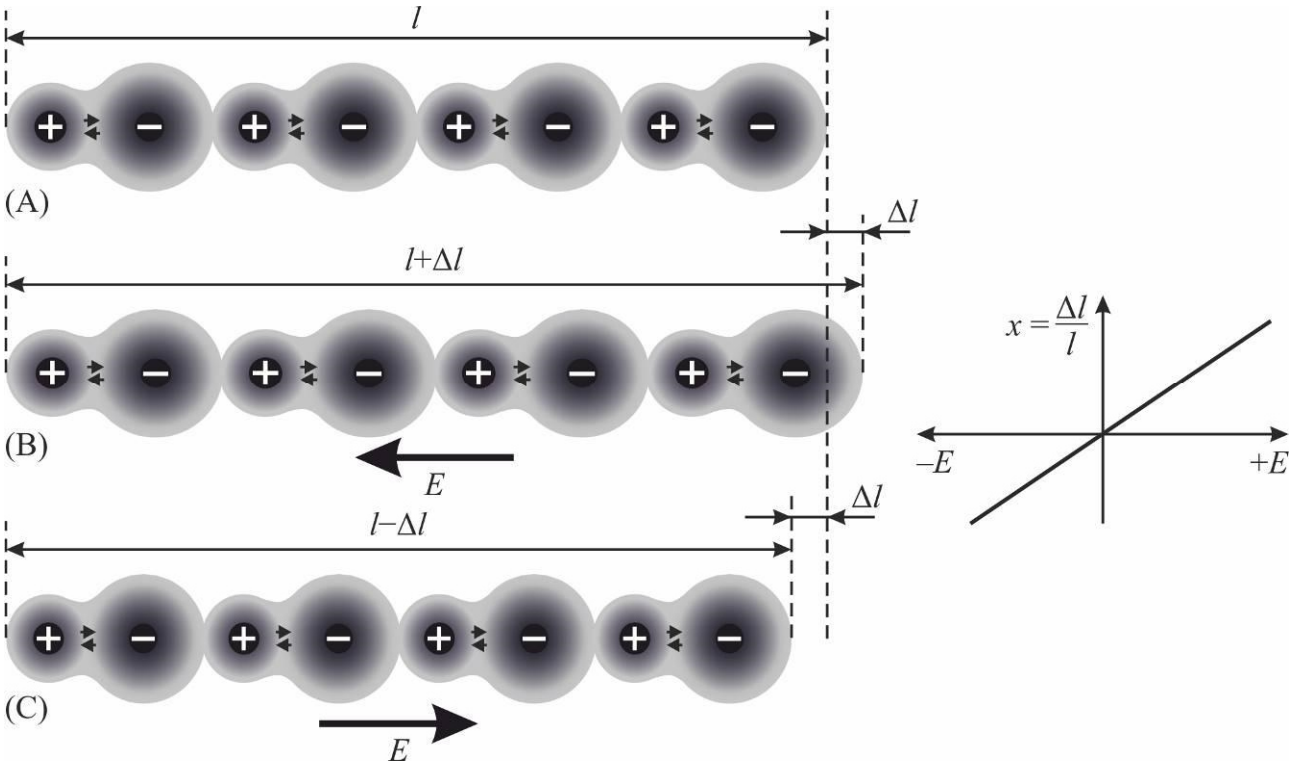

Fig. 4.14. Simplified model of ionic chain with hybridized bonding that leads to polar properties of crystals: A – non-deformed hybridized bonds in the absence of any external effects; B – mechanical stretching of chain or its elongation due to thermal expansion; C – compression of the chain leads to deformation and electric polarization of opposite sign

4. *Ferroelectric* ("non-linear" pyroelectric) also can be imagined by *combined pictures* shown in Fig. 4.14, but its intrinsic polar-sensitive bonding is "gentle", i.e., it is *not sufficiently stable* and can *change its own orientation* to the opposite in the applied electrical field, demonstrating the hysteresis loop and very large dielectric permittivity.

Therefore, in contrast to shown in Fig. 4.14 a very stable polar-sensitive structure, which can only be destroyed by the melting or evaporation of a crystal, the *pliable* structure of a ferroelectric can be radically changed at high hydrostatic pressure and when temperature increases above the Curie point: in both cases, the polar-sensitive bonds of ions become broken and crystal acquires centrosymmetric struture. But the impact of a *sufficiently strong electric field*, without breaking the polarity, changes its direction as shown in Fig. 4.15.

In other words, the increase of temperature and corresponding increase in the intensity of thermal chaotic movement violates the relatively *weak* polar-sensitive correlation between the neighboring ions that leads to the phase transition at Curie point into the non-polar phase. Similarly, the increase of hydrostatic pressure also promotes structural disordering by reducing the space required for the formation of

mixed ionic-covalent bonds, i.e. "squeezes out" polar-sensitive bond and by this destroys in the ferroelectric its weakly-stable ordering of polar-sensitive bonds, which leads to transition into disordered phase.

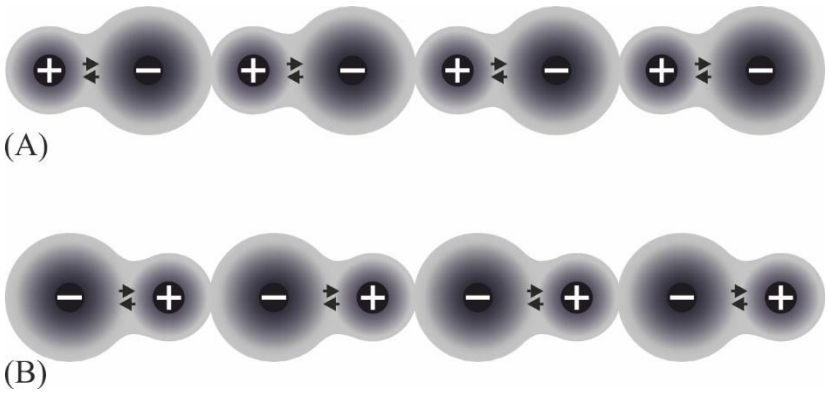

Fig. 4.15. Simplified model of switchable (weakly resistant) polar-sensitive bonds in ferroelectric: A – initial arrangement of mixed (covalent-ionic) bonding in 1D polar crystal chain; B – opposite orientation of covalent-ionic hybridized bonds generated by a sufficiently strong electrical field (larger than coercive field). The simplest 1D model does not allow describing the switching dynamics itself, accompanied by the dielectric and electromechanical hysteresis

5. ***Conception of intermediate type of bonds*** agrees with the assumption of ions deformation due their polarization that may occur, for example, by the distortion of more pliable electronic orbitals in anions due to different electronegativity of adjacent ions. At that, the electronic density between ionic residues increases, i.e., the mixed covalent-ionic bond, possessing greater degree of charge separation, turns into polar-sensitive bond. Due to the fact that these bonds are partially-covalent, they retain the definite orientation, which promotes their strengthenind, supporting to withstand to chaotic thermal motion in crystal lattice. Due to fact that these bonds are partially-ionic, in them, firstly, the polarizability increases since, in addition to electrons, the ions are shifted as well, and, secondly, increases the rate of reaction upon external action on crystal is determined by the inertia of ions motion of (but not by fast electrons), so that they determine phonon spectrum of polar crystal lattice.

Polar-sensitive bonds can arise in crystals which have *small coordination number* (CN, showing number of nearest neighbors to given atom). Thus, to the polar dielectrics and semiconductors, the "open" structures correspond: this provides a sufficient space for electronic orbits interaction. If in the usual *densely-packed* crystalline structures this number is large (CN = 8–6 for ordinary dielectrics), then, for example, in piezoelectric sphalerite and in pyroelectric wurtzite the the coordination number is only CN = 4.

The polar-sensitive structure manifests itself in the crystals as an ability to provide electrical (vector type) response to the non-electrical scalar or more complicated (tensor type) of actions. It's obvious that hybridized ionic-covalent bonding causes the reduction in crystal symmetry, so the polar crystals always belong to the non-centrosymmetric classes of crystals.

The noncentrosymmetric structure of some crystals is caused precisely by the presence of specific interatomic bonds, that is, ion-covalent (hybridized) bond is main cause of the pyroelectric, ferroelectric, and piezoelectric properties in the crystals. For example, the piezoelectric effect arises as the electrical response to the uniform or directional mechanical action on the polar crystal. Its mechanism is that the displacement of ions compresses (or stretches) their *asymmetric* bonds, as a result of which the electric charges are induced on the surface of a crystal. On the contrary, if the atomic bonds in a crystal are the *centrosymmetric*, no electrical response is possible for any *uniform* mechanical effect: the electrical effects from various charges displacement in this case *compensate* each other.

4.4 Modeling of polar-sensitive bonds

From 32 classes of crystals of symmetry, 11 classes are centrosymmetric classes and 21 are non-centrosymmetric classes. At that, only in 20 non-central classes odd electromechanical effect (piezoelectricity) is possible: $x = d \square E$ (i.e., strain x in them is proportional to applied electrical field E while d is piezoelectric module). Furthermore, from 20 piezoelectric classes of crystals 10 classes belong to pyroelectric classes of symmetry (they have *special* polar axis), while others 10 non-central classes can be referred as “exclusively” piezoelectrics: they have only *polar-neutral* axes which compensate each other. This means that, taking into account compensation effect from all these axes, polar-neutral crystal does not respond to the *uniform* change of temperature or onto hydrostatic pressure influence (as it happens also in centrosymmetric crystals).

The deep-laid physical nature of intrinsic polarity in some crystals in many respects remains unclear. It will suffice to mention that occasionally even the homeopolar diamond can have a form of pyroelectric wurtzite (class symmetry 6*mm*) in addition to its principal form of *m*3*m* diamond structure. Moreover, among many piezoelectrics several monatomic crystals exist: to piezoelectric structure of quartz-type (32 class of point symmetry) crystals Te and Se belong. In mentioned examples of non-ionic crystals, undoubtedly, only the dissymmetry of electronic atomic shells can be responsible for intrinsic polarity of these crystals.

However, below only the crystals with *mixed ionic-covalent bonds* will be discussed. At that, basically the polar-neutral crystals (in other words, "exclusively" piezoelectrics) will be considered, and original method will be indicated: how to measure any single component of polar-sensitivity in polar-neutral crystals. In addition to determining of "hidden" polarity, it will be shown that a possibility exists to obtain pyroelectric response onto uniform thermal action from non-pyroelectric crystals that might have some new applications.

1. ***Models based on asymmetry*** in the distribution of electronic density along atomic bonds are free from assumption as to internal electrical field, so their intrinsic polarity no need be compensated by free charges. Although asymmetric polar-sensitive bonding is not a result of any internal field; nevertheless, it can provide polar response to non-electrical homogeneous external impact (thermal, mechanical or other) that in principle is impossible in centrosymmetric crystals.

Non-centrosymmetric allocation of electrical charges in polar-sensitive structures can be presented by different simplified structural models [5]:

(1) Quasi-one-dimensional structural ordering, which corresponds to the vector (dipole-like) response onto external influences; simplest model uses linear unidirectional polar bond between two ions, Fig. 4.16A.

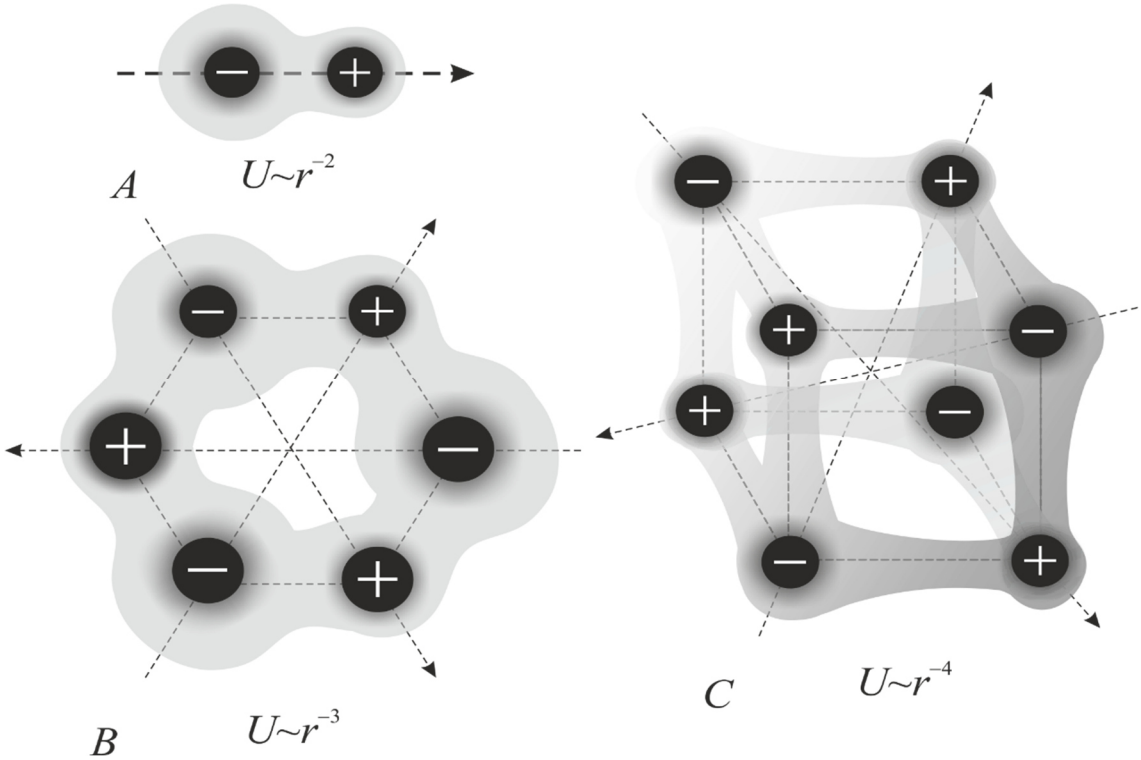

Fig. 4.16. Simplified representation of polar-sensitive structures in crystals: A – 1D dipole-like model; B – 2D polarity modeling; C – 3D polar construction; polar-sensitive directions presented by arrows while specified rate of energy decrease with distance $U(r)$ is shown by power function

(2) Two-dimensional structural arrangement of polar-sensitive bonds allowing describe electrical response onto scalar action by the model which consists of six ions, having asymmetric bonds and located in one plane, Fig. 4.16B.

(3) Three-dimensional asymmetric polar-sensitive bonding, modeled by eight ions, representing spatial polar-neutral structure, Fig. 4.16C.

Such modeling of electrical charge allocations looks quite ordinary when describing dynamic properties of electronic shells, for instance, to explain the nature of Van der Waals bonding by quantum polar fluctuating in electronic shells. Being applied to *polar crystals*, this modeling describes spatial orientation of asymmetric hybridized ionic-covalent bonds. Thus one-, two- and three- dimensional distributions of polar-sensitive bonds in a space is presented by directionality of structural bonds that will be used further to describe various properties of functional (polar) dielectrics.

2. *Dipole-type structural predisposition* (Fig. 4.16A) is the simplest case which corresponds to the quasi-one-dimensional disposition of polar-sensitive bonds in a crystal. This is a well-known conception of pyroelectricity – *internal ability* of a structure *to electrical response* (polarization) on non-electrical action. This case is used here only as a way of description of polar crystal reaction onto *homogeneous* dynamic influence: on changing in time uniform heating (or cooling) that leads to pyroelectric effect. Similarly can be described also crystal reaction onto changing in time uniform compression or stretching on crystal, i.e., dynamic hydrostatic influence, which gives volumetric piezoelectric effect.

Physical properties, which usually are described by dipole-like model of polar-sensitivity, can be described by *material polar vectors*. They might be considered as properties “built-into crystal structure”. Exactly this predisposition of 1D oriented polar-sensitive bonds results in their reaction of vector type on any external scalar influence onto pyroelectric crystal. Relevant crystals belong to 10 pyroelectric classes of symmetry (including ferroelectrics as sub-class of pyroelectrics). The ability of such crystals to give electrical (polar) response $\mathrm{d}M_i$ onto homogeneous hydrostatic pressure $\mathrm{d}p$ can be described by material-type tensor of first rank (vector) $d_{Vi} = \mathrm{d}M_i/\mathrm{d}p$ which characterizes volumetric piezoelectric effect with module d_{Vi}. This property is inherent only in crystals of pyroelectric symmetry.

Similarly, the ability of 1D-system of polar-sensitive bonds to electrical response on temperature change $\mathrm{d}T$ corresponds to a certain, also “material”, vector $\mathrm{d}M_i/\mathrm{d}T$ and can be described by indicatory surface (indicatrix), consisting of two spheres, as shown in Fig. 4.17A. These two spheres are located above and below the symmetry plane *m* and characterized by equation $\gamma(\phi) = = dM_i/dT = \gamma_{max} \cos\phi$. It is

evident that polar-sensitivity spatial distribution can be described just by same way. The upper sphere is indicatory surface for upper orientation of M_i, while bottom sphere means only the change in a sign of pyroelectric coefficient γ_i, if internal polarity has opposite direction. Material vector γ_i has maximum in direction, coinciding with internal polarity direction. So γ_{max} should be measured in the cut of a crystal made perpendicularly to polar axis. Angle ϕ is angle between ordinate and slanting crystal's cut, in which pyroelectric effect is studied.

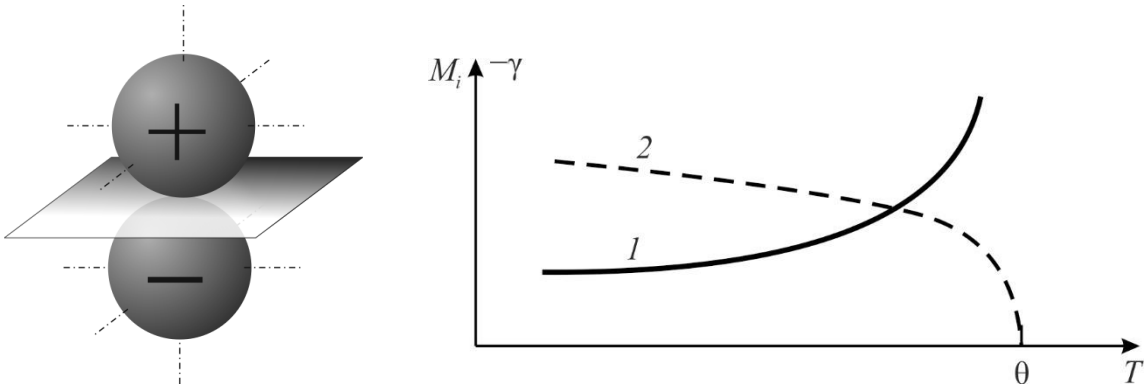

(A) (B)

Fig. 4.17. 1D modeling of polar-sensitive bonding: A – indicatory surface of material vector; B – temperature dependence of pyroelectric coefficient (line *1*) and internal polarity (line *2*)

Figure 4.17B shows the example of "gentle" (nonlinear) pyroelectric-ferroelectric, in which of polar-sensitivity disappears after phase transition at $T = \theta$, and therefore $M_i(T)$ can be measured quantitative concerning this zero. In "persistent" (linear) pyroelectrics, value of $M_i(T)$ can not be measured quantitatively (since this dependence is interrupted only at melting of a crystal).

It should be mentioned also that energy of dipole-to-dipole interaction not very fast decreases with distance: namely, as $\sim r^{-2}$, Fig. 4.16A. Such peculiarity has significant influence on the *temperature dependence* of intrinsic polar-sensitivity, when thermal chaotic movement aspires to destroy internal ordering in structure. It is notable that 1D-ordering long time looks like relatively stable, because it is capable more strongly withstand to inescapable disorienting by 3D thermal fluctuations.

That is why usual (linear) pyroelectric can preserve its internal polar-sensitivity up to the melting of a crystal. However, if chaotic 3D thermal disordering, nevertheless, still can overcome a steadiness (internal energy) of self-ordering of polar quasi-1D system (this is case of ferroelectrics, Fig. 4.17B), then its collapse happens very fast (critically) that leads to phase transition into non-polar phase. At that, it is important to note that in temperature interval of ordered phase the

dependence of polar-sensitivity on temperature subordinate to Landau law: $M_i(T) = M_{max}(\Theta - T)^{1/2}$, i.e., with Landau critical index "0.5".

Further need to consider others, less studied polar crystals, which are *not pyroelectrics* but belong to so called "exclusively" piezoelectrics. In this case more complicated allocation of polar-sensitivity needs another modeling than simplest arrangement of dipole-type polar-sensitive bonds. As noted above in connection with Fig. 4.16B, the intrinsic polarity of such piezoelectrics can be represented as by the plane 2D model (based on structure of quartz) so by the spatial 3D model (based on sphalerite structure); correspondingly, they can be described by second and third ranks tensors.

As seen in Fig. 4.16B and C, correspondent intrinsic electrical moments, described by these higher-rank tensors, are totally compensated (in contrast to dipole-type structural arrangement). In both these cases any scalar action (e.g., hydrostatic pressure or uniform heating) can not arise in such crystals any response of vector character. Only vector or tensor types of outside actions, such as temperature *gradient* (vector grad T) or mechanical stress X_{ij} (second-rank tensor) are capable to discover "hidden" internal polar-sensitivity, which awakes its vector-type response, i.e., to induce voltage on crystal surface in open-circuit crystal or generate electrical current in close-circuit crystal.

Presented below modelling of internal (or "latent", or "hidden") polarity describes an ability of low-symmetric crystal to make electrical response to variety of external actions that are *variable in time*. It should be noted that, if external impact after its switching on (or changed), afterwards remains constant, polarization does not manifest itself – unlike electrical conductivity, which exists all the time at external factor action (fields, illumination, radiation, heat gradient, etc.).

3. S***ituated in-plane (2D) polar-sensitivity*** is typical characteristic of some piezoelectric which are not pyroelectrics (for instance, quartz). Crystals of a quartz-symmetry are berlinite ($AlPO_4$), cinnabar (HgS), tellurium (Te), etc. Suppose that these crystals are investigating by *uniform* thermal action, realized under special condition of *partial limitation of thermally induced strain*. According to Curie principle, symmetry of response includes common elements of action symmetry and symmetry of crystal. In this case, action is scalar but symmetry of crystal response is artificially changed by a limitation of its possible deformations.

Spatial distribution of internal polar-sensitivity in quartz-type crystals can be described in polar coordinates as $M_{ij}(\theta,\phi) = M_{max}\sin^3\theta\cos3\phi$, Fig. 4.18A, where θ is the azimuth angle and ϕ is the plane angle. Using radius vector directed from center of shown figure, one can determine the magnitude of polar-sensitivity in any

slanting cut of quartz-type crystals. In particular, the maxims of piezoelectric effect are seen along any one of three polar-neutral axes of *X*-type. At that, no piezoelectric effect is possible in the directions of *Y* and *Z* axes.

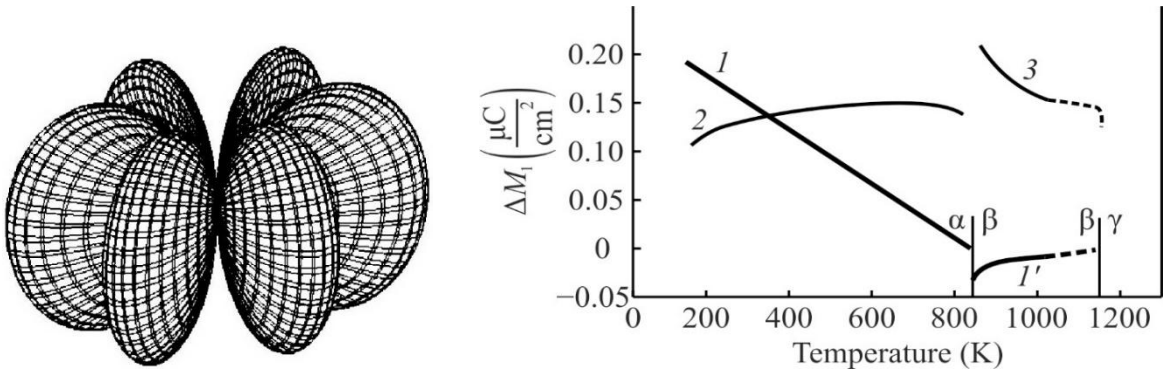

(A) (B)

Fig. 4.18. Internal polar-sensitivity in quartz: A – indicatory surface; B – temperature dependence:
1 – M_1 found in [100]-cut plate in *α*- quartz; *1`* – M_1 found in [110] rod in high-temperature *β*-quartz; *2* – artificial pyroelectric coefficient of [100]-thin cut, *3* – piezoelectric module d_{14}

In case of 2D allocation of polar-sensitive bonds, the energy of their interaction decreases with distance *much faster* then in case of 1D interaction: $U \sim r^{-3}$, Fig. 4.16B. This condition has significant effect on the interaction of polar-sensitive bonds in their plane. Such kind of polar-sensitivity (described by *second rank* tensor M_{ij}) can be suppressed by 3D thermal fluctuations more easily than in case of 1D internal polarity. It is remarkable that correlation between 2D internal polar-sensitivity also ceases at definite critical temperature, so crystals with 2D-polarity experiencing phase transition into another symmetry state, as it is seen in Fig. 1.13B on example of quartz.

At that, "effective pyroelectric coefficient γ_1" vanishes in vicinity of $\alpha \rightarrow \beta$ phase transition of quartz at temperature of $\theta_1 \approx$ 850 K. It is also notable that very special temperature dependence is observed for components of polar-sensitivity $M_{[100]} = \Delta M_1$. Calculated from $\gamma_1(T)$, the $\Delta M_1 = \int \gamma_1 dT$ decreases with temperature *linearly*: $\Delta M_1 \sim (\theta - T)$, that is, with "Landau's" *critical index* 1.

Previously such linear temperature dependence has been observed for spontaneous polarization of *improper ferroelectrics*. It should be noted that all piezoelectrics of quartz symmetry (SiO_2, $AlPO_4$ and HgS) have additional to $\alpha \rightarrow \beta$ *high-temperature* transition, namely $\beta \rightarrow \gamma$. In their *β*-phase quartz and berlinite still remain piezoelectrics, but with intrinsic polar-sensitivity described by 3D distribution in a space. At that, highest-temperature *γ*-phase in these crystals already is non-polar.

4. ***Spatially-distributed (3D) polar-sensitivity*** can be seen in some others piezoelectrics (which also are non-pyroelectrics), for instance, in the $A^{III}B^{V}$ sphalerite-symmetry semiconductors (like gallium arsenide) or in KDP type piezoelectrics (KH_2PO_4 and many of its analogues in *paraelectric* phase). They are characterized by third rank material-type tensor $M_{ijk} = M_{111}\sin\theta\cdot\sin2\theta\cdot\cos2\phi$ and can be described by indicatrix shown in Fig. 4.19A.

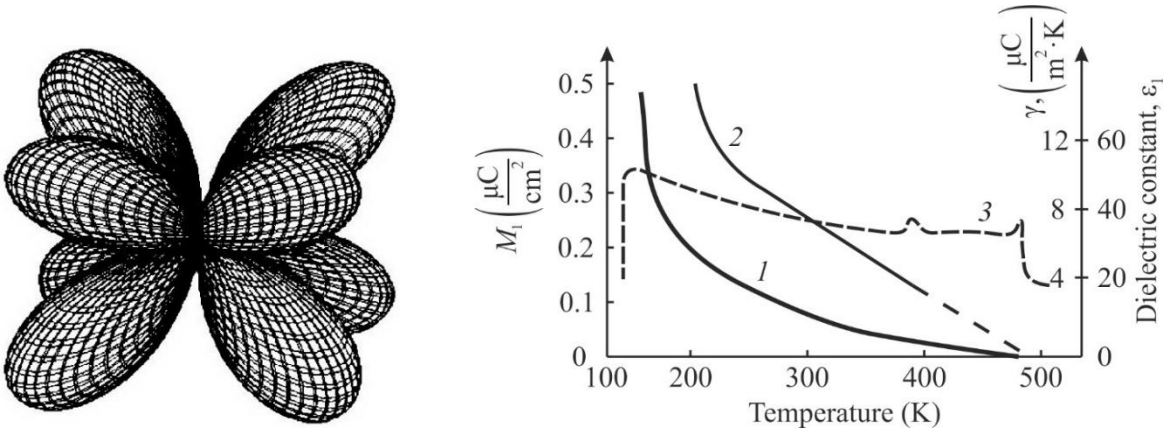

(A) (B)

Fig. 4.19. Intrinsic polarity in paraelectric phase of KDP crystal: A – indicatory surface; B – temperature characteristics of partially clamped crystal: *1* – polar-sensitivity $|M| \sim (\theta - T)^2$; *2* – effective pyroelectric coefficient; *3* – permittivity ε_1 at microwaves

Well known ferroelectrics of KDP type (and close to them antiferroelectrics of ADP type) at room temperature belong to polar-neutral crystals and are "exclusively" piezoelectrics. Their polar-sensitivity is totally compensated and spatially distributed as shown in Fig. 4.19A.

In this case, correlation between polar-sensitive bonds decreases with distance rather fast (as r^{-4}, Fig. 4.16C) that testifies rather weak internal stability of 3D-arranged polar-sensitive bonding, which can be more easily destroyed by the same 3D thermal fluctuations.

Figure 4.19B shows some properties of KDP crystal above its ferroelectric phase transition, where this crystal is the piezoelectric of 422 class of symmetry (only below 150 K it turns into ferroelectric). It is seen that internal polar-sensitivity very gradually vanishes by law $P \sim (\theta - T)^2$, i.e., with critical index "2".

It was found [8] that crystals of KDP type in their paraelectric phase, similarly to quartz-type crystals, have *high-temperature phase transition*, at which their polar-neutral 422 class changes their symmetry to non-polar class of symmetry.

Measurement KDP crystal at microwaves (at lower frequencies proton conductivity interferes with measurements) shows first usual slow decrease of permittivity $\varepsilon_1(T)$, but then it abruptly decreases at temperature of $\theta \approx 480$ K,

evidently in connection with high-temperature phase transition. The presence of this transition is confirmed by measuring thermal expansion coefficient, which has deep minimum at above mentioned temperature.

Common feature of all models shown in Figs. 4.17 – 4.19 is the availability of critical temperature, at which coordination between adjacent polar-sensitive bonds is disrupted with temperature increase. At that, in some crystals, the temperature steadiness of polar-sensitive bonds allocations always can be described by critical law $M(T) \sim (\theta - T)^n$.

It means that really phase transition temperature θ exists, which corresponds to the vanishing of tensor M_{ijk} with temperature rise. It is established that critical parameter is $n = 1$, if polar-sensitive bonds are arranged in a plane (two-dimensional case, 2D, quartz-type crystals).

In the event of spatial (3D) arrangement of polar-sensitive bonds (KDP and $A^{III}B^{V}$ type crystals are examples), critical exponent is $n = 2$. These two cases differ essentially from the 1D dipole-type polar-sensitive bonds in ferroelectrics that shows well known critical law $M_i(T)$ with $n = 0.5$ (Landau critical index).

4.5 Summary and self-test questions

1. Any dielectric is able to polarization in the external *electrical* field, but only some of dielectrics – polar types – can be polarized in *non-electrical* manner. Unique properties of polar crystals (pyroelectrics, piezoelectrics, etc.) can be described by a peculiar polar-sensitive internal structure, capable to generate electrical response onto non-electrical homogeneous (scalar) actions.

2. Electrical polarization means that electrical charges separation occurs (which however remain unfree). When electrical voltage switches on, through a dielectric a reactive current flows caused by shifting of electrical charges; next, when voltage switches off, this is also accompanied by flow of depolarization current; inasmuch as electrical polarization is a response only to the *change* in the electrical voltage.

3. Polarization, induced by external electrical field, is necessarily accompanied by mechanical deformation of a dielectric – this is the *electrostriction* (electrically induced mechanical strain), which indicates that polarized state of a dielectric is non-equilibrium (stressed) state, so polarization of dielectric, which is included in closed circuit, disappears instantly as soon as external electrical field is turned off.

4. When electrical field is applied to solid dielectric, closely connected charges of structural units are displaced relatively to each other, whereby dielectric becomes polarized. Arisen by this way electrical moment is conditioned by contributions from: electrons displaced from their equilibrium positions in atoms, ions deviated from their equilibrium state in crystal lattice, and dipoles which changed their orientation in the external electrical field.

5. Electrons, ions and dipoles can acquire induced electrical moment (i.e., polarized state) through various mechanisms: (1) elastic reversible displacement of bound electric charges, (2) displacement of weakly bound charges with participation of their thermal motion, and (3) macroscopic displacement of free charges that later localize on defect places in dielectric. It should be noted that in polar dielectrics all this processes can occur *without* electrical field application but under the action of varying temperature, uniform pressure, mechanical stress, exposure of sufficiently high energy irradiation, etc.

6. The *dielectric anisotropy* usually arises in dielectrics under external fields influence, but it always is present in polar dielectrics. This means that in non-centrosymmetric dielectrics their electrical, thermal and mechanical characteristics show dependence on the directions of action and response. Any vector is defined by three parameters – projections on coordinate axes. Transformation from one vector to another is described as $D_i = \varepsilon_0 \varepsilon_{ij} E_j$; in the anisotropic media components ε_{ij} are shown with two indices: one comes from vector E_j “action", while another from "response" vector D_i, which directions may not correspond to direction of action.

7. The *dielectric nonlinearity* is associated with permittivity dependence on electrical field. In principle, $\varepsilon(E)$ change should be observed in all dielectrics, however, in most of them nonlinearity is small. Nevertheless, in some *polar dielectrics* (ferroelectrics and paraelectrics) dielectric nonlinearity can be essential and found applications in electronics.

8. The *boundary conditions* are especially important in case of functional dielectrics polarization: these conditions can be electrical, mechanical and thermal. Two *electrical* boundary conditions are: (1) electrical field $E = 0$ that means polar crystal is electrically free and it is a source of current; (2) electrical induction $D = 0$, i.e., the polar crystal is electrically disconnected and it is a source of voltage.

9. Two *mechanical boundary* conditions are: (1) stress $X = 0$ that means mechanically free state of polar crystal; (2) strain $x = 0$, i.e., polar crystal is mechanically clamped. Two *thermal boundary* conditions are: (1) isothermal condition with invariable temperature ($\delta T = 0$); (2) entropy S = const that corresponds to adiabatic condition.

10. All dielectrics and semiconductors are able to creation in them *electrical moment* $P_i = \chi_{ij} \cdot E_j$ induced by electrical field; this property is described by second rank symmetric tensor of dielectric susceptibility χ_{ij} (or the same tensor of dielectric permittivity $\varepsilon_{ij} = 1 + \chi_{ij}$).

11. Polar *dielectrics-pyroelectrics* have ability to make electrical moment $P_i = \gamma_i \cdot \delta T$ induced in them by change of temperature δT; this property is described by first rank material tensor: *pyroelectric coefficient* γ_i, i.e., electrical susceptibility to temperature change. Polar dielectrics-pyroelectrics also have ability to create in them induced electrical moment $P_i = \zeta_i \cdot p$ due to change of hydrostatic pressure p, described by first rank material tensor: *piezoelectric pressure coefficient* ζ_i, i.e., sensitivity to change in pressure.

12. Polar *dielectrics-piezoelectrics* show ability to create in them electrical moment induced by mechanical stress: $P_i = d_{ikl} \cdot X_{kl}$. This property is described by third rank material tensor: *piezoelectric module* d_{ikl} (it can also be called as susceptibility to mechanical stress).

13. In fact, any experimental investigations of pyroelectric or piezoelectric effects do not allow directly determine the value of their “spontaneous polarization”, but experiments characterize only the magnitude of *dynamic response* of peculiar polar-sensitive internal crystalline structure.

14. When explaining various properties of polar crystals, you can do without the concept of "spontaneous polarization", i.e., to imagine that in polar crystal the "permanent polarization" *exists*. It looks also reasonable the assumption that electrical polarization *appears* as a response to external (not even electrical). This is due to peculiar distribution of polar-sensitive internal bonds having distinction in ions affinity for electrons, i.e., electronegativity.

15. To explain more complex manifestations of crystals properties, it needs to take into account a special structure of *cores*: total number of electrons in atom, degree of screening of external electrons from action of nucleus, etc. The electronegativity is the property of an atom to attract electrons; it depends on the atomic number (the number of protons in the nucleus), on the degree of screening of internal electrons, and on the structure of external electron orbitals. Atoms with more electronegativity are more strongly atoms attract electrons.

16. Non-centrosymmetric structures are formed owing to compensation of atomic electronegativity by polar-sensitive bonding in the process of polar crystal formation (while it is growing from liquid or steam state of a material). At that, dependently on chemical composition of a crystal, the variety of combinations may occur between the ions of crystals having two- or three-dimensional polar-active

constructions (which, when external actions exerts on them, can produce electrical responses, describable by tensors of different ranks). Non-centrosymmetric structures of polar crystals are demonstration of *mixed ionic-covalent bonds* between their ions. These bonds are strongly directional and, therefore, such structures lead to different manifestations of asymmetry and complexity of polar crystal structures.

17. When electrical field is affected on "persistant arranged" polar structure, its electrical polarization usually looks like a linear effect (as in ordinary dielectrics). It may seem, however, that the exception are ferroelectrics, in which a *switching* of their “gently arranged" polarization is seen: their low-stable enantiomorphic structure can change its polar-sensitive direction. Outwardly this event manifests itself as dielectric *hysteresis loop*, which allows measure the ability of polar-sensitive structure to react on external actions and indirectly can characterize its features.

18. In ordinary ionic or covalent crystals *specific polar properties* can be obtained by applying to them direct electrical field E. At that, resulting induced polarization is accompanied by *electrostriction*, which is quadratic effect: relative deformation of crystal increases in applied field *parabolically*: $x = R \cdot E^2$ (in contrast to polar crystals, in which field-induced deformation depends on applied field *linearly* showing piezoelectric effect: $x = d \cdot E$). Mechanical strain in case of electrostriction does not change its sign when electrical field changes sign – unlike piezoelectric effect.

19. It can be shown that linear electromechanical effect (which is peculiar property of polar crystals) can be interpreted as *linearized electrostriction*. The point is that electrical field changes original *symmetry* of a crystal due to its electrical polarization. In this way, under fixed external voltage, the structure of a crystal turns into *artificially created polar* structure (it becomes an electrically-induced non-centrosymmetric structure). In dielectrics that have large permittivity electrically induced piezolectric effect can become "gigantic", and this feature is really used now in electronics. Similarly, in the presence of electrical bias field in *any* crystal the *pyroelectric* effect also can be induced, that finds application in modern thermal sensors.

20. In compliance with such electrically induced piezoelectric and pyroelectric effects, one can suppose that *usual* piezoelectric effect also can be explained as the “linearized electrostriction”. This assumption might be advanced according to conception that fundamental reason of crystal intrinsic polar-sensitivity is the asymmetry in electronic density distribution along the polar bonds between

ions, which have different electronegativity (this mechanism replaces externally applied field).

21. *Mixed covalent-ionic bonds*, which in polar crystals is main property, guarantee piezoelectric and pyroelectric properties without external electrical field application to a crystal. In this way, instead of external electrical field, which need to be applied to ionic or covalent crystals in order to force them to have polarized (although non-equilibrium) state, in the case of mixed covalent-ionic crystals their polar-sensitive state *remains stable* without any external field, being ensured by fundamental property of ions – their electronegativity.

22. Polar-sensitive bonds arise in such crystals, which have small coordination number (CN) that shows number of nearest neighbors to given atom. Thus to polar dielectrics and semiconductors an "open" structures correspond: they provide sufficient space for electronic orbits interaction. If in usual densely-packed crystalline structures this number is large (CN = 12 for metals and CN = 8–6 for ordinary dielectrics), then, for example, coordination number in piezoelectric sphalerite structure and in pyroelectric wurtzite structure CN = 4.

23. Exactly the presence of polar-sensitive bonds determines the non-centrosymmetric structure of some crystals: hybridized ionic-covalent bonds are the main cause of pyroelectric, ferroelectric and piezoelectric properties. For example, mechanical action on a polar crystal leads to an electrical (piezoelectric) response. Its mechanism lies in the fact that the displacement of ions deforms their *asymmetric bonds* and by this way leads to the appearance of electric charges on the surfaces of a crystal. In opposite case, when the ionic bonds of the crystal are the centrosymmetric, the mechanoelectric polarization is impossible because the electrical effects of the displacement of charges compensate each other.

24. Non-centrosymmetric allocation of electrical charges in polar-sensitive structures can be presented by different simplified structural models: (1) quasi-one-dimensional structural ordering, which corresponds to vector (dipole-like) response onto external influences; (2) two-dimensional structural arrangement of polar-sensitive bonds allowing describe electrical response onto scalar action by model, which consists of six ions, having asymmetric bonds and located in one plane; (3) three-dimensional asymmetric polar-sensitive bonding, modeled by eight ions, representing a spatial polar-neutral structure.

25. In some polar crystals can be seen a critical temperature, at which coordination between adjacent polar-sensitive bonds is disrupted with temperature increase. In these cases temperature steadiness of polar-sensitive bonds allocations can be described by critical law $M(T) \sim (\theta - T)^n$. It means that the phase transition

temperature θ exists, which corresponds to vanishing of tensor M_{ijk} with temperature rise. It is established that critical parameter is $n = 1$, if polar-sensitive bonds are arranged in a plane; in the event of spatial (3D) arrangement of polar-sensitive bonds critical exponent is $n = 2$. These two cases differ essentially from the 1D dipole-type polar-sensitive bonds in ferroelectrics that shows a well known critical law $M_i(T)$ with $n = 0.5$ (Landau critical index).

Chapter 4. Self-test questions

1. What are the difficulties of the theory of spontaneous polarization of pyroelectrics?
2. How and why are polar-sensitive bonds formed?
3. What is the electronegativity and what is its role in the formation of polar crystals?
4. How do piezoelectric effect and electrostriction relate? Can they be justified by a common model?
5. What critical exponents describe the temperature dependence of polar moments - tensors of different ranks?

CHAPTER 5. POLAR CRYSTALS PECULIARITIES

Contents

Various experimental evidences of polar-sensitivity existence in crystals are considered: the structural affinity of piezoelectrics and pyroelectrics; the chemical features of polar crystals confirming proximity of their properties; the increase in volume while self-ordering of polar-sensitive bonds; the piezoelectric and electrocaloric contributions to polar crystals permittivity; the high-frequency dielectric absorption; the dependence of polar crystal elastic properties on various electrical boundary conditions, etc. Features of charge transfer in the polar-sensitive crystals are explained: physical nature of giant change of conductivity in critistors, posistors and varistors as well as in others field-controllable switching elements, particularly those which exhibit colossal magnetoresistance; the nature of high sensibility of nanostructured sensors based on zinc oxide is discussed. The nature of *electrically induced* polar properties is investigated: electrically induced piezoelectric module in paraelectrics and relaxor ferroelectrics; electrical control by resonant frequency of piezoelectric resonators and filters. The *thermomechanically induced* pyroelectricity is examined: an original method of pyroelectric response and volumetric piezoelectric effect obtaining in polar-neutral piezoelectrics (non-pyroelectrics) is described. Two- and three-dimensional structural arrangements of polar-sensitive bonds in polar-neutral piezoelectric are analyzed; artificial pyroelectric effect for 10 classes of polar-neutral piezoelectric crystals are calculated and experimentally tested in quartz and gallium arsenide type crystals. This effect can be used in single-chip pyroelectric and piezoelectric single and matrix sensors.

Various experimental evidences of polar-sensitivity existence in some crystals will be considered: structural affinity of piezoelectrics and pyroelectrics; chemical features of polar crystals confirming the proximity of their properties; an increase in volume while self-ordering of polar-sensitive bonds; piezoelectric and electrocaloric contributions to polar crystals permittivity; high-frequency dielectric absorption;

dependence of polar crystal elastic properties on various electrical boundary conditions, etc. Some important features of *charge transfer* in polar-sensitive crystals will be explained: physical nature of giant change of conductivity in critistors, posistors and varistors as well as in others field-controllable switching elements, particularly those which exhibit colossal magnetoresistance; the nature of high sensibility of nanostructured sensors based on zinc oxide is discussed.

The *electrically induced* polar properties will be also discussed in this Chapter: electrically induced piezoelectric module in paraelectrics and relaxor ferroelectrics, electrical control by resonant frequency of piezoelectric resonators and filters. The *mechanically induced* pyroelectricity will be examined in details: an original method of obtaining pyroelectric response and volumetric piezoelectric effect in the polar-neutral piezoelectrics (non-pyroelectrics) will be described. Two- and three-dimensional structural arrangements of polar-sensitive bonds in the polar-neutral piezoelectric are analyzed; artificial pyroelectric effect for 10 classes of polar-neutral piezoelectric crystals are calculated and experimentally tested in the quartz and gallium arsenide type crystals. It will be shown that this effect can be used in the single-chip pyroelectric and piezoelectric sensors.

5.1 Experimental evidences of polar-sensitivity

Polar properties of well-known pyroelectrics and ferroelectrics, described by the first-rank tensor (i.e., dipole moment vector $M_i = P_i$) do not need additional evidences. However, in the "exclusive" piezoelectrics, which are not pyroelectrics, the existence of polar-sensitivity, that is a capability to electrical response onto homogeneous non-electric action, needs some additional experimental grounds [4]. At that, all electrical measurements are limited only by vector-type responses – by the detection of voltage or current. That is why it is not surprisingly that totally compensated internal polar-sensitivity is not so easy be detected in this case. However, there are some others, indirect evidences of polar-sensitivity existence in the non-central crystals.

1. *Structural affinity* *of piezoelectrics and pyroelectrics* follows, for example, from the polymorphism of $\bar{4}3m$ (piezoelectric) and $6mm$ (pyroelectric) structures. Such proximity of piezoelectricity and pyroelectricity demonstrates zinc sulphide (zinc blende) crystal: interatomic interaction in ZnS provides such configuration of a crystal, in which both structures (sphalerite and wurtzite) can coexist.

In case of sphalerite, the *piezoelectric* internal polar-sensitive structure of ZnS can be described by 3D spatial distribution: this simulation might be represented by

four 3-fold polar axes of [111]-type, which are crossed at the angle of 105.5°, as shown in Fig. 5.1A. Such intrinsic three-dimensional polar structure is absolutely *self-compensated* and in this case zinc sulphide should be attributed to the "exclusive" piezoelectrics. However, second principal structure of ZnS (in which for simplicity only positive polar-sensitive directions are shown) is *pyroelectric* wurtzite. The structure includes not only [111]-type polar axes, but in addition the *dipole type* of polar-sensitivity component as well, directed along one of these axes, Fig. 5.1B; such zinc sulphide is already undoubtedly related to the pyroelectrics.

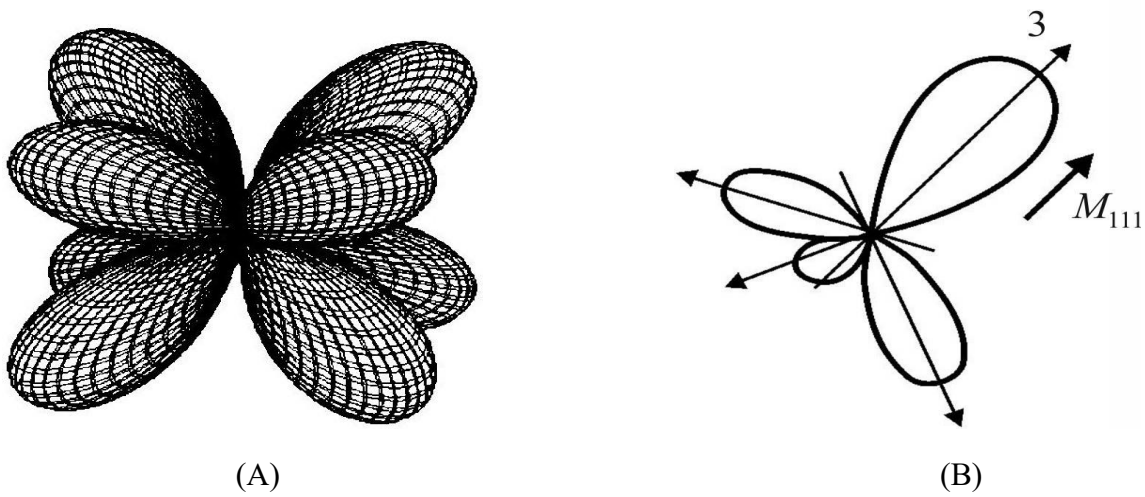

Fig. 5.1. Spatial distribution of 3D type polar-sensitivity (only the positive directions of polar axes are shown): A – total compensation of polar-sensitivity in sphalerite; B – non-compensated "dipole-type" component M_{111} of polar-sensitivity in wurtzite (shown only positive directions)

The difference between the atomic distances of the two main forms of zinc blende is actually so small that these structures with different symmetries can alternate with each other in the same crystal, demonstrating polymorphism. As a result, it turns out that there is no big difference between the pyroelectric and piezoelectric state of this crystal. Accordingly, it seems unconvincing to consider the amplification of polarity in one of polar-neutral directions in wurtzite as the appearance of a spontaneous polarization.

2. *Chemical features* of the polar crystals are another important factor, confirming the proximity of different polar-sensitive structures properties.

In the *pyroelectric* crystals, the surfaces of crystalline plate, which is oriented perpendicularly to the polar axes, have different chemical properties (in particular, different rates of *chemical etching*). As is known, the ferroelectric is a pyroelectric that breaks into domains. At that, selective etching is well known characteristic of the ferroelectrics, what is used to detect their domain structure: chemical etching occurs with different speeds for "+" and "–"orientation of domains.

By the same way, in the *piezoelectric* quartz crystal (which is *not pyroelectric*) the etching occurs much more rapidly on the "positive" side of the polar *X*-axis, while the rate of etching is much slower on the "negative" side of the *X*-axis. In this way the figures of etching seen on quartz are quite different for "+" and "–" surfaces. The dependence in surface chemical activity of given piezoelectric indicates, firstly, the directivity of polar-sensitive bonds in it, and, secondly, non-symmetric distribution of binding energy of ions in electrically positive or negative direction. This phenomenon can also be explained as a “proximity” effect: the propagation of the influence of polar (non-centrosymmetric) crystal property onto its immediate environment) that has no relation to “internal field existence” in a crystal.

[***Note***. Consider, for example, the (111)-cut of cubic but non-polar NaCl crystal: then one side of such a plate would be completely covered by the Na^+ ions while the other by the Cl^- ions, creating, it would seem, both internal and external electric field, and having different chemical activity. But in the reality this does not happen: centrosymmetric NaCl crystal self-neutralizes its surfaces of the (111) slices, so does not create any “proximity” effect, and does not become artificial pyroelectric. So, the peculiarities of polar crystals are explained precisely by the asymmetry in electron density distribution in the elementary unit sell of a crystal, which creates peculiar properties, including the proximity effect].

In contrast to cubic non-polar NaCl crystal, also cubic but polar-sensitive GaAs crystal shows considerable distinction in chemical properties between two surfaces of the (111)-cut plates. This peculiarity is taken into account while electrodes deposition on the gallium arsenide: the adhesion of one or another metal on “positive” and “negative” surfaces of (111)-cut of GaAs is significantly different, so on them it is necessary to use different technologies of electrodes deposition.

Here it is pertinent to mention that direct measurements of the electrical charge density on the fresh cleavages of the pyroelectric tourmaline crystal were made: these measurements showed charge density ~ 0.01 $\mu C/cm^2$ [Jelud].

3. *Increase in volume* (which means decrease in density) is a characteristic property of the self-ordering of the polar-sensitive bonds in crystal [6]. For instance, at ferroelectrics phase transitions into low-temperature polar phase crystal increases its volume as compared with high-temperature nonpolar phase: this is conditioned by the ordering of previously disordered interatomic bonds. Such expansion of a solid upon cooling is quite unusual phenomenon, since in the majority of cases density of solids increases with cooling due to a decrease in the intensity of thermal oscillations of the atoms.

It is noteworthy that during transition to the antiferroelectric phase from the high-temperature paraelectric phase, the volume of crystal decreases: i.e. antipolar (counter) ordering is denser than in polar phase. At that, by applying strong electrical field, antiferroelectric shows a compelled transition into ferroelectric phase: at that the jump of volume becomes so significant that it thermodynamically leads to a large electrocaloric effect with a significant cooling by electrical field (that is interesting for practical use in refrigerators).

The issue of volume increase in the ordered structures can be considered also more broadly: for example, the ferromagnets also usually expand when cooled from the paramagnetic phase, and this is used in the technique for obtaining alloys with a low coefficient of thermal expansion. In connection with this, it is noteworthy that even during crystallization the density of polar crystals decreases as they grow from their liquid phase (for example, GaAs crystal can swim on surface of its melt like ice in water). The point is that in liquid phase the interatomic polar-sensitive bonds can not establish their strict orientation due to intensive thermal motion in disordered liquid structure.

The process of crystal growth from liquid or vapor phase is undoubtedly influenced by the proximity effect just discussed above. During crystallization polar crystal spontaneously expands due to establishment of strong orientation of its polar-sensitive bonds, so crystal density becomes less than the density of a melt. It is also important to add that crystal growth occurs much more rapidly exactly in the direction of polar (or polar-neutral) bonds: as in pyroelectrics so in piezoelectrics, and this determines the form of polar crystal. At that for the manifestation of chemical properties in polar-sensitive crystals is not fundamental importance whether the crystal is the pyroelectric or only the piezoelectric.

4. ***Dielectric permittivity*** frequency dependence of polar-sensitive crystals differs from usual dielectrics. Electrical polarization is the separation of bound electrical charges that is accompanied by deformation of a crystal (strain). Therefore, polarization is not only electrical but electro-mechanical phenomenon. In case of polar-sensitive crystal, electrical energy, given to a crystal by electrical field, is stored not only in the microscopic displacements of bound charges, but in the macroscopic deformation of a crystal as a whole. This deformation is elastically reversible, so it makes *electromechanical contribution* to the permittivity.

When dielectric properties of polar-sensitive crystals are studied at *lower frequencies* (below the frequency of possible electromechanical resonances), the ε^X of *mechanically free* crystal is measured (stress $X = 0$). In this case crystal's electromechanical reaction e^2/ε_0 contributes to the dielectric constant ("*e"* is the

piezoelectric strain module). In the same time, at rather high frequencies (above the electromechanical resonances), the ε^x is determined (crystal is *clamped*, its strain $x = 0$). At high frequencies the own mechanical inertia of test sample makes impossible its electromechanical reaction.

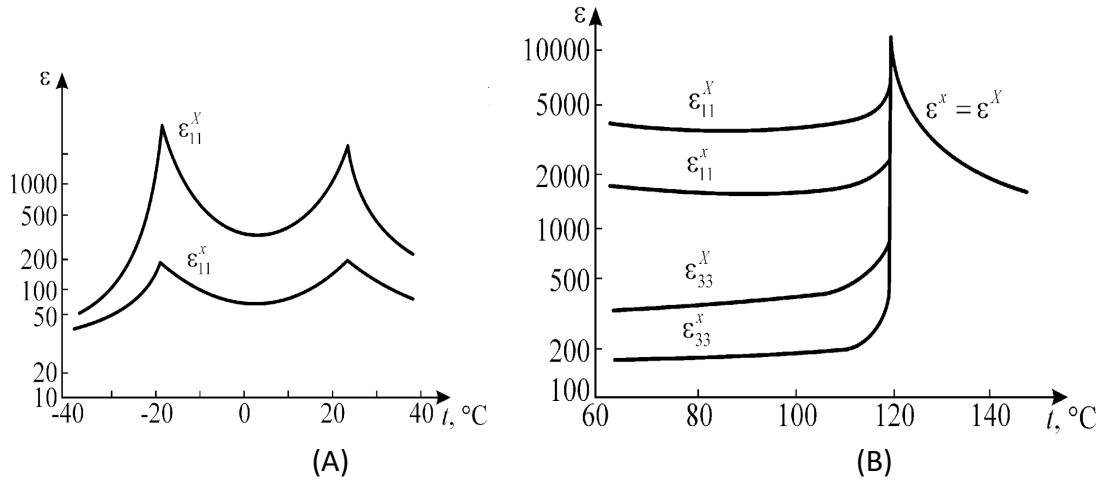

Fig. 5.2. Temperature dependence of dielectric permittivity in free (at frequency of 10^3 Hz) and clamped (at 10^{10} Hz) crystals: A – Rochelle salt, B – barium titanate

The comparison of dielectric constants of free and clamped polar crystals is shown in Fig. 5.2 for most well-known and well-studied polar crystals-ferroelectrics. In Rochelle salt piezoelectric effect is observed in entire temperature range, so everywhere dielectric permittivity of free and clamped crystal differs greatly, Fig. 5.2A. In the vicinity of ferroelectric Curie points the effect of clamping is very large: $\varepsilon^X/\varepsilon^x \approx 50$. In other well known crystal – barium titanate, $BaTiO_3$ – above the Curie point (in cubic center-symmetric phase) piezoelectric effect is absent, and $\varepsilon^X = \varepsilon^x = \varepsilon$. But below Curie point in single-domain $BaTiO_3$ crystal near room temperature the ratio $\varepsilon^X/\varepsilon^x$ is about 2 (while in polarized $BaTiO_3$ piezoelectric ceramics $\varepsilon^X/\varepsilon^x < 2$).

A very large dielectric permittivity ε^X may occur in a mechanically free crystal, but only at low frequencies; however in the region of very high frequencies, the dielectric constant ε^x is significantly reduced. In this case, permittivity's frequency dependence shows a series of electromechanical resonances, as follows from Fig. 5.3, where the study of the KH_2PO_4 (KDP crystal) is shown, we note that in this case the ratio $\varepsilon^X/\varepsilon^x \approx 100$ is record high.

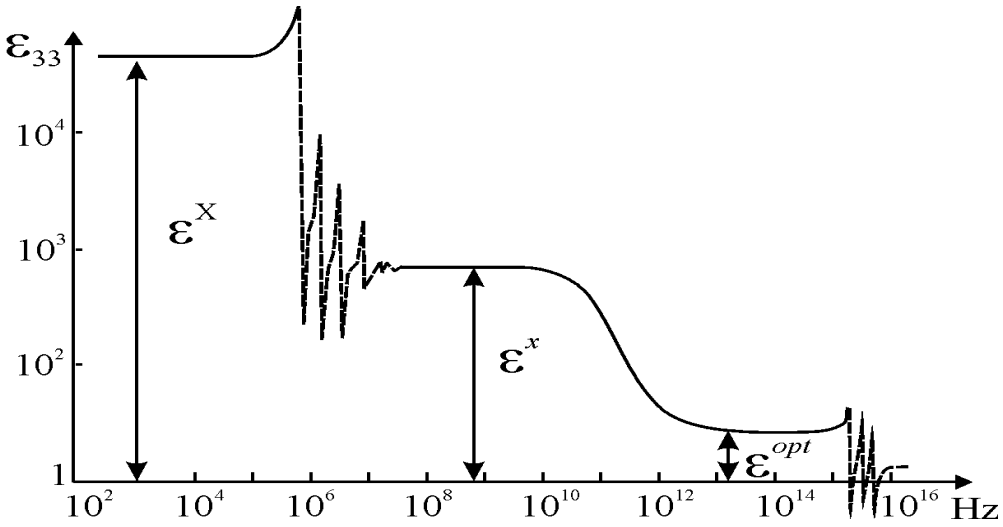

Fig. 5.3. Dielectric spectrum of KDP crystal near its Curie point: in the frequency range of $10^5 \ldots 10^8$ Hz a series of piezoelectric resonances is observed [8]

Given in Fig. 5.2 and Fig. 5.3 examples show very large electromechanical contributions to low-frequency dielectric constant of polar-sensitive crystals. However, in most cases the difference between ε^X and ε^x is not so great.

Another possible influence on polar crystal permittivity is the "electro-thermal contribution" ε_{ET} that is called also as *electro-caloric* contribution. This refers to difference $\varepsilon^T - \varepsilon^S = \varepsilon_{ET}$ between the permittivity ε^T measured under isothermal conditions when T = const and dielectric has enough time to exchange energy with the environment, and the permittivity ε^S measured in adiabatic conditions, at the constant entropy (S = const), i.e., when heat exchange with the environment is impossible.

Electro-caloric contribution to permittivity might be essential when ε is large and its dependence $\varepsilon(T)$ is big, for example, near the ferroelectric phase transition. Sometimes the difference between ε^T and ε^S might reach 10...50% (for example, just below ferroelectric phase transition).

5. *High-frequency dielectric absorption* is another remarkable feature of polar-sensitive dielectrics. In polar crystals, there is a fundamental microwave absorption, which greatly exceeds this absorption of centrosymmetric crystals. As a result, the dielectric losses in microwaves are large and have a quasi-Dedye character due to the interaction of optical and acoustic phonons. The frequency dependence of the dielectric loss is shown in Fig. 5.4 as the imaginary part of the complex dielectric constant $\varepsilon^* = \varepsilon' - i\varepsilon''$. In the polar-sensitive crystals microwave dielectric losses show additional maximum of quasi-Debye type absorption due to interaction between optical and acoustical phonons.

Experimental evidence shown in the Fig. 5.4 is a comparison of microwave properties of two semiconductors. One is the non-polar crystal silicon, Fig. 5.4 A, which that is characterized only by covalent bonding between atoms, therefore its dielectric losses are caused exclusively by the conductivity (σ). Correspondingly, in silicon the loss factor decreases with frequency, but increases with temperature:

$$\varepsilon''(\omega,T) \approx \sigma_0 \exp[a(T - T_0)]/[\varepsilon_0\omega],$$

where σ_0 is conductivity at room temperature T_0, ε_0 is electrical constant, and a is peculiar parameter for given semiconductor.

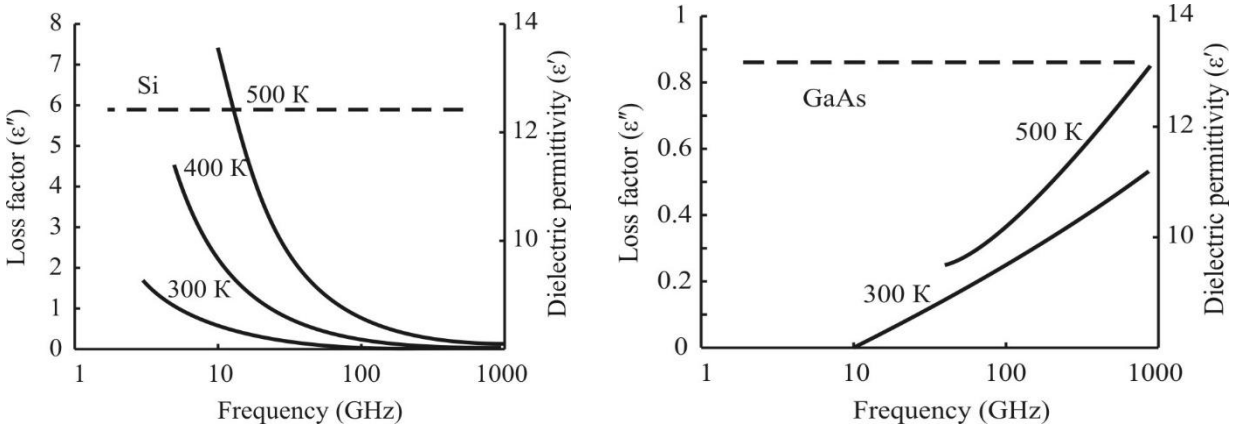

Fig. 5.4. Frequency dependence of microwave absorption ε″ (solid line) in non-polar silicon (A) polar crystal *s/i*-GaAs (B); dashed line shows permittivity

Other example is gallium arsenide – polar-sensitive crystal-semiconductor, Fig. 5.4B, in which conductivity a thousand times less than in silicon. Since the influence of conductivity on the microwave absorption of this crystal is negligible, it would be expected that in the millimeter wave range the absorption of gallium arsenide should be very small. In fact, however, microwave losses of GaAs are increased and ε″(ω,T) increases even more with frequency rise.

The fact is that in the polar-sensitive crystals on millimetre waves the losses of polarization are manifested due to interaction of acoustic and optical phonons. In the non-polar crystals, optical phonons, which excited by ultra-high frequency electrical field, very weakly dissipate received energy on acoustic phonons, which are electrically inactive in the non-piezoelectric crystals, and play the role of a "thermal reservoir" of crystal lattice. In polar crystals, on the contrary, due to absence of centre of symmetry in elementary cell, acoustic and optical phonons are coupled, so that the super high frequency energy, imparted to crystal, is more efficiently converted into the heat: this is the microwave losses.

Loss factor increasing with frequency can be described by Debye formula:

$$\varepsilon''(\omega,T) \approx (\omega/\omega_D) \exp(-U/k_BT),$$

where ω_D is Debye frequency, k_B is Boltzmann constant, U is potential barrier of relaxation. As can be seen from the experiments (Fig. 5.4B), in the polar-sensitive crystals the microwave (fundamental) loss factor increases with frequency ascending and with temperature rise.

6. *Elastic properties* of the polar crystals are also very remarkable. In similar in chemical composition and structure of crystalline structures polar crystals the elastic stiffness (c) is usually lesser than in the non-polar crystals; correspondingly, their elastic compliance (s) is bigger. Both these parameters in the polar crystals essentially depend on the electrical conditions in which the crystal is located: whether it is short-circuited (s^D, c^D) or open-circuited (s^E, c^E). If the polar crystal is short-circuited, its elastic compliance will be bigger than in the case of the open-circuited crystal ($s^D > s^E$). The reason is that electrical voltage, generated by a strain in the case of open-circuited crystal, increases its harshness (resistance to deformation). Experimental example of this effect is shown on Fig. 5.5.

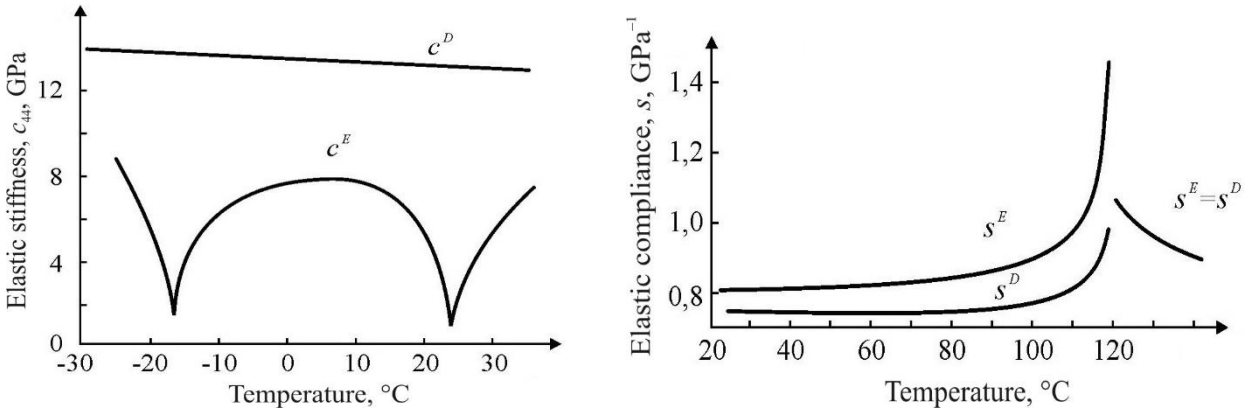

(A) (B)

Fig. 5.5. Effect of electrical conditions on polar crystals elastic properties; A – Rochelle salt elastic stiffness in its polar direction; B – barium titanate elastic compliance

Experiments show essential difference in the elastic stiffness in the well-known ferroelectric Rochelle Salt crystal: $c^D > c^E$, Fig. 5.5 A. In the entire range of investigation this crystal is polar, at that, above 24° C it is paraelectric while below –18° C it is antiferroelectric, while between these temperatures Rochelle Salt is ferroelectric. The most impressive difference between c^D and c^E is seen in the Curie points where elastic stiffness of short-circuited crystal decreases in 8 times. As known, the elastic stiffness determines the speed of sound in a crystal; it can be seen from the Fig. 5.5 A that in short-circuited crystal this speed varies critically at the points of phase transitions. The above change in c^E can be considered as greatest of known; in fact, in the most of polar crystals, the difference between c^D and c^E is not so large, but quite noticeable.

Second example of *electrical conditions* influence on the elastic properties of polar-sensitive crystals is shown in Fig. 5.5 B. The significant difference between the elastic compliance of an electrically open and a short-circuited crystal can be seen in the polar phase of barium titanate (below its Curie point). In the polar (ordered) phase of barium titanate, the piezoelectric effect is observed, and in the non-polar phase this effect is absent, so $s^E = s^D$. However, below temperature of phase transition barium titanate turns into tetragonal polar-sensitive phase that is characterized by the piezoelectric effect, so elastic compliance becomes quite different: $s^E > s^D$. The most critical reduction of the compliance s^D is seen in Curie point.

There are many other examples how electrical conditions influence on polar crystals mechanical and thermal properties. For one's turn, mechanical boundary conditions also may strongly affect as on electrical so on thermal properties. By that polar crystals differ from a great number of non-polar crystals and non-crystalline dielectrics. Further, it will be shown that polar crystals exhibit unusual properties in the field of electrical conductivity as well.

5.2 Charge transfer in polar-sensitive crystals

While study electrical polarization mechanisms in dielectrics (including piezoelectrics, pyroelectrics and ferroelectrics) to simplify the task the electrical conductivity of material usually no need to take into account. In turn, while studying electrical conductivity of semiconductors, as a rule, no attention is paid to the phenomenon of their electrical polarization. In most cases, these assumptions are justified; however, there are quite rare but nonetheless important cases, when the interdependence of intrinsic polarity and conductivity becomes essential physical phenomenon. For example, should not neglect by intrinsic polarity while classification of semiconductors: the non-polar semiconductors (such as Si or Ge) are characterized by the *non-direct band gap* electronic energy spectrum, while main feature of the polar semiconductors, such as $A^{III}B^{V}$ crystals (possessing piezoelectric symmetry) and $A^{II}B^{VI}$ crystals (with pyroelectric symmetry) are the crystals with *direct band gap*.

It will be considered further, how polar-sensitive structure can affect electrical resistance (or conductance) of the non-centrosymmetric crystals. It should be noted that this phenomenon manifests itself somewhat *differently* in the ordinary and in the elevated electric fields. At that, strong influence of internal polarity is seen both

on the *temperature* dependence of resistivity (used in the electronics components *critistors* and *posistors*) and on the *field-dependence* of resistivity (that is used in electronics in the varistors). It should be noted that understanding of the mechanisms of internal polarity action on the electrical charges transfer can be important for improving relevant materials parameters.

As first example, the influence of intrinsic polarity on the *temperature behavior of resistivity* is considered. Figure 5.6 demonstrates different types of thermistors – electronic components that are widely used to measure temperature by means of resistivity alteration. Temperature dependence of electrical resistance in the *metals* has been used for a long time: their resistivity increases with temperature (curve *1*) thanks to scattering of conduction electrons by lattice vibrations; although this effect is rather weak, the *positive* temperature coefficient of resistance in metals finds application in sensors. Much wider application such thermistors are found, in which the *negative* temperature coefficient of resistance is used, so they are called the *negistors*, curve *2* in Fig. 5.6. Usually they are made of semiconductor oxides, in which resistance decreases noticeably with increasing temperature. The physical nature of $R(T)$ decrease in negistors is the increase of free electrons concentration in the semiconductor with temperature rise. At that, electrical polarity of material does not have significant effect on the $R(T)$ dependence.

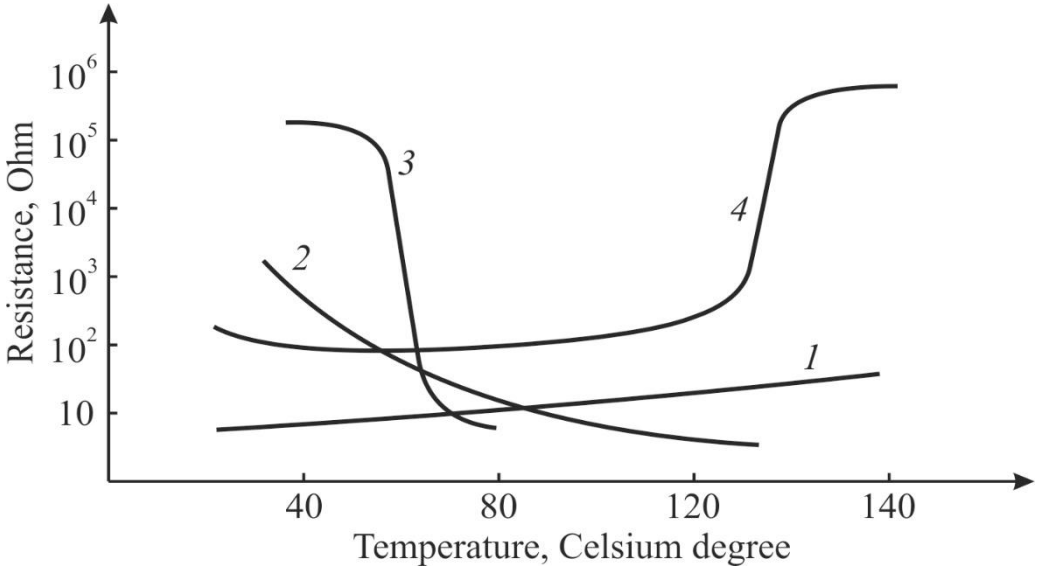

Fig. 5.6. Temperature dependence of resistance: *1* – platinum wire thermistor; *2* – negistor utilizing transition-metals oxides; *3* – critistor based on vanadium dioxide; *4* – posistor utilizing doped barium titanate [10]

As can be seen from Fig. 5.6, there are some materials, in which the resistivity is much more sensitive to the change of temperature, and they are, in particular, the polar-sensitive materials *critistors* (curve *3*) and the *posistors* (curve *4*): they have

large negative or positive temperature coefficients of resistance. It is natural to assume that this feature can be explained by the influence of polarity on conductivity. It is important to note that in all shown in Fig. 5.6 temperature characteristics the magnitude of electrical fields and currents practically *does not matter*: in variuos electrical field they demonstrate the *linear* properties.

However, in some other cases, just the polar-sensitivity determines the nonlinear properties in the oxide dielectrics-semiconductors.

Therefore, second example is related to the effect of intrinsic polarity on the *non-linear behaviour of resistivity*. Figure 5.7 demonstrates broadly how strong electrical field can affect electrical resistance of different materials.

Dielectrics usually retain a very high resistance up to very high field strengths (curve *1*), but there is a limit: the phenomenon of electrical breakdown due to electronic avalanches, when the resistance of the dielectric drops to zero. Similarly, in semiconductors (curve *2*), irreversible breakdown with the decrease in resistance due to generation of new charge carries in electrical field is also observed. The influence of the polarity of the electrical strength of crystals is not considered here.

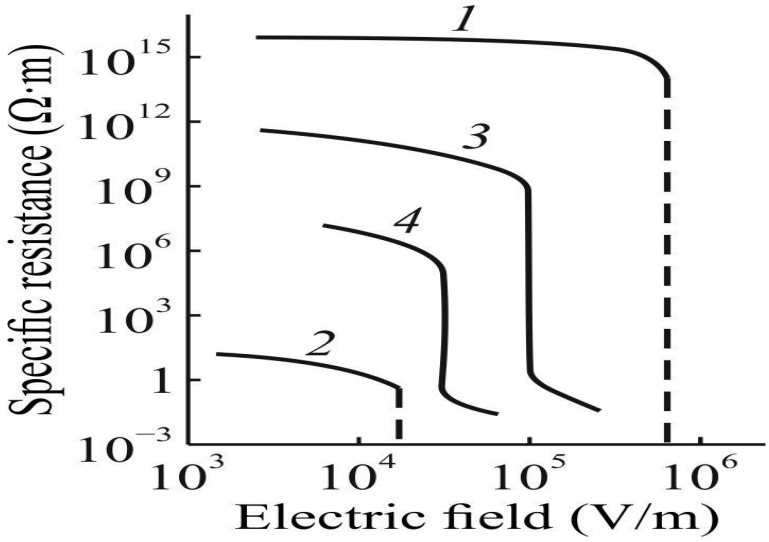

Fig. 5.7. Field dependence of resistance: *1* – typical dielectric; *2* – typical; semiconductor; *3* – zinc oxide varistor; *4* – silicon nitride

It's quite another matter, when the resistance can be changed in thousands times *without electrical breakdown.* This phenomenon is might be due to a peculiar electro-physical process (curve *3* in Fig. 5.7); in another case, it might be ascribed to the tunneling effect (curve *4* in Fig. 5.7). Unlike irreversible effect of electrical breakdown, these $R(E)$ transfer from the insulating state to the conducting state is reversible, because dielectric/semiconductor does not undergo to any destruction, as it happens in case of electrical breakdown.

Materials, which resistance is characterized by the curves *3* and *4* in Fig. 5.7, are dielectrics in a wide range of electrical fields until anomalous changes in conductivity. In this regard, note that different interatomic bonds of solid dielectrics affect the electrical conductivity in different ways. Ionic bonds promote the transition of electrons to their polaron state, which significantly *reduces conductivity*: the electrons mobility in the ionic dielectrics is only (1–10) $cm^2V^{-1}s^{-1}$. Conversely, in the covalent crystals, their "open" internal structure does not contribute to the formation of small radius low-mobility polarons, but contributes to very high electrons mobility: 10^4–10^5 $cm^2V^{-1}s^{-1}$. In both cases, there is a correlation between the mobility and the affinity of atoms to electrons.

At the same time, covalent bonding at which *two* atoms share two valence electrons, has different extreme cases: firstly, covalent bond may approach to the metallic bonding, when *all* atoms share between them all valence electrons, and, secondly, covalent bond may approach to the ionic bond, when one atom completely delegates its valence electrons to another atom.

Two important properties of ionic dielectrics: their increased polarizability and their low conductivity are *interdependent*. Indeed. the electron (or hole) generated in dielectric as a result of any activation processes becomes less mobile, since it polarizes by its field the surrounding nanosize region in the crystal. It is obvious that such a charge carrier is forced to move along together with the region polarized by it, forming a *small radius polaron*. The low mobility of such charge carriers makes possible, in turn, the long existence of electrostatic field in dielectrics (in the conductors this field is shielded by free charge carriers).

Thus, the relatively stable state in a dielectric with low electronic conductivity is due precisely to the ionic polarization. Heating a crystal or exposing it to a strong electrical field can disrupt this stability, because under external energy exposure electrons can free themselves from their polarized environment: polarons transfer into highly mobile electrons, and the dielectric turns into a more conducting medium.

In some especial cases the stable non-conducting state in dielectric may be compromised even in a weak electrical field and without essential heating. Exactly this exceptional case corresponds to crystals with polar-sensitive properties. In such polar dielectrics, even small change in the external conditions (pressure, temperature, mechanical stress or electrical field) can lead to a huge increase of conductivity (up to 10^4–10^9 times), and dielectric turns into conductive matter but without breakdown. Large jump of conductivity (or resistivity) usually, but not obligatory, is accompanied by the change in the structure of crystal; that is associated

with peculiar re-arrangement of electronic interaction between particles, which can lead to the alteration in crystal symmetry.

Now it would be interesting to find out why this transformation in some crystals is a rare exception. The unusual dependence of resistivity on electrical voltage, i.e., its change by hundreds and thousands of times, takes place in non-centrosymmetric polar crystals with a pyroelectric or piezoelectric structure. In fact, mentioned in Fig. 5.7, silicon nitride SiC has a pyroelectric wurtzite structure while vanadium dioxide VO_2 refers to triclinic piezoelectric symmetry, Unusual dependences $R(T)$, which were presented in Fig. 5.6, characteristic firstly, for zinc oxide ZnO with a polar pyroelectric structure, passing with increasing voltage to another, but also polar sphalerite (piezoelectric) structure, and secondly for barium titanate $BaTiO_3$, which is a ferroelectric with pyroelectric structure.

Thus, the explanation of unusual jump-like change in conductivity in some polar crystals reduces to the clarification principal physical cause: why the polar-sensitivity, leading to the non-centrosymmetricity, might have especially strongly influence on the electrical conductivity. An evident reason for the lack of center of symmetry in crystal is a special kind of atomic bonding – polar-sensitive bonds. This kind of interatomic bonding represents the intermediate case between ionic and covalent bonds: as noted above, the pure-ionic, as well as the pure-covalent crystals always demonstrate a centrosymmetric structure, and this means that in such crystals there is no intrinsic (hidden) polarity.

Non-centrosymmetric structures are the result of mixed ионшс-covalent bonds between the atoms of a crystal. Like the covalent bond, these mixed bonds are *directional*, which leads to the asymmetry of polar crystal structures. In turn, the nonuniform probability density of the distribution of electrons in the interatomic bonds is due to the difference in the electronegativity of atoms. In addition, this density asymmetry of electronic clouds is the main cause of *internal polarity* in crystals. Electrical conductivity in dielectrics and semiconductors, having an activational character, must depend on the affinity of atoms to electrons: in order to form a free charge carrier, it is necessary to tear an electron from its own atom or ion. At the same time, the crystals discussed here are not monoatomic, but are chemical compounds. Therefore, the importance is not only of the electronegativity of individual atoms (measured on the Pauling scale), but the difference of this parameter in neighboring ions.

Consequently, a distinctive feature of polar crystals is a certain system of polar-sensitive bonds. The spatial distribution of polar bonds in a crystal can be complex, but its distinguishing feature is the absence of a center of symmetry. This

feature has a decisive influence on the physical characteristics of polar crystals, including their resistivity.

In discussed case, the most important is the influence of polar-sensitivity on the crystal resistivity. If internal polarity is distributed in a complex manner, than charge carriers is obliged to lead the way through the alternating bipolar nano-size districts that dramatically decreases their mobility – just as electron in the antiferromagnetic with difficulties leads its way through the anti-parallel magnetized lattice. On the contrary, if internal polarity is quite ordered (or becomes ordered by the external field) than charge carrier mobility should be much higher – just like big electroconductivity is peculiar to the ferromagnetic with parallel ordered spins.

Below it will be shown how the model of polar-sensitive bonding can be applied to explanation, firstly, the critical temperature dependence of resistivity and, secondly, the stimulated by electrical field, large jumps of conductivity in the polar crystals, listed in Fig. 5.6 and 5.7.

First and foremost, the critistor effect in the vanadium oxides is considered as phase transition of insulator-to-metal type At lower temperature VO_2 and V_2O_3 are the wide-gap semiconductors (almost dielectrics), but when temperature increases they exhibit metallic-type behaviour: the energy band gap in these crystals almost disappears. As a result, in a narrow temperature interval their resistivity changes in thousands times; at that, the critical temperature (within a limited range) can be controlled by the chemical composition. It is natural to assume that this feature is due to peculiarity of interatomic bonds in vanadium oxides.

As well known, the covalent bond, in which the adjoining atoms are divided by a pair of valence electrons, on one hand, is close to the metallic bond, in which all valence electrons are generalized in the lattice of a metal. But, on other hand, the covalent bond is close also to the ionic bond as well, in which cation entirely delivers its valence electrons to anion, and together they constitute the dielectric ionic lattice. It would seem that exactly this feature of covalent bond could be used to explain discussed phase transition in vanadium oxide. However, crystals with dielectric-metal type transition having strong $R(T)$ dependence are extremely rare case. The point is that a key role in this phenomenon belongs to the hybridized covalent-ionic bonds, which give rise to polar-sensitivity and to non-centrosymmetric structure creation.

Indirect confirmation of this mechanism is the dependence of VO_2 conductivity on pressure, which pretty easy converts this oxide into metal. Upon crystal compression, its atoms become closer to each other and, as a result, there is not enough space for hybridized ionic-covalent polar bonds mutual orientation: all

valence electrons become generalized in the electronic gas filling a lattice: now this is already metallic bonds (as it was noted. polar bond ordering leads to increase in crystal volume; respectively, crystal compression destroys the ordering of polar-sensitive bonds).

In Fig. 5.8 temperature dependence of conductivity σ in VO_2 crystal is compared with σ dependence on hydrostatic pressure. Experiments show that at very high pressure (as well as in very big electrical field) dielectric phase in the vanadium dioxide cannot be realized. This means that not only a critical temperature exists (as seen in Fig. 5.6, curve *3*), but also the critical field and the critical pressure exist (when VO_2 shows sharp increase of conductivity). As it will be shown later, just such dependence on pressure is a characteristic of polar-sensitive coupling in ferroelectrics (their phase transition at higher pressure is shifted to low temperatures).

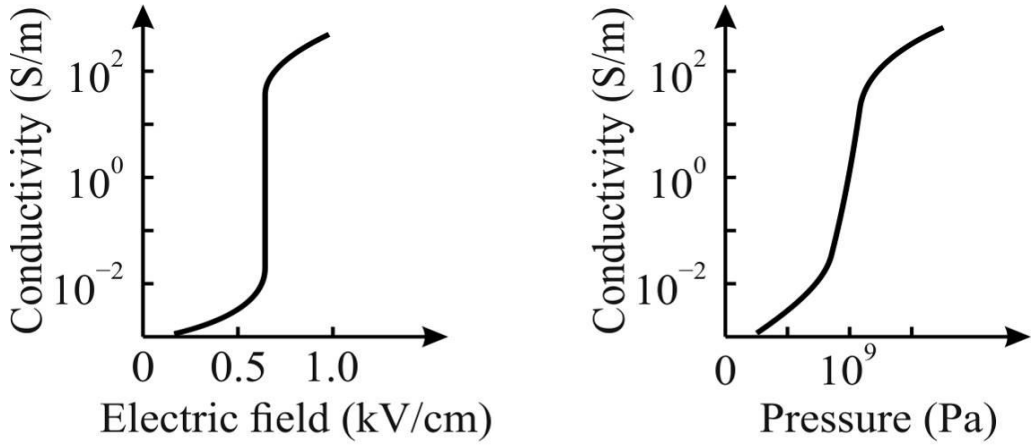

Fig. 5.8. Changing VO_2 conductivity in electrical field (A), and with increase of pressure (B) [11]

When comparing the characteristics of vanadium oxide of critistor, it should be noted that shown in Fig. 5.6, curve *3* relates to the *ceramic* material, in which $R(T)$ dependence is somewhat blurred in comparison with single crystal: its inverse characteristic $\sigma(T) \sim 1/R(T)$ is shown in Fig. 5.8A. It is seen that in the single crystals this physical phenomenon manifests itself more sharply than in ceramics.

Thus, the mechanism of temperature-induced phase transition in the vanadium dioxide looks like this: in the insulating state of VO2 rather complex destribution of polar-sensitive bonds of 3D-orientations promotes extremely low mobility of the polaron-type charge carries. The point is that vanadium dioxide in its lower-temperature (dielectric) state has several competing phases with dominating of the monoclinic polar-sensitive structure. Exactly the instability of these phases with

their variability and mutual transitions contributes to formation charge carriers with bound (polaron) states. Next, when temperature rises, growing energy results in fast liberation electrons, creating their avalanche with the stepped decrease of resistivity (i.e., with $\sigma(T)$ spasmodic increase).

External electrical field also supports to liberation of charge carriers from their bound state, so even at temperatures much low then natural jump of conductivity (in the dielectric phase of VO_2) the electrical field forcedly and fast switches VO_2 into its conducting phase. At that, the electrically controlled and fast changing "dielectric-to-metallic" reflection of infrared and optical waves from VO_2 surface is reached: thus, arises the element with electrically guided optical reflection.

Exactly in complicated polar-sensitive structure a strong coupling of charge carriers with their close neighbours in the lattice is formed. Very low mobility of formed polarons stipulates large resistivity of VO_2 at lower temperature. Due to a delicate balance of this unstable state, the mechanism of high conductivity appearance resembles the “cards house destruction” or the “domino effect”. When electrons become unfettered, their interaction with the surrounding nano-areas becomes screened; as a result, the avalanche-like increase of free charge carriers occurs. Arising with temperature increase, the high-conductive (“quasi-metallic”) phase of VO_2 is characterized by the *non-polar* tetragonal rutile-like structure. It should be also noted that a definite influence on the electrical conductivity is also exerted by the magnetic ordering in VO_2, which at lowered temperature is antiferromagnetic, while at increased temperature it is paramagnetic.

It is important to note two features: firstly, the dielectric-to-metal transition is *very fast* and completely *reversible*: when VO_2 cooling, its dielectric phase instantly returns. Secondly, transition from the dielectric phase to the electrically conducting phase can be easily stimulated by the external electrical field, which releases the electrons from their polaron state. During this transition, the electrical resistivity, the opacity, etc, can be changed up to several orders of magnitude. Due to these properties vanadium oxide is used as a surface with electrically controlled reflection that can be applied in various sensors, and so on. Based on vanadium dioxide fast optical shutters, modulators, cameras and data storage devices are elaborated.

Thus, vanadium dioxide refers to the ***field-controllable switching elements***. As controlling factor for resistivity the electrical field acts, which changes resistivity into hundreds of times. As shown in Fig. 5.9A, the *curve* “$E \approx 0$”, located below temperature 60° C, vanadium dioxide is dielectric (“D”), but above 65° C it exhibits quasi-metallic behaviour: the band gap in the electronic energy spectrum in

vanadium oxide almost disappears. As a result, in narrow temperature interval the resistance of VO_2 decreases rapidly, passing to the metallic phase ("M").

However, if external *electrical field* is applied to the VO_2 (usually sample is the thin film with interdigital electrodes), the transition from "D" phase into "M" phase will start at much lower temperature, for example at ~35°C, and the resistance under controlling field decreases in thousands times, as shown by vertical line *1* → *2* in Fig. 5.9A. Such a displacement of the phase transition in the electrical field is the physical basis for vanadium oxides application as the switching elements: externally applied electrical bias field promotes charge carriers liberation from their bounded state, so fast switching takes place to the conducting state. As mentioned, electrically controlled optical reflection from VO_2 film is used in controlling optical devices.

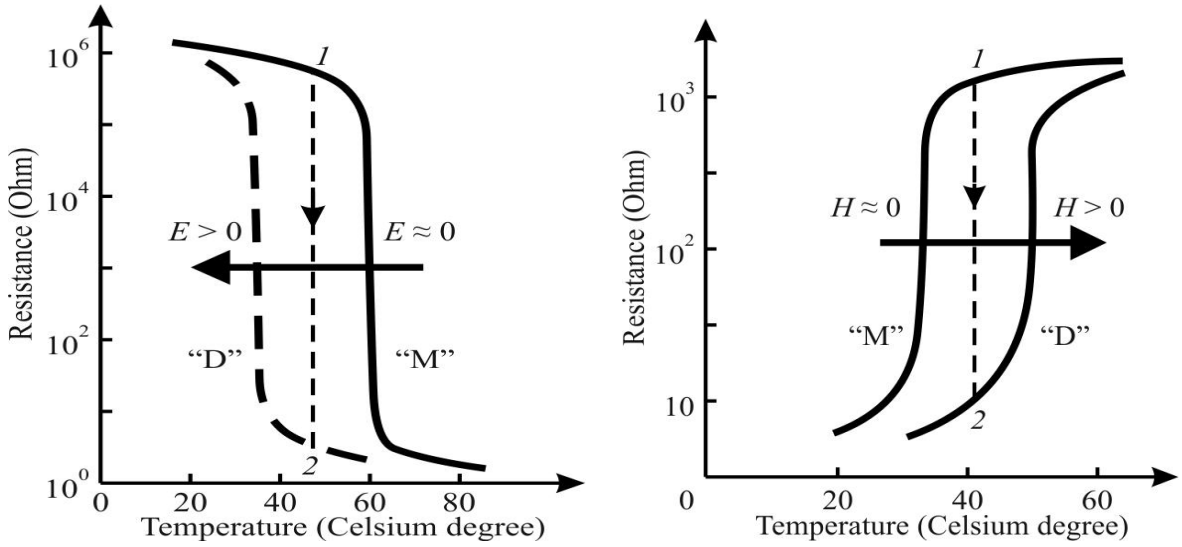

Fig. 5.9. Resistance control by external fields: A – electrical bias field manages *R* value in VO_2; B – magnetic bias field manages *R* value in $(La_{1-x},Ca_x)MnO_3$ (dotted line *1* → *2* shows large fall in resistance)

It should be noted that in the polar-sensitive crystals a significant control by the resistivity is possible not only by using electrical field, but by applying *magnetic bias field*. Example of *magnetic control* by electrical resistance in manganites with a perovskite structure is shown in Fig. 5.9B. These compounds are the important family of oxides with *colossal magnetoresistance*. Among such compounds, interesting polar compounds of the type $(La_{1-x},Ca_x)MnO_3$, where concentration of Ca may vary within $0 \le x \le 1$. With this variation, the physical properties of manganites change dramatically; in particular, phase transitions with different types of magnetic and dielectric ordering are seen. In this case, the magnetic ordering is due to double electron transfer through the intermediate oxygen ion $Mn^{+3} \Leftrightarrow O^{-2} \Leftrightarrow Mn^{+4}$. At low

temperatures, the magnetically ordered phase $(La_{1-x},Ca_x)MnO_3$ has the reduced electrical resistance (which is typical for ferromagnetic ordering) while at elevated temperatures, the compound under consideration is the wide-gap semiconductor (almost a dielectric). An application from outside the magnetic field returns this compound to a magnetically ordered phase with low electrical resistance.

Therefore, in addition to electrical control by the resistivity in V_2O, in the case of $(La_{1-x},Ca_x)MnO_3$ compound the magnetic way of resistivity controlling is applied. Indeed, the parallel ordering of electronic spins inthe "M"-phase of compound corresponds to a low electrical resistance, Fig. 5.9B, left part, at $H = 0$. However, when temperature rises, growing thermal movement in the manganite lattice destroys the double-exchange mechanism, and ferromagnetic (conducting) phase is turning into the non-magnetic (nearly dielectric, "D") phase; correspondingly, the sharp increase of resistance occurs. However, by the magnetic bias field applying in the higher-temperature "D"- phase the magnetic ordering in the manganite can be forcibly returned, see Fig. 4*b*, *curve* $H > 0$. At that, the resistance falls down in hundred times, as it is shown by the dotted line *1* → *5*. Induced by magnetic field "insulator-conductor" transition is otherwise called the colossal magnetoresistanse. Large change of resistivity under the controlling magnetic field can be used in many electronic devices.

Thus, in the polar-sensitive material, both electrical and magnetic fields may shift the temperature of "insulator-conductor" type phase transformation, leading to the enormous changing of resistivity. At that, the phase with reduced resistivity may be located as at elevated temperature so at lower temperature.

The listed mechanisms of dielectrics polarity strong influence on electrical resistivity make it possible at last to consider the ***posistor****s,* mentioned above in connection with Fig. 5.6, curve *4* (note that such electronic ceramics with the *positive* temperature coefficient of resistivity is used not only in electronics but in electrical engineering). Quite unusual for dielectrics and semiconductors availability to obtain such temperature range, in which their resistivity *increases* with temperature rise (instead of usual exponential decrease) is observed not only in the manganites of $(La_{1-x},Ca_x)MnO_3$ type but also in doped ferroelectrics of $BaTiO_3$ type.

In ordinary ferroelectrics, near their the phase transition anomaly of electrical resistivity usually is small: ferroelectric transition in most cases does not significantly change general activation-type $R(T)$ *decrease* with growing temperature, Fig. 5.10A, the dotted part of line. Electronic energy band gap in most of ferroelectrics is big, and, therefore, they usually can be considered as dielectrics both above and below their phase transition.

However, using doping, it is possible significantly reduce resistance in ferroelectric that is shown by a solid line in Fig. 5.10A. At that, near the ferroelectric Curie point (~ 400 K in $BaTiO_3$) a sharp increase in $R(T)$ is seen (in ~ 10^3 times). As already noted, in most cases posistor effect is used in doped ferroelectrics *ceramics* of barium titanate type (not in crystals). It is important to note that the state with low resistance is peculiar only to polar-sensitive phase, while at transition to non-polar phase the resistance stepwise increases. (Typical for usual dielectrics activation-type resistance falls down is seen only at further heating, significantly higher than Curie point).

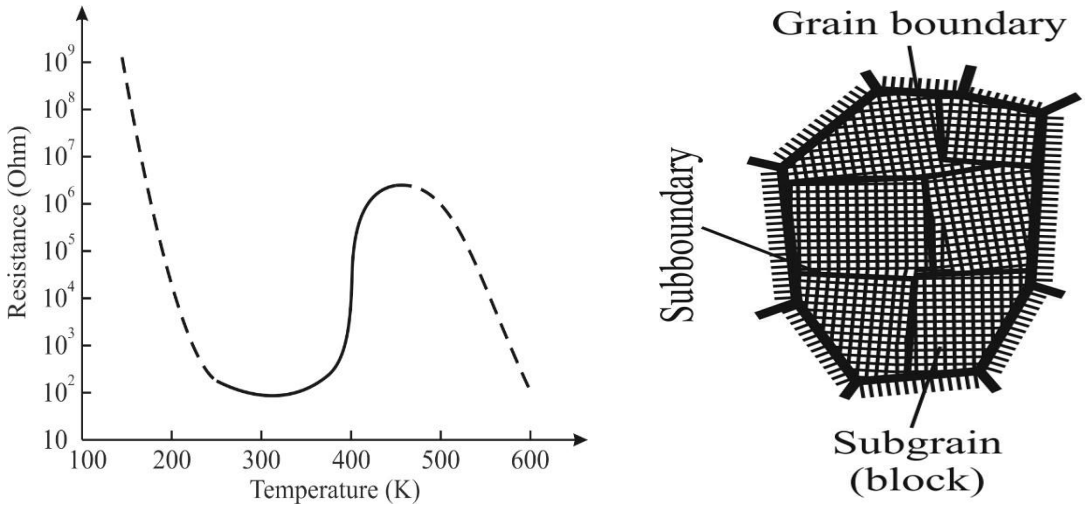

(A) (B)

Fig. 5.10. Resistance temperature dependence in dysprosium doped barium titanate (A) and scheme of crystallite (grain) with (mosaic) structure inside crystallite (B)

In case of ferroelectrics, strong influence of polar-sensitive ordering on the resistivity is obvious. Experiments show that one-directed polar-sensitive bonds in the structure with tetragonal symmetry of 4*m* class do not promote polaron states formation, giving increased conductivity in doped ferroelectric. When phase transition into high-temperature non-polar *m*3*m* phase occurs, the ordering in polar-sensitive bonds disappears, and charge carriers transform into polarons with increased effective mass. At that, exactly the polycrystalline structure essentially contributes in the disordering, under which the favorable conditions are created for charge carriers binding and correspondent increase of electrical resistance.

With a further increase in temperature above the limits of use of a posistor, in the end, the polaron states are destroyed by thermal motion, and the resistance decreases as in all semiconductors and dielectrics, Fig. 5.10, $t > 500$ °C.

In the posistor effect, a decisive role of the grain boundaries of polycrystalline ferroelectric is seen: they are relatively “transparent” for charge carriers movement

in the ordered polar phase, but become practically “locked” in the non-polar phase, creating polarons. The scheme of crystallite is shown in Fig. 5.10B: this is a rather complex formation, having both “widened” boundaries and densely located “narrow” dividing walls, which also introduce disorder into structure. Both grain boundaries and interblock boundaries have chemical composition similar to basic ferroelectric, but they have high concentration of structural defects. The main reason for the low resistance of boundaries in the polar phase is the *proximity effect*[*)], already discussed above in connection with polar crystals surface chemical peculiarities. As a result, highly ordered in the polar phase interatomic bonds induce inside weakly-ordered boundaries the polar type regularity, which causes lower electrical resistance. When, with temperature increase, thermal motion destroys the ordering of polar-sensitive bonds in body of crystallite, the ordering is even more disturbed in the numerous wide and narrow boundaries, so the resistance suddenly rises.

The temperature of the sharp increase in posistors resistance could be changed by applying various doped ferroelectric solid solutions. For example, in the composition (Ba, Pb) TiO_3, the resistance jump can be increased up to 600 K, while in the composition (Ba, Sr) TiO_3, the temperature jump of resistance can be reduced down to 300 K. Thus, ceramic posistors can be designed for applications in a wide range of temperatures. Pozistors – unusual ceramic elements with low "cold" electrical resistance and high "hot" resistance – are used in thermal control systems, in devices that prevent thermal and current overload, in engine-start systems, in measurement technology, as well as in automatic control systems. Posistors are also used to protect against overvoltage and to avoid high short circuit current: when the posistor is connected in series with the load, the current in the circuit is limited to a safe level [1].

For the same goal – electrical current limiting in the critical situations – others polar conductive materials are used, namely, the ***varistors***, i.e., ceramic dielectrics-semiconductors, in which the drastic change in conductivity not means any phase transition (as it occurs in VO_2 or in doped $BaTiO_3$). In case of varistors, the significant jump of electronic conductivity (millions of times) is observed, for instance, in the carborundum (SiC) or in the zinc oxide (ZnO). The comparison of their behavior in strong electrical fields with ordinary dielectrics and semiconductors was shown in Fig.5.11

[***Note.*** Proximity effect is well known in magnetism, when a magnet induces magnetization in closely adjacent non-magnetic material; this effect is also known in superconductivity, when ordinary metal closest to superconductor also becomes

superconductor; in liquid crystalline substances, when ordering, peculiar to one phase, affects ordering of neighboring phase, etc].

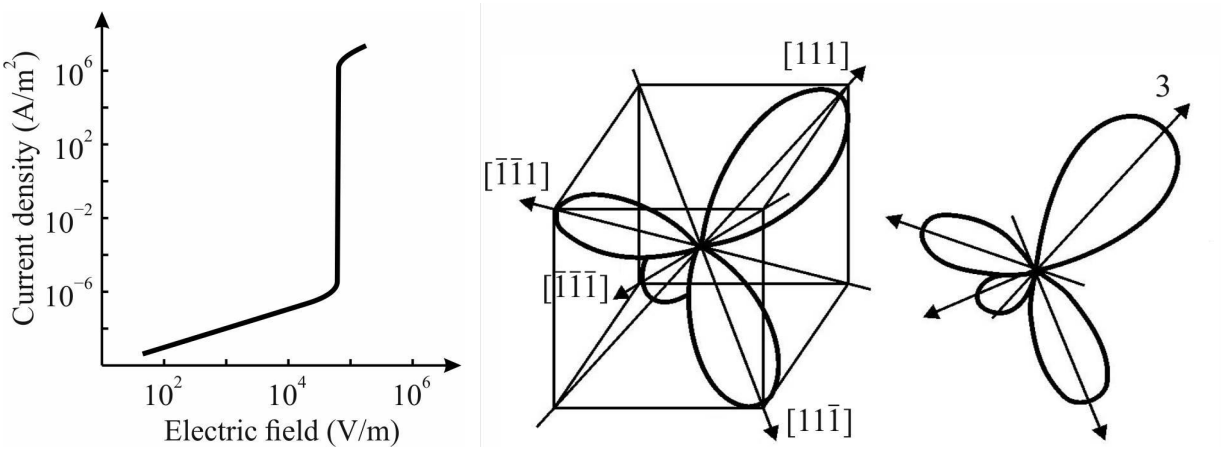

(A) (B) (C)

Fig. 5.11. Zink oxide non-linear property: A – current-voltage characteristic; B, C – polarity changing from polar-neutral sphalerite into polar wurtzite (only positive directions of polar axes are shown)

Both of mentioned materials belong to non-centrosymmetric classes of symmetries with *mutable structure*, which can be changed from the sphalerite (piezoelectric) structure into the wurtzite (pyroelectric) structure.

Varistors are characterized by linear (ohmic) current-voltage dependence, both at reduced level and at increased level of electrical fields: $j \sim E$, Fig. 5.11A. However, it is important that in a low electrical field the varistor has a high electrical resistance: its resistance is close to the dielectric, but in a strong electric field the resistance of varistor decreases millions of times and it becomes a typical semiconductor. In this transformation, the electrical breakdown of the varistor does not occur, since the growth of the electrical current in it is limited. The characteristic *j(E)* is reversible: the increased current passing through the varistor remains stable. Therefore, physical phenomenon of stepped grows of electrical current in the varistor is essentially different from conventional electrical breakdown.

The features of carborundum varistors and zinc oxide varistors are similar, but the jump of resistance in zinc oxide varistors is much bigger. At that, zinc oxide crystal has big electronic energy band gap (~ 3.4 eV). Advantages, associated with large band gap, include the higher breakdown voltages and the ability to stand in increased electrical fields, as well as the possibility of their applications in the higher-temperatures and higher-power conditions.

To explain an enormous nonlinearity of electrical conductivity in ZnO, the following should be noted. Zinc oxide crystallizes in two main structures: cubic sphalerite and hexagonal wurtzite, both belongs to the non-centrosymmetric classes of symmetries. In both cases, polar-sensitive bonds are mixed in the complex 3D structure, which corresponds to structural motives shown in Fig. 5.11B. The modification of the sphalerite (zinc blende) is polar-neutral material (of piezoelectric symmetry), while zinc oxide has 1D-oriented motive of polar wurtzite symmetry (of pyroelectric type). It is important to keep in mind that this material rather easily can *alternate* its structures under the influences of external factors: for example at high pressure (about 10 GPa) any polar properties in zinc oxide disappear, and crystal acquires the electrically neutral rock salt structure. This indicates the *high sensitivity* of ZnO structure to any external impacts what does this material to be important for applications in the electronic devices.

Figure 5.11B demonstrates possible physical mechanism, explaining how the external electrical field, being applied to the zinc oxide in its insulating phase, induces a change in the internal polarity distribution, which in its turn has strong impact on the electrical conductivity. Of eight possible [111]-type directions of inner polarity (Fig.5.11B, left) one directions obviously should be settled close to the direction of applied field, which strengthens the polar-sensitivity in this direction (following axis *3*) at the expense of others axes, Fig. 5.11B, right (where for convenience only positive directions of polar axes are shown).

Thus, the high-resistance phase of ZnO is the dielectric-sphalerite, in which electrical transfer of charge carries occurs in the complex and competing 3D structure: these charge carries are the excitons with large binding energy ~ 60 meV. Sphalerite phase can be electrically transformed into the low-resistance phase, consisting of mainly 1D-oriented polar wurtzite.

As already mentioned above (when posistor effect was discussed in polar higher-conducting phase of doped barium titanate), one-dimensional polar ordering prevents the binding of charge carriers into polaron state; at that, polarity of wurtzite agrees with this case.

On the contrary, very complicated polarity orientations in the sphalerite structure (Fig. 5.11B, left) deepens potential barriers of polaron state and essentially lowers charges mobility. Thus, mechanism of nonlinearity in ZnO might represent electrically induced switching from the sphalerite structure into the wurtzite structure.

Varistors are widely applied to protect electrical circuits from sudden jumps of voltage: when voltage increases, the current flows through varistor, but not others elements of circuit.

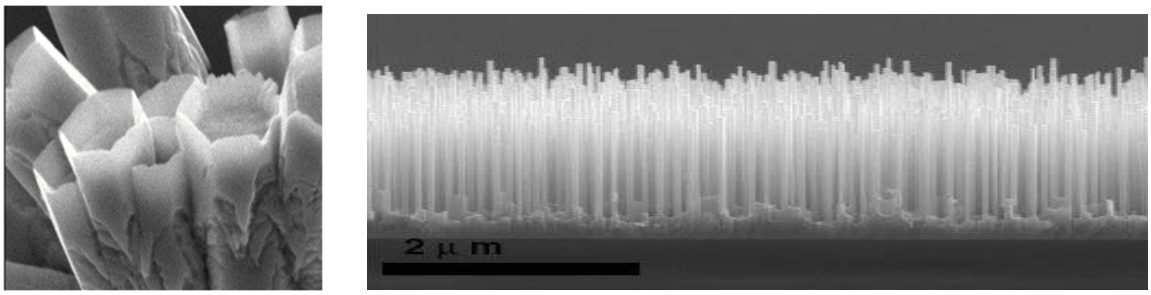

(A) (B)

Fig. 5.12. Zinc oxide nanostructures used in sensors: *A* – hexagonal nanocrystals; *B* – very thin tubular nanocrystals [12]

The finely balanced polar-sensitive structure of zinc oxide, which is always ready for the strong change of its electrical properties under the external influence, is used also in the sensors for various purposes, especially in the nano-structural state, Fig. 5.12. Very thin films of zinc oxide (and, particularly, its nanostructures) are used as components in the solar elements, in the piezoelectric nano-generators, as well as luminescent materials, light-emitting diodes, lasers, etc. Note that superfine ZnO nanocrystals shown in Fig. 5.12B are thousands of times thinner than human hair.

At that, the nanoparticles of zinc dioxide demonstrate structures with quite developed surfaces and very tender forms, Fig. 5.12A, which despite its small size and unusual shape, retains the regularity of its structure inherent in bulk crystal. As already mentioned, the piezoelectric and pyroelectric properties of polar crystals are strongly influenced by boundary conditions. Apparently for this reason, the piezoelectric module in ZnO nanostructures is larger compared to a conventional bulk crystal.

Internal polar bonds in the ZnO nanostructures are very sensitive to temperature, light, humidity, and even to the composition of surrounding gas. As already discussed in connection with the properties of varistors, zinc oxide varies greatly its electrical conductivity with structural changes from the sphalerite to the wurtzite structures. In this case, in the ultrathin nanostructures, the balance of symmetry can be easily broken, as was shown above in Fig. 5.12B, which can serve as a physical model for the functioning of ZnO sensors.

5.3 Electrically induced polar properties

It was already indicated in Chapter 1 that *polar properties* in the non-polar dielectric can be induced by a bias field through the electrostriction, which is deformation of a crystal in the electrical field. When this field is small and relative dielectric permittivity ε is less than 10, effect of electrostriction is very small and can be neglected. However, in the electronics many materials with a large permittivity ($\varepsilon \sim 10^3$–10^4) are applied; in this case the electrostriction (which is proportional to ε^2) becomes large.

1. *Electrostriction* is a quadratic ("even") effect, and it is different from the inverse piezoelectric effect, which is characterized by a linear ("odd") dependence of the deformation on the electrical field. In the case of electrostriction, the sign of the deformation $x(E^2)$ does not depend on the polarity of electrical field, while in most dielectrics, then expansion is observed along the applied field ($x_3 > 0$), while in the transverse direction the compression is observed (x_1, $x_2 < 0$). The value of electrostriction is usually small: it is an order of magnitude smaller than the piezoelectric deformation. Only in very large electrical fields, the deformation of electrostriction can be compared with the piezoelectric deformation: in quartz, in a field of 35 kV/cm these deformations become equal.

In the analytical description of electrostriction, the same boundary conditions are accepted as in the case of the piezoelectric effect. It is advisable to consider only the electrostriction in *mechanically free* dielectrics ($X = 0$). Electrostriction dependence of the strain x on polarization P or electrical field E is described by two equations according to whether the dielectric is electrically clamped or free; in thise cases the following equations can be obtained:

$$x_{ij} = Q_{ijkl}P_kP_l + Q'_{ijklgh}P_kP_lP_gP_h + \dots;$$
$$x_{ij} = R_{ijkl}E_kE_l + R'_{ijklgh}E_kE_lE_gE_h + \dots; \qquad (5.1)$$

In these series, it is usually sufficient to consider only the first terms of the expansion, since the electrostriction is rather small. However, in the ferroelectric relaxors, the electrostriction is gigantic; that is why in the series above, the first three terms of the expansion in the series are considered:

$$x(E) = RE^2 + R'E^4 + R''E^6 \qquad (5.2)$$

It's obvious that coefficients of electrostriction Q_{ijkl} and R_{ijkl} ($i, j, k, l = 1, 2, 3$) are the fours-rank tensors. The electrostriction tensors Q_{ijkl} and R_{ijkl}, in principle, have 81 components, but due to the diagonal symmetry of the deformation tensor, only 36 components remain in them. Others tensors of the fourth rank – elastic constants – are usually represented by components of matrices of c_{mn} and s_{nm} type,

where $m, n = 1, 2, ...6$; they are also symmetrical, therefore, even crystals with the lowest symmetry can have a maximum of 21 independent elastic constants. In contrast, the tensors that describe electrostriction, Q_{ijkl} and R_{ijkl}, in the limiting case of the smallest symmetry, can have all $6 \times 6 = 36$ independent components. But in practice, this difficult case does not occur: the majority of these components are usually zero. With increasing crystal symmetry, the number of nonzero components Q_{ijkl} and R_{ijkl} decreases significantly, but it never happens (as in the case of the piezoelectric module d_{ijl}) when *all* components of the electrostriction tensor go to zero.

Electrostriction for the highest symmetry medium (isotropic medium) is described by only two components of the tensar: Q_{11} and Q_{12} (respectively, R_{11} and R_{12}); which correspond to the longitudinal expansion and lateral compression of the dielectric in an electricфд field. Since in practice the giant electrostriction of relaxor ferroelectrics with a diffuse phase transition is usually used, the above two parameters turn out to be sufficient.

The so-called “fundamental” electrostriction can be considered as tensor Q_{mn}, since its components differ only slightly for different solids and weakly depend on changes in external conditions. Even in ferroelectrics, the components Q_{mn} change little with temperature and frequency and are practically independent of fields. This allows us to consider exactly this tensor as main characteristic of electromechanical interaction of atoms, ions or molecules in a given dielectric.

The components of the tensor R_{mn}, in contrast to Q_{mn}, strongly depend on the dielectric permittivity and, therefore, they depend on the temperature and frequency of the applied electrical field. That is why in the ferroelectrics with a high permittivity ($\varepsilon \sim 10^4$), electrostriction reaches (and may even exceed) the strain that is possible with the piezoelectric effect. Giant electrostriction is important for electronic devices, because it can be used in actuators.

2. *Electrical control* of the piezoelectric effect is of not only scientific, but also technical interest. A change in the piezoelectric properties of a material upon application of an electric field finds application in devices based on surface acoustic waves (SAW), in electrically controlled delay lines as well as in convolvers and electrically tunable piezoelectric filters [6].

The physical mechanisms of electrical control of the piezoelectric effect are different in paraelectrics and piezoelectrics, but in essence they reduce to controlling the speed of sound in a material in which an electric field changes elastic compliance. Typical cases of a change in the speed of sound by bias electrical field in different dielectrics are shown in Fig. 5.13. The piezoelectric crystal of lithium

niobate has a polar-sensitive structure with symmetry of 3*m*. The speed of sound $\Delta v/v_0(E)$ in a $LiNbO_3$ crystal changes in the electric field by only a fraction of a percent, 5.13A, which is enough to control SAW devices. The linear dependence $v(E)$ indicates that the energy of oriented polar-sensitive bonds in a polar $LiNbO_3$ crystal significantly exceeds the external control energy.

Another case is shown in Fig. 5.13B when piezoelectric effect is *induced* by external electrical field in the *non-polar* (centrosymmetric) dielectric. Due to the electrostriction, the bias electrical field transforms the structure of *any* isotropic dielectric into the non-centrosymmetric structure, and induces in it *electromechanical coupling* – i.e., the piezoelectric activity. In Fig. 5.13B induced piezoelectric effect is so great that for its description it is necessary to use formula (5.2).

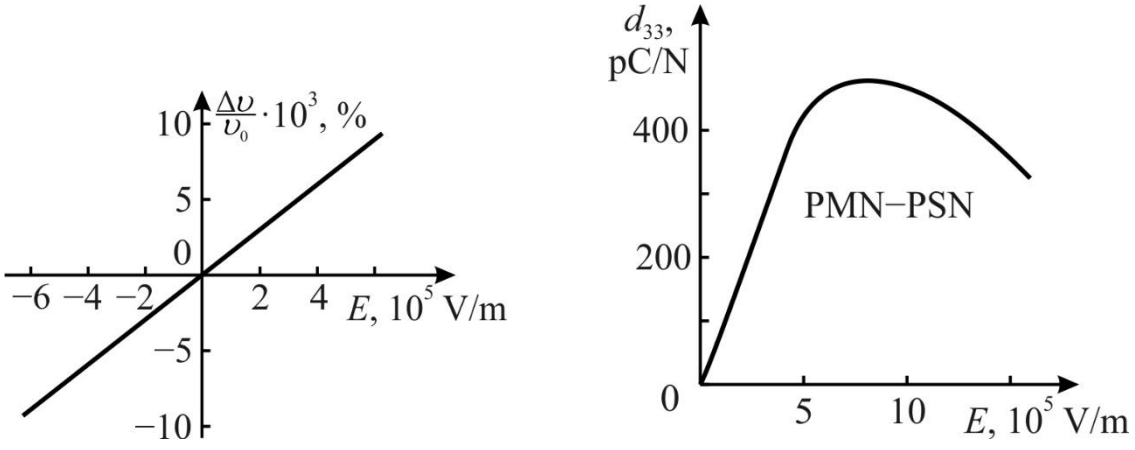

(A) (B)

Fig. 5.13. Electrically tuneable and induced piezoelectric effect: A – lithium niobate crystal used in controlled delay lines; B – diffused phase transition ceramics

In the same time, in dielectrics with low permittivity the induced piezoelectric effect is so small that it is difficult to even find, as the electrostriction negligible. It is appropriate to remember that in Chapter 1 in Fig. 1.9A some *intermediate case* was given: induced piezoelectric effect in the dielectrics with a permeability of about 100. The comparison of characteristics of widely used in electronics ceramics was given: the titanium oxide (TiO_2, rutile with $\varepsilon \sim 100$), the calcium titanate (perovskite, $CaTiO_3$ with $\varepsilon \sim 150$) and the strontium titanate ($SrTiO_3$ with $\varepsilon \sim 300$) were shown. It is this type of ceramics which are interesting for using in the *electrically controlled* piezoelectric resonators and filters: while bias field is applied the element of circuit demonstrates strong piezelectricity, but once this field is turned off, the piezoelectric effect fast disappears. In this case, resonant frequency of the piezoelectric element can be controlled by the applied electric bias field.

The ***piezoelectric modulus*** *for electrically induced piezoelectric effect* can be calculated from the equation of electrostriction (5.1), omitting, for simplicity, the indices of tensor components, as in case of formula (5.2). The deformation is the even function of polarization, which can be described by arapidly convergent serie:

$$x = QP^2 + Q'P^4 + \ldots .$$

In case of rather small alternating electrical field $E_{\square}$, it suffices to restrict to first member of the expansion: $x = QP^{5\cdot}$ Electrostriction $x_{\square}$ in an alternating electrical field is linearized, and can be represented as the piezoelectric effect:

$$x_{\square} = 2QP_yP_{\square} = d{\cdot}E_{\square},$$

where parameter d acts as the piezoelectric modulus, caused by the electrostriction Q:

$$d \ \square \ 2Q\varepsilon_0^2\varepsilon^{5\cdot}E, \qquad (5.3)$$

where $E = E_{\text{bias}}$ is the electrical field which induces the piezoelectric effect.

3. *Relaxor ferroelectrics peculiarities.* Piezoelectric module induced in a crystal by electrical field is proportional to the field strength and the *square* of permittivity. Therefore, the field-induced "piezoelectric effect" is the higher, the higher the dielectric permittivity. As stated earlier in Chapter 1, in the dielectrics with increased dielectric constant (ε = 100–300) the induced piezoelectric module is approximately 0.3 pC/N; however, in a specially developed electrostrictive ceramics $PbMg_{1/3}Nb_{2/3}O_3 – PbSc_{1/2}Nb_{1/2}O_3$ (PSN–PMN) where ε = 30.000, the piezoelectric module in electrical field (E_{bias} = 10^6 V/m, Fig. 5.13B), is close in magnitude to the piezoelectric materials commonly used in the technique (in PZT d_{31} □ 500 pC/N). In this case, the induced piezoelectric effect in crystals of ferroelectric relaxors is even greater.

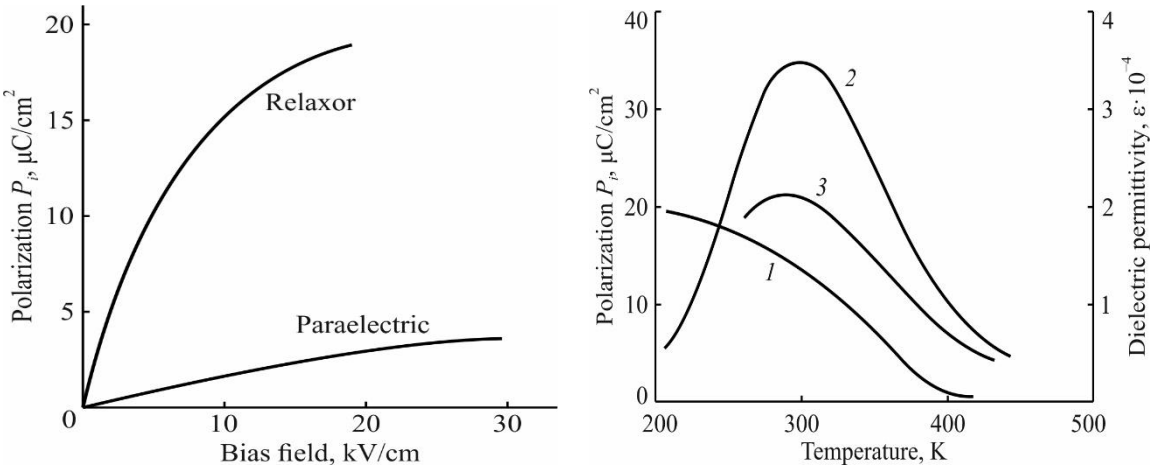

(A) (B)

Fig. 5.14. Relaxor ferroelectric characteristics: A – comparison of electrically induced polarization P_i in PMN with paraelectric BST; B – PMN properties: *1* – induced by 10 kV/cm polarization P_i; 2 – permittivity at E_{bbias} = 0; 3 – permittivity at E_{bias} = 10 kV/cm

The comparison of induced polarization in relaxor ferroelectric PMN with similar polarization of paraelectric material $Ba(Ti_{0.6},Sr_{0.4})O_3$ = BST (that also has rather big ε ~ 10.000) is shown in Fig. 5.14 (data are obtained by pyrolectric coefficient measurement). The electrically induced polarization P_{imd} in the PMN far exceeds this polarization in the BST: the reason is that relaxor ferroelectrics have much greater permittivity (~20.000-40.000). Moreover, in the relaxor ferroelectric polarization P_{imd} depends on temperature as well as in the conventional ferroelectrics, Fig. 5.14B.

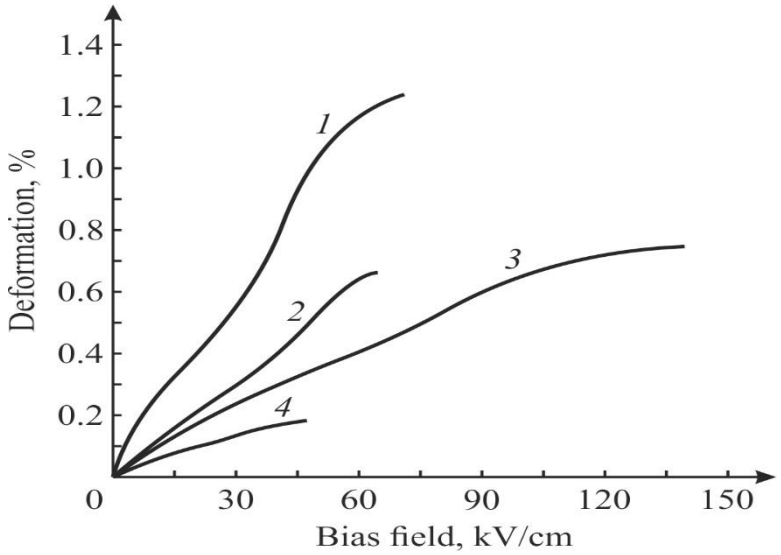

Fig. 5.15. Electromechanical effect in relaxors: *1* – crystal PZN-4.5% PT; *2* – crystal PZN; *3* – crystal PMN-24% PT; *4* – piezoceramics PZT-8

For technical purposes, it is important that in a field of electrical bias, the relaxor demonstrates not only the piezoelectric, but also the electrically induced *pyroelectric* effect; the value of which may exceed the pyroelectric coefficient of conventional pyroelectric. At the same time, compared with the induced pyroelectric effect used in the BST type paraelectrics, the induced pyroelectric effect in PMN is more thermostable due to the smaller oblique dependence P_{imd} (T).

It was shown that theoretical calculation for electrically induced piezoelectric effect gives for artificial piezoelectric module $d = 2Q\sum_0^2\sum^2\oplus$. It is obvious that electrically induced piezoelectricity is substantial only in dielectrics with a very high permittivity. However, in the paraelectric materials induced piezoelectricity appears and disappears practically *without inertia*. But in the relaxor ferroelectrics response time is about several microseconds. Nevertheless, in some of PMN-PSN relaxor ferroelectric with ∑ ε 40.000 piezoelectric modulus riches d = 2000 pC/N (more then as in best piezoelectric ceramics of PZT type). For example, high strain in the electrical field shows crystals $PbZn_{1/3}Nb_{2/3}O_3$–4,5%$PbTiO_3$ (PZN–4,5%PT). Its

electrically tuneable deformation in 10 times more than deformation in widely used piezoelectric ceramics PZT-8 and, unlike piezoelectric, allows large controllability without hysteresis.

Thus, both paraelectrics and relaxor ferroelectrics under bias electrical field produce *induced piezoelectric effect*, which immediately disappears after switching off this field. The speed of such control of the piezoelectric effect depends on the inertia of polarization, and its magnitude is limited by the dispersion of permittivity, which appears at frequencies of about hundreds of kilohertz. From the point of view of physics, the electrically induced piezoelectric effect is interesting because it allows explain the microscopic nature of electromechanical coupling in solids (physical models and thermodynamic theory of this will be discussed further in Chapter 4). From the point of view of technical applications, this effect is important for electromechanical drives and electrically tunable piezoelectric resonators and filters, allowing control of the resonant frequency and bandwidth.

5.4 Thermomechanically induced pyroelectricity

It is important to note the fact that pyroelectric effect corresponds to the *quasi-one-dimensional model* of polar-sensitive bonds orientation. This means that such effect is possible in 10 classes of *pyroelectric symmetry* crystals; and one would assume that pyroelectric effect (and volumetric piezoelectric effect as well) is impossible for two-dimensional and three-dimensional models of polar bonds arrangement. The main thing that will be shown in this section is that by the creating for polar-neutral crystal the *special boundary conditions* the "artificial pyroelectric effect" can be obtained in non-centrosymmetric crystals in all remaining 10 polar-neutral classes of crystals.

1. ***First two-dimensional*** structural arrangement of the polar-sensitive bonds will be considered (correspondent simplest model was shown in Fig. 5.11B and 5.13). In the actual ("exclusive") piezoelectric, the primary pyroelectric effect is always absent ($\gamma_i^{(1)} = 0$) and in mechanically clamped condition the secondary pyroelectric effect also looks to be impossible ($\gamma_i^{(2)} = e_{im}\alpha_m = 0$). However, in the *partial clamping conditions* any piezoelectric is liable to show "secondary type" pyroelectric effect, because the sum $e_{im}\alpha_m \neq 0$. Just this is the "*artificial* pyroelectric effect" [13].

From 10 classes of "exclusive" piezoelectrics, exactly the quartz is simplest example for explanation of internal polarity nature. Trigonal α-quartz, which belongs to 32 class of symmetry, is electrically active only in the [100]-type

directions that corresponds to (100)-plate of quartz, which is known as a “Curie cut”. This cut should be prepared perpendicularly to any one of three two-fold polar axes: *1*, *1′* or *1″* (distribution of polar activity in quartz crystal was presented in Fig. 5.13A).

Further it will be shown how it is possible to measure the components of the polar-sensitivity in the polar-neutral crystal.

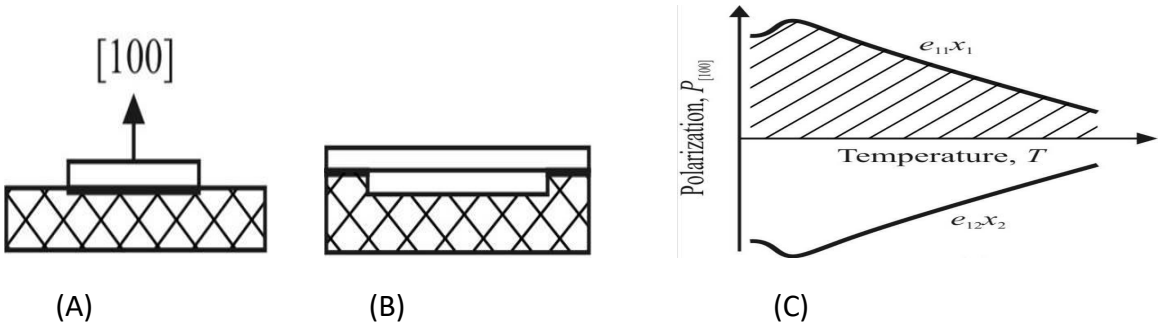

Fig. 5.16. Partially clamped quartz samples: A – tangential strain in thin plate is forbidden by plate soldering to substrate; B – membrane variant of partial clamping; C – thermally induced polar response conditioned by piezoelectric effect

In the standard crystallographic setup of quartz crystal the matrix of piezoelectric coefficients e_{im} consists of one longitudinal (e_{11}), one transverse (e_{12}) and three share components of piezoelectric strain modulus (e_{14}, e_{25} and e_{26}):

$$e_{im} = \begin{bmatrix} e_{11} & e_{12} & 0 & e_{14} & 0 & 0 \\ 0 & 0 & 0 & 0 & e_{25} & e_{26} \\ 0 & 0 & 0 & 0 & 0 & 0 \end{bmatrix}.$$

Transverse component e_{12} equals to longitudinal one but has opposite sign: $e_{12} = -e_{11}$. Besides, only one of share piezoelectric modules (e_{14}) is independent, others share components are $e_{25} = -e_{14}$ and $e_{26} = 2e_{11}$. So the only two components of given matrix (2) are independent.

Before proceeding further, it is necessary to show that *any* homogeneous influence (uniform change of temperature or hydrostatic pressing) can not induce the electrical response in a specimen of quartz even being taken from the Curie cut.

First of all, any share strain cannot be excited in a sample, if external influence has the scalar type. So only the longitudinal and the transverse electrical response should to be taken into account. In the non-clamped quartz sample (i.e., in free-stress state) the longitudinal piezoelectric effect ($e_{11}x_1$) and the transverse effect ($-e_{12}\,x_1$) *compensates* each other. It is illustrated in the Fig. 5.16C, which characterises uniform thermal influence on quartz sample: one part of piezoelectric response

($e_{11}x_1$) induced by thermal deformation x_1 equals to another part ($e_{12}x_1$) but with opposite sign.

Since a rather complex phenomenon is discussed here, it makes sense to give the additional proof that any electrical response in actual piezoelectric really is compensated in the case of scalar influence, as shown in Fig. 5.16C. First of all note that from the matrix for piezoelectric strain modulus e_{im} it follows that polarization component $P_3 = 0$ (in $Z = 3$ direction quartz shows no piezoelectric effect) as well as for component $P_2 = 0$, because shear strains e_{23} and e_{26} can not be excited by the uniform action. It remains to analyze the polarization component P_1.

Induced mechanically (by direct piezoelectric effect) this component of electrical polarization can be given by

$$P_1 = e_{1m}x_m = e_{11}x_1 + e_{12}x_2 + e_{13}x_3 + e_{14}x_4 + e_{15}x_5 + e_{16}x_6 = e_{11}x_1 + e_{12}x_5.$$

This sum depends on mechanical boundary conditions, in which crystal is located:

(*i*) In case when crystal is totally clamped, any mechanically induced polarization is impossible: $P_1 = 0$ due to $x_m = 0$.

(*ii*) It is essential to show that in case of free-stress condition (when quartz crystal can be deformed) any polar response is also absent ($P_1 = 0$).

Firstly, many components of the piezoelectric strain module of quartz crystal are zero: it is seen from the above matrix that $e_{13} = e_{15} = e_{16} = 0$. Secondly, in the above equation the share strain $x_4 = 0$ because any share strain should be absent in the case when external action is uniform.

Thirdly, in free-stress quartz crystal the strains x_1 and x_2 in the (100)-plane are equal: $x_1 = x_5$. In fact, that in case of uniform thermal action ($x_m = \alpha_m dT$) these strains are equal due to the parity of correspondent components of quartz thermal expansion coefficients: $\alpha_1 = \alpha_2$ (however, $\alpha_1 \neq \alpha_3$).

In fourth, in the event of uniform stretching (or compression), again, the strains $x_1 = x_2$ due to the equality of correspondent quartz elastic stiffness components: $c_{11} = c_{25}$. Strains could be calculated from the equation $x_m = c_{mn}X_n$, where X_n is the uniform (hydrodynamic) stress. Thus, excitation in the actual piezoelectric the homogeneous deformation (by thermal or elastic way) does not lead to its polar response, since the piezoelectric contributions from strains $e_{11}x_1$ and $e_{12}x_2$ into the polarization P_1 compensate each other, Fig. 5.16C.

(*iii*) However, in the *partially clamped* quartz crystal the thermally induced polarization will not be zero ($P_1 \neq 0$), and just this circumstance is used here to examine internal compensated (latent) polarity that, in principle, makes possible the use partially clamped quartz (and others polar-neutral piezoelectrics) in the thermal or pressure sensors.

The fundamental idea is that artificial limitation (by mechanical boundary conditions) of any one of strain (x_1 or x_2) should transform the plate of piezoelectric quartz into the artificially created "pyroelectric" crystal [14].

Suppose that one of two types of deformations can not be realized in the piezoelectric plate. For example, it is possible to suppress the tangential strains ($x_2 = 0$ and $x_3 = 0$), if piezoelectric plate is firmly fixed on the massive incompressible substrate with zero coefficient of thermal expansion (in given case as substrate the fused silica in which $\alpha \approx 0$, Fig. 5.16A). In this case the uniform heating or cooling (as well as hydrostatic compression) will lead to the polar response appearance: $P_{[100]} = e_{11}x_1$. Similarly, the prohibition on the normal strain ($x_1 = 0$) with a possibility of tangential strain would cause the response of opposite polarity: $P_{[100]} = e_{12}x_2$, but experimental realization of second case is more difficult.

In practice, it is easier to limit the plane strain x_2, if piezoelectric plate soldered onto a fused silica. The only deformation that can be realized in this case is the thickness strain x1 directed along polar-neutral axis "1", which by this way is turned into the single polar axis. Therefore, substantial reducing of one type of deformations transforms piezoelectric crystal into artificial pyroelectric. This effect can be defined also as the polarization of partially clamped actual piezoelectric by the uniform change of its temperature. Partial clamping is provided by the non-uniform mechanical boundary condition, limiting some of thermal strains of a crystal, which becomes uniformly but anisotropic stressed.

Artificial thermo-piezoelectric effect can be characterized by the coefficient γ^* which is equivalent to the pyroelectric coefficient, which depends on electrical, elastic and thermal properties of the non-central crystal, as well as on the way of its deformation limitation:

$$\gamma^* = d_{im}\lambda^*_m, \qquad (5.4)$$

where d_{im} is piezoelectric modulus and λ^*_m is effective thermo-elastic coefficient of partially clamped crystal.

The spatial distribution of the sensitivity of artificial pyroelectric effect in the crystals of quartz type symmetry (such as berlinite ($AlPO_4$), cinnabar (HgS), tellurium (Te), etc.) can be found similarly to quartz crystal. It is possible to find "pyroelectric coefficients" in these crystals, even in any slanting plates. The spatial distribution of $\gamma^*(\theta,\phi)$ that characterizes artificial pyroelectric coefficient in the quartz type crystals can be presented in polar coordinates: $\gamma^*(\theta,\phi) = \gamma^*_{max}\sin^3\theta \cdot \cos 3\phi$, where θ is azimuth angle and ϕ is plane angle. This spatial pattern is equivalent to longitudinal piezoelectric modulus distribution that was shown in Fig. 1.13A. Through the radius vector directed from the center of this figure it is

possible to determine the size of the artificial effect in any cut of quartz-type crystals. It is obvious that maxims of the effect occur along any of three *X*-axes.

In order to get effective pyroelectric coefficient $\gamma^* = dP_i/dT$, the thermodynamic equations for the non-centrosymmetric (but not pyroelectric) crystal should be used. With assumption that crystal is short-circuited ($E = 0$), the exact solution is given below:

$$\begin{aligned} \mathrm{d}x_n &= s_{nm}\,\mathrm{d}X_m + \alpha_m\,\mathrm{d}T; \\ \mathrm{d}P_i &= d_{im}\,\mathrm{d}X_m, \end{aligned} \qquad (5.5)$$

where s_{nm} is components of elastic compliance tensor. Solving equations (5.5) for trigonal crystal class (which include quartz crystal) leads to following expression:

$$\gamma^*_{100} = d_{11}(\alpha_1 s_{33} - \alpha_3 s_{13})\,[s_{11}\square s_{33} - (s_{13})^2]^{-1}. \qquad (5.6)$$

For quartz crystal one can obtain $\gamma^*_{100} = 5.6$ μC/m^{2}K, in others crystals of 32 symmetry class this parameter is bigger: $\gamma^*_{100} = 5.7$ μC/m^{2}K in berlinite, 8.7 μC/m^{2}K in cinnabar, and 10 μC/m^{2}K for tellurium crystal. This parameter is not very small, because the first known pyroelectric tourmaline has pyroelectric coefficient $\gamma = 4$ μC/m^{2}K, while in wurtzite crystal (ZnS) usual pyroelectric response is characterized by $\gamma = 0.3$ μC/m^{2}K.

In quartz, as in other piezoelectrics the thermomechanically induced pyroelectric effect was studied by a quasistatic method, in which the pyroelectric coefficient is determined by the time during which the pyroelectric current charges the measuring capacitor [12]. Electronic equipment includes the Peltier element used for heating and cooling. Samples, having a plate shape about 100 microns thick and the area of ~ 1 cm^2 with copper electrodes, soldered onto silica glass substrates were investigated.

Temperature dependence of artificial pyroelectric response of partially clamped in the (100)-cut of quartz crystal is shown in Fig. 5.17 along with the rest of the key parameters. Investigation shows that artificial pyroelectric coefficient γ^*_{100} changes with temperature very slowly while the alteration of some others components of tensors might be very complicated. In a wide temperature range artificial "pyroelectric" coefficient $\gamma^*_1$is almost constant, but it is seen a tendency to it decrease at low temperatures, perhaps due to reduction of thermal expansion coefficient. In vicinity of quartz $\alpha \rightarrow \beta$ phase transition at temperature $\theta_1 \approx 850$ K the γ_1^* breaks off. It is remarkable that for thermally induced polarity $P_{[100]} = \Delta P_1 = \int \gamma^*_1 dT$ the simplest linear temperature dependence is observed: $\Delta P_1 \sim (\theta - T)$ with a critical index $n = 1$.

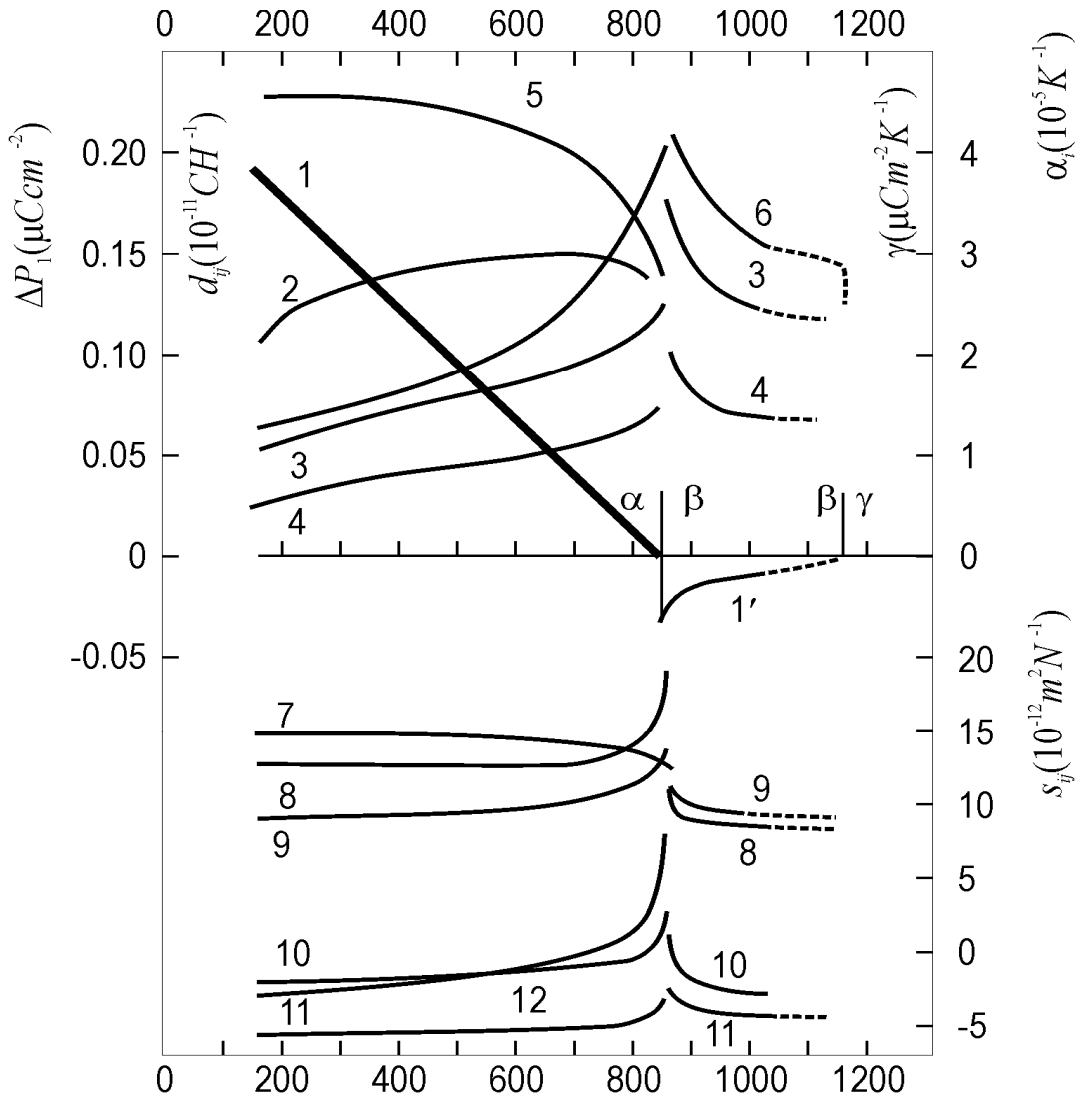

Fig. 5.17. Latent (hidden) intrinsic polarity temperature dependence for quartz (curve 1) in comparison with dependences of other thermal and elastic parameters of this crystal:

1 – ΔP_1 found in [100]-cut thin plate of quartz in α-phase;

1`– ΔP_1 found in [110] oriented rod in high-temperature β-phase of quartz;

2 – artificial pyroelectric coefficient γ_1*of partially clamped [100]-cut of quartz in α-phase;

3, 4 – thermal expansion coefficients α_1 (3) и α_3 (4) of quartz crystal;

5, 6 – piezoelectric modulus d_{11} (5) и d_{14} (6) of quartz α-phase;

7–12 – elastic compliance components: 0,5□s_{66} (7), s_{11} (8), s_{33} (9), s_{12} (10), s_{13} (11), s_{44} (12)

It should be noted that piezoelectrics of quartz symmetry (SiO_2 and $AlPO_4$), in addition to $\alpha \rightarrow \beta$ phase transition have the second high-temperature transformation between their β and γ phases. Temperature dependence of artificial pyroelectric response (Fig. 4.5, curve *1′*) characterises quartz in its β-phase with temperature dependence of 3D moment M_{ijk}. It is described by another equation; $P_{13} \sim (\theta_2 - T)^2$ with $\theta_2 = 1140$ K. As seen from Fig. 4.5 (curve *1′*), this electrical moment vanishes at the $\beta \rightarrow \gamma$ phase transition. In the quartz crystal high-temperature γ-phase is non-polar. Again, it is necessary to note that the study of volumetric piezoelectric

effect needs the non-compressible substrate, so only theoretical estimation on this effect can be provided [15].

2. Second consider here is ***three-dimensional*** structural arrangement of polar-sensitive bonds in the polar-neutral piezoelectric. As the first example, well studied ferroelectric KH_2PO_4 (KDP) will be described, but in its *paraelectric phase* (above the Curie point). At room temperature and above it KDP is only a piezoelectric, which belongs to the polar-neutral 422 class of symmetry. In addition to several crystals of KDP type, the antiferroelectrics of ADP (NH_3PO_4) type have analogous piezoelectric properties. Their polar-sensitivity corresponds to the 3D arrangement.

In the standard installation, the piezoelectric module matrix of these crystals shows no longitudinal and no transverse effects:

$$d_{mi} = \begin{pmatrix} 0 & 0 & 0 & d_{14} & 0 & 0 \\ 0 & 0 & 0 & 0 & d_{25} & 0 \\ 0 & 0 & 0 & 0 & 0 & 0 \end{pmatrix}; \; d_{25} = d_{14}\,.$$

To find the artificial pyroelectric effect, one needs to *change* the standard setup of a crystal, for example, by turning axes *1* and *2* around the axis *3* at angle of $\pi/4$. In these crystals one needs to select piezoelectric element not in a form of thin plate, but as the long rectangular rod, extending along one of new axes of *1′* or *2′*, while electrodes should be deposited on the surface of piezoelectric element perpendicularly to axis *3′* = *4*.

By limiting of longitudinal deformation of KDP sample, made in the form of rectangular rod, it is possible to obtain artificial the pyroelectric effect with coefficient

$$\gamma^*_3 = 2\, d_{36}\alpha_1(2s_{11} + 2s_{12} + s_{66})^{-1}. \qquad (5.7)$$

Figure 5.18 shows main properties of KDP crystal *above* its ferroelectric phase transition, where this crystal is only a piezoelectric. Investigations show that in this paraelectric phase the KDP crystal can be transformed into the artificial pyroelectric with coefficient $\gamma^*_3 = 6$ μC/m^{2}K, while in ADP crystal $\gamma^*_3 = 17$ μC/m^{2}K. Moreover, it is found that crystals of KDP type in their paraelectric phase also have (as quartz) the high-temperature phase transition, at which this polar-neutral crystal changes its symmetry from the 422 class into non-polar class of symmetry. This is confirmed by the measurements KDP dielectric constant ε_1 which at temperature increase jumps down at temperature of $\theta \approx 480$ K, while internal polarity vanishes very gradually by low $P \sim (\theta - T)^2$ with the same θ. To verify the quadraticity of this dependence, the curve *1* in Fig. 5.18 is shown in scale $P^{1/2}(T)$, which really turned out to be linear [15].

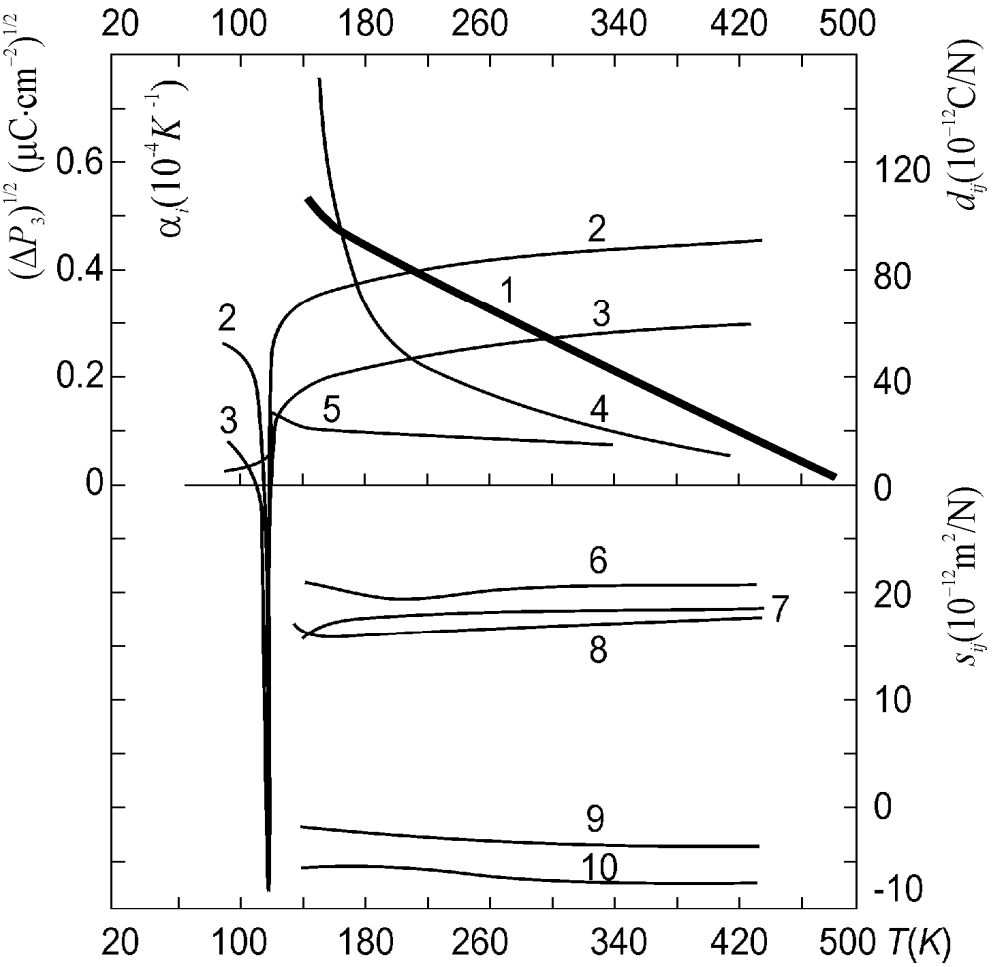

Fig. 5.18. Latent intrinsic polarity temperature dependence of KDP crystal in comparison with other thermal and elastic parameters of this crystal:

1 – ΔP_3 obtained by study KDP rod oriented in [110] direction;

2, 3 – thermal expansion coefficients α_3 (2) and α_1 (3) of KDP crystal;

4, 5 – piezoelectric modulus d_{36} (4) and d_{14} (5) of KDP crystal;

6-12 – elastic compliance: $0.5 s_{66}$ (7), s_{11} (8), s_{33} (9), s_{12} (10), s_{13} (11), s_{44} (12)

Spatial (3D) polar-sensitive bonds conception can be applied for many others polar-neutral piezoelectrics. For instance, in the crystals of 23 cubic class of symmetry the polar-neutral directions correspond to four axes of order 3, and it can be shown that artificial "pyroelectric coefficient" is given by the equation:

$$\gamma^*_{[111]} = 2\sqrt{3}\, d_{14}\alpha\, (4s_{11} + 8s_{12} + s_{44})^{-1}. \qquad (5.8)$$

It is interesting to notice that parameter γ^*_{111} is rather big in the sillenite type crystals. Some of them, such $Bi_{12}GeO_{20}$ and $Bi_{12}SiO_{20}$, are widely used in electronics. Artificial pyroelectric coefficient in $Bi_{12}GeO_{20}$ is estimated as $\gamma^* \approx 25$ μC/m^{5}·K, however, among these classes of piezoelectric crystals it is possible to find crystals with artificial "pyroelectric" coefficient up to 100 μC/m^{5}·K.

Among possible practical applications of artificial pyroelectricity the most promising are the semi-insulated (*s/i*) semiconductors of GaAs group ($A^{III}B^{V}$). The

point is that they might be used as pyroelectric converters in the upper layer of sandwich composition, which can be integrated with amplifiers (in bottom layer) using semiconductor with high-mobility electrons.

These crystals have sphalerite structure that belongs to polar-neutral $\bar{4}3m$ group of symmetry. In the specially oriented plates and by using a restriction of some thermal deformations, the $A^{III}B^{V}$ crystal is capable to produce pyroelectric signal. At that, the voltage sensitivity of *s/i*-GaAs, for instance, is close to pyroelectric ceramics: GaAs plate with thickness of 100 microns at temperature change several degrees shows electrical potential 2 B. This can be of interest for implementation in the multi-element planar integral thermal far IR detectors. It is assumed that in a special way oriented semi-insulating layers or micro-regions embedded in gallium arsenide integrated circuit together with amplifiers and switching devices may form a mosaic microstructure of non-selective and highly sensitive infrared detectors.

Polar-sensitive bonds in piezoelectric-active $A^{III}B^{V}$ type semiconductors of sphalerite structure are directed along each of threefold axes of cubic crystal. However, polar-sensitivity in a crystal is completely compensated; therefore, any scalar influence to it, including uniform temperature change, can not produce electrical response. Nevertheless, this compensation of electrical polarity can be broken in the specially oriented plates (layers), in which thermal deformations are limited. As a result, along one of three-fold polar axis the electrical response appears, just that is the artificial pyroelectric effect.

High-symmetry cubic crystals of class $\bar{4}3m$ is characterized by the isotropy of thermal expansion coefficient: $\alpha_m = \alpha$ (in GaAs $\alpha = 5.8 \cdot 10^{-6}$ K^{-1} at 300 K). In these crystals elastic compliance $s_{mn}^{E,T}$ tensor is reduced to three independent components (in GaAs $s_{11}^{E,T} = 12 \cdot 10^{-11}$, $s_{12}^{E,T} = -4.6 \cdot 10^{-11}$ and $s_{33}^{E,T} = 17 \cdot 10^{-11}$ m^2/N). In the main installation of $A^{III}B^{V}$ crystal piezoelectric properties are described by matrix:

$$d_{im} = \begin{bmatrix} 0 & 0 & 0 & d_{14} & 0 & 0 \\ 0 & 0 & 0 & 0 & d_{25} & 0 \\ 0 & 0 & 0 & 0 & 0 & d_{36} \end{bmatrix}, \qquad (5.9)$$

This matrix represents the third rank tensor of piezoelectric coefficients. In this installation for (100), (010) and (001) crystal plates all longitudinal (d_{11}, d_{22}, d_{33}) as well as all transverse (d_{12},, d_{13}, d_{21}, d_{23}, d_{31}, d_{23}) modules are zero. Therefore, usually used in electronics and in most of experiments [100]-oriented plates of $A^{III}B^{V}$ semiconductors are *non-sensitive* to any homogeneous mechanical influence, except the shear action (which correspond to share modules $d_{14} = d_{25} = d_{36}$). It is obvious

from the matrix (5.9) that no response is possible, if the external influence on crystal has scalar character. In other words, being applied to standard (100)-plates of $A^{III}B^{V}$ crystals any partial clamping cannot invoke its polar response. Meanwhile, the crystal plates of (100) orientation are conceptually the sole chips using for GaAs type devices. It is not improbable that this is the main reason for mentioned polar effects previously were out of consideration.

Due to the cubic symmetry in standard installation of crystal the piezoelectric module components are equal: $d_{14} = d_{25} = d_{36}$ and, therefore, they might be denoted simply as d. In gallium arsenide $d = 5.7 \cdot 10^{-12}$ C/N, i.e. it surpasses even quartz piezoelectric module ($d_{SiO2} = 5.4 \cdot 10^{-12}$ C/N). From equation (6) one cannot see any opportunity of artificial pyroelectric effect in the GaAs, since the matrix contains only shear piezoelectric components that can not be excited by homogeneous heat exposure. As shown before, artificial pyroelectric effect, generally, occurs due to the de-compensation of the contributions from longitudinal and transverse piezoelectric effects, described by left half of matrix (6.6). But in this case (in *standard installation* of $A^{III}B^{V}$ crystal) all components of longitudinal and transverse piezoelectric module are zero.

But in another orientation of crystallographic axes to which standard matrix (5.9) can be converted, both longitudinal and transverse components of piezoelectric module appear. These components are maximal in the slice of a crystal, oriented perpendicularly to the axis of the third order (which is spatial diagonal of cube), since greatest polar-sensitivity in $A^{III}B^{V}$ crystal coincides with these directions. This polarity is due mixed ionic-covalent bonding between A·B ions, and anisotropy of electronic density distribution is such that this density is increased in the vicinity of B-ion. When describing effect of partial limitation of deformations on piezoelectric properties of polar crystal, it is more convenient to use not the piezoelectric modulus d, (describing relationship between mechanical stress X and induced by it polarization $P_i = d_{in}X_n$) but the piezoelectric constant e, which relates deformation x to polarity: $P_i = e_{in}x_n$, where $e_m = d_{in}c_{mn}$ and c_{mn} is elastic stiffness. The matrix of piezoelectric constantfor the main crystal setting corresponds to the piezoelectric modulus (5.9)

$$e_{im} = \begin{matrix} 0 & 0 & 0 & e_{14} & 0 & 0 \\ 0 & 0 & 0 & 0 & e_{15} & 0 \\ 0 & 0 & 0 & 0 & 0 & e_{36} \end{matrix}$$

This matrix represents the third rank tensor of piezoelectric coefficients. In this instance, for (100) = (010) = (001) crystal plates as longitudinal (e_{11}, e_{22}, e_{33}) so transverse (e_{12}, e_{13}, e_{21}, e_{23}, e_{31}, e_{23}) modules are zero. That is why (100) type of

GaAs plate is not sensitive to any mechanical strains except the twist ones. The lasts corresponds to the share modules $e_{14} = e_{25} = e_{36}$ but they could not provide any response under *homogeneous* influences. Partial clamping is also useless if it is applied to the standard (100) plates of III-V crystals.

Figure 5.19A and B shows such orientation of the $A^{III}B^{V}$ crystal, which should be prepared to invoke its polar response. Polar cut of $A^{III}B^{V}$ crystal should be oriented by such a way, at which [111]-axis is perpendicular to studied plane. In case of volumetric piezoelectric effect investigation this (111)-plate has to be fixed onto the "ideally hard" substrate (in trial experiments the hard steel might be used, but in microelectronic piezoelectric sensors it is expedient to use the membrane, clamped along its boundaries). In similar fashion, the *s/i*-GaAs (or GaN) crystalline (111)-plate could be activated for "pyroelectric" response, if a rigid substrate, shown in Fig. 5.19B, would have very small thermal expansion coefficient ($\alpha \sim 0$). In our first experiments the fused silica was used as a substrate, but in microelectronic practical devices the pyro-active *s/i* (dielectric) layer of Ga(AsP) or (GaAl)As layer can be directly deposited on the substrate made of GaAs crystal, followed by the etching and forming membrane clamped along the boundaries.

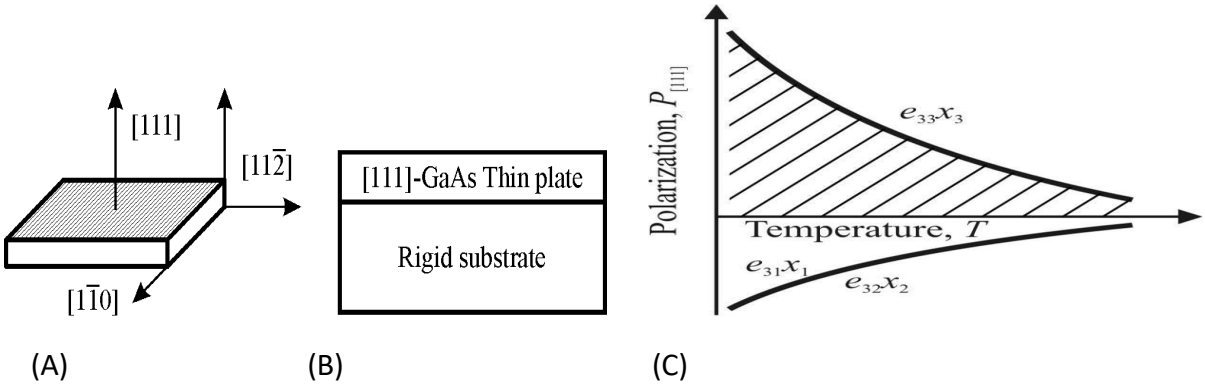

Fig. 5. 19. Partial (in plane) clamping realization: A – orientation of *s/i*-GaAs [111]-cut; B – plate soldered to rigid substrate, C – internal polarity change decompensated by partial clamping

Such partial clamping makes impossible the plane strains ($x_1 = x_2 = 0$), so electrical response from uniform pressure (or thermal deformation) can be realized only perpendicularly to the plane: $M_3 = e_{33}x_4$. It is obvious that created artificially composite structure (Fig. 5.19A) can be used for volumetric piezoelectric effect investigation (or to study the artificial pyroelectric response).

In the any form of free-stress sample the longitudinal piezoelectric effect (e_{33}) and *two* transverse effects (e_{31} and e_{32}) compensate each other: $e_{31} + e_{32} = \square\, e_{34}$. It is illustrated in Fig. 5.19C, which describes thermal investigation of GaAs (111)-plate: one part of piezoelectric polarization ($e_{33}x_3$, induced by thermal deformation x_3) equals to other parts ($e_{31}x_1 + e_{32}x_2$) but with opposite sign (in this case, index "3"

corresponds to the [111]-axis). Strain components in free-stress cubic crystal are equal: $x_1 = x_2 = x_3$, because excitation is homogeneous. That is why, in non-pyroelectric crystal the sum of piezoelectric coefficients of transverse and longitudinal piezoelectric coefficients is zero:

$$e_{31} + e_{32} + e_{33} = 0 \qquad (e_{31} = e_{32} = -\tfrac{1}{2}\, e_{33}).$$

As a result, piezoelectric effect, produced by longitudinal strain component $x_3 = \alpha \mathrm{d}T$ is compensated by effect of two transverse strain components $x_1 = x_2 = \alpha \mathrm{d}T$; therefore no electrical response is possible. Consequently, free-stress polar (111)-plate of GaAs type crystals is not sensible to the homogeneous excitations.

However, the artificial limitation of any one of mentioned strain components (x_3 or $x_1 + x_2$) can transform piezoelectric (111)-plate of GaAs type crystal into artificially created "pyroelectric". In practice, it is easier to limit the plane strain ($x_1 + x_2$) by a simple mechanical design. In this case, the only thickness strain x_3 can be excited, and just in the direction of polar axis "3" ([111]-direction) which is transformed into a "peculiar" polar axis. This effect is impossible as in the free-stress so in the free-strain crystals: both artificial effects are the result of non-isotropic partial clamping. Only partially clamped piezoelectric crystal manifests artificial pyroelectricity or volumetric piezoelectric effect.

Shown in Fig. 5.19 partial clamping violates polar neutrality ($e_{31}x_1 + e_{32}x_2 = 0$) and makes it possible to manifest artificial pyroelectric effect as $M_i = e_{33}x_4$. Greatest effect in crystals of $\bar{4}3m$ class of symmetry can be achieved in such a special installation, in which one of new axis *3′* coincides with polar-neutral axes of [111]. With this new installation, the axis *1′* should be directed normally to axis passing through the *3′* plane of symmetry of a cube, while orientation of new axis *2′* is predetermined by Descartes coordinate system.

For further calculations, it is expedient to return to the matrix of piezoelectric module. After above procedure application, the matrix of piezoelectric module for $\bar{4}3m$ crystal in new installation is:

$$d_{i'm'} = \begin{bmatrix} 0 & 0 & 0 & 0 & -\frac{d}{\sqrt{3}} & \frac{2d}{\sqrt{6}} \\ \frac{d}{\sqrt{6}} & -\frac{d}{\sqrt{6}} & 0 & -\frac{d}{\sqrt{3}} & 0 & 0 \\ -\frac{d}{2\sqrt{3}} & -\frac{d}{2\sqrt{3}} & \frac{d}{\sqrt{3}} & 0 & 0 & 0 \end{bmatrix}. \qquad (5.10)$$

All components of this new matrix are expressed in the terms of shear module *d*, taken from the basic installation of the crystal (6.6). The third row of the matrix (5.10) characterizes piezoelectric properties of such crystal plate, which is cut

perpendicularly to axis $3' = [111]$ and characterized by longitudinal piezoelectric module $d_{3'3'} = d/\sqrt{3}$ and by transverse effect $d_{3'1'} = d_{3'2'} = -d/2\sqrt{4}$. Piezoelectric shear components in third row of this matrix are absent.

Piezoelectric shear components in third row of this matrix are absent.

Thus, in ideal conditions, the determination of artificial pyroelectric coefficient $\gamma_{APE} = \mathrm{d}M_i/\mathrm{d}T$ is possible, when thermo-electrical response from tangential strain is completely suppressed by the rigid substrate: $\mathrm{d}x_1 = \mathrm{d}x_2 = 0$. At uniform change of temperature the only allowed strain is the $\mathrm{d}x_3$ (hereinafter for simplicity there is no indexes). Since thermal deformation is allowed only in the direction "3", the corresponding component of mechanical stress tensor X_3 is zero. Another boundary condition is the $E_3 = 0$, i.e. crystal is assumed electrically free (close-circuited), as usually supposed at thermodynamic analysis of piezoelectric and pyroelectric effects. Corresponding equations are presented below:

$$\mathrm{d}x_n = s_{mn}^{E,T}\,\mathrm{d}X_m + \alpha_n^E\,\mathrm{d}T,$$
$$\mathrm{d}M_i = d_{in}^T\,\mathrm{d}X_n. \qquad (5.11)$$

Here x_n and X_m are the strain and stress tensor components, parameters $s_{mn}^{E,T}$ is the elastic compliance, d_{in}^T is the piezoelectric module and α_n^E is the thermal expansion, indices E and T indicate that parameters assume constancy of electrical field and temperature. For crystals of $\bar{4}3m$ group at chosen boundary conditions equations (5.11) can be specified:

$$\mathrm{d}x_1 = s_{11}^{E,T}\,\mathrm{d}X_1 + s_{12}^{E,T}\,\mathrm{d}X_2 + \alpha\mathrm{d}T = 0,$$
$$\mathrm{d}x_2 = s_{12}^{E,T}\,\mathrm{d}X_1 + s_{22}^{E,T}\,\mathrm{d}X_2 + \alpha\mathrm{d}T = 0,$$
$$\mathrm{d}x_3 = s_{31}^{E,T}\,\mathrm{d}X_1 + s_{32}^{E,T}\,dX_2 + \alpha\mathrm{d}T,$$
$$\mathrm{d}M_3 = d_{31}^T\,\mathrm{d}X_1 + d_{32}^T\,\mathrm{d}X_2. \qquad (5.12)$$

It is necessary to take into account that in the cubic crystals $s_{11}^{E,T} = s_{22}^{E,T}$ and $X_1 = X_2$; for artificial piezoelectric coefficient in a new installation of a crystal (and return back to broken indexes) it is possible to obtain

$$\gamma_{3'} = \mathrm{d}M_{3'}/\mathrm{d}T = 2\,d_{3'1'}\,\alpha/(s_{1'1'}^{E,T} + s_{1'2'}^{E,T}).$$

After conversion of incoming in formula parameters, all tensor components should be presented in the standard installation of a crystal (which is usually listed in the reference books):

$$\gamma_{111} = 2\sqrt{3}\,d_{14}\alpha/(4s_{11}^{E,T} + 8s_{12}^{E,T} + s_{44}^{E,T}). \qquad (5.13)$$

For gallium arsenide this coefficient is $\gamma_{111} = 1.5\ \mu\mathrm{C}\cdot\mathrm{m}^{-2}\cdot\mathrm{K}^{-1}$ (estimates show that in the gallium nitride this coefficient is much higher). It should be noted that similar calculation of artificial pyroelectric coefficient for quartz crystal results in the $\gamma_{100} = 5.6\ \mu\mathrm{C}\cdot\mathrm{m}^{-2}\cdot\mathrm{K}^{-1}$ and can be observed along three polar-neutral axes, while in the well-known pyroelectric tourmaline its pyroelectric coefficient is 4

μC□m^{-2}□K^{-1} and the maximum effect is possible only along one particular polar axis. In the gallium arsenide artificial pyroelectric effect in the directions of basic axes [100], [010] and [001] is impossible. The maximum of this effect in the $A^{III}B^{V}$ crystals corresponds to four [111]-type polar-neutral axes.

Indicatory surface of $\gamma(\theta,\phi)$ for polar-neutral cubic crystals constitutes of eight identical surfaces which start from the centre of a cube to its vertices at the angle of 105.2°.

It is possible to find $\gamma(\theta,\phi)$ in any direction for crystal of gallium arsenide group: the magnitude of "pyroelectric" coefficient can be determined as a radius-vector emanating from centre of cube to the intersection with indicatory surface. Being compared with quartz, the indicative surface of gallium arsenide crystals group is more complicated, because it characterizes the artificial pyroelectric effect along four polar-neutral axes (and each has two possible directions).

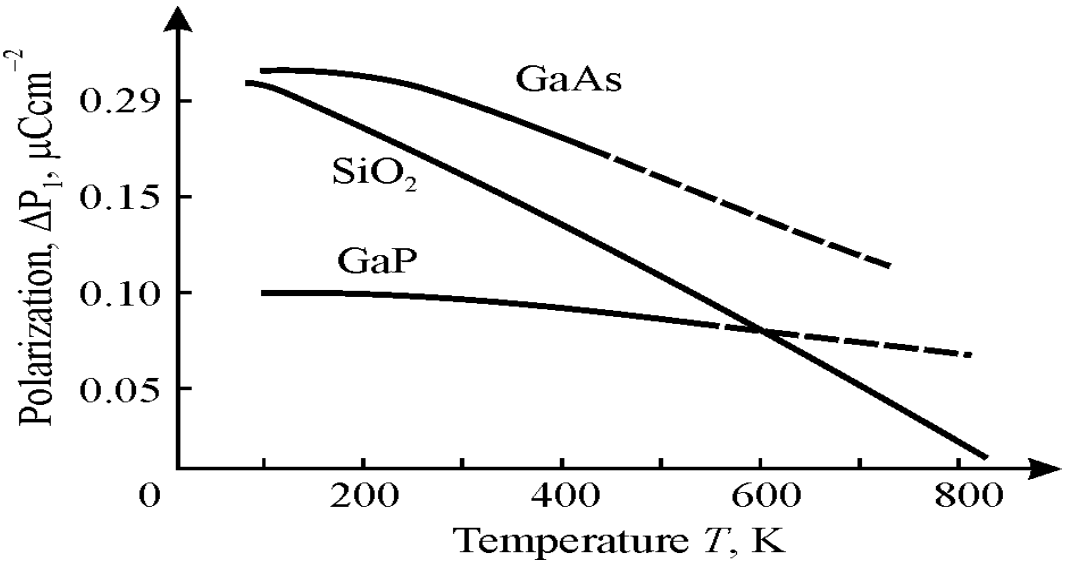

Fig. 5.20. Temperature dependencies of component M_{111} for GaAs and GaP crystals in comparison to M_{100} of SiO_2 (α-quartz) crystal

With temperature increase the internal polar-sensitivity decreases in all studied piezoelectrics. It should be recalled that in the quartz this polarity vanishes at the temperature of $\alpha \rightarrow \beta$ transition, Fig. 5.17, while in the KDP crystal γ_{100} also vanishes at high-temperature phase transition, Fig. 5.18.

It can be assumed that in piezoelectric crystals of the gallium arsenide group their internal polar sensitivity disappears at the melting point. In Fig. 5.20, temperature dependence of polar moments M_{111} of GaAs and GaP crystals and component M_{100} of internal polarity of quartz crystal is compared.

In the molten state, any stable polar formations are impossible, but it is noteworthy that the growth of polar crystal from a melt forms the polar bonds which

lead to an increase in the volume of material and, accordingly, a lower crystal density compared to its melt density.

3. Polar-sensitivity can be revealed in **others non-centrosymmetric crystals**. For instance, in trigonal crystals of polar class 3*m,* in addition to usual pyroelectric effect, seen along polar axis [001], the artificial pyroelectric response can be observed in the [010]-direction which is perpendicular to the [001] axis. The equation for artificial pyroelectric effect calculation gives:

$$\gamma^*_2 = \mathrm{d}P/\mathrm{d}T = d_{22}(\alpha_1 s_{33} - \alpha_3 s_{13})(s_{11}s_{33} - s_{13}^2)^{-1}.$$

In some crystals of polar class 3*m* it is possible to get such data: in proustite crystal (Ag_3AsS_3) $\gamma^*_2 = 10$ μC□m^{-2}□K^{-1}; in pyrargyrite crystal (Ag_3SbS_3) $\gamma^*_2 = 15$ μC□m^{-2}□K^{-1}; in lithium tantalate ($LiTaO_3$) $\gamma^*_2 = 20$ μC□m^{-2}□K^{-1}, and in lithium niobate ($LiNbO_3$) $\gamma^*_2 = 40$ μC□m^{-2}□K^{-1}. Note that the order of magnitude for such polar response is *comparable* to conventional pyroelectric response: in the lithium niobate, for example,

$\gamma_3 = 50$ μC□m^{-2}□K^{-1}.

In case of anisotropic restriction of thermal deformations artificial pyroelectric response can be observed in any piezoelectric, but analysis of this effect very often needs to use non-standard installation of a crystal.

For example, in the cubic piezoelectric class 23, to which the crystal bismuth germanate ($Bi_{12}GeO_{20}$) belongs, polar-sensitive direction is [111]-type axis, and the maximum of effect is observed just in this direction:

$$\gamma^*_{[111]} = 2\sqrt{3}\,\alpha \cdot d_{14}\,(4s_{11} + 8s_{12} + s_{44})^{-1},$$

At temperature near 300 K in piezoelectric Bi12GeO20 this parameter equals γ*[111] = 20 μC·m−2·K−1 that exceeds many times effects in quartz and GaAs.

The aim of pyroelectric response in partially clamped piezoelectrics depends not only on orientation of piezoelectric element, but also on its shape.

For example, for a long rectangular rod of quartz crystal (symmetry class 32), the artificial pyroelectric coefficient can be determined from equation:

γ1' = d11α1s11−1.

It is assumed that the rod is oriented along axis 2 while electrodes coated the surface perpendicularly to the axis 1; at this orientation and form of sample γ*1' = 5.4 μC·m−2·K−1.

The expressions for artificial pyroelectric effect calculation for all 10 classes of actual piezoelectrics (those which do not possess of pyroelectric effect) are shown in Table 5.1.

Table 5.1

Artificial pyroelectric effect for 10 classes of actual piezoelectric crystals [16]

Symmetry classes, axes orientation (x,y,z)	Sample and its orientation as to basic axes	Calculation expressions for APE coefficient $\gamma_{n\,APE}$	Piezoelectric, γ_{nAPE} [$\mu C/m^2 \cdot K$)] found at 300 K
32 (for basic coordinate System)	Rectangular rod with length l along y and thickness along x	$\gamma_1 = \frac{d_{11}^T \cdot \alpha_1^E}{s_{11}^{E,T}}$	SiO_2, $\gamma_1 = 5.4$
	Disk with normal d directed along x	$\gamma_1 = \frac{d_{11}^T (\alpha_1^E s_{33}^{E,T} - \alpha_3^E s_{13}^{E,T})}{s_{11}^{E,T} \cdot s^{E,T}_{33} - (s_{13}^{E,T})^2}$	SiO_2, $\gamma_1 = 5.7$
$\bar{4}2m$ (axes x and y are rotated around axis z at the angle of 45°)	Rectangular rod with length l and normal d directed along axis z *a*) l is directed on x, *б*) l is directed on y.	$\gamma_3 = \frac{\pm 2 d_{36}^T \cdot \alpha_1^E}{2 s_{11}^{E,T} + 2 s_{12}^{E,T} + s_{66}^{E,T}}$	KDP, *a*) $\gamma_3 = -6$ *б*) $\gamma_3 = +6$ ADP, *a*) $\gamma_3 = -17$ *б*) $\gamma_3 = +17$
$\bar{4}3m$ and 23 (axis z is directed on The third fold axis)	Disk, d directed along z	$\gamma_3 = \frac{-2\sqrt{3} \cdot d_{14}^T \cdot \alpha^E}{4 s_{11}^{E,T} + 8 s_{12}^{E,T} + s_{44}^{E,T}}$	Tl_3TaSe_4, $\gamma_3 = -23{,}5$; $Bi_{12}GeO_{20}$, $\gamma_3 = -20$
222 (axes x and y are turned around axis z at the angle of 45°)	Rectangular rod with normal d directed along axis z and length l directed *a*) l along axis x, *б*) l along axis y	$\gamma_3 = \frac{\pm d_{36}^T (\alpha_1^E + \alpha_2^E)}{s_{11}^{E,T} + s_{22}^{E,T} + 2 s_{12}^{E,T} + s_{66}^{E,T}}$ *a*) corresponds to sign «+» *b*) corresponds to sign «–»	
622 and 422 (axes y and z are turned around axis x at the angle of 45°)	Rectangular rod with normal d directed along axis x and length l directed *a*) l along axis y, *б*) l along axis z	$\gamma_3 = \frac{\pm d_{14}^T (\alpha_1^E + \alpha_3^E)}{s_{11}^{E,T} + s_{33}^{E,T} + s_{44}^{E,T} + 2 s_{13}^{E,T}}$ *a*) corresponds to sign «+» *b*) corresponds to sign «–»	
$\bar{4}$ (standard)	Rectangular rod with normal d directed along axis z and length l directed *a*) l along axis x, *б*) l along axis y	$\gamma_1 = \frac{-d_{31}^T \cdot \alpha_1^E}{s_{11}^{E,T}} = R$ *b*) $\gamma_1 = -R$	
$\bar{6}m2$ and $\bar{6}$ (standard)	Disk, normal d is oriented along axis y	$\gamma_1 = \frac{d_{22}^T (\alpha_1^E s_{33}^{E,T} - \alpha_3^E s_{13}^{E,T})}{s_{11}^{E,T} \cdot s_{33}^{E,T} - (s_{13}^{E,T})^2}$	

Both in crystals free from any mechanical stresses and in the crystals completely clamped, new effects are impossible, because the artificial effects are the

result of anisotropic *partial clamping*. Thus only partially clamped piezoelectric exhibits the artificial pyroelectricity or volumetric piezoelectric effect.

Therefore, in any polar crystals the variations in the polar-sensitivity under the thermal (δT) or the pressure (δT) change provide pyroelectric effect ($P_i = \gamma_i \delta T$) or volumetric piezoelectric effect ($P_i = \zeta_i \delta p$). In this case point, P_i is the change of vector value. Thus, pyroelectric coefficient γ_i as well as volumetric piezoelectric coefficient ξ_i are also vectors, and they are inherent to pyroelectrics only.

That is why pyroelectric can transform scalar influences (δT or δp) into a vector type of responses, which are electrical voltage or electrical current.

5.5 Possible applications of artificially formed polarity

It is established, theoretically and experimentally, that in any piezoelectric the volumetric piezoelectric effect and the artificial pyroelectric effect can be realized (note that earlier these effects were considered possible only in crystals and textures of pyroelectric symmetry).

The application of partial limitation of deformations method (partial clamping of crystal) opens new possibilities for the use of piezoelectric (non-pyroelectric) crystals in electronics, because all semiconductors of $A^{III}B^{VI}$ group (among which are such promising semiconductors as gallium nitride) are the "exclusive" piezoelectrics: hence, in a single-crystal monolithic device it is possible to combine the acoustic or thermal sensor with the signal amplifier.

From Table 5.2, one can judge the place of described above new effects among the well-known and well-studied mechanoelectric and thermoelectric effects in the dielectrics and wide energy band semiconductors.

[***Note.*** The table does not include effects caused by fields (electrical and magnetic), as well as some weak effects, for instance, flexoelectrical effect which occurs in any crystalline dielectric as thin layers polarization during their bending].

. Left part of Table 5.2 lists the possibilities of piezoelectric effect obtaining (both conventional and volumetric) in various materials. It is noteworthy that the volumetric piezoelectric effect can be obtained only in 10 classes of crystals of pyroelectric symmetry and polar texture (∞:m symmetry): only them are suitable for the use in acoustic receivers and pressure meters. In the remaining 10 symmetry classes of "exclusive" piezoelectric crystals hydrostatic pressure does not lead to any electrical response, since it is compensated in their polar-neutral structure. Finally, the applied direct electric field induces the uniaxial polarity in any solid dielectric and, as a consequence, the manifestation of electrically induced piezoelectric effect

(that is linearized electrostriction). In the relaxor ferroelectrics which have large permittivity this effect can transcend the ordinary piezoelectric effect.

Table 5.2

Electrical responses in polar-sensitive dielectrics (classification)

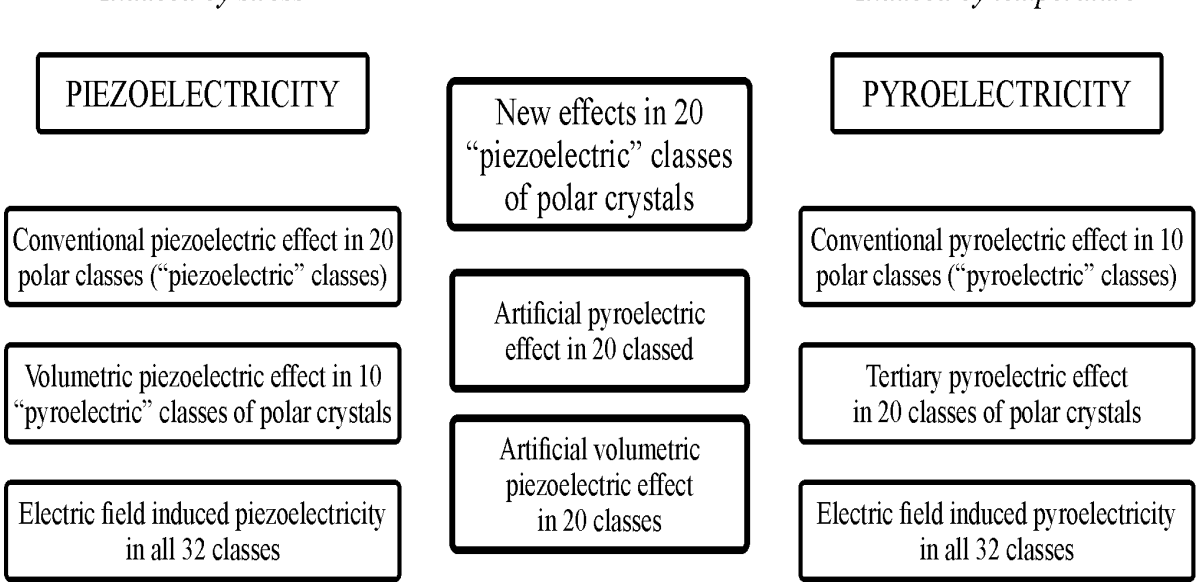

Right part of Table 5.2 lists the possibilities of obtaining *pyroelectric effects*, which under uniform thermal action is usually manifested in the 10 classes of pyroelectrics and in the polar textures. If, however, thermal action is inhomogeneous, for example, it is characterized by a temperature gradient, then the electrical response appears in *any* non-centrosymmetric crystal, including the "pure-piezoelectric" crystals. This tertiary effect is known for a long time and sometimes called actinoelectricity [5]. It is caused by the temperature *gradient* that is due to non-uniform heating. However, this effect is relatively small; in spite of this, it is used sometimes for powerful laser pulses detecting, using the highly heat-resistant quartz crystal (others polar crystals could be damaged). Finally, under applied direct electrical field the induced uniaxial polarity appears in any dielectric, with the manifestation of electrically induced pyroelectric effect. In the relaxor ferroelectrics this effect can compete with pyroelectric effect of best polar crystals.

In the center of Table 5.2, the effects possible in the crystals of 20 non-centrosymmetric classes under conditions of partial deformation *restriction* are listed. First of all, this is, certainly, the *artificial pyroelectric effect*, obtained not by the application of external electrical field (when it always arises) but by the artificial restriction of a certain type of deformations. In fact, this is, certainly, a secondary pyroelectric effect, which usually can not be manifested in the polar-neutral crystals, since it is totally compensated. But artificially it is possible to forbid a certain part

of deformations, as a result of which the de-compensation occurs, i.e. the polar response. In the short-circuited circuit with a polar crystal, under the uniform thermal action, a current is generated, while the electrical potential is generated in the open-circuited crystal.

Therefore, in the polar crystals, their internal polar-sensitive structure is non-compensated only in the pyroelectrics, but it is totally self-compensated in the so-called "exclusive" piezoelectrics. At that, this self-compensation in them is a total, being not dependent on would a crystal is in a stress-free state or in a strain-free state. Nevertheless, the non-isotropic partial clamping destroys self-compensation of intrinsic polarity. Exactly this de-compensation allows observe in such crystals the vector response to the scalar influence, Table 5.3.

Table 5.3

Main parameters of artificial pyroelectrics in comparison with usual pyroelectrics

Crystal	γ, μ**Cm^{-2}K^{-1}**	ε	F_V, **m^{2}C^{-1}**	F_D.**10^{-5}, Pa$^{-1/2}$**
Artificial pyroelectric effect in partially clamped piezoelectrics				
$Bi_{12}SiO_{20}$	27	42	0.08	5.2
$NH_{14}H_2PO_{14}$	17	50	0.02	0.6
s/i-GaAs	1.5	13	0.016	0.1
43*m* crystals	0.5–25	7–8	0.01– 0.1	0.1– 4
α-SiO_2	5.6	4.5	0.033	7
Usual pyroelectric effect in ferroelectrics				
TGS	500	50	0.4	6
PVDF	30	12	0.1	0.9
$LiTaO_3$	230	48	0.2	5
PZT ceramics	380	300	0.6	6

The effects described above open new possibilities to sensor devices elaboration. In them such piezoelectric crystals as quartz crystal and semi-insulating $A^{III}B^{V}$ crystals could find application (for instance, gallium arsenide or gallium nitride which is habitual materials in the microelectronics and micromachining). Technologically, by partial clamping using, it is possible to convert the layers of these crystals into the artificial pyroelectrics that with the use of hybrid or monolithic technology are comparable with semiconductor devices. A layer with pyroelectric properties can be an acoustic receiver (as part of a piezotransistor) or serve as a thermal sensor – as part of a pyrotransitor. Calculated and experimental results need for pyroelectric sensors are shown in Table 5.3, where C_V is specific heat, F_V =

$\gamma \cdot (C_V \varepsilon)^{-1}$ is the responsibility while $F_D = \gamma \cdot C_V (\varepsilon \cdot \tan\delta)^{-1/2}$ characterizes signal-to-noise ratio of pyroelectric detectors at 300 K and the modulation frequency of 1 kHz.

The polar (piezoelectric and pyroelectric) properties of $A^{III}B^{V}$ crystals in electronic devices were apparently not used. However, the polar-sensitive structure of any wide-band gallium arsenide-type crystal can be used to convert mechanical or temperature effects into electrical signals. In this case, $A^{III}B^{V}$ semiconductor compounds can be considered as dielectrics, and only the phenomenon of electrical polarization might be taken into account.

This assumption is close to reality in the *s/i*-GaAs and even more for in GaAs solid solutions with AlAs (especially for the GaN crystal). The piezoelectric activity of these semiconductors is usually not taken into account due to their increased conductivity (polarization can be shielded by free charges). But it should be borne in mind that in *s/i*-GaAs shielding effect becomes insignificant at frequency above 1 kHz, while the AlGaAs crystal can be used as a piezoelectric and "pyroelectric" sensor even at a frequency of 20 Hz.

Thus, temperature dependence of piezoelectric polar-sensitivity can be used in the microelectronics for thermal sensors. By the similar way, piezoelectric polar-sensitivity dependence on the pressure can by applied in the mechanical sensors.

In addition to sensors, as a result of the above studies, one more important circumstance has been discovered. Significant polar sensitivity in the crystals of $A^{III}B^{V}$ group is observed along any of the [111] directions, whereas in the standard-used direction of [100] type these crystals do not respond to the vibration and temperature changes. Nevertheless, with planar chip technology, it may turn out that some layers of devices are oriented in the [111] direction. In this case, in such devices the electrical noise can occur due to the vibrations and, possibly, due to local temperature changes.

This feature should be taken into account when designing devices using semiconductors of the $A^{III}B^{V}$ group. Eventually, these peculiarities might be used to noises investigation which arises due to chaotic disturbance of internal polarisation.

5.6 Functional dielectrics in electronics

The dielectrics, intended for use in electrical and electronic devices, must have good electrical insulating properties: very low electrical conductivity and high electrical strength. At the same time, in present-day electronic technology, quite others properties of dielectrics gained especial importance, namely, those, allowing

their use for *conversion of energy or information*; these dielectrics may be considered as ***functional materials***.

The functional (or active, or adaptive, or controlled, or smart) dielectrics actively react to the changes of temperature, pressure, mechanical stress, electrical and magnetic fields, light illumination and even smell. Functional dielectrics can be classified as pyroelectrics, ferroelectrics, piezoelectrics, electrets, quantum-electronics materials, microwave dielectrics with tuneable permittivity, etc.

Active dielectrics perform different functions. For example, the *piezoelectrics* convert mechanical energy into electrical energy and vice versa that is used in piezoelectric filters, ultrasound emitters, piezoelectric transformers, piezoelectric motors, etc.

Another example is the *pyroelectrics*, which convert heat into electricity and applied as sensitive detectors of radiation, thermal-vision devices, etc. Nonlinear properties of *ferroelectrics* and paraelectrics, constant electrical field produced by *electrets* allow use these functional dielectrics for modulation, detection, amplification, registering, storing, displaying and other types of electrical conversion of signals carrying information.

In is necessary also to mention the use of functional dielectrics in multifunctional electronic devices and active search for new technological solutions with these dielectrics application in the field of information technologies.

Main property of any dielectrics is their electrical *polarization,* i.e., effect of *separation* of electrical charges which remain bonded in spite of their shifting. As a result, the *electrical moment* appears (as product of charges magnitude by their displacement); volumetric density of this moment is polarization *P*.

One unusual feature of functional dielectrics is that electrical polarization in them can occur not only being induced by electrical field, but also by others reasons. A comparison of conventional (non-polar) dielectrics and two categories of polar dielectrics are shown in Table. 5.4. Essential distinction between active (functional) dielectrics and ordinary dielectrics is obvious.

[***Note:*** parameter $\boldsymbol{\gamma}$ is the pyroelectric coefficient; $\boldsymbol{\zeta}$ is the volumetric piezoelectric module; ***d*** is the piezoelectric module; ***c*** is the elastic stiffness; *C* is the specific heat. In this table not taken into account:

(1) *flexoelectricity* possible in all dielectrics under non-homogeneous mechanical action;

(2) *actinoelectricity* that occurs in piezoelectrics under the grad***T*** action and

(3) *photopolarization* effect in polar (non-centrosymmetric) dielectrics].

Table 5.4

Electrical polarization *P* as a response on various actions

Actions	Non-polar crystals	Piezoelectrics	Pyroelectrics
Scalar action: Temperature $\mathbf{d}T$ Pressure $\mathbf{d}p$	– –	_ _	Pyroelectric effect: $\mathbf{d}P = \gamma\,\mathbf{d}T$ Volume piezoelectric effect: $\mathbf{d}P = \zeta\mathbf{d}T$
Vector action: Electrical field E	$P = \varepsilon_0\varepsilon E$	$P = \varepsilon_0\chi E + (e^2/c)E$	$P = \varepsilon_0\chi E + (e^2/c)E + (\gamma^2 T)E/(\varepsilon_0 C)$
Tensor action Mechanical stress X	–	$P = dX$	$P = d'X$

In many applications of functional dielectrics (as sensors, actuators, filters, transformers, motors, etc.), they are subjected to external thermal, electrical, mechanical and other influences – scalar, vector, or tensor types. Table I1 shows that conventional dielectric electrically reacts *only* on electrical field action: $E \Rightarrow P$, while polar piezoelectrics and pyroelectrics, besides the $E \Rightarrow P$ response, are capable of electrical response on other actions: mechanical $X \Rightarrow P$ and thermal $dT \Rightarrow dP$. At the same time, piezoelectrics respond to electrical action not by ordinary polarization only $P = \varepsilon_0\chi E$, but also produces electromechanical response $P' = (e^2/c)E$, while pyroelectric, in addition, gives even more: electrothermal response $P'' = (\gamma^2 T)E/(\varepsilon_0 C)$.

In view of possibility to use some of dielectrics as the functional (converting) elements in electronics, one should identify and describe their properties not only in terms of exclusively electrical characteristics, but also take account of their capability to manifest various electrical, mechanical and thermal properties. These materials are important also for miniaturization of microwave and telecommunications equipments. In this case, decisive role is played by value of permittivity (ε) since planar dimensions of microwave devices are reduced exactly by factor ε. In some functional dielectrics (paraelectrics) big value of ε can be obtained together with low dielectric losses that has important technical application in highfrequency devices. Some functional dielectrics allow *electrical control* by permittivity that can be used for electrically controlled microwave devices.

For all mentioned reasons, in the field of electronics materials science recent technology shows considerable interest in ferroelectrics, paraelectrics, piezoelectrics and pyroelectrics, precisely because of their new applications in the instrumentation

engineering and electronics, as well as owing to significant progress in the field of modern microelectronic and nanoelectronic technologies.

Functional materials are particularly relevant to modern and future instrumentation based on the micromachining. In this trend, microelectronic group-technology is used for variety of technical fields. Based on modern equipment, micromachining is organically connected with microelectronics and nanoelectronics.

Among contemporary applications of functional dielectrics, one should note following main areas of particular relevance: ferroelectric and paraelectric thin films *integrated* with semiconductors; micro-systems combining sensors, processors and actuators; *microwave* microelectronics, based on functional dielectric components; *nano-dielectrics* which are perspective for sensors, computer memories and electrical power generation.

Engineers, specialized in application of materials science into electronics and information technologies, need to get modern views about the nature of electrical polarization, electrical charges transfer mechanisms, thermal properties of functional dielectrics, mechanisms of dielectric losses, as well as about intrinsic mechanisms of polarization in non-centrosymmetric crystals, which are responsible to convert thermal, mechanical, optical and other actions into electrical signals.

In order to extend the use of functional dielectrics in the field of nanoelectronics, it is necessary to have a versatile and profound presentation about physical processes that provide electrical, mechanoelectrical, thermoelectrical, photoelectrical and other conversion phenomena in the polar crystals.

It might be that most striking features of polar dielectrics is, firstly, the *mutual influence* of mechanical, electrical and thermal properties on each other and, secondly, the dependence of these properties on the *conditions* in which polar crystals are studied or applied. To demonstrate this interdependence, basic mechanical, electrical and thermal *linear effects* in the non-polar and polar dielectrics are symbolically compared in Fig. 5.21. It is seen that in the ordinary dielectrics these properties are independent, but in the polar crystals they are connected by quite complex interactions.

Figure 5.21A symbolically shows that in solid dielectric its elastic mechanical deformation x (strain) is proportional to applied mechanical stress $x = s \cdot X$, where s is elastic compliance.

Note that this linear relationship can also be written in reverse direction: $X = c \cdot x$ as Hooke's law, where c is elastic stiffness. Similarly, in a dielectric, electrically induced polarization P is proportional to magnitude of applied electrical field: P

$=\varepsilon_0\chi\square E$, where χ is dielectric susceptibility while ε_0 is electrical constant in SI. If electrical polarization would be induced *non-electrically*, then another recording of this linear connection will be more convenient: $E=\varepsilon_0^{-1}\xi\square P$ where $\xi=\chi^{-1}$ is dielectric impermeability.

Finally, thermal properties are described by proportionality of amount of heat δQ in a crystal appeared due to ambient temperature change: $\delta Q = C\square\delta T$ where C is specific heat.

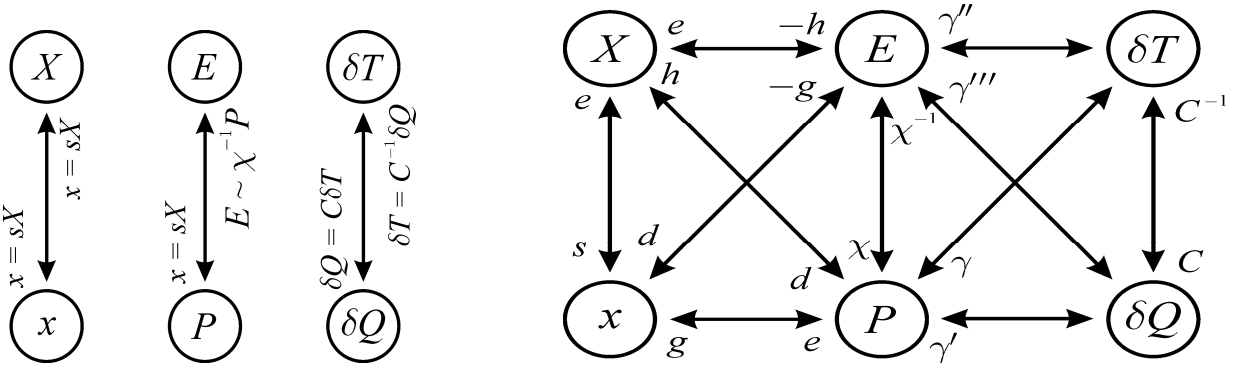

(A) (B)

Fig. 5.21. Linking diagram for mechanic, electrical and thermal effects: A – in non-polar dielectric; B – in polar dielectric

In polar crystals, their mechanical, electrical and thermal properties are *interdependent*, so possible diagram of their interaction looks like two squares connecting by one side, Fig. 5.21B. This scheme shows how complicated is description of non-centrosymmetric (polar) crystals properties.

The *piezoelectricity* is symbolically described by left the square in Fig. 5.21B. Two horizontal and two crossed-connecting lines with arrows present eight linear piezoelectric effects that may be observed in polar crystals at different conditions. The number of piezoelectric effects equals *eight*, since this effect can be *direct* or *converse* (2), crystal can be electrically *open-circuited* or *short-circuited* (2), as well as crystal mechanically can be *free* or *clamped* (2), so that: 2×2×2 = 8.

These effects are described by four piezoelectric coefficients-modules (*d, e, g, h*); at that, simplified equations of the direct effects are: $P = d\square X$, $P = e\square x$, $E = -g\square x$, $E_j = -h\square X$ and for the converse effect equations are: $x = d\square E$, $X = e\square E$, $x = g\square P$, $X = h\square P$. However, all above mentioned *four* modules can be calculated through each other and through known elastic constants, for example, in simplified form: $d_{in} = \varepsilon\varepsilon\square g = e\square s = \varepsilon\varepsilon\square h\square s$, and so on. As can be seen, the description of electromechanical effects in polar crystals (even in linear case) is not easy task.

In polar-sensitive crystals, the description of electrothermal effects is also not simple. The *pyroelectric* effect occurs when disturbance factor is the thermal action

on a crystal while response has electrical nature. The *electrocaloric* effect is the converse effect: it arises, when electrical field acts on the pyroelectric, while results is heating or *cooling* of polar crystal. Both these effects are symbolically presented in the right square in Fig. 5.21B.

Firstly, two horizontal lines and two crossed-connected lines with the arrows symbolically characterize four options in pyroelectric effect implementation: polar crystal can be electrically *open-circuited* or *short-circuited*; besides, pyroelectric effect can occur in two different thermal conditions: *adiabatic* with $\delta Q = 0$ or *isothermal* with $\delta T = 0$. So pyroelectric effect might be described by *four* equations: $P = \gamma \cdot \delta T$, $P_i = \gamma' \cdot \delta Q$, $E = \gamma'' \cdot \delta T$ and $E = \gamma''' \cdot \delta Q$, in which different pyroelectric coefficients correspond to various boundary conditions.

Secondly, four lines with arrows, shown in the right part of Fig. 5.21B, are used here for symbolical description of *electrocaloric* effect. As pyroelectric effect, this effect may be described by *four* different linear relationships (depending on thermal and electrical boundary conditions).

However, this effect under normal conditions (at temperature ~300 K) is as rather weak and not considered here in more detail. (However, in Chapter 4, large electrocaloric effect will be discussed, arising when the antiferroelectric is switching electrically into the ferroelectric phase that can be considered as possible basis for electrocaloric refrigerator).

Important consequence of these relationships is dependence of crystal *fundamental parameters* on thermal, electrical of mechanical processes passing in polar crystals at different boundary conditions. For example, dielectric susceptibility of free crystal χ^X (that means the stress $X = 0$) and of clamped crystal χ^x (that means the strain $x = 0$) can differ, at that $\chi^X > \chi^x$.

Similarly, in polar crystals their elastic stiffness in Hooke's law depends on electrical conditions: in open-circuited crystal elastic stiffness (c^P) differs from it in closed-circuited crystal (c^E).

Moreover, when Hooke's law is studied in polar crystal, its elastic stiffness depends on isothermal (c^T) or adiabatic (c^S) conditions. Even most conservative parameter of a crystal — its heat capacity C at normal temperatures — turns out to be dependent on electrical and thermal boundary conditions in which crystal is studied. For example, in open-circuited polar crystal its specific heat C^E differs from specific heat C^P of close-circuited crystal. In the same manner, the difference is seen in specific heat of mechanically free (C^X) and mechanically clamped (C^x) polar crystals.

5.7 Summary and self-test questions

1. Experimental evidences of the polar-sensitivity in crystals are the *structural affinity* of the piezoelectrics and pyroelectrics with an example of zinc sulfide uniting in polymorphic structure the regions with sphalerite and wurtzite symmetry; as well as the *chemical features* of polar crystals demonstrating different chemical sensitivity on the surfaces of opposite polarity.

2. Polar-sensitive bonds ordering leads to the *increased volume* at the transition into polar phase; such crystals are characterized by the electromechanic and electrocaloric *contributions* into the *permittivity* as well as big high-frequency dielectric *absorption*.

3. Charge transfer in some polar-sensitive crystals may depend on the symmetry of the polar phase: the large *decrease* of resistivity in the *critistors* of vanadium dioxide type occurs from its triclinic (piezoelectric) symmetry; while large *increase* of resistivity in the *posistors* is due to doped barium titanate transition from the polar tetragonal (pyroelectric) structure into the non-polar cubic phase.

4. Zinc oxide which is best material for *varistors* (with giant change in resistivity) has polar wurtzite (pyroelectric) structure with possible transformation into another but also polar sphalerite (piezoelectric) state. Others field-controllable switching elements, which exhibit the colossal magnetoresistance as well as high sensibility of nanostructured sensors based on the zinc oxide also belong to the polar-sensitive crystals.

5. The *electrically induced* polar properties are caused by the *linearized electrostriction*: In dielectric with high permittivity in a strong electrical field, both the piezoelectric effect and the pyroelectric effect can be induced. They are proportional to the applied field and the square of the dielectric permittivity. In the paraelectrics and especially in the relaxor ferroelectrics electrically induced piezoelectric module can reach and even surpass piezoelectric module of usual piezoelectrics.

6. Interesting for practical application in electronics is the possibility of *electrical control* by the piezoelectric effect: using this principle it is possible to implement tunable piezoelectric resonators and filters and various SAW devices.

7. The *mechanically induced* pyroelectricity (and the volumetric piezoelectric effect) is possible to obtain in any polar-neutral piezoelectric (which is not pyroelectric). For this, the original method of partial limitation of thermal (or elastic) deformations is applied, due to which one of the polar-neutral axes is transformed into the polar axis.

8. Obtaining the artificial pyroelectric effect (or volumetric piezoelectric effect) is achieved in a composite system "non-deformable substrate – oriented plate of polar-neutral crystal". These studies can be realized in two- and three-dimensional structural arrangements of polar-sensitive bonds; as a result, the artificial pyroelectric effect for 10 classes of polar-neutral piezoelectric crystals is calculated.

9. Main thing is that by the creating for piezoelectric crystal *special boundary conditions* the “pyroelectric effect” can be obtained in all 10 polar-neutral classes of crystals. Therefore, in any polar crystals, the changes in polar-sensitivity under thermal (δT) or pressure (δT) variation provide the pyroelectric effect ($P_i = \gamma_i \delta T$) or the volumetric piezoelectric effect ($P_i = \zeta_i \delta p$). At that, pyroelectric coefficient γ_i as well as volumetric piezoelectric coefficient ξ_i are the material vectors which inherent to the polar crystals only. That is why polar-sensitive crystal can transform scalar influences (δT or δp) into the vector type of responses, which are electrical voltage or electrical current.

10. Temperature dependence of the piezoelectric polar-sensitivity can be used in microelectronics for thermal sensors. By similar way, polar-sensitivity dependence on pressure can by applied in the mechanical sensors. Significant polar sensitivity in crystals of $A^{III}B^{V}$ group is observed along any of [111] directions, whereas in the standard-used direction of [100] type in these crystals do not respond to mechanical vibrations and temperature changes.

11. In the planar chip technology, it may turn out that some layers of devices are oriented in the [111] direction. In this case, in such devices the electrical noise can occur due to the vibrations and, possibly, due to local temperature changes. This feature should be taken into account when designing devices using semiconductors of $A^{III}B^{V}$ group.

Chapter 5. Self-test questions

1. What are the features of the closeness of pyroelectrics and piezoelectrics?
2. How does polarity affect the properties of critisters and varistors?
3. What are the mechanisms for controlling the piezoelectric effect?
4. Compare regular and polar crystals for the connections between electrical, mechanical and thermal properties?
5. How piezoelectric polar-sensitivity can be used in microelectronics for thermal sensors?

CHAPTER 6. PIEZOELECTRICS: PHYSICS AND APPLICATIONS

Contents

The basic physical mechanisms of the piezoelectric effect are considered. Piezoelectric is a solid-state transducer of mechanical energy into electrical energy (direct effect) or, vice versa. the electromechanical transducer (converse effect). In this case, the mechanically induced electrical polarization is directly proportional to the strain, i.e., this is the odd (linear) effect which is possible only in the non-central symmetric material. Piezoelectric effect is characterized by the various piezoelectric modules — third-rank tensors — depending on the combination of boundary conditions, under which piezoelectricity is used or studied. The interrelation of the mechanical and the electrical properties of piezoelectrics is characterized by the electromechanical *coupling coefficient*, the square of which shows how much of energy applied to the piezoelectric is converted into another kind of energy. Parameters of some piezoelectric materials can be controlled by the electrical field that is used in controlled piezoelectric filters and surface acoustic wave devices.

Model description of the piezoelectricity is given for one-directional (1D) polar-sensitive bonds, representing the *longitudinal* piezoelectric effect; for the polar bonds oriented in-plane (2D) can be seen also the *transverse* piezoelectric effect and, at last, for spatial (3D) distribution of polar bonds, apart from mentioned two effects, the *shear* piezoelectric effect is poosible. The *electro-induced* piezoelectric effect and the method of *strain partial limitation* allowing to get the volumetric piezoelectric effect are considered. In addition to the linear converse piezoelectric effect, the quadratic electrostriction effect is analyzed, when the induced strain is proportional to square of field strength. Naturally, the sign of this deformation does not change when electrical polarity changes. In the electrical bias field, the electrostriction looks like the piezoelectric effect. In this case, the magnitude of such electrically induced piezoelectric effect in the relaxor ferroelectrics (possessing large permittivity) can be giant.

The discovery of piezoelectricity dates back to 1880 when Pierre and Jacques Curie find out this effect in the quartz crystals. Technical application of piezoelectrics started in 1920 with the ultrasonic transducer (invented by P. Langevin) was applied for the transmitting and receiving signals in the water, and from Cady's work on the use of piezoelectric filters in the telephony.

Piezoelectricity is researching issue, which is the intersection of two classical scientific fields: first, the mechanics of deformed solid body, and secondly –the electrodynamics of continuous media. Differential equations of electrodynamics establish a link between the vectors of electrical field E, electrical induction D, magnetic field H and magnetic induction B. Almost all piezoelectrics are dielectrics, so piezoelectric effects occur at the speeds much slower then the speed of light. In this case, the magnetic effects can be ignored, and, instead of electrodynamics, the equation of *electrostatics in dielectric* can be applied when $\mathrm{rot}E = 0$, $\mathrm{div}D = 0$.

Theory of the elasticity was stimulated in the 20–40s of the XIX century with the works of Cauchy, Poisson and Green. The interaction of electrical charges and mechanical pressure in the piezoelectric crystals was described in mathematical form by Pockels, while the quantitative ratios are given by Voigt in 1910–1920; these equations are fundamental for constructing the mathematical model of piezoelectric effect. It should be noted that in this section only the *homogeneous* mechanical deformations and homogeneous electrical fields (identical throughout a crystal) are considered. In the case of heterogeneous deformations, in addition to the piezoelectric effect and electrostriction, other electromechanical phenomena are possible, for example, the *flexoelectrical* effect (which is very important for liquid crystals). In the case of a gradient of temperature in piezoelectric, the *tertiary* pyroelectric effect occurs (*actinoelectricity*). However, flexoelectricity and actinoelectricity are not considered here.

Piezoelectric is a solid-state transducer of mechanical energy into electrical energy (the direct effect) or, vice versa, electromechanical transducer (the converse effect). At that, mechanically induced electrical polarization is directly proportional to strain, i.e., this is the odd (linear) effect which is possible only in the non-centrosymmetric material. Piezoelectric effect is characterized by various piezoelectric modules — third-rank tensors, depending on the combination of boundary conditions under which piezoelectricity is used or studied [2]. The interrelation of mechanical and electrical properties in piezoelectrics is characterized by the electromechanical coupling coefficient, the square of which shows how much the energy applied to piezoelectric is converted into another kind of energy.

Parameters of piezoelectric effect can be controlled by the electrical field by changing piezoelectric filters and the surface acoustic wave parameters.

Piezoelectricity, together with electrostriction, refers to the electromechanical properties of crystals. Electrostriction is the *universal* property of all dielectrics, since the deformation in applied electrical field partly is a manifestation of electrical polarization, when electrically charged particles are forcedly shifted from their initial positions in the process of their separation. Being quadratic (even) effect, the electrostriction does not have any opposite effect. On contrary, the linear (odd) piezoelectric effect can be either direct or converse. All electromechanical effects substantially depend on the electrical and mechanical boundary conditions.

The model description of the piezoelectricity is given for:

– *longitudinal* piezoelectric effect in one-directional polar crystal;
– *transverse* piezoelectric effect in the plane oriented polar bonds model;
– *shear* piezoelectric effect in spatially distributed polar bonds model;
– *electrically induced* piezoelectric effect in high-permittivity dielectrics;
– *volumetric effect* in polar-neutral crystals under partial limitation of strain.

Therefore, in addition to *linear converse* piezoelectric effect, the electro-mechanical effects include the *quadratic* electrostriction effect, in which electrically induced strain is proportional to the square of field strength. Naturally, the sign of this deformation does not change when electrical polarity changes. In constant electric bias field, the electrostriction looks like piezoelectric effect. In this case, the magnitude of such electrically induced piezoelectric effect can be very large in the peculiar case of paraelectrics and relaxor ferroelectrics, which have large permittivity.

6.1 General characteristics of piezoelectricity

As known, only the crystals, belonging to the 21 non-central symmetric classes of point symmetry, can have properties described by the *odd-rank* tensors. Off them, 20 classes exhibit the *piezoelectric effect*, quantitative characteristic of which is the third-rank tensor[)] of piezoelectric coefficients d_{ijk}.

[***Note.*** These 20 piezoelectric classes also include 10 pyroelectric symmetry classes, described by the first rank (also odd-rank) tensors γ_i and ζ_j for pyroelectric and electrocaloric effects, correspondingly. The generality of the above theoretical reasoning is confirmed by the fact that the remaining one of the 21 off-central (but not piezo- and non-pyroelectric) symmetry classes shows the electromechanical effect, which is also described by the odd-rank tensor but already of the 5th rank. At

that, all material's tensors of the odd-ranks vanish in the crystals, which have the centre of symmetry; therefore, the linear electromechanical effects (as well as linear thermoelectric effects) in the central symmetric media *is impossible*].

The fact is that the piezoelectric effect cannot occur in the central symmetric crystals since any centre gomogeneous mechanical action onto the central symmetric crystal leads to the symmetry group also with a centre of symmetry. In other words, after any *uniform* (scalar) deformation, the central symmetric crystal remains the central symmetric one. Therefore, the presence of centre of symmetry in the deforming crystal means that there is no reason for mechanically induced electrical polarization, because *no polar directions* exist in such a crystal.

At that, the manifestation of piezoelectric effect in the *pyroelectric* crystal is obvious, since it has a *peculiar polar axis,* so any deformation of them leads to the electrical polarization. Note, that in the *polar-neutral* crystals the polar-sensitive directions also exist, although they are totally compensated*). Piezoelectric effect in these crystals occurs, when the *directional* (non-scalar) external influence (acting in a certain direction) makes the polar-neutral structure of such crystal as "*uncompensated*". Thus, as a result of the directed mechanical influence, in the polar-neutral crystal a *special* polar direction arises along of previously compensated axis. Therefore, all polar-neutral crystals should be attributed to the piezoelectrics.

1. *Piezoelectric materials* include the bulk ceramics, ceramic thin films, multilayer ceramics, single crystals, polymers and ceramics-polymer composites. In recent years a large number of different piezoelectric film materials have been developed and tested for different micro-systems and microelectronic components. Film and bulk piezoelectrics can be used also in the microwave devices. Of particular importance are piezoelectric composites of various classes, in which parameters can be obtained that are far superior to those of homogeneous piezoelectric materials [3]. New relaxor-ferroelectric ceramics and crystals exhibit extremely high efficiency of piezoelectric energy conversion, which is of interest, in particular, for medical imaging devices and for other applications, such as special drives for industrial non-destructive testing.

[***Note.*** An exception among 21 crystallographic classes, which do not have the centre of symmetry (while only 20 classes show piezoelectricity), is the cubic class with point group 432, in which the appearance of *linear* piezoelectric activity is prohibited by *others elements* of symmetry. Mechanically induced polarization can be obtained in this class only in such a case, when applied mechanical stress would be *asymmetric*. Moreover, this "mysterious" non-centrosymmetric but non-piezoelectric class of crystals, in reality, may behave like piezoelectric but in the

strong electrical field. The description of converse piezoelectric effect by simple linear relation $x = dE$ in the strong electrical fields should be considered only as the first term of odd series: $x = dE + d'E^3 + d''E^5 + \ldots$. Really, in weak electrical field, for the non-centrosymmetric class 432 first term of this series is $d = 0$, but already the *second term* of this series, namely the d' is non-zero].

2. *Practical application* of instruments and devices that use piezoelectric effect in their designs is very wide and constantly expanding. Most important scientific and technical fields of piezoelectric effect use are:

· *piezo-electronics* (piezoelectric technique of the bulk acoustic waves), including development piezoelectric receivers, piezoelectric transformers and piezoelectric motors, adaptors, microphones, piezoelectric resonators and piezoelectric filters;

· *acousto-electronics* (piezoelectric technique of surface waves), which are developed microelectronic data converters: delay lines, filters, sensors of external influences, convolvers, etc.;

· *acousto-optics*, which uses interaction of optical waves with acoustic waves that allows developing of deflectors, optical filters and other optical devices;

· *modern energy devices* such as piezoelectric power generators, piezoelectric motors, etc.

Main areas of piezoelectrics applications in *electronics* are classified in Fig. 6.1 which enumerates far from complete using of piezoelectrics. As known, some products, such as watches, cameras, mobile phones, televisions, computers, and piezoelectric lighters have become the objects of everyday life. Many electronic devices are not possible without the use of piezoelectric elements.

These include radiators and the antennas of sonar, frequency stabilizers in computers, electronic devices and the reference time, power line filters and delay lines in the radio and telephone communications, sensors to measure acceleration, vibration, acoustic emission non-destructive testing, piezo-transformers and piezo-motors, medical ultrasound imaging and medical instruments for various purposes, etc.

Functional assignments of piezoelements located in the watches, piezoelectric switches, televisions and mobile phones are quite diverse, but in basis of these devices lie same physical phenomenon – piezoelectricity, that is, ability of some crystals, ceramics, textures and composite produce electricity by their shape or size changing. Conversely, they can change their size or shape under the influence of electrical voltage.

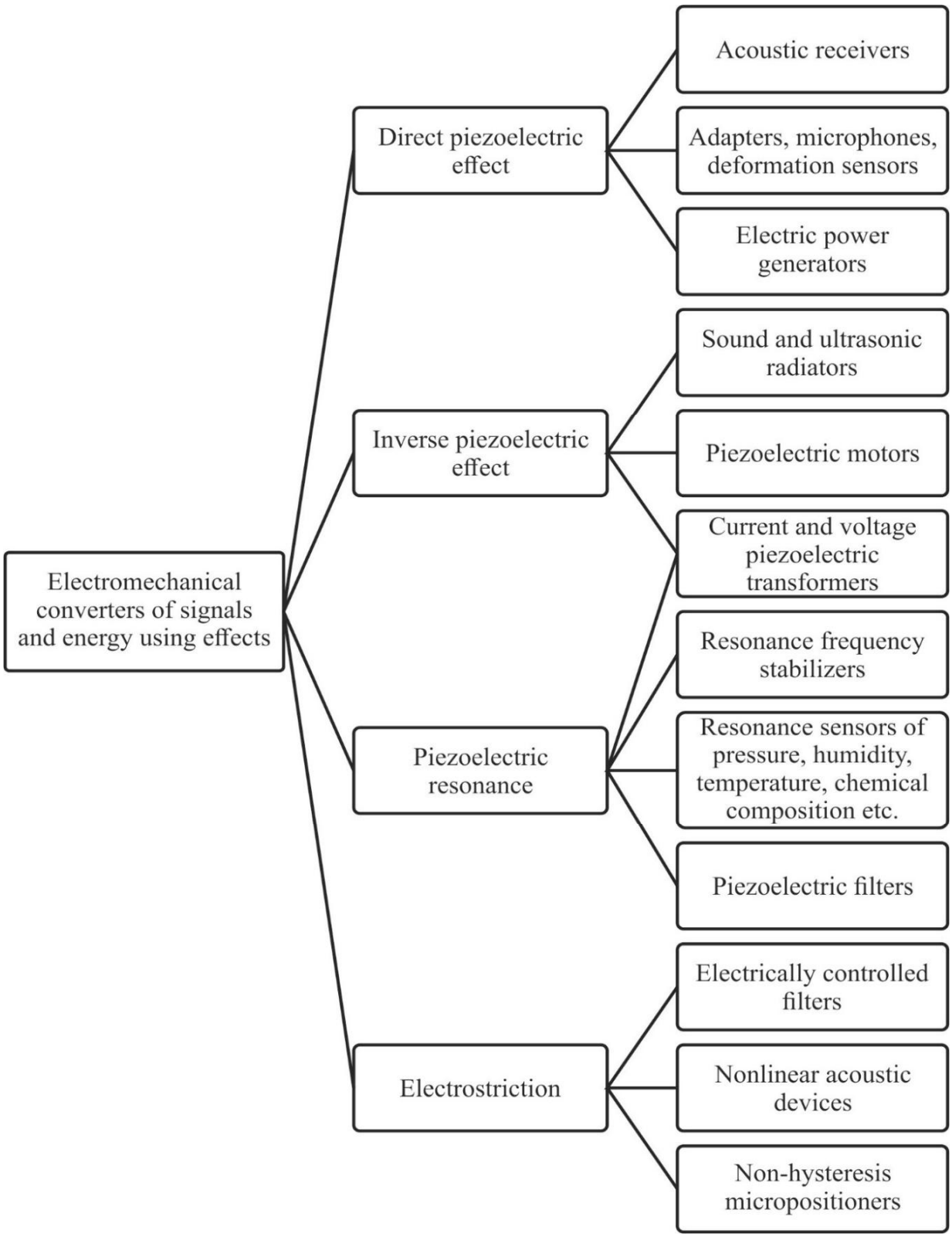

Fig. 6.1. **Piezoelectrics applications in electronics**

Can only mention some uses of piezoelectric effect in *microelectronics*:

· Miniature piezoelectric emitters that are effective at high frequencies and have small dimensions (such as installed in children's toys and music sheets);

· Precision positioning systems, for example, in the needle positioning system in scanning tunneling microscope or for positioners to move hard disk driver;

· Supplying in widescreen printers, printed on solvent ink and inks with ultraviolet hardening.

· Microwave miniature resonant devices based on thin AlN and ZnO films.

Relatively new scientific direction is appeared – the *piezoelectronics*. Among modern applications, it is necessary to highlight the most important trends:

· Thin piezoelectric films, integrated with semiconductors;

· Microsystems that combine sensors, processors and actuators;

· Ultrahigh-frequency components based on active dielectrics;

· Nanosized piezoelectrics where various electronic devices are planned.

One of modern directions of piezoelectronics is converting any motion into electrical current. For example, conversion of human energy into the power supply of various electronic devices: special piezoelectric gears designed for soldiers will allow the use of electric current generated by their movement and thereby get rid of excessive weight of batteries. Significant advantages can be achieved using nanotechnologies: it is established that as size of piezoelectric converter is reduced, its ability to generate energy increases. It has been experimentally shown that nanoparticles of about 20 nanometers in size produce twice as much current as a monolithic piezoelectric. Dozens of ways of applying nanotechnologies have been proposed – from charging the energy of a mobile phone from voice of consumer and to a device that allows reading human thoughts (which is extremely important for neurology).

Some examples of modern *energy devices* based on piezoelectrics are:

· Dampers of vibrations for helicopters and airplanes; in particular, special design of bearing has been developed in which the friction is weakened by the vibration, for creation of which does not require special mechanisms (bearing sleeves are made of piezoelectric material, at that, electrical voltage makes the piezoelectric shrink and expand, creating a vibration that decreases friction);

· Piezoelectric converters, installed in the jet aircraft in order to save energy (and, consequently, fuel), in which vibrations of fuselage and wings are directly transformed into electricity;

· Powered traffic lights are developed, whose batteries are charged from the noise of cars at the street intersections;

· Experiments were carried out to convert the energy of sea waves into electricity (tidal power plants in the USA). Next example is piezoelectric system

operating experimentally in Japan on the crossroads of railway stations to convert the energy of platform vibrations into electricity.

However, this book is not devoted to hundreds of piezoelectronic devices consideration, but it covers only the *physical bases* of electromechanical transformations in the polar crystals and textures.

3. *Piezoelectricity is the linear electromechanical effect* (or, what is same, the *mechanoelectrical effect*) in the non-centrosymmetric crystals. In this connection, it is advisable to recall that:

· *Electrical properties* characterize the movement of charged particles in a matter caused by external electrical field. First property is the electrical polarization, i.e., *charge separation,* representing the *reversible* elastic shift of bound charges. Second electrical property is the electrical conductivity*,* i.e., *directional movement of free charges,* which is the *irreversible* phenomenon that in context of piezoelectricity can be neglected.

At that, of crystals electrical properties, only the dielectric polarization is relevant to the piezoelectric effect. Polarization is described by second-rank (even) tensors of permittivity ε_{ij} or dielectric susceptibility χ_{ij} ($i, j = 1, 2, 3$).

When describing the electrical polarization as applied to piezoelectricity, only the fast (practically non-inertia) mechanisms of the elastic displacement of electrons and ions should be taken into account that makes it possible to disregard the fundamental dielectric dispersion $\varepsilon(\omega)$ in the almost entire frequency range of piezoelectrics applications (up to 100 GHz).

· *Mechanical properties* are characterized by the features of internal bonds between atoms (or between molecules) of a material. At that, the *elasticity* should be attributed to the *reversible* mechanical properties, while others mechanical effects: fluidity and fracture are the *irreversible* properties (last effects are not taken into account when considering piezoelectricity).

When describing elastic properties, a discrete structure of crystal is usually ignored, so crystal is considered as continuous homogeneous medium (*continuum approximation*).

This approach is justified up to frequencies near 10^{12} Hz, which is much greater than usual operation frequency of conventional piezoelectronics, acoustoelectronics, acoustooptics (up to 100 GHz).

Therefore, while describing piezoelectricity, only the reversible (mechanical and electrical) properties of crystals should be taken into account, so the piezoelectric effect is also a *reversible* property.

· *Elastic parameters*, of many mechanical properties, are most important to describe piezoelectric effect; they are characterized by even material tensors of fourth rank: the *elastic stiffness* c_{mn} and the *elastic compliance* s_{mn} ($m, n = 1, 2, \ldots 6$). It is appropriate to recall that c_{mn} and s_{mn} are the parameters of Hooke's law, which joins two even second-rank tensors: mechanical *stress* X_m and mechanical *strain* x_n: $X_m = c_{mn}x_n$, or converse equation: $x_n = s_{mn}X_m$.

Mechanism of elasticity looks like this: the deformation of a crystal alters atomic mutual arrangement, as a result, the forces arise, which try to restore the body into its original position. These forces, occurring in the deformed body, are called *internal*, and magnitude of these forces, being calculated per unit area, is called *stress*.

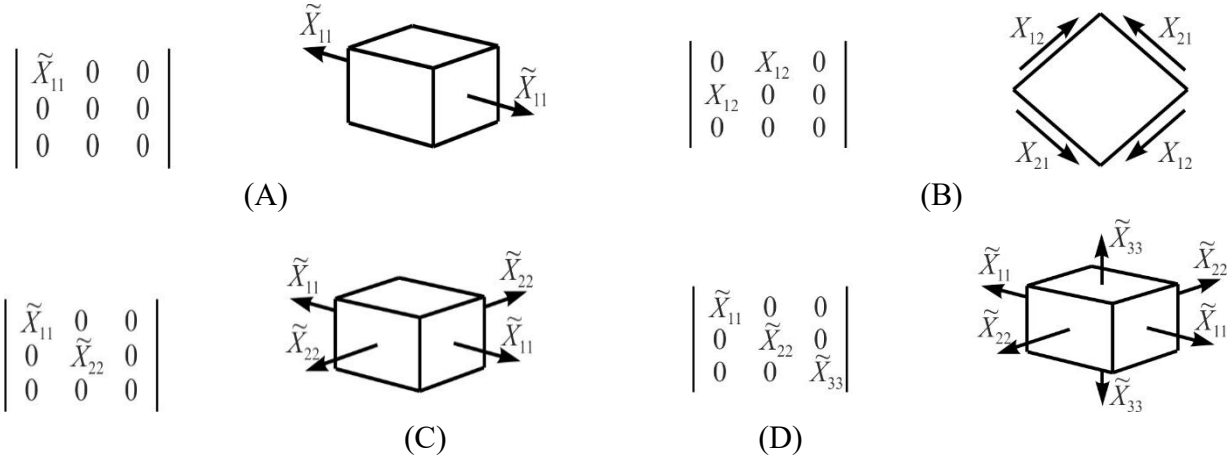

Fig. 6.2. Matrix representation of stress tensor with geometric explanation of components.

Homogeneous mechanical stresses, being the second-rank tensor X_{ij}, can be very diverse, always remaining the *centrosymmetric action* on a piezoelectric*). When all components of tensor X_{ij} are given with regard to principal axes, some important cases can be shown, Fig. 6.2: A – *line-stressed* state (uniaxial stress), as example might be uniformly tensile rod; B – *pure shear* stress which is perpendicular to the plane of figure; C – *plane-stressed* state (biaxial stress); D – *volumetric*-stressed state (three-axes stress).

Hydrostatic action, at which $X_{11} = X_{22} = X_{33} = -p$ (pressure) is non shown in Fig. 6.2, its matrix is similar to Fig. 6.2D, but X_{jj} directions in this case are oriented opposite to shown in figure, and all components have same magnitude.

Relative deformation is dimensionless, while the unit of stress measurement is N/m^2 and the same unit of measurement is also maintained for *elastic rigidity*: $[c] = H/m^2 = Pa$ (Pascal).

Elastic compliance is defined as $s = Pa^{-1}$; because of the smallness of Pascal unit, the unit "gigapascal" is often used which equals to 10^9 Pa. Knowing all

components of one of elastic tensors, for example, the tensor of elastic stiffness c_{mn}, it is possible to calculate components of the converse tensor; in a given case, the tensor of elastic compliance: $s_{mn} = (-1)^{i+j} \Delta c_{mn} / \square c_{mn}$, where $\square c_{mn} \square$ is determinant of matrix and Δc_{mn} is minor of this matrix without m-line and n-column.

In addition to tensors of compliance and stiffness, for some calculations, related to research and practical application of piezoelectric effect, some other elastic parameters of piezoelectric are significant, which can be calculated with the help of known c_{mn} or s_{mn}.

Density of elastic energy W of deformed (or stressed) crystal can be determined from the expression for elementary mechanical work done by forces X for deformation x: $dW = Xdx$. By the integrating of this expression, it can be obtained $W_{elast} = -\frac{1}{2} xX$. Depending on a task and using Hooke's law in two forms: $x = sX$ or $X = cx$, two equation can be obtained for the density of elastic energy: $W_{elast} = \frac{1}{2} cx^2 = \frac{1}{2} sX^2$.

Volumetric compressibility $<s>$ is a significant parameter for evaluating properties of piezoelectrics, for example, for their use as emitters or receivers of elastic waves.

This compressibility characterizes dependence of relative change in the volume ΔV of crystal or texture under the action of hydrostatic pressure p: $\Delta V = - ps$. Volumetric compressibility is formed as the invariant of elastic compliance tensor: $<s> = s_{11} + s_{22} + s_{33} + 2(s_{12} + s_{13} + s_{31})$. For cubic crystals and isotropic solids the compressibility looks more simple $<s> = 3(s_{11} + 2s_{12})$.

Volumetric modulus of elasticity K is introduced as a parameter converse to compressibility. Parameter K also can be determined by tensor of elastic stiffness. For the cubic crystals, $K = (c_{11} + 2c_{12})/3$. Modulus of elasticity characterizes the ability of material to resist the change in its volume; this parameter is also called as volumetric compression module.

Module K characterizes the ability of object to such change in its volume that is not accompanied by the change in form of sample under the influence of normal directional stress that is same in all directions (this occurs, for example, under hydrostatic pressure conditions).

Module K is equal to the ratio of volumetric stress to the value of relative volume compression. It should be noted that volumetric elastic modulus of the non-binding fluid is different from zero while for incompressible fluid it is infinite.

Poisson's coefficient v is used to characterize elastic properties of a material. As know, under the action of tensile force the body begins to stretch longitudinally, while (in the vast majority of cases) the cross-section of material decreases.

Poisson's coefficient shows how the transverse section of a deformed body changes during its stretching (or compression). Its value is equal to ratio of relative cross-section of compression e' (in case of one-way stretching) to relative longitudinal elongation e, that is, $v = |e'|/e$.

In the case of absolutely brittle material, the Poisson's coefficient is 0, and for absolutely elastic material $v = 0.6$. For most steels this coefficient lies in region of 0.3; for rubber it is approximately equal to 0.6. Poisson's coefficient is measured in relative units: mm/mm, m/m.

For high-symmetric crystals and isotropic solids, other characteristics of elasticity are used:

The *shear modulus* or rigidity module (denoted as G or μ) characterizes the strained state of pure shear, that is, the ability of material to resist the shape change while maintaining its volume.

The shear modulus is defined as a ratio of shear stress to share deformation, which is defined as the change in forward angle between the planes in which tensile stresses are applied, applied to two mutually orthogonal planes. The shear modulus is one of components of viscosity phenomenon.

The *Young's modulus* (E) characterizes resistance of a material to stretching (or compression) during elastic deformation, or the property of object to deform along the axis under the action of force along the same axis; is defined as the ratio of stress to elongation.

For cubic crystals, E equals to each of first three diagonal components of elastic stiffness which are same: $E = c_{11} = c_{22} = c_{33}$. Often, Young's modulus, which characterizes ability to resist tensile deformation, is called simply *modulus of elasticity*.

In conclusion, it is worth noting that deformation, occurring due to the action of external force, *quickly disappears* to zero when this force is removed – this is the case of so-called "*perfectly elastic solid* ".

Only in the perfectly elastic materials Hooke's law is valid: relative deformation (strain) is proportional to mechanical stress, and their behaviour during deformation *does not depend on the strain rate*. Exactly this ideal case is implied in further discussion of piezoelectric effect.

6.2 Model description of piezoelectricity

Manifestations of piezoelectric properties are quite diverse; that is why, the electromechanical interaction first will be simulated for the case of *one-directionally* oriented polar-sensitive bonds (*longitudinal* piezoelectric effect), next the model of polar-sensitive bonds *oriented in-plane* (*transverse* piezoelectric effect) will be described, and at last the case of *spatial distribution* of polar-sensitive bonds (*shear* piezoelectric effect) will be considered.

1. ***Longitudinal piezoelectric effect*** can be explained by a model shown in Fig. 6.3, where symbolically one-dimensional crystal is presented which has length l and supplied by electrodes (model represents equally oriented joint polar-sensitive bonds). Under the action of longitudinal mechanical stress $+X$ crystal lengthens by value Δl, Fig. 6.3B, creating electrical moment, which is the mechanically induced electrical polarization P. It is compensated by the electrical charges of opposite sign which appear on electrodes.

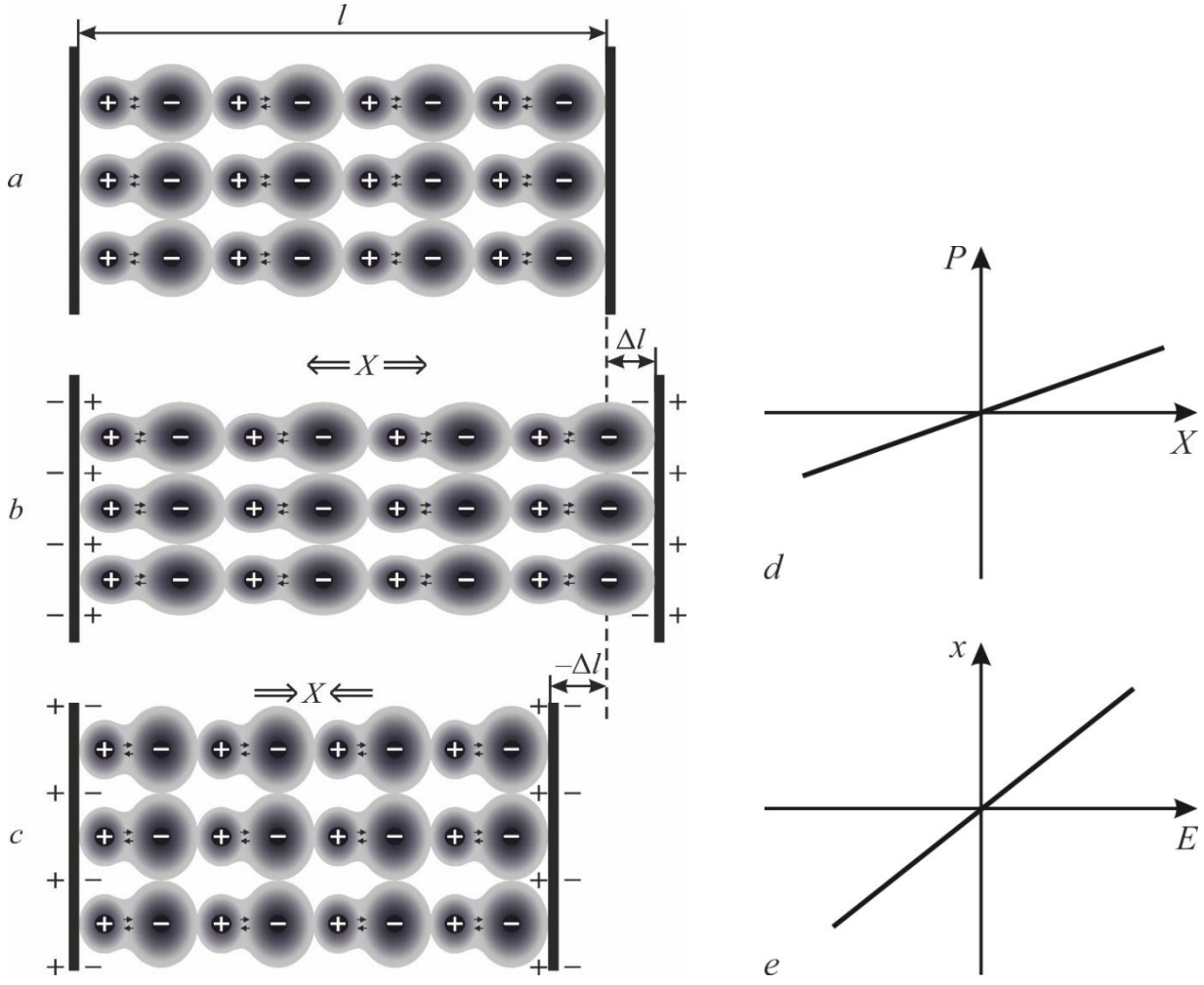

Fig. 6.3. Simple model of direct longitudinal piezoelectric effect, explanations are given in the text

If a given model, piezoelectric is investigated or used in the mode of *strain sensor*, when induced charges flow into input of amplifier (in this case crystal is the *source of current*). If studied crystal would be electrically open, then electrical potential will occur and it will exists for some time (this is the *voltage-source* mode), but afterwards induced voltage gradually decreases being neutralized due to a small but still final electrical conductivity. In any case, polarization dependence on stress is *linear*, as shown in Fig. 6.3D: $P = d \square X$ where d is piezoelectric module. The change in the sign of mechanical stress, Fig. 6.3C leads to the compression of model crystal and to change of electrical polarization sign, as well as to change of sign of compensating charges. As can be seen from Fig. 6.3D, the dependency $P(X)$ remains linear.

Since piezoelectric effect is reversible, the previous test, performed mentally with the model shown in Fig. 6.3, could be carried out in the reverse order, i.e., by applying electrical field and obtaining longitudinal deformation, which depends on the sign of field, i.e., to simulate the *converse piezoelectric effec*t: $x = d \square E$, where $\Delta l/l$ is mechanical strain, Fig. 6.7E.

It should be noted that simplest model presented here for the *longitudinal* piezoelectric effect can describe also the *volumetric* piezoelectric effect, since the uniform compression leads, in particular, to change in the *length* of a chain and produce corresponding electrical response (at that, any change in transverse dimensions remains electrically neutral).

As already noted, the piezoelectric effect may be not only longitudinal, but also might be the transverse and the share effects.

2. *Transverse piezoelectric effect* can be explained using *planar* model resembling structural features of hexagonal α-quartz); simplified explanation of this effect is presented in Fig. 6.4, where the *hexagon* with positive silicon ions and negative ions of oxygen forms planar *non-centrosymmetric structure*.

[***Note***. When piezoelectric effect describing in literature [1–4], it should be noted that usually any microscopic models are avoided, so explanations are limited to piezoelectric symmetry given by formal crystallography. However, at present, when piezoelectric effect is investigated and used in the *nanoscale structures*, the microscopic models might be useful].

Next the two-dimensional square sample made of piezoelectric-active material is considered, Fig. 6.4B, in which the *inscribed hexagon* symbolically shows mutual arrangement of electrical charges with three polar-neutral axes x', x'' and x'''.

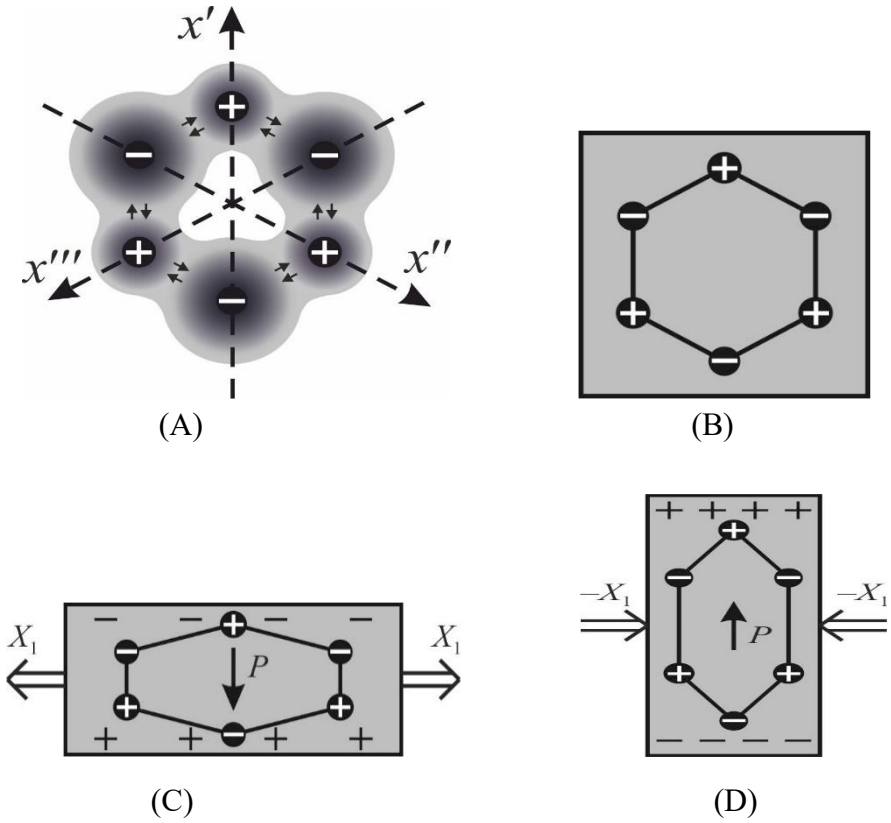

Fig. 6.4. Simplified model of transverse piezoelectric effect: A – model cross section of quartz perpendicularly of 6-order axis; B – "piezoactive square" model C, D – longitudinal stress induces transverse polarizations

Original structure shown in Fig. 6.4B is *electrically neutral*, moreover, under *uniform* (scalar type) compression or tension, which can change the volume of considered square, it remains totally electrically neutral. Thus, in discussed model, the volumetric piezoelectric effect can not arise (in contrast to quasi-one-dimensional structure shown earlier in Fig. 6.3, where the *pyroelectric symmetry* is used.

In basis of discussed here structure is the α-quartz, which has rather complex spiral structure, but main “structural motive” is the hexagon, in which silicon and oxygen ions can be alternating traced: there are two oxygen ions per silicon ion. So in the symbolic projection of two layers of this spiral structure, Fig. 6.4A, the sign “+” should be understood as ion Si^{+4} while the sign “–“ means two oxygen ions having sign “–4”.

The directional (tensor type) mechanical action onto considered piezoelectric-active square sample, Fig. 6.4C, produces the *transverse effect* (not longitudinal). Due to stretching stress applied along the horizontal axis, the electrical polarization is induced, however, not in same direction, but perpendicularly to it. When the sign of stress changes, Fig.6.4D, induced polarity also changes its sign: this is the linear

transverse piezoelectric effect. Longitudinal piezoelectric effect in this model also would be possible, if mechanical stress ill be applied along the $x - x'$ axis.

3. *Share piezoelectric effect* can be explained by images shown in Fig. 6.6. As model sample, the piezoelectric-active cube is used now, which structure has *three polar-neutral axes*, (i.e., this cube is a cut from crystal having quartz symmetry). At that, one of axes of a cube is directed along *x*-direction (i.e., along one of direction of crystal internal polarity). As well as in the case of "piezoelectric square" considered before, this piezoelectric-active cube not reacts electrically to any *scalar* action (i.e., neither pyroelectric nor volumetric piezoelectric effect are possible in this sample). But the *directional* (tensor) actions allow in this model get both the longitudinal and the transverse piezoelectric effects.

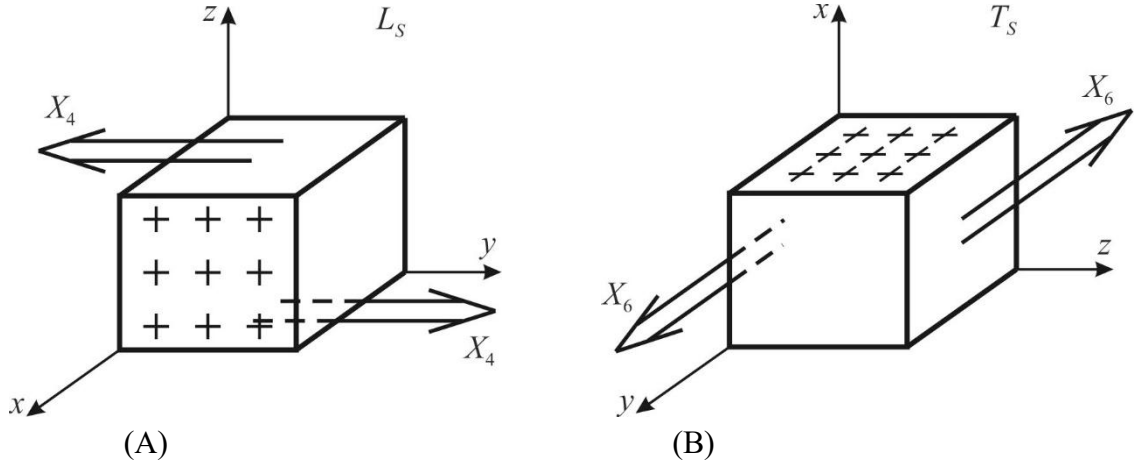

Fig. 6.5. Models representation of longitudinal (A) and transverse (B) shear piezoelectric effects

However, in the case shown in Fig. 6.5, the sample made of piezoelectric-active cube is used here only to the explanation of *shear-type* mechanical action. Firstly, such action may be applied *perpendicularly* to *x*-axis of a chosen sample, and exactly along it mechanically induced electrical polarization occurs, Fig. 6.9A. That's why corresponding piezoelectric effect is called the *longitudinal shear effect*, L_S. However, another share piezoelectric effect is also possible, namely, the *transverse share effect,* L_T, shown in Fig. 6.5B.

In general case of low-symmetric crystal, *three* longitudinal *L*-effects, *six* transverse *T*-effects, *three* longitudinal shear L_S-effects and *six* transverse shear L_T-effects can be observed. In the crystals of lowest symmetry and in some slanting cut of others polar crystals the maximum number of piezoelectric modules can be 16. However, in practically applied piezoelectrics, when the basic installation of crystal is used, this quantity is much smaller what will be shown below.

4. ***Induced by electrical field piezoelectric effect*** in external electrical field manifests essentially in dielectrics which have big permittivity (peculiar for paraelectrics and relaxor ferroelectrics) in form of linearized electrostriction Q_e [5, 8].

The deformation as an *even* function of polarization can be given by the fast converging series: $x = Q_eP^2 + Q_e'P^4 + ...$ In not very large electrical fields, it might be confined by the first member of this series.

When discussion of possible application of piezoelectrics, suppose that polarization contains two components: the first (P_b) is induced by bias (controlling) electrical field, which leads to induced piezoelectricity, and the second component ($P_\sim$) which is due to "dynamic field" $E_\sim$ exciting dynamic piezoelectric response:

$$x = Q_e (P_b + P_\sim)^2 = Q_eP_b^2 + 2Q_eP_bP_\sim + Q_eP_\sim^2.$$

If not take into account parametric interactions, that is, assuming $P_b >> P_\sim$, last term in a given expression can be neglected. In addition, it can be supposed that polarization $P_\sim$, which excites piezoelectric response, is fast-changing influence compared to P_b ($P_\sim$ usually changes much faster than controlling field). In this case, the determined by P_b deformation of paraelectric can be considered constant ($x_b = Q_eP_b^2$). Thus, electrostriction for variable field looks like linearized and may be perceived as piezoelectric effect:

$$x = 2Q_eP_bP_\sim = d \cdot E_\sim,$$

where d plays the role of piezoelectric module caused by electrostriction Q_e and depending on bias electrical field strength. Taking into account that in the paraelectrics $\varepsilon >> 1$, it is possible to have

$$P_b = \varepsilon_0(\varepsilon - 1)E_b \approx \varepsilon_0\varepsilon E_b; \quad P_\sim = \varepsilon_0(\varepsilon - 1)E_\sim \approx \varepsilon_0\varepsilon E_\sim; \quad x_\sim = dE_\sim \approx 2Q\varepsilon_0^2\varepsilon^2E_bE_\sim.$$

Denoting further a field which induces piezoelectric effect through $E_b = E$, the artificial piezoelectric module is

$$d = 2Q_e\varepsilon_0^2\varepsilon^2E.$$

In cases of electrically induced piezoelectricity and electrical control by parameters of piezoelectric devices, following physical effects are used:

· *Forced induction of noncentrosymmetric structure* in nonpolar dielectric by strong electrical field application. As known, external field transforms the structure of any dielectric into artificially polar structure, causing piezoelectric activity. At that, external electrical field by influence on the speed of sound can change the frequency of "piezoelectric resonator" (made of non-polar dielectric) using electrically induced piezoelectric effect. Electrostriction of ordinary dielectrics is small, but in some dielectrics such as rutile ($\varepsilon = 100$) or strontium titanate ($\varepsilon = 300$) the electrically induced piezoelectricity is perceptible [9, 10].

· *Sound velocity change* by external electrical field in classical piezoelectrics (quartz, langasite, potassium dihydrogen phosphate, niobium lithium, silicosilenite) by means of electrical control of elasticity coefficients (Young's modulus) of crystal. In normal piezoelectric material, due to large internal bonding, this effect is small but allows, for example, change a little the frequency of piezoelectric resonator. At that, due to high electromechanical quality factor of these piezoelectrics (such as quartz or lithium niobate) this effect of frequency control becomes technically applicable, for example, in the SAW convectors (processors for pulse convolution).

· *Domains polarization change* in the ferroelectrics using electrical field by influencing domain orientation. The control field changes both velocity and attenuation of sound, which causes electrical reorganization of piezoelectric devices. However, electrical control of piezoelectric effect in ferroelectrics is characterized by hysteresis and relatively low operation speed, due to inertia of domain reorientations.

· *Electroinduced piezoelectric effect in paraelectrics* is particular but important case of piezoelectric effect induced by electrical field. In this case electrical field changes the frequency of *soft transverse optical mode* of lattice oscillation that strongly affects all properties of paraelectric. Electrical control of resonant frequency of piezoelectric resonators made of paraelectrics reaches several percents, that is two orders of magnitude higher than frequency conversion of resonators made from classical piezoelectric crystals and is order of magnitude superior to frequency controlling of resonators made from ferroelectric ceramics.

A distinctive feature of electrically induced piezoelectric effect is the possibility of piezoelectric activity appearance (in particular, piezoelectric resonance) only at the moment of switching on of electrical control voltage; at that, the speed of control of resonator parameters can exceed frequency of 10 kHz.

6.3 Direct piezoelectric effect

Piezoelectric effect is always the result of *force action* onto a polar crystal; at that, the force might be mechanical stress or electrical voltage, while the responses of a crystal are electrical polarization or mechanical strain. The *direct* piezoelectric effect is a result of the *mechanical action*; to simplify the problem, further only the *homogeneous* and *centrosymmetric* actions on the piezoelectric will be considered. As was previously shown in Fig. 6.1, in relation to particular piezoelectric sample, mechanical stresses might be longitudinal, transverse, share and hydrostatic.

The simplest case of *longitudinal* piezoelectric effect is demonstrated in Fig. 6.6: in a sample made of polar crystal, under the action of negative or positive stress the electrical polarization appears which shows *linear* dependence on a stress.

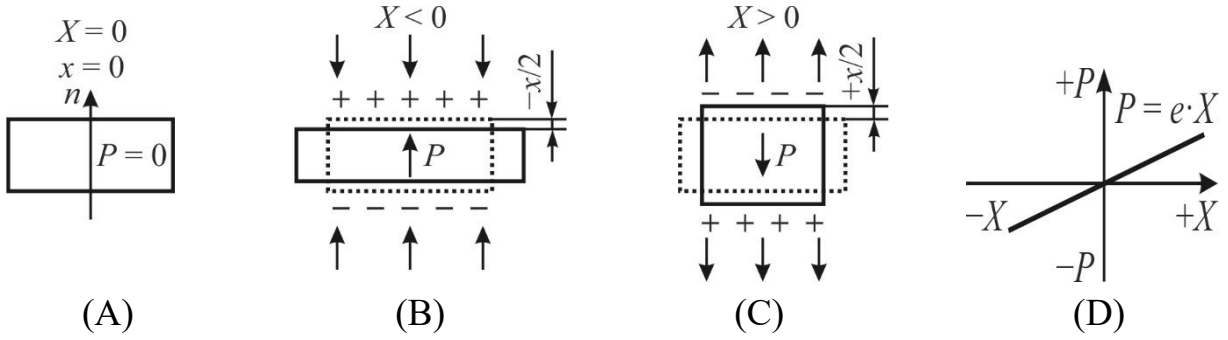

Fig. 6.6. Direct piezoelectric effect: A – plate of polar crystal with vertical directed polar axis in unexcited state; B – compressive stress $-X$ is applied to the plate; C – tensile stress $+X$ is applied to the plate; D – linear dependence of induced polarization on applied stress

In accordance with first observation of piezoelectric effect by Curie brothers, the equations of direct piezoelectric might have a form:

$$P_i = d_{ijk} X_{jk}, \qquad (6.1)$$

where P_i are components of polarization vector (tensor of first rank); $i,j,k = 1, 2, 3$ in accordance with the Cartesian x, y and z axes; X_{jk} are components of mechanical stress (second rank tensor) and d_{ijk} are components of piezoelectric module (tensor of third rank). It will be recalled that repeating indices j and k in the expression (6.1) meant summation; thus presented in shortened form equations of direct piezoelectric effect in their expanded form would be looked like three equations and each of them has six terms in their right-hand side. Correspondingly, there must be 27 coefficients, which connect three components of polarization vector P_i and the nine components of stress tensor X_{jk}:

	X_{11}	X_{12}	X_{13}	X_{21}	X_{22}	X_{23}	X_{31}	X_{32}	X_{33}
P_1	D_{111}	d_{112}	D_{113}	d_{121}	d_{122}	d_{123}	d_{131}	d_{132}	d_{133}
P_2	D_{211}	d_{212}	d_{213}	d_{221}	d_{222}	d_{223}	d_{231}	d_{232}	d_{233}
P_3	D_{311}	d_{312}	d_{313}	d_{321}	d_{322}	d_{323}	d_{331}	d_{332}	d_{333}

If these 27 components would be represented in the form of matrix – it will look as three-dimensional image inconvenient for practical use. However, in fact, due to the *symmetry* of stress tensor: $X_{jk} = X_{kj}$ the tensor of piezoelectric modules is symmetric for last two indices: $d_{ijk} = d_{ikj}$ that decreases possible number of independent components of piezoelectric modulus tensor to 18 (all of them really exists in the crystals of lowest symmetry).

In this case, significantly simplified *matrix representation* of piezoelectric modules is commonly accepted, as more convenient is to use *shortened* matrix record of a third-rank tensor, At that, first index of tensor d_{ijk} remains unchanged over the value of i = 1, 2, 3, but two other indices j and k, which also have values 1, 2 and 3, "collapse" in one index m = 1, 2, ..., 6 according to rule given in Table 6.1.

Table 6.1

Replacement of tensor indices on matrices ones

Tensor indices *i, j, k, l*	11	22	33	23 and 32	31and 13	12 and 21
Matrices indices *m, n*	1	2	3	4	5	6

In the matrix record, equation of direct piezoelectric effect takes the form:

$$P_i = d_{im} X_m. \qquad (6.2)$$

Now in the right side of these equations there are not nine but six members of sum. Moreover, it can be seen clearly that, in fact, the number of independent piezoelectric modules even for lowest symmetry crystals can be no more than 16. Each of these components is the coefficient of proportionality between corresponding component of electrical polarization P_i and mechanical stress component X_m which generates the polarization P_i:

	X_1	X_2	X_3	X_4	X_5	X_6
P_1	d_{11}	d_{12}	D_{13}	d_{14}	d_{15}	d_{16}
P_2	d_{21}	d_{22}	D_{23}	d_{24}	d_{25}	d_{26}
P_3	d_{31}	d_{32}	D_{33}	d_{34}	d_3	d_{36}

Thus, such important characteristic of polar crystals as piezoelectric module cannot be described by *one number* (as density or melting point of a crystal), but it is complex characteristic represented by either a matrix or a bulky figure, such as shown in Fig. 6.7.

In fact, the number of non-zero components of matrix of piezoelecric modules can be quite small, if choose not slant plate of a crystal, but its main crystallographic installation. At that, the lower symmetry, the smaller number of non-zero components in matrix. As an example, the matrix of piezoelectric modules of quartz (SiO_2) is shown:

$$d_{im} = \begin{bmatrix} d_{11} & d_{12} & 0 & d_{14} & 0 & 0 \\ 0 & 0 & 0 & 0 & d_{25} & d_{26} \\ 0 & 0 & 0 & 0 & 0 & 0 \end{bmatrix}, \text{ where: } \begin{cases} d_{11} = -d_{12} \\ d_{25} = -d_{14} \\ d_{26} = 2d_{11} \end{cases} \qquad (6.3)$$

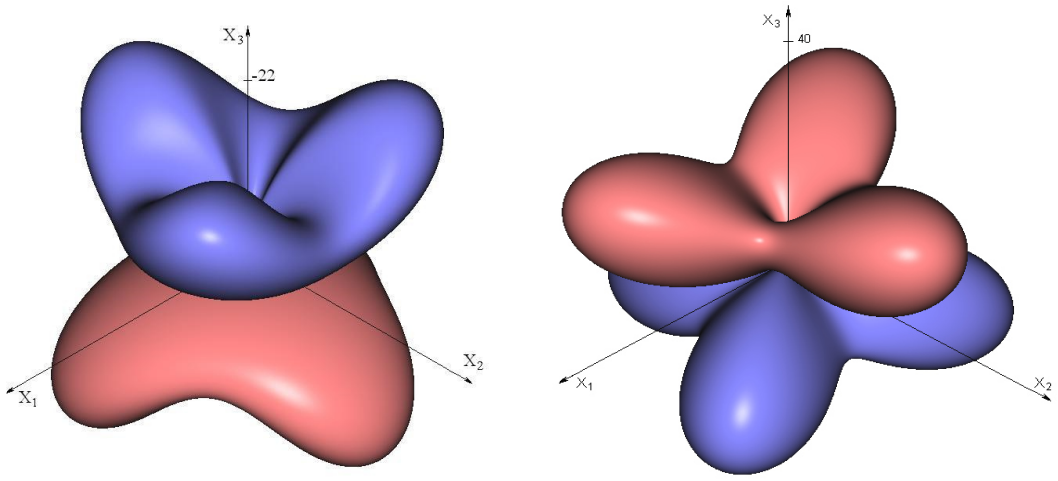

(A) (B)

Fig. 6.7. Indicative surfaces of transverse (A) and longitudinal (A) piezoelectric effects in $LiNbO_3$ [5]

As seen, of 18 possible components of possible piezoelectric modulus in the main installation of quartz crystal only five positions in matrix (6.3) are non zero, at that, only two components of d_{im} remain independent. Strong anisotropy of piezoelectric properties of quartz is clearly traceable: along the axis $Z = 3$ no linear electromechanical reactions are possible while as longitudinal so transverse piezoelectric effects are manifested only along the axis $X = 1$.

1. *Figures of merit in piezoelectrics* are the quite different parameters.

Piezoelectric module d_{11} characterizes the longitudinal piezoelectric effect, i.e., polarization induced along same direction, in which mechanical stress acts. Longitudinal effect is sometimes also called the *L*-effect. The components d_{22} and d_{33} have similar physical meaning characterizing: the longitudinal piezoelectric effects along axes, respectively, *2* and *3*. Therefore, if indexes in matrix record of piezoelectric modulus are same, then these components describe one of three possible longitudinal piezoelectric effects.

Piezoelectric module d_{12} characterizes the *transverse* piezoelectric effect or *T*-effect. In this case elastic stress is applied along axis *2* while piezoelectric effect is observed along axis *1*, perpendicular to axis *2*. Others transverse piezoelectric modules are characterized by coefficients d_{13}, d_{21}, d_{31} and d_{32}, which are components of d_{im} matrix. They express appearance of polarization along one of the axes *1*, *2* or *3* under influence of stretch-compression stresses along one of the axes perpendicular to response axis.

Piezoelectric modulus d_{14} in equation (6.3) characterizes one of the *share* piezoelectric effects; in quartz, two others share modules d_{25} and d_{26} do not equal zero; others share modules $d_{13} = d_{15} = d_{24} = d_{26} = d_{34} = d_{35} = d_{36} = 0$. By example of

share piezoelectric modulus one can see that piezoelectric polarization may occur not only under compression-stretching stress action, but also under the influence of rotatory shifts. Physical meaning of d_{14} looks like this: the pair of forces, applied along axis *2,* induces electrical polarization along axis *1*. Share piezoelectric effect is observed and widely used in many crystals and textures; for instance, widely used in engineering polarized ferroelectric ceramics has two share modules d_{15} and d_{24} and matrix of its piezomodules is same as in barium titanate crystal ($BaTiO_3$):

$$d_{im} = \begin{bmatrix} 0 & 0 & 0 & 0 & d_{15} & 0 \\ 0 & 0 & 0 & d_{24} & 0 & 0 \\ d_{31} & d_{32} & d_{33} & 0 & 0 & 0 \end{bmatrix}, \text{ where: } \begin{cases} d_{24} = d_{15} \\ d_{32} = d_{31} \end{cases}$$

Except for this example, two matrices of piezoelectric modules of most studied piezoelectrics are given below:

For Rochelle Salt (RS) in temperature range of t = (–18 — +24) °C:

$$d_{im} = \begin{pmatrix} d_{11} & d_{12} & d_{13} & d_{14} & 0 & 0 \\ 0 & 0 & 0 & 0 & d_{25} & d_{26} \\ 0 & 0 & 0 & 0 & d_{35} & d_{36} \end{pmatrix};$$

For potassium dihydrogen phosphate crystals (KDP) at any temperature above Curie point (150 K):

$$d_{im} = \begin{pmatrix} 0 & 0 & 0 & d_{14} & 0 & 0 \\ 0 & 0 & 0 & 0 & d_{25} & 0 \\ 0 & 0 & 0 & 0 & 0 & 0 \end{pmatrix}; \text{ at that, } d_{25} = d_{14}.$$

In barium titanate, share piezoelectric modules d_{15} and d_{24} are different from zero, while in the piezoelectric phase of KDP crystals (above Curie temperature) only one share module d_{36} is different from zero. In general case of study or application of *slanting cuts* of piezolectric crystals (as well as in crystals of lowest symmetry) there can be *nine* shear modules: three longitudinal shear modules (L_S) and six transverse shear modules (T_S), Fig. 6.8A shows their difference. Note that the L_S-effect corresponds to modules d_{14}, d_{25} and d_{36} and they are characterized by the fact that induced piezoelectric polarization vector is parallel to the displacement axis and perpendicular to the shear plane. Transverse share displacement, that is, the T_S-effect corresponds to piezoelectric modulus d_{15}, d_{16}, d_{24}, d_{26}, d_{34} and d_{36}. In this case, vector of polarization is perpendicular to displacement axis and lies in displacement plane.

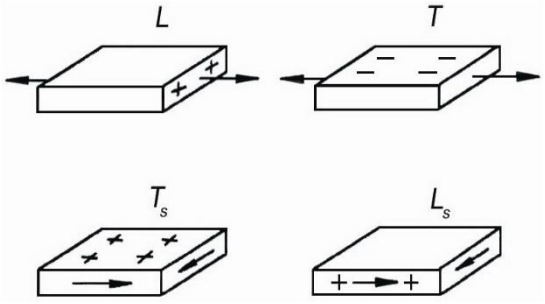

(A)

	X_1	X_2	X_3	X_4	X_5	X_6
P_1	L	T	T	L_s	T_s	T_s
P_2	T	L	T	T_s	L_s	T_s
P_3	T	T	L	T_s	T_s	L_s

(B)

Fig. 6.8. Different types of piezoelectric modules: A – mutual arrangement of initiating deformation and electrical response; B – conditional location of longitudinal and transverse piezoelectric modules in the matrix [7]

The dimensions of piezoelectric modulus follows from relation: $d = P/X$, where $[P] = \text{C/m}^2$ and $[X] = \text{N/m}^2$, therefore $[d] = \text{C/N}$. Piezoelectric modules of different crystals and textures can be significantly differentiated by magnitude and sign: for example, in the ammonium hydrophosphate (ADP) main piezoelectric modules $d_{14} = -1.34\times10^{-12}$ C/N and $d_{36} = 20\times10^{-12}$ C/N (other components of matrix are zero). From these data seen that selected unit of measurement of piezoelectric modulus is too large. Therefore, in practice, it is more convenient to use a unit of pC/N (picoculone per Newton), where 1 pC = 10^{-12} C. For example, in barium titanate $d_{33} = 150$ pC/N, $d_{31} = 70$ pC/N and $d_{15} = 250$ pC/N, at that $d_{24} = d_{25}$ and $d_{32} = d_{31}$.

Expression (6.2) describes only one of four possible variants of direct piezoelectric effect characterizing, namely, for electrically free ($E = 0$) crystal: $P_i = d_{im}\square X_m$. Others *idealized* boundary conditions leads to three more equations also describing direct piezoelectric effect:

$$P_i = e_{in}\square x_n;$$
$$E_j = -g_{jm}\square X_m; \qquad (6.4)$$
$$E_j = -h_{jn}\square x_n.$$

Here and in future only matrix record of the components of third rank tensors e_{in}, g_{jm} and h_{jn} is used. These piezoelectric coefficients, like piezoelectric modulus d_{im}, characterize piezoelectric properties of noncentrosymmetric crystals and textures. Units of measurement of all these piezoelectric parameters are:

$$d = \text{C/N}, \qquad g = \text{V·m/N}, \qquad e = \text{C/m}^2; \qquad h = \text{V/m}.$$

In the literature, these modules are called differently [Uchno], but mostly as d is piezoelectric module, g is piezoelectric stress constant, e is piezoelectric strain constant and h is piezoelectric voltage constant. All of these piezoelectric parameters

can be independently determined experimentally, the principles of these measurements are shown in Fig. 6.9.

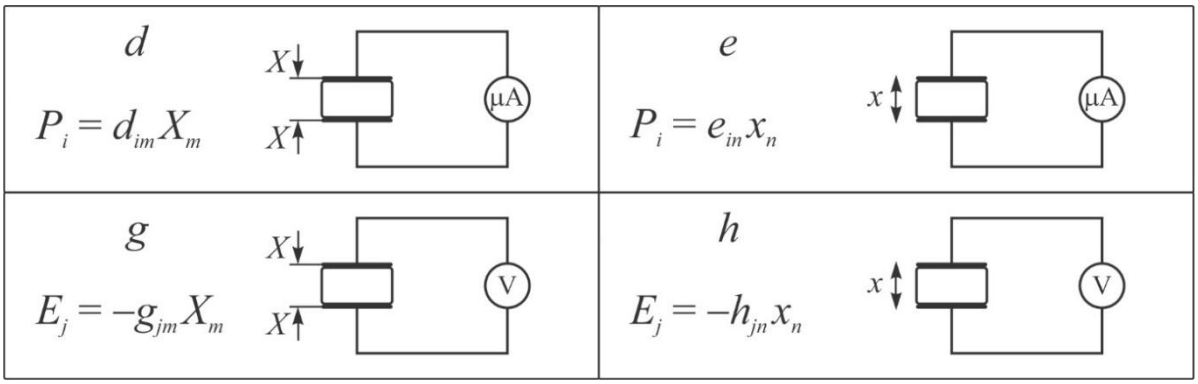

Fig. 6.9. Experimental determination of various modules in case of direct piezoelectric effect [5]

In accordance with considered in Chapter 1 boundary conditions, while d_{im} measuring the component of mechanical stress tensor X_m, acting on piezoelectric, is determined, as well as the component of electrical polarization vector P_i arising from this action, Fig. 6.9, *d* (at that, stress intensity component X_m is measured as result of division of force F acting on area S of piezoelectric element). This method of piezoelectric module measuring is a static; exactly such method was used while piezoelectric effect was first detecting.

To determine the piezoelectric constant e_{in} ($P_i = e_{in} x_n$) using induced by *strain* x_n direct piezoelectric effect, crystal must be electrically free ($E = 0$) and mechanically free ($X = 0$). Mechanical deformation) can be determined by dilatometer, while measuring of induced polarization is reduced to the definition of electrical charge arising on piezoelectric surface, whose value is measured by current passing through microammeter μA, Fig. 6.9, *e* (as known, polarization equals to surface charge density on electrodes). In turn, when coefficients g_{im} and h_{jn} determination, the voltmeter V can be used, which shows potential $U = E \cdot t$ induced by crystal deformation or by mechanical stress, accordingly. The larger the thickness of sample *t,* the higher is potential *U*.

[***Note***. A question might arise as to how deformation appears in a piezoelectric, if vector of electrical field and tensor of mechanical deformation do not act to the polar crystal. The fact is that homogeneous (scalar) change of temperature leads to crystal thermal expansion-compression, so electrical polarization in it appears by secondary pyroelectric effect, as well as hydrostatic (scalar) change of pressure results in strain x_n – this is volumetric piezoelectric effect].

In addition to direct measurements, each of four piezoelectric coefficients can be *calculated* using others coefficients, if elastic parameters (c_{mn} or s_{mn}) and tensor of permittivity ε_{ij} (or converse tensor $\beta_{ij} = \varepsilon_{ij}^{-1}$) are known. For example, from equation (6.1) $P_i = d_{im}X_m$ and from Hook's low $X_m = c_{mn}x_n$ follows $P_i = d_{im}c_{mn}x_n$. Comparing this expression with equation (6.4), it is possible to obtain one of equations connecting two piezoelectric coefficients: $e_{in} = d_{im}c_{mn}$.

However, in this and other similar relationships, the conditions at which components c_{mn} and s_{mn} are defined cannot be ignored: for the short-circuited ($E = 0$) or the open-circuited piezoelectric ($D = 0$), since $c^E_{mn} \neq c^D_{mn}$ and $s^E_{mn} \neq s^D_{mn}$. Others relations between piezoelectric coefficients include components of tensors ε_{ij} or β_{ij}, which differ for mechanically free (ε^X_{ij} or β^X_{ij} when $X = 0$) and mechanically clamped crystals and textures (ε^x_{ij} or β^x_{ij} that means $x = 0$).

In accordance with relation (6.2), which corresponds to direct piezoelectric effect and taking into account electrically free crystal, it should be determined that elastic stiffness will be included in this relation with a superscript E. Consequently, this ratio must be written in form: $e_{in} = d_{im}c^E_{nm}$. Similarly, to determine piezoelectric module d_{im} in direct piezoelectric effect piezoelectric also needs to be electrically free ($E = 0$), so the piezoelectric module must be determined as follows: $d_{im} = e_{mj}s^E_{mn}$

Other ratios of piezoelectric coefficients are given below in more complete equations, which take into account the conditions for determining the dielectric and elastic parameters:

$$d_{mj} = \varepsilon_0\varepsilon^X_{ij}g_{mi} = e_{nj}s^E_{mn} = \varepsilon_0\varepsilon^x_{ij}h_{ni}s^E_{mn};$$
$$e_{mi} = \varepsilon_0\varepsilon^x_{ij}h_{mj} = d_{ni}c^E_{mn} = \varepsilon_0\varepsilon^X_{ij}g_{nj}c^E_{mn};$$
$$g_{mi} = (\beta^X_{ij}/\varepsilon_0)d_{mj} = h_{ni}s^D_{mn} = (\beta^x_{ij}/\varepsilon_0)e_{nj}s^D_{mn};$$
$$h_{mj} = (\beta^x_{ij}/\varepsilon_0)e_{mi} = g_{ni}c^D_{mn} = (\beta^x_{ij}/\varepsilon_0)d_{ni}c^E_{mn}.$$

2. *Electromechanical coupling factor K_{coup}* is one of important figures of merit as for piezoelectric materials so for elements of piezoelectric devices. It reflects the *interconnection* of electrical and mechanical properties in non-centrosymmetric crystals and textures which demonstrate piezoelectric effect. Electromechanical coupling can be investigated by various experimental and theoretical methods.

Due to piezoelectric is the energy convertor, its electrical and elastic properties need to be considered together. The point is that in polar-sensitive crystal any change in its mechanical state leads to change in its electrical state, and vice versa [7]. The square of electromechanical coupling factor shows what amount of energy brought to piezoelectric (W_{br}) is converted into other type of energy (W_{conv}):

$$K^2_{coup} = W_{conv}/W_{br}$$

At that, any energy losses (mechanical damping and dielectric losses) are not included in this expression, so the K_{coup} it is not efficiency coefficient.

In case of *direct piezoelectric effect*, the mechanical energy received by piezoelectric is spent not only onto deformation (when elastic energy W_{elas} is accumulated) but also spent onto electrical polarization, which causes the accumulation of electrical energy W_{elec}:

$$K_{\text{coup}}^2 = \frac{W_{\text{elec}}}{W_{\text{elec}}} = \frac{W_{\text{elec}}}{W_{\text{elas}} + W}. \tag{6.5}$$

Coupling factor K_{coup} might be different at various boundary conditions when crystal might be mechanically free or clamped and electrically short-circuited or open-circuited. As electrical so elastic energy are defined by the quadratic forms. Energy of electrical polarization can be expressed through the electrical field E and induction D, using permittivity ε and inverse permittivity β :

$$W_{\text{elec}} = \frac{1}{2}ED = \frac{1}{2}\varepsilon_0\varepsilon E^2 = \frac{1}{2}\left(\frac{\varepsilon_0}{\beta}\right)D^2. \tag{6.6}$$

By the same way, mechanical energy is defined by strain x or stress X, as well as by stiffness and compliance characterizing elastic process:

$$W_{\text{elas}} = \frac{1}{2}xX = \frac{1}{2}cx^2 = \frac{1}{2}sX^2, \tag{6.7}$$

In addition to these relations, electromechanical coupling factor can be defined as the ratio of elastic energy density to density of elastic and electrical energy:

$$K_{\text{coup}}^2 = \frac{W_{\text{em}}^2}{W_{\text{elas}}W}.$$

where in mechanically clamped piezoelectric $W_{em} = d \cdot X \cdot E$ while for mechanically free piezoelectric $W_{em} = e \cdot h \cdot E$, at that $d = P/X$ and $e = P/x$.

Although factor K_{coup} is a scalar parameter, it depends on direction of external influences and on other causes. For example, polarized ferroelectric ceramics (which is a texture of $\infty \cdot m$ symmetry) can be identified by 12 different coupling coefficients, depending on the system of boundary conditions (and possible forms of piezoelectric sample), as well as on manner of clamping and fixing. Numerical values of K_{coup} are defined by piezoelectric material properties. Most crystals, ceramics and textures used in practice have K_{coup} = 0.1–0.5, although in some crystals in their particular orientation K_{coup} reaches value of 0.8– 0.96.

In case of a *direct* piezoelectric effect, the electromechanical coupling factor can be calculated, if main parameters of piezoelectric are known. Taking into account the contribution to polarization from direct piezoelectric effect $P_{piezo} = d \square X$, equation of electrical induction $D = \varepsilon_0 E + P = \varepsilon_0 \varepsilon E$ takes the form:

$$D = \varepsilon_0 \varepsilon E + d \square X. \quad (6.8)$$

Accordingly, in the equation for linear deformation (Hooke's law $x = s \square X$) the piezoelectric contribution to deformation from converse piezoelectric effect $x_n = d \square E$ should be taken into account:

$$x = s \square X + d \square E. \quad (6.9)$$

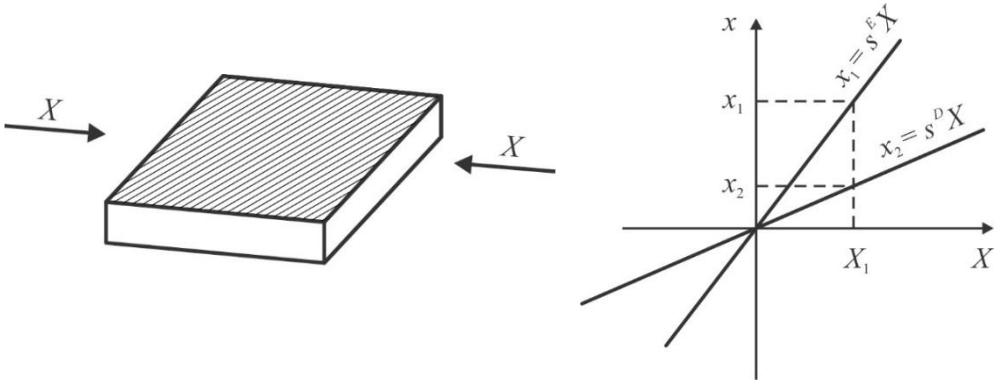

(A) (B)

Fig. 6.10. Difference in elastic compliance in piezoelectric: A – mechanical action on piezoelectric plate; B – Hooke's law in open-circuited (s^D) and in close-circuited (s^E) polar crystal [5]

Next, direct piezoelectric effect in sample plate made of noncentrosymmetric crystal will be considered, Fig. 6.10. Suppose that homogeneous mechanical stress X acts on piezoelectric plate, as a result of which it deforms remaining electrically opened ($D = 0$). Accordingly, from equation $D = \varepsilon_0 E + P = \varepsilon_0 \varepsilon E$ it is possible to obtain $E = -(d/\varepsilon_0 \varepsilon)X$. By substituting it in the (6.9), obtain next relation

$$x = (s - d^2/\varepsilon_0 \varepsilon) \square X. \quad (6.10)$$

In the brackets there is new tensor of elastic compliance, corrected for piezoelectric effect. As can be seen from formula (6.10), due to piezoelectric reaction the compliance of plate *decreases* (correspondingly, its stiffness increases). Therefore, by applying mechanical force $X = X_1$ the plate does not deform to value of $x = x_1$ (as if it were in the absence of piezoelectric effect), but only to value $x = x_2 < x_1$. The work of external forces brought to a plate (W_{br}) spents not only on the elastic deformation with accumulation of *elastic* energy (W_{elas}), but also on creation of *electrical* energy of polarization (W_{elrc}). Under these conditions, deformation of piezoelectric plate becomes lesser ($x - x_1$) as reduced elastic energy compensates appearance of electrical energy.

Using equation (6.10) and formula for elastic energy ½ $s \cdot X^2$, it is possible to determine the mechanoelectric contribution to energy:

$$W_{elas} = W_{br} - W_{eec} = ½\, s \cdot X^2 - ½\, (d^2/\varepsilon_0\varepsilon)X^2.$$

Changed energy in this case, obviously, is electrical energy W_{elec}. Substituting obtained expressions into formula (6.5), the coupling factor can be found:

$$K^2_{coup} = W_{elec}/(W_{elas} + W_{elec}) = ½\, (d^2/\varepsilon_0\varepsilon)X^2/(½\, sX^2) = d^2/(\varepsilon_0\varepsilon \cdot s). \qquad (6.11)$$

It should be noted that the ratio of energies in (6.11) does not depend on the amplitude of fields (mechanical stress X or electrical field E). Thus, coupling factor K_{coup} is a parameter *characterizing given piezoelectric*.

Multiply the numerator and denominator in the formula (6.11) on ½ E^2X^2:

$$K^2_{coup} = (½\, d{\cdot}E{\cdot}X)^2/[(½\, \varepsilon_0\varepsilon E^2)(\, ½\, s \cdot X^2)] = W^2_{em}/(W_{elec}{\cdot}W_{elas}).$$

Denominator represents a product of energies $W_{elec} = ½\, \varepsilon_0\varepsilon E^2$ and $W_{elast} = ½\, s \cdot X^2$, while the numerator corresponds to electromechanical energy $W_{em} = ½\, d \cdot E \cdot X$.

3. *Elastic properties dependence on electrical boundary conditions.* While studied mechanical properties of piezoelectric, a significant difference in the elastic compliance of short-circuited (s^E) and open-circuited (s^D) polar crystals is observed. Under the influence of outside stress, Fig. 6.10A, strain is linearly increased, Fig. 6.10B in accordance with a Hooke's law. However, if piezoelectric is electrically close-circuited, its elastic compliance will be bigger than in the case when crystal is open-circuited. The reason is that the piezoelectric voltage generated by mechanical strain in open-circuited crystal *increases its harshness* (resistance to deformation).

By comparing of expressions (6.11) and (6.10), it is possible to verify that elastic compliance reduces in $(1 - K^2_{coup})$ times: $d^2/\varepsilon_0\varepsilon = K_{coup} \cdot s$. However, in case of close-circuited crystal ($E = 0$), piezoelectricity does not affect elastic compliance s^E. In same way, for considered case compliance s^D of open-circuited piezoelectric ($D = 0$) is reduced. Expression (6.10) can be rewritten:

$$x = (s^E - d^2/\varepsilon_0\varepsilon)X = (s^E - K^2_{coup}\, s^E)X = s^D X;$$

$$s^D = s^E(1 - K^2_{coup}).$$

From above relations the important expression follows for electromechanical coupling factor:

$$(s^E - s^D)/\, s^E = K^2_{coup}. \qquad (6.12)$$

Correspondingly, elastic stiffness c_{mn} (where $m,\ n = 1, 2, \ldots 6$), which is the tensor converse to tensor of elastic compliance s_{mn}, also can be obtained from formula (6.13):

$$(c^D{}_{mn} - c_{mn}{}^E)/\, c^D{}_{mn} = K^2_{св}. \qquad (6.13)$$

In Chapter 2, Fig. 2.5B large difference between elastic stiffness of close-circuited (c^E_{14}) and open-circuited (c^D_{14}) in Rochelle Salt crystal was shown. In this

figure, throughout a given range of temperatures Rochelle Salt is piezoelectric. In the Curie points elastic stiffness c^E_{14} of close-circuited crystal changes very much, being almost at order of magnitude different from c^D_{14}. Therefore, the strong influence of *electrical conditions* on the *mechanical properties* of ferroelectrics is evident.

Since the speed of elastic (sound) waves is are determined by elastic stiffness c and density ρ of a crystal

$$v_{sound} = (c/\rho)^{1/2},$$

then difference in elastic stiffness $c^D - c^E$ leads to the differences in speed of sound in the open-circuited and close-circuited crystals. From Fig. 2.5 in Chapter 2 it follows that velocity of sound in the direction, corresponding to stiffness component c_{44} of Rochelle Salt in both Curie points decreases several times as compared with room temperature. This means that due to piezoelectric effect elastic stiffness of piezoelectric might vary considerably.

4. ***Main applications of direct piezoelectric effect.*** There are various engineering approaches for comparing piezoelectric materials [11–14]. For piezoelectrics intended for use as acoustic *signal receivers*, it is necessary to provide high sensitivity at low noise levels. If such piezoelectric receivers are employed in the liquid environments, they are called *hydrophones*, if such devices are used in the air, they are called *microphones.* In general, in electronics, instrumentation, medical technology, such use of piezoelectrics can be generalized by such concepts as *piezoelectric sensors*.

In order to assess suitability of piezoelectric element, following quality factor is often used for receiver material: $d_{i\mu}/\varepsilon_{i\mu}{}^{1/2} = K_{res}$; this parameter characterizes efficiency in the mode of receiver, that is, to convert mechanical energy into electrical one. Taking captured the most famous piezoelectric quartz as the unit of K_{res}, it can be obtained that this value for piezoelectric ceramic is 4–6 times higher than for quartz: for lithium niobate crystal 8 times higher, for a PVDF polymer film 12 times higher, and 25 times for Rochelle Salt. By these data should be guided during the design and application of piezoelectric receivers or sensors.

Piezoelectric sensors use direct piezoelectric effect, at that piezoelectric modules g and h should be used for most convenient parameters for assessing the sensory capability of those or other piezoelectric devices. Direct piezoelectric effect was considered above in the idealized boundary conditions, and following equations for piezoelectric effect were given: $E_i = -g_{im} \cdot X_m$ and $E_i = -h_{in} \cdot x_n$. In this case, the piezoelectric voltage constant g_{im} is defined as the ratio of piezoelectric module d_{nj} to dielectric constant ε_{nj}: $g_{im} = d_{mj}/\varepsilon_{ij}$ and characterizes the electrical field E arising

in a piezoelectric under applied stress X. Therefore, the dimension [g] is: (V/m)/(N/m) = V□m/N. Another piezoelectric constant, h, can be defined also as the product of the coefficient g on corresponding Young module for certain direction in the crystal; respectively, and the dimension h equals: V/m.

Piezoelectric crystals are *direct converters* of mechanical energy into electrical one. The efficiency of such transformation can be expressed through mechanoelectric coupling coefficient of K_{ME}, the square of which equates the product of piezoelectric modules g and h; $K^2_{ME} = d_{mj}□h_{mj}$. The listed coefficients are important characteristics for such cases when it is necessary to ensure high efficiency of energy transfer, for example, in the acoustic and ultrasound sensors. For practical devices, exactly the charge q_x generated on the surface of piezoelectric converter is important; it is proportional to the force F_x, which acts along the x-axis: $q_x = d□F_x$. A piezoelectric plate with electrodes deposited on it is capacitor C. The voltage V on this capacitor is determined by expression: $V = Q/C = d□F/C$. In turn, capacity can be expressed through dielectric permittivity ε, surface of electrode S and thickness of crystal l (only the electrode area is taken into account, but not area of crystal itself, since piezoelectric induced charge accumulates only on electrodes): $C = \varepsilon\varepsilon_0 S□l$. Then expression for electrical voltage on piezoelectric sensor takes form: $V = d□F/\varepsilon\varepsilon_0 S$.

Piezoelectric sensory elements can be used either in a simple lamellar form or in the form of multilayer structure, in which individual plates are joined together by means of electrodes placed between them. For example, in Fig. 6.11A shows the two-layer power sensor. When external force is applied to this sensor, one of its parts is expanded while other is compressed, which leads to doubling of output signal (double sensors can be activated in parallel or sequentially). Piezoelectric sensor has very high output impedance; so to coordinate with subsequent electronic circuits it is necessary to use special interfaces representing voltage converters in current, or voltage amplifiers with high input resistance.

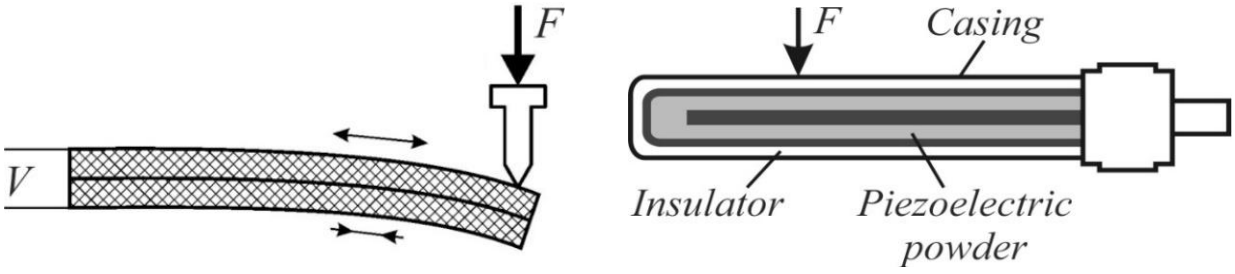

(A) (B)

Fig. 6.11. Piezoelectric sensors: A – two-layer (bimorph) piezoelectric force sensor; B – piezoelectric cable (*F* is dynamic mechanical load) [12]

Next example, in Fig. 6.11B, shows piezoelectric application in *seismic cables*. They are essentially vibration or power sensors implemented as cables, in which electrical signal appears on the internal conductor, Fig. 6.11B. Piezoelectric cable consists of metal casing covered outside by layer of insulation, and inside contains the densely pressed piezoelectric ceramic powder enveloping inner metallic rod. To give such a cable piezoelectric properties, its sensitive component (ceramic powder) must pass the thermal polarization procedure. Sensor does not register constant (not changing in time) force: the only dynamic change in mechanical force generates electrical signal. Mechanoelectrical sensors are used for a variety of purposes: monitoring vibration of compressors and engines for analysis of traffic flow on motorways, etc.

Piezoelectric materials for force sensors need peculiar combination of properties, namely, the large ratio of piezoelectric modulus to permittivity. Such is, for example, lithium sulfate crystals (Li2SO4), which are often used in hydrophones. This piezoelectric is used also for detector heads in the ultrasonic defectoscopy. Next example is lithium tetraborate crystals (Li2B4O7), which have been developed for use in the receiving mode. This crystal has small value of permittivity ($\varepsilon 33 = 10$) and relatively small piezoelectric module: d33 = 34 pC, but the special for hydrophones parameter g33 = 0.27 V/m² in Li2B4O7 is greater than for others piezoelectrics. For comparison, piezoelectric module of widely used piezoelectric ceramics (d33 = 450 pC/N) is 13 times larger but parameter g33 = 0.03 V/m² is 10 times smaller than in lithium tetraborate.

Vibration sensors that use piezoelectric effect are widely applied in airplanes, electric generators, accelerometers etc. These sensors operate in frequency range of 2Hz–5kHz and are characterized by high attenuation of noise, high linearity and wide temperature range (especially when quartz crystals are used as sensitive elements). When piezoelectric crystals are applied in the accelerometers, they are located between the casing and *inertial mass,* which makes acting force proportional to acceleration. Ceramic piezoelectric films are also used in accelerometers: in this case they are the *microsensors* usually deposited on silicon. During formation of integrated silicon microsensors, thin film of piezoelectric ceramic are usually deposited onto silicon console. Piezoelectric signal is amplified by microelectronic circuit embedded in same microdevice with piezoelectric sensor.

Acoustic sensors application is much wider than simply detecting vibrations and sound signals. Such are the micro-scale apparatus and devices based on surface acoustic waves, realized on the principle of detecting mechanical vibrations in solids. Such sensors are used to measure displacements, to determine the

concentrations of components, to measure mechanical stress, force and temperature. Solid-state detectors often form the basis of more complex sensors, such as chemical analyzers, biological research, etc. According to characteristics of surface waves propagation, it is possible to obtain necessary information about biological objects or chemical components on the surface of a film. The use of high-sensitivity piezoelectric devices allows achievement a significant success in the visualization of ultrasonic fields, which resulted in significant increase in resolution, in particular in case of use of acoustic holography techniques, for increasing operating frequency of probing beams.

In medicine, progressive development of piezoelectric receivers has greatly facilitated wide introduction of various types of ultrasound flow detection and acoustic emission analysis as well as cardiography and acoustic visualization of internal organs, into practice (including medical). This ensured a sharp increase in the possibilities of medical diagnostics for prevention of complicated cases. Piezoelectric sensors are used in biomedical engineering and "sensorization robots", which have been developing intensively lately. Introducing a piezoelectric catheter with a shell of polarized polyvinylidene fluoride in the middle of the blood vessel, it was possible to implement a precision diagnosis of valve stenosis, cardiomyopathy, and so on. On the basis of polyvinylidene fluoride, a polyfunctional thermotactyl sensor ("artificial skin") for prosthetics and robots is developed. Promising results are obtained during the treatment of bone fractures in the case of wrapping fragments of fissile bones, a bimorphic piezoelectric polymeric film; there is a sharp acceleration of the growth of the osteons in the direction of the force lines of the piezoelectric field, which accelerates the recovery of the patient.

Piezoelectric microphones work in acoustic range that is perceived by humans; however, this name can be used for ultrasonic and infrasound wave detectors. In essence, the microphone is the pressure sensor adapted to convert sound waves in a wide spectral range. Microphones are characterized by sensitivity, direction, bandwidth, dynamic range, size, cost, etc. An important condition for the use of microphones is the harmonization of acoustic impedances of the medium and device. For sound receivers, the value of the acoustic resistance determines the conditions for reconciliation with the medium.

Piezoelectric films made of polyvinylidene fluoride (PVDF) and copolymers have been used for many years to produce pickups for musical instruments. PVDF-based piezoelectric pickups have a very high quality reproduction partly because they have very low *Q*-factor: they do not have their own resonance (as in ceramic pickups), and therefore there is virtually no distortion of signals.

Piezoelectric macrocomposite materials have high hydrostatic sensitivity, for example, ceramics with a structure of "coral" (macrocomposite), where ceramic framework is placed in polymer matrix, which reduces effective permittivity. Macrocomposites also use other materials for hydrophones, created on the basis of thin rods of polarized ceramics, variously bonded and placed in a solid polymer matrix. These materials are significantly superior to sensitivity in the mode of reception not only the usual piezoceramic, but also lithium tetraborate. *Microcomposite* materials are piezoelectric glassceramics: texture of needle microcrystals of lithium tetraborate or other crystals in a glass-phase matrix obtained by rapid melt-fixing under conditions of a sharp temperature gradient. In piezoelectric glassceramics $\sum_{33} = 10$ and $d_{33} = 20$ pC/N so important parameter $g_{33} = 0.1$ V⊕m/N.

Piezoelectric generators of high voltage are very simple in their design and can provide both high voltage (for creating, for example, a spark) and significant power that can be used in the piezoelectric damper of vibrations. Figure 6.12A shows principal design of piezoelectric ignition system: as a rule, two piezoelectric cylinders are designed to work in parallel. Using piezoelectric ceramic cylinders with a diameter of about 10 mm and a length of about 15 mm, it is possible to obtain electrical impulses of 15 – 25 kV in time interval near 50 microseconds.

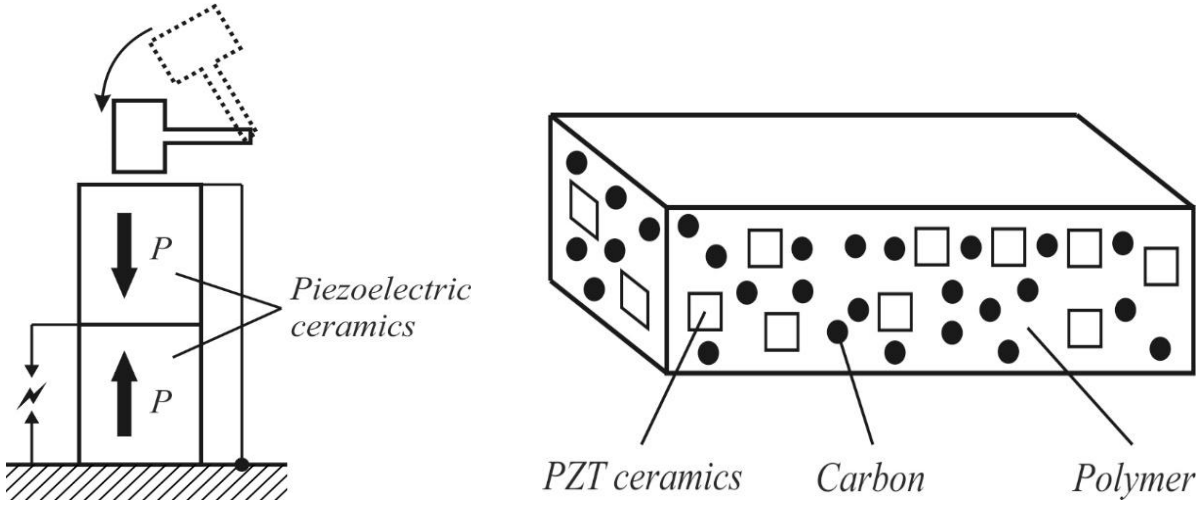

(A) (B)

Fig. 6.12. Application of direct piezoelectric effect at high energies: A – piezoelectric lighter, shown direction of ceramics polarization; B – principle composition of piezoelectric composite for damping of vibrations [3]

Mechanical vibrations dampers are important application of piezoelectric composites. The vibrational object must be elastically connected with the piezoelectric, forming a single system. At that the vibration is transmitted to piezoelectric material and mechanical vibrational energy is converted into electrical

energy due to the direct piezoelectric effect: it is alternating electrical voltage. To suppress vibrations, a *resistive material* is introduced into the oscillatory system, for example, carbon, as shown in Fig. 6.12B; at that, the flexible polymers are used for composite elasticity. Thus, the energy of mechanical vibrations is quickly transformed by piezoelectric and resistor into a heat and vibrations quickly decay. Piezoelectric dampers are used not only in aviation, particularly, in helicopters, but also in industry as well as in household appliances (damping vibrations of mountain skis).

Possible applications of direct piezoelectric effect are difficult to recalculate. The experiments on obtaining piezoelectric energy using energy of sea waves are known: as mechano-electric energy converter, multi-layer thin polymer film (PVDF type), whose area is hundreds of square meters, is used. Experiments were also conducted with the use of a PVDF film for submerged piezoelectric tidal wave power plant immersed in seawater with high power. Successfully were studied implanted into the human body film converters, which convert the mechanical energy of breathing into electrical energy, for example, for driving a continuously acting insulin batcher and the like.

6.4 Converse piezoelectric effect

In case of the *converse* piezoelectric effect, the driving force mainly is the electrical field E, while induced response usually is the mechanical deformation x (or if latter is impossible, mechanical stress arises). As already mentioned before, applied to *any dielectric* electrical voltage causes its deformation, since charged particles of a material are displaced in the process of electrical polarization. Due to this mechanism in all dielectrics the *quadratic* electromechanical effect occurs (electrostriction) but usually it is very small.

However, in the dielectrics with non-centrosymmetric structure another effect is important, namely, the *linear* electromechanical effect. This converse piezoelectric effect was second observation made by Curie brothers, and its equation can be written as:

$$x_n = d_{nj}E_j\,,$$

where $i = 1, 2, 3$ and $n = 1, 2, \ldots 6$ accordingly to matrix marks, d_{nj} is piezoelectric module in matrix record. It is seen that component of strain x_n is directly proportional to magnitude of electrical field E_j applied to piezoelectric. Simplest model of converse longitudinal piezoelectric effect is shown in Fig. 6.13.

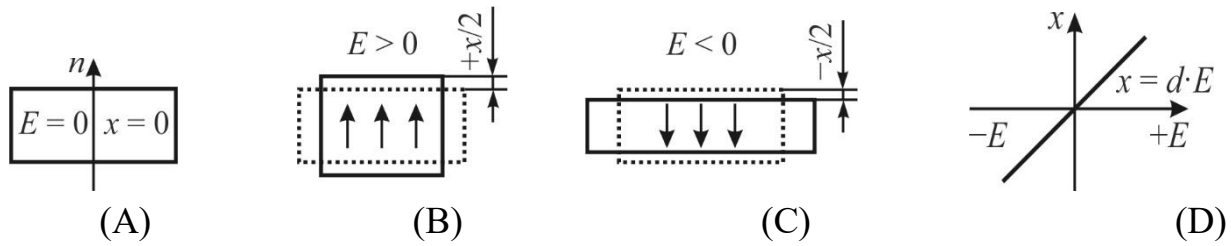

Fig. 6.13. Converse piezoelectric effect: A – polar crystal with vertically directed polar axis *n*; B – applied electrical field leads to crystal expansion; C – when sign of electrical field changes, crystal contract;
D – linear electrical field–strain dependence

The figure shows symbolically how piezoelectric sample is expanded or compressed under the action of electrical field applied along the polar axis *n* of a crystal. The sign of deformation changes with the change in electrical polarity (note that in real experiments, even in strong electrical field value of relative deformation *x* does not exceed one per cent).

1. ***Fundamentals of converse piezoelectric effect.*** Equation (6.14) corresponds to the piezoelectric effect in mechanically free ($X = 0$) and open-circuited ($D = 0$) crystal and includes the same piezoelectric modulus *d* as in the case of direct piezoelectric effect. However, this equation represents only one of possible descriptions of linear electromechanical interaction in noncentrosymmetric crystals and textures. At various boundary conditions, the converse piezoelectric effect can be described by four equations:

$$x_n = d_{nj}E_j; \qquad X_m = e_{mj}E_j;$$
$$x_n = g_{ni}P_i; \qquad X_m = h_{mi}P_i,$$

where d_{nj}, g_{ni}, e_{mj} and h_{mj} are piezoelectric coefficients used in previous Section to describe direct piezoelectric effect.

The converse piezoelectric effect, as well as the direct one, in principal, allows determine all piezoelectric coefficients from experiments, Fig. 6.14.

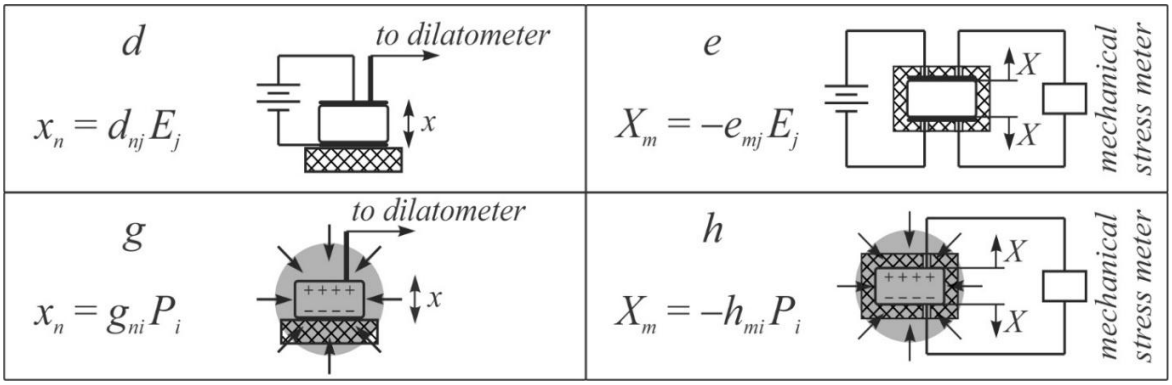

Fig. 6.14. Experimental methods of piezoelectric coefficients measurement, using converse piezoelectric effect

For example, to measure piezoelectric module, Fig. 6.11, *d*, it is necessary, firstly, to know electrical field applied to crystal: $E = U/t$ (where U is electrical voltage supplied from low-impedance source, t is thickness of a sample). Secondly, mechanical deformation Δt induced by electrical field should be obtained using dilatometer that allows find dimensionless relative deformation $x = \Delta t/t$.

The piezoelectric constant e_{mj} in case of converse piezoelectric effect is more difficult to determine, Fig. 6.14, *e,* since crystal must be mechanically clamped ($x = 0$). Therefore, measuring element that determines mechanical force F which is created by piezoelectric of area S ($X = F/S$) must be mounted in the massive casing which prevents piezoelectric deformation. It is obvious that experimental realization of such a method in the static mode is not reasonable, but the *dynamic* mode of measurement can be successfully carried out at *elevated frequencies* – higher than frequencies of own mechanical resonances of piezoelectric sample (when it can not be deformed).

In principal, it is possible, using converse piezoelectric effect, to determine experimentally piezoelectric coefficients g_{ni} and h_{mi}. In these experiments, the sample of piezoelectric might be polarized by external *scalar action* (uniform variation of hydrostatic pressure). In the case of g_{ni} measurement, the deformation should be found by dilatometer, Fig. 6.14, *g*; while in the second case a pressure needs to be found, Fig. 6.14, *h*.

The use *four* different piezoelectric coefficients for piezoelectric effect description is justified by various examples of piezoelectrics technical application. For example, when choosing piezoelectric material for the ultrasound *emitters,* which are usually used in sonar (in home appliances – in washing machines), rather big mechanical deformations must be generated by the converse piezoelectric effect under influence of electrical voltage. In this case, in order to evaluate the effectiveness of various piezoelectric materials, they must be comparing by the magnitude of piezoelectric module d (according to equation $x = d \cdot E$).

Piezoelectric cells are also applied as ultrasound *receivers*, but the requirements for them are peculiar: it is necessary to use direct piezoelectric effect to obtain maximum electrical voltage from piezoelectric element – the "effort sensor", which uses piezoelectric coefficient g. In this case the best piezoelectrics are those which have highest coefficient $g = d/\varepsilon_0\varepsilon$. In other cases, for example, to evaluate the performance of piezoelectric adapters, the coefficients h and e might be important.

Above mentioned equations of piezoelectric effect (both direct and converse) characterize different connections between mechanical parameters X and x and

electrical parameters of P and E. To summarize the problem, these equations can be presented in the form of diagram – the *piezoelectric square* (Fig. 6.15) in the corners of which parameters x, X, P and E are located.

The left vertices of a square show the mechanical stress and strain with their linear relationship, depicted by the straight line, symbolically characterizes different representation of Hooke's law: $x = s \square X$ or $x = c \square x$. The right tops of square pictured in Fig. 6.15 corresponds to electrical field E and polarization P, as well as the connecting line reflects electrical interaction: $P = \varepsilon_0 \chi E$ or $E = (\varepsilon_0 \chi)^{-1} P$.

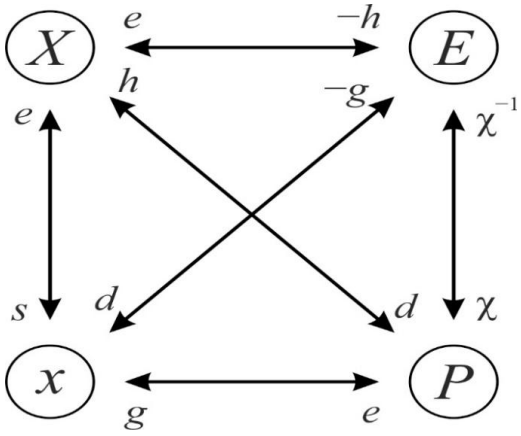

Fig. 6.15. Relationship of main parameters describing piezoelectric effects [7]

Horizontal lines as well as diagonals of a square in Fig. 6.15 characterize eight linear equations of direct and converse piezoelectric effects. Near the straight lines of these connections all piezoelectric coefficients are depicted. The piezoelectric coefficient, located closer to arrow near connection line, must be multiplied by the parameter nearest to it. For example, upper line of piezoelectric square corresponds to two equations of piezoelectric effect $P = d \square E$ and $X = h \square P$, while the lowest line symbolizes equations $x = d \square E$ and $E = - h \square x$.

In previous Section, several matrixes of piezoelectric modules are shown for the *principal installations* of some crystals, and it was seen that most of 18 possible components in these matrices are zero. For example, in quartz crystal there are only 5 of non-zero components of piezoelectric modules (of which 2 are independent), in barium titanate they are respectively 5 and 3, while in KDP crystal only 2 and 1. It is obvious that a considerable interest is: how much of *non-zero components* of piezoelectric modules can be seen in all 20 classes of noncentrosymmetric crystals, in which piezoelectricity can be observed.

All these classes are listed in Table. 6.2; there notations are given in the international classification, where main symmetry elements of these classes listed. Table 6.2 shows the number of non-zero components of *permittivity* tensor for all 20 piezoelectric classes of crystals, as well as for elastic stiffness (or compliance)

tensors and the number of non-zero components of piezoelectric coefficients tensors. From the Table 6.2 it follows that with increasing symmetry of crystals the number of independent components of tensors becomes smaller. The number of non-zero components of piezoelectric modules reduces to 2 or 3 of which only one component is independent in last classes of piezoelectric crystals; such piezoelectrics are the easiest objects to study.

Table 6.2.

The number of components of basic "material" tensors of piezoelectric crystal classes [7]

Crystal symmetry	Syngony of lattice	Number of non-zero components ε_{ij}	Number of independent components ε_{ij}	Number of non-zero components c_{mn}	Number of independent components c_{mn}	Number of non-zero components d_{in}	Number of independent components d_{in}
1	Triclinic	9	6	36	21	18	18
2 *M*	Monoclinic	5 5	4 4	20 20	13 13	8 10	8 10
222 *Mm*2	Ortho-rhombic	3 3	3 3	12 12	9 9	3 5	3 5
4 422 □4 4*mm* □42*m*	Tetragonal	3 3 3 3 3	2 2 2 2 2	16 12 16 12 12	7 6 7 6 6	7 2 7 5 3	4 1 4 3 2
3 32 3*m*	Trigonal (rhombo-hedral)	3 3 3	2 2 2	24 18 18	7 6 6	13 5 8	6 2 4
6 □6 622 6*mm* □6*m*2	Hexagonal	3 3 3 3 3	2 2 2 2 2	12 12 12 12 12	5 5 5 5 5	7 6 2 5 3	4 2 1 3 1
23 □43*m*	Cubic	3 3	1 1	12 12	3 3	3 3	1 1
∞□*m*	Polarized ceramics	3	2	16	7	5	3

The matrix of elastic stiffness c_{mn} and its converse matrix of elastic compliance s_{mn}, in principal, would have of 6×6 components but these matrixes are symmetric with respect to main diagonal; therefore, in general case, maximal number of independent components in them equals 21 (that is really seen in triclinic crystals).

The increase in number of symmetry elements in crystals causes the growth of zero components of c_{mn} or s_{mn} matrixes and the decrease of independent

components number. As a result, for most symmetric cubic crystals in the matrix of elastic stiffness only three independent components of 12 nonzero are counted. In the case of *centrosymmetric* crystals (these symmetry classes in Table 6.2 are not given), all 18 components of piezoelectric coefficients are zero, that is, they have no linear electromechanical effect (piezoelectric effect) but in them there should be the quadratic effect – electrostriction.

Ferroelectric ceramics is considered as main piezoelectric material. Typically, the non-polarized (isotropic) ferroelectric ceramics after synthesis has "sphere symmetry" (the largest possible symmetry in solids).

Technologically ceramics can be converted into the noncentrosymmetric *texture* $\infty \cdot m$ that has "cone symmetry", where there is axis of symmetry of infinite order (∞) and symmetry plane m passing through this axis. In the process of this technology, strong electrical field is applied to the ceramics at elevated temperatures.

As a result, ferroelectric domains, which initially were oriented in ceramics chaotically, become reorient along applied field, forming rather stable unipolar texture of domains.

After switching off polarization field this structure is long-term stored its polar properties and has a set of elastic parameters and piezoelectric coefficients, which corresponds to tetragonal crystals of class 4*m*.

2. ***Effective permittivity in piezoelectrics***. Different mechanisms of electrical polarization were considered above in Section 1. However, in the polar-sensitive crystals (piezoelectrics and pyroelectrics), to the “basic permittivity”, which is due to *microscopic* processes of polarization (ionic, electron, dipole), the *macroscopic* polarization is added, which are conditioned by the electromechanical ε_{EM} or electrothermal ε_{ET} reaction of polar sample studied as a whole.

Next only piezoelectric dielectric contribution $\sum EM$ will be considered (electrothermal contribution $\sum ET$ is discussed in Chapter 4).

Electrical induction is characterized by equation $D = \sum 0 \sum E$, where $\varepsilon 0$ is electrical constant in SI and ε is permittivity conditioned by some elementary polarization mechanisms.

In such piezoelectric which can be freely deformed in applied electrical field, it is necessary to take into account also the piezoelectric effect: $P = ex$, where e is piezoelectric coefficient and x is mechanical deformation:

$$D = \sum 0 \sum E + ex. \qquad (6.14)$$

In the same way, piezoelectric coefficient e can be found from electrical contribution to mechanical stress, using converse piezoelectric effect $X = - eE$. As a result, general stress in piezoelectric is:

$$X = cx - eE.$$

The condition of free deformation of piezoelectric in electrical field is the absence of mechanical stress in it (X = 0); as a result of which next equation implies:

$$x = eE/c.$$

By substituting of this expression into equation (6.14), it can be obtained:

$$D = \sum 0 \sum E + (e2/c) = (\sum 0 \sum + e2/c)E \qquad (6.15)$$

As can be seen from this expression and from Fig. 6.16, piezoelectric reaction increases electrical induction. In the mechanically clamped crystal, when strain is impossible (x = 0), electrical field E1 induces D1 = ∑0∑E1x. However, in the mechanically free crystal (X = 0) in the same field of E1 the induction is greater: it is D2 = ∑0∑E1X.

Piezoelectric reaction is additional mechanism to the electrical polarization, because it imitates corresponding contribution to permittivity. If piezoelectric is mechanically clamped, then ε = εx, but if it is free, then ε = εX. The above equations imply the relation betweenεx and εX:

$$\sum X = \sum x + e2/\sum 0c \qquad (6.16)$$

In practice, at low frequency the ∑X is measured, since the piezoelectric reaction of sample under study is easy establishing, and the electromechanical deformation contributes to permittivity increase.

But at sufficiently high frequency (higher than frequencies of all piezoelectric resonances), when sample's own mechanical inertia does not allow its strain in external field (x = 0), the permittivity ∑x is measured.

Experimental comparison of dielectric permittivity of free and clamped piezoelectric crystals was shown in Section 2 in Fig. 2.5 on examples of well-known ferroelectrics.

At that, in the Rochelle Salt crystal piezoelectric effect is observed throughout studied temperature range, and everywhere in range of research ∑X > ∑x.

In the vicinity of Curie ferroelectric points, the effect of mechanical clamping is particularly large: ∑X/∑x H 50.

In other studied crystal, barium titanate, above Curie point in cubic (centrosymmetric) phase ∑X = ∑x = ∑ since there is no piezoelectric effect. But below Curie point in the single-domain (polarized) BaTiO3 crystal near room temperature this ratio is approximately two. In the polarized ferroelectric ceramics this ratio is ∑X/∑x < 2.

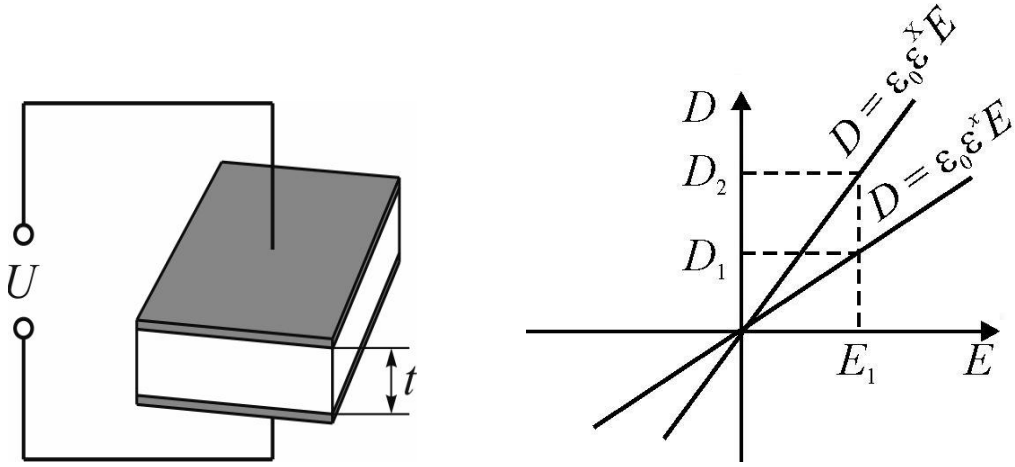

(A) (B)

Fig. 6.16. Electromechanical contribution to permittivity: electrical induction D depending on electrical field E for mechanically free (X = 0) and clamped (x = 0) piezoelectric

3. ***Electromechanical interaction at converse piezoelectric effect.*** Relations (6.5) and (6.12) were obtained when considering direct piezoelectric effect. In a similar way, it is possible to determine the K_{coup} from converse piezoelectric effect, when the *electrical energy* is brought to crystal and, in addition, leads to its elastic deformation. Since piezoelectric is assumed to be mechanically free, initial equations change in comparison with (6.8) and (6.9). In the equation to electrical induction $D = \varepsilon_0\varepsilon E$, the piezoelectric effect of mechanically free crystal should be taken into account: $D = \varepsilon_0\varepsilon E + ex$ (6.14). Moreover, to the mechanical stress, as shown above, the electroelactic contribution to stress $X_n = cx - eE$ needs to be added. As a result, the piezoelectric reaction appears as additional mechanism of electrical polarization, which causes appropriate contribution to permittivity $\varepsilon^X = \varepsilon^x + e^2/\varepsilon_0 c$ (6.16). The condition of free deformation of piezoelectric in electrical field is the equation $X = 0$, so it was obtained $D = \varepsilon_0\varepsilon E + (e^2/c)E = (\varepsilon_0\varepsilon + e^2/c)E,$ (6.15)

Expression (6.15) allows determine electromechanical coupling factor for the converse piezoelectric effect:

$$W_{br} = W_{elec} + W_{elas} = \tfrac{1}{2}\,\varepsilon_0[\varepsilon^x + e^2/(\varepsilon_0 c)]E^2 = \tfrac{1}{2}\,\varepsilon_0\varepsilon^X E^2,$$

where $W_{elec} = \tfrac{1}{2}\,\varepsilon_0\varepsilon^x E^2$ и $W_{elas} = \tfrac{1}{2}\,(e^2/c)E^2$.

As a result:

$$K^2_{coup} = W_{elast}/(W_{elas} + W_{elec}) = e^2/\{\varepsilon_0 c[\varepsilon^x + e^2/(\varepsilon_0 c)]\}.$$

Obtained relations make it possible to determine K_{coup} from the ratio between dielectric constant of free and clamped crystals

$$\varepsilon^X = \varepsilon^x + K^2_{coup}\,\varepsilon^X; \quad \varepsilon^X - \varepsilon^x/\varepsilon^X = K^2_{coup}. \qquad (6.17)$$

From formulas obtained it is possible to get the ratio of mutual energy of electromechanical energy W_{EM} to product of mechanical (elastic) energy of electrical energy:

$W^2_{EM}/(W_{elast}\cdot W_{EM}) = K^2_{cou}/(1 - K^2_{cou})$.

It is seen that in this case the formula differs from the formula obtained during the analysis of direct piezoelectric effect.

The following is considered the variation of elastic medium with density ρ under action of stress X:

$$\rho(d^2x/dt^2) = X, \qquad (6.\ 18)$$

similar to oscillator equation, which describes the variations of mass m associated with elastic force cx: $m(d^2x/dt^2) = -cx$. The role of mass in equation (6.18) is the density ρ. Substituting expression $X = cx - eE$ in (6.18), one can find:

$$\rho(d^2x/dt^2) = cx - eE,$$

and from expression (6.15), taking into account the absence of free charges in the elastic medium (div$D = 0$, $D = 0$), we have:

$$D = \varepsilon_0\varepsilon E + ex = 0.$$

The latter equations mean that spatially variable electric fields excite acoustic waves in a piezoelectric and, conversely, elastic deformations of a piezoelectric medium are accompanied by waves of electric fields. From the general solution of these equations in the approach of plane waves follows the Christoffel equation:

$$(\Gamma - \rho v^2)x = 0, \qquad (6.19)$$

where $\Gamma = c + e/\varepsilon_0\varepsilon$ is the Christoffel tensor (modified tensor of elastic stiffness).

Although equation (6.19) is written for mechanical deformations, electrical potential propagates in piezoelectric with same velocity as elastic displacement. From equation (6.19) it follows that $\Gamma = c(1+K^2_{coup})$. Substituting changed speed $v + \Delta v$ and taking into account that in the absence of the piezoelectric effect and $\Gamma = c$, it is possible to obtain the relation:

$$2\Delta v/v_0 + (\Delta v/v_0)^2 = K^2_{coup}.$$

Typically, the change in velocity of elastic waves in piezoelectrics is small. Therefore, in the above expression one can ignore the term $(\Delta v/v_0)^2$ and assume that $K^2_{coup} \approx 2\Delta v/v_0$.

4. *Simplest devices consideration*. Electromechanical coupling coefficient in piezoelectric devices characterizes the conversion energy of piezoelectric better than a set of elastic, dielectric, and piezoelectric constants. For example, the width of frequency band of electromechanical filter or converter directly depends on the corresponding coupling factor. Moreover, by means of coupling coefficients it is possible to compare piezoelectric materials, which have essentially different permittivity and modulus of elasticity. At that, it should be borne in mind that coupling coefficient is not a tensor, and formulas for tensors transformation in this case can not be used.

The influence of boundary conditions on the magnitude of coupling factor is illustrated by consideration of relatively simple but from the point of view of technique the most important case: the characteristics of *polarized ferroelectric ceramics* having symmetry $\infty\square m$. Depending on shape of ceramic piezoelectric element, on direction of its polarization, on location of electrodes, etc. coupling coefficient may be longitudinal, transverse, radial, thickness, and so on. Piezoelectric ceramics has 11 different coupling coefficients that describe piezoelectric effects in case of electrical field applied *parallel* to polarization axis *Z*, and another coupling factors for electrical field directed perpendicular to axis *Z*. Each of these coefficients corresponds to a certain system of boundary conditions.

As example, a rectangular plate with electrodes deposited perpendicularly to the axis of polarization is considered when mechanical stress is applied along the plate, Fig. 6.14A.

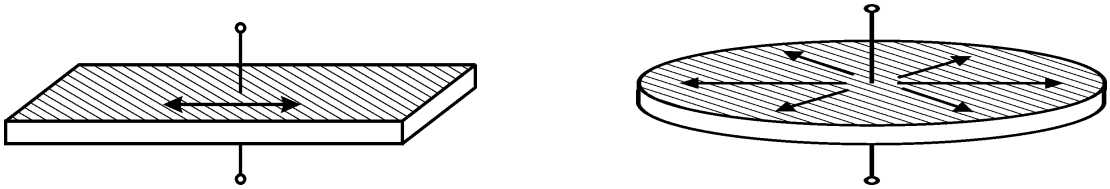

(A) (B)

Fig. 6.17. Piezoelectric oscillations: A – ceramic plate polarized in thickness, B – ceramic disk polarized in thickness (electrodes are shown by shading, deformation is indicated by arrows) [5]

The plate can freely expand in the longitudinal direction, and it is assumed that all other mechanical stresses are zero. Electrical field is applied to the electrodes, in this case the *transverse* coefficient of electromechanical coupling equals to:

$$K_{31} = d_{31}(\varepsilon_{33}s_{11})^{-1/2} . \qquad (6.20)$$

Next, the piezoelectric disk is considered, shown in Fig. 6.17B, with planar system of stresses $X_1 = X_2$ (and assuming that $X_3 = 0$). In this case, symmetry requires that deformation $x_1 = x_2$ and deformation $x_3 = 0$. For the planar deformation, radial coupling coefficient should be determined (in plane perpendicular to polarization axis) in which there is the isotropic mechanical stress:

$$K_{rad} = k_{31}\{2/(1-\sigma)\}^{1/2} \qquad (6.21)$$

where $\sigma = -s_{12}/s_{11}$ is Poisson's coefficient.

For another stresses system, when $X_1 = X_2 = 0$ but $X_3 \neq 0$, the deformation can be realized in the thickness and all deformations in the plane are absent: ($x_1 = x_2 = 0$, but $x_3 \neq 0$). In this case the *thickness coupling coefficient* is determined which characterizes the energy transformation for the case of one-dimensional deformation, and equals to:

$$K_t = h_{33}(\varepsilon_{33}/c_{11})^{-1/2} . \qquad (6.22)$$

Coupling coefficient in the disk thickness K_t corresponds to plate vibration on thickness, while the electrodes are deposited onto largest surfaces, and plate is polarized between these electrodes. Figure 6.18A can serve as illustration of this case, provided that piezoelectric oscillations occur on the higher mode (the main, lower mode is planar mode for which coupling coefficient K_{31} acts). Mode of oscillation in thickness, corresponding to K_t, is observed at much higher frequency, when lateral surfaces of disk can be considered as fixed.

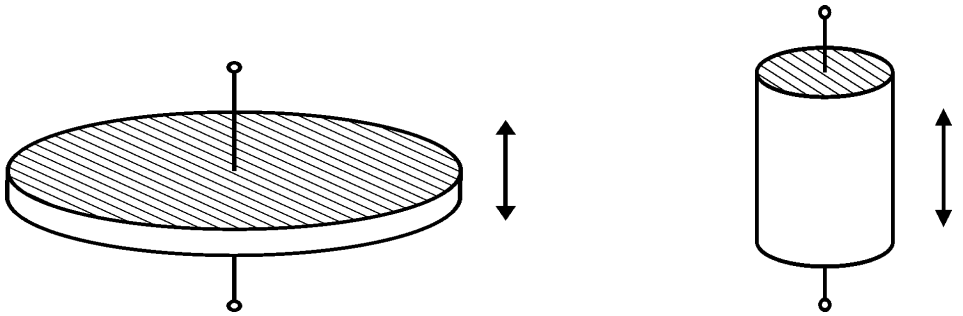

(A) (B)

Fig. 6.18. Examples of piezoelectric oscillations: A – disk polarized and deforming in thickness, B – cylinder polarized in length (electrodes are shown by shading, arrows indicate deformation) [5]

Another important in practice coupling coefficient for piezoelectric elements can be determined by examining the case of one-dimensional stress oriented parallel to Z axis; illustration of this case can be seen in Fig. 6.18B. Characteristic for this case longitudinal coupling is:

$$K_{33} = d_{33}\,(\varepsilon_{33}/s_{33})^{-1/2}. \qquad (6.23)$$

In all above equations, it is assumed that coupling coefficient has the same sign as corresponding piezoelectric modulus d, although, generally speaking, coupling coefficient has no sign. Since in the *dynamic* conditions of vibrations, due to various types constraints, not all mechanical energy is converted into electrical energy (and vice versa), then dynamical coupling coefficients must be smaller than corresponding static coefficients. Differences between them depend on values of coupling coefficients, but usually dynamic coefficients are less then static by 20–25%.

It is clear from the above discussion that there are a large number of coupling factors, and some of them outperform others. In technical applications of piezoelectrics for a given electrical and mechanical conditions it is always possible find a system of mechanical stresses, which corresponds to greatest piezoelectric coupling coefficient.

5. ***Applications of converse piezoelectric effect*** in electronics are based on electrical energy conversion into mechanical energy, mostly for generating sound

and ultrasound in a liquid or air environment [11–14]. Piezoelectrics are also used in contact with a solid, in which ultrasonic or hypersonic waves are excited; in addition, converse piezoelectric effect is a physical basis of piezoelectric drives and motors. The effectiveness of piezoelectric transducer in the mode of radiation is characterized by the coefficient of quality $d_{im}/s_{\text{nm}} = K_{rad}$. Comparison of radiating power of different piezoelectrics might be taken with unit $K_{rad} = 1$ for most famous piezoelectric – quartz. Other piezoelectrics surpass quartz in 2–20 times, however, newly developed crystals of relaxor ferroelectrics more than 50 times more effective than quartz. Nevertheless, most used material is piezoelectric ceramics. As additional criteria for comparing piezoelectric materials, radiation parameter $K^2_{rad}/\tan\delta$ can be applied, which characterizes electromechanical efficiency of transducer, as well as mechanical quality factor Q_m, which determine the acoustomechanical efficiency of emitter.

Energy transformers, depending on frequency range, are subdivided into four types: (1) *sound converters*, i.e., zoomers, vibrators, cellular microphones, high-frequency speakers, sirens, and so on; (2) devices for *ultrasonic technology,* which are used in high intensity emitters for welding and cutting, washing and cleaning of materials, liquid level sensors, dispersion sprays, fog generators, inhalers, air humidifiers; (3) *ultrasonic distance meters* in air environment used as distance meters for motor vehicles, sensors of presence and movement in security systems, as a level meter, as devices for remote control, in the devices for scaring birds, animals and agricultural pests, etc.; (4) *high-frequency ultrasound* devices applied for equipment for testing materials and non-destructive testing, diagnostics in medicine and industry, delay lines, etc.

In liquid medium, the piezoceramics are mainly used as ultrasound emitters having high electromechanical coupling coefficient and high mechanical *Q*-factor. Such emitters are applied in ultrasonic hydrolocation (sonars) and for distant underwater communication. Ultrasound is widely used also in industry to clean the surface.

In solid environment, the thin films of piezoelectrics-semiconductors films (zinc oxide, cadmium sulfide or aluminum nitride) are applied, in most cases for elastic waves operating in ultrahigh frequency range (microwave), i.e., in the hypersound range. In some cases, very thin plates of lithium niobate, obtained by ionic digestion, are utilized in microwave range to generate hypersonic in a media. If sound emitter is a thin film deposited on the surface of solid medium, then, in addition to piezoelectric ceramics, it is advisable to use vapor-deposited CdSe crystalline films and other piezoelectrics, the sputtering technology of which is well

worked out in electronics. Piezoelectric emitters of sound and ultrasound are a part of piezoelectric converters used for radiation of acoustic oscillations, primarily in liquid and solid media.

Piezoelectric emitters made from single crystals are used in the higher-frequency range until the strength limit is affected (in frequencies greater than 200 MHz thickness of transmitter-emitter is several micrometers). In the microwave range, piezoelectric emitters are used on basis of piezoelectrics-semiconductors (with a wide electronic zone). The application of a thin high-strength piezoelectric, working at resonant frequency of longitudinal or transverse oscillations, allows reach frequencies up to 75 GHz. Piezoelectric emitters of these types are used mainly in the acoustoelectronics – in devices operating on SAW.

Scanning acoustic microscope with high-resolution is one of the most striking achievements of modern piezoelectronics because it becomes possible the non-destructive control of submicron elements up to nanometer sizes, which allows investigations without surface damage of scanned crystals chips which do not withstand the effects of electron microscope bundles, as well as X-ray or Auger Probe.

Piezoelectric actuators are solid devices similar to actuators based on magnetostriction and actuators based on thermal expansion. The range of controlled displacement in piezoelectric actuators is similar, but in comparison with magnetic and thermal actuators, in the case of piezoelectrics applying, the precision of displacement is much better. That is why piezoelectric actuators are used in tunnel and atomic force microscopes, which are well known for their high (atomic) resolution. One more advantage of piezoelectric actuators is also their high speed.

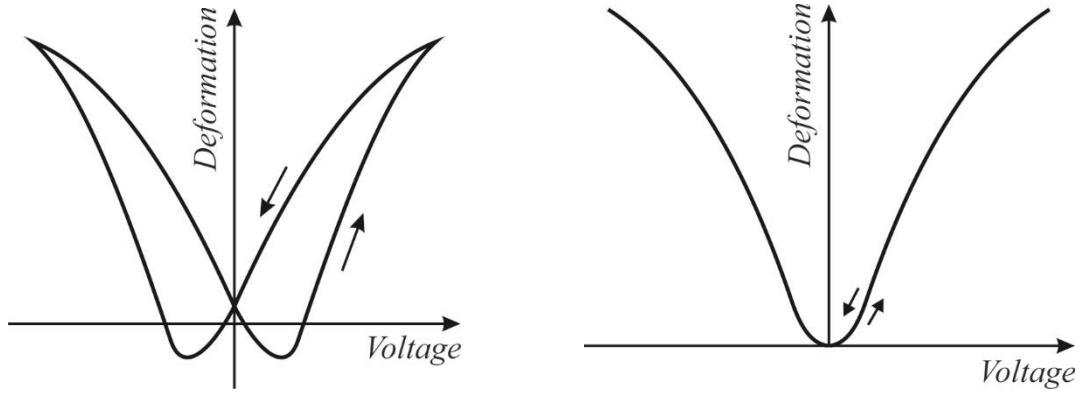

(A) (B)

Fig. 6.19. Comparison of electrically controlled deformation: A – usual piezoelectric ceramics; B – electrostrictive relaxor ferroelectric material of PMN–PT type

This unique feature, together with multi-layer actuator technology, offers important applications for them. The main drawbacks of piezoelectric materials are

high electrical voltage, small deformation and hysteresis, i.e., the ambiguous deformation dependence on control field, Fig. 6.19A. Therefore, considerable efforts of developers are aimed, firstly, at increasing displacement and secondly in development of non-hysteresis materials, Fig. 6.19B.

Piezoelectric actuators are divided on three main groups: the *axial*, in which piezoelectric modulus d_{33} is used, the *transverse* actuators using d_{31}, and the *bending* actuators also using d_{31}. Axial and transverse actuators have common name – multilayer packets, because they are typed in package of many piezoelectric elements (discs, rods, plates or bars). The deformation in axial actuator is provided in longitudinal direction, at that, batch actuators develop a lot of effort. In Fig. 6.20A the principle of construction of axial packet actuator is shown.

Significantly greater deformation can be obtained in the case of piezoelectric plate *bending;* in this case, distinguish: the separate piezoelectric plate (monomorph), the piezoelectric plate coupled with passive elastic plate (unimorph), two counter-polarized ceramics plates (bimorph) and several polarized piezoelectric plates (multimorph), Fig. 6.20B. Bending actuators develop smaller force, but give considerable displacement (hundreds of microns). In general, bending actuators belong to a group of low-power. There are also actuators with a new type of lamellar bimorph, in which the metallic frame forbids lateral deformation and therefore greatly enhance longitudinal deformation ("muni-actuator") [3].

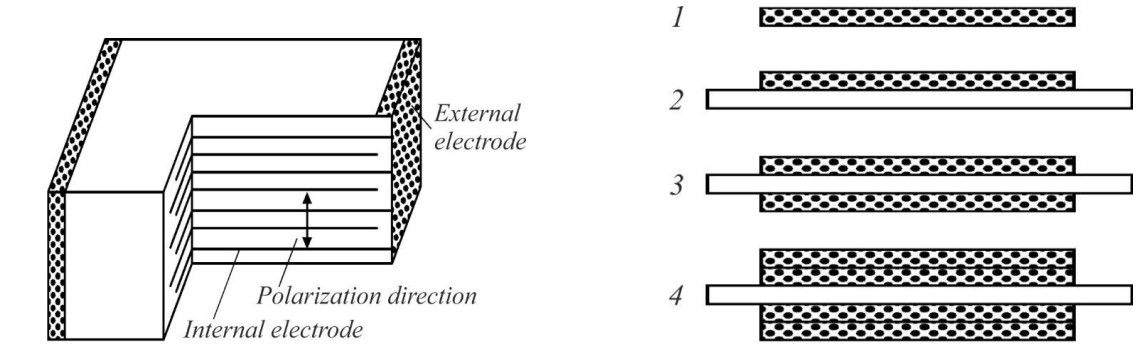

Fig. 6.20. Piezoelectric actuators A – packet of elements, B – bending devices (*1* – monomorph, *2* – unimorph, *3* – bimorph, *4* – multimorph) [3]

Piezoelectric micro-positioners provide the possibility of obtaining electrically controlled mechanical deformations. Relative deformation in strong electrical fields in piezoelectric and ceramics can reach 10^{-3}–10^{-2}; usually electromechanical elements connected in a battery (to reduce control voltage) can develop considerable effort. Such micro-positioners are used in optical communication systems and optical instrumentation, since electrically controlled

mechanical shifts are compared or even exceed optical wavelengths. In particular, they are irreplaceable for the development of multi-elemental orbital telescopes with an aperture of tens of meters.

Piezoelectric motors utilize piezoelectric plate mechanical oscillations which turn into the circular motion of rotor; that is, no wire winding or magnetic fields in such engines. The main material for piezomotors is polarized piezoelectric ceramics. The contact point of oscillating ceramic plate with revolving rotor should be made of steadfast materials (metals or metal cermets) resistant to wear: the life time of piezomotors depends on durability of this mechanical contact. First ultrasonic piezoelectric motors were invented in Igor Sikorsky National Technical University of Ukraine "KPI" by Dr. V.V. Lavrinenko. Then quite various piezoelectric engines were developed: non-reversible and reversible, with passive rotor and active stator, with active rotor and passive stator, with electrical excitation of oscillations of one and two types, and others.

In piezoelectric engines quite different oscillations of piezoelectric elements can be used: compression-stretching, bending, shear, torsional and radial oscillations. The combination of these types of oscillations made it possible to create a large number of different designs of piezomotors, many of which are currently only undergoing engineering review. It is important to develop more durable materials, which will bring the life of the piezoelectric motor to modern level. In electronic devices, piezomotors are used in watches and cameras, tape drives and other mechanical drives, tape recorders and electrophones; they are also used in robotics. Advantages of piezoengines are the economy and simplicity of construction, high stability, the ability to instantly switch on and stop, and absence of magnetic fields (which is especially important for electromechanical magnetic recording devices).

6.5 Electromechanical resonance

Resonance is a sharp increase in the amplitude of forced oscillations, which occurs when the frequency of external influence is brought into some values (resonance frequencies), which are determined by the properties of a system. The increase in the amplitude of oscillations is only a consequence of resonance, but its cause is coincidence of the external frequency (exciting system) with the internal (own) frequency of oscillatory system. With the help of the resonance phenomenon, it is possible to amplify even very weak periodic oscillations. While resonance at a certain frequency, oscillatory system is particularly sensitive to the effect of

excitatory force. The degree of sensitivity in the theory of oscillations is described by the magnitude called *Q*-factor.

Resonance oscillations in a solid elastic body are observed when frequency of the excitatory force is close to frequency of its own oscillations. Any mechanical element is characterized by mass, elasticity and indicator that characterizes irreversible energy losses, for example, friction or emission radiation to the environment. Each mechanical element (mass, elasticity, friction) gives the counteraction (reaction) to the force that affects it, and therefore the oscillatory velocity of their movement depends not only on the magnitude of external force, but also on the reaction of a mechanical element. For solids, the mechanical resistance of any element is defined as the ratio of force to the oscillatory velocity.

Since the mass, elasticity and frictional reactions of mechanical oscillations are of different nature, mechanical resonance has complex nature. In the case of external periodic force, mechanical resistance, due to mass, increases with frequency and equals the product of mass at circular frequency. Due to elasticity the mechanical resistance, on the contrary, is conversely proportional to circular frequency and flexibility of an element.

At low frequencies the reaction of a mass of element is negligible and may not be taken into account, so the value of reaction is determined by elasticity of element. As frequency increases, the reaction of elasticity decreases but mass reaction increases, and finally comes the moment, when at certain frequency mechanical actions of mass and elasticity are equal and compensate each other. Formally, this compensation is due to a difference in the signs of these resistances. Physically, compensation is explained by the fact that at low frequencies external force overcomes only elastic forces and bias coincide with the phase with external force. When the frequency of external force becomes large, it has to overcome mainly the inertia of a mass, adding acceleration. In this case, acceleration phase coincides with phase of external force, while phase of displacement becomes opposite phase of external force (acceleration is second derivative of displacement in time). Consequently, directions of mass and elasticity reactions are opposite.

Resonance phenomenon in the electrical circuit of piezoelectric element is due to resonance of its mechanical oscillations. In the case of piezoelectric resonance, the amplitude of oscillations at same value of exciting electrical field sharply increases, at that, displacement remains in-phase. As a result, dielectric contribution ε_{EM} at resonance frequency ω_r rises sharply. With the increase in displacement frequency of the polar bonds, they become anti-phase relative to exciting field, and ε_{EM} acquires the negative value (anti-resonance at frequency ω_a).

The resonance properties of a piezoelectric quasi-one-dimensional rod can be described by the resonant circuit with two capacitors and inductance. Piezoelectric resonances are repeated if the length l of piezoelectric rod becomes multiplicative, i.e., if $l = \lambda$, $l = 3\lambda/2$, $l = 2\lambda$, and so on. This is accompanied by multiple resonance surges for frequency dependence permittivity (see Fig. 2.3 in Chapter 2). Gradually, with increasing frequency, amplitudes of these bursts is becoming smaller and the electromechanical dielectric contribution is gradually disappearing. It is obvious that frequency of resonances associated with ε_{EM} dependent not only on properties of a crystal, but also on its geometric dimensions.

1. ***Quality factor (or Q-factor)*** of the resonance is important characteristic of oscillatory system, which determines the resonance band and shows how many times energy reserves in a system are greater than the loss of energy in one period of oscillation. If the losses of mechanical or electrical origin in the resonator would absent, then mechanical stresses at the moment of resonance will reach infinitely great value, and resonator would be destroyed. However, mechanical and electrical losses are always present, and such phenomenon is never seen.

Current in the electric circuit of the resonator at resonance always has a finite value and active character, which is determined by presence of losses. Quality is conversely proportional to the rate of attenuation of proper oscillations in the system. That is, the higher the Q-factor of oscillatory system the lower energy loss for each period, and the more slowly oscillations are dying. The general formula for the Q-factor of any vibrational system:

$$Q = 2\pi \square f \square W/P_d, \tag{6.24}$$

where f is frequency of oscillations, W is energy stored in oscillatory system, P_d is dissipation energy. In electric resonance circuit energy dissipates through the final resistance of a circuit; in bulk electromagnetic resonators energy is lost in the walls of resonator, in its material and in contact elements. In the piezoelectric, the oscillation suppression is due to internal friction in a crystal or ceramic.

As well known, for sequential oscillation circuits in electrical RLC circuit, when all three elements are included sequentially: $Q = R^{-1}(L/C)^{1/2}$, where R, L and C are resistance, inductance and capacitance of the resonance circuit, respectively. For a parallel circuit, in which inductance, capacitance and resistance are included in parallel: $Q = R(L/C)^{1/2}$. In the case of electrical circuit, it is much easier to measure the amplitude (current or voltage) than energy or power. Since power and energy are proportional to the square of amplitude of oscillation, the band on amplitude-frequency characteristic (AFC) will be distanced from a peak at about 3 dB. Therefore, another (equivalent) definition of Q factor is used, which relates the width

of amplitude resonance curve Δω at the level with resonance frequency $\omega = 2\pi f$, that is $Q = \omega/\Delta\omega = \omega/2\delta$, where δ is decay damping.

2. *Resonance in piezoelectrics.* Piezoelectric energy converter usually has pronounced resonance properties near internal frequency of oscillations of mechanical system. They are determined by the speed of sound in piezoelectric material and the type of electromechanical oscillations (longitudinal, transverse, radial, bend, etc.).

Experiments show that generalized conductivity of piezoelectric element in the circuit of alternating current, which frequency smoothly varies widely, linearly *increases* with increasing frequency; that is, conductivity has a *reactive* capacitive character. However, this expected logically capacitive type conductivity is violated at some frequencies, at which initially a sharp increase in conductivity occurs, followed by a sharp drop in it, Fig. 6.21. At the moment when conductivity becomes maximal, its character changes – it becomes active. Such active nature of conductivity is also observed at time when it is minimal; in the interval between maximum and minimum values conductivity is *inductive*. Therefore, conduction changes are typically resonant in nature.

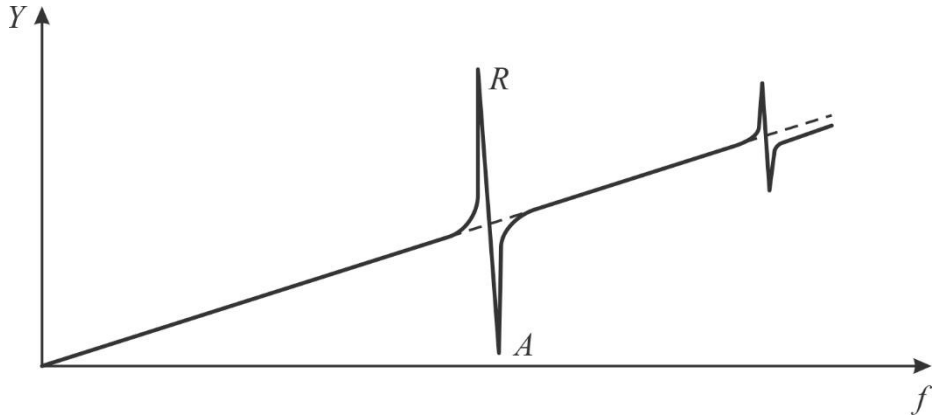

Fig. 6.21. Frequency dependence of conductivity *Y* of piezoelectric element: in points *R* (resonance) and *A* (antiresonance) conductivity is active, between these points its character is inductive while at frequencies below point *R* and above point *A* conductivity is capacitive

To describe characteristics of electrical long lines and circuits with distributed parameters, the equivalent electrical circuits is widespread used, comprised of elements with lumped parameters. Common is also to use such equivalent circuits for piezoelectric resonators, considering that piezoelectric element is usually the mechanical vibrational system with distributed parameters such as mass, elasticity and loss control parameter, for example, friction or acoustic radiation.

In the frequency domain close to resonance, the nature of piezoelectric resonator conductivity change is similar to conductivity of electrical sequential oscillation circuit, shunt by a capacitor. This allows use as a basis for describing

conductivity or resistance in the vicinity of frequencies close to resonance the equivalent electrical circuit (substitution scheme) composed of elements with lumped parameters (inductance, capacitance, and resistance) whose values are constant and independent of amplitude of oscillations and frequencies. Such equivalent circuit in the form of a vibration circuit is depicted in Fig. 6.22A.

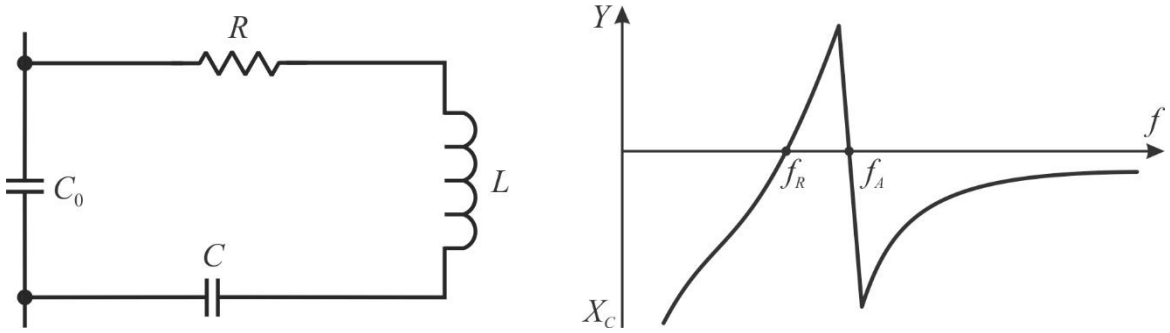

(A) (B)

Fig. 6.22. Piezoelectric resonance: A – equivalent electrical circuit; B – frequency dependence of reactive resistance of the piezoelectric resonator

At frequency $f = f_r$ there is a mechanical resonance, and the current in electrical circuit of piezoelectric resonator reaches maximum value. When frequency increases up to $f_a > f_r$, called the *antiresonance* frequency, impedance of resonator becomes maximal, and current in its circuit is minimal. Piezoelectric resonance corresponds to two resonant frequencies f_r and f_a, at which the resistance of resonator is active. The first resonance, observed at lower frequency, is characterized by low impedance, and the second – at higher frequency – has high resistance.

In other words, lower frequency resonance of equivalent scheme of Fig. 6.22 is caused by the *voltage* resonance (sequential resonance) of circuit, consisting of series of inductance L, capacitance C and resistance R. This branch is called dynamic or piezoelectric; at that, listed elements do not exist physically and their parameters can be determined only in conditions of resonance excitation. The second resonance taking place at higher frequency is the resonance of *currents* or the parallel resonance, occurring in parallel circuit, one branch of which contains capacitance C_0, and the other is consistent connection of the elements L, C and R. This resonance is characterized by high resistance.

Elements of equivalent electrical circuit are called *equivalent* electrical (or dynamical) parameters of the resonator. These are dynamic (equivalent) inductance, dynamic (equivalent) capacity, dynamic (equivalent) resistance and parallel capacity C_0. The reactive dynamic parameters L and C are determined by the elastic, dielectric and piezoelectric coefficients, as well as by the density of piezoelectric. The values

of these parameters essentially depend on orientation of a cut of piezoelectric element, on the type and frequency of excited mechanical vibrations, on the size of elements and electrodes. The dynamic resistance of R depends on internal friction and sources of other mechanical losses. Losses of electrical origin in piezoelectric resonator are usually small and not taken into account. Only for some types of crystals and piezoelectric ceramics electrical losses are noticeable, and then they should be taken into account.

Dynamic resistance can be measured directly, for example, with a bridge meter of full resistance. Dynamic inductance and capacitance can be measured only by indirect methods. The value $\Delta f = f_a - f_r$ is called the *resonance interval*. The quality of piezoelectric resonator is determined by peculiarity of its frequency characteristic, Fig. 6.17B, and by value of efficiency. Knowledge of frequencies f_a and f_r allows determine a number of important characteristics of resonator, and in the first place coefficient of electromechanical coupling: $K_{EM} \approx (2\Delta f/f_p)^{1/2}$. Resonance frequency is calculated from the formula $f_r = 1/2\pi(L_1C_1)^{1/2}$ while mechanical Q factor is defined as $Q_M = 1/(2\pi f_r C_0 R_1)$.

Of the four equivalent parameters, specified in Fig. 6.22, only the parallel capacity C_0 has concrete physical embodiment: its value is determined by intermediate capacitance of piezoelectric as well as by capacitance of housing and mounting. It can be directly measured with some approximation by known methods. In the case of "effective" piezoelectrics, the capacity C_0 varies markedly with frequency: at frequencies below resonance it is larger while at frequencies above resonance lesser. The measurements of parallel capacitance can not be performed at resonant frequency: it should be measured at frequencies far from resonance. For "effective" piezoelectrics this capacity must be measured at a frequency higher than resonance, that is, under conditions of completely clamped piezoelectric.

Equivalent scheme given in Fig. 6.22 is considered to be simplified, but it satisfactorily describes frequency dependence of full resistance of resonators near the resonance, and the hardware designers in most cases satisfy the knowledge of values of its equivalent parameters. In some cases, equivalent circuit has to be complicated by introducing into it parameters of other elements, for example inductance of additional circuits (previous and following), and also the capacitance between full device and piezoelectric element. In addition, piezoelectric resonators usually have several resonances due to oscillations of various types or overtones of any kind of oscillation. In this case, equivalent scheme, which reflects presence of several resonances, looks like a parallel connection of a number of dynamic branches shunted by a common parallel capacity.

Experimentally, parameters of piezoelectric resonator are determined by methods of resonances – antiresonances, changes in electrical load, and the method of circular diagrams, etc.

3. ***Applications of piezoelectric resonance*** due to very high Q-factor of mechanical vibrational systems, is significantly greater than electrical vibrational circuits, because sometimes Q is characterized by values from thousands to hundreds of thousands [3, 13]. Therefore, amplitudes of mechanical oscillations of piezoelectric cell at mechanical resonance are Q times greater than amplitude of its oscillations outside of resonance region. Electrical quantities that characterize oscillations of piezoelectric element, such as electrical current, are related directly to mechanical stresses and deformations. At the moment of mechanical resonance current through piezoelectric increases and frequency response of current acquires resonant character, exactly corresponding to characteristic of mechanical resonance oscillations. Such is, in general, the picture of resonance phenomena observed in piezoelectric resonator, which explains the origin of resonance in electrical circuit.

Piezoelectric resonance is widely used in the radio engineering, electronics, electroacoustics, and microelectronics: filters and resonators, generators and resonant piezoelectric converters, piezoelectric transformers and even motors. In resonators, mainly crystals are used (quartz, lithium niobate, etc.) or piezoelectric ceramics with small losses. For example, quartz resonators are used as resonant circuits and generators of high-frequency oscillations. The high quality factor (10^5–10^6) of quartz resonator determines small deviation of generator frequency from its nominal value: (10^{-3}–10^{-5}) %, when ambient temperature, pressure and humidity change. Widely used miniature quartz resonators with oscillation frequencies of 30 kHz – 8 MHz are used in electronic clocks, in systems of electronic ignition of internal combustion engines and others. Quartz and others piezoelectric resonators are also used in the acoustoelectronic devices for filtration and signal processing: monolithic piezoelectric filters, as well as in filters and resonators on surface acoustic waves (SAW). Main advantage of resonators on SAW is possibility of their use in frequency stabilization devices and narrowband filtering in the frequency range 100–1500 MHz.

Piezoelectric filters made of piezoelectric ceramics and manufactured for frequency range of 1 kHz – 10 MHz usually are multi-layered. At the same time, at lower frequency bands up to 3.5 kHz bimorphic elements are used in which piezoelectric performs resonant oscillations of a bend-type along its face. In the range of 40–200 kHz, piezoelectric resonators are used with longitudinal oscillations along the length, while at frequencies 200–800 kHz piezoelectric resonators in form

of disks with radial oscillations are realized. At frequencies above 1 MHz mainly thickness vibrations of piezoelectric rings are used. Considered filters differ in simplicity of construction, have small dimensions (in comparison with *LC*-filters) and stable working characteristics.

In most cases, piezoelectric elements have only two electrodes, and resonators with such elements are electrical double-poles devices. But in some cases, resonators use piezoelectric elements with a large number of electrodes, having separate leads, for example, with four electrodes. Such resonators with multi-element piezoelectric should be regarded as electrical multi-polar devices. Resonators with four-electrode piezoelectric element are often used in the generators and filters, since they allow replacement of two resonators of one frequency with single four-pole resonator, as well as eliminate unwanted ohmic bonds with a phase shift of 180° between two pairs of terminals, using also voltage transformations and conversion of resistance.

Acoustic resonance, electrically excited at the expense of piezoelectric effect, is employed in various electronic devices. Piezoelectric resonators have been used in radio engineering for more than 90 years. Their main purpose is to stabilize the frequency of radio generators. Miniature quartz frequency stabilizers are applied in most watches, mobile phones and computers. The quality and stability of piezoelectric resonators can be very high. This allows them to be utilized as sensors in various devices by which they measure pressure, acceleration, displacement, temperature and velocity of gases and liquids, determine their chemical composition, etc., since the parameters of environment affect the quality factor and actual frequency of resonator.

Precision resonance sensors also employ resonance. Among them, the resonant precision sensors of *force*, both active and passive, are implemented. As known, piezoelectric devices can not measure stationary processes: this means that piezoelectric force sensors can convert only changing force to variable electrical signal, but they do not react to constant magnitude of external force. The range of measurement depends on frequency of mechanical resonance in applied piezoelectric crystal, for example, quartz. The principle of such sensors is based on the fact that when mechanical loading on quartz crystals, where certain sections used as resonators in electronic generators, the shift in their resonant frequency occurs. Frequency offset is due to dependence of some parameters of crystal on the magnitude of external forces. For example, coefficient of rigidity depends on applied load, whereas density and geometric parameters change under these conditions insignificantly. There exists special direction for each cut of crystal, along which the maximum of sensitivity of piezoelectric resonator is observed.

Frequency stabilizers mainly use crystalline quartz. Previously, for manufacture of resonators used natural quartz (rock crystal). Now quartz is artificially hydrothermal. Different design quartz resonators can overlap the frequency range 10^3 – 10^9 Hz. They use not only simple oscillations of the type "compression-stretching" of quartz plates in length, width or thickness, but also bending, twisting or shear oscillations of complicated by the design resonators.

The widespread use of quartz is due to rare combination of unique properties in it, which ensure the achievement of mechanical Q-factor up to $Q_m \sim 10^7$ and more with the presence of a number of crystallographic orientations (sections) that change very little resonant frequency in operating temperature intervals. Modern quartz resonators provide long-term stability of the frequency up to 10^{-8} and short-term stability another two to three orders higher. The high level of quartz growing technology and production of resonators, including micro-miniaturals (for example, for electronic clocks), makes it almost indispensable in frequency stabilization devices and precision narrowband filters. To increase thermostability of piezoelements, plates of quartz are cut at angle of 5° to X-axis. For special purposes, also are applied sections of 18° X and others. The most thermostable is AT-cut of quartz when its plates are cut along X-axis at angle of $\theta = 35°$ to Z-axis. Moreover, another double-reversed ST-section has become widespread.

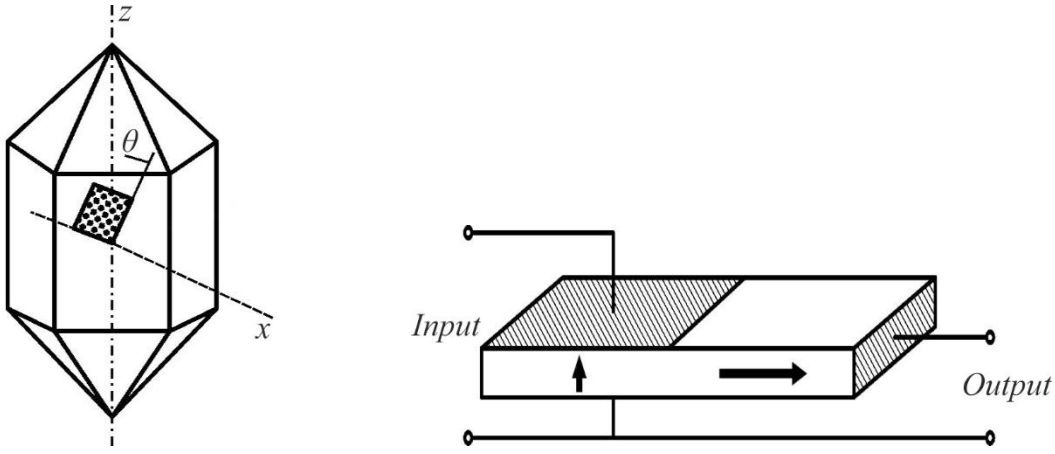

(A) (B)

Fig. 6.23. Piezoelectric resonance: A – orientation of thermostable AT-cut in quartz, B – simplest model of piezoelectric transformer [5]

Piezoelectric transformers use resonant properties of electromechanical devices. These elements in electronic devices play the role of low-power and small-scale *sources of electrical energy*. From electromagnetic transformers, they distinguish by the scheme of energy conversion: "electrical–*acoustical*–electrical", which causes a significant simplification of the design of piezoelectric transformer,

Fig. 6.23B, which does not have any wires or windings required in electromagnetic transformers. By peculiarities of application and constructive features, the piezoelectric *voltage* and *current* transformers can be distinguished. The most common characteristic of piezoelectric transformers is magnitude of piezoelectric efficiency: $K_{31}Q_m$, where K_{31} is coefficient of transverse electromechanical coupling and Q_m is mechanical Q-factor for transverse oscillations of piezoelectric element.

Piezoelectric plate-type transformer in simplest case has two pairs of electrodes – exciter and generator, Fig. 6.23B. Using *converse* piezoelectric effect, the exciter creates mechanical deformation in a plate, which covers the entire volume of piezoelectric element in a form of resonant wave (piezoelectric transformers operate in acoustic resonance mode). In the generator section of piezoelectric transducer, as a result of *direct* piezoelectric effect, the alternating signal arises, which galvanically is divided from input voltage.

The general characteristics of piezotransformers depend on electric quality factor, which determines their efficiency, and also depends on coefficient of electromechanical coupling and mechanical quality of particular piezoelectric material and on the type of oscillation. As a working material in piezotransformers, different types of piezoelectric ceramics are applied, since exactly ceramics allows constructively combine both elements of this device – exciter and generator – in one plate (disk, rod). This is due to technological possibility of multi-direction task of orientation of piezoelectric polarization vector in the process of manufacturing the components of corresponding mono-block piezoelectric element.

The use of modern piezoelectric ceramics materials allows realize the magnitude of transformation factor in voltage more than 1000, which ensures that output voltage exceeds 10 kV. In addition to *voltage* transformer mode, these devices are successfully used as transformers of electrical *current*.

Classification of piezoelectric transformers in *working frequency* is as follows:

· Low-frequency transformers, calculated on the resonance frequency below 10 kHz, in particular, for industrial frequencies 1000, 400 and 50 Hz. These very low-frequency piezoelectric elements usually operate in oscillations of *bending*. The bimorphic and multilayer devices can be mechanically free or mechanically loaded (to reduce operating frequency).

· Middle-frequency piezoelectric transformers have frequency range 10 ... 500 kHz and are constructed with single-layer or multilayer piezoelectric cells, operating on the longitudinal acoustic oscillations of the main mode or in higher modes of oscillation.

· High-frequency piezo-transformers for frequency range more than 500 kHz use thin piezoelectric plates with their higher frequency modes of longitudinal acoustic vibrations in width, or multilayer structures working on oscillations in the thickness of piezoelectric element.

On the *power transferred* to load, following designs of piezoelectric transformers can be distinguished:

· Low-power (up to 1 W) which usually are made of single-layer piezoelectric elements having their own weight less than one gram;

· Average power (1–50 W) representing the single-cassette piezoelectric transducer containing up to six piezoelectric elements;

·) High power (more than 50 W) which are combined multi- cassette transformers.

Specific transmitted power of piezoelectric transformers is (1–10) W/g or (15–75) W/cm*3*, according to the efficiency value 90–95%. Also known are combined piezoelectric transformers that unite both main types of transformers, but they are much more complicated and not well-proven in technology. Main application of piezotransformers issecondary sources of electrical power of radioelectronic devices. Piezoelectric transformers are also used in high voltage generators for gas discharge lamps.

6.6 Thermodynamic description of piezoelectric effect

Direct piezoelectric effect is defined as a response of polar crystal onto external mechanical action while converse piezoelectric effect is that the electric field produces a proportional to it deformation. At that, the polar-neutral ("exclusive") piezoelectrics which are 10 of 20 classes of polar crystals do not react onto hydrostatic pressure, i.e. onto homogeneous (scalar) mechanical action, and therefore they cannot serve as vibration sensors in the air or in the liquid medium. Remaining 10 of the 20 classes of polar crystals are not only piezoelectrics but the pyroelectrics and only they are able to exhibit the volume piezoelectric effect as a response to hydrostatic action, so appropriate sensors are made exactly of them. However, polar-neutral piezoelectrics are also characterized by a set of important for electronic applications properties that manifest themselves in them both under directed mechanical action and under the influence of an electrical field.

As shown in the Introduction in connection with of Fig. I.1, direct and converse pyroelectric effects, depending on electrical and mechanical conditions, can be described by *eight* different equations. All of them can be obtained by various thermodynamic potentials analysis. As opposed to microscopic theories, the atomic

structure of material is not taken into account in thermodynamics, but a material is regarded as continuum which has certain properties. In case of piezoelectricity, this continuum is anisotropic: its electrical, thermal and elastic properties depend on the direction of applied forces and fields.

Thermodynamic potentials. It is assumed that thermal, elastic and electrical properties of piezoelectricity can be described by *six* parameters: two thermal characteristics (T – temperature, S – entropy), two mechanical properties (X – stress, x – strain) and two electrical properties (E – electrical field, D – electrical induction).

If dielectric gets some amount of heat $\mathrm{d}Q$, the change in its internal energy $\mathrm{d}U$, according to first principle of thermodynamics, is described by expression:

$$\mathrm{d}U = \mathrm{d}Q + \mathrm{d}W = \mathrm{d}Q + X\mathrm{d}x + E\mathrm{d}D, \qquad (6.25)$$

where $\mathrm{d}W$ is work carried out by electrical ($E\mathrm{d}D$) and mechanical ($X\mathrm{d}x$) forces. As only *reversible* processes are reviewed here (this includes both electrical polarization and mechanical strain), so $\mathrm{d}Q = T\mathrm{d}S$ in accordance with second principle of thermodynamics. As a result, the change in internal energy (6.25) can be represented as a function of the six basic parameters of the dielectric:

$$\mathrm{d}U = T\mathrm{d}S + X\mathrm{d}x + E\mathrm{d}D, \qquad (6.26)$$

where selected basic parameters are S, x and D. The remaining parameters (T, X and E) are defined as the derivatives of internal energy U on entropy S, strain x and electrical induction D. During differentiation, one parameter is assumed as constant of other two parameters denoted by the corresponding way:

$$\begin{aligned} T &= (\partial U/\partial S)_{x,D}; \\ X_n &= (\partial U/\partial x_n)_{S,D}; \\ E_i &= (\partial U/\partial D_i)_{S,x}. \end{aligned} \qquad (6.27)$$

These ratios in a brief form are three equation of state of polar dielectric: thermal, elastic and electrical. Earlier in the Section 1.3 the variety of boundary conditions were discussed: electrical, mechanical and thermal. Correspondingly, of three pairs of related parameters: $T \Leftrightarrow S$, $X \Leftrightarrow x$ and $D \Leftrightarrow E$, the three *independent* parameters might be chosen, at that, by the *eight* ways. The objectives of different boundary conditions describing thermal, elastic and electrical properties of polar crystals determines the choice of eight different thermodynamic functions (potentials), with which one can express the basic equation of state of piezoelectricity. Obtained above equation is just one of them:

$$\begin{aligned} &\mathrm{d}U = T\mathrm{d}S + X\mathrm{d}x + E\mathrm{d}D; && \mathrm{d}H = T\mathrm{d}S - x\mathrm{d}X - D\mathrm{d}E; \\ &\mathrm{d}H_1 = T\mathrm{d}S - x\mathrm{d}X + E\mathrm{d}D; && \mathrm{d}H_2 = T\mathrm{d}S + X\mathrm{d}x - D\mathrm{d}E; \\ &\mathrm{d}A = -S\mathrm{d}T + X\mathrm{d}x + E\mathrm{d}D; && \mathrm{d}G = -S\mathrm{d}T - x\mathrm{d}X - D\mathrm{d}E; \\ &\mathrm{d}G_1 = -S\mathrm{d}T - x\mathrm{d}X + E\mathrm{d}D; && \mathrm{d}G_2 = -S\mathrm{d}T + X\mathrm{d}x - D\mathrm{d}E, \end{aligned} \qquad (6.28)$$

where H – enthalpy, H_1 – elastic enthalpy, H_2 – electric enthalpy, A – Helmholtz free energy; G – Gibbs free energy, G_1 – elastic Gibbs energy, G_2 – electrical Gibbs energy. Indexes at the vector and tensor parameters are omitted for simplicity.

From equation (6.10) three equations of state were obtained (6.27). With an increasing number of thermodynamic functions up to eight, the number of equations of state also increases. For example, if independent variables would be selected as electrical induction D, strain x and temperature T; then thermodynamic potential should be nominated Helmholtz free energy, and equation of state of a dielectric differs from equations (6.27):

$$-S = (\partial A/\partial T)_{x,D};$$
$$X_m = (\partial A/\partial x_m)_{T,D};$$
$$E_i = (\partial A/\partial D_i)_{T,x}.$$

Equation of state can be written as linear differentials of independent variables:

$$\mathrm{d}S = (\partial S/\partial T)_{D,x}\,\mathrm{d}T + (\partial S/\partial x_m)_{D,T}\,\mathrm{d}x_m + (\partial S/\partial D_i)_{x,T}\,\mathrm{d}D_i;$$
$$\mathrm{d}X_n = (\partial X_n/\partial T)_{D,x}\,\mathrm{d}T + (\partial X_n/\partial x_m)_{D,T}\,\mathrm{d}x_m + (\partial X_n/\partial D_i)_{x,T}\,\mathrm{d}D_i; \qquad (6.29)$$
$$\mathrm{d}E_j = (\mathrm{d}E_j/\partial T)_{D,x}\,\mathrm{d}T + (\mathrm{d}E_j/\partial x_m)_{D,T}\,\mathrm{d}x_m + (\mathrm{d}E_j/\partial D_i)_{x,T}\,\mathrm{d}D_i.$$

As number of potentials is eight, then full number of such equations is 26. The coefficients in these equations are the generalized state of compliance: they define various fields (electrical, mechanical and thermal). The most important ones are mentioned earlier in connection with description of piezoelectrics: second rank tensors (ε_{ij}, α_{ij}), tensors of third rank (d_{in}, e_{im}, h_{jn}, g_{jn}, fourth rank tensors (c_{mn} and s_{mn}). Here the indices are $i, j, k = 1, 2, 3$, while $m, n = 1, 2, ..., 6$, and they are used for matrix presentation of parameters.

As shown above, thermodynamic potentials (6.28) with Helmholtz free energy are responsible to describe not only piezoelectric effect, but pyroelectric effect, ferroelectric phase transitions, and other phenomena in polar crystals. To describe only the piezoelectric effects, some changes need to be done considering the primary four potentials as adiabatic ones ($\mathrm{d}S = 0$), and following four potentials as isothermal ($\mathrm{d}T = 0$) ones.

Specifically, with this example – Helmholtz free energy – based on $\mathrm{d}T = 0$, the piezoelectric effect is described by:

$$\mathrm{d}X_n = c^D{}_{mn}\,\mathrm{d}x_m - h_{in}\,\mathrm{d}D_i;$$
$$\mathrm{d}E_j = -h_{jm}\,\mathrm{d}x_m + (\beta^x{}_{ij}/\varepsilon_0)\,\mathrm{d}D_i,$$

in which coefficients elastic stiffness $c^D{}_{mn} = (\partial X_n/\partial x_m)_D = (\partial^2 A/\partial x_n \partial x_m)_D$ that are determined at constant induction, while the parameter $(\beta^x{}_{ij}/\varepsilon_0) = (\partial E_i/\partial D_j)_x = (\partial^2 A/\partial D_i \partial D_j)_x$ is *converse permittivity* of clamped crystal. The parameter h_{jm} is one of four piezoelectric coefficients that also refer to one of generalized compliances:

$$h_{jm} = -(\partial X_n/\partial D_j)_x = -(\partial E_i/\partial x_n)_D = -(\partial^2 A/\partial x_n \partial D_i).$$

Thus, one of four piezoelectric coefficients (*d, e, g, h*) is discovered. The same pair of equations can be obtained from free energy expression and from other thermodynamic potentials, the number of which in the terms of d$S = 0$ and d$T = 0$ is reduced to five. As a result of the thermodynamic relations, four pairs of basic equations of piezoelectric effect follow as:

$$D_i = d_{in} X_n + \varepsilon_0 \varepsilon_{ij} E_j ; \qquad x_m = s^E_{mn} X_n + d_{jm} E_j ;$$

$$D_i = \varepsilon_0 \varepsilon^x_{ij} E_j + e_{im} x_m ; \qquad X_n = c^E_{nm} x_m - e_{jn} E_j ;$$

$$E_j = (\beta^x_{ji}/\varepsilon_0) D_i - h_{jm} x_m ; \qquad X_n = c^D_{nm} x_m - h_{in} D_i ;$$

$$E_j = (\beta^x_{ji}/\varepsilon_0) D_i - g_{jn} x_n ; \qquad x_m = s^D_{mn} X_n - g_{im} D_i .$$

Therefore, all four piezoelectric coefficients are possible to estimate.

Thus, thermodynamic (phenomenological) theory allows without clarifying the molecular mechanisms get all basic equations that describe direct and converse piezoelectric effect at the macroscopic level. These equations are used in engineering calculations, and parameters of these equations can serve as a basis for comparing the properties of various piezoelectric materials.

6.7 Summary and self-test questions

1. *Piezoelectric effect* occurs in crystals or polarized ceramics for which the electrical voltage appears across the material when pressure is applied. Similar to pyroelectric effect, this phenomenon is due to asymmetric structure of material that allows ions to move more easily along one axis than along the others. As pressure is applied, opposite sides of piezoelectric acquire the opposite charges resulting in a voltage appears across the material.

2. *Piezoelectric* converts mechanical energy into electrical or, conversely, electrical energy into a mechanical one. Mechanoelectric effect was firstly observed, which for this reason was called "direct" piezoelectric effect. The piezoelectric effect is the odd (linear) effect, in which the mechanically induced polarization is directly proportional to the deformation; vice versa, while converse piezoelectric effect, the electrically induced deformation is directly proportional to the magnitude of the electrical field. Both piezoelectric effects may happen only in noncentrosymmetric crystals and structures.

3. *Electrostriction* is observed in all dielectrics and it is an even effect, in which deformation of dielectric caused by electrical field is quadratically dependent on the magnitude of this field. Thus, sign of electrostrictive deformation does not change with the change of sign of a field. Electrostription differs from piezoelectric effect by the fact that it does not have converse effect, that is, this effect is exclusively electromechanical, but not "mechanoelectric".

4. Piezoelectric effect is described by *piezoelectric constants* – tensors of the third rank. Mathematical relations describing piezoelectricity or electrostriction depend on the combination of certain boundary conditions, in which piezoelectric is used or investigated. The main mechanical conditions are reduced either to the possibility of deformation (if crystal is free) or to their impossibility (when crystal is clamped). The boundary electrical conditions are that the crystal can be short-circuited or open-circuited.

5. *Piezoelectricity* is the linear electromechanical effect. At that, of electrical properties of crystals, only the dielectric polarization (characterized by permittivity) is relevant to the piezoelectric effect. Mechanical properties of piezoelectrics include elasticity, hardness, durability and others; but for piezoelectric effect the most important mechanical properties are the *elasticity* (which depends on binding forces of atoms in a crystal) and the *velocity* of elastic waves in piezoelectric (which, in addition to elasticity, depends on specific density).

6. External mechanical influence on piezoelectric is characterized by the *tensor of mechanical stress.* This symmetric tensor of second rank in its physical nature differs from symmetric second-rank tensor of permittivity, whose structure is consistent with the *internal symmetry* of a crystal. So permittivity tensor is the *material* tensor, while tensor of mechanical stresses is the *field* tensor, characterizing structure of forces applied to crystal from outside. From Hooke's law, which confirms linear proportionality of deformation and mechanical stress, two tensors are very important for piezoelectrics: the tensor of elastic stiffness c_{mn} (also called Young modulus) and the tensor of elastic compliance s_{mn}. Both of them are symmetric material tensors of fourth rank. Others important for applications special parameters of piezoelectrics are: *volumetric modulus of elasticity K, volumetric compressibility* $<s>$ and *Poisson's coefficient v,* all of them are used to characterize the elastic properties of piezoelectric material.

7. In various cases of technical application off piezoelectrics, depending on the symmetry of action of external mechanical forces, five important cases should be distinguished: *linear-stressed* state (uniaxial tension), *plane-stressed* state (two-axis stress), *volume-stressed* state (three-dimensional stress) and stress of *pure shear*. A separate important case is the *hydrostatic pressure*, in which all components of stress are the same $X_{11} = X_{22} = X_{33} = –p$, where p is specific pressure. Depending on symmetry of the mechanical load, as well as symmetry of piezoelectric, the deformation in it (which is also symmetric tensor of second rank) can be classified as one-dimensional, two-dimensional, and three-dimensional. Two-dimensional deformation of tensile-compression must be taken into account in modern planar microelectronic technology.

8. Piezoelectric effect can be induced by the electrical field in any solid dielectric as the "*linearized electrostriction*". In some of paraelectrics and in the relaxor ferroelectrics the magnitude of electrically induced piezoelectric effect may outweigh piezoelectric effect of best piezoelectric materials. Piezoelectric effect manifestations can be controlled by bias electrical field: for example, the frequency of piezoelectric resonance becomes tuneable, or parameters of filters based on surface acoustic waves might be controlled. Effectiveness of electrical control of piezoelectric effect is most significant in dielectrics with large permittivity.

9. Mechanical property (elasticity) and electrical property (polarization) of piezoelectric crystals are interrelated, and, therefore, they can be *considered together*. This relationship is characterized by electromechanical coupling coefficient K_{EM} – one of most important parameters of piezoelectric materials and devices. In case of direct piezoelectric effect, applied to piezoelectric mechanical energy is spent not only on elastic deformation, but also creates electrical polarization, which causes electrical energy accumulation. Conversely, supplied to piezoelectric electrical energy (in case of converse piezoelectric effect) is spent not only for its polarization, but also to its elastic deformation and elastic energy accumulation.

10. The square of electromechanical coupling factor K_{EM}^2 shows what part of energy, attached to piezoelectric, is converted into the energy of other kind. However, this parameter is not performance factor: firstly, because losses of electrical or mechanical power are not considered, and, secondly, actual conversion efficiency of piezoelectric depends not only the K_{EM}, but largely is on the shape, orientation and other peculiarities of piezoelectric element.

11. *Polar crystals and textures* are distinguished by the fact that their electrical, elastic and thermal characteristics are interdependent. Moreover, during the study (or the use of devices) only electrical effect (for example, polarization) reveals that the corresponding electrical parameters depend on boundary mechanical and thermal conditions: for example, permittivity of mechanically free crystal (ε^X) differs from permeability of clamped piezoelectric crystal ε^x (which can not be deformed), and always $\varepsilon^X > \varepsilon^x$. By the same way, elastic stiffness of piezoelectric (or its elastic compliance) depends on its electrical state (short-circuited or open-circuited) and therefore $c^E \neq c^D$; in some cases they differ several times.

12. *Thermodynamic* (phenomenological) theory allows, without specifying the molecular mechanisms, obtain all basic equations describing direct and converse piezoelectric effect at macroscopic level. These equations are used in engineering

calculations, and parameters of these equations can be the basis for comparing the properties of different piezoelectric materials.

13. For application in electronics and instrumentation, many piezoelectrics of different structures have been developed: crystals, ceramics, polymer materials, films, composites. One of most important piezoelectric crystals is quartz, which combines large mechanical Q-factor ($Q_m \sim 10^7$) with high thermal stability of resonant frequency in the operating temperature intervals. In electronics, piezoelectric crystals niobium tantalite, lithium tantalite and lansacite, whose unique characteristics provide wide implementation of acousto-electronic devices, are widely employed.

14. *Piezoelectric ceramics* is most important material for modern piezoelectric devices. In order to meet the needs of technology, dozens of compositions of piezoelectric ceramics are developed with different set of parameters, which provide: converters of mechanical vibrations of environment into electrical signals; converters of electrical signals into elastic waves or in mechanical displacements; devices that use electromechanical resonance.

15. *Polymer piezoelectric films* of PVDF-type (and their corresponding copolymers) are characterized by simple technology, low acoustic impedance and are widely applied in piezoelectric polymer sensors and many other devices.

16. *Electrostriction materials* acquire now great importance, because they differ from piezoelectrics by the absence of hysteresis in deformation-electrical field dependence. They are relaxor ferroelectrics with disordered structure characterized by blurred temperature maximum $\varepsilon(T)$ in the vicinity of phase transition and record high electromechanical coupling coefficient.

17. Parameters of piezoelectrics *can be controlled* by bias electrical field: for example, piezoelectric filters characteristics can be changed as well as surface acoustic wave parameters. Electrical controlling by piezoelectric properties is most manifested in dielectrics with high permittivity.

18. External electrical field, changing the velocity of elastic waves propagation, makes it possible to control resonant frequency or phase of bulk piezoelectric filters or surface acoustic waves. This effect can be used in frequency and phase modulators, parametric amplifiers for implementation in new electronic devices. Electro-induced piezoelectric effect can be applied also in parametric devices. Since electromechanical coupling factor depends on permittivity ($K \sim \varepsilon^{3/2}$), the most promising dielectrics for parametric devices are those which have $\varepsilon \approx 10^3 – 10^4$.

19. *Piezoelectric sensors* are widely employed in electronics, instrumentation, in medical technology. In these sensors direct piezoelectric effect is used with most convenient parameters piezoelectric modulus g, which characterizes electrical voltage occur under applied pressure, and the modulus h showing voltage per unit strain. Piezoelectric devices employed in liquid media are called *hydrophones*, piezoelectric devices, used in the air are called *microphones.* They are capable of operating in very wide range of frequencies – from hertz to gigahertz.

20. *Converse piezoelectric effect* is applied, for most part, to generate sound and ultrasound in the liquid or air environment. As ultrasound emitters, mainly the piezoelectric ceramics with high electromechanical coupling coefficient and large mechanical Q-factor are employed. Such emitters are used in ultrasonic sonar and in a distant underwater connection.

21. *Piezoelectric actuators* are based on converse piezoelectric effect and widely applied in electronics and modern instrumentation, as well as in robotics and engineering. Piezoelectric actuators differ in their precision of movement; that is why they applied in tunnel and atomic force microscopes having high (atomic) resolution.

22. *Piezoelectric motors* have advantages due to absence of induction windings and magnetic fields. These motors convert high-frequency electric current into mechanical rotation; at that, working element is the piezoelectric ceramics, which converts electrical energy into mechanical with high efficiency (90%) exceeding this parameter for many types of engines.

23. *Piezoelectric transformers*, which allow effectively replace electromagnetic transformers, are used in many cases. These devices operate predominantly in the resonant mode using as direct so converse piezoelectric effects.

Chapter 6. Self-test questions

1. What and how many parameters characterize piezoelectric effects?
2. What is the role of the boundary conditions for the piezoelectric effect and its application?
3. What are the methods for independently measuring all piezoelectric modules?
4. What is the peculiarity of using piezoelectric sensors?
5. How many and which piezoelectric devices are contained in a smartphone?

CHAPTER 7. PYROELECTRICS: PHYSICS AND APPLICATIONS

Contents

Pyroelectrics represent one of the important classes of functional dielectrics because they efficiently react to the changes in *temperature* (as well as on pressure and other mechanical actions). These are polar dielectrics, which can be defined also as the materials which allow directly convert energy, representing mainly the thermoelectric and, vice versa, the electrothermal power converter. Transformative function of polar crystals is due to their peculiar physical structure and chemical composition. Four different mechanisms of pyroelectric effect are discussed. This effect and inverse to it electrocaliric effect are reviewed in the aspect of their use in electronic devices at various boundary conditions (adiabatic and isothermal development, mechanically free or clamped crystals study, short-circuited or open-circuited circumstances). The nature of thermoelectrical coupling in polar-sensitive crystals and its influence on the dielectric permittivity and thermal properties crystals are also described by various models and thermodynamic calculations. The principles of operation of the main types of pyroelectric sensors are considered: the motion detector sensors, infrared thermometers for high precision pyrometery; pyroelectric vidicons in both vacuum and microelectronic design, etc. Physical mechanisms and applications of electrically induced pyroelectric and electrocaloric effects at various conditions are also depicted.

The possibilities of electrocaloric effect are discussed in connection of its possible application in miniature solid-state refrigeration systems.

Extraordinary properties of the natural mineral tourmaline, which when heated attracts small particles, were already known in antiquity (2000 years ago). But for the first time this phenomenon was explained as *electrical* phenomenon in 18th century by Linnaeus and Aepinus, while the term "*pyroelectric*" arose 200 years ago in works of D. Brewster (Greek word "pyro" means "fire"). Pyroelectrics are the solid-state *direct converters* of the thermal energy into the electrical energy). First theory of pyroelectricity was developed by W. Thomson and W. Voigt at the end of the 19-th century.

[***Note.*** In addition to pyroelectricity, the *thermoelectricity* is widely used as the solid-state converter of thermal energy into electrical energy. In the thermoelectric devices, the electronic processes in the *semiconductors* are used, occurring under conditions of a temperature gradient (temperature difference). In this case, the generation of electricity occurs continuously – in the stationary conditions. In the pyroelectric devices, the electrical *polarization-depolarization* effect are used in the *non-stationary conditions*, when the dynamic and periodic temperature *changes* are obviously required].

As among the minerals, so among the artificially synthesized crystals, the pyroelectrics are relatively rare crystals. Mineral pyroelectrics consist mainly of tourmalines (alumoborosilicates of the type $NaMg[Al_3B_3.Si_6(OOH)_{30}]$ with various impurities), and of synthetic pyroelectrics the lithium sulfate ($LiSO_4 \times H_2O$), lithium niobate ($LiNbO_3$), potassium tartaric acid ($K_4C_8O_{12} \times H_2O$). Among pyroelectrics are the broadband semiconductors of $A^{II}B^{VI}$ type (CdS, ZnO, etc.), but their pyroelectric effect is small. It is interesting to note that the crystalline sugar ($C_5H_{10}O_5$) is pyroelectric, and for that very reason it is used in the homeopathic medicines. Recently, a significant progress has been made in the use of *artificial* pyroelectric materials in the form of thin films, using gallium nitride (GaN) and cesium nitrate ($CsNO_3$), as well as some polymers: polyvinyl fluoride and derivatives of cobalt phthalocyanine.

Any *ferroelectric* is a potential pyroelectric, but in order to use ferroelectrics as the pyroelectric element it need to be single domain. Otherwise, the pyroelectric effect is mutually compensated due to the multitude of differently oriented ferroelectric domains. However, it is possible to prepare singe domain ferroelectrics in various ways, including polarization by electrical field at increased temperature; moreover current technologies for pyroelectric crystals-ferroelectrics producing usually use such methods of growing crystals, which immediately provides their monodomain structure.

Pyroelectrics represent one of important classes of functional dielectrics, because they efficiently react to the changes in *temperature* (as well as on the change in pressure and under other mechanical actions). These are polar dielectrics, which can be defined also as the materials, which allow directly convert energy, representing mainly the hermoelectric and, vice versa, the electrothermal power converter. Transformative function is due to a peculiar physical structure and chemical composition of polar crystals.

The p*yroelectric* effect and inverse to it the *electrocaliric* effect are reviewed below in the aspect of their use in the electronic devices at various boundary

conditions (adiabatic and isothermal development, mechanically free or clamped crystals study, short-circuited or open-circuited circumstances). The nature of the thermoelectrical coupling in the pyroelectrics and its influence on the dielectric permittivity and thermal properties of polar crystals are also described by various models and thermodynamic calculations. Physical mechanisms and applications of *electrically induced* pyroelectric and electrocaloric effects at various conditions are also depicted.

7.1 General characteristics of pyroelectricity

In the polar dielectric, temperature raising or lowering changes the intensity of particles thermal motion, and, therefore, changes the orientation of polar-sensitive bonds (or polar molecules) as well as the distance between them, leading to appearance of *thermally induced polarization*. As a result of such pyroelectric effect, on the surfaces of polar crystal the uncompensated electrical charges appear. Covered by electrodes pyroelectric element usually is connected to amplifier and through the input impedance of amplifier a pyroelectric *current* flows. In the case of disconnected crystal, the pyroelectric *voltage* appears on the crystal surface; however, over time, if the temperature of a crystal remains invariable, this pyroelectric potential decreases gradually to zero.

Energy description of this process means that thermal energy is converted by pyroelectric directly into the electrical energy due to its electrically active intrinsic structure therefore, pyroelectric is thermoelectric (or vice versa electrothermal) power converter. At that, own peculiar internal electrical structure of crystals-pyroelectrics is energetically advantageous [5].

Crystallographic consideration of this phenomenon comes down to a particular structure of a crystal, which obligatory must have the presence of polar axis possible only in correspondent crystallographic class. Therefore, according to Neumann principle, the point symmetry groups of pyroelectric crystals should be the subgroups of $\infty\square m$ limit group, which describes symmetry of polar vector. Pyroelectric crystals have next symmetry elements allowed for them: single axis of symmetry of any order and planes of symmetry passing through this axis and parallel to it. Such crystals belong to the ten polar point symmetry groups shown in Fig. 7.1A. In crystals with centre of symmetry pyroelectricity does not occur, as well as there are no pyroelectric crystals among the cubic classes of crystals [3].

As can be seen from the left part of Fig. 7.1A, one of five types of axes (allowed by spatial symmetry of crystals) in the pyroelectric should be the *single*

polar axis; correspondently, five groups of pyroelectric classes of crystals are designated as follows: 1, 2, 3, 4, 6. These numbers indicates the order of polar axis and comply with triclinic, monoclinic, trigonal, tetragonal and hexagonal classes of symmetry. Listed five various axes of symmetry can *lie in planes* of symmetry (denoted by *m*), forming five more possible classes of pyroelectrics: *m*, *mm*2, 3*m*, 4*mm* and 6*m* seen in Fig. 7.1A on the right.

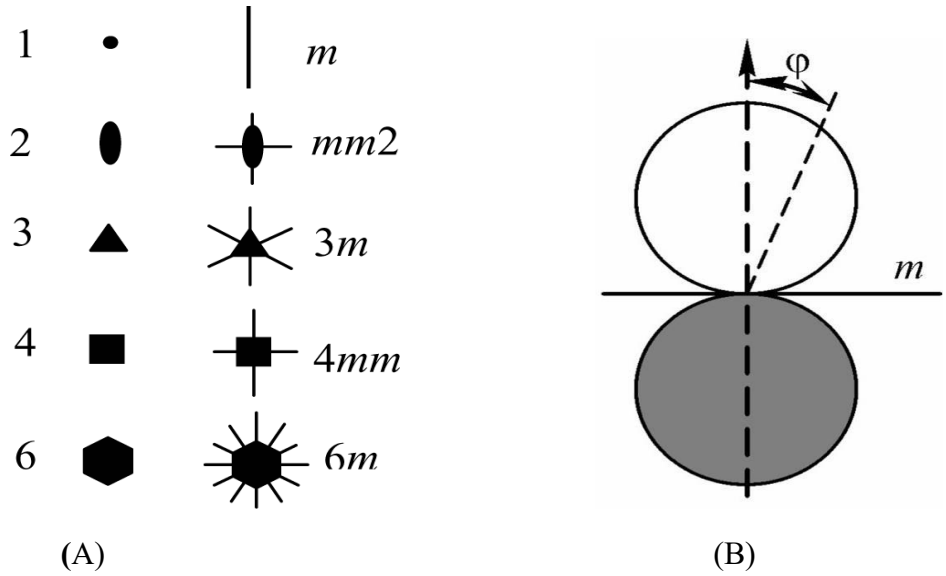

Fig. 7.1. Pyroelectric crystals formal description: A – ten polar symmetry classes, number indicates the order of symmetry axis, while *m* is the plane of symmetry; B – guide surface (indicatrix) for pyroelectric coefficient $\gamma(\phi)$; black area shows negative part of pyroelectric coefficient [1]

Thus, the symmetry of a crystal limits arbitrariness in the orientation of polar vector, which must either be directed *along* the axis of symmetry or lie in the *plane* of symmetry. When changing external conditions, in particular, temperature or pressure, only *limited* measurements of polar response are permissible. If made action is non-directional, being described by scalar magnitude (that corresponds to uniform heating or hydrostatic pressure), then changes in the polar response must be consistent with the symmetry of crystal. In the crystals of eight pyroelectric classes, in which shown number indicates polar axis (Fig, 7.1A), the polar response can vary only in a magnitude, but not in its direction, which must always coincide with the direction of the existing axis of symmetry. However, in the crystals with only *plane* of symmetry (point group *m*), greater freedom is allowed: polar vector can vary both in magnitude and in direction, remaining, nevertheless, invariably in the plane of symmetry. Regarding the crystals included into triclinic system (group 1), one can say that this symmetry does not impose any restrictions in the orientation of polar

vector, i.e., it is not conditioned by any crystallographic chosen direction. As a result, at temperature or pressure changes, the polar vector can be described in a space by arbitrary curve.

Pyroelectric effect maximally manifests itself only in one direction of crystal structure, namely, along the polar axis, where maximum of pyroelectric coefficient is seen: γ_{max}, Fig. 7.1B. In the direction transverse to polar axis $\gamma = 0$; note that in practice sometimes considered more rational to use the slanting cuts of pyroelectric crystals where $\gamma(\phi) = \gamma_{max}\cos\phi$.

Among known 32 classes of crystals, 20 classes are piezoelectric ones, and of them 10 classes are the pyroelectric (called the "pyroelectric group", Fig. 7.1A. Common feature of this group of crystals is the lack of certain elements of symmetry: the centre of symmetry, the transverse planes of symmetry and any axes of symmetry of infinite number, perpendicular or oblique with respect to current axis.

It should be noted that, besides the polar *crystals*, the *polarized ferroelectric ceramics* also have pyroelectric properties (at increased temperature and under externally applied electrical field most of ferroelectric domains in ceramics become and then stay oriented). Formed pyroelectric *texture* has the group of polar symmetry $\infty\square m$ (∞ is order of symmetry axis). Because of mechanical strength and high chemical resistance, the polarized ferroelectric ceramics very often are used in the pyrometry, although usually pyroelectric sensitivity of the ceramics is less than in the ferroelectric crystals. In addition to polarized ferroelectric ceramics, some *polymeric films*, for example, polyvinylidene fluoride, have significant pyroelectric effect. Their advantage is elasticity and their lack is aging (decrease with time transformative properties).

As is well known, only crystals belonging to non-centrosymmetric classes can have properties described by the odd-rank tensors. Therefore, the crystals of all acentric classes exhibit a piezoelectric effect, the quantitative characteristic of which is the third-rank tensor of piezoelectric module. An exception among crystallographic classes that do not have a centre of symmetry (the total number of which is 21) is the only cubic class with point group 432, which prohibits the appearance of piezoelectric activity by others elements of symmetry it has. Like all material tensors of odd rank, the tensor of piezoelectric coefficients is impossible in the crystals having a centre of symmetry.

However, among pyroelectric crystals, there are those crystals, in which external electrical field can change the direction of polarization onto opposite. These are the ferroelectrics, and their repolariztion occurs due to the fact that their polar structure is only slightly distorted in comparison with non-polar phase. Therefore,

free energy of such a crystal in the polar phase turns out to be comparable with the free energy of the non-polar phase, because the energy barrier separating these modifications has rather small value. This leads to the fact that the restructuring of crystal lattice relatively easily can be done by the external field.

Pyroelectric effect applications are based mainly on the reason that thermal energy, being radiated in the form of infrared waves, is invisible to human eyes. So, the pyroelectric sensors can work as a hidden device and they are widely used for security and automation applications. The field of pyroelectric effect using in electronics includes mainly temperature sensors and far-infrared (IR) detectors used in imaging devices. The advantages of pyroelectric sensors as compared to semiconductor-based IR devices consist primarily in the possibility of using them without special cooling — at normal temperature. In addition, based on the principle of *heating by any radiation*, the pyroelectric sensors are non-selective and so the *wide-range* devices, which can register not only thermal, but also microwave, *x*-ray and optical radiation, including high-power laser illumination. A very important feature of pyroelectric devices is much faster response than other temperature sensors and high overload resistance [6].

The basic device of the pyroelectric sensor is simple, Fig. 7.2A: it is a plate of pyroelectric supplied with electrodes and irradiated by the studied heat flow. To quickly establish thermal equilibrium, the sensor element is thin enough (usually tens of micrometers) while for matrix-based IR image devices this element can have an equally small area. In the case when the observed object is stationary, the external irradiation of sensor should be intermittent, i.e., modulated with a certain frequency (usually several tens of hertz), so, when the irradiation stops for a short time, pyroelectric element would have enough time to return to its thermal equilibrium (correspondent chopper can be mechanical or piezoelectric). Deposited on element electrodes are connected to amplifier: usually it is the field effect transistor with high input resistance.

The time-dependent pyroelectric response to thermal radiation incident on the sensor element is shown in Fig. 7.2B. As long as irradiation is not present, the pyroelectric is in the thermodynamic equilibrium when the energy of ions attraction in polar-sensitive bonds (governed by difference in ions electro-negativity, see Chapter 1), is completely balanced by the energy of phonons (thermal chaotic motion in a lattice). An increase or decrease in temperature causes a disturbance of this equilibrium, as a result of which pyroelectric induces electrical polarization, shown in Fig. 7.2A in a form of bound electrical charges on the surface of

pyroelectric element, these charges are compensated by the electrical charges on electrodes.

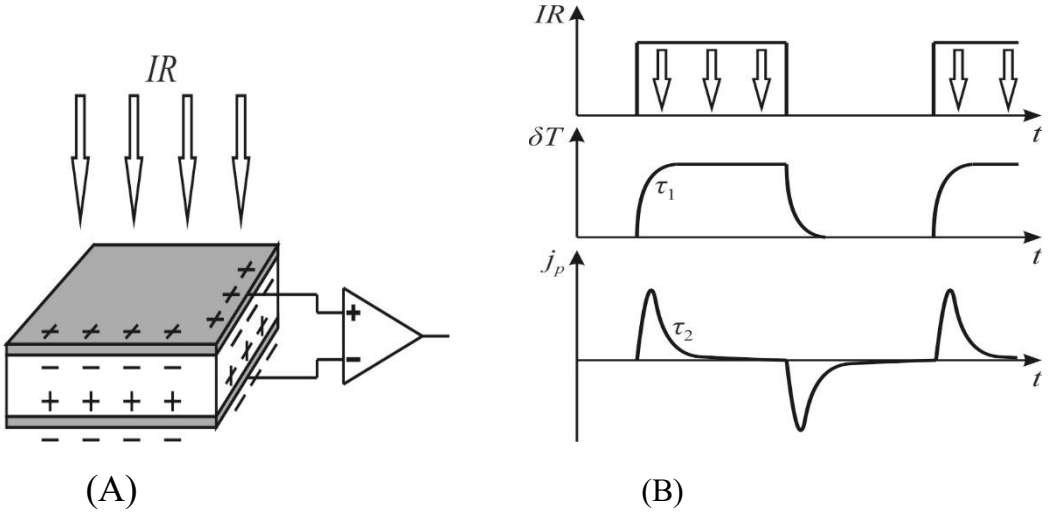

Fig. 7.2. Principle of pyroelectric sensor operation: A – sensor is irradiated by heat flux *IR* and signal goes to amplifier; B – time-dependence of heat flux *IR* modulated by square modulator, δT is temperature changes of sensor and j_p is pyroelectric current

As seen in Fig. 7.2B, sensor's temperature approximately reproduces intensity of incident energy according to law: $\delta T(t) \sim [1 - e(-t/\tau_1)]$ with a delay time τ_1, which depends on heat capacity and thermal conductivity of pyroelectric and electrodes. With a small delay, the pyroelectric current $j_p(t)$ quickly increases to a maximum, but then it gradually drops to almost zero with the relaxation time τ_2 depending on capacity of pyroelement and on input resistance of amplifier. When pyroelectric element cools and returns to the thermal equilibrium with medium, new peak of pyroelectric current occurs but of opposite polarity; then the pattern repeats followint to modulation that has meander character.

Among the far infrared pyroelectric devices are the *motion detector sensors*, which can detect the movement of human beings, animals and anything, which radiates thermal infrared radiation [7]. Other class of devices are the *infrared thermometers* of high precision need for pyrometery: non-contact temperature measurements in the areas where physical contact is not possible, such as moving objects, extremely heated substances, etc. (sensitivity of pyroelectric thermometers reaches 10^{-6} K). Pyroelectric sensors practically solve the problem of detecting low-power heat energy fluxes including measurements of the shape and power of short (10^{-5} – 10^{-9} s) *laser radiation pulses* and can be applied for lasers power measurement that have a repetitively pulsed energy up to 25 kHz.

However, the ***pyroelectric vidicons*** in both vacuum and microelectronic design can be considered as main applications of pyroelectrics. Pyroelectric

transducers of the infrared image (thermal imagers) are intended for the conversion of thermal (or radiation) images into the electrical signals or in the visible images on a television screen. Infrared vision ("dark vision") is of great importance in the medicine and various technologies.

In the vacuum pyrovidicons, the possibility of using pyroelectric effect to registrate spatial distribution of the radiation in infrared imaging systems is realized. To be detected, the thermal image is projected onto the thin plate of pyroelectric – the target. Thermal image creates on this target the electrical relief, which is distribution of pyroelectric charges; this relief modulates the current in the electronic beam, which scans pyroelectric target. It is important to note that absorbed by target radiation flux causes the changes over time thermal relief. As a result of the transformation: "infrared radiation – electrical signal" on the screen of video control device with a period of the frame formed visible image of the thermal relief).

[***Note.*** The areas of application of pyroelectric vidicons are, for example, aeroregistration of fires, which allow, on the background of dense smoke, to detect a source of fire and to target fire extinguishing agents, to determine the boundaries of underground fires in coal mines, etc. Remote registration of infrared illumination during construction and operation of buildings can reduce the cost of their heating. Pyroelectric vidicons are also used to control various technological processes. For example, they are important for assessing the status of high-voltage transmission lines according to infrared data obtaind from vidicon located on helicopter, as well as for checking of isolation of powerful electric machines. They are used also for automated technological control of electronic components which are under electric voltage. Pyroelectric imagers are widely used in medical practice to provide a successful diagnosis of cardiovascular and cancerous diseases] [8].

Despite low energy efficiency of thermoelectric conversion, the pyroelectricity should not be considered a weak effect. For example, the tourmaline plate of 1 mm thick being heated to 10 degrees creates potential of 1.2 kV [3] and this despite the fact that tourmaline has relatively small pyroelectric coefficient. In case of strong pyroelectric – triglycine sulfate (TGS) – its rapid heating may cause electrical breakdown due to arisen pyroelectric potential. Perhaps for this reason, the possibilities of creating pyroelectric generators in which the pyroelectric can be repeatedly heated and cooled to generate useful electrical energy have been investigated.

Possible advantages of such pyroelectric generators for power generation (compared to conventional heat engines and electric generators) include: low operating temperatures, less bulky equipment and fewer moving parts. Such

generators use a principle of multi-stage devices, optimizing conditions of energy exchange between successive cascades. To compare competitiveness of pyroelectrics with other types of similar devices, it is possible to give data of different types of soli-state energy converters: the radioisotope-thermoelectric has mass 200 kg/kW and efficiency up to 3%; photovoltaic semiconductor (solar cells) have mass 10 kg/kW, and efficiency up to 40%; pyroelectric multi-stage cascade gas mass 4 kg/kW and efficiency up to 10%. Nevertheless, pyroelectric devices are far from industrial applications.

It is interesting to note that pyroelectrics were used to create large electric fields needed to control deuterium ions in the process of nuclear fusion. With this purpose the pyroelectric crystal was applied, which under certain conditions develops such pyroelectric voltage which is sufficient for the occurrence of cold-temperature thermonuclear fusion [9].

In this case, a pyroelectric is used to create high-intensity electrical field in order to accelerate the deuterium ions to bombard a target that also contains deuterium. In this case, two deuterium nuclei can merge into one, forming nucleus of helium-3 and high-energy neutron. In one experiment, pyroelectric potassium tantalate was rapidly heated on 40 °C and the tungsten needle created a field of 25 GV/m. The device turned out to be a useful neutron generator, but could not be a source of energy since it requires much more energy than it produces.

7.2 Pyroelectric effect modeling

As mentioned earlier, the pyroelectric effect can be *naturally* observed in the polar crystals, (as well as in the polarized ferroelectric ceramics and in the polar polymers). Moreover, this effect can also be *artificially* induced in the non-polar dielectrics by electrical bias field, as well as by the partial restriction of certain type of deformations in the polar-neutral piezoelectrics (the latter case was already considered in detail in Chapter 2). Next the basic models of natural pyroelectricity in polar crystals will be first considered and then the electroinduced pyroelectric effect.

In short, the physical mechanism of pyroelectric effect is as follows: under constant external conditions (temperature, pressure, etc.), the structure of a polar crystal corresponds to its energy minimum. At the same time, polar-sensitive interatomic bonds, striving for mutual ordering, are in subtle equilibrium with thermal chaotic motion of atoms in the crystal lattice. When this equilibrium changes, caused for example by a change in temperature (i.e., a change in thermal

energy), the polar crystal immediately reacts with the appearance of an electrical polarization — the bound charges on the crystal surface.

1. ***Simplified model*** of usual pyroelectric effect considers the one-dimensional structural arrangement of polar-sensitive bonds, shown previously in Chapter 1 by utterly simple model in Fig. 1.11A and next presented in more detail in Fig. 1.17. Traditionally, the pyroelectric effect is explained by two mechanisms: firstly, by change in the *orientation* of polar-sensitive bonds due to alteration in thermal chaotic motion, and, secondly, due to piezoelectric effect caused by *thermal deformation* of polar crystal. Correspondingly, these effects are called as the *primary* and the *secondary* effects which are described by pyroelectric coefficients $\gamma^{(1)}$ and $\gamma^{(2)}$. In case of mechanically free crystal, both of these mechanisms contribute to thermally-induced electrical response: $\gamma = \gamma^{(1)} + \gamma^{(2)}$. Polar-sensitive structure of pyroelectric (that looks like *hidden* internal polarity) is able to provide electrical (vector) response to external scalar impacts; in a given case – when temperature changes.

The *primary* mechanism of pyroelectricity, i.e., the change in orientation of polar-sensitive structural units, manifests itself *regardless* of mechanical conditions in which crystal is located. It should be noted that primary effect is most noticeable *above* Debye temperature ($T > \theta_D$), when thermal fluctuations in crystal (phonons) become sufficiently active.

The *secondary* mechanism of pyroelectricity, i.e., the piezo-transformed thermal deformation, is possible in the *mechanically free* crystals only. Usually (but not always) this effect prevails at lower temperatures ($T < \theta_D$).

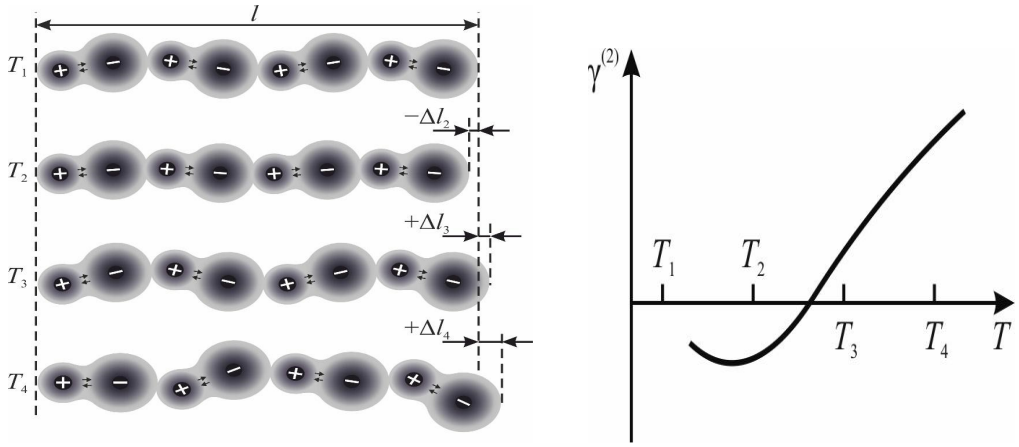

(A) (B)

Fig. 7.3. One-dimensional model of pyroelectricity (A): T_1 – polar-sensitive chain with length l at very low temperature; T_2 – partial ordering of polar-sensitive bonds accompanied by chain compression on $-\Delta l_2$; while T_3, T_4 – thermally activated disordering with chain elongation on $+\Delta l_3$ and $+\Delta l_4$; B – secondary pyroelectric coefficient temperature dependence

Both mechanisms are schematically illustrated in Fig. 7.3 by temperature transformations of one-dimensional model: the chain having length l and made of polar pairs is shown. It is assumed that in the initial state of polar crystal (at very low temperature T_1) quantum oscillations of crystal lattice prevent complete ordering of polar-sensitive bonds).

[*Note.* This fact is confirmed by the impossibility of achieving perfect ordering, for example, in the *virtual ferroelectrics* $KTaO_3$ and $SrTiO_3$ where polar ordering is failed due to quantum oscillations].

Next, as can be seen from Fig.7.3, when temperature rises to T_2, the *partial ordering* of polar-sensitive structure occurs, at which its length decreases on $-\Delta l_2$. In Chapter 3 various explanations were given for this compression – due to ordering of polar bonds or due to establishment of closer covalent connection. Further increase of temperature, accompanied by essential increase of phonons concentration, leads to model chain thermal expansion (nature of which is described before in Chapter 3). Then this extension continues at T_3 and T_4 in Fig. 7.3.

2. *Secondary pyrolectric effect* can be explained by the one-dimensional model presented above as *piezoelectric* response of a chain. Indeed, any mechanical stretching or compression of model chain leads to additional change in specific electrical moment: $\Delta M_{i2} \sim \Delta l/l$. Thus, not only from general considerations, but also from given simple model it follows that *any pyroelectric should have piezoelectric properties* (but opposite conclusion would be unfair in normal conditions).

In case of secondary pyrolectric effect, the proportionality of electrical moment ΔM_{i2} to the temperature increment ΔT is a result of *linear* dependence of thermal deformation on temperature: $\Delta l \sim \alpha \Delta T$, where α is coefficient of thermal expansion, as well as a result of also *linear* dependence of mechanically induced electrical moment ΔM_{i2} on relative deformation (strain) that means direct piezoelectric effect: $\Delta M_{i2} \sim e \Delta l/l$, where e is piezoelectric strain constant. From these two formulas it is possible to obtain simple linear equation for secondary pyroelectric effect: $\Delta M_i = \gamma^{(2)} \Delta T$, where $\gamma^{(2)} = e\alpha$ is secondary pyroelectric coefficient produced by piezoelectric conversion of thermal strain. Practically dependence of $\gamma^{(2)}(T)$ follows temperature dependence of thermal expansion coefficient $\alpha(T)$, which in polar crystals at low temperatures is negative but than changes by the law $\gamma^{(2)} \sim \alpha \sim T^3$.

Some examples of $\gamma^{(2)}(T)$ dependences in pyroelectric crystals are shown in Fig. 7.4. Usually at low temperatures the pyroelectricity decreases significantly down to negative values. At that, the largest secondary pyroelectric coefficient is seen in the lithium sulfate crystal, which at normal temperatures has technical

applications as thermal sensor (due to its low dielectric permittivity and high stability). In the pyroelectrics-semiconductors of $A^{II}B^{VI}$ group (CdS is their representative) as well as in others *hexagonal crystals*, which $\gamma^{(2)}(T)$ dependence is shown in Fig. 7.4B, the pyroelectric effect is much smaller than in lithium sulfate (note that special characteristics $\gamma^{(2)}(T)$ of beryllium oxide is due to its very large Debye temperature).

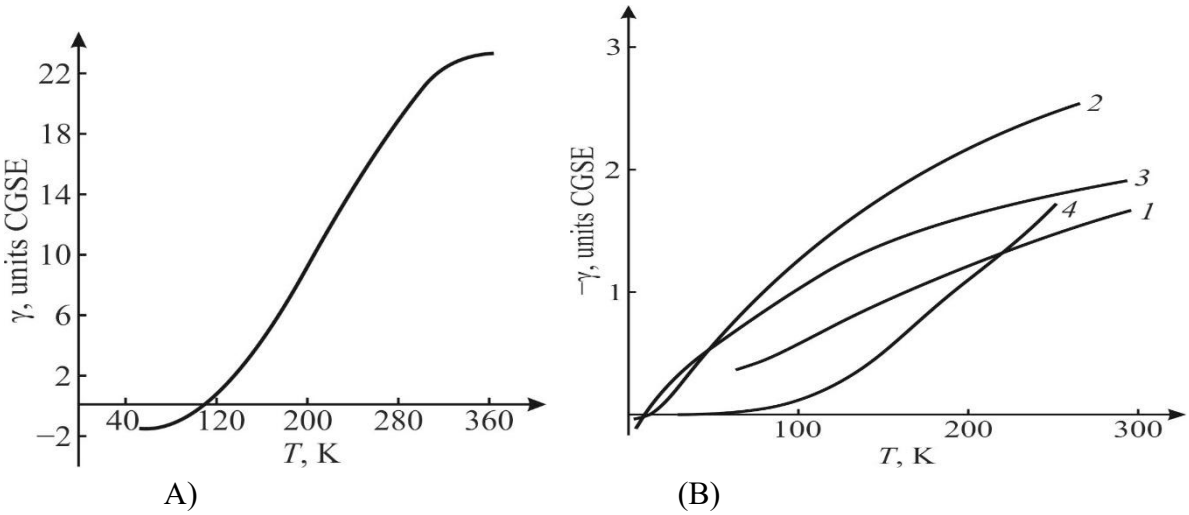

Fig. 7.4. Secondary pyroelectric coefficient temperature dependence [3]: A – lithium sulfate crystal, Li_2SO_4-H_2O; B – tourmaline, $NaMg[Al_3B_3 \square SiO_2(OOH)_{30}]$ (*1*), ZnO (*2*), CdS (*3*), BeO (*4*)

It is noteworthy that in most polar crystals, which were discussed in detail in Section 3, thermal expansion coefficient at low temperature becomes negative. Accordingly, their pyroelectric coefficient $\gamma^{(2)}(T)$ changes its sign, as it seen in Fig. 7.3; moreover, it should be noted that the change in sign of pyroelectric coefficient could hardly be explained, adhering to the model of spontaneous polarization.

Thus, secondary pyroelectric coefficient can be measured as difference between the pyroelectric coefficients of mechanically free and clamped crystal. This coefficient can be also calculated from equation of piezoelectric response: $M_i = e_{im} x_m$, where e_{im} are components of piezoelectric module (third rank tensor) and x_m is component of strain (second rank tensor). Under thermal influence this effect is excited by thermally induced strains in a crystal: $x_m = \alpha_m dT$, where α_m is component of thermal expansion coefficient (which is also second rank tensor). It should be noted that, traditionally, components of symmetric second rank tensors (such as strain x_m, stress X_n and others) are denoted by a single index which, however, has six values: $m, n = 1, 2 ...., 6$, while the components of first-rank tensors (vectors) are usually characterized by the index that has 3 values: $i = 1, 2, 3$. As a result, components of secondary pyroelectric coefficient are written as follows: $\gamma_i^{(2)} = e_{im}\alpha_m$

3. ***Primary pyroelectric effect*** needs to be discussed in more detail. The bonding energy of polar bonds determines their resilience to chaotic thermal motion, and these bonds react to external action by such a change, which is accompanied by the electrical response, i.e., by induced polarization. Weakening or strengthening of polar-sensitive structure steadiness depends on the intensity of thermal motion in crystal. At that, in first approximation, thermally induced elementary electrical polar moment dm can be considered as proportional to intensity of thermal motion: dm ~ k_BT. The density of thermally induced electrical moment of 1D polar chain M_{i1} can be obtained by the summing elementary moments along chain: $M_{i1} = \gamma^{(1)}\Delta T$, where ΔT is some temperature interval and $\gamma^{(1)}$ is the *primary* pyroelectric coefficient, emergent due to electrical reaction of polar-sensitive crystal.

The reaction of "more persistent" polar-sensitive bonds to external influence (in this case, to temperature change) is much weaker than the reaction of "more pliant" polar bonds. Therefore, in "more persistent" pyroelectrics the primary coefficient $\gamma^{(1)}$ is much less than in the "more pliant" pyroelectrics, which, as a rule, are ferroelectrics. Indeed, in the ferroelectrics, in the end, thermal chaotic motion destroys any correlation of polar-sensitive bond in Curie point. (In this regard, it should be noted that in ferroelectrics, because of weakness of their polar bonding, the external electrical field is able to reorient the direction of these bonds to opposite one, forming dielectric hysteresis loop).

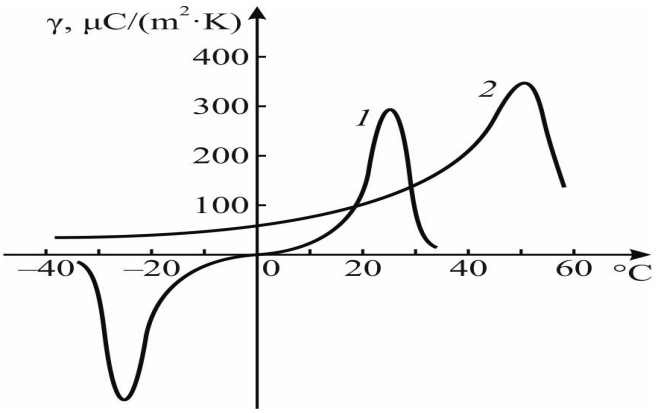

Fig. 7.5. Pyroelectric coefficient temperature dendence [3]: *1* – Rochele salt ($KNaC_4H_4O_6 \square H_2O$); *2* – triglycine sulfate $(NU_3CH_2COOH)_3 \square H_2SO_4$

Currently, dozens of pyroelectric crystals have been investigated and many compositions have been developed. However, the Fig. 7.5 shows only the classic examples: pyroelectric coefficients for two well-studied crystals: Rochelle salt (RS) and triglycine sulfate (TGS). The study of RS is only of academic interest, especially in the sense that two phase transitions are observed in this crystal: ferroelectric phase transition at +24 °C and antiferroelectric phase transition at –18 °C. In this regard,

pyroelectric coefficient in the RS changes its sign. In the TGS crystal primary pyroelectric coefficient reaches record value among crystalline pyroelectrics ($\gamma \sim$ 350 μQ/(m^{2}K). In addition, for practical applications, it is very convenient that maximum of pyroelectric coefficient $\gamma^{(1)}(T)$ in TGS crystals is located in the region of normal temperatures.

Summing up this discussion and taking into account both classical mechanisms of pyroelectricity, for thermally induced polarization it is possible to obtain

$$\Delta M_i = (\gamma^{(1)} + \gamma^{(2)})\Delta T$$

Electrical moment induced by temperature change in the *linear* ("persistant") pyroelectrics (such as tourmaline or lithium sulfate crystals) mostly is due to the thermal deformation of a crystal. On the contrary, in the *non-linear* ("pliant") pyroelectrics (which include ferroelectrics), temperature induced electrical moment is caused mainly by the thermal disordering of dipole-type oriented polar-sensitive structure. At that, large change of polar-sensitivity with temperature in *ferroelectrics* near their Curie point is described by equation $\Delta M_i \sim (\theta - T)^{0.5}$, where θ is Curie-Weiss temperature and power "0.5" is Landau critical index. In all above cases, a behavior of pyroelectrics corresponds to one-dimensional polarity model.

4. ***Electrically induced artificial pyroelectric effect*** finds application in the infrared image matrix sensors which use the paraelectric ceramics. The thing is that such matrix consists of thousands of identical miniature pyroelectric elements, each of which is connected to its own amplifier (that also have the form of correspondent matrix). Ceramics are used because in a crystal it is difficult to ensure the uniformity of all the elements due to the inevitable changes in the conditions of crystal growth.

The designs of IR imagers are known, where the *ferroelectric* ceramics are used below its Curie temperature, in which it is, nevertheless, necessary to maintain the same polarization of all elements by electrically bias fild application In this case, it is advisable to speak of an *electrically supported* pyroelectric effect. Some companies use for such microelectronic imagers lead titanate based ceramics, for example, $Pb(Ti.Zr)O_3$; such instruments provide infrared observations with a temperature contrast better than 1 °C.

For even greater sensitivity, it is possible to choose a material with the highest dependence of permittivity on temperature*), such are the ferroelectrics in their *paraelectric phase*, where dependence of $\varepsilon(T)$ is described by the Curie-Weiss law, Fig. 7.6A. For example, the company Texas Instruments for this purpose applied a ceramic solid solution $Ba_{0.67}Sr_{0.33}TiO_3$ (BST) with Curie point near 20 C and

permittivity maximum of about 25,000 [6]. However, above Curie point, the polar-sensitive bonds in paraelectric are disordered, so that the external *electrical bias field* E_b must be applied to induce the pyroelectric effect (in case of BST optimal $E_b \sim 4$ kV/cm.

[Note. Since the pyroelectric coefficient is $\gamma = dP/dT \approx (\varepsilon_0 d\varepsilon/dT)E$, the external electrical field E, in principle, always induces pyroelectricity, but this effect is usually imperceptibly small, since typically in crystals $\varepsilon \sim 10$ and it very weakly depends on temperature. The exceptions are the ferroelectrics where a huge $\varepsilon \sim 10^4$ changes dramatically with temperature according to the Curie-Weiss law, as a result of which the induced pyroelectric effect becomes so large that it finds important technical applications].

Dotted line in Fig. 7.6A shows temperature dependence of polarization *without* external bias field application while solid line characterizes polarization at bias field. This field shifts the phase transition towards higher temperatures, and such a reduction of $P(T)$ allows record the temperature change on $+\delta T$ or $-\delta T$ by the measuring of pyroelectric current induced by changing of polarization ($+\delta P$ or $-\delta P$). At selected working point (at temperature T_b and the displacement field E_b) the induced polarization equals P_b being *non-equilibrium* without external electrical support.

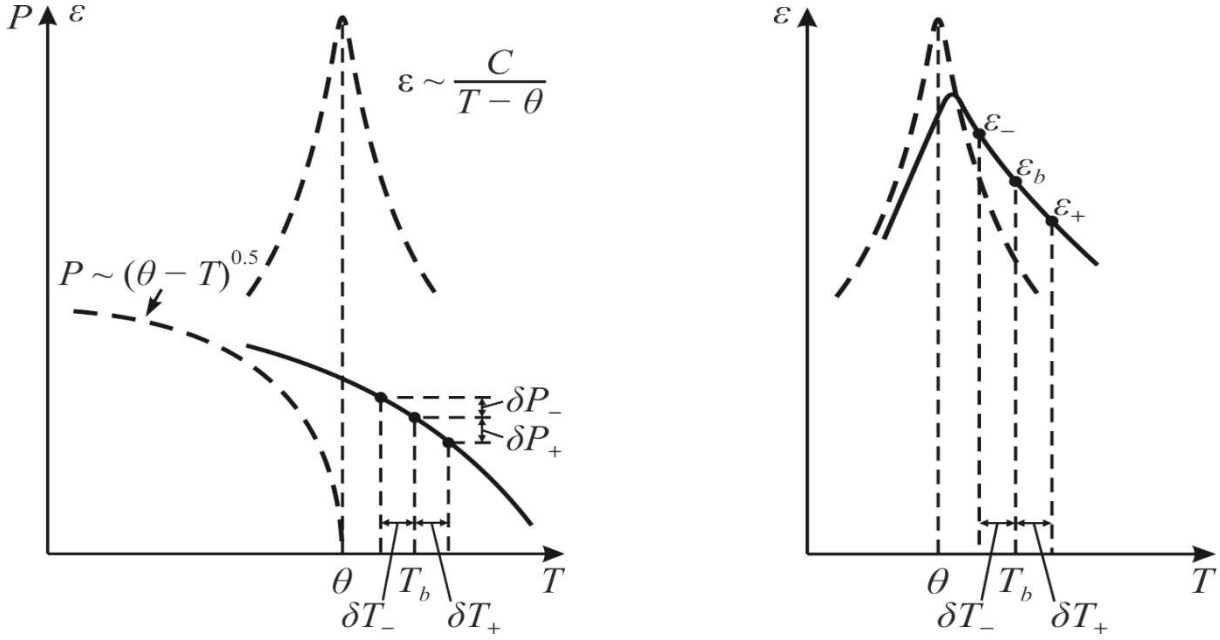

Fig. 7.6. Electrically induced pyroelectric effect in paraelectric phase of ferroelectric: A – dielectric permittivity ε and reversible polarization P temperature dependence; B – dielectric permittivity ε
(dotted line – without bias field, solid line – at bias field)

The electrical field E_b that holds induced by it polarization at given temperature T_b resists to polar bonds natural disordering caused by thermal random motion of crystal lattice. The change in this temperature on $\pm\delta T$ due to external heating or cooling disrupts this equilibrium, and when a new equilibrium is established the polarization changes on $\pm\delta P$, which leads to registration of new temperature by signal current flowing through correspondent transistor.

It should be noted that the mechanism of electrically induced pyroelectric response can be explained differently, Fig.7.6B. Peculiar for ferroelectrics temperature maximum of permittivity under the action of electrical displacement field expands and shifts towards high temperatures. At selected operating point with field E_b and base temperature T_b, permittivity equals ε_b, so sensor element has capacitance $C_b \sim \varepsilon_b$ and contains electrical charge $Q_b \sim C_b$. If sensor's temperature rises by $+\delta T$, capacitance of element decreases by δC, at that the excess charge $-\delta Q_b$ flows to the input circuit of amplifier registering the increase in temperature. Similarly, when temperature decreases by $-\delta T$, capacitance of pyroelectric element increases, and bias electrical field additionally infects it with a charge $+\delta Q_b$, which is registered by amplifier in the form of electrical signal of opposite polarity.

In military technology, microelectronic matrix (non-vacuum) pyroelectric vidicons are widely used: matrix devices allow investigate the spatial distribution of radiation. Such sensitive receivers of radiation can consist of many pyroelements that form the *pyroelectric line* (with a number of elements of several dozen) or the pyroelectric matrix (10^3 - 10^5 elements). In such matrices, thousands of miniature pyroelectric cells are placed on one silicon plate of the processor. Each elementary pyroelement is connected to the input of correspondent integral transistor so that the plate of square inch is a solid state IR TV receiver. Such non-cooled receivers have a very high sensitivity that grows like a square root of the number of elements, and can distinguish between the temperature contrast of 0.1–0.2 degrees.

5. ***Thermomechanical induced artificial pyroelectric effect*** is described in detail in Chapter 2. At that in any piezoelectric (including non-pyroelectrics) the artificial pyroelectric effect can be obtained which might have interest for practical applications. Comparing the magnitude of such mechanically induced pyroelectric effect with the ordinary pyroelectric effect can be made by the example of a lithium niobate crystal. In the $LiNbO_3$ crystal, in addition to the pyroelectric polar axis, there are also three polar-neutral axes, and in crystal slices made perpendicular to any of these axes while limiting thermal deformation (for example, by stick of such a slice onto silica glass substrate, it is possible to get the artificial pyroelectric effect with

pyroelectric coefficient $\gamma^*_2 = 40$ μC□m^{-2}□K^{-1}, which is only slightly inferior to the usual pyroelectric effect of $LiNbO_3$ equal to $\gamma_3 = 50$ μC□m^{-2}□K^{-1} [10, 11].

At the same time, thermomechanical induced pyroelectric effect opens up completely new possibilities in the use of wide-gap semiconductors-piezoelectrics. In them, artificial effect is not small: in gallium arsenide this coefficient is $\gamma^*_{111} =$ 1.5 μC□m^{-2}□K^{-1} n comparison with well-known pyroelectric tourmaline with $\gamma = 4$ μC□m^{-2}□K^{-1}. In the crystal of bismuth germanate ($Bi_{12}GeO_{20}$) this parameter equals $\gamma^*_{[111]} = 20$ μC□m^{-2}□K^{-1} that exceeds many times effects in quartz and GaAs. It can be supposed that temperature dependence of piezoelectric polar-sensitivity can be used in the microelectronics for thermal sensors [12–14]. Thus, the physical mechanisms of the pyroelectric effect can be varied.

7.3 Pyroelectric effect thermodynamic description

Pyroelectric effect is defined as the electrical response of polar crystal onto uniform alteration of crystal temperature. As was shown in Introduction when Fig. I.1 discussion the pyroelectric effect can be described by *four* different equations (depending on thermal and electrical conditions). Since pyroelectric effect can be primary and secondary, the mechanical boundary conditions have to be taken into account in these equations. Thermodynamic consideration of pyroelectric effect is advisable to carry out taking into account those boundary conditions that are used in the most common case of pyroelectrics application in a thermal sensor.

In the mechanically free crystal (when stress $X_m = 0$) in the electrically free conditions (crystal is situated in a closed circuit when $E_i = 0$), arising pyroelectric current is defined by the pyroelectric coefficient $\gamma_i^{X,E}$, where superscripts indicate the permanency of electrical field and mechanical stress during thermodynamic processes of pyroelectric response and subscript means that the pyroelectric coefficient is a vector. In fact, the electrical field and the mechanical stress are not always zero, but it is assumed that they remain unchanged; for example, the polycrystalline pyroelectric sensor array usually needs the unaltered electrical displacement field to orient ferroelectric domains, at that, this target is experiencing constant mechanical stress because it is deposited on a substrate.

As follows from simple model of pyroelectricity, shown in Fig. 7.2, traditionally is accepted the phenomenological division of pyroelectric effect into the primary and secondary effects with coefficients $\gamma^{(1)}$ и $\gamma^{(2)}$ correspondingly:

$$\gamma_i^{X,E} = \gamma_i^{(1)} + \gamma_i^{(2)} = \gamma_i^{x} + d^{T}_{im} . c_{mn}^{X,E} . \alpha_n^{X,E}, \qquad (7.1)$$

$i = 1, 2, 3;$ $m, n = 1, 2, \ldots 6.$

The contribution of primary pyroelectric effect can be found during mechanically clamped crystal study when strain is absent ($x_n = 0$), i.e., $\gamma^{(1)} = \gamma_i^x$. The contribution of secondary effect can be found experimentally as a difference between pyroelectric coefficients of free and clamped crystal: $\gamma_i^{(2)} = \gamma_i^{X,E} - \gamma_i^x$ that can be calculated using formula (7.1) with known components of piezoelectric modulus d^T_{im}, elastic stiffness $c_{mn}^{X,E}$, and thermal expansion coefficient $\alpha_n^{X,E}$ (superscripts correspond different boundary conditions). Usually in the linear ("persistant") pyroelectrics $\gamma = 10^{-7}$–10^{-5} C·m^{-7}·K^{-1} while in the non-linear ("pliant") pyroelectrics-ferroelectrics $\gamma = 10^{-5}$–10^{-3} C·m^{-7}·K^{-1}.

It should be recalled that symmetry requirements permit both primary and secondary pyroelectric effects only in 10 of 20 piezoelectric classes of crystals. At that, in the pyroelectric crystal a "peculiar polar direction" exists, along which pyroelectric response shows maxim, Fig. 7.1B. In the remaining 10 piezoelectric but not pyroelectric classes of crystals any scalar (homogeneous) influence, including temperature, can not result in a vector (electrical) response under *homogeneous* boundary conditions, i.e., if the crystal is mechanically completely free or entirely clamped. In order to excite electrical response in the piezoelectric by thermal influence, the temperature gradient or the inhomogeneous boundary conditions are needed.

Pyroelectric is a transducer of thermal energy into electrical energy. When using the electrocaloric effect, which is inverse effect to pyroelectric effect, the electrical energy is converted into a heat. The efficiency of these conversions is characterized by the coefficient of electro-thermal bonding $K_{TE} = K_{ET}$. Power coefficient of thermoelectric conversion K_{TE}^2 shows what part of thermal energy $\mathrm{d}W_\mathrm{T}$ delivered to the reformative element is converted into the electrical energy $\mathrm{d}W_E$:

$$K_{ET}^2 = \mathrm{d}W_E/\mathrm{d}W_T. \qquad (7.2)$$

In view of some difficulties associated with determination of K_{ET} in the dynamic regime of work, the thermoelectric conversion efficiency might be estimated using quasi-static thermodynamic relations derived on basis of Gibbs thermodynamic potential (G) or on basis of electrical potential of Gibbs (G_2), which describes equilibrium properties of crystals.

There are eight thermodynamic potentials, corresponding to eight combinations of conjugate thermodynamic variables D and E, X and X, S and T; three of which might be selected as the dependent variables, and remaining three as the independent variables. For *potential G* the *independent* variables of are stress (X), electrical field (E) and temperature (T), while the *dependent* variables are strain

(x), electrical displacement (D) and entropy (S). In the case of *potential* G_2 the *independent* variables of are strain (x), electrical field (E) and temperature (T), while the *dependent* variables are stress (X), electrical displacement (D) and entropy (S). The increment of thermodynamic potentials is determined by a work done by reformative element under certain boundary conditions specific for functional given element:

$$\mathrm{d}G = -x_i\,\mathrm{d}X_i - D_n\,\mathrm{d}E_n - S\,\mathrm{d}T\,,$$
$$\mathrm{d}G_2 = X_i\,\mathrm{d}x_i - D_m\mathrm{d}E_m - S\,\mathrm{d}T,$$

where

$$x_j = -\partial G/\partial X_j\;;\;\; D_m = -\partial G/\partial E_m;\;\; S = -\partial G/\delta T,$$

and, correspondingly

$$X_j = -\partial G_2/\delta x_j\;;\;\; D_m = -\partial G_2/\delta E_m;\;\; S = -\partial G_2/\delta T\;;$$

where: $i, j = 1, 2, 3$ and $n, m = 1, 2,\ldots 6$.

The choice of potentials (of possible eight) to estimate the work carried out by thermodynamic system is determined by the mechanical, electrical and thermal boundary conditions under which the element of a device works. The change of independent variables (X, E, T) that corresponds to the equation of state for the dependent variables (x, D, S), where the superscripts X, E, T denote the so-called boundary conditions which must be invariable, while crystal parameters are measured:

$$\begin{aligned}\mathrm{d}x_n &= s_{nm}^{E,T}\,\mathrm{d}X_m + d_{in}^{X,T}\,\mathrm{d}E_i + \alpha_n^{X,E}\,\mathrm{d}T;\\ \mathrm{d}D_n &= d_{nj}^{E,T}\,\mathrm{d}X_j + \varepsilon_{nm}^{X,T}\,\mathrm{d}E_m + \gamma_n^{X,E}\,\mathrm{d}T;\\ \mathrm{d}S &= \alpha_j^{X,E}\mathrm{d}X_j + \gamma_n^{X,T}\,\mathrm{d}E_n + C^{X,E}\,\mathrm{d}T/T.\end{aligned} \qquad (7.3)$$

In above expressions (7.3), the following notations are applied:

$$s_{nm}^{E,T} = \mathrm{d}x_n/\mathrm{d}X_m = -\partial^2 G/\partial X_m \partial X_n$$

– the elastic stiffness, fourth rank tensor;

$$d_{nj}^{X,T} = d_{nj}^{T} = dx_n/dE_i = dD_j/dX_n = -\partial^2 G/\partial X_n \partial E_i$$

– the piezoelectric modulus, third rank tensor;

$$\varepsilon_{ij}^{X,T} = \partial D_i/\partial E_j = -\partial^2 G/\partial E_i \partial E_j$$

– the permittivity tensor, second rank tensor;

$$\alpha_n^{X,E} = \alpha_{n'}^{E} = dx_n/dT = -\partial^2 G/dT\partial X_n$$

– the thermal expansion tensor of free crystal, second rank tensor;

$$\gamma_i^{X,E} = \gamma_{i'}^{E} = \mathrm{d}D_i/\mathrm{d}T = \partial S/\partial E_i = -\partial^2 G/\partial T \partial E_i$$

– the pyroelectric coefficient, tensor of the first rank;

$$C^{X,E} = T\mathrm{d}S/\delta T = -T\,\partial^2 G/\partial T^2$$

– the specific volumetric heat capacity, scalar (tensor of zero rank).

The transformations of piezoelectric strain tensor are: $e_{nj}^{x,T} = e_{nj}^{E,T} = e_{nj}^{E}$.

Taking into account that shape and volume of pyroelectric element do not change ($x = 0$, i.e., crystal is mechanically clamped), from above equations in case of $E = 0$ it is possible to obtain the contribution to thermally induced polarization P_i from the *primary* pyroelectric effect:

$$\mathrm{d}P_i = \gamma_i^x \, \mathrm{d}T, \qquad (7.4)$$

where $\gamma_i^x = \gamma_i^{(1)}$.

The above equations allow also find *piezoelectric contribution* to the pyroelectric coefficient, as well as to the dielectric permittivity and to the volumetric specific heat capacity of a crystal. The measurements of pyroelectric effect are usually carried out at the condition $E = 0$. When using equations (7.4), it is possible to obtain the following relationship between pyroelectric coefficient of mechanically free ($X = 0$) crystal and mechanically clamped ($x = 0$) crystal:

$$\gamma_i^X = \gamma_i^x + e_{mi}{}^T \alpha_{m'}{}^E, \qquad (7.5)$$

which means $\gamma = \gamma^{(1)} + \gamma^{(2)}$, because expression $e_{mj}{}^T \alpha_{m'}{}^E = \gamma^{(2)}$ describes the contribution of *secondary* pyroelectric effect.

At constant temperature, the permittivity of mechanically free ($\varepsilon_{nm}^{X,T}$) crystal and clamped ($\varepsilon_{nm}^{x,T}$) crystal are related as follows:

$$\varepsilon_{ij}^{X,T} = \varepsilon_{ij}^{x,T} + d_{ni}{}^T e_{nj}{}^T, \qquad (7.6)$$

where $d_{ni}{}^T e_{nj}{}^T$ is the piezoelectric contribution to permittivity.

For heat capacity of electrically short-circuited ($E = 0$) and mechanically free ($X = 0$) pyroelectric crystal the following relation holds:

$$C^{E,X} = C^{E,x} + T\alpha_m{}^E c_m{}^{E,T}.$$

Note that the difference between the $C^{E,X}$ and $C^{E,x}$ is small, so that in the notation of volume specific heat it is possible to keep only one superscript: C^E.

From the above equations it follows that the use of pyroelectric element in the absence of mechanical stress ($X = 0$) and when electrical field is absent ($E = 0$), the accumulation of electrical energy in the pyroelectric element $\mathrm{d}W_E$ is described by the potential G, that in a given boundary conditions corresponds to expression:

$$\mathrm{d}W_E = D_i \, \mathrm{d}E_i = (\mathrm{d}P_i)^2/\varepsilon_o\varepsilon_{ij}^{X,T} = (\gamma_i^{X,E})^2(\mathrm{d}T)^2/\varepsilon_o\varepsilon_{ij}^{X,T}, \qquad (7.7)$$

where $\mathrm{d}P_i = \mathrm{d}D_i$ and $\mathrm{d}W_E$ is obtained quantity of electrical energy in the process of pyroelectric effect.

The thermal energy $\mathrm{d}W_\mathrm{T}$ that is spent on energy storage in crystal by the definition equals to $\mathrm{d}S \cdot \mathrm{d}T$; under a given boundary conditions it corresponds to expression:

$$\mathrm{d}S \cdot \mathrm{d}T = (\alpha_m^{X,E}\mathrm{d}X_m + \gamma_i^{X,T}\,\mathrm{d}E_i + C^{X,E}\mathrm{d}T/T) \cdot \mathrm{d}T,$$

where the increments dX_m and dE_i respectively represents the appearance of stress and electrical field in crystal. Estimation of the amount of $(\alpha_m^{X,E}\, dX_m + \gamma_i^{X,T}\, dE_i)$ in different pyroelectric crystals shows that it does not exceed a fraction of percent of value $(C^{X,E}dT/T)$, so

$$dW_т = C^{X,E}\,(dT)^2/T_p, \qquad (7.8)$$

where $T_p = T$ is the operating temperature of the element and $dW_т$ is the obtained quantity of thermal energy.

Thus, when the pyroelectric element is mechanically free ($X = 0$), the equation (7.2) after substitution of equations (7.7) and (7.8) can be written as follows:

$$K_{ET}^2 = [(\gamma_i^{X,E})^2(dT)^2/\varepsilon_o\varepsilon_{ij}^{X,T}]/[C^{X,E}(dT)^2/T_p] = (\gamma_i^{X,E})^2 T_p/\varepsilon_o\varepsilon_{ij}^{X,T}C^{X,E}.$$

Similarly, the factor of electro-thermal conversion for mechanically clamped crystal element is:

$$K_{ET}^2 = [(\gamma_i^{x,E})^2(dT)^2/\varepsilon_o\varepsilon_{ij}^{x,T}]/[C^{x,E}(dT)^2/T_p] = (\gamma_i^{x,E})^2 T_p/\varepsilon_o\varepsilon_{ij}^{x,T}C^{x,E}.$$

Calculations show that even in best pyroelectrics electro-thermal conversion factor is small: in TGS crystal $K_{ET}^2 = 4\%$, in SBN ($Sr_{0.5}Ba_{0.5}Nb_2O_6$) $K_{ET}^2 = 1.2\%$ and in $LiTaO_3$ $K_{ET}^2 = 1\%$. In others pyroelectrics this factor is even smaller: in $BaTiO_3$ $K_{ET}^2 = 0.25\%$ and in polymer PVDF $K_{ET}^2 = 0.2\%$. Relatively low efficiency of thermoelectric conversion is due to a physical nature of this phenomenon in dielectric crystals that are "electrically persistant" in relation to the external influences. Note in this regard that the efficiency of energy conversion is much higher in the case of piezoelectric effect. Corresponding electromechanical coupling coefficient K_{EM} much exceeds the pyroelectric coupling coefficient K_{ET}. The value of K_{EM} sometimes reaches ~ 0.95, and in case of piezoelectric resonance in crystals that have high electro-mechanical quality this coefficient increases to almost 1.

In spite of low efficiency, pyroelectric effect is used primarily for the detection and measurement of heat flow, and, under certain conditions, for direct transition of thermal energy into electricity. The "direct" conversion of heat into electricity is used in thermal imaging and in highly sensitive temperature sensor. The advantage of pyroelectric sensors is that they use a thermal signal to convert electrical signals to dielectrics in which electrical conductivity is virtually absent and the “shot noise” produced by the charge carriers is reduced to zero. As well known, the most important characteristic for the sensor is the "signal-to-noise" ratio, which in the pyroelectrics exceeds this parameter of semiconductor sensors (the latter usually need to be cooled)

The efficiency of pyroelectric sensors, which convert the infrared radiation into the electrical energy, is evaluated by special "quality parameters" commonly

called as *figures of merit.* In addition to the main parameter (pyroelectric coefficient γ) the figures of merit using are really necessary.

For example, the temperature change of pyroelectric element under heating conditions the greater, the lower its volumetric specific heat C_V, as well as the voltage generated by the element becomes greater, the lower is its permittivity ε. Depending on where the pyroelectric material is used, the figures of merit are different.

In the case of *low impedance* amplifier application for the efficiency of sensor next figure of merit should be used: *current sensitivity* $S_I = \gamma/C_V$. However in the case of *low impedance* amplifier another figure of merit is actual: *voltage sensitivity* $S_V = \gamma/(C_V\varepsilon_0\varepsilon)$.

For thermal imaging matrix device the Landau coefficient $\alpha_L = (T - \theta)/\varepsilon_0 C$ (where C – is Curie-Weiss constant) is important which characterises temperature dependence of permittivity, so that the figure of merit is $\gamma/(C_V\alpha_L\varepsilon_0\varepsilon)$.

At last, for large-distant temperature sensor, in which most important is the low noise in pyroelectric, it is recommended to use following figure of merit: $\gamma/[C_V(\varepsilon_0\varepsilon\tan\delta)^{1/2}]$, where $\tan\delta$ is dielectric losses characteristic.

Table 7.1 presents a number of options for pyroelectrics with these quality parameters.

The first group of pyroelectrics presented in Table 7.1 includes ferroelectrics with a non-linear dependence $P(E)$: crystals of triglycinesulfate group, lithium niobate and lithium tantalate, potassium nitrate, lead titanate, polarized zirconate-titanate ceramics.

In ferroelectrics, mainly the primary pyroelectric effect is used, especially large near the Curie point, where the temperature change of polar-sensitive bonds is expressed very strongly and pyroelectric coefficient reaches a maximum.

The *linear* crystalline pyroelectrics (in which dependence $P(E)$ is linear) can be attributed to the *second group* of pyroelectrics.

In them, the polar-sensitive bonds have same direction throughout a crystal (unlike ferroelectrics, which are usually divided into domains), and this direction cannot be changed by external electrical field. Pyroelectric coefficient of linear pyroelectrics varies a little with temperature, never falling to zero, as in ferroelectrics.

These pyroelectrics include $A^{II}V^{VI}$ crystals with wurtzite structure (such as CdS) as well as lithium sulfate, lithium tetraborate, and others. In linear pyroelectric the contribution of secondary pyroelectric effect is relatively large and can exceed the contribution of primary pyroelectric effect.

Table 7.1

Basic parameters of pyroelectrics used to manufacture sensors:

γ – pyroelectric coefficient, ε – permittivity, λ – thermal conductivity, C_V – volumetric heat capacity, S_j – current sensitivity, S_V – voltage sensitivity (all data given at room temperature)

Pyroelectric	γ, $10^{-5}\times$ $C/(m^2 \cdot K)$	ε	λ, $W/\mu C$	C_V, $10^6\times$ $\times J/(m^3 \cdot K)$	$\gamma/C_V = S_j$, $10^{-11}\ A \cdot m/W$	$\gamma/(C_V\varepsilon) = S_V$, $10^{-12}\ A \cdot m/W$
TGS $T_C = 49°C$	40	35	0,4	2,5	16	4,6
DTGS $T_C = 61°C$	27	18	0,4	2,5	10,8	6,0
LaTGS $T_C = 49,5°C$	70	35	~0,4	2,6	27,5	7,8
DLaTGS $T_C = 49,2°C$	25	22	~0,4	2,6	9,8	4,5
TGFB $T_C = 73,8°C$	21	15	~0,4	1,7	12,5	8,3
TGSe $T_C = 22°C$	30	400	~0,4	1,8	16,8	0,4
$LiTaO_3$ $T_C = 618°C$	22	52	4,2	3,2	6,9	1,3
$LiNbO_3$ $T_C = 1210°C$	8	30	~ 4,0	2,8	2,9	0,9
$Sr_{1/2}Ba_{1/2}Nb_2O_6$ $T_C = 116°C$	60	400	~2,0	2,34	25,6	0,6
PLZT (6/80/20) $T_C = 120°C$	76	1000	1,2	2,6	29	0,3
PLZT (4/65/35) $T_K = 225°C$	52	680	1,2	2,6	20	0,3
PCD 33/14 $T_K = 420°C$	17	250	~2,0	3,2	5,3	2,0
PVDF	3	11	0,13	2,4	1,3	1,0

Polar polymers (such as PVDF films) and polar composite materials can be attributed to the *third group* of pyroelectric materials. They need additional special treatment: stretching the film in several times with its subsequent polarization, as a result of which the polymer film acquires pyroelectric properties.

The pyroelectric coefficient of polymeric materials is lower than that of polar single crystals and pyroelectric ceramics, but the films have excellent mechanical properties, being flexible materials.

For comparing of physical mechanisms of pyroelectricity in different pyroelectric materials, as well as for evaluating the possibilities of their technical

application in Fig. 7.7 the temperature dependences of the current and voltage efficiency of pyroelements are given.

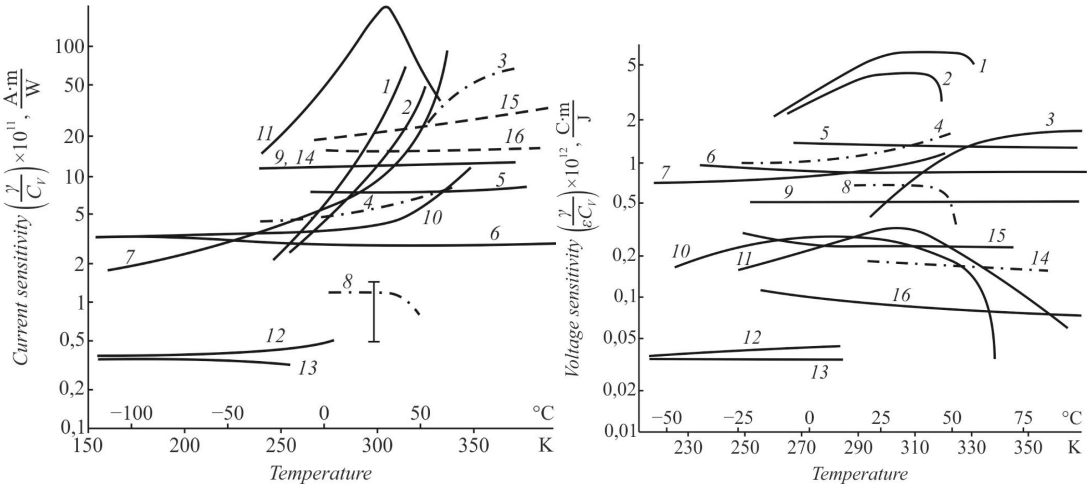

(A) (B)

Fig. 7.7. Temperature dependence of current (A) and voltage (B) sensitivity in different pyroelectrics: 1 – DTGS; 2 – TGS; 3 – $BaTiO_3$; 4 – $Li_2SO_4 \oplus H_2O$; 5 – $LiTaO_3$; 6 – $LiNbO_3$; 7 – $Pb_5Ge_3O_{11}$; 8 – $PVDF_2$; 9 – $SbNbO_4$; 10 – $Sn_2P_2S_6$; 11 – $Sr_{0,75}Ba_{0,25}Nb_2O_6$; 12 – CdO; 13 – ZnO; 14 – PZT-5; 15 – PZT-4; 16 – PZTG-1306.

It is noteworthy that crystals with the maximum of current sensitivity $\gamma/C_V = Sj$ do not belong to the thermostable materials. Typically, they are ferroelectrics with Curie point θ of about 300 K. The pyroelectric coefficient is maximal near theθ, because in this temperature range the ability to temperature polarization is most seen. The change in specific heat of material has little effect on temperature change of quality parameter γ/C_V. To the pyrodetectors, crystals with a maximum of this parameter the triglycinsulfate (TGS), deuterated triglycerol sulfate (DTGS), strontium-barium niobate (SBN) belong. Therefore, in this case the sensitive receivers need external some thermal stabilization. In ferroelectric crystals of barium titanate ($BaTiO_3$) and lead germanate ($Pb_5Ge_3O_{11}$) with a rather low Curie point (400 and 450 K. respectively) the thermostability of γ/C_V characteristic is not very good. On the contrary, the thermostatically stable crystals are lithium tantalate ($LiTaO_3$) and lithium niobate (LiNbO3), as well as lead stbioniobate crystals ($SbNbO_4$), but the latter are not sufficiently developed technologically.

The current sensitivity of the pyroelectric elements, made of tantalate and lithium niobate, is in an order of magnitude inferior to the crystals of SBN and TGS. For comparison, in Fig. 7.7 the γ/C_V characteristics non ferroelectric (but pyroelectric) crystals are shown: cadmium sulfide (CdS) and zincite (ZnS). These pyroelectrics are very thermostable but have low sensitivity; moreover, with increasing temperature their electrical conductivity increases. However, these pyroelectrics also deserve attention, because they can be relatively easily obtained

in the form of thin layers by modern microelectronic technology. Micron thickness of CdS and ZnS films can be relatively easy integrated into a monolithic structure with silicon.

Another dependences that are shown in Fig. 7.7B are the temperature variation of quality parameter of volt-watt sensitivity $\gamma/(C_V\varepsilon) = S_V$. In this case, the temperature peak of parameter γ in the vicinity of Curie point ferroelectric is compensated by the temperature dependence of its dielectric constant ε. With this parameter, crystals of TGS type have a clear advantage over other pyroelectrics. However, these crystals are mechanically fragile, water soluble and, if possible, they are desirable to be replaced by the chemically and mechanically durable pyroelectrics such as single crystals $LiTaO_3$, $SbNbO_4$ and tin thiogipophosfate ($Sn_2P_2S_6$).

Since most pyroelectrics belong to ferroelectrics, it is advisable to apply the thermodynamic Landau theory developed to describe the properties of the ferroelectrics to analyze, in part, the temperature dependence of figures of the merit. Since most of the ferroelectrics, used in pyroelectric sensors, belong to crystals with a second-order phase transition, then the Landau's proposed expansion of free energy F in a series on the fluctuations in polarization has the following form:

$$F(P,T) = \tfrac{1}{2}\,\alpha_L P^2 + \tfrac{1}{4}\,\beta_L P^4, \qquad (7.9)$$

where temperature dependent parameter Landau $\alpha_L = \alpha_0(T - \theta) = (T - \theta)/\varepsilon_0 C$ (θ and C are temperature and Curie-Weiss constant respectively; β_L is temperature dependent parameter Landau. Considering that electrical field can be defined as derivative $\partial F/\partial P$, expression (7.9) can be rewritten as $E = \alpha_L P + \beta_L P^3$. For electrically free crystal ($E = 0$) it is possible to obtain:

$$[(T - \theta)/\varepsilon_0 C]P + \beta_L P^3 = 0. \qquad (7.10)$$

Inverse dielectric susceptibility is $\chi^{-1} = dE/dP = d^2F/dP^2 = \alpha_L + 3\beta_L P^2$ but it is possible to consider that $\chi \approx \varepsilon$, since $\varepsilon = 1 + \chi$ and permittivity of ferroelectrics is very large: $\varepsilon >> 1$. In the polar phase (when $T < \theta$) the condition of minimum free energy follows: $P = (T - \theta)^{0.5}/\varepsilon_0 C$. Since dielectric permittivity is defined as

$$\varepsilon \cong (\partial P/\partial E)/\varepsilon_0 = \alpha_L + 3\beta_L P^2,$$

then temperature dependence of dielectric constant below temperature θ gets a look as $\varepsilon = C/[2(T - \theta)]$.

According to Debye theory, heat capacity temperature increasing can be given as: $\Delta C_V = (\partial F/\partial T)$. Since from the Landau theory follows that $P^2 = -\alpha_L/\beta_L$ the expression (8.5) will look like

$$F(P,T) = \tfrac{1}{2}\,\alpha_L P^2 + \tfrac{1}{4}\,\beta_L P^4 = \tfrac{1}{2}\,\alpha_L\,(-\alpha_L/\beta_L) + \tfrac{1}{4}\,\beta_L\,(-\alpha_L/\beta_L)^2 = -\tfrac{1}{4}\,\alpha_L^2/\beta_L.$$

As a result of the differentiation of this equation by temperature, we have:

$$\Delta C_V = (\partial F/\partial T) = \tfrac{1}{2}(\theta - T)/\beta_L(\varepsilon_0 C)^2,$$

$$C_V = C_{V0} + \Delta C_V = C_{V0} + ½(\theta - T)/\beta_L(\varepsilon_0 C)^2.$$

The substitution of the indicated temperature dependences C_V, ε and $\gamma = \partial P/\partial T$ in the formula for the basic parameters of the quality of pyroelectrics (see Table 7.1) allows give their temperature dependence in the form:

$$\gamma = \partial P/\partial T = ½(\beta_L \varepsilon_0 C)^{-1/2}(\theta - T)^{-1/2};$$

$$\gamma/C_V = ½(\beta_L \varepsilon_0 C)^{-1/2}(\theta - T)^{-1/2}/[C_{V0} + ½(\theta - T)/\beta_L(\varepsilon_0 C)^2];$$

$$\gamma/C_V \varepsilon_0 \varepsilon = \beta_L^{-1/2}(\varepsilon_0 C)^{-3/2}(\theta - T)^{1/2}/[C_{V0} + ½(\theta - T)/\beta_L(\varepsilon_0 C)^2].$$

It is seen that to maximize the efficiency of the transformation of the heat signal into an electrical signal the pyroelectric receiver should have not only high pyroelectric coefficient, but also low heat capacity, low dielectric constant (which determines the capacity of the pyroelectric cell and the pyroelectric signal generated on it). Some improvements of the characteristics of the pyroelectric element can be obtained using composite pyroelectric ceramics and polymers. In addition, it should be noted that besides primary pyroelectric effect ($\gamma^{(1)}$), in mechanically free crystal there is also the secondary pyroelectric effect ($\gamma^{(2)}$) due to piezoelectric contribution into pyrocoefficient/ The contribution to pyroelectricity from secondary pyroelectric effect usually is less than the contribution from the primary pyroelectric effect.

Thus, thermodynamic and others calculations and estimates provide an opportunity to explain the features of pyroelectrics, and also allow engineers to choose pyroelectric materials for certain devices.

7.4 Electrocaloric effect

According to Curie principle, any linear physical effect in crystals must have the opposite effect. For example, opposite to the direct piezoelectric effect is the inverse piezoelectric effect. Similarly, the inverse to pyroelectric effect is the electrocaloric effect. In this way, pyroelectric not only converts thermal energy into electrical energy, but vice versa.

In short, the physical mechanism of electrocaloric effect is as follows: constant electrical field applied from the outside to a polar crystal *violates its equilibrium state* under given conditions, which is established thermodynamically at a given temperature and pressure and corresponds to the energy minimum. In this case, the mutual ordering of polar-sensitive interatomic bonds, existing in the equilibrium structure of a pyroelectric, changes. If the applied field is directed accordingly to internal orientation of polar bonds, then it increases total energy of a crystal and it heats up. If this field is directed oppositely, then crystal energy decreases which is expressed in its cooling.

Understanding the physical mechanism and taking into account the influence of this effect is important for describing and predicting some properties of polar crystals, especially in case of phase transitions. Controlled by voltage, the electrocaloric cooling (or heating) depends on the polarity of applied electrical field and crystal polarity. At that, the alternating voltage can generate in crystal the *temperature wave*. Electrocaloric effect can be used for temperature control by electrical voltage, basically to achieve better cooling.

The electrocaloric effect consists in the changing of temperature ΔT of pyroelectric crystal when the electric field ΔE is applied to it. In accordance with this, the equation for electrocaloric effect is

$$\Delta T = \xi \Delta E, \text{ or in the differential form } \xi = \mathrm{d}T/\mathrm{d}E,$$

where ξ is coefficient of electrocaloric effect. Electrocaloric (as well as pyroelectric) properties have only the crystals of polar classes: 1, 2, 3, 4, 6, *m*, 2*m*, 3*m*, 4*m*, 6*m*.

It is possible to find a relationship between electrocaloric coefficient (ξ) and pyroelectric coefficient (γ). The possibility to induce electrical polarization P in the polar0 sensitive crystal reflects the *change* in the heat content in a crystal that is described by the entropy S. At that, the internal energy U of a crystal remains *unchanged* that makes it is possible to write down next relations:

$$\mathrm{d}U = 0 = E\mathrm{d}P + T\mathrm{d}S,$$

from which it follows

$$T = -E\left(\frac{\mathrm{d}P}{\mathrm{d}S}\right), \text{ and } \quad \frac{\partial T}{\partial E} = -\frac{\mathrm{d}P}{\mathrm{d}S} = -\left(\frac{\partial P}{\partial T}\right)\cdot\left(\frac{\partial T}{\partial S}\right).$$

Taking into account the fact that $\partial T/\partial E = \xi$ and $\partial P/\partial T = \gamma$, from thermodynamic relations can be obtained: $dS = dQ/T$, where $\mathrm{d}Q$ is heat increment equal $\rho C J \mathrm{d}T$ (ρ is crystal density, C is heat capacity of crystal and J is the mechanical equivalent heat). Next it is possible to get

$$\xi = -\gamma T/(\rho C J).$$

It's clear that electrocaloric and pyroelectric coefficients are proportional to each other but have opposite signs. Therefore, crystals with big pyroelectric effect exhibit also big electrocaloric effect. The crystal is a single system: if it is *heated* (or cooled), then the change in its internal polarity occurs due to the electrocaloric effect that leads to *cooling* (or heating) of crystal; as a result of which it will tend to maintain its temperature (Le Chatelier's principle). Therefore, when electrical field is applied to a crystal, the electrocaloric effect can lead to both heating and cooling of a pyroelectric, depending on how the ordered polar bonds of a crystal are directed with respect to the applied field. If this field coincides with the orientation of polar-sensitive bonds, the temperature of crystal will increase, but if electrical field is

directed oppositely to their direction, crystal cools. It is natural that just electrocaloric *cooling* may have interest for technical applications; therefore it needs to evaluate exactly this possibility.

In the *linear* ("persistent") pyroelectrics, in accordance with a smallness of the pyroelectric effect, the electrocaloric effect is also small: calculations show that pyroelectric even in a very strong electrical field (already close to electrical breakdown field) can change its temperature only on tenths of degree of Kelvin that obviously not have any technical interest. However, in the *nonlinear* ferroelectrics (and antiferroelectrics), in which the maximum value of permittivity reaches many thousands, the electrocaloric effect is large enough to discuss seriously its possible use in *technical* cooling devices (large electrocaloric effect is described, for example, in [15]). Therefore, it needs to dwell in more detail the electrocaloric effect exactly in the ferroelectric materials.

As known, in the vicinity of phase transitions in ferroelectrics the latent heat of a transition is released or absorbed: it can be considered that this heat is required to compensate the electrocaloric effect. From this point of view, phase transition looks like this: *heated* from outside crystal loses the ordering of its polar bonds and, therefore, it is cooled due to electrocaloric effect, as a result of which *heat is consumed without heating the crystal*. When the crystal is *cooled* through a phase transition, the reverse occurs. Since the temperature of phase transition can be shifted, when external electric field is applied, the process of heat release and heat absorption can be controlled electrically.

As noted, in the *nonlinear* ("pliant") pyroelectrics-ferroelectrics, the maximum of electrocaloric effect is observed in the vicinity of phase transition: it is caused by the appearance (or disappearance) of polar-sensitive bonds ordering. Without application of external electric field, during external cooling from paraelectric phase into ferroelectric phase, the crystal heats up by approximately parts of degree, but it also cools by same amount during the phase transition from ordered (ferroelectric) phase into the disordered paraelectric phase. At that, the change in temperature makes it possible directly (using the knowledge of crystal specific heat) to estimate the latent heat of phase transformation.

When electrical *field is applied* near ferroelectric phase transition, such heating-cooling effect becomes significant: using available fields, due to the electrocaloric effect in ferroelectric it is possible to change temperature by 1–2 °C. Such a change is usually called as the *shift of Curie point* under applied electrical field: when phase transition temperature shifts to higher temperatures. With regard

to technical applications, using cyclical operations in cooling device, this shift in temperature is already of technical interest.

Low temperatures are needed both for low-temperature electronics and for home appliances. It is important to receive solid-state coolers that prevent the use of both environmentally harmful freon and machine equipment of conventional refrigeration units (with compressors). Interest in electrocaloric cooling; changing in the temperature of dielectric in adiabatic conditions in the case of application or removal of an electric field has been noted for a long time, but above all, in relation to the reception of more low temperatures.

The dependence of the change in temperature dT for one cycle of application of direct electrical field can be described as follows:

$$\mathrm{d}T = -(T/C)(\mathrm{d}P/\mathrm{d}T)\,\mathrm{d}E,$$

where P is induced polarization, and C is heat capacity of used dielectric. Early experiments showed that in most of pyroelectrics and ferroelectrics when applying to electrical field up to 25 kV/cm the electrocaloric lowering of temperature does not exceed 0.5 K, and the only in a narrow range of temperatures near their Curie point. However, calculations show that the value of dT is less than 1 K is not sufficient for commercial applications of pyroelectric materials in temperature range 290-310 K.

The literature provides guidance on obtaining low temperatures in an operationally important temperature range from liquid nitrogen to freon temperatures using ferroelectric materials. Rather big values of the electrocaloric effect (2.6°C) near the phase transition of antiferroelectric ceramics of the $Pb(Zr,Sn,Ti)O_3$ system, as well as in the ceramics $Pb(Sc,Nb)O_3$.

For example, large electrocalyrical effect has recently been obtained with cycle temperature of about 4°C. This field-induced phase transitions from the antiferroelectric into the ferroelectric phase with enlarged electrocaloric effect was obtained recently in $(Pb,La)(Zr,Sn,Ti)O_3$ [15].

The technical interest in such effects is due to the fact that solid-state refrigeration systems based on the elastocaloric, magnetocaloric and electrocaloric materials offer potential advantages over conventional vapor-compression cooling technologies.

At that, the electrocaloric effect (electrical field inducing adiabatic temperature change in dielectric material) has some advantages, such as high cooling efficiency and easy miniaturization that need for portable cooling devices.

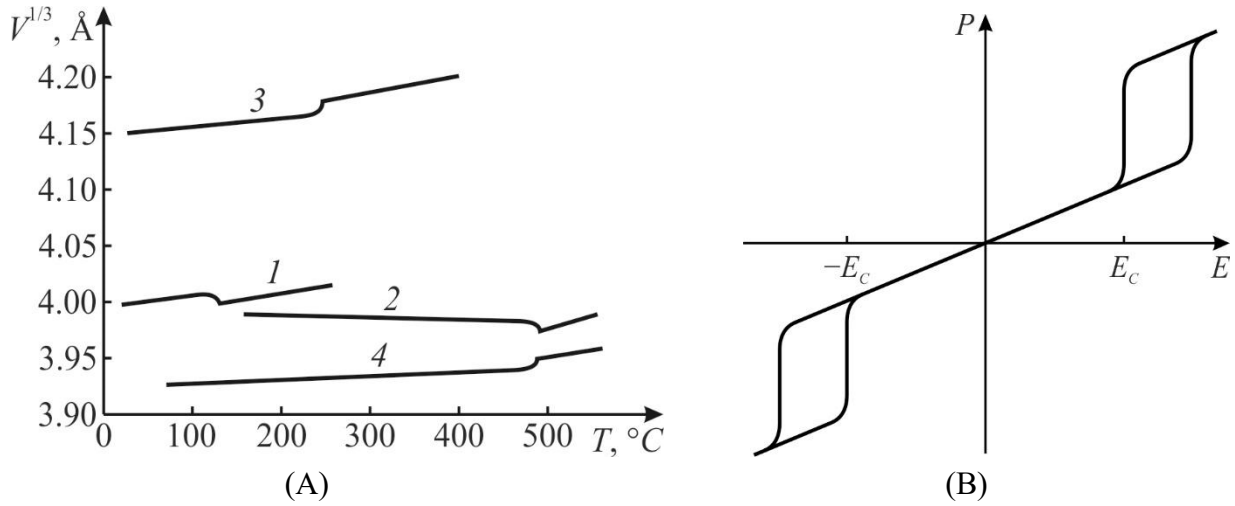

Fig. 7.8. Explanation of field-induced electrocaloric effect: A – temperature dependence of cubic root on unit cell volume in ferroelectrics $BaTiO_3$ (*1*) and $PbTiO_3$ (*2*), and in antiferroelectrics $PbZrO_3$ (*3*) and $NaNbO_3$ (*4*); B – double hysteresis loop of antiferroelectric

Consider physical basis of this effect. In the vicinity of phase transition, all thermodynamic functions of a crystal change, but *differently* for ferroelectrics and antiferroelectrics.

The convincing example is the *change in volume*: Fig. 7.8A shows temperature dependence of the unit cell volume for two ferroelectrics and two antiferroelectrics.

It is seen that the volume of ferroelectric polar phase *increases* as compared with the non-polar phase, while volume of anti-polar phase *decreases*. Obviously, the greatest change in thermodynamic functions can be expected during the transition from antipolar phase into polar phase and vice versa, which can be realized during phase transitions antiferroelectric ↔ferroelectric induced by electrical field application.

Figure 7.8B demonstrates correspondent electrical characteristics in a form of double dielectric hysteresis loop: in the field interval $-E$ □ $+E$, the material is the antiferroelectric but it transforms into the ferroelectric polar phases both at positive and negative voltages.

Thermodynamically, this corresponds to large electrocaric effect), which can already be considered as the alternative to other cooling methods (such as large magnetocaloric effect).

[***Note.*** Figure 7.8A shows different changing in volume δV near phase the transitions which are close to first type. The relationship between the change in volume δV and temperature change δT can be qualitatively traced from thermodynamic equation of state: $pV = RT$. Since the pressure p is constant and the

R is universal constant, $\delta V/\delta T = const$. It means that increments of δV should result in corresponding change in δT].

Another interesting physical aspect of the electrocalorytic effect is temperature hysteresis in the ferroelectrics, experiencing a phase transition close to first type phase transition [3]. This temperature hysteresis expresses the fact that during heating and cooling the ordering of polar-sensitive bonds occurs at different temperatures.

It can be explained taking into account the electrocaloric effect, which is rather big in such crystals. Indeed, when crystal is heated, the transition from ordered (ferroelectric) phase occurs at temperature slightly higher than "true" transition temperature, because due to electrocaloric effect crystal cools a little and uses its ability to remain ferroelectric at temperatures higher than "true" temperature of phase transition.

On the contrary, when cooling from paraelectric phase, ferroelectric crystal tends to remain in its paraelectric phase: whenever the *ordering* of polar-sensitive occurs in it due to electrocaloric effect crystal heats up that contributes to the preservation in it the paraelectric phase.

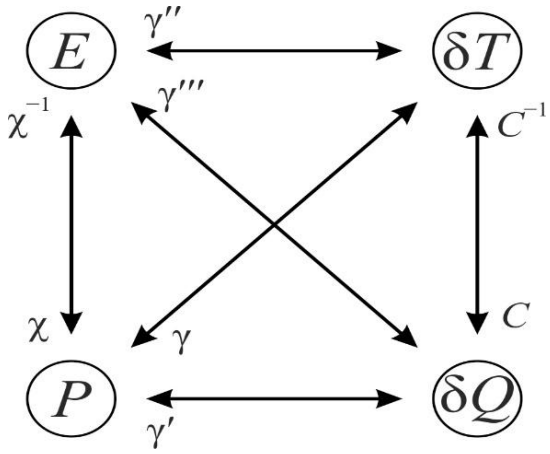

Fig. 7.9. Relationship of main parameters describing pyroelectric and electrocaloric effects

In conclusion of discussion of this topic, is appropriate to recall that in the polar crystals electrocaloric effect influences the value of *permittivity*. When thermal equilibrium is entirely established at the time of electrical field application (at very low frequency), pyroelectric crystal absorbs applied electrical energy and converts it into thermal energy.

This is the *isothermal* way of polarization of polar crystal, which is characterised by isothermal permittivity ε^T which is detectable at rather low frequency. On the contrary, in case of rather fast changing of applied electrical field,

the energy process has adiabatic character (when thermal equilibrium has no time to be set).

While measurements, it looks like a decrease of the capacitance of pyroelectric element, i.e., the decrease of its permittivity. Therefore, adiabatic permittivity ε^S can be determined at increased frequency, at that the difference $\Delta\varepsilon_{EC} = (\varepsilon^T - \varepsilon^S)$ is the electrocaloric part of low frequency permittivity; it might be essential only in pyroelectrics, depending on their specific heat and pyroelectric coefficient: $\Delta\varepsilon_{EC} = (\gamma^2 T)/(\varepsilon_0 C)$.

7.5 Summery and self-test questions

1. Pyroelectricity is the property of a polar crystal to *produce electrical energy* when it is subjected to the *change* of thermal energy. It is possible also to define *pyroelectric* effect as the ability of crystals to generate electricity, when they are *dynamically* heated or cooled; at that pyroelectric becomes polarized positively or negatively in proportional to *change* in temperature.

2. Pyroelectricity looks like *thermoelectric* power conversion; at that, this effect is a linear one, so according to Curie principle, a reversed effect must exist, namely, the *electrocaloric* effect, which the *electrothermal* energy conversion characterises.

3. Physical mechanism of pyroelectric effect is as follows: under constant external conditions (temperature, pressure, etc.), the structure of polar crystal corresponds to its energy minimum. At the same time, polar-sensitive interatomic bonds, striving for their mutual ordering, are in the *subtle equilibrium* with thermal chaotic motion of atoms in crystal lattice. When this equilibrium changes, caused for example by change in temperature (i.e., change in thermal energy), the polar crystal immediately reacts by appearance of electrical polarization — bound charges on the crystal surface.

4. Physical mechanism of electrocaloric effect is as follows: electrical field applied from the outside to a polar crystal *violates its equilibrium state* established thermodynamically under certain conditions at given temperature and pressure, which corresponds to the energy minimum. In this case, mutual ordering of polar-sensitive interatomic bonds, existing in the equilibrium structure, changes. If applied electrical field is directed accordingly to internal orientation of polar bonds, then it increases total energy of a crystal and it heats up. If this field is directed oppositely, then crystal energy decreases which is expressed in its cooling.

5. The nature of thermoelectrical coupling in the polar-sensitive crystals and their thermal properties can be described by various models: the *primary* effect, the *secondary* effect, as well as electrically and mechanically induced *artificial* pyroelectric effects. Hidden (or latent) intrinsic polarity in pyroelectric is only their ability to provide electrical (vector) response to any non-electrical (scalar) *dynamic* influence (such as uniform change of temperature).

6. *Primary* pyroelectric effect reflects the strength of bonding energy of polar bonds and their resilience to the chaotic thermal motion: these bonds react to external action by such a change, which is accompanied by electrical response, i.e., by the induced polarization. *Secodary* pyroelectric effect is the piezoelectrically transformed thermal deformation.

7. *Electrically induced* artificial pyroelectric effect exists in all solid dielectrics, but has practical meaning only in the dielectrics with very high permittivity (10^3–10^4). Electrical field keeps induced polar state of dielectric in the opposition to thermal motion in crystal; any violation of this equilibrium with temperature changes leads to the electrical response: the artificial pyroelectricity.

8. *Thermomechanically induced* pyroelectric effect manifests itself in any piezoelectric material and arises along the polar-neutral axes (in the pyroelectrics – along special polar axis, being in this case secondary pyroelectric effect). Partial limitation of thermal deformation turns the polar-neutral axis into a polar one. This effect can be of practical importance in wide-band semiconductors-piezoelectrics of AIIIBV type, allowing in monolithic (one-crystal) devices combining pyroelectric element with amplifier.

9. Very small changes in temperature can produce the perceptible pyroelectric potential: *infrared sensors* are designed from such pyroelectric materials, when heat of a human or animal from several feet away is enough to generate voltage. Among wide variety of thermal sensors, using pyroelectric effect, *motion detector* sensors can be identified as well as *infrared thermometers* for high precision pyrometery, *pyroelectric vidicons* in both vacuum and microelectronic design, etc.

10. *Electrocaloric* effect has a certain prospects for use in the miniature solid-state refrigeration systems. Using electrically induced phase transition from ferroelectric to anti-ferroelectric phase, a cooling up to 4 °C can be obtained in the single transition period.

11. Research and application of dielectrics is commonly held under the *adiabatic* conditions when entropy not changes: $\delta S = 0$. Therefore, from experiments, the adiabatic permittivity ε^S is measured. In such dielectrics, which polarization strongly depends on temperature, another – *isothermal* – process of

polarization might be important, when $\delta T = 0$ and permittivity is isothermal: ε^T. Isothermal permittivity is always greater than adiabatic: $\varepsilon^T > \varepsilon^S$. In the vicinity of ferroelectric phase transition the difference between ε^T and ε^S can reach 10–50%, so it should be taken into account.

Chapter 7. Self-test questions

1. What and how many parameters characterize the pyroelectric and electrocaloric effects?
2. What is the role of the boundary conditions for the pyroelectric effect and its application?
3. Haw can be obtained the pyroelectric effect in piezoelectric?
4. Haw can be obtained the pyroelectric effect in paraelectric?
5. What is the peculiarity of using pyroelectric far-infrared imaging devices?

AFTERWORDS

The basics of the modern approach to the physics of dielectrics as substances with special behavior in the electrical field are given: in dielectrics, there is a limited space shift of the electric charges – electrical *polarization*, and, at the same time, there is almost no movement of free charges through a matter – electrical *conductivity*.

Dielectrics include all gases, many liquids, as well as crystals, polycrystals, ceramics, glass, composites, amorphous substances and some substances compacted from nanocrystalline structures. In the crystalline dielectrics, the band gap of electronic spectrum is greater than ~ 3 eV.

Under normal conditions, the conductivity of dielectrics is lower than 10^{-10} S/m, so the electrical bias current exceeds the electrical conductivity current, and the electrostatic field in dielectrics can exist for a long time.

Dielectrics are also a medium for electromagnetic field propagating over long distances. This book considers the solid dielectrics only.

Structure. Crystals are characterized by almost perfect order of their internal construction. Therefore, the *crystals* can be described by a three-dimensional (3D) periodic spatial structure.

Characteristic of crystals is the translational ordering: an elementary cell of several atoms is "infinitely" translated in all directions, creating a regular crystal lattice.

The *polycrystals* consist of a large number of small crystals (crystallites); at that, macroscopic structure of polycrystals is disordered, but the microscopic components of their structure (crystallites, blocks) represent the small crystals with a clearly defined microscopic structure and the same properties as in large single crystal.

The *vitreous* and amorphous states of solid dielectrics are characterized by the absence of distant (translational) symmetry. These bodies are characterized only by a short order in the arrangement of atoms.

For two-dimensional (2D) systems, a strictly ordered structure is possible only in the plane. If such a planar system is nano-dimensional in the thickness, and is repeated many times in dielectric or semiconductor crystal (creating a superstructure), then its electronic properties can characterize so-called "quantum well", which is also related to the 2D nanostructures.

One-dimensional (1D) nanostructures include linearly oriented systems, in which translational ordering is observed only along one direction.

There are also known systems, in which the dimensions along all three directions are commensurate with the distance between the atoms. Such zero-dimensional (0D) systems can be "quantum dots", in which only 10 to 10^3 atoms are ordered.

A solid body is a collection of a very large number of structural units – atoms, ions or molecules – which are *strongly connected* to each other.

At that, properties of an isolated atom usually affect the nature of a solid body composed of these atoms, but only to a certain extent: the point is that in a solid body the properties of the atom are significantly affected by its environment (crystal lattice).

Therefore, to describe different properties of solids, it is necessary to use methods which are applicable to understanding the behavior of the system of many particles.

Although a solid is a system of strongly interacting particles, the theory of solids (including dielectrics) solves the problem of how to reduce description of a system of strongly interacting particles to a description of the systems of weakly interacting *quasiparticles*.

Quasiparticles. Well known properties of most crystals (strength, hardness, elasticity, etc.) determine the name of the physical state of matter: a solid. But in any solid body there are many different interactions between the particles that determine the electrical and thermal properties of matter.

Therefore, to explain the features of solids, it is assumed that they have other states ("hidden") which resemble the properties of the basic physical states of matter: *gases* of quasiparticles and quantum *liquids* (electrons in metal), as well as the electron-hole *plasma* (in semiconductors).

Quasiparticles are the collective motions of many solid particles (for example, the oscillations of the atoms of the crystal lattice).

Although many atoms are involved in each oscillation, this motion still has an atomic scale, because the average energy of each oscillation (phonon) is approximately equal to kW.

For particles, the number of which in any state is unlimited, the Bose-Einstein statistics is applie, and such particles are called *bosons*.

If the particles are subject to the Pauli principle (that is, only one particle can be in a certain state), then the Fermi-Dirac statistic is applied to them, and the particles are called *fermions.*

Fermions include, first of all, electrons, which are charged by collective excitations in the crystal and have different (including anisotropic) effective mass.

Among bosons the photons were considered which are the electromagnetic waves that can propagate in both vacuum and dielectric..

The bosons include also *phonons* representing elastic waves in crystals, that is main heat reservoir of a solid body, as well as *magnons* (spin waves), which can exist in the ferromagnets, antiferromagnets, and ferromagnets.

There are phenomena in which many quasiparticles are involved. For example, heat is transferred by phonons, electrons, and magnons. However, the transfer of electric charge is realized mostly by electrons, while magnetic moment of ferromagnets is responsible for magnons.

Another example of collective motion in crystals is the electronic excitation of an atom or molecule, which occurs, for example, due to the absorption of a quantum of light.

This excitation is not localized in a particular cell of the crystal, but moves from cell to cell in the form of a Frenkel *exciton*. The average energy of an exciton is of the same order as the energy of the excited state of an individual atom.

According to classical laws, the average energy of thermal motion of a particle is equal to $k_B T$, and therefore the internal thermal energy of the body is $E \sim N k_B T$, where N is the number of particles in the body.

However, as temperature decreases, the simple linear dependence $E(T)$ becomes broken, because the internal energy of a solid body approaches zero much faster than the linear law.

This fact is explained by the discrete (quantum) nature of the energy spectrum of solids. The fact is that with decreasing temperature the collective motions of atoms or ions (quasiparticles) become "freeze".

This usually occurs at temperatures below 100…200 K, but for some crystals nonlinearity as a function of $E(T)$ is also observed in the range of higher temperatures.

The greater the energy difference between the energy levels of the equivalent oscillator, the higher the temperature of corresponding motion "freezing". Because of this, the quantum motions in solids can be observed at quite different temperatures.

Symmetry. The creation of crystalline and other ordered bodies from atoms is accompanied by a decrease in energy compared to non-interacting atoms.

The minimum energy corresponds only to a certain arrangement of atoms (ions, molecules) relative to each other, which is accompanied by a significant redistribution of electron density between the particles.

Crystallization of matter, i.e., the transformation of a disordered set of atoms (liquid or gas) into regular crystal lattices, occurs due to the desire of the system of atoms to reduce energy with decreasing temperature.

The structure of a crystal is determined by the forces acting between atomic particles, and the nature of these forces is explained by quantum mechanics.

The periodic arrangement of atoms in space allows for a certain classification of the types of symmetry of the crystal. Determining the symmetry of crystal structures can be a difficult problem – an elementary cell can consist of dozens of atoms or ions.

The symmetry of the crystal is a set of virtual operations, after which the crystal passes into itself. Elements of symmetry are rotations around the axes of symmetry, images in the planes of symmetry (helical axes, planes of mirror sliding and translation).

The combination of "rotating" elements of symmetry (axes, images) with translations leads to limitations in the placement of atoms. For example, crystals can have only axes of symmetry of the second, third, fourth and sixth ranks (the axis of the first order is trivial).

According to "point symmetry", all crystals must belong to one of 32 classes. All possible types of spatial symmetry of crystal lattice structures (230 of them) were determined by the crystallographer Fedorov. Such a distant order applies only to perfectly ordered crystals and can be considered macrosymmetry. In real cases, the arrangement of the nearest atoms (microsymmetry) is broken both dynamically and quasi-statically.

Movement in crystals. Different types of particle motion are possible in crystals; moreover, for one reason or another, in real crystals the particles are not always placed in an ideal order (which corresponds to the minimum energy).

Irregular placement of atoms in crystal lattices (atom in the internode, vacancy, dislocation, boundary between individual crystallites) is called crystal *lattice defects*. In the places of defects the energy of the crystal is increased, but under normal conditions the atoms cannot rearrange and create a more energetically advantageous configuration.

To do this, atoms would have to overcome large potential barriers compared to the dynamic thermal energy of their motion, which is equal to $k_B T$. Only special technological methods allow to create almost defect-free crystals.

The microsymmetry of crystals is broken not only by defects, but also dynamically – in the case of any movement of atoms – and any peculiarities in the arrangement of the neighboring atoms affect their possible movements. Atoms and

ions make small oscillations and rotations around their equilibrium positions, which are described by the oscillator model.

At a sufficiently high temperature, atoms can oscillate so much that they lose their equilibrium state and jump either into the space between atoms (in this case, atoms in the internodes), or into randomly free adjacent equilibrium positions.

Such jumps at room and lower temperatures are quite rare, but become more frequent as the temperature approaches the melting point of a crystal. As the temperature increases, the amplitude of oscillations of atoms increases, and when this amplitude reaches 3–7% of the interatomic distance, the crystal usually melts.

With decreasing temperature, the amplitude of oscillations of atoms decreases significantly. But even in the case of approaching absolute zero temperature, the atoms do not stop moving.

This quantum motion of atoms is called zero oscillations. The inability to stop motion at zero temperature is a manifestation of the quantum properties of matter and does not correspond to the notion of classical physics that at a temperature of $T = 0$ K there must be a complete order in the arrangement of already stationary atoms. Quantum motion can significantly affect the passage of low-temperature phase transitions.

Another violation of the notion of "classical order" in crystals can be vacancies, when the crystal has random defects in the placement of atoms, consisting in the absence of atoms in some nodes of the crystal lattice. If a neighboring atom jumped on the vacant node, the vacancy moved to the vacated place.

The role of vacancies is very large in the diffusion of atoms in solids. In order for a vacancy to move, the atom must overcome a significant potential barrier. Therefore, these processes are rare at low temperatures, and the diffusion coefficient quickly approaches zero with decreasing temperature.

Mechanical properties of solids correspond to the internal connections between molecules and atoms of a matter; these include mainly elasticity, strength, hardness and viscosity, and others. Depending on the symmetry of the external mechanical forces, there are: linear-stress, plane-stress and volume-stress states, as well as net shear stress and hydrostatic pressure.

The response to the external stress can be *strain* (deformation), which, according to Hooke's law, is directly proportional to the mechanical stress and is classified into one-dimensional, two-dimensional and three-dimensional.

To consider dielectric devices in electronics, the most important mechanical properties are *elasticity* (which depends on the bond strength of atoms in crystals)

and the *speed* of elastic waves in crystals (which, in addition to elasticity, is affected by the density).

The propagation of one-dimensional, surface, and bulk elastic waves in solids, as well as the resonant properties of solid rods, beams, membranes, etc., are also described by the *elastic stiffness tensor*. Electrically excited elastic waves are widely used in modern acoustoelectronic, acousto-optical, microwave and other microelectronic devices.

Thermal properties of solids are due to the internal energy of motion of molecules, atoms and electrons, and are characterized by heat capacity, thermal conductivity and thermal expansion. *Heat capacity* is the ability to accumulate heat energy in a material when it is heated.

Several theories of lattice heat capacity of a solid are considered. First, this is the law of constancy of heat capacity, derived from the classical representations and with some accuracy is valid only for normal and elevated temperatures. Secondly, this is Einstein's quantum theory of heat capacity - the first successful attempt to apply quantum laws to the description of low-temperature heat capacity.

Third, it is Debye's quantum heat capacity theory, which agrees better with experiments at low temperatures than Einstein's theory. Finally, the dynamic theory of the Bourne crystal lattice is considered as the most perfect attempt to describe the dynamics of the crystal lattice, including the theory of heat capacity.

Thermal conductivity is the transfer of a heat by structural particles of matter (molecules, atoms, electrons) in the process of their thermal motion.

The coefficient of *thermal expansion* characterizes the features of the internal bonds of atoms, ions or molecules, including the amount of energy of these bonds. This energy is largely determined by such a fundamental parameter of the crystal as its melting point.

Electrons in dielectric crystals. The motions of different atomic particles in a solid are so different that it is often possible to neglect the motion of others by studying some particles.

For example, the velocity of atoms or ions in a solid is very small compared to the velocity of electrons, and therefore, considering the motion of electrons, the ions can be considered stationary (*adiabatic* approximation).

The accuracy of this approximation is determined by the parameter $(m/M)^{1/2}$ that is the ratio of the mass of the electron m to the mass of the ion M.

Analysis of the Schrödinger equation for electron in a crystal (Bloch's theorem) shows that the wave function in this case depends on some vector $\boldsymbol{k}$, the

modulus of which has the dimension of the inverse length, and therefore a *quasi-momentum* is introduced.

This concept is very useful for considering many aspects of electronic solid state theory. To greatly simplify the description of the motion of electrons in a crystal allowed the introduction of the concept of *effective mass,* i.e., a mass that must be attributed to the electron, so that its motion in the crystal under the action of external forces took the form of Newton's second law.

The concept of the effective mass has proved very fruitful in solid state physics and, in particular, in semiconductor physics.

The solutions of the Schrödinger equation have the form of Bloch waves for the real values of wave vector within the consolidated band, and the corresponding values of the electron energy form the allowed *energy zones*: for electrons on valence bonds - the valence band, and for the first excited state of valence electrons - the conduction band.

In metals, these zones overlap while in semiconductors and dielectrics, there is an energy gap (or *band gap*) between the valence band and the conduction band. There are no electron wave states in the band gap, and it can be considered as an energy barrier between the electrons bound at the valence levels and the free electrons to which the conduction band corresponds.

Dielectrics can have a different structure (crystals, glass, ceramics, polymers) and differ in that they may have an *electrostatic field*, moreover, in dielectric crystals the band gap is greater than 3 eV, and their electrical conductivity under normal conditions is less than 10^{-10} S/m. At the alternating voltage, the electric bias current in dielectrics exceeds the conductivity current.

The most important characteristic of dielectrics is the dielectric constant ε; accordingly, the most important of the electrical effects in dielectrics is the *electrical polarization*.

Elastic (deformation) polarization is weakly dependent on temperature, and is also the least inertial type of polarization, and therefore it determines the high-frequency and optical properties of dielectrics.

The mechanisms of thermal (relaxation) polarization are mainly due to the structural defects of dielectrics and lead to ε dispersion and dielectric losses at low frequencies and radio frequencies.

Dielectric permeability frequncy variance is an interdependent change of real and imaginary parts ε^* in case of frequency change.

The main property of the $\varepsilon^*(\omega)$ dispersion is the fulfillment of the Cramers–Kronig relations, which must satisfy any dispersion equation. In a wide range of

frequencies and in different crystallographic directions, several sections of the dispersion $\varepsilon^*(\omega)$ are usually observed in dielectrics, which form the *dielectric spectrum*.

In a strong electric field, if a certain threshold value of the voltage in the dielectric is reached, the *electrical breakdown* occurs: the magnitude of the current passing through the dielectric increases catastrophically and the electric discharge (spark or arc) passes through the dielectric.

The main physical mechanism of the first stage of breakdown (loss of electrical strength) is the shock ionization by electrons, as a result of which the concentration of charge carriers increases sharply due to the occurrence of the electron avalanche.

This form of breakdown of dielectrics is called electronic breakdown, which is characterized by a very short time of development of processes of loss of electrical strength.

Functional (active) dielectrics are able to convert energy and information carried by electrical signals. Piezoelectrics convert mechanical energy into electrical or, conversely, electrical energy into mechanical energy. The piezoelectric effect is observed in the *non-centrosymmetric* crystals and structures and is an odd (linear) effect.

The piezoelectric effect can be controlled by an external electrical field, for example, by changing the piezo-resonance frequency or the parameters of filters based on surface acoustic waves.

The efficiency of electrical control of the piezoelectric effect is most significant in the dielectrics with high dielectric constant.

Pyroelectric is also a solid-state energy converter. If piezoelectricity is associated with the electromechanical transformation, the pyroelectrics demonstrate thermoelectric coversion. Such energy conversion in a solid is possible only if the dielectric (crystal, polycrystal or polymer) has polar-sensitive structure.

Thermoelectric conversion is a pyroelectric effect, and the inverse electrothermal conversion of energy is the electrocaloric effect.

Ferroelectrics are characterized by switchable polar-sensitive structure, the direction of which can be changed by the externally applied electric field. In addition to ferroelectrics, the electrets have their own residual polarization. In contrast to the non-equilibrium residual polarization of electrets, the polar-sensitive structure of non-centre symmetric polar dielectrics characterizes by their stable (thermodynamically stable) state.

Ferroelectrics are distinguished from pyroelectrics by their ability to repolarization: the reorientation of their polar-sensitivity polarization under the action of an electrical field. At that, the *dielectric hysteresis* is observed.

Phase transitions. In the most cases, at a certain temperature, all degrees of freedom of atomic particles in a solid can be divided into two groups. For some degrees of freedom, the interaction energy U_{int} is small compared to k_BT, and for others it was large (the k_BT parameter is a measure of the thermal motion energy).

If $U_{int} << k_BT$, then corresponding degrees of freedom behave as a set of particles of an "ideal gas", and applicability of notion of *quasiparticles* is obvious. If $U_{int} >> k_BT$, then the corresponding degrees of freedom are ordered, but this motion can also be described by the introduction of *quasiparticles*.

A difficult for the theory is the case when the interaction energy $U_{int} \sim k_BT$, which usually corresponds to the phenomenon of *phase transition in a solid*. It should be noted that in all substances near certain temperatures, the physical properties do not change smoothly, but change abruptly.

This abrupt alteration in material properties is called a *phase transition* and such changes are inevitable when the aggregate state of matter changes. The typical example of a phase transition is the liquid–vapor transition; the liquid–crystal transition (crystallization) is another such example.

Both of these transitions belong to the transitions of the *first order*, when the phases located before and after the transition point are *significantly different* from each other. One phase replaces another simply because it is more energy efficient. For the transition to take place, the potential barrier separating these phases must be overcome. Therefore, in the vicinity of the phase transition of the first kind, both the supercooling and the overheating are possible.

Solid state physics is mainly concerned with the study of phase transitions in one aggregate state — the solid.

Of particular interest are the phase transitions in which a new property appears in the crystal, such as a spontaneous magnetic moment in the case of a transition from a paramagnetic state to a ferromagnetic state. In other cases, during the transition there is a switchable electric moment (in ferroelectrics), spontaneous deformation (in ferroelastics) or the ability to conduct current without resistance (in superconductors), and so on.

All these transitions belong to the transitions of the *second order:* at the Curie temperature T_C one of the phases ceases to exist and it is replaced by another. At the T_C point phases are indistinguishable; but if one move away from this point, the discrepancy between the properties of both phases increases.

Thus, in the ferromagnets below the Curie point the spontaneous magnetization appears and increases as it cools, in the ferroelectric crystals, if the temperature is lower than the Curie temperature T_C, a switchable electric moment increases, although at temperatures $T = T_C$ and above it equals zero.

Near the point of phase transition of the second order, a solid behaves in such a way that any descriptions based on the quasiparticles cannot adequately correspond to the experimental situation. Usually the nearest neighboring crystal particles in crystal are considered to be such *strongly interacting* that the interaction of more distant particles can be *even neglected*.

However, near the phase transition, the interaction of the nearest particles is compensating by each other, and against this background, the interaction of atomic particles placed at more long distance from each other becomes *dominant*.

In the case of such a transition, the anomalous increase in the role of collective motions is confirmed by the experiment: a maximum of heat capacity and a strong anomaly of the coefficient of thermal expansion, the magnetic permeability of ferromagnets and dielectric permittivity of ferroelectrics at the Curie point tend to infinity, etc. That is why the usual model of quasiparticles has difficulty in describing second-order phase transitions.

GENERAL REFERENCES

1. N.W. Ashcroft, N.D. Mermin, Solid State Physics, Holt and Winston, New York, 1976.

2. C. Kittel, Introduction to Solid State Physics, Wiley, New York, 1996.

3. O. Madelung, Introduction to Solid State Theory, Springer Series in Solid State Sciences, Vol. 2, Springer, Berlin, Heidelberg, New York, 1978.

4. R.P. Feynman, The Feynman Lectures on Physics 'Mainly Electromagnetism and Matter', Calif. Addison-Wesley, Redwood City, 1989.

5. S.M. Sze, Physics of Semiconductor Devices, John Wiley & Sons, New York, 1981.

6. H. Frohlich, Theory of dielectrics, Clarendon Press, Oxford, 1986.

7. M. Ali Omar. Elementary solid state physics. Addison-Wesley Pub. Co. – 1975.

8. Waser Rainer. Nanoelectronics and information technology. Advanced electronic materials and novel devices. – Weinheim: Wiley-VCH, 2005.

9. H. S. Nalva. Nanostructured materials and nanotechnology. San Diego: Academic Press, 2002.

10. A.K. Jonscher, Dielectric relaxation in solids, Chelsea Dielectrics Press, London, 1983.

11. M. Born and K. Huang, Dynamical theory of crystal lattices, Press Oxford, 1988.

12. A.R. Von Hippel. Dielectrics and waves. John Willey & Sons. New York. 1954.

13. W.F. Brown. Dielectrics. Handbuch der Physik. Springer, Berlin. 1956.

14. W. Franz. Dielectrisher Durschlag. Handbuch der Physik. 1956.

15. J.F. Nye. Physical properties of crystals. Oxford press. Bristol, 1957.

16. J.C. Sleter. Insulators, semiconductors and metals. McGraw-Hill, London, 1967.

17. L.H. Van Vlack. Materials science for engineers. Addison-Wesley Publ. Company. 1972.

18. C. Kittel. Introduction to solid state physics. John Willey & Sons. New York. 1975.

19. M.E. Lines, A.M. Glass. Principles and applications of ferroelectrics and related materials. Clarendon, Oxford 1977.

20. Y.M. Poplavko. Physics of Dielectrics (in Russian). High school, Kiev. 1980.

21. I. S. Rez and Y.M. Poplavko. Dielectrics. Main properties and electronic applications (in Russian). Edited “Radio i svyaz”, Moscow. 1989.

22. R. E. Newnham. Properties of materials. Anysotropy, symmetry, structure. Oxford press, 2004.

23. Y.M. Poplavko. Dielectric spectroscopy of solids. Basic theory and method application (in Russian). Edited LAMBERT Academic Publishing, 2013.

24. Y.M. Poplavko. Polar crystals. Physical nature and new effects. Edited LAMBERT Academic Publishing, 2014.

25. Y.M. Poplavko. Dielectrics at Microwaves. Thermostable ceramics, ferroelectrics, films, composites. Edited LAMBERT Academic Publishing, 2014.

26. Y.M. Poplavko. L.P. Pereverzeva, I.P. Raevskiy. Physics of active dielectrics (in Russian) Ed. “South Federal University of Russia”, Postov-na-Donu. 2009.

27. Y.M. Poplavko. Physics of active dielectrics. Edited LAMBERT Academic Publishing, 2015.

References to Chapter 1

1. Y.M. Poplavko, Electronic materials. Principles and applied science, ELSEVIER, 2019.

2. J.C. Burfoot and G.W. Taylor, Polar dielectrics and their application, Macmillan Press, New Jersey, 1979.

3. Y.M. Poplavko and Y.V. Didenko. Spontaneous Polarization or Manifestation of Peculiar Internal Structure? Third Intern. Conf. on Information and Telecommunication Technologies and Radio Electronics (UkrMiCo’2018); Ukraine, Odessa.

4. Y.M. Poplavko and Y.I. Yakimenko, Piezoelectrics, Polytechnic Institute, Kiev, 2013.

5. Y.M. Poplavko, L.P. Pereverzeva, I.P. Raevskiy, Physics of active dielectrics, South Federal University of Russia, Postov-na-Donu, 2009.

6. K.M. Rabe, C.H. Ahn, J.-M. Triscons (Eds.), Physics of ferroelectrics: a modern perspectives, Springer, 2007.

7. D.G. Schlom, L.-Q. Chen, C.J. Fennie at. al. Elastic strain engineering of ferroic oxides. MRS Bukketin, vol. 39 Feb. 2014, p. 118.

8. L.P. Pereverzeva and Y.M. Poplavko, Pyroelectricity in non-central crystals, Acta Physica Polonica A, 1993, 84, No 2, p. 287.

References to Chapter 2

1. A. Von Hippel, Dielectrics and waves, Jon Wiley, New York. 1954.

2. R. Kremer and A. Schönhals (Editors), Broadband Dielectric Spectroscopy. Springer-Verlag Berlin Heidelberg, 2003, p. 729.

3. A.K. Jonscher, Dielectric relaxation in solids. Chelsea Dielectrics Press, London, 1983.

4. Van Vlack, Materials science for engineers, Addison-Wesley Publishing Co., Massachusetts, 1975

5. H. Frelich, Theory of dielectrics. Dielectric constant and dielectric loss. 2nd ed. Oxford, 1959.

References to Chapter 3

1. V.F. Lvovich. Impedance spectroscopy. Applications to Electrochemical and Dielectric Phenomena, John Wiley & Sons, Inc., Hoboken, New Jersey, 2012, p. 323.

2. R. Kremer & A. Schönhals (Editors). Broadband Dielectric Spectroscopy. Springer-Verlag Berlin Heidelberg, 2003, p. 729.

3. K.S. Cole, R.H. Cole Dispersion and absorption in dielectrics. J. Chem. Phys. 1941. 9, 341–351

4. R.M. Fuoss, J.G. Kirkwood. Electrical Properties of Solids. VIII. Dipole moments in polyvinyl chloride-diphenyl systems. J. Am. Chem. Soc. 1941, 63, 2, 385-394.

5. D.W. Davidson, R.H. Cole. Dielectric relaxation in glycerol, propylene glycol, and n-propanol. J. Chem. Phys. 1951, 19, 1484–1490.

6. S. Havriliak, and S. A Negami, Complex plane representation of dielectric and mechanical relaxation processes in some polymers. Polymer, 1967, 8, 161-210.

References to Chapter 4

1. Y.M. Poplavko, Electronic materials. Principles and applied science, ELSEVIER, 2019.

2. K. Uchino, Ferroelectric devices, Marcel Dekker, New York, 2000.

3. M.E. Lines and A.M. Glass, Principles and application of ferroelectrics and related materials, Clareton Press, Oxford, 1977.

4. I.S. Jeludev, Basic of ferroelectricity, Atomizdat, Moscow, 1973.

5. W.O. Cady, Piezoelectricity, Amazon com, New York, 1946.

6. Y.M. Poplavko and Y.I. Yakimenko, Piezoelectrics, Polytechnic Institute, Kiev, 2013.

7. Y.M. Poplavko, L.P Pereverzeva, A.S. Voronov, Y.I. Yakimenko, Material Sciences, part II, Dielectrics, Polytechnik, Kiev, 2007.

References to Chapter 5

1. Y.M. Poplavko, L.P. Pereverzeva, I.P. Raevskiy, Physics of active dielectrics, South Federal University of Russia, Postov-na-Donu, 2009.

2. Y.M. Poplavko, L. Pereverzeva, N.-I. Cho, Y.S.You, Feasibility of microelectronic quartz temperature and pressure sensors. Jpn. J. Appl. Phys., Vol. 37, 1998, p. 4041.

3. Y.M. Poplavko and L.P. Pereverzeva, Pyroelectricity of partially clamped piezoelectrics, Ferroelectrics (USA), 1992, Vol. 130, p. 361.

4. Y.M. Poplavko, N.-I. Cho, Clamping influence on ferroelectric integrated film microwave properties, Semiconductor Science and Technology, 1999, Vol. 14, p. 961.

5. Y.M. Poplavko and L.P. Pereverzeva, Termopiezoelectric transducers. Ferroelectrics (USA), 1992, Vol. 131, p. 331.

References to Chapter 6

1. W.O. Cady, Piezoelectricity, Amazon com, New York, 1946.

2. J.C. Burfoot and G.W. Taylor, Polar dielectrics and their application, Macmillan Press, New Jersey, 1979.

3. K. Uchino, Ferroelectric devices, Marcel Dekker, New York, 2000.

4. I.S. Jeludev, Basics of ferroelectricity, Atomizdat, Moscow, 1973.

5. Y.M. Poplavko and Y.I. Yakimenko, Piezoelectrics, Polytechnic Institute, Kiev, 2013.

6. I.S. Rez and Y.M. Poplavko, Dielectrics**:** Main properties and electronics applications, Radio e Svjaz, Moscow, 1989.

7. Y.M. Poplavko. Eletronic materials. Principles and applied science. Elsevier, 2019.

8. Y.M. Poplavko, L.P. Pereverzeva, I.P. Raevskiy, Physics of active dielectrics, South Federal University of Russia, Postov-na-Donu, 2009.

9. Y.M. Poplavko, L. Pereverzeva, N.-I. Cho, Y.S.You, Feasibility of microelectronic quartz temperature and pressure sensors. Jpn. J. Appl. Phys., Vol. 37, 1998, p. 4041.

10. Y.M. Poplavko and L.P. Pereverzeva, Termopiezoelectric transducers, Ferroelectrics (USA), 1992, Vol. 131, p. 331.

11. Yoshimitsu Kikuchi, Ultrasonic transducers, Corona Publishing Company, Tokyo, 1969.

12. Jacob Fraden, AIP Handbook of modern sensors: physics, designs and applications, American Institute of Ohysics, New York, 1993

13. N. Setter. Piezoelectric materials in devices, EPFL, Swiss Federal Institute of Technology, Lausanne, 2002.

14. M.E. Lines and A.M. Glass, Principles and application of ferroelectrics and related materials, Clareton Press, Oxford, 1977.

References to Chapter 7

1. Y.M. Poplavko. Electronic materials. Principles and applied science, ELSEVIER, 2019.

2. J.C. Burfoot and G.W. Taylor, Polar dielectrics and their application, Macmillan Press, New Jersey, 1979.

3. I.S. Jeludev, Basics of ferroelectricity, Atomizdat, Moscow, 1973.

4. I.S. Rez and Y.M. Poplavko, Dielectrics**:** Main properties and electronics applications, Radio e Svjaz, Moscow, 1989.

5. M.E. Lines and A.M. Glass, Principles and application of ferroelectrics and related materials, Clareton Press, Oxford, 1977.

6. K. Uchino, Ferroelectric devices, Marcel Dekker, New York, 2000.

7. C. F. Tsai and M. S. Young (December 2003). Pyroelectric infrared sensor-based thermometer for monitoring indoor objects. Review of Scientific Instruments. 74 (12): 5267–5273.

/8 Y.M. Poplavko, L.P Pereverzeva, A.S. Voronov, Y.I. Yakimenko, Material Sciences, part II, Dielectrics, Polytechnik, Kiev, 2007.

9. B. Naranjo, S. Putterman and T. Venhaus, Pyroelectric fusion using a tritiated target, Nuclear Instruments and Methods in Physics Research Section A: Accelerators, Spectrometers, Detectors and Associated Equipment, Vol. 632, Issue 1, (11 March 2011), pp. 43-46.

10. Y.M. Poplavko and L.P. Pereverzeva, Pyroelectricity of partially clamped piezoelectrics, Ferroelectrics (USA), 1992, Vol. 130, p. 361.

11. Y.M. Poplavko, L. Pereverzeva, N.-I. Cho, Y.S.You, Feasibility of microelectronic quartz temperature and pressure sensors. Jpn. J. Appl. Phys., Vol. 37, 1998, p. 4041.

12. L.P. Pereverzeva, Y.M. Poplavko, Pyroelectricity in non-central crystals, Acta Physica Polonica A, 1993, 84, No 2, p. 287.

13. Y.M. Poplavko and L.P. Pereverzeva, Pyroelectric response of piezoelectrics. Ferroelectrics (USA), 1992, Vol. 134, p. 207.

14. Y.M. Poplavko and L.P. Pereverzeva, Termopiezoelectric transducers, Ferroelectrics (USA), 1992, Vol. 131, p. 331.

15. Fansping Zhuo, Qiang Li, Huimin Qiao et.al. Field-induced phase transitions and enhanced double negative electrocaloric effects in (Pb,La)(Zr,Sn,Ti)O_3 antiferroelectric single crystal. Appl. Phys. Lett., 2018, 112, 133901.